

Group Theory

M.S. Dresselhaus
G. Dresselhaus
A. Jorio

Group Theory

Application to the Physics of Condensed Matter

With 131 Figures and 219 Tables



Springer

Professor Dr. Mildred S. Dresselhaus
Dr. Gene Dresselhaus

Massachusetts Institute of Technology Room 13-3005
Cambridge, MA, USA
E-mail: millie@mgm.mit.edu, gene@mgm.mit.edu

Professor Dr. Ado Jorio

Departamento de Física
Universidade Federal de Minas Gerais
CP702 – Campus, Pampulha
Belo Horizonte, MG, Brazil 30.123-970
E-mail: adojorio@fisica.ufmg.br

ISBN 978-3-540-32897-1

e-ISBN 978-3-540-32899-8

DOI 10.1007/978-3-540-32899-8

Library of Congress Control Number: 2007922729

© 2008 Springer-Verlag Berlin Heidelberg

This work is subject to copyright. All rights are reserved, whether the whole or part of the material is concerned, specifically the rights of translation, reprinting, reuse of illustrations, recitation, broadcasting, reproduction on microfilm or in any other way, and storage in data banks. Duplication of this publication or parts thereof is permitted only under the provisions of the German Copyright Law of September 9, 1965, in its current version, and permission for use must always be obtained from Springer. Violations are liable to prosecution under the German Copyright Law.

The use of general descriptive names, registered names, trademarks, etc. in this publication does not imply, even in the absence of a specific statement, that such names are exempt from the relevant protective laws and regulations and therefore free for general use.

Production and Typesetting: LE-T_EX Jelonek, Schmidt & Vöckler GbR, Leipzig, Germany
Cover design: WMX Design GmbH, Heidelberg, Germany

Printed on acid-free paper

9 8 7 6 5 4 3 2 1

springer.com

The authors dedicate this book
to John Van Vleck and Charles Kittel

Preface

Symmetry can be seen as the most basic and important concept in physics. Momentum conservation is a consequence of translational symmetry of space. More generally, every process in physics is governed by selection rules that are the consequence of symmetry requirements. On a given physical system, the eigenstate properties and the degeneracy of eigenvalues are governed by symmetry considerations. The beauty and strength of group theory applied to physics resides in the transformation of many complex symmetry operations into a very simple linear algebra. The concept of *representation*, connecting the symmetry aspects to matrices and basis functions, together with a few simple theorems, leads to the determination and understanding of the fundamental properties of the physical system, and any kind of physical property, its transformations due to interactions or phase transitions, are described in terms of the simple concept of symmetry changes.

The reader may feel encouraged when we say group theory is “simple linear algebra.” It is true that group theory may look complex when either the mathematical aspects are presented with no clear and direct correlation to applications in physics, or when the applications are made with no clear presentation of the background. The contact with group theory in these terms usually leads to frustration, and although the reader can understand the specific treatment, he (she) is unable to apply the knowledge to other systems of interest. What this book is about is teaching group theory in close connection to applications, so that students can learn, understand, and use it for their own needs.

This book is divided into six main parts. Part I, Chaps. 1–4, introduces the basic mathematical concepts important for working with group theory. Part II, Chaps. 5 and 6, introduces the first application of group theory to quantum systems, considering the effect of a crystalline potential on the electronic states of an impurity atom and general selection rules. Part III, Chaps. 7 and 8, brings the application of group theory to the treatment of electronic states and vibrational modes of molecules. Here one finds the important group theory concepts of *equivalence* and *atomic site* symmetry. Part IV, Chaps. 9 and 10, brings the application of group theory to describe periodic lattices in both real and reciprocal lattices. Translational symmetry gives rise to a linear momentum quantum number and makes the group very large. Here the

concepts of *cosets* and *factor groups*, introduced in Chap. 1, are used to factor out the effect of the very large translational group, leading to a finite group to work with each unique type of wave vector – the group of the wave vector. Part V, Chaps. 11–15, discusses phonons and electrons in solid-state physics, considering general positions and specific high symmetry points in the Brillouin zones, and including the addition of spins that have a 4π rotation as the identity transformation. Cubic and hexagonal systems are used as general examples. Finally, Part VI, Chaps. 16–18, discusses other important symmetries, such as time reversal symmetry, important for magnetic systems, permutation groups, important for many-body systems, and symmetry of tensors, important for other physical properties, such as conductivity, elasticity, etc.

This book on the application of Group Theory to Solid-State Physics grew out of a course taught to Electrical Engineering and Physics graduate students by the authors and developed over the years to address their professional needs. The material for this book originated from group theory courses taught by Charles Kittel at U.C. Berkeley and by J.H. Van Vleck at Harvard in the early 1950s and taken by G. Dresselhaus and M.S. Dresselhaus, respectively. The material in the book was also stimulated by the classic paper of Bouckaert, Smoluchowski, and Wigner [1], which first demonstrated the power of group theory in condensed matter physics. The diversity of applications of group theory to solid state physics was stimulated by the research interests of the authors and the many students who studied this subject matter with the authors of this volume. Although many excellent books have been published on this subject over the years, our students found the specific subject matter, the pedagogic approach, and the problem sets given in the course user friendly and urged the authors to make the course content more broadly available.

The presentation and development of material in the book has been tailored pedagogically to the students taking this course for over three decades at MIT in Cambridge, MA, USA, and for three years at the University Federal of Minas Gerais (UFMG) in Belo Horizonte, Brazil. Feedback came from students in the classroom, teaching assistants, and students using the class notes in their doctoral research work or professionally.

We are indebted to the inputs and encouragement of former and present students and collaborators including, Peter Asbeck, Mike Kim, Roosevelt Peoples, Peter Eklund, Riichiro Saito, Georgii Samsonidze, Jose Francisco de Sampaio, Luiz Gustavo Cançado, and Eduardo Barros among others. The preparation of the material for this book was aided by Sharon Cooper on the figures, Mario Hofmann on the indexing and by Adelheid Duhm of Springer on editing the text. The MIT authors of this book would like to acknowledge the continued long term support of the Division of Materials Research section of the US National Science Foundation most recently under NSF Grant DMR-04-05538.

Cambridge, Massachusetts USA,
Belo Horizonte, Minas Gerais, Brazil,
August 2007

Mildred S. Dresselhaus
Gene Dresselhaus
Ado Jorio

Contents

Part I Basic Mathematics

| | | |
|----------|--|----|
| 1 | Basic Mathematical Background: Introduction | 3 |
| 1.1 | Definition of a Group | 3 |
| 1.2 | Simple Example of a Group | 3 |
| 1.3 | Basic Definitions | 6 |
| 1.4 | Rearrangement Theorem | 7 |
| 1.5 | Cosets | 7 |
| 1.6 | Conjugation and Class | 9 |
| 1.7 | Factor Groups | 11 |
| 1.8 | Group Theory and Quantum Mechanics | 11 |
| 2 | Representation Theory and Basic Theorems | 15 |
| 2.1 | Important Definitions | 15 |
| 2.2 | Matrices | 16 |
| 2.3 | Irreducible Representations | 17 |
| 2.4 | The Unitarity of Representations | 19 |
| 2.5 | Schur's Lemma (Part 1) | 21 |
| 2.6 | Schur's Lemma (Part 2) | 23 |
| 2.7 | Wonderful Orthogonality Theorem | 25 |
| 2.8 | Representations and Vector Spaces | 28 |
| 3 | Character of a Representation | 29 |
| 3.1 | Definition of Character | 29 |
| 3.2 | Characters and Class | 30 |
| 3.3 | Wonderful Orthogonality Theorem for Character | 31 |
| 3.4 | Reducible Representations | 33 |
| 3.5 | The Number of Irreducible Representations | 35 |
| 3.6 | Second Orthogonality Relation for Characters | 36 |
| 3.7 | Regular Representation | 37 |
| 3.8 | Setting up Character Tables | 40 |

| | | |
|----------|---|-----------|
| 3.9 | Schoenflies Symmetry Notation | 44 |
| 3.10 | The Hermann–Mauguin Symmetry Notation | 46 |
| 3.11 | Symmetry Relations and Point Group Classifications | 48 |
| 4 | Basis Functions | 57 |
| 4.1 | Symmetry Operations and Basis Functions | 57 |
| 4.2 | Basis Functions for Irreducible Representations | 58 |
| 4.3 | Projection Operators $\hat{P}_{kl}^{(\Gamma_n)}$ | 64 |
| 4.4 | Derivation of an Explicit Expression for $\hat{P}_{kl}^{(\Gamma_n)}$ | 64 |
| 4.5 | The Effect of Projection Operations on an Arbitrary Function | 65 |
| 4.6 | Linear Combinations of Atomic Orbitals for Three Equivalent Atoms at the Corners of an Equilateral Triangle . . | 67 |
| 4.7 | The Application of Group Theory to Quantum Mechanics | 70 |

Part II Introductory Application to Quantum Systems

| | | |
|----------|--|-----------|
| 5 | Splitting of Atomic Orbitals in a Crystal Potential | 79 |
| 5.1 | Introduction | 79 |
| 5.2 | Characters for the Full Rotation Group | 81 |
| 5.3 | Cubic Crystal Field Environment for a Paramagnetic Transition Metal Ion | 85 |
| 5.4 | Comments on Basis Functions | 90 |
| 5.5 | Comments on the Form of Crystal Fields | 92 |
| 6 | Application to Selection Rules and Direct Products | 97 |
| 6.1 | The Electromagnetic Interaction as a Perturbation | 97 |
| 6.2 | Orthogonality of Basis Functions | 99 |
| 6.3 | Direct Product of Two Groups | 100 |
| 6.4 | Direct Product of Two Irreducible Representations | 101 |
| 6.5 | Characters for the Direct Product | 103 |
| 6.6 | Selection Rule Concept in Group Theoretical Terms | 105 |
| 6.7 | Example of Selection Rules | 106 |

Part III Molecular Systems

| | | |
|----------|--|------------|
| 7 | Electronic States of Molecules and Directed Valence | 113 |
| 7.1 | Introduction | 113 |
| 7.2 | General Concept of Equivalence | 115 |
| 7.3 | Directed Valence Bonding | 117 |
| 7.4 | Diatom Molecules | 118 |
| 7.4.1 | Homonuclear Diatomic Molecules | 118 |
| 7.4.2 | Heterogeneous Diatomic Molecules | 120 |

| | | |
|----------|---|------------|
| 7.5 | Electronic Orbitals for Multiaatomic Molecules | 124 |
| 7.5.1 | The NH_3 Molecule | 124 |
| 7.5.2 | The CH_4 Molecule | 125 |
| 7.5.3 | The Hypothetical SH_6 Molecule | 129 |
| 7.5.4 | The Octahedral SF_6 Molecule | 133 |
| 7.6 | σ - and π -Bonds | 134 |
| 7.7 | Jahn–Teller Effect | 141 |
| 8 | Molecular Vibrations, Infrared, and Raman Activity | 147 |
| 8.1 | Molecular Vibrations: Background | 147 |
| 8.2 | Application of Group Theory to Molecular Vibrations | 149 |
| 8.3 | Finding the Vibrational Normal Modes | 152 |
| 8.4 | Molecular Vibrations in H_2O | 154 |
| 8.5 | Overtones and Combination Modes | 156 |
| 8.6 | Infrared Activity | 157 |
| 8.7 | Raman Effect | 159 |
| 8.8 | Vibrations for Specific Molecules | 161 |
| 8.8.1 | The Linear Molecules | 161 |
| 8.8.2 | Vibrations of the NH_3 Molecule | 166 |
| 8.8.3 | Vibrations of the CH_4 Molecule | 168 |
| 8.9 | Rotational Energy Levels | 170 |
| 8.9.1 | The Rigid Rotator | 170 |
| 8.9.2 | Wigner–Eckart Theorem | 172 |
| 8.9.3 | Vibrational–Rotational Interaction | 174 |

Part IV Application to Periodic Lattices

| | | |
|----------|--|------------|
| 9 | Space Groups in Real Space | 183 |
| 9.1 | Mathematical Background for Space Groups | 184 |
| 9.1.1 | Space Groups Symmetry Operations | 184 |
| 9.1.2 | Compound Space Group Operations | 186 |
| 9.1.3 | Translation Subgroup | 188 |
| 9.1.4 | Symmorphic and Nonsymmorphic Space Groups | 189 |
| 9.2 | Bravais Lattices and Space Groups | 190 |
| 9.2.1 | Examples of Symmorphic Space Groups | 192 |
| 9.2.2 | Cubic Space Groups and the Equivalence Transformation | 194 |
| 9.2.3 | Examples of Nonsymmorphic Space Groups | 196 |
| 9.3 | Two-Dimensional Space Groups | 198 |
| 9.3.1 | 2D Oblique Space Groups | 200 |
| 9.3.2 | 2D Rectangular Space Groups | 201 |
| 9.3.3 | 2D Square Space Group | 203 |
| 9.3.4 | 2D Hexagonal Space Groups | 203 |
| 9.4 | Line Groups | 204 |

| | | |
|-----------|---|------------|
| 9.5 | The Determination of Crystal Structure and Space Group | 205 |
| 9.5.1 | Determination of the Crystal Structure | 206 |
| 9.5.2 | Determination of the Space Group | 206 |
| 10 | Space Groups in Reciprocal Space and Representations | 209 |
| 10.1 | Reciprocal Space | 210 |
| 10.2 | Translation Subgroup | 211 |
| 10.2.1 | Representations for the Translation Group | 211 |
| 10.2.2 | Bloch's Theorem and the Basis of the Translational Group | 212 |
| 10.3 | Symmetry of \mathbf{k} Vectors and the Group of the Wave Vector | 214 |
| 10.3.1 | Point Group Operation in \mathbf{r} -space and \mathbf{k} -space | 214 |
| 10.3.2 | The Group of the Wave Vector G_k and the Star of k | 215 |
| 10.3.3 | Effect of Translations and Point Group Operations on Bloch Functions | 215 |
| 10.4 | Space Group Representations | 219 |
| 10.4.1 | Symmorphic Group Representations | 219 |
| 10.4.2 | Nonsymmorphic Group Representations and the Multiplier Algebra | 220 |
| 10.5 | Characters for the Equivalence Representation | 221 |
| 10.6 | Common Cubic Lattices: Symmorphic Space Groups | 222 |
| 10.6.1 | The Γ Point | 223 |
| 10.6.2 | Points with $k \neq 0$ | 224 |
| 10.7 | Compatibility Relations | 227 |
| 10.8 | The Diamond Structure: Nonsymmorphic Space Group | 230 |
| 10.8.1 | Factor Group and the Γ Point | 231 |
| 10.8.2 | Points with $k \neq 0$ | 232 |
| 10.9 | Finding Character Tables for all Groups of the Wave Vector . . | 235 |

Part V Electron and Phonon Dispersion Relation

| | | |
|-----------|---|------------|
| 11 | Applications to Lattice Vibrations | 241 |
| 11.1 | Introduction | 241 |
| 11.2 | Lattice Modes and Molecular Vibrations | 244 |
| 11.3 | Zone Center Phonon Modes | 246 |
| 11.3.1 | The NaCl Structure | 246 |
| 11.3.2 | The Perovskite Structure | 247 |
| 11.3.3 | Phonons in the Nonsymmorphic Diamond Lattice | 250 |
| 11.3.4 | Phonons in the Zinc Blende Structure | 252 |
| 11.4 | Lattice Modes Away from $\mathbf{k} = 0$ | 253 |
| 11.4.1 | Phonons in NaCl at the X Point $k = (\pi/a)(100)$ | 254 |
| 11.4.2 | Phonons in BaTiO ₃ at the X Point | 256 |
| 11.4.3 | Phonons at the K Point in Two-Dimensional Graphite . | 258 |

| | | |
|-----------|---|------------|
| 11.5 | Phonons in Te and α -Quartz Nonsymmorphic Structures | 262 |
| 11.5.1 | Phonons in Tellurium | 262 |
| 11.5.2 | Phonons in the α -Quartz Structure | 268 |
| 11.6 | Effect of Axial Stress on Phonons | 272 |
| 12 | Electronic Energy Levels in a Cubic Crystals | 279 |
| 12.1 | Introduction | 279 |
| 12.2 | Plane Wave Solutions at $\mathbf{k} = 0$ | 282 |
| 12.3 | Symmetrized Plane Solution Waves along the Δ -Axis | 286 |
| 12.4 | Plane Wave Solutions at the X Point | 288 |
| 12.5 | Effect of Glide Planes and Screw Axes | 294 |
| 13 | Energy Band Models Based on Symmetry | 305 |
| 13.1 | Introduction | 305 |
| 13.2 | $\mathbf{k} \cdot \mathbf{p}$ Perturbation Theory | 307 |
| 13.3 | Example of $\mathbf{k} \cdot \mathbf{p}$ Perturbation Theory for a Nondegenerate Γ_1^+ Band | 308 |
| 13.4 | Two Band Model: Degenerate First-Order Perturbation Theory | 311 |
| 13.5 | Degenerate second-order $\mathbf{k} \cdot \mathbf{p}$ Perturbation Theory | 316 |
| 13.6 | Nondegenerate $\mathbf{k} \cdot \mathbf{p}$ Perturbation Theory at a Δ Point | 324 |
| 13.7 | Use of $\mathbf{k} \cdot \mathbf{p}$ Perturbation Theory to Interpret Optical Experiments | 326 |
| 13.8 | Application of Group Theory to Valley–Orbit Interactions in Semiconductors | 327 |
| 13.8.1 | Background | 328 |
| 13.8.2 | Impurities in Multivalley Semiconductors | 330 |
| 13.8.3 | The Valley–Orbit Interaction | 331 |
| 14 | Spin–Orbit Interaction in Solids and Double Groups | 337 |
| 14.1 | Introduction | 337 |
| 14.2 | Crystal Double Groups | 341 |
| 14.3 | Double Group Properties | 343 |
| 14.4 | Crystal Field Splitting Including Spin–Orbit Coupling | 349 |
| 14.5 | Basis Functions for Double Group Representations | 353 |
| 14.6 | Some Explicit Basis Functions | 355 |
| 14.7 | Basis Functions for Other Γ_8^+ States | 358 |
| 14.8 | Comments on Double Group Character Tables | 359 |
| 14.9 | Plane Wave Basis Functions for Double Group Representations | 360 |
| 14.10 | Group of the Wave Vector for Nonsymmorphic Double Groups | 362 |

| | |
|---|-----|
| 15 Application of Double Groups to Energy Bands with Spin | 367 |
| 15.1 Introduction | 367 |
| 15.2 $E(\mathbf{k})$ for the Empty Lattice Including Spin–Orbit Interaction | 368 |
| 15.3 The $\mathbf{k} \cdot \mathbf{p}$ Perturbation with Spin–Orbit Interaction | 369 |
| 15.4 $E(\mathbf{k})$ for a Nondegenerate Band Including Spin–Orbit Interaction | 372 |
| 15.5 $E(\mathbf{k})$ for Degenerate Bands Including Spin–Orbit Interaction | 374 |
| 15.6 Effective g -Factor | 378 |
| 15.7 Fourier Expansion of Energy Bands: Slater–Koster Method | 389 |
| 15.7.1 Contributions at $d = 0$ | 396 |
| 15.7.2 Contributions at $d = 1$ | 396 |
| 15.7.3 Contributions at $d = 2$ | 397 |
| 15.7.4 Summing Contributions through $d = 2$ | 397 |
| 15.7.5 Other Degenerate Levels | 397 |

Part VI Other Symmetries

| | |
|--|-----|
| 16 Time Reversal Symmetry | 403 |
| 16.1 The Time Reversal Operator | 403 |
| 16.2 Properties of the Time Reversal Operator | 404 |
| 16.3 The Effect of \hat{T} on $E(\mathbf{k})$, Neglecting Spin | 407 |
| 16.4 The Effect of \hat{T} on $E(\mathbf{k})$, Including the Spin–Orbit Interaction | 411 |
| 16.5 Magnetic Groups | 416 |
| 16.5.1 Introduction | 418 |
| 16.5.2 Types of Elements | 418 |
| 16.5.3 Types of Magnetic Point Groups | 419 |
| 16.5.4 Properties of the 58 Magnetic Point Groups $\{A_i, M_k\}$ | 419 |
| 16.5.5 Examples of Magnetic Structures | 423 |
| 16.5.6 Effect of Symmetry on the Spin Hamiltonian for the 32 Ordinary Point Groups | 426 |
| 17 Permutation Groups and Many-Electron States | 431 |
| 17.1 Introduction | 432 |
| 17.2 Classes and Irreducible Representations of Permutation Groups | 434 |
| 17.3 Basis Functions of Permutation Groups | 437 |
| 17.4 Pauli Principle in Atomic Spectra | 440 |
| 17.4.1 Two-Electron States | 440 |
| 17.4.2 Three-Electron States | 443 |
| 17.4.3 Four-Electron States | 448 |
| 17.4.4 Five-Electron States | 451 |
| 17.4.5 General Comments on Many-Electron States | 451 |

| | |
|--|-----|
| 18 Symmetry Properties of Tensors | 455 |
| 18.1 Introduction | 455 |
| 18.2 Independent Components of Tensors Under Permutation Group Symmetry | 458 |
| 18.3 Independent Components of Tensors: Point Symmetry Groups | 462 |
| 18.4 Independent Components of Tensors Under Full Rotational Symmetry | 463 |
| 18.5 Tensors in Nonlinear Optics | 463 |
| 18.5.1 Cubic Symmetry: O_h | 464 |
| 18.5.2 Tetrahedral Symmetry: T_d | 466 |
| 18.5.3 Hexagonal Symmetry: D_{6h} | 466 |
| 18.6 Elastic Modulus Tensor | 467 |
| 18.6.1 Full Rotational Symmetry: 3D Isotropy | 469 |
| 18.6.2 Icosahedral Symmetry | 472 |
| 18.6.3 Cubic Symmetry | 472 |
| 18.6.4 Other Symmetry Groups | 474 |
| A Point Group Character Tables | 479 |
| B Two-Dimensional Space Groups | 489 |
| C Tables for 3D Space Groups | 499 |
| C.1 Real Space | 499 |
| C.2 Reciprocal Space | 503 |
| D Tables for Double Groups | 521 |
| E Group Theory Aspects of Carbon Nanotubes | 533 |
| E.1 Nanotube Geometry and the (n, m) Indices | 534 |
| E.2 Lattice Vectors in Real Space | 534 |
| E.3 Lattice Vectors in Reciprocal Space | 535 |
| E.4 Compound Operations and Tube Helicity | 536 |
| E.5 Character Tables for Carbon Nanotubes | 538 |
| F Permutation Group Character Tables | 543 |
| References | 549 |
| Index | 553 |

Part I

Basic Mathematics

Basic Mathematical Background: Introduction

In this chapter we introduce the mathematical definitions and concepts that are basic to group theory and to the classification of symmetry properties [2].

1.1 Definition of a Group

A collection of elements A, B, C, \dots form a group when the following four conditions are satisfied:

1. The product of any two elements of the group is itself an element of the group. For example, relations of the type $AB = C$ are valid for all members of the group.
2. The associative law is valid – i.e., $(AB)C = A(BC)$.
3. There exists a unit element E (also called the identity element) such that the product of E with any group element leaves that element unchanged $AE = EA = A$.
4. For every element A there exists an inverse element A^{-1} such that $A^{-1}A = AA^{-1} = E$.

In general, the elements of a group will not commute, i.e., $AB \neq BA$. But if all elements of a group commute, the group is then called an *Abelian* group.

1.2 Simple Example of a Group

As a simple example of a group, consider the permutation group for three numbers, $P(3)$. Equation (1.1) lists the $3! = 6$ possible permutations that can be carried out; the top row denotes the initial arrangement of the three numbers and the bottom row denotes the final arrangement. Each permutation is an element of $P(3)$.

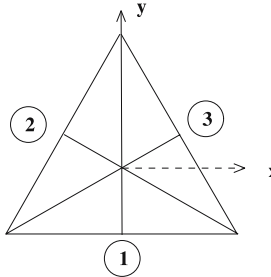


Fig. 1.1. The symmetry operations on an equilateral triangle are the rotations by $\pm 2\pi/3$ about the origin and the rotations by π about the three twofold axes. Here the axes or points of the equilateral triangle are denoted by numbers in *circles*

$$\begin{aligned}
 E &= \begin{pmatrix} 1 & 2 & 3 \\ 1 & 2 & 3 \end{pmatrix} & A &= \begin{pmatrix} 1 & 2 & 3 \\ 1 & 3 & 2 \end{pmatrix} & B &= \begin{pmatrix} 1 & 2 & 3 \\ 3 & 2 & 1 \end{pmatrix} \\
 C &= \begin{pmatrix} 1 & 2 & 3 \\ 2 & 1 & 3 \end{pmatrix} & D &= \begin{pmatrix} 1 & 2 & 3 \\ 3 & 1 & 2 \end{pmatrix} & F &= \begin{pmatrix} 1 & 2 & 3 \\ 2 & 3 & 1 \end{pmatrix} . \quad (1.1)
 \end{aligned}$$

We can also think of the elements in (1.1) in terms of the three points of an equilateral triangle (see Fig. 1.1). Again, the top row denotes the initial state and the bottom row denotes the final position of each number. For example, in symmetry operation D , 1 moves to position 2, and 2 moves to position 3, while 3 moves to position 1, which represents a clockwise rotation of $2\pi/3$ (see caption to Fig. 1.1). As the effect of the six distinct symmetry operations that can be performed on these three points (see caption to Fig. 1.1). We can call each symmetry operation an *element* of the group. The $P(3)$ group is, therefore, identical with the group for the symmetry operations on a equilateral triangle shown in Fig. 1.1. Similarly, F is a counter-clockwise rotation of $2\pi/3$, so that the numbers inside the circles in Fig. 1.1 move exactly as defined by Eq. 1.1.

It is convenient to classify the products of group elements. We write these products using a *multiplication table*. In Table 1.1 a multiplication table is written out for the symmetry operations on an equilateral triangle or equivalently for the permutation group of three elements. It can easily be shown that the symmetry operations given in (1.1) satisfy the four conditions in Sect. 1.1 and therefore form a group. We illustrate the use of the notation in Table 1.1 by verifying the *associative law* $(AB)C = A(BC)$ for a few elements:

$$\begin{aligned}
 (AB)C &= DC = B \\
 A(BC) &= AD = B . \quad (1.2)
 \end{aligned}$$

Each element of the permutation group $P(3)$ has a one-to-one correspondence to the symmetry operations of an equilateral triangle and we therefore say that these two groups are *isomorphic* to each other. We furthermore can

Table 1.1. Multiplication^a table for permutation group of three elements; $P(3)$

| | E | A | B | C | D | F |
|-----|-----|-----|-----|-----|-----|-----|
| E | E | A | B | C | D | F |
| A | A | E | D | F | B | C |
| B | B | F | E | D | C | A |
| C | C | D | F | E | A | B |
| D | D | C | A | B | F | E |
| F | F | B | C | A | E | D |

^a $AD = B$ defines use of multiplication table

use identical group theoretical procedures in dealing with physical problems associated with either of these groups, even though the two groups arise from totally different physical situations. It is this generality that makes group theory so useful as a general way to classify symmetry operations arising in physical problems.

Often, when we deal with symmetry operations in a crystal, the geometrical visualization of repeated operations becomes difficult. Group theory is designed to help with this problem. Suppose that the symmetry operations in practical problems are elements of a group; this is generally the case. Then if we can associate each element with a matrix that obeys the same multiplication table as the elements themselves, that is, if the elements obey $AB = D$, then the matrices representing the elements must obey

$$M(A) M(B) = M(D) . \quad (1.3)$$

If this relation is satisfied, then we can carry out all geometrical operations analytically in terms of arithmetic operations on matrices, which are usually easier to perform. The one-to-one identification of a generalized symmetry operation with a matrix is the basic idea of a *representation* and why group theory plays such an important role in the solution of practical problems.

A set of matrices that satisfy the multiplication table (Table 1.1) for the group $P(3)$ are:

$$E = \begin{pmatrix} 1 & 0 \\ 0 & 1 \end{pmatrix} \quad A = \begin{pmatrix} -1 & 0 \\ 0 & 1 \end{pmatrix} \quad B = \begin{pmatrix} \frac{1}{2} & -\frac{\sqrt{3}}{2} \\ -\frac{\sqrt{3}}{2} & -\frac{1}{2} \end{pmatrix}$$

$$C = \begin{pmatrix} \frac{1}{2} & \frac{\sqrt{3}}{2} \\ \frac{\sqrt{3}}{2} & -\frac{1}{2} \end{pmatrix} \quad D = \begin{pmatrix} -\frac{1}{2} & \frac{\sqrt{3}}{2} \\ -\frac{\sqrt{3}}{2} & -\frac{1}{2} \end{pmatrix} \quad F = \begin{pmatrix} -\frac{1}{2} & -\frac{\sqrt{3}}{2} \\ \frac{\sqrt{3}}{2} & -\frac{1}{2} \end{pmatrix} . \quad (1.4)$$

We note that the matrix corresponding to the identity operation E is always a unit matrix. The matrices in (1.4) constitute a matrix representation of the group that is isomorphic to $P(3)$ and to the symmetry operations on

an equilateral triangle. The A matrix represents a rotation by $\pm\pi$ about the y axis, while the B and C matrices, respectively, represent rotations by $\pm\pi$ about axes 2 and 3 in Fig. 1.1. D and F , respectively, represent rotation of $-2\pi/3$ and $+2\pi/3$ around the center of the triangle.

1.3 Basic Definitions

Definition 1. *The order of a group \equiv the number of elements in the group. We will be mainly concerned with finite groups. As an example, $P(3)$ is of order 6.*

Definition 2. *A subgroup \equiv a collection of elements within a group that by themselves form a group.*

Examples of subgroups in $P(3)$:

$$\begin{aligned} E & (E, A) (E, D, F) \\ & (E, B) \\ & (E, C) \end{aligned}$$

Theorem. *If in a finite group, an element X is multiplied by itself enough times (n), the identity $X^n = E$ is eventually recovered.*

Proof. If the group is finite, and any arbitrary element is multiplied by itself repeatedly, the product will eventually give rise to a repetition. For example, for $P(3)$ which has six elements, seven multiplications must give a repetition. Let Y represent such a repetition:

$$Y = X^p = X^q, \quad \text{where } p > q. \quad (1.5)$$

Then let $p = q + n$ so that

$$X^p = X^{q+n} = X^q X^n = X^q = X^q E, \quad (1.6)$$

from which it follows that

$$X^n = E. \quad (1.7)$$

□

Definition 3. *The order of an element \equiv the smallest value of n in the relation $X^n = E$.*

We illustrate the order of an element using $P(3)$ where:

- E is of order 1,
- A, B, C are of order 2,
- D, F are of order 3.

Definition 4. The period of an element $X \equiv$ collection of elements $E, X, X^2, \dots, X^{n-1}$, where n is the order of the element. The period forms an Abelian subgroup.

Some examples of periods based on the group $P(3)$ are

$$\begin{aligned} &E, A \\ &E, B \\ &E, C \\ &E, D, F = E, D, D^2. \end{aligned} \tag{1.8}$$

1.4 Rearrangement Theorem

The rearrangement theorem is fundamental and basic to many theorems to be proven subsequently.

Rearrangement Theorem. If E, A_1, A_2, \dots, A_h are the elements of a group, and if A_k is an arbitrary group element, then the assembly of elements

$$A_k E, A_k A_1, \dots, A_k A_h \tag{1.9}$$

contains each element of the group once and only once.

Proof. 1. We show first that every element is contained.

Let X be an arbitrary element. If the elements form a group there will be an element $A_r = A_k^{-1}X$. Then $A_k A_r = A_k A_k^{-1}X = X$. Thus we can always find X after multiplication of the appropriate group elements.

2. We now show that X occurs only once. Suppose that X appears twice in the assembly $A_k E, A_k A_1, \dots, A_k A_h$, say $X = A_k A_r = A_k A_s$. Then by multiplying on the left by A_k^{-1} we get $A_r = A_s$, which implies that two elements in the original group are identical, contrary to the original listing of the group elements.

Because of the rearrangement theorem, every row and column of a multiplication table contains each element once and only once. \square

1.5 Cosets

In this section we will introduce the concept of cosets. The importance of cosets will be clear when introducing the factor group (Sect. 1.7). The cosets are the elements of a factor group, and the factor group is important for working with space groups (see Chap. 9).

Definition 5. If \mathcal{B} is a subgroup of the group G , and X is an element of G , then the assembly $EX, B_1 X, B_2 X, \dots, B_g X$ is the right coset of \mathcal{B} , where \mathcal{B} consists of E, B_1, B_2, \dots, B_g .

A coset need not be a subgroup. A coset will itself be a subgroup \mathcal{B} if X is an element of \mathcal{B} (by the rearrangement theorem).

Theorem. *Two right cosets of given subgroup either contain exactly the same elements, or else have no elements in common.*

Proof. Clearly two right cosets either contain no elements in common or at least one element in common. We show that if there is one element in common, all elements are in common.

Let $\mathcal{B}X$ and $\mathcal{B}Y$ be two right cosets. If $B_kX = B_\ell Y$ = one element that the two cosets have in common, then

$$B_\ell^{-1}B_k = YX^{-1} \quad (1.10)$$

and YX^{-1} is in \mathcal{B} , since the product on the left-hand side of (1.10) is in \mathcal{B} . And also contained in \mathcal{B} is $EYX^{-1}, B_1YX^{-1}, B_2YX^{-1}, \dots, B_gYX^{-1}$. Furthermore, according to the rearrangement theorem, these elements are, in fact, identical with \mathcal{B} except for possible order of appearance. Therefore the elements of $\mathcal{B}Y$ are identical to the elements of $\mathcal{B}YX^{-1}X$, which are also identical to the elements of $\mathcal{B}X$ so that all elements are in common. \square

We now give some examples of cosets using the group $P(3)$. Let $\mathcal{B} = E, A$ be a subgroup. Then the right cosets of \mathcal{B} are

$$\begin{aligned} (E, A)E &\rightarrow E, A & (E, A)C &\rightarrow C, F \\ (E, A)A &\rightarrow A, E & (E, A)D &\rightarrow D, B \\ (E, A)B &\rightarrow B, D & (E, A)F &\rightarrow F, C, \end{aligned} \quad (1.11)$$

so that there are three distinct right cosets of (E, A) , namely

$$\begin{aligned} (E, A) &\quad \text{which is a subgroup} \\ (B, D) &\quad \text{which is not a subgroup} \\ (C, F) &\quad \text{which is not a subgroup.} \end{aligned}$$

Similarly there are three left cosets of (E, A) obtained by $X(E, A)$:

$$\begin{aligned} (E, A) \\ (C, D) \\ (B, F) \end{aligned} \quad (1.12)$$

To multiply two cosets, we multiply constituent elements of each coset in proper order. Such multiplication either yields a coset or joins two cosets. For example:

$$(E, A)(B, D) = (EB, ED, AB, AD) = (B, D, D, B) = (B, D). \quad (1.13)$$

Theorem. *The order of a subgroup is a divisor of the order of the group.*

Proof. If an assembly of all the distinct cosets of a subgroup is formed (n of them), then n multiplied by the number of elements in a coset, \mathcal{C} , is exactly

the number of elements in the group. Each element must be included since cosets have no elements in common.

For example, for the group $P(3)$, the subgroup (E, A) is of order 2, the subgroup (E, D, F) is of order 3 and both 2 and 3 are divisors of 6, which is the order of $P(3)$. \square

1.6 Conjugation and Class

Definition 6. *An element B conjugate to A is by definition $B \equiv XAX^{-1}$, where X is an arbitrary element of the group.*

For example,

$$A = X^{-1}BX = YBY^{-1}, \quad \text{where } BX = XA \quad \text{and} \quad AY = YB.$$

The elements of an Abelian group are all selfconjugate.

Theorem. *If B is conjugate to A and C is conjugate to B , then C is conjugate to A .*

Proof. By definition of conjugation, we can write

$$\begin{aligned} B &= XAX^{-1} \\ C &= YBY^{-1}. \end{aligned}$$

Thus, upon substitution we obtain

$$C = YXAX^{-1}Y^{-1} = YXA(YX)^{-1}.$$

\square

Definition 7. *A class is the totality of elements which can be obtained from a given group element by conjugation.*

For example in $P(3)$, there are three classes:

1. E ;
2. A, B, C ;
3. D, F .

Consistent with this class designation is

$$ABA^{-1} = AF = C \tag{1.14}$$

$$DBD^{-1} = DA = C. \tag{1.15}$$

Note that each class corresponds to a physically distinct kind of symmetry operation such as rotation of π about equivalent twofold axes, or rotation

of $2\pi/3$ about equivalent threefold axes. The identity symmetry element is always in a class by itself. An *Abelian* group has as many classes as elements. The identity element is the only class forming a group, since none of the other classes contain the identity.

Theorem. *All elements of the same class have the same order.*

Proof. The order of an element n is defined by $A^n = E$. An arbitrary conjugate of A is $B = XAX^{-1}$. Then $B^n = (XAX^{-1})(XAX^{-1}) \dots n$ times gives $XA^nX^{-1} = XEX^{-1} = E$.

Definition 8. *A subgroup \mathcal{B} is self-conjugate (or invariant, or normal) if $X\mathcal{B}X^{-1}$ is identical with \mathcal{B} for all possible choices of X in the group.*

For example (E, D, F) forms a self-conjugate subgroup of $P(3)$, but (E, A) does not. The subgroups of an Abelian group are self-conjugate subgroups. We will denote self-conjugate subgroups by \mathcal{N} . To form a self-conjugate subgroup, it is necessary to include entire classes in this subgroup.

Definition 9. *A group with no self-conjugate subgroups \equiv a simple group.*

Theorem. *The right and left cosets of a self-conjugate subgroup \mathcal{N} are the same.*

Proof. If N_i is an arbitrary element of the subgroup \mathcal{N} , then the left coset is found by elements $XN_i = XN_iX^{-1}X = N_jX$, where the right coset is formed by the elements N_jX , where $N_j = XN_kX^{-1}$.

For example in the group $P(3)$, one of the right cosets is $(E, D, F)A = (A, C, B)$ and one of the left cosets is $A(E, D, F) = (A, B, C)$ and both cosets are identical except for the listing of the elements. \square

Theorem. *The multiplication of the elements of two right cosets of a self-conjugate subgroup gives another right coset.*

Proof. Let $\mathcal{N}X$ and $\mathcal{N}Y$ be two right cosets. Then multiplication of two right cosets gives

$$\begin{aligned} (\mathcal{N}X)(\mathcal{N}Y) &\Rightarrow N_iXN_\ell Y = N_i(XN_\ell)Y \\ &= N_i(N_mX)Y = (N_iN_m)(XY) \Rightarrow \mathcal{N}(XY) \end{aligned} \quad (1.16)$$

and $\mathcal{N}(XY)$ denotes a right coset. \square

The elements in one right coset of $P(3)$ are $(E, D, F)A = (A, C, B)$ while $(E, D, F)D = (D, F, E)$ is another right coset. The product $(A, C, B)(D, F, E)$ is (A, B, C) which is a right coset. Also the product of the two right cosets $(A, B, C)(A, B, C)$ is (D, F, E) which is a right coset.

1.7 Factor Groups

Definition 10. *The factor group (or quotient group) is constructed with respect to a self-conjugate subgroup as the collection of cosets of the self-conjugate subgroup, each coset being considered an element of the factor group. The factor group satisfies the four rules of Sect. 1.1 and is therefore a group:*

1. Multiplication – $(\mathcal{N}X)(\mathcal{N}Y) = \mathcal{N}XY$.
2. Associative law – holds because it holds for the elements.
3. Identity – $E\mathcal{N}$, where E is the coset that contains the identity element. \mathcal{N} is sometimes called a *normal divisor*.
4. Inverse – $(X\mathcal{N})(X^{-1}\mathcal{N}) = (\mathcal{N}X)(X^{-1}\mathcal{N}) = \mathcal{N}^2 = E\mathcal{N}$.

Definition 11. *The index of a subgroup \equiv total number of cosets $=$ (order of group)/(order of subgroup).*

The order of the factor group is the index of the self-conjugate subgroup.

In Sect. 1.6 we saw that (E, D, F) forms a self-conjugate subgroup, \mathcal{N} . The only other coset of this subgroup \mathcal{N} is (A, B, C) , so that the order of this factor group = 2. Let $(A, B, C) = \mathcal{A}$ and $(E, D, F) = \mathcal{E}$ be the two elements of the factor group. Then the multiplication table for this factor group is

| | | |
|---------------|---------------|---------------|
| | \mathcal{E} | \mathcal{A} |
| \mathcal{E} | \mathcal{E} | \mathcal{A} |
| \mathcal{A} | \mathcal{A} | \mathcal{E} |

\mathcal{E} is the identity element of this factor group. \mathcal{E} and \mathcal{A} are their own inverses. From this illustration you can see how the four group properties (see Sect. 1.1) apply to the factor group by taking an element in each coset, carrying out the multiplication of the elements and finding the coset of the resulting element. Note that this multiplication table is also the multiplication table for the group for the permutation of two objects $P(2)$, i.e., this factor group maps one-on-one to the group $P(2)$. This analogy between the factor group and $P(2)$ gives insights into what the factor group is about.

1.8 Group Theory and Quantum Mechanics

We have now learned enough to start making connection of group theory to physical problems. In such problems we typically have a system described by a Hamiltonian which may be very complicated. Symmetry often allows us to make certain simplifications, without knowing the detailed Hamiltonian. To make a connection between group theory and quantum mechanics, we consider the group of symmetry operators \hat{P}_R which leave the Hamiltonian invariant. These operators \hat{P}_R are symmetry operations of the system and the \hat{P}_R operators commute with the Hamiltonian. The operators \hat{P}_R are said to

form *the group of the Schrödinger equation*. If \mathcal{H} and \hat{P}_R commute, and if \hat{P}_R is a Hermitian operator, then \mathcal{H} and \hat{P}_R can be simultaneously diagonalized.

We now show that these operators form a group. The identity element clearly exists (leaving the system unchanged). Each symmetry operator \hat{P}_R has an inverse \hat{P}_R^{-1} to undo the operation \hat{P}_R and from physical considerations the element \hat{P}_R^{-1} is also in the group. The product of two operators of the group is still an operator of the group, since we can consider these separately as acting on the Hamiltonian. The associative law clearly holds. Thus the requirements for forming a group are satisfied.

Whether the operators \hat{P}_R be rotations, reflections, translations, or permutations, these symmetry operations do not alter the Hamiltonian or its eigenvalues. If $\mathcal{H}\psi_n = E_n\psi_n$ is a solution to Schrödinger's equation and \mathcal{H} and \hat{P}_R commute, then

$$\hat{P}_R\mathcal{H}\psi_n = \hat{P}_R E_n \psi_n = \mathcal{H}(\hat{P}_R \psi_n) = E_n(\hat{P}_R \psi_n). \quad (1.17)$$

Thus $\hat{P}_R\psi_n$ is as good an eigenfunction of \mathcal{H} as ψ_n itself. Furthermore, both ψ_n and $\hat{P}_R\psi_n$ correspond to the *same* eigenvalue E_n . Thus, starting with a particular eigenfunction, we can generate all other eigenfunctions of the same degenerate set (same energy) by applying all the symmetry operations that commute with the Hamiltonian (or leave it invariant). Similarly, if we consider the product of two symmetry operators, we again generate an eigenfunction of the Hamiltonian \mathcal{H}

$$\begin{aligned} \hat{P}_R \hat{P}_S \mathcal{H} &= \mathcal{H} \hat{P}_R \hat{P}_S \\ \hat{P}_R \hat{P}_S \mathcal{H} \psi_n &= \hat{P}_R \hat{P}_S E_n \psi_n = E_n(\hat{P}_R \hat{P}_S \psi_n) = \mathcal{H}(\hat{P}_R \hat{P}_S \psi_n), \end{aligned} \quad (1.18)$$

in which $\hat{P}_R \hat{P}_S \psi_n$ is also an eigenfunction of \mathcal{H} . We also note that the action of \hat{P}_R on an arbitrary vector consisting of ℓ eigenfunctions, yields a $\ell \times \ell$ matrix representation of \hat{P}_R that is in block diagonal form. The representation of physical systems, or equivalently their symmetry groups, in the form of matrices is the subject of the next chapter.

Selected Problems

- 1.1.** (a) Show that the trace of an arbitrary square matrix X is invariant under a similarity (or equivalence) transformation UXU^{-1} .
 (b) Given a set of matrices that represent the group G , denoted by $D(R)$ (for all R in G), show that the matrices obtainable by a similarity transformation $UD(R)U^{-1}$ also are a representation of G .
- 1.2.** (a) Show that the operations of $P(3)$ in (1.1) form a group, referring to the rules in Sect. 1.1.
 (b) Multiply the two left cosets of subgroup (E, A) : (B, F) and (C, D) , referring to Sect. 1.5. Is the result another coset?

- (c) Prove that in order to form a normal (self-conjugate) subgroup, it is necessary to include only entire classes in this subgroup. What is the physical consequence of this result?
- (d) Demonstrate that the normal subgroup of $P(3)$ includes entire classes.

1.3. (a) What are the symmetry operations for the molecule AB_4 , where the B atoms lie at the corners of a square and the A atom is at the center and is not coplanar with the B atoms.

- (b) Find the multiplication table.
- (c) List the subgroups. Which subgroups are self-conjugate?
- (d) List the classes.
- (e) Find the multiplication table for the factor group for the self-conjugate subgroup(s) of (c).

1.4. The group defined by the permutations of four objects, $P(4)$, is isomorphic (has a one-to-one correspondence) with the group of symmetry operations of a regular tetrahedron (T_d). The symmetry operations of this group are sufficiently complex so that the power of group theoretical methods can be appreciated. For notational convenience, the elements of this group are listed below.

$$\begin{aligned}
 e &= (1234) & g &= (3124) & m &= (1423) & s &= (4213) \\
 a &= (1243) & h &= (3142) & n &= (1432) & t &= (4231) \\
 b &= (2134) & i &= (2314) & o &= (4123) & u &= (3412) \\
 c &= (2143) & j &= (2341) & p &= (4132) & v &= (3421) \\
 d &= (1324) & k &= (3214) & q &= (2413) & w &= (4312) \\
 f &= (1342) & l &= (3241) & r &= (2431) & y &= (4321) .
 \end{aligned}$$

Here we have used a shorthand notation to denote the elements: for example $j = (2341)$ denotes

$$\begin{pmatrix} 1 & 2 & 3 & 4 \\ 2 & 3 & 4 & 1 \end{pmatrix} ,$$

that is, the permutation which takes objects in the order 1234 and leaves them in the order 2341:

- (a) What is the product vw ? wv ?
- (b) List the subgroups of this group which correspond to the symmetry operations on an equilateral triangle.
- (c) List the right and left cosets of the subgroup (e, a, k, l, s, t) .
- (d) List all the symmetry classes for $P(4)$, and relate them to symmetry operations on a regular tetrahedron.
- (e) Find the factor group and multiplication table formed from the self-conjugate subgroup (e, c, u, y) . Is this factor group isomorphic to $P(3)$?

Representation Theory and Basic Theorems

In this chapter we introduce the concept of a representation of an abstract group and prove a number of important theorems relating to irreducible representations, including the “Wonderful Orthogonality Theorem.” This mathematical background is necessary for developing the group theoretical framework that is used for the applications of group theory to solid state physics.

2.1 Important Definitions

Definition 12. *Two groups are isomorphic or homomorphic if there exists a correspondence between their elements such that*

$$\begin{aligned} A &\rightarrow \hat{A} \\ B &\rightarrow \hat{B} \\ AB &\rightarrow \hat{A}\hat{B} , \end{aligned}$$

where the plain letters denote elements in one group and the letters with carets denote elements in the other group. If the two groups have the same order (same number of elements), then they are isomorphic (one-to-one correspondence). Otherwise they are homomorphic (many-to-one correspondence).

For example, the permutation group of three numbers $P(3)$ is *isomorphic* to the symmetry group of the equilateral triangle and *homomorphic* to its factor group, as shown in Table 2.1. Thus, the homomorphic representations in Table 2.1 are *unfaithful*. Isomorphic representations are *faithful*, because they maintain the one-to-one correspondence.

Definition 13. *A representation of an abstract group is a substitution group (matrix group with square matrices) such that the substitution group is homomorphic (or isomorphic) to the abstract group. We assign a matrix $D(A)$ to each element A of the abstract group such that $D(AB) = D(A)D(B)$.*

Table 2.1. Table of homomorphic mapping of $P(3)$ and its factor group

| permutation group element | | factor group |
|---------------------------|---------------|---------------|
| E, D, F | \rightarrow | \mathcal{E} |
| A, B, C | \rightarrow | \mathcal{A} |

The matrices of (1.4) are an isomorphic representation of the permutation group $P(3)$. In considering the representation

$$\left. \begin{array}{c} E \\ D \\ F \end{array} \right\} \rightarrow (1) \quad \left. \begin{array}{c} A \\ B \\ C \end{array} \right\} \rightarrow (-1)$$

the one-dimensional matrices (1) and (-1) are a homomorphic representation of $P(3)$ and an isomorphic representation of the factor group \mathcal{E}, \mathcal{A} (see Sect. 1.7). The homomorphic one-dimensional representation (1) is a representation for any group, though an unfaithful one.

In quantum mechanics, the matrix representation of a group is important for several reasons. First of all, we will find that an eigenfunction for a quantum mechanical operator will transform under a symmetry operation similar to the application of the matrix representing the symmetry operation on the matrix for the wave function. Secondly, quantum mechanical operators are usually written in terms of a matrix representation, and thus it is convenient to write symmetry operations using the same kind of matrix representation. Finally, matrix algebra is often easier to manipulate than geometrical symmetry operations.

2.2 Matrices

Definition 14. Hermitian matrices are defined by: $\tilde{A} = A^*$, $\tilde{A}^* = A$, or $A^\dagger = A$ (where the symbol $*$ denotes complex conjugation, \sim denotes transposition, and \dagger denotes taking the adjoint)

$$A = \begin{pmatrix} a_{11} & a_{12} & \cdots \\ a_{21} & a_{22} & \cdots \\ \vdots & \vdots & \ddots \end{pmatrix}, \quad (2.1)$$

$$\tilde{A} = \begin{pmatrix} a_{11} & a_{21} & \cdots \\ a_{12} & a_{22} & \cdots \\ \vdots & \vdots & \ddots \end{pmatrix}, \quad (2.2)$$

$$A^\dagger = \begin{pmatrix} a_{11}^* & a_{21}^* & \cdots \\ a_{12}^* & a_{22}^* & \cdots \\ \vdots & \vdots & \ddots \end{pmatrix}. \quad (2.3)$$

Unitary matrices are defined by: $\tilde{A}^* = A^\dagger = A^{-1}$;
 Orthonormal matrices are defined by: $\tilde{A} = A^{-1}$.

Definition 15. The dimensionality of a representation is equal to the dimensionality of each of its matrices, which is in turn equal to the number of rows or columns of the matrix.

These representations are *not unique*. For example, by performing a similarity (or equivalence, or canonical) transformation $UD(A)U^{-1}$ we generate a new set of matrices which provides an equally good representation. A simple physical example for this transformation is the rotation of reference axes, such as (x, y, z) to (x', y', z') . We can also generate another representation by taking one or more representations and combining them according to

$$\begin{pmatrix} D(A) & \mathcal{O} \\ \mathcal{O} & D'(A) \end{pmatrix}, \quad (2.4)$$

where $\mathcal{O} = (m \times n)$ matrix of zeros, not necessarily a square zero matrix. The matrices $D(A)$ and $D'(A)$ can be either two distinct representations or they can be identical representations.

To overcome the difficulty of non-uniqueness of a representation with regard to a similarity transformation, we often just deal with the *traces* of the matrices which are invariant under similarity transformations, as discussed in Chap. 3. The *trace* of a matrix is defined as the sum of the diagonal matrix elements. To overcome the difficulty of the ambiguity of representations in general, we introduce the concept of *irreducible* representations.

2.3 Irreducible Representations

Consider the representation made up of two distinct or identical representations for every element in the group

$$\begin{pmatrix} D(A) & \mathcal{O} \\ \mathcal{O} & D'(A) \end{pmatrix}.$$

This is a reducible representation because the matrix corresponding to each and every element of the group is in the same block form. We could now carry out a similarity transformation which would mix up all the elements so that the matrices are no longer in block form. But still the representation is reducible. Hence the definition:

Definition 16. If by one and the same equivalence transformation, all the matrices in the representation of a group can be made to acquire the same block form, then the representation is said to be *reducible*; otherwise it is *irreducible*. Thus, an irreducible representation cannot be expressed in terms of representations of lower dimensionality.

We will now consider three irreducible representations for the permutation group $P(3)$:

$$\begin{aligned}
 \Gamma_1 : & \quad \begin{matrix} E \\ (1) \end{matrix} & \begin{matrix} A \\ (1) \end{matrix} & \begin{matrix} B \\ (1) \end{matrix} \\
 \Gamma_{1'} : & \quad \begin{matrix} (1) \\ (1) \end{matrix} & \begin{matrix} (-1) \\ (-1) \end{matrix} & \\
 \Gamma_2 : & \quad \begin{pmatrix} 1 & 0 \\ 0 & 1 \end{pmatrix} & \begin{pmatrix} -1 & 0 \\ 0 & 1 \end{pmatrix} & \begin{pmatrix} \frac{1}{2} & -\frac{\sqrt{3}}{2} \\ -\frac{\sqrt{3}}{2} & -\frac{1}{2} \end{pmatrix} \\
 & \quad \begin{matrix} C \\ (1) \end{matrix} & \begin{matrix} D \\ (1) \end{matrix} & \begin{matrix} F \\ (1) \end{matrix} \\
 \Gamma_1 : & \quad \begin{matrix} (1) \\ (-1) \end{matrix} & \begin{matrix} (1) \\ (1) \end{matrix} & \begin{matrix} (1) \\ (1) \end{matrix} \\
 \Gamma_{1'} : & \quad \begin{pmatrix} \frac{1}{2} & \frac{\sqrt{3}}{2} \\ \frac{\sqrt{3}}{2} & -\frac{1}{2} \end{pmatrix} & \begin{pmatrix} -\frac{1}{2} & \frac{\sqrt{3}}{2} \\ -\frac{\sqrt{3}}{2} & -\frac{1}{2} \end{pmatrix} & \begin{pmatrix} -\frac{1}{2} & -\frac{\sqrt{3}}{2} \\ \frac{\sqrt{3}}{2} & -\frac{1}{2} \end{pmatrix} .
 \end{aligned} \tag{2.5}$$

A reducible representation containing these three irreducible representations is

$$\Gamma_R : \begin{pmatrix} 1 & 0 & 0 & 0 \\ 0 & 1 & 0 & 0 \\ 0 & 0 & 1 & 0 \\ 0 & 0 & 0 & 1 \end{pmatrix} \begin{pmatrix} 1 & 0 & 0 & 0 \\ 0 & -1 & 0 & 0 \\ 0 & 0 & -1 & 0 \\ 0 & 0 & 0 & 1 \end{pmatrix} \begin{pmatrix} 1 & 0 & 0 & 0 \\ 0 & -1 & 0 & 0 \\ 0 & 0 & \frac{1}{2} & -\frac{\sqrt{3}}{2} \\ 0 & 0 & -\frac{\sqrt{3}}{2} & -\frac{1}{2} \end{pmatrix} \dots , \tag{2.6}$$

where Γ_R is of the form

$$\left(\begin{array}{c|c|c} \Gamma_1 & 0 & \mathcal{O} \\ \hline 0 & \Gamma_{1'} & \mathcal{O} \\ \hline \mathcal{O} & \mathcal{O} & \Gamma_2 \end{array} \right) . \tag{2.7}$$

It is customary to list the irreducible representations contained in a reducible representation Γ_R as

$$\Gamma_R = \Gamma_1 + \Gamma_{1'} + \Gamma_2 . \tag{2.8}$$

In working out problems of physical interest, each irreducible representation describes the transformation properties of a set of eigenfunctions and corresponds to a distinct energy eigenvalue. Assume Γ_R is a reducible representation for some group G but an irreducible representation for some other group G' . If Γ_R contains the irreducible representations $\Gamma_1 + \Gamma_{1'} + \Gamma_2$ as illustrated earlier for the group $P(3)$, this indicates that some interaction is breaking up a fourfold degenerate level in group G' into three energy levels in group G : two nondegenerate ones and a doubly degenerate one. Group theory does not tell us what these energies are, nor their ordering. Group theory only specifies the symmetries and degeneracies of the energy levels. In general, the higher the symmetry, meaning the larger the number of symmetry operations in the group, the higher the degeneracy of the energy levels. Thus when a perturbation is applied to lower the symmetry, the degeneracy of the energy levels tends to be reduced. Group theory provides a systematic method for determining exactly how the degeneracy is lowered.

Representation theory is useful for the treatment of physical problems because of certain orthogonality theorems which we will now discuss. To prove the orthogonality theorems we need first to prove some other theorems (including the unitarity of representations in Sect. 2.4 and the two Schur lemmas in Sects. 2.5 and 2.6).

2.4 The Unitarity of Representations

The following theorem shows that in most physical cases, the elements of a group can be represented by unitary matrices, which have the property of preserving length scales. This theorem is then used to prove lemmas leading to the proof of the “Wonderful Orthogonality Theorem,” which is a central theorem of this chapter.

Theorem. *Every representation with matrices having nonvanishing determinants can be brought into unitary form by an equivalence (similarity) transformation.*

Proof. By unitary form we mean that the matrix elements obey the relation $(A^{-1})_{ij} = A_{ij}^\dagger = A_{ji}^*$, where A is an arbitrary matrix of the representation. The proof is carried out by actually finding the corresponding unitary matrices if the A_{ij} matrices are not already unitary matrices.

Let A_1, A_2, \dots, A_h denote matrices of the representation. We start by forming the matrix sum

$$H = \sum_{x=1}^h A_x A_x^\dagger, \quad (2.9)$$

where the sum is over all the elements in the group and where the adjoint of a matrix is the transposed complex conjugate matrix $(A_x^\dagger)_{ij} = (A_x)_{ji}^*$. The matrix H is Hermitian because

$$H^\dagger = \sum_x (A_x A_x^\dagger)^\dagger = \sum_x A_x A_x^\dagger. \quad (2.10)$$

Any Hermitian matrix can be diagonalized by a suitable unitary transformation. Let U be a unitary matrix made up of the orthonormal eigenvectors which diagonalize H to give the diagonal matrix d :

$$\begin{aligned} d &= U^{-1} H U \\ &= \sum_x U^{-1} A_x A_x^\dagger U \\ &= \sum_x U^{-1} A_x U U^{-1} A_x^\dagger U \\ &= \sum_x \hat{A}_x \hat{A}_x^\dagger, \end{aligned} \quad (2.11)$$

where we define $\hat{A}_x = U^{-1}A_xU$ for all x . The diagonal matrix d is a *special* kind of matrix and contains only real, positive diagonal elements since

$$\begin{aligned} d_{kk} &= \sum_x \sum_j (\hat{A}_x)_{kj} (\hat{A}_x^\dagger)_{jk} \\ &= \sum_x \sum_j (\hat{A}_x)_{kj} (\hat{A}_x)^*_{kj} \\ &= \sum_x \sum_j |(\hat{A}_x)_{kj}|^2. \end{aligned} \quad (2.12)$$

Out of the diagonal matrix d , one can form two matrices ($d^{1/2}$ and $d^{-1/2}$) such that

$$d^{1/2} \equiv \begin{pmatrix} \sqrt{d_{11}} & & \mathcal{O} \\ & \sqrt{d_{22}} & \\ \mathcal{O} & & \ddots \end{pmatrix} \quad (2.13)$$

and

$$d^{-1/2} \equiv \begin{pmatrix} \frac{1}{\sqrt{d_{11}}} & & \mathcal{O} \\ & \frac{1}{\sqrt{d_{22}}} & \\ \mathcal{O} & & \ddots \end{pmatrix}, \quad (2.14)$$

where $d^{1/2}$ and $d^{-1/2}$ are real, diagonal matrices. We note that the generation of $d^{-1/2}$ from $d^{1/2}$ requires that none of the d_{kk} vanish. These matrices clearly obey the relations

$$(d^{1/2})^\dagger = d^{1/2} \quad (2.15)$$

$$(d^{-1/2})^\dagger = d^{-1/2} \quad (2.16)$$

$$(d^{1/2})(d^{1/2}) = d \quad (2.17)$$

so that

$$d^{1/2}d^{-1/2} = d^{-1/2}d^{1/2} = \hat{1} = \text{unit matrix}. \quad (2.18)$$

From (2.11) we can also write

$$d = d^{1/2}d^{1/2} = \sum_x \hat{A}_x \hat{A}_x^\dagger. \quad (2.19)$$

We now define a new set of matrices

$$\hat{\hat{A}}_x \equiv d^{-1/2} \hat{A}_x d^{1/2} \quad (2.20)$$

and

$$\hat{A}_x^\dagger = (U^{-1}A_xU)^\dagger = U^{-1}A_x^\dagger U \quad (2.21)$$

$$\hat{\hat{A}}_x^\dagger = (d^{-1/2} \hat{A}_x d^{1/2})^\dagger = d^{1/2} \hat{\hat{A}}_x^\dagger d^{-1/2}. \quad (2.22)$$

We now show that the matrices \hat{A}_x are unitary:

$$\begin{aligned}
 \hat{A}_x \hat{A}_x^\dagger &= (d^{-1/2} \hat{A}_x d^{1/2})(d^{1/2} \hat{A}_x^\dagger d^{-1/2}) \\
 &= d^{-1/2} \hat{A}_x d \hat{A}_x^\dagger d^{-1/2} \\
 &= d^{-1/2} \sum_y \hat{A}_x \hat{A}_y \hat{A}_y^\dagger \hat{A}_x^\dagger d^{-1/2} \\
 &= d^{-1/2} \sum_y (\hat{A}_x \hat{A}_y) (\hat{A}_x \hat{A}_y)^\dagger d^{-1/2} \\
 &= d^{-1/2} \sum_z \hat{A}_z \hat{A}_z^\dagger d^{-1/2}
 \end{aligned} \tag{2.23}$$

by the rearrangement theorem (Sect. 1.4). But from the relation

$$d = \sum_z \hat{A}_z \hat{A}_z^\dagger \tag{2.24}$$

it follows that $\hat{A}_x \hat{A}_x^\dagger = \hat{1}$, so that \hat{A}_x is unitary.

Therefore we have demonstrated how we can always construct a unitary representation by the transformation:

$$\hat{A}_x = d^{-1/2} U^{-1} A_x U d^{1/2}, \tag{2.25}$$

where

$$H = \sum_{x=1}^h A_x A_x^\dagger \tag{2.26}$$

$$d = \sum_{x=1}^h \hat{A}_x \hat{A}_x^\dagger, \tag{2.27}$$

and where U is the unitary matrix that diagonalizes the Hermitian matrix H and $\hat{A}_x = U^{-1} A_x U$. \square

Note: On the other hand, not all symmetry operations can be represented by a unitary matrix; an example of an operation which cannot be represented by a unitary matrix is the time inversion operator (see Chap. 16). Time inversion symmetry is represented by an antiunitary matrix rather than a unitary matrix. It is thus not possible to represent all symmetry operations by a unitary matrix.

2.5 Schur's Lemma (Part 1)

Schur's lemmas (Parts 1 and 2) on irreducible representations are proved in order to prove the “Wonderful Orthogonality Theorem” in Sect. 2.7. We next prove Schur's lemma Part 1.

Lemma. *A matrix which commutes with all matrices of an irreducible representation is a constant matrix, i.e., a constant times the unit matrix. Therefore, if a non-constant commuting matrix exists, the representation is reducible; if none exists, the representation is irreducible.*

Proof. Let M be a matrix which commutes with all the matrices of the representation A_1, A_2, \dots, A_h \square

$$MA_x = A_xM . \quad (2.28)$$

Take the adjoint of both sides of (2.28) to obtain

$$A_x^\dagger M^\dagger = M^\dagger A_x^\dagger . \quad (2.29)$$

Since A_x can in all generality be taken to be unitary (see Sect. 2.4), multiply on the right and left of (2.29) by A_x to yield

$$M^\dagger A_x = A_x M^\dagger , \quad (2.30)$$

so that if M commutes with A_x so does M^\dagger , and so do the Hermitian matrices H_1 and H_2 defined by

$$\begin{aligned} H_1 &= M + M^\dagger \\ H_2 &= i(M - M^\dagger) , \end{aligned} \quad (2.31)$$

$$H_j A_x = A_x H_j , \quad \text{where } j = 1, 2 . \quad (2.32)$$

We will now show that a commuting Hermitian matrix is a constant matrix from which it follows that $M = H_1 - iH_2$ is also a constant matrix.

Since H_j ($j = 1, 2$) is a Hermitian matrix, it can be diagonalized. Let U be the matrix that diagonalizes H_j (for example H_1) to give the diagonal matrix d

$$d = U^{-1} H_j U . \quad (2.33)$$

We now perform the unitary transformation on the matrices A_x of the representation $\hat{A}_x = U^{-1} A_x U$. From the commutation relations (2.28), (2.29), and (2.32), a unitary transformation on all matrices $H_j A_x = A_x H_j$ yields

$$\underbrace{(U^{-1} H_j U)}_d \underbrace{(U^{-1} A_x U)}_{\hat{A}_x} = \underbrace{(U^{-1} A_x U)}_{\hat{A}_x} \underbrace{(U^{-1} H_j U)}_d . \quad (2.34)$$

So now we have a diagonal matrix d which commutes with all the matrices of the representation. We now show that this diagonal matrix d is a constant matrix, if all the \hat{A}_x matrices (and thus also the A_x matrices) form an irreducible representation. Thus, starting with (2.34)

$$d \hat{A}_x = \hat{A}_x d \quad (2.35)$$

we take the ij element of both sides of (2.35)

$$d_{ii}(\hat{A}_x)_{ij} = (\hat{A}_x)_{ij}d_{jj} , \quad (2.36)$$

so that

$$(\hat{A}_x)_{ij}(d_{ii} - d_{jj}) = 0 \quad (2.37)$$

for all the matrices A_x .

If $d_{ii} \neq d_{jj}$, so that the matrix d is not a constant diagonal matrix, then $(\hat{A}_x)_{ij}$ must be 0 for all the \hat{A}_x . This means that the similarity or unitary transformation $U^{-1}A_xU$ has brought all the matrices of the representation \hat{A}_x into the same block form, since any time $d_{ii} \neq d_{jj}$ all the matrices $(\hat{A}_x)_{ij}$ are null matrices. Thus by definition the representation A_x is reducible. But we have assumed the A_x to be an irreducible representation. Therefore $(\hat{A}_x)_{ij} \neq 0$ for all \hat{A}_x , so that it is necessary that $d_{ii} = d_{jj}$, and Schur's lemma *Part 1* is proved.

2.6 Schur's Lemma (Part 2)

Lemma. *If the matrix representations $D^{(1)}(A_1), D^{(1)}(A_2), \dots, D^{(1)}(A_h)$ and $D^{(2)}(A_1), D^{(2)}(A_2), \dots, D^{(2)}(A_h)$ are two irreducible representations of a given group of dimensionality ℓ_1 and ℓ_2 , respectively, then, if there is a matrix of ℓ_1 columns and ℓ_2 rows M such that*

$$MD^{(1)}(A_x) = D^{(2)}(A_x)M \quad (2.38)$$

for all A_x , then M must be the null matrix ($M = \mathcal{O}$) if $\ell_1 \neq \ell_2$. If $\ell_1 = \ell_2$, then either $M = \mathcal{O}$ or the representations $D^{(1)}(A_x)$ and $D^{(2)}(A_x)$ differ from each other by an equivalence (or similarity) transformation.

Proof. Since the matrices which form the representation can always be transformed into unitary form, we can in all generality assume that the matrices of both representations $D^{(1)}(A_x)$ and $D^{(2)}(A_x)$ have already been brought into unitary form. \square

Assume $\ell_1 \leq \ell_2$, and take the adjoint of (2.38)

$$[D^{(1)}(A_x)]^\dagger M^\dagger = M^\dagger [D^{(2)}(A_x)]^\dagger . \quad (2.39)$$

The unitary property of the representation implies $[D(A_x)]^\dagger = [D(A_x)]^{-1} = D(A_x^{-1})$, since the matrices form a substitution group for the elements A_x of the group. Therefore we can write (2.39) as

$$D^{(1)}(A_x^{-1})M^\dagger = M^\dagger D^{(2)}(A_x^{-1}) . \quad (2.40)$$

Then multiplying (2.40) on the left by M yields

$$MD^{(1)}(A_x^{-1})M^\dagger = MM^\dagger D^{(2)}(A_x^{-1}) = D^{(2)}(A_x^{-1})MM^\dagger , \quad (2.41)$$

which follows from applying (2.38) to the element A_x^{-1} which is also an element of the group

$$MD^{(1)}(A_x^{-1}) = D^{(2)}(A_x^{-1})M. \quad (2.42)$$

We have now shown that if $MD^{(1)}(A_x) = D^{(2)}(A_x)M$ then MM^\dagger commutes with all the matrices of representation (2) and $M^\dagger M$ commutes with all matrices of representation (1). But if MM^\dagger commutes with all matrices of a representation, then by Schur's lemma (Part 1), MM^\dagger is a constant matrix of dimensionality $(\ell_2 \times \ell_2)$:

$$MM^\dagger = c \hat{1}, \quad (2.43)$$

where $\hat{1}$ is the unit matrix.

First we consider the case $\ell_1 = \ell_2$. Then M is a square matrix, with an inverse

$$M^{-1} = \frac{M^\dagger}{c}, \quad c \neq 0. \quad (2.44)$$

Then if $M^{-1} \neq \mathcal{O}$, multiplying (2.38) by M^{-1} on the left yields

$$D^{(1)}(A_x) = M^{-1}D^{(2)}(A_x)M \quad (2.45)$$

and the two representations differ by an equivalence transformation.

However, if $c = 0$ then we cannot write (2.44), but instead we have to consider $MM^\dagger = 0$

$$\sum_k M_{ik}M_{kj}^\dagger = 0 = \sum_k M_{ik}M_{jk}^* \quad (2.46)$$

for all ij elements. In particular, for $i = j$ we can write

$$\sum_k M_{ik}M_{ik}^* = \sum_k |M_{ik}|^2 = 0. \quad (2.47)$$

Therefore each element $M_{ik} = 0$ so that M is a null matrix. This completes proof of the case $\ell_1 = \ell_2$ and $M = \mathcal{O}$.

Finally we prove that for $\ell_1 \neq \ell_2$, then $M = \mathcal{O}$. Suppose that $\ell_1 \neq \ell_2$, then we can arbitrarily take $\ell_1 < \ell_2$. Then M has ℓ_1 columns and ℓ_2 rows. We can make a square $(\ell_2 \times \ell_2)$ matrix out of M by adding $(\ell_2 - \ell_1)$ columns of zeros

$$\ell_1 \text{ columns} \\ \ell_2 \text{ rows} \left(\begin{array}{cccc} 0 & 0 & \cdots & 0 \\ 0 & 0 & \cdots & 0 \\ M & 0 & 0 & \cdots & 0 \\ \vdots & \vdots & & \vdots \\ 0 & 0 & \cdots & 0 \end{array} \right) = N = \text{square } (\ell_2 \times \ell_2) \text{ matrix.} \quad (2.48)$$

The adjoint of (2.48) is then written as

$$\begin{pmatrix} M^\dagger \\ 0 & 0 & 0 & \cdots & 0 \\ 0 & 0 & 0 & \cdots & 0 \\ \vdots & \vdots & \vdots & & \vdots \\ 0 & 0 & 0 & \cdots & 0 \end{pmatrix} = N^\dagger \quad (2.49)$$

so that

$$NN^\dagger = MM^\dagger = c \hat{1} \quad \text{dimension } (\ell_2 \times \ell_2). \quad (2.50)$$

$$\begin{aligned} \sum_k N_{ik} N_{ki}^\dagger &= \sum_k N_{ik} N_{ik}^* = c \hat{1} \\ \sum_{ik} N_{ik} N_{ik}^* &= c \ell_2. \end{aligned}$$

But if we carry out the sum over i we see by direct computation that some of the diagonal terms of $\sum_{k,i} N_{ik} N_{ik}^*$ are 0, so that c must be zero. But this implies that for every element we have $N_{ik} = 0$ and therefore also $M_{ik} = 0$, so that M is a null matrix, completing the proof of Schur's lemma *Part 2*.

2.7 Wonderful Orthogonality Theorem

The orthogonality theorem which we now prove is so central to the application of group theory to quantum mechanical problems that it was named the “Wonderful Orthogonality Theorem” by Van Vleck, and is widely known by this name. The theorem is in actuality an orthonormality theorem.

Theorem. *The orthonormality relation*

$$\sum_R D_{\mu\nu}^{(\Gamma_j)}(R) D_{\nu'\mu'}^{(\Gamma_{j'})}(R^{-1}) = \frac{h}{\ell_j} \delta_{\Gamma_j, \Gamma_{j'}} \delta_{\mu\mu'} \delta_{\nu\nu'} \quad (2.51)$$

is obeyed for all the inequivalent, irreducible representations of a group, where the summation is over all h group elements A_1, A_2, \dots, A_h and ℓ_j and $\ell_{j'}$ are, respectively, the dimensionalities of representations Γ_j and $\Gamma_{j'}$. If the representations are unitary, the orthonormality relation becomes

$$\sum_R D_{\mu\nu}^{(\Gamma_j)}(R) \left[D_{\mu'\nu'}^{(\Gamma_{j'})}(R) \right]^* = \frac{h}{\ell_j} \delta_{\Gamma_j, \Gamma_{j'}} \delta_{\mu\mu'} \delta_{\nu\nu'} . \quad (2.52)$$

Example. To illustrate the meaning of the mathematical symbols of this theorem, consider the orthogonality between the Γ_1 and $\Gamma_{1'}$ irreducible representations for the $P(3)$ group in Sect. 2.5 using the statements of the theorem (2.52):

$$\begin{aligned} \sum_R D_{\mu\nu}^{(\Gamma_1)}(R) D_{\mu'\nu'}^{(\Gamma_{1'})*}(R) &= [(1) \cdot (1)] + [(1) \cdot (1)] + [(1) \cdot (1)] \\ &\quad + [(1) \cdot (-1)] + [(1) \cdot (-1)] + [(1) \cdot (-1)] = 0. \end{aligned} \quad (2.53)$$

Proof. Consider the $\ell_{j'} \times \ell_j$ matrix

$$M = \sum_R D^{(\Gamma_{j'})}(R) X D^{(\Gamma_j)}(R^{-1}), \quad (2.54)$$

where X is an arbitrary matrix with $\ell_{j'}$ rows and ℓ_j columns so that M is a rectangular matrix of dimensionality $(\ell_{j'} \times \ell_j)$. Multiply M by $D^{(\Gamma_{j'})}(S)$ for some element S in the group:

$$\underbrace{D^{(\Gamma_{j'})}(S)M}_{\ell_{j'} \times \ell_j} = \sum_R D^{(\Gamma_{j'})}(S) D^{(\Gamma_{j'})}(R) X D^{(\Gamma_j)}(R^{-1}). \quad (2.55)$$

We then carry out the multiplication of two elements in a group

$$\underbrace{D^{(\Gamma_{j'})}(S)M}_{\ell_{j'} \times \ell_j} = \sum_R D^{(\Gamma_{j'})}(SR) X D^{(\Gamma_j)}(R^{-1}S^{-1}) D^{(\Gamma_j)}(S), \quad (2.56)$$

where we have used the group properties (1.3) of the representations Γ_j and $\Gamma_{j'}$. By the rearrangement theorem, (2.56) can be rewritten

$$D^{(\Gamma_{j'})}(S)M = \underbrace{\sum_R D^{(\Gamma_{j'})}(R) X D^{(\Gamma_j)}(R^{-1})}_{M} D^{(\Gamma_j)}(S) = M D^{(\Gamma_j)}(S). \quad (2.57)$$

Now apply Schur's lemma Part 2 for the various cases. \square

Case 1. $\ell_j \neq \ell_{j'}$ or if $\ell_j = \ell_{j'}$, and the representations are not equivalent.

Since $D^{(\Gamma_{j'})}(S)M = M D^{(\Gamma_j)}(S)$, then by Schur's lemma Part 2, M must be a null matrix. From the definition of M we have

$$0 = M_{\mu\mu'} = \sum_R \sum_{\gamma,\lambda} D_{\mu\gamma}^{(\Gamma_{j'})}(R) X_{\gamma\lambda} D_{\lambda\mu'}^{(\Gamma_j)}(R^{-1}). \quad (2.58)$$

But X is an arbitrary matrix. By choosing X to have an entry 1 in the $\nu\nu'$ position and 0 everywhere else, we write

$$X = \begin{pmatrix} 0 & 0 & 0 & 0 & 0 & 0 & \dots \\ 0 & 0 & 0 & 1 & 0 & 0 & \dots \\ 0 & 0 & 0 & 0 & 0 & 0 & \dots \\ 0 & 0 & 0 & 0 & 0 & 0 & \dots \\ \vdots & \vdots & \vdots & \vdots & \vdots & \vdots & \end{pmatrix}, \quad X_{\gamma\lambda} = \delta_{\gamma\nu} \delta_{\lambda\nu'}. \quad (2.59)$$

It then follows by substituting (2.59) into (2.58) that

$$0 = \sum_R D_{\mu\nu}^{(\Gamma_{j'})}(R) D_{\nu'\mu'}^{(\Gamma_j)}(R^{-1}). \quad (2.60)$$

Case 2. $\ell_j = \ell_{j'}$ and the representations Γ_j and $\Gamma_{j'}$ are equivalent.

If the representations Γ_j and $\Gamma_{j'}$ are equivalent, then $\ell_j = \ell_{j'}$ and Schur's lemma part 1 tells us that $M = c\hat{1}$. The definition for M in (2.54) gives

$$M_{\mu\nu'} = c\delta_{\mu\mu'} = \sum_R \sum_{\gamma,\lambda} D_{\mu\gamma}^{(\Gamma_{j'})}(R) X_{\gamma\lambda} D_{\lambda\mu'}^{(\Gamma_{j'})}(R^{-1}). \quad (2.61)$$

Choose X in (2.59) as above to have a nonzero entry at $\nu\nu'$ and 0 everywhere else. Then $X_{\gamma\lambda} = c'_{\nu\nu'} \delta_{\gamma\nu} \delta_{\lambda\nu'}$, so that

$$c''_{\nu\nu'} \delta_{\mu\mu'} = \sum_R D_{\mu\nu}^{(\Gamma_{j'})}(R) D_{\nu'\mu'}^{(\Gamma_{j'})}(R^{-1}), \quad (2.62)$$

where $c''_{\nu\nu'} = c/c'_{\nu\nu'}$. To evaluate $c''_{\nu\nu'}$ choose $\mu = \mu'$ in (2.62) and sum on μ :

$$\underbrace{c''_{\nu\nu'} \sum_{\mu} \delta_{\mu\mu}}_{\ell_{j'}} = \sum_R \sum_{\mu} D_{\mu\nu}^{(\Gamma_{j'})}(R) D_{\nu'\mu}^{(\Gamma_{j'})}(R^{-1}) = \sum_R D_{\nu'\nu}^{(\Gamma_{j'})}(R^{-1}R). \quad (2.63)$$

since $D^{(\Gamma_{j'})}(R)$ is a representation of the group and follows the multiplication table for the group. Therefore we can write

$$c''_{\nu\nu'} \ell_{j'} = \sum_R D_{\nu'\nu}^{(\Gamma_{j'})}(R^{-1}R) = \sum_R D_{\nu'\nu}^{(\Gamma_{j'})}(E) = D_{\nu'\nu}^{(\Gamma_{j'})}(E) \sum_R 1. \quad (2.64)$$

But $D_{\nu'\nu}^{(\Gamma_{j'})}(E)$ is a unit $(\ell_{j'} \times \ell_{j'})$ matrix and the $\nu'\nu$ matrix element is $\delta_{\nu'\nu}$. The sum of unity over all the group elements is h . Therefore we obtain

$$c''_{\nu\nu'} = \frac{h}{\ell_{j'}} \delta_{\nu\nu'}. \quad (2.65)$$

Substituting (2.65) into (2.62) gives:

$$\frac{h}{\ell_{j'}} \delta_{\mu\mu'} \delta_{\nu\nu'} = \sum_R D_{\mu\nu}^{(\Gamma_{j'})}(R) D_{\nu'\mu'}^{(\Gamma_{j'})}(R^{-1}). \quad (2.66)$$

We can write the results of Cases 1 and 2 in compact form

$$\sum_R D_{\mu\nu}^{(\Gamma_j)}(R) D_{\nu'\mu'}^{(\Gamma_{j'})}(R^{-1}) = \frac{h}{\ell_j} \delta_{\Gamma_j, \Gamma_{j'}} \delta_{\mu\mu'} \delta_{\nu\nu'}. \quad (2.67)$$

For a unitary representation (2.67) can also be written as

$$\sum_R D_{\mu\nu}^{(\Gamma_j)}(R) D_{\mu'\nu'}^{(\Gamma_{j'})*}(R) = \frac{h}{\ell_j} \delta_{\Gamma_j, \Gamma_{j'}} \delta_{\mu\mu'} \delta_{\nu\nu'}. \quad (2.68)$$

This completes the proof of the wonderful orthogonality theorem, and we see explicitly that this theorem is an orthonormality theorem.

2.8 Representations and Vector Spaces

Let us spend a moment and consider what the representations in (2.68) mean as an orthonormality relation in a vector space of dimensionality h . Here h is the order of the group which equals the number of group elements. In this space, the representations $D_{\mu\nu}^{(\Gamma_j)}(R)$ can be considered as elements in this h -dimensional space:

$$V_{\mu,\nu}^{(\Gamma_j)} = \left[D_{\mu\nu}^{(\Gamma_j)}(A_1), D_{\mu\nu}^{(\Gamma_j)}(A_2), \dots, D_{\mu\nu}^{(\Gamma_j)}(A_h) \right]. \quad (2.69)$$

The three indices Γ_j, μ, ν label a particular vector. All distinct vectors in this space are orthogonal. Thus two representations are orthogonal if any one of their three indices is different. But in an h -dimensional vector space, the maximum number of orthogonal vectors is h . We now ask how many vectors $V_{\mu,\nu}^{(\Gamma_j)}$ can we make? For each representation, we have ℓ_j choices for μ and ν so that the total number of vectors we can have is $\sum_j \ell_j^2$ where we are now summing over representations Γ_j . This argument yields the important result

$$\sum_j \ell_j^2 \leq h. \quad (2.70)$$

We will see later (Sect. 3.7) that it is the *equality* that holds in (2.70). The result in (2.70) is extremely helpful in finding the totality of irreducible (non-equivalent) representations (see Problem 2.2).

Selected Problems

2.1. Show that every symmetry operator for every group can be represented by the (1×1) unit matrix. Is it also true that every symmetry operator for every group can be represented by the (2×2) unit matrix? If so, does such a representation satisfy the Wonderful Orthogonality Theorem? Why?

2.2. Consider the example of the group $P(3)$ which has six elements. Using the irreducible representations of Sect. 2.3, find the sum of ℓ_j^2 . Does the equality or inequality in (2.70) hold? Can $P(3)$ have an irreducible representation with $\ell_j = 3$? Group $P(4)$ has 24 elements and 5 irreducible representations. Using (2.70) as an equality, what are the dimensionalities of these 5 irreducible representations (see Problem 1.4)?

Character of a Representation

We have already discussed the arbitrariness of a representation with regard to similarity or equivalence transformations. Namely, if $D^{(\Gamma_j)}(R)$ is a representation of a group, so is $U^{-1}D^{(\Gamma_j)}(R)U$. To get around this arbitrariness, we introduce the use of the trace (or character) of a matrix representation which remains invariant under a similarity transformation. In this chapter we define the character of a representation, derive the most important theorems for the character, summarize the conventional notations used to denote symmetry operations and groups, and we discuss the construction of some of the most important character tables for the so-called point groups, that are listed in Appendix A. *Point groups* have no translation symmetry, in contrast to the *space groups*, that will be discussed in Chap. 9, and include both point group symmetry operations and translations.

3.1 Definition of Character

Definition 17. *The character of the matrix representation $\chi^{\Gamma_j}(R)$ for a symmetry operation R in a representation $D^{(\Gamma_j)}(R)$ is the trace (or the sum over diagonal matrix elements) of the matrix of the representation:*

$$\chi^{(\Gamma_j)}(R) = \text{trace } D^{(\Gamma_j)}(R) = \sum_{\mu=1}^{\ell_j} D^{(\Gamma_j)}(R)_{\mu\mu}, \quad (3.1)$$

where ℓ_j is the dimensionality of the representation Γ_j and j is a representation index. From the definition, it follows that representation Γ_j will have h characters, one for each element in the group. Since the trace of a matrix is invariant under a similarity transformation, the character is invariant under such a transformation.

3.2 Characters and Class

We relate concepts of class (see Sect. 1.6) and character by the following theorem.

Theorem. *The character for each element in a class is the same.*

Proof. Let A and B be elements in the same class. By the definition of class this means that A and B are related by conjugation (see Sect. 1.6)

$$A = Y^{-1}BY, \quad (3.2)$$

where Y is an element of the group. Each element can always be represented by a unitary matrix D (see Sect. 2.4), so that

$$D(A) = D(Y^{-1}) D(B) D(Y) = D^{-1}(Y) D(B) D(Y). \quad (3.3)$$

And since a similarity transformation leaves the trace invariant, we have the desired result for characters in the same class: $\chi(A) = \chi(B)$, which completes the proof. \square

The property that all elements in a class have the same character is responsible for what van Vleck called “the great beauty of character.” If two elements of a group are in the same class, this means that they correspond to similar symmetry operations – e.g., the class of twofold axes of rotation of the equilateral triangle, or the class of threefold rotations for the equilateral triangle.

Sometimes a given group will have more than one kind of twofold symmetry axis. To test whether these two kinds of axes are indeed symmetrically inequivalent, we check whether or not they have the same characters.

We summarize the information on the characters of the representations of a group in the celebrated *character table*. In a character table we list the irreducible representations (IR) in column form (for example, the left-hand column of the character table) and the class as rows (top row labels the class). For example, the character table for the permutation group $P(3)$ (see Sect. 1.2) is shown in Table 3.1. (Sometimes you will see character tables with the columns and rows interchanged relative to this display.)

Table 3.1. Character table for the permutation group $P(3)$ or equivalently for group “ D_3 ” (see Sect. 3.9 for group notation)

| class \rightarrow | \mathcal{C}_1 | $3\mathcal{C}_2$ | $2\mathcal{C}_3$ |
|---------------------|-----------------|------------------|------------------|
| IR \downarrow | $\chi(E)$ | $\chi(A, B, C)$ | $\chi(D, F)$ |
| Γ_1 | 1 | 1 | 1 |
| $\Gamma_{1'}$ | 1 | -1 | 1 |
| Γ_2 | 2 | 0 | -1 |

Table 3.2. Classes for group “ D_3 ” or equivalently for the permutation group $P(3)$ and for the symmetry operations of the equilateral triangle

| notation for each class of | D_3 | equilateral triangle | $P(3)^a$ |
|---------------------------------|--------|--|-----------|
| class 1 E ($N_k = 1$) | $1C_1$ | (identity class) | (1)(2)(3) |
| class 2 A, B, C ($N_k = 3$) | $3C_2$ | (rotation of π about twofold axis) | (1)(23) |
| class 3 D, F ($N_k = 2$) | $2C_3$ | (rotation of 120° about threefold axis) | (123) |

^aFor the class notation for $P(3)$ see Chap. 17

We will see in Sect. 3.9 that this group, more specifically this *point* group is named D_3 (Schoenflies notation). In Table 3.1 the notation $N_k C_k$ is used in the character table to label each class C_k , where N_k is the number of elements in C_k . If a representation is irreducible, then we say that its character is *primitive*. In a character table we limit ourselves to the primitive characters. The classes for group D_3 and $P(3)$ are listed in Table 3.2, showing different ways that the classes of a group are presented.

Now that we have introduced character and character tables, let us see how to use the character tables. To appreciate the power of the character tables we present in the following sections a few fundamental theorems for character.

3.3 Wonderful Orthogonality Theorem for Character

The “Wonderful Orthogonality Theorem” for character follows directly from the wonderful orthogonality theorem (see Sect. 2.7). There is also a second orthogonality theorem for character which is discussed later (see Sect. 3.6). These theorems give the basic orthonormality relations used to set up character tables.

Theorem. *The primitive characters of an irreducible representation obey the orthogonality relation*

$$\sum_R \chi^{(\Gamma_j)}(R) \chi^{(\Gamma_{j'})}(R^{-1}) = h \delta_{\Gamma_j, \Gamma_{j'}} \quad (3.4)$$

or

$$\sum_R \chi^{(\Gamma_j)}(R) \chi^{(\Gamma_{j'})}(R)^* = h \delta_{\Gamma_j, \Gamma_{j'}} , \quad (3.5)$$

where Γ_j denotes irreducible representation j with dimensionality ℓ_j .

This theorem says that unless the representations are identical or equivalent, the characters are orthogonal in h -dimensional space, where h is the order of the group.

Example. We now illustrate the meaning of the Wonderful Orthogonality Theorem for characters before going to the proof. Consider the permutation group $P(3)$. Let $\Gamma_j = \Gamma_1$ and $\Gamma_{j'} = \Gamma_{1'}$. Then use of (3.13) yields

$$\begin{aligned} \sum_k N_k \chi^{(\Gamma_j)}(\mathcal{C}_k) \left[\chi^{(\Gamma_{j'})}(\mathcal{C}_k) \right]^* &= \underbrace{(1)(1)(1)}_{\text{class of } E} + \underbrace{(3)(1)(-1)}_{\text{class of } A, B, C} + \underbrace{(2)(1)(1)}_{\text{class of } D, F} \\ &= 1 - 3 + 2 = 0. \end{aligned} \quad (3.6)$$

It can likewise be verified that the Wonderful Orthogonality Theorem works for all possible combinations of Γ_j and $\Gamma_{j'}$ in Table 3.1.

Proof. The proof of the wonderful orthogonality theorem for character follows from the Wonderful Orthogonality Theorem itself (see Sect. 2.7). Consider the wonderful orthogonality theorem (2.51)

$$\sum_R D_{\mu\nu}^{(\Gamma_j)}(R) D_{\nu'\mu'}^{(\Gamma_{j'})}(R^{-1}) = \frac{h}{\ell_j} \delta_{\Gamma_j, \Gamma_{j'}} \delta_{\mu\mu'} \delta_{\nu\nu'} . \quad (3.7)$$

Take the diagonal elements of (3.7)

$$\sum_R D_{\mu\mu}^{(\Gamma_j)}(R) D_{\mu'\mu'}^{(\Gamma_{j'})}(R^{-1}) = \frac{h}{\ell_j} \delta_{\Gamma_j, \Gamma_{j'}} \delta_{\mu\mu'} \delta_{\mu'\mu} . \quad (3.8)$$

Now sum (3.8) over μ and μ' to calculate the traces or characters

$$\sum_R \sum_{\mu} D_{\mu\mu}^{(\Gamma_j)}(R) \sum_{\mu'} D_{\mu'\mu'}^{(\Gamma_{j'})}(R^{-1}) = \frac{h}{\ell_j} \delta_{\Gamma_j, \Gamma_{j'}} \sum_{\mu\mu'} \delta_{\mu\mu'} \delta_{\mu'\mu} , \quad (3.9)$$

where we note that

$$\sum_{\mu\mu'} \delta_{\mu\mu'} \delta_{\mu'\mu} = \sum_{\mu} \delta_{\mu\mu} = \ell_j , \quad (3.10)$$

so that

$$\sum_R \chi^{(\Gamma_j)}(R) \chi^{(\Gamma_{j'})}(R^{-1}) = h \delta_{\Gamma_j, \Gamma_{j'}} , \quad (3.11)$$

completing the proof. Equation (3.11) implies that the primitive characters of an irreducible representation form a set of *orthogonal* vectors in *group-element* space, the space spanned by h vectors, one for each element of the group, also called Hilbert space (see Sect. 2.8). Since any arbitrary representation is equivalent to some unitary representation (Sect. 2.4), and the character is preserved under a unitary transformation, (3.11) can also be written as

$$\sum_R \chi^{(\Gamma_j)}(R) \left[\chi^{(\Gamma_{j'})}(R) \right]^* = h \delta_{\Gamma_j, \Gamma_{j'}} . \quad (3.12)$$

Since the character is the same for each element in the class, the summation in (3.12) can be written as a sum over classes k

$$\sum_k N_k \chi^{(\Gamma_j)}(\mathcal{C}_k) \left[\chi^{(\Gamma_{j'})}(\mathcal{C}_k) \right]^* = h \delta_{\Gamma_j, \Gamma_{j'}}, \quad (3.13)$$

where N_k denotes the number of elements in class k , since the representation for R is a unitary matrix, $\chi^{(\Gamma_{j'})}(R^{-1}) = [\chi^{(\Gamma_{j'})}(R)]^*$ (see Sect. 2.2). Also, since the right-hand side of (3.13) is real, we can take the complex conjugate of this equation to obtain the equivalent form

$$\sum_k N_k \left[\chi^{(\Gamma_j)}(\mathcal{C}_k) \right]^* \chi^{(\Gamma_{j'})}(\mathcal{C}_k) = h \delta_{\Gamma_j, \Gamma_{j'}}. \quad (3.14)$$

□

The importance of the results in (3.11)–(3.14) cannot be over-emphasized:

1. Character tells us if a representation is irreducible or not. If a representation is reducible then the characters are not primitive and will generally not obey this orthogonality relation (and other orthogonality relations that we will discuss in Sect. 3.6).
2. Character tells us whether or not we have found all the irreducible representations. For example, the permutation group $P(3)$ could not contain a three-dimensional irreducible representation (see Problem 1.2), since by (2.70)

$$\sum_j \ell_j^2 \leq h. \quad (3.15)$$

Furthermore, character allows us to check the uniqueness of an irreducible representation, using the following theorem.

Theorem. *A necessary and sufficient condition that two irreducible representations be equivalent is that the characters be the same.*

Proof. Necessary condition: If they are equivalent, then the characters are the same – we have demonstrated this already since the trace of a matrix is invariant under an equivalence transformation.

Sufficient condition: If the characters are the same, the vectors for each of the irreducible representations in h -dimensional space cannot be orthogonal, so the representations must be equivalent. □

3.4 Reducible Representations

We now prove a theorem that forms the basis for setting up the characters of a *reducible* representation in terms of the primitive characters for the irreducible representations. This theoretical background will also be used in constructing irreducible representations and character tables, and is essential to most of the practical applications of group theory to solid state physics.

Theorem. *The reduction of any reducible representation into its irreducible constituents is unique.*

Thus, if $\chi(\mathcal{C}_k)$ is the character for some class in a reducible representation, then this theorem claims that we can write the character for the reducible representation $\chi(\mathcal{C}_k)$ as a linear combination of characters for the *irreducible* representations of the group $\chi^{(\Gamma_i)}(\mathcal{C}_k)$

$$\chi(\mathcal{C}_k) = \sum_{\Gamma_i} a_i \chi^{(\Gamma_i)}(\mathcal{C}_k), \quad (3.16)$$

where the a_i coefficients are non-negative integers which denote the number of times the irreducible representation Γ_i is contained in the reducible representation. Furthermore we show here that the a_i coefficients are unique. This theorem is sometimes called the decomposition theorem for reducible representations.

Proof. In proving that the a_i coefficients are unique, we explicitly determine the values of each a_i , which constitute the characters for a reducible representation. Consider the sum over classes k :

$$\sum_k N_k \left[\chi^{(\Gamma_j)}(\mathcal{C}_k) \right]^* \chi(\mathcal{C}_k) = S_j. \quad (3.17)$$

Since $\chi(\mathcal{C}_k)$ is reducible, we write the linear combination for $\chi(\mathcal{C}_k)$ in (3.17) using (3.16) as

$$\begin{aligned} S_j &= \sum_k N_k \left[\chi^{(\Gamma_j)}(\mathcal{C}_k) \right]^* \sum_{\Gamma_i} a_i \chi^{(\Gamma_i)}(\mathcal{C}_k) \\ &= \sum_{\Gamma_i} a_i \left\{ \sum_k N_k \left[\chi^{(\Gamma_j)}(\mathcal{C}_k) \right]^* \chi^{(\Gamma_i)}(\mathcal{C}_k) \right\}. \end{aligned} \quad (3.18)$$

We now apply the Wonderful Orthogonality Theorem for Characters (3.13) to get

$$\sum_{\Gamma_i} a_i h \delta_{\Gamma_i, \Gamma_j} = a_j h = \sum_k N_k \left[\chi^{(\Gamma_j)}(\mathcal{C}_k) \right]^* \chi(\mathcal{C}_k) = S_j \quad (3.19)$$

yielding the decomposition relation

$$a_j = \frac{1}{h} \sum_k N_k \left[\chi^{(\Gamma_j)}(\mathcal{C}_k) \right]^* \chi(\mathcal{C}_k) = \frac{S_j}{h} \quad (3.20)$$

and completing the proof of the theorem. Thus the coefficients a_i in (3.16) are uniquely determined. In other words, the number of times the various irreducible representations are contained in a given reducible representation can be obtained directly from the character table for the group.

This sort of decomposition of the character for a reducible representation is important for the following type of physical problem. Consider a *cubic crystal*. A cubic crystal has many symmetry operations and therefore many classes and many irreducible representations. Now suppose that we squeeze this crystal and lower its symmetry. Let us further suppose that the energy levels for the cubic crystal are degenerate for certain points in the Brillouin zone. This squeezing would most likely lift some of the level degeneracies. To find out how the degeneracy is lifted, we take the representation for the cubic group that corresponds to the unperturbed energy and treat this representation as a reducible representation in the group of lower symmetry. Then the decomposition formulae (3.16) and (3.20) tell us immediately the degeneracy and symmetry types of the split levels in the perturbed or stressed crystal. (A good example of this effect is crystal field splitting, discussed in Chap. 5.) \square

3.5 The Number of Irreducible Representations

We now come to another extremely useful theorem.

Theorem. *The number of irreducible representations is equal to the number of classes.*

Proof. The Wonderful Orthogonality Theorem for Character (3.14)

$$\sum_{k'=1}^k N_{k'} \left[\chi^{(\Gamma_i)}(\mathcal{C}_{k'}) \right]^* \chi^{(\Gamma_j)}(\mathcal{C}_{k'}) = h \delta_{\Gamma_i, \Gamma_j} \quad (3.21)$$

can be written as

$$\sum_{k'=1}^k \left[\sqrt{\frac{N_{k'}}{h}} \chi^{(\Gamma_i)}(\mathcal{C}_{k'}) \right]^* \left[\sqrt{\frac{N_{k'}}{h}} \chi^{(\Gamma_j)}(\mathcal{C}_{k'}) \right] = \delta_{\Gamma_i, \Gamma_j}. \quad (3.22)$$

Each term

$$\sqrt{\frac{N_{k'}}{h}} \chi^{(\Gamma_i)}(\mathcal{C}_{k'})$$

in (3.22) gives the k' th component of a k -dimensional vector. There can be only k such vectors in a k -dimensional space, since the $(k+1)$ th vector would be linearly dependent on the other k vectors. If there were less than k such vectors, then the number of independent vectors would not be large enough to span the k -dimensional space. To express a reducible representation in terms of its irreducible components requires that the vector space be spanned by irreducible representations. Therefore the number of irreducible representations must be k , the number of classes.

For our example of the permutation group of three objects, we have three classes and therefore only three irreducible representations (see Table 3.1). We have already found these irreducible representations and we now know that any additional representations that we might find are either *equivalent* to these representations or they are *reducible*. Knowing the number of distinct irreducible representations is very important in setting up character tables.

As a corollary of this theorem, the number of irreducible representations for Abelian groups is the number of symmetry elements in the group, because each element is in a class by itself. Since each class has only one element, all the irreducible representations are one dimensional. \square

3.6 Second Orthogonality Relation for Characters

We now prove a second orthogonality theorem for characters which sums over the irreducible representations and is extremely valuable for constructing character tables.

Theorem. *The summation over all irreducible representations*

$$\sum_{\Gamma_j} \chi^{(\Gamma_j)}(\mathcal{C}_k) \left[\chi^{(\Gamma_j)}(\mathcal{C}_{k'}) \right]^* N_k = h \delta_{kk'} \quad (3.23)$$

yields a second orthogonality relation for the characters. Thus, the Wonderful Orthogonality Theorem for Character yields an orthogonality relation between rows in the character table while the second orthogonality theorem gives a similar relation between the columns of the character table.

Proof. Construct the matrix

$$Q = \begin{pmatrix} \chi^{(1)}(\mathcal{C}_1) & \chi^{(1)}(\mathcal{C}_2) & \cdots \\ \chi^{(2)}(\mathcal{C}_1) & \chi^{(2)}(\mathcal{C}_2) & \cdots \\ \chi^{(3)}(\mathcal{C}_1) & \chi^{(3)}(\mathcal{C}_2) & \cdots \\ \vdots & \vdots & \end{pmatrix}, \quad (3.24)$$

where the irreducible representations label the rows and the classes label the columns. Q is a square matrix, since by (3.22) the number of classes (designating the column index) is equal to the number of irreducible representations (designating the row index). We now also construct the square matrix

$$Q' = \frac{1}{h} \begin{pmatrix} N_1 \chi^{(1)}(\mathcal{C}_1)^* & N_1 \chi^{(2)}(\mathcal{C}_1)^* & \cdots \\ N_2 \chi^{(1)}(\mathcal{C}_2)^* & N_2 \chi^{(2)}(\mathcal{C}_2)^* & \cdots \\ N_3 \chi^{(1)}(\mathcal{C}_3)^* & N_3 \chi^{(2)}(\mathcal{C}_3)^* & \cdots \\ \vdots & \vdots & \end{pmatrix}, \quad (3.25)$$

where the classes label the rows, and the irreducible representations label the columns. The ij matrix element of the product QQ' summing over classes is then

$$(QQ')_{ij} = \sum_k \frac{N_k}{h} \chi^{(\Gamma_i)}(\mathcal{C}_k) \left[\chi^{(\Gamma_j)}(\mathcal{C}_k) \right]^* = \delta_{\Gamma_i, \Gamma_j} \quad (3.26)$$

using the Wonderful Orthogonality Theorem for Character (3.13). Therefore $QQ' = \hat{1}$ or $Q' = Q^{-1}$ and $Q'Q = \hat{1}$ since $QQ^{-1} = Q^{-1}Q = \hat{1}$, where $\hat{1}$ is the unit matrix. We then write $Q'Q$ in terms of components, but now summing over the irreducible representations

$$(Q'Q)_{kk'} = \sum_{\Gamma_i} \frac{N_k}{h} \chi^{(\Gamma_i)}(\mathcal{C}_k) \left[\chi^{(\Gamma_i)}(\mathcal{C}_{k'}) \right]^* = \delta_{kk'} \quad (3.27)$$

so that

$$\sum_{\Gamma_i} \chi^{(\Gamma_i)}(\mathcal{C}_k) \left[\chi^{(\Gamma_i)}(\mathcal{C}_{k'}) \right]^* = \frac{h}{N_k} \delta_{kk'} , \quad (3.28)$$

which completes the proof of the second orthogonality theorem. \square

3.7 Regular Representation

The regular representation provides a recipe for finding all the irreducible representations of a group. It is not always the fastest method for finding the irreducible representations, but it will always work.

The *regular representation* is found directly from the multiplication table by rearranging the rows and columns so that the identity element is always along the main diagonal. When this is done, the group elements label the columns and the inverse of each group element labels the rows. We will illustrate this with the permutation group of three objects $P(3)$ for which the multiplication table is given in Table 1.1. Application of the rearrangement theorem to place the identity element along the main diagonal gives Table 3.3. Then the matrix representation for an element X in the regular representation is obtained by putting 1 wherever X appears in the multiplication Table 3.3

Table 3.3. Multiplication table for the group $P(3)$ used to generate the regular representation

| | E | A | B | C | D | F |
|--------------|-----|-----|-----|-----|-----|-----|
| $E = E^{-1}$ | E | A | B | C | D | F |
| $A = A^{-1}$ | A | E | D | F | B | C |
| $B = B^{-1}$ | B | F | E | D | C | A |
| $C = C^{-1}$ | C | D | F | E | A | B |
| $F = D^{-1}$ | F | B | C | A | E | D |
| $D = F^{-1}$ | D | C | A | B | F | E |

and 0 everywhere else. Thus we obtain

$$D^{\text{reg}}(E) = \begin{pmatrix} 1 & 0 & 0 & 0 & 0 & 0 \\ 0 & 1 & 0 & 0 & 0 & 0 \\ 0 & 0 & 1 & 0 & 0 & 0 \\ 0 & 0 & 0 & 1 & 0 & 0 \\ 0 & 0 & 0 & 0 & 1 & 0 \\ 0 & 0 & 0 & 0 & 0 & 1 \end{pmatrix}, \quad (3.29)$$

which is always the unit matrix of dimension $(h \times h)$. For one of the other elements in the regular representation we obtain

$$D^{\text{reg}}(A) = \begin{pmatrix} 0 & 1 & 0 & 0 & 0 & 0 \\ 1 & 0 & 0 & 0 & 0 & 0 \\ 0 & 0 & 0 & 0 & 0 & 1 \\ 0 & 0 & 0 & 0 & 1 & 0 \\ 0 & 0 & 0 & 1 & 0 & 0 \\ 0 & 0 & 1 & 0 & 0 & 0 \end{pmatrix} \quad (3.30)$$

and so on. By construction, only $D^{\text{reg}}(E)$ has a non-zero trace!

We now show that the regular representation is indeed a representation. This means that the regular representation obeys the multiplication table (either Table 1.1 or 3.3). Let us for example show

$$D^{\text{reg}}(BC) = D^{\text{reg}}(B)D^{\text{reg}}(C). \quad (3.31)$$

It is customary to denote the matrix elements of the regular representation directly from the definition $D^{\text{reg}}(X)_{A_k^{-1}, A_i}$, where A_k^{-1} labels the rows and A_i labels the columns using the notation

$$D^{\text{reg}}(X)_{A_k^{-1}, A_i} = \begin{cases} 1 & \text{if } A_k^{-1}A_i = X \\ 0 & \text{otherwise.} \end{cases} \quad (3.32)$$

Using this notation, we have to show that

$$D^{\text{reg}}(BC)_{A_k^{-1}, A_i} = \sum_{A_j} D^{\text{reg}}(B)_{A_k^{-1}, A_j} D^{\text{reg}}(C)_{A_j^{-1}, A_i}. \quad (3.33)$$

Now look at the rearranged multiplication table given in Table 3.3. By construction, we have for each of the matrices

$$D^{\text{reg}}(B)_{A_k^{-1}, A_j} = \begin{cases} 1 & \text{if } A_k^{-1}A_j = B \\ 0 & \text{otherwise,} \end{cases} \quad (3.34)$$

$$D^{\text{reg}}(C)_{A_j^{-1}, A_i} = \begin{cases} 1 & \text{if } A_j^{-1}A_i = C \\ 0 & \text{otherwise.} \end{cases} \quad (3.35)$$

Therefore in the sum $\sum_{A_j} D^{\text{reg}}(B)_{A_k^{-1}, A_j} D^{\text{reg}}(C)_{A_j^{-1}, A_i}$ of (3.33), we have only nonzero entries when

$$BC = (A_k^{-1} A_j) \underbrace{(A_j^{-1} A_i)}_1 = A_k^{-1} A_i. \quad (3.36)$$

But this coincides with the definition of $D^{\text{reg}}(BC)$:

$$D^{\text{reg}}(BC)_{A_k^{-1}, A_i} = \begin{cases} 1 & \text{if } A_k^{-1} A_i = BC \\ 0 & \text{otherwise.} \end{cases} \quad (3.37)$$

Therefore D^{reg} is, in fact, a representation of the group A_1, \dots, A_h , completing the proof.

The following theorem allows us to find all the irreducible representations from the regular representation.

Theorem. *The regular representation contains each irreducible representation a number of times equal to the dimensionality of the representation.*

(For the group $P(3)$, this theorem says that D^{reg} contains $D^{(\Gamma_1)}$ once, $D^{(\Gamma_1')}$ once, and $D^{(\Gamma_2)}$ twice so that the regular representation of $P(3)$ would be of dimensionality 6.)

Proof. Since D^{reg} is a reducible representation, we can write for the characters (see (3.16))

$$\chi^{\text{reg}}(\mathcal{C}_k) = \sum_{\Gamma_i} a_i \chi^{(\Gamma_i)}(\mathcal{C}_k), \quad (3.38)$$

where \sum_{Γ_i} is the sum over the irreducible representations and the a_i coefficients have been shown to be unique (3.20) and given by

$$a_i = \frac{1}{h} \sum_k N_k \left[\chi^{(\Gamma_i)}(\mathcal{C}_k) \right]^* \chi^{\text{reg}}(\mathcal{C}_k). \quad (3.39)$$

We note that $N_E = 1$ for the identity element, which is in a class by itself. But by construction $\chi^{\text{reg}}(\mathcal{C}_k) = 0$ unless $\mathcal{C}_k = E$ in which case $\chi^{\text{reg}}(E) = h$. Therefore $a_i = \chi^{(\Gamma_i)}(E) = \ell_i$, where $\chi^{(\Gamma_i)}$ is the trace of an ℓ_i dimensional unit matrix, thereby completing the proof.

The theorem (3.38) that we have just proven tells us that the regular representation contains each irreducible representation of the group at least once. To obtain these irreducible representations explicitly, we have to carry out a similarity transformation which brings the matrices of the regular representation into block diagonal form. It turns out to be very messy to extract the matrices of the regular representation – in fact, it is so tedious to do this operation that it does not even make an instructive homework problem.

It is much easier to write down the matrices which generate the symmetry operations of the group directly.

Consider for example the permutation group of three objects $P(3)$ which is isomorphic to the symmetry operations of a regular triangle (Sect. 1.2). The matrices for D and F generate rotations by $\pm 2\pi/3$ about the z axis, which is \perp to the plane of the triangle. The A matrix represents a rotation by $\pm\pi$ about the y axis while the B and C matrices represent rotations by $\pm\pi$ about axes in the $x-y$ plane which are $\pm 120^\circ$ away from the y axis. In setting up a representation, it is advantageous to write down those matrices which can be easily written down – such as E, A, D, F . The remaining matrices such as B and C can then be found through the multiplication table. \square

We will now make use of the regular representation to prove a useful theorem for setting up character tables. This is the most useful application of the regular representation for our purposes.

Theorem. *The order of a group h and the dimensionality ℓ_j of its irreducible representations Γ_j are related by*

$$\sum_j \ell_j^2 = h. \quad (3.40)$$

We had previously found (2.70) that $\sum_j \ell_j^2 \leq h$. The regular representation allows us to prove that it is the equality that applies.

Proof. By construction, the regular representation is of dimensionality h which is the number of elements in the group and in the multiplication table. But each irreducible representation of the group is contained ℓ_j times in the regular representation (see (3.38)) so that

$$\chi^{\text{reg}}(E) = h = \sum_{\Gamma_j} \underbrace{a_j}_{\ell_j} \underbrace{\chi^{\Gamma_j}(E)}_{\ell_j} = \sum_{\Gamma_j} \ell_j^2, \quad (3.41)$$

where one ℓ_j comes from the number of times each irreducible representation is contained in the regular representation and the second ℓ_j is the dimension of the irreducible representation Γ_j .

We thus obtain the result

$$\sum_j \ell_j^2 = h, \quad (3.42)$$

where \sum_j is the sum over irreducible representations. For example for $P(3)$, we have $\ell_1 = 1$, $\ell_{1'} = 1$, $\ell_2 = 2$ so that $\sum \ell_j^2 = 6 = h$. \square

3.8 Setting up Character Tables

For many applications it is sufficient to know just the character table without the actual matrix representations for a particular group. So far, we have only

set up the character table by taking traces of the irreducible representations – i.e., from the definition of χ . For the most simple cases, the character table can be constructed using the results of the theorems we have just proved – without knowing the representations themselves. In practice, the character tables that are needed to solve a given problem are found either in books or in journal articles. The examples in this section are thus designed to show the reader how character tables are constructed, should this be necessary. Our goal is further to give some practice in using the theorems proven in Chap. 3.

A summary of useful rules for the construction of character tables is given next.

- (a) The number of irreducible representations is equal to the number of classes (Sect. 3.5). The number of classes is found most conveniently from the classification of the symmetry operations of the group. Another way to find the classes is to compute all possible conjugates for all group elements using the group multiplication table.
- (b) The dimensionalities of the irreducible representations are found from $\sum_i \ell_i^2 = h$ (see (3.42)). For simple cases, this relation uniquely determines the dimensionalities of the irreducible representations. For example, the permutation group of three objects $P(3)$ has three classes and therefore three irreducible representations. The identity representation is always present, so that one of these must be one-dimensional (i.e., the matrix for the identity element of the group is the unit matrix). So this gives $1^2 + ?^2 + ?^2 = 6$. This equation only has one integer solution, namely $1^2 + 1^2 + 2^2 = 6$. No other solution works!
- (c) There is always a whole row of 1s in the character table for the identity representation.
- (d) The first column of the character table is always the trace for the unit matrix representing the identity element or class. This character is always ℓ_i , the dimensionality of the $(\ell_i \times \ell_i)$ unit matrix. Therefore, the first column of the character table is also filled in.
- (e) For all representations other than the identity representation Γ_1 , the following relation is satisfied:

$$\sum_k N_k \chi^{(\Gamma_i)}(\mathcal{C}_k) = 0, \quad (3.43)$$

where \sum_k denotes the sum on classes. Equation (3.43) follows from the wonderful orthogonality theorem for character and taking the identity representation Γ_1 as one of the irreducible representations.

If there are only a few classes in the group, (3.43) often uniquely determines the characters for several of the irreducible representations; particularly for the one-dimensional representations.

- (f) The Wonderful Orthogonality Theorem for character works on rows of the character table:

$$\sum_k \left[\chi^{(\Gamma_i)}(\mathcal{C}_k) \right]^* \chi^{(\Gamma_j)}(\mathcal{C}_k) N_k = h \delta_{\Gamma_i, \Gamma_j} . \quad (3.44)$$

This theorem can be used both for orthogonality (different rows) or for normalization (same rows) of the characters in an irreducible representation and the complex conjugate can be applied either to the $\chi^{(\Gamma_i)}(\mathcal{C}_k)$ or to the $\chi^{(\Gamma_j)}(\mathcal{C}_k)$ terms in (3.44) since the right hand side of (3.44) is real.

- (g) The second orthogonality theorem works for columns of the character table:

$$\sum_{\Gamma_i} \left[\chi^{(\Gamma_i)}(\mathcal{C}_k) \right]^* \chi^{(\Gamma_i)}(\mathcal{C}_{k'}) = \frac{h}{N_k} \delta_{kk'} . \quad (3.45)$$

This relation can be used both for orthogonality (different columns) or normalization (same columns), as the wonderful orthogonality theorem for character.

- (h) From the second orthogonality theorem for character, and from the character for the identity class

$$\chi^{(\Gamma_i)}(E) = \ell_i \quad (3.46)$$

we see that the characters for all the other classes obey the relation

$$\sum_{\Gamma_i} \chi^{(\Gamma_i)}(\mathcal{C}_k) \ell_i = 0 , \quad (3.47)$$

where \sum_{Γ_i} denotes the sum on irreducible representations and ℓ_i is the dimensionality of representation Γ_i . Equation (3.47) follows from the wonderful orthogonality theorem for character, and it uses the identity representations as one of the irreducible representations, and for the second any but the identity representation ($\Gamma_i \neq \Gamma_1$) can be used.

With all this machinery it is often possible to complete the character tables for simple groups without an explicit determination of the matrices for a representation.

Let us illustrate the use of the rules for setting up character tables with the permutation group of three objects, $P(3)$. We fill in the first row and first column of the character table immediately from rules #3 and #4 in the earlier list (see Table 3.4).

In order to satisfy #5, we know that $\chi^{(\Gamma_1')}(\mathcal{C}_2) = -1$ and $\chi^{(\Gamma_1')}(\mathcal{C}_3) = 1$, which we add to the character table (Table 3.5).

Table 3.4. Character table for $P(3)$ – Step 1

| | \mathcal{C}_1 | $3\mathcal{C}_2$ | $2\mathcal{C}_3$ |
|-------------|-----------------|------------------|------------------|
| Γ_1 | 1 | 1 | 1 |
| Γ_1' | 1 | | |
| Γ_2 | 2 | | |

Table 3.5. Character table for $P(3)$ – Step 2

| | \mathcal{C}_1 | $3\mathcal{C}_2$ | $2\mathcal{C}_3$ |
|---------------|-----------------|------------------|------------------|
| Γ_1 | 1 | 1 | 1 |
| $\Gamma_{1'}$ | 1 | -1 | 1 |
| Γ_2 | 2 | 0 | -1 |

Table 3.6. Character table for $P(3)$

| | \mathcal{C}_1 | $3\mathcal{C}_2$ | $2\mathcal{C}_3$ |
|---------------|-----------------|------------------|------------------|
| Γ_1 | 1 | 1 | 1 |
| $\Gamma_{1'}$ | 1 | -1 | 1 |
| Γ_2 | 2 | 0 | -1 |

Table 3.7. Multiplication table for the cyclic group of three rotations by $2\pi/3$ about a common axis

| | E | C_3 | C_3^2 |
|---------|---------|---------|---------|
| E | E | C_3 | C_3^2 |
| C_3 | C_3 | C_3^2 | E |
| C_3^2 | C_3^2 | E | C_3 |

Now apply the second orthogonality theorem using columns 1 and 2 and then again with columns 1 and 3, and this completes the character table, thereby obtaining Table 3.6.

Let us give another example of a character table which illustrates another principle that not all entries in a character table need to be real. Such a situation can occur in the case of cyclic groups. Consider a group with three symmetry operations:

- E – identity,
- C_3 – rotation by $2\pi/3$,
- C_3^2 – rotation by $4\pi/3$.

See Table 3.7 for the multiplication table for this group. All three operations in this cyclic group C_3 are in separate classes as can be easily seen by conjugation of the elements. Hence there are three classes and three irreducible representations to write down. The character table we start with is obtained by following Rules #3 and #4 (Table 3.8). Orthogonality of Γ_2 to Γ_1 yields the algebraic relation: $1 + a + b = 0$.

Since $C_3^2 = C_3C_3$ and $C_3^2C_3 = E$, it follows that $b = a^2$ and $ab = a^3 = 1$, so that $a = \exp(2\pi i/3)$. Then, orthogonality of the second column with the first yields $c = \exp(4\pi i/3)$ and orthogonality of the third column with the first column yields $d = [\exp(4\pi i/3)]^2$. From this information we can readily complete the Character Table 3.9, where $\omega = \exp[2\pi i/3]$. Such a group

Table 3.8. Character table for Cyclic Group C_3

| | E | C_3 | C_3^2 |
|------------|-----|-------|---------|
| Γ_1 | 1 | 1 | 1 |
| Γ_2 | 1 | a | b |
| Γ_3 | 1 | c | d |

Table 3.9. Character table for cyclic group C_3

| | E | C_3 | C_3^2 |
|------------|-----|------------|------------|
| Γ_1 | 1 | 1 | 1 |
| Γ_2 | 1 | ω | ω^2 |
| Γ_3 | 1 | ω^2 | ω |

often enters into a physical problem which involves time inversion symmetry, where the energy levels corresponding to Γ_2 and Γ_3 are degenerate (see Chap. 16).

This idea of the cyclic group can be applied to a four-element group: E , C_2 , C_4 , C_4^3 – to a five-element group: E , C_5 , C_5^2 , C_5^3 , C_5^4 – and to a six-element group: E , C_6 , C_3 , C_2 , C_3^2 , C_6^5 , etc. In each case, use the fact that the N th roots of unity sum to zero so that each Γ_j is orthogonal to Γ_1 and by the rearrangement theorem each Γ_j is orthogonal to $\Gamma_{j'}$. For the case of Bloch's theorem, we have an N -element group with characters that comprise the N th roots of unity $\omega = \exp[2\pi i/N]$.

All these cyclic groups are Abelian so that each element is in a class by itself. The representations for these groups correspond to the multiplication tables, which therefore contain the appropriate collections of roots of unity.

The character tables for all the point groups used in this chapter are listed in Appendix A. The notation used in these tables is discussed in more detail in the next sections.

3.9 Schoenflies Symmetry Notation

There are two point group notations that are used for the symmetry operations in the character tables printed in books and journals. One is the Schoenflies symmetry notation, which is described in this section and the other is the Hermann–Mauguin notation that is used by the crystallography community and is summarized in Sect. 3.10. For the Schoenflies system the following notation is commonly used:

- E = Identity
- C_n = rotation through $2\pi/n$. For example C_2 is a rotation of 180° . Likewise C_3 is a rotation of 120° , while C_6^2 represents a rotation of 60° followed

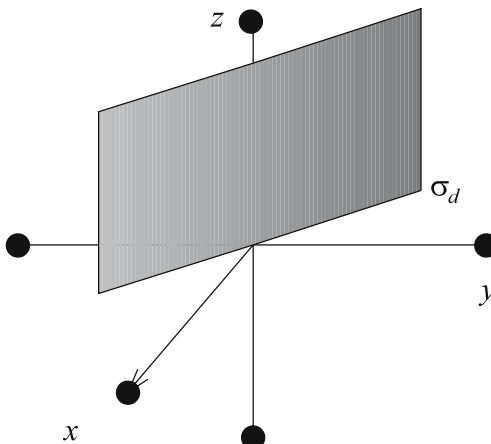


Fig. 3.1. Schematic illustration of a dihedral symmetry axis. The reflection plane containing the diagonal of the square and the fourfold axis is called a dihedral plane. For this geometry $\sigma_d(x, y, z) = (-y, -x, z)$

by another rotation of 60° about the same axis so that $C_6^2 = C_3$. In a Bravais lattice it can be shown that n in C_n can only assume values of $n = 1, 2, 3, 4$, and 6 . The observation of a diffraction pattern with fivefold symmetry in 1984 was therefore completely unexpected, and launched the field of quasicrystals, where a six-dimensional space is used for obtaining crystalline periodicity.

- σ = reflection in a plane.
- σ_h = reflection in a “horizontal” plane. The reflection plane here is perpendicular to the axis of highest rotational symmetry.
- σ_v = reflection in a “vertical” plane. The reflection plane here contains the axis of highest rotational symmetry.
- σ_d is the reflection in a diagonal plane. The reflection plane here is a vertical plane which bisects the angle between the twofold axes \perp to the principal symmetry axis. An example of a diagonal plane is shown in Fig. 3.1. σ_d is also called a dihedral plane.
- i is the inversion which takes

$$\begin{cases} x \rightarrow -x \\ y \rightarrow -y \\ z \rightarrow -z \end{cases}.$$

- S_n is the improper rotation through $2\pi/n$, which consists of a rotation by $2\pi/n$ followed by a reflection in a horizontal plane. Alternatively, we can define S_n as a rotation by $4\pi/n$ followed by the inversion.
- iC_n = compound rotation–inversion, which consists of a rotation followed by an inversion.

In addition to these point group symmetry operations, there are several space group symmetry operations, such as translations, glide planes, screw axes, etc. which are discussed in Chap. 9. The point groups, in contrast to the space groups, exhibit a point that never moves under the application of all symmetry operations. There are *32 common point groups* for crystallographic systems ($n = 1, 2, 3, 4, 6$), and the character tables for these 32 point groups are given in many standard group theory texts. For convenience we also list the character tables for these point groups in Appendix A (Tables A.1–A.32). Tables A.22–A.28 are for groups with fivefold symmetry axes and such tables are not readily found in group theory books, but have recently become important, because of the discovery of quasicrystals, C_{60} , and related molecules. Note that the tables for fivefold symmetry are: C_5 (Table A.22); C_{5v} (Table A.23); $C_{5h} \equiv C_5 \otimes \sigma_h$; D_5 (Table A.24); D_{5d} (Table A.25); D_{5h} (Table A.26); I (Table A.27); and I_h (Table A.28). Recurrent in these tables is the “golden mean,” $\tau = (1 + \sqrt{5})/2$ where $\tau - 1 = 2 \cos(2\pi/5) = 2 \cos 72^\circ$. These are followed by Tables A.33 and A.34 for the semi-infinite groups $C_{\infty v}$ and $D_{\infty h}$, discussed later in this section.

Certain patterns can be found between the various point groups. Groups C_1, C_2, \dots, C_6 only have n -fold rotations about a simple symmetry axis C_n (see for example Table A.15) and are cyclic groups, mentioned in Sect. 3.8. Groups C_{nv} have, in addition to the n -fold axes, vertical reflection planes σ_v (e.g., Table A.16). Groups C_{nh} have, in addition to the n -fold axes, horizontal reflection planes σ_h and include each operation C_n together with the compound operations C_n followed by σ_h (Tables A.3 and A.11 illustrate this relation between groups). The groups S_2, S_4 , and S_6 have mostly compound operations (see Tables A.2, A.17, and A.20). The groups denoted by D_n are dihedral groups and have non-equivalent symmetry axes in perpendicular planes (e.g., Table A.18). The group of the operations of a square is D_4 and has in addition to the principal fourfold axes, two sets of non-equivalent twofold axes (Table A.18). We use the notation C'_2 to indicate that these twofold axis are in a different plane (see also Table A.12 for group D_3 , where this same situation occurs). When non-equivalent axes are combined with mirror planes we get groups like D_{2h}, D_{3h} , etc. (see Tables A.8 and A.14). There are five cubic groups T, O, T_d, T_h , and O_h . These groups have no principal axis but instead have four threefold axes (see Tables A.29–A.32).

3.10 The Hermann–Mauguin Symmetry Notation

There is also a second notation for symmetry operations and groups, namely the *Hermann–Mauguin or international notation*, which is used in the International Tables for X-Ray Crystallography, a standard structural and symmetry reference book. The international notation is what is usually found in crystallography textbooks and various materials science journals. For that reason

Table 3.10. Comparison between Schoenflies and Hermann–Mauguin notation

| rotation | Schoenflies | Hermann–Mauguin |
|---------------------------------|---------------|-----------------|
| | C_n | n |
| rotation–inversion | iC_n | \bar{n} |
| mirror plane | σ | m |
| horizontal reflection | | |
| plane \perp to n -fold axes | σ_h | n/m |
| n -fold axes in | | |
| vertical reflection plane | σ_v | nm |
| two non-equivalent | | |
| vertical reflection planes | $\sigma_{v'}$ | nmm |

Table 3.11. Comparison of notation for proper and improper rotations in the Schoenflies and International systems

| proper rotations | | improper rotations | |
|------------------|-------------|--------------------|---------------|
| international | Schoenflies | international | Schoenflies |
| 1 | C_1 | $\bar{1}$ | S_2 |
| 2 | C_2 | $\bar{2} \equiv m$ | σ |
| 3 | C_3 | $\bar{3}$ | S_6^{-1} |
| 3_2 | C_3^{-1} | $\bar{3}_2$ | S_6 |
| 4 | C_4 | $\bar{4}$ | S_4^{-1} |
| 4_3 | C_4^{-1} | $\bar{4}_3$ | S_4 |
| 5 | C_5 | $\bar{5}$ | S_{10} |
| 5_4 | C_5^{-1} | $\bar{5}_4$ | S_{10}^{-1} |
| 6 | C_6 | $\bar{6}$ | S_3^{-1} |
| 6_5 | C_6^{-1} | $\bar{6}_5$ | S_3 |

it is also necessary to become familiar with this notation. The general correspondence between the two notations is shown in Table 3.10 for rotations and mirror planes. The Hermann–Mauguin notation \bar{n} means iC_n which is equivalent to a rotation of $2\pi/n$ followed by or preceded by an inversion. A string of numbers like 422 (see Table A.18) means that there is a fourfold major symmetry axis (C_4 axis), and perpendicular to this axis are two inequivalent sets of twofold axes C'_2 and C''_2 , such as occur in the group of the square (D_4). If there are several inequivalent horizontal mirror planes like

$$\frac{2}{m}, \quad \frac{2}{m}, \quad \frac{2}{m},$$

an abbreviated notation mmm is sometimes used [see notation for the group D_{2h} (Table A.8)]. The notation 4mm (see Table A.16) denotes a fourfold axis

and two sets of vertical mirror planes, one set through the axes C_4 and denoted by $2\sigma_v$ and the other set through the bisectors of the $2\sigma_v$ planes and denoted by the dihedral vertical mirror planes $2\sigma_d$. Table 3.11 is useful in relating the two kinds of notations for rotations and improper rotations.

3.11 Symmetry Relations and Point Group Classifications

In this section we summarize some useful relations between symmetry operations and give the classification of point groups. Some useful relations on the commutativity of symmetry operations are:

- (a) Inversion commutes with all point symmetry operations.
- (b) All rotations about the same axis commute.
- (c) All rotations about an arbitrary rotation axis commute with reflections across a plane perpendicular to this rotation axis.
- (d) Two twofold rotations about perpendicular axes commute.
- (e) Two reflections in perpendicular planes will commute.
- (f) Any two of the symmetry elements σ_h , S_n , C_n ($n = \text{even}$) implies the third.

If we have a major symmetry axis C_n ($n \geq 2$) and there are either twofold axes C_2 or vertical mirror planes σ_v , then there will generally be more than one C_2 or σ_v symmetry operations. In some cases these symmetry operations are in the same class and in the other cases they are not, and this distinction can be made by use of conjugation (see Sect. 1.6).

The classification of the 32 crystallographic point symmetry groups shown in Table 3.12 is often useful in making practical applications of character tables in textbooks and journal articles to specific materials.

In Table 3.12 the first symbol in the Hermann–Mauguin notation denotes the principal axis or plane. The second symbol denotes an axis (or plane) perpendicular to this axis, except for the cubic groups, where the second symbol refers to a $\langle 111 \rangle$ axis. The third symbol denotes an axis or plane that is \perp to the first axis and at an angle of π/n with respect to the second axis.

In addition to the 32 crystallographic point groups that are involved with the formation of three-dimensional crystals, there are nine symmetry groups that form clusters and molecules which show icosahedral symmetry or are related to the icosahedral group I_h . We are interested in these species because they can become part of crystallographic structures. Examples of such clusters and molecules are fullerenes. The fullerene C_{60} has full icosahedral symmetry I_h (Table A.28), while C_{70} has D_{5h} symmetry (Table A.26) and C_{80} has D_{5d} symmetry (Table A.25). The nine point groups related to icosahedral symmetry that are used in solid state physics, as noted earlier, are also listed in Table 3.12 later that double line.

Table 3.12. The extended 32 crystallographic point groups and their symbols^(a)

| system | Schoenflies symbol | Hermann–Mauguin symbol ^(b) | | examples |
|--------------|--------------------|---------------------------------------|-------------|--|
| | | full | abbreviated | |
| triclinic | C_1 | 1 | 1 | Al_2SiO_5 |
| | $C_{i}, (S_2)$ | $\bar{1}$ | $\bar{1}$ | |
| monoclinic | $C_{1h}, (S_1)$ | m | m | KNO_2 |
| | C_2 | 2 | 2 | |
| | C_{2h} | $2/m$ | $2/m$ | |
| orthorhombic | C_{2v} | $2mm$ | mm | I, Ga |
| | $D_2, (V)$ | 222 | 222 | |
| | $D_{2h}, (V_h)$ | $2/m\ 2/m\ 2/m$ | mmm | |
| tetragonal | C_4 | 4 | 4 | CaWO_4 |
| | S_4 | $\bar{4}$ | $\bar{4}$ | |
| | C_{4h} | $4/m$ | $4/m$ | |
| | $D_{2d}, (V_d)$ | $\bar{4}2m$ | $\bar{4}2m$ | |
| | C_{4v} | $4mm$ | $4mm$ | |
| | D_4 | 422 | 42 | |
| | D_{4h} | $4/m\ 2/m\ 2/m$ | $4/mmm$ | |
| rhombohedral | C_3 | 3 | 3 | AsI_3 FeTiO_3 |
| | $C_{3i}, (S_6)$ | $\bar{3}$ | $\bar{3}$ | |
| | C_{3v} | $3m$ | $3m$ | |
| | D_3 | 32 | 32 | |
| | D_{3d} | $\bar{3}2/m$ | $\bar{3}m$ | |
| hexagonal | $C_{3h}, (S_3)$ | $\bar{6}$ | $\bar{6}$ | ZnO, NiAs CeF_3 $\text{Mg}, \text{Zn}, \text{graphite}$ |
| | C_6 | 6 | 6 | |
| | C_{6h} | $6/m$ | $6/m$ | |
| | D_{3h} | $\bar{6}2m$ | $\bar{6}2m$ | |
| | C_{6v} | $6mm$ | $6mm$ | |
| | D_6 | 622 | 62 | |
| | D_{6h} | $6/m\ 2/m\ 2/m$ | $6/mmm$ | |

Footnote (a): The usual 32 crystallographic point groups are here extended by including 9 groups with 5 fold symmetry and are identified here as icosahedral point groups.

Footnote (b): In the Hermann–Mauguin notation, the symmetry axes parallel to and the symmetry planes perpendicular to each of the “principal” directions in the crystal are named in order. When there is both an axis parallel to and a plane normal to a given direction, these are indicated as a fraction; thus $6/m$ means a sixfold rotation axis standing perpendicular to a plane of symmetry, while $\bar{4}$ denotes a fourfold rotary inversion axis. In some classifications, the rhombohedral (trigonal) groups are listed with the hexagonal groups. Also show are the corresponding entries for the icosahedral groups (see text).

Table 3.12. (continued)

| the extended 32 crystallographic point groups and their symmetries | | | | |
|--|--------------------|------------------------|--------------|-----------------------------|
| system | Schoenflies symbol | Hermann–Mauguin symbol | | examples |
| | | full | abbreviated | |
| cubic | T | 23 | 23 | NaClO_3 |
| | T_h | $2/m\bar{3}$ | $m3$ | FeS_2 |
| | T_d | $\bar{4}3m$ | $\bar{4}3m$ | ZnS |
| | O | 432 | 43 | $\beta\text{-Mn}$ |
| | O_h | $4/m\bar{3}2/m$ | $m3m$ | NaCl , diamond, Cu |
| icosahedral | C_5 | 5 | 5 | |
| | $C_{5i}, (S_{10})$ | $\bar{1}0$ | $\bar{1}0$ | |
| | C_{5v} | $5m$ | $5m$ | |
| | C_{5h}, S_5 | $\bar{5}$ | $\bar{5}$ | |
| | D_5 | 52 | 52 | |
| | D_{5d} | $\bar{5}2/m$ | $\bar{5}/m$ | C_{80} |
| | D_{5h} | $\bar{1}02m$ | $\bar{1}02m$ | C_{70} |
| | I | 532 | 532 | |
| | I_h | | | C_{60} |

It is also convenient to picture many of the point group symmetries with stereograms (see Fig. 3.2). The stereogram is a mapping of a general point on a sphere onto a plane going through the center of the sphere. If the point on the sphere is above the plane it is indicated as a +, and if below as a o. In general, the polar axis of the stereogram coincides with the principal axis of symmetry. The first five columns of Fig. 3.2 pertain to the crystallographic point group symmetries and the sixth column is for fivefold symmetry.

The five first stereograms on the first row pertaining to groups with a single axis of rotation show the effect of two-, three-, four-, and sixfold rotation axes on a point +. These groups are cyclic groups with only n -fold axes. Note the symmetry of the central point for each group. On the second row we have added vertical mirror planes which are indicated by the solid lines. Since the “vertical” and “horizontal” planes are not distinguishable for C_1 , the addition of a mirror plane to C_1 is given in the third row, showing the groups which result from the first row upon addition of horizontal planes. The symbols \oplus indicate the coincidence of the projection of points above and below the plane, characteristic of horizontal mirror planes.

If instead of proper rotations as in the first row, we can also have improper rotations, then the groups on row 4 are generated. Since S_1 is identical with C_{1h} , it is not shown separately; this also applies to $S_3 = C_{3h}$ and to $S_5 = C_{5h}$ (neither of which are shown). It is of interest to note that S_2 and S_6 have inversion symmetry but S_4 does not.

The addition of twofold axes \perp to the principal symmetry axis for the groups in the first row yields the stereograms of the fifth row where the twofold

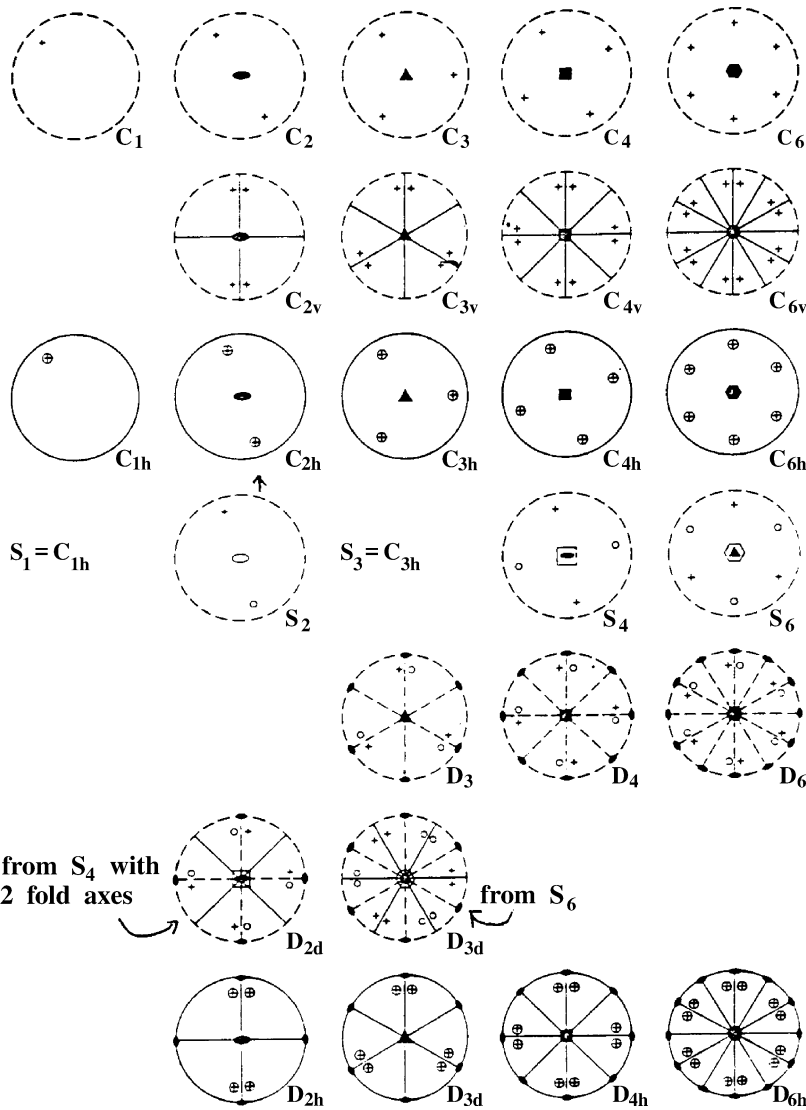


Fig. 3.2. The first five columns show stereographic projections of simple crystallographic point groups

axes appear as dashed lines. Here we see that the higher the symmetry of the principal symmetry axis, the greater the number of twofold axes D_5 (not shown) that would have 5 axes separated by 72° .

The addition of twofold axes to the groups on the fourth row yields the stereograms of the sixth row, where D_{2d} comes from S_4 , while D_{3d} comes from S_6 . Also group D_{5d} (not shown) comes from S_{10} . The addition of twofold axes

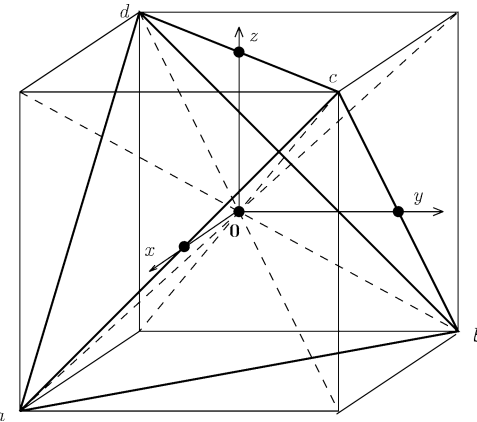


Fig. 3.3. Schematic diagram for the symmetry operations of the group T_d

to S_2 results in C_{2h} . The stereograms on the last row are obtained by adding twofold axes \perp to C_n to the stereograms for the C_{nh} groups on the third row. D_{5h} (not shown) would fall into this category. The effect of adding a twofold axis to C_{1h} is to produce C_{2v} .

The five point symmetry groups associated with cubic symmetry (T , O , T_d , T_h and O_h) are not shown in Fig. 3.2. These groups have higher symmetry and have no single principal axis. The resulting stereograms are very complicated and for this reason are not given in Fig. 3.2. For the same reason the stereograph for the I and I_h icosahedral groups are not given. We give some of the symmetry elements for these groups next.

The group T (or 23 using the International notation) has 12 symmetry elements which include:

| | | |
|----------------------|----------------|---------------------------------------|
| 1 | identity | |
| 3 | twofold axes | (x, y, z) |
| 4 | threefold axes | (body diagonals – positive rotation) |
| 4 | threefold axes | (body diagonals – negative rotations) |
| <hr/> | | |
| 12 symmetry elements | | |

The point group T_h (denoted by $m3$ in the abbreviated International notation or by $2/m3$ in the full International notation) contains all the symmetry operations of T and inversion as well, and is written as $T_h \equiv T \otimes i$, indicating the direct product of the group T and the group C_i having two symmetry elements E, i (see Chap. 6). This is equivalent to adding a horizontal plane of symmetry, hence the notation $2/m$; the symbol 3 means a threefold axis (see Table 3.11). Thus T_h has 24 symmetry elements.

The point group T_d ($\bar{4}3m$) contains the symmetry operations of the regular tetrahedron (see Fig. 3.3), which correspond to the point symmetry for diamond and the zincblende (III–V and II–VI) structures. We list next the 24 symmetry operations of T_d :

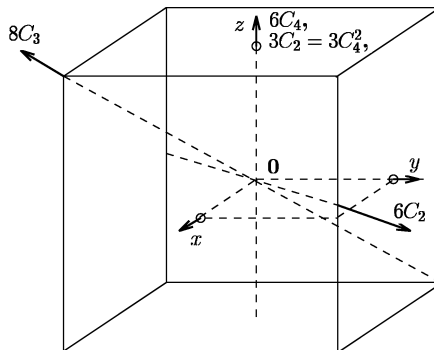


Fig. 3.4. Schematic for the symmetry operations of the group O

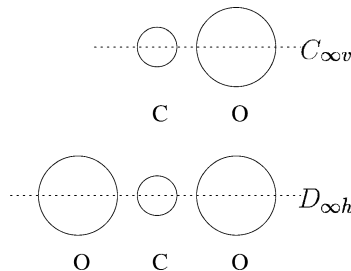


Fig. 3.5. Schematic diagram of the CO molecule with symmetry $C_{\infty v}$ and symmetry operations E , $2C_{\phi}$, σ_v , and the linear CO_2 molecule in which the inversion operation together with $(E, 2C_{\phi}, \sigma_v)$ are also present to give the group $D_{\infty h}$

- identity,
- eight C_3 about body diagonals corresponding to rotations of $\pm 2\pi/3$,
- three C_2 about x, y, z directions,
- six S_4 about x, y, z corresponding to rotations of $\pm\pi/2$,
- six σ_d planes that are diagonal reflection planes.

The cubic groups are O (432) and O_h ($m3m$), and they are shown schematically in Fig. 3.4.

The operations for group O as shown in Fig. 3.4 are E , $8C_3$, $3C_2 = 3C_4^2$, $6C_2$, and $6C_4$. To get O_h we combine these 24 operations with inversion to give 48 operations in all. We note that the second symbol in the Hermann–Mauguin (International) notation for all five cubic groups is for the $\langle 111 \rangle$ axes rather than for an axis \perp to the principal symmetry axis.

In addition to the 32 crystallographic point groups and to the eight fivefold point groups, the character tables contain listings for $C_{\infty v}$ (Table A.33) and $D_{\infty h}$ (Table A.34) which have full rotational symmetry around a single axis, and therefore have an ∞ number of symmetry operations and classes. These two groups are sometimes called the semi-infinite groups because they have

an infinite number of operations about the major symmetry axis. An example of $C_{\infty v}$ symmetry is the CO molecule shown in Fig. 3.5.

Here the symmetry operations are E , $2C_\phi$, and σ_v . The notation C_ϕ denotes an axis of full rotational symmetry and σ_v denotes the corresponding infinite array of vertical planes. The group $D_{\infty h}$ has in addition the inversion operation which is compounded with each of the operations in $C_{\infty v}$, and this is written as $D_{\infty h} = C_{\infty v} \otimes i$ (see Chap. 6). An example of a molecule with $D_{\infty h}$ symmetry is the CO_2 molecule (see Fig. 3.5).

Selected Problems

- 3.1.** (a) Explain the symmetry operations pertaining to each class of the point group D_{3h} . You may find the stereograms on p. 51 useful.
 (b) Prove that the following irreducible representations E_1 and E_2 in the group D_5 (see Table A.24) are orthonormal.
 (c) Given the group T (see Table A.29), verify that the equality

$$\sum_j \ell_j^2 = h$$

is satisfied. What is the meaning of the two sets of characters given for the two-dimensional irreducible representation E ? Are they orthogonal to each other or are they part of the same irreducible representation?

- (d) Which symmetry operation results from multiplying the operations σ_v and σ_d in group C_{4v} ? Can you obtain this information from the character table? If so, how?

- 3.2.** Consider an A_3B_3 molecule consisting of $3A$ atoms at the corners of a regular triangle and $3B$ atoms at the corners of another regular triangle, rotated by 60° with respect to the first.

- (a) Consider the A and B atoms alternately occupy the corners of a planar regular hexagon. What are the symmetry operations of the symmetry group and what is the corresponding point group? Make a sketch of the atomic equilibrium positions for this case.
 (b) If now the A atoms are on one plane and the B atoms are on another parallel plane, what are the symmetry operations and point group?
 (c) If now all atoms in (a) are of the same species, what then are the symmetry operations of the appropriate point group, and what is this group?
 (d) Which of these groups are subgroups of the highest symmetry group? How could you design an experiment to test your symmetry group identifications?

- 3.3.** (a) What are the symmetry operations of a regular hexagon?
 (b) Find the classes. Why are not all the two-fold axes in the same class?

- (c) Find the self-conjugate subgroups, if any.
- (d) Identify the appropriate character table.
- (e) For some representative cases (two cases are sufficient), check the validity of the “Wonderful Orthogonality and Second Orthogonality Theorems” on character, using the character table in (d).

3.4. Suppose that you have the following set of characters: $\chi(E) = 4$, $\chi(\sigma_h) = 2$, $\chi(C_3) = 1$, $\chi(S_3) = -1$, $\chi(C'_2) = 0$, $\chi(\sigma_v) = 0$.

- (a) Do these characters correspond to a representation of the point group D_{3h} ? Is it irreducible?
- (b) If the representation is reducible, find the irreducible representations contained therein.
- (c) Give an example of a molecule with D_{3h} symmetry.

3.5. Consider a cube that has O_h symmetry.

- (a) Which symmetry group is obtained by squeezing the cube along one of the main diagonals?
- (b) Which symmetry group is obtained if you add mirror planes perpendicular to the main diagonals, and have a mirror plane crossing these main diagonals in the middle.

Basis Functions

In the previous chapters we have discussed symmetry elements, their matrix representations and the properties of the characters of these representations. In this discussion we saw that the matrix representations are not unique though their characters are unique. Because of the uniqueness of the characters of each irreducible representation, the characters for each group are tabulated in character tables. Also associated with each irreducible representation are “basis functions” which can be used to generate the matrices that represent the symmetry elements of a particular irreducible representation. Because of the importance of basis functions, it is customary to list the most important basis functions in the character tables.

4.1 Symmetry Operations and Basis Functions

Suppose that we have a group G with symmetry elements R and symmetry operators \hat{P}_R . We denote the irreducible representations by Γ_n , where n labels the representation. We can then define a set of basis vectors denoted by $|\Gamma_n j\rangle$. Each vector $|\Gamma_n j\rangle$ of an irreducible representation Γ_n is called a component or partner and j labels the component or partner of the representation, so that if we have a two-dimensional representation, then $j = 1, 2$. All partners collectively generate the matrix representation denoted by $D^{(\Gamma_n)}(R)$. These basis vectors relate the symmetry operator \hat{P}_R with its matrix representation $D^{(\Gamma_n)}(R)$ through the relation

$$\hat{P}_R |\Gamma_n \alpha\rangle = \sum_j D^{(\Gamma_n)}(R)_{j\alpha} |\Gamma_n j\rangle. \quad (4.1)$$

The basis vectors can be abstract vectors; a very important type of basis vector is a *basis function* which we define here as a basis vector expressed explicitly in coordinate space. *Wave functions* in quantum mechanics, which are basis functions for symmetry operators, are a special but important example of such basis functions.

In quantum mechanics, each energy eigenvalue of Schrödinger's equation is labeled according to its symmetry classification, which is specified according to an irreducible representation of a symmetry group. If the dimensionality of the representation is $j > 1$, the energy eigenvalue will correspond to a j -fold degenerate state, with j linearly independent wave-functions. The effect of the symmetry operator \hat{P}_R on one of these wave functions (e.g., the α th wave function) will generally be the formation of a linear combination of the j wave functions, as is seen in (4.1).

Like the matrix representations and the characters, the basis vectors also satisfy orthogonality relations

$$\langle \Gamma_n j | \Gamma_{n'} j' \rangle = \delta_{nn'} \delta_{jj'} , \quad (4.2)$$

and this relation is proved in Sect. 6.2 in connection with selection rules. In quantum (wave) mechanics, this orthogonality relation would be written in terms of the orthogonality for the wave functions

$$\int \psi_{n,j}^*(\mathbf{r}) \psi_{n',j'}(\mathbf{r}) d^3r = \delta_{nn'} \delta_{jj'} , \quad (4.3)$$

where the wave functions $\psi_{n,j}$ and $\psi_{n',j'}$ correspond to different energy eigenvalues (n, n') and to different components (j, j') of a particular degenerate state, and the integration is usually performed in 3D space. The orthogonality relation (4.3) allows us to generate matrices for an irreducible representation from a complete set of basis vectors, as is demonstrated in Sect. 4.2.

4.2 Use of Basis Functions to Generate Irreducible Representations

In this section we demonstrate how basis functions can be used to generate the matrices for an irreducible representation.

Multiplying (4.1) on the left by the basis vector $\langle \Gamma_{n'} j' |$ (corresponding in wave mechanics to $\psi_{n',j'}^*(\mathbf{r})$), we obtain using the orthogonality relation for basis functions (4.2):

$$\langle \Gamma_{n'} j' | \hat{P}_R | \Gamma_n \alpha \rangle = \sum_j D^{(\Gamma_n)}(R)_{j\alpha} \langle \Gamma_{n'} j' | \Gamma_n j \rangle = D^{(\Gamma_{n'})}(R)_{j'\alpha} \delta_{nn'} . \quad (4.4)$$

From (4.4) we obtain a relation between each matrix element of $D^{(\Gamma_n)}(R)_{j\alpha}$ and the effect of the symmetry operation on the basis functions:

$$D^{(\Gamma_n)}(R)_{j\alpha} = \langle \Gamma_n j | \hat{P}_R | \Gamma_n \alpha \rangle . \quad (4.5)$$

Thus by taking matrix elements of a symmetry operator \hat{P}_R between all possible partners of an irreducible representation as shown by (4.5) the matrix

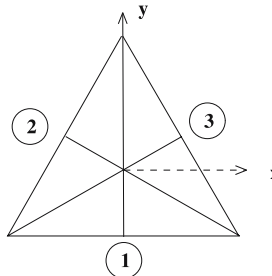


Fig. 4.1. Symmetry operations of an equilateral triangle. The notation of this diagram defines the symmetry operations in Table 4.1. Each vertex is labeled by the same number as its axis

representation $D^{T_n}(R)_{j\alpha}$ can be generated. In practice, this turns out to be the easiest way to obtain these matrix representations for the symmetry elements.

As an example of how basis vectors or basis functions can generate the matrices for an irreducible representation, consider a planar molecule with threefold symmetry such that the symmetry operations are isomorphic to those of an equilateral triangle and also isomorphic to $P(3)$ (see Chap. 1). Thus there are six symmetry operations and six operators \hat{P}_R (see Sect. 1.2). The proper point group to describe all the symmetry operations of a regular planar triangle could be $D_{3h} = D_3 \otimes \sigma_h$. However, since the triangle is a 2D object, the horizontal mirror plane may not be an important symmetry operation and we can here simplify the algebra by using the group D_3 which has six symmetry elements. Group theory tells us that the energy levels can never be more than twofold degenerate. Thus no threefold or sixfold degenerate levels can occur because the largest dimensionality of an irreducible representation of $P(3)$ is 2 (see Problem 2.2). For the one-dimensional representation Γ_1 , the operator \hat{P}_R leaves every basis vector invariant. Thus any constant such as the number one forms a suitable basis function. For many practical problems we like to express our basis functions in terms of functions of the coordinates (x, y, z) . Some explanation is needed here about the meaning of (x, y, z) as a basis function. To satisfy the orthonormality requirement, the basis functions are vectors with unit length and the matrices which represent the symmetry operations are unitary matrices. The transformation properties of the x , y , and z components of an arbitrary vector under the symmetry operations of the group are the same as those for the unit vectors x , y , and z .

In this connection it is convenient to write out a basis function table such as Table 4.1. On the top row we list the functions to be investigated; in the first column we list all the symmetry operations of the group (see Fig. 4.1 for notation). If we denote the entries in the table by $f'(x, y, z)$, then Table 4.1 can be summarized as

$$\hat{P}_R f(x, y, z) = f'(x, y, z) , \quad (4.6)$$

Table 4.1. Symmetry operations \hat{P}_R of the group of the equilateral triangle on basis functions taking (x, y, z) into (x', y', z')

| \hat{P}_R | x' | y' | z' | x'^2 | y'^2 | z'^2 |
|----------------|-------------------------------|-------------------------------|------|---|---|--------|
| $E = E$ | x | y | z | x^2 | y^2 | z^2 |
| $C_3 = F$ | $\frac{1}{2}(-x + \sqrt{3}y)$ | $\frac{1}{2}(-y - \sqrt{3}x)$ | z | $\frac{1}{4}(x^2 + 3y^2 - 2\sqrt{3}xy)$ | $\frac{1}{4}(y^2 + 3x^2 + 2\sqrt{3}xy)$ | z^2 |
| $C_3^{-1} = D$ | $\frac{1}{2}(-x - \sqrt{3}y)$ | $\frac{1}{2}(-y + \sqrt{3}x)$ | z | $\frac{1}{4}(x^2 + 3y^2 + 2\sqrt{3}xy)$ | $\frac{1}{4}(y^2 + 3x^2 - 2\sqrt{3}xy)$ | z^2 |
| $C_{2(1)} = A$ | $-x$ | y | $-z$ | x^2 | y^2 | z^2 |
| $C_{2(2)} = B$ | $\frac{1}{2}(x - \sqrt{3}y)$ | $\frac{1}{2}(-y - \sqrt{3}x)$ | $-z$ | $\frac{1}{4}(x^2 + 3y^2 - 2\sqrt{3}xy)$ | $\frac{1}{4}(y^2 + 3x^2 + 2\sqrt{3}xy)$ | z^2 |
| $C_{2(3)} = C$ | $\frac{1}{2}(x + \sqrt{3}y)$ | $\frac{1}{2}(-y + \sqrt{3}x)$ | $-z$ | $\frac{1}{4}(x^2 + 3y^2 + 2\sqrt{3}xy)$ | $\frac{1}{4}(y^2 + 3x^2 - 2\sqrt{3}xy)$ | z^2 |

where the symmetry operations \hat{P}_R label the rows. From Table 4.1 we can then write down the matrix representations for entries on each irreducible representation. In the trivial case of the identity representation, the (1×1) matrix 1 satisfies $\hat{P}_R 1 = 1$ for all \hat{P}_R so that this homomorphic representation always applies, i.e., $|\Gamma_1\rangle = 1$.

To find the basis functions for the $\Gamma_{1'}$ representation (i.e., the representation of the factor group for $P(3)$), we note that (E, D, F) leaves z invariant while (A, B, C) takes z into $-z$, so that z forms a suitable basis function for $\Gamma_{1'}$, which we write as $|\Gamma_{1'}\rangle = z$. Then application of (4.5) yields the matrices for the irreducible representation $\Gamma_{1'}$

$$\langle z|(E, D, F)|z\rangle = 1, \quad \langle z|(A, B, C)|z\rangle = -1. \quad (4.7)$$

Thus the characters (1) and (-1) for the (1×1) irreducible representations are obtained for $\Gamma_{1'}$. We note that *in the case of (1×1) representations, the characters and the representations are identical*.

To find the two-dimensional representation Γ_2 we note that all the group operations take (x, y) into (x', y') . Table 4.1 shows the results of each \hat{P}_R operator acting on x, y, z to yield x', y', z' and \hat{P}_R acting on x^2, y^2, z^2 to yield x'^2, y'^2, z'^2 . Table 4.1 thus can be used to find the matrix representation for Γ_2 by taking as basis functions $|\Gamma_2, 1\rangle = |x\rangle$ and $|\Gamma_2, 2\rangle = |y\rangle$. We now illustrate the use of Table 4.1 to generate the matrix $D^{(\Gamma_2)}(C_3^{-1}) = D$ where D is a clockwise rotation of $2\pi/3$ about the z -axis:

$$D|x\rangle = -1/2(x + \sqrt{3}y) \quad \text{yields first column of matrix representation}$$

$$D|y\rangle = 1/2(\sqrt{3}x - y) \quad \text{yields second column of matrix representation}$$

so that

$$D^{(\Gamma_2)}(C_3^{-1}) = D = \begin{pmatrix} -\frac{1}{2} & \frac{\sqrt{3}}{2} \\ -\frac{\sqrt{3}}{2} & -\frac{1}{2} \end{pmatrix}. \quad (4.8)$$

To clarify how we obtain all the matrices for the irreducible representations with Γ_2 symmetry, we repeat the operations leading to (4.8) for each of the symmetry operations \hat{P}_R . We thus obtain for the other five symmetry operations of the group \hat{P}_R using the same basis functions (x, y) and the notation of Fig. 4.1:

$$D^{(\Gamma_2)}(E) = \begin{pmatrix} 1 & 0 \\ 0 & 1 \end{pmatrix}, \quad (4.9)$$

$$D^{(\Gamma_2)}(C_2(2) = B) = \begin{pmatrix} \frac{1}{2} & -\frac{\sqrt{3}}{2} \\ -\frac{\sqrt{3}}{2} & -\frac{1}{2} \end{pmatrix}, \quad (4.10)$$

$$D^{(\Gamma_2)}(C_3 = F) = \begin{pmatrix} -\frac{1}{2} & -\frac{\sqrt{3}}{2} \\ \frac{\sqrt{3}}{2} & -\frac{1}{2} \end{pmatrix}, \quad (4.11)$$

$$D^{(\Gamma_2)}(C_2(1) = A) = \begin{pmatrix} -1 & 0 \\ 0 & 1 \end{pmatrix}, \quad (4.12)$$

$$D^{(\Gamma_2)}(C_2(3) = C) = \begin{pmatrix} \frac{1}{2} & \frac{\sqrt{3}}{2} \\ \frac{\sqrt{3}}{2} & -\frac{1}{2} \end{pmatrix}. \quad (4.13)$$

As mentioned before, x and y are both basis functions for representation Γ_2 and are called the *partners* of this irreducible representation. The number of partners is equal to the dimensionality of the representation.

In Table 4.1 we have included entries for $\hat{P}_R x^2$, $\hat{P}_R y^2$, $\hat{P}_R z^2$ and these entries are obtained as illustrated below by the operation $D = C_3^{-1}$:

$$Dx^2 = \left(-\frac{x}{2} - \frac{\sqrt{3}}{2}y \right)^2 = \left(\frac{x^2}{4} + \frac{\sqrt{3}}{2}xy + \frac{3}{4}y^2 \right), \quad (4.14)$$

$$Dy^2 = \left(-\frac{y}{2} + \frac{\sqrt{3}}{2}x \right)^2 = \left(\frac{y^2}{4} - \frac{\sqrt{3}}{2}xy + \frac{3}{4}x^2 \right), \quad (4.15)$$

$$D(x^2 + y^2) = x^2 + y^2, \quad (4.16)$$

$$\begin{aligned} D(xy) &= \left(-\frac{x}{2} - \frac{\sqrt{3}}{2}y \right) \left(-\frac{y}{2} + \frac{\sqrt{3}}{2}x \right) \\ &= \frac{1}{4} \left(-2xy - \sqrt{3}[x^2 - y^2] \right), \end{aligned} \quad (4.17)$$

$$D(x^2 - y^2) = -\frac{1}{4} \left(2[x^2 - y^2] - 4\sqrt{3}xy \right), \quad (4.18)$$

$$D(xz) = \left(-\frac{x}{2} - \frac{\sqrt{3}}{2}y \right) z, \quad (4.19)$$

$$D(yz) = \left(-\frac{y}{2} + \frac{\sqrt{3}}{2}x \right) z. \quad (4.20)$$

Using (4.1) we see that $\hat{P}_R(x^2 + y^2) = (x^2 + y^2)$ for all \hat{P}_R so that $(x^2 + y^2)$ is a basis function for Γ_1 or as we often say transforms according to the irreducible representation Γ_1 . Correspondingly $z(x^2 + y^2)$ transforms as $\Gamma_{1'}$ and z^2

transforms as Γ_1 . These transformation properties will be used extensively for many applications of group theory. It is found that many important basis functions are given directly in the published character tables. Like the matrix representations, the basis functions are not unique. However, corresponding to a given set of basis functions, the matrix representation which is generated by these basis functions will be unique.

As before, the characters for a given representation are found by taking the sum of the diagonal elements of each matrix in a given representation:

$$\chi^{(\Gamma_n)}(R) \equiv \text{tr } D^{(\Gamma_n)}(R) = \sum_j D^{(\Gamma_n)}(R)_{jj} = \sum_j \langle \Gamma_n j | \hat{P}_R | \Gamma_n j \rangle. \quad (4.21)$$

Since the trace is invariant under a similarity transformation, the character is independent of the particular choice of basis functions or matrix representations.

If instead of a basis function (which generates irreducible representations) we use an arbitrary function f , then a reducible representation will result, in general. We can express an arbitrary function as a linear combination of the basis functions. For example, any linear function of x, y, z such as $f(x, y, z)$ can be expressed in terms of linear combinations of basis vectors x, y, z and likewise any quadratic function is expressed in terms of quadratic basis functions which transform as irreducible representations of the group. For example for the group $P(3)$ (see Table 4.1), quadratic forms which serve as basis functions are $(x^2 + y^2)$ and z^2 which both transform as Γ_1 ; z transforms as Γ_1' ; (xz, yz) and $(xy, x^2 - y^2)$ both transform as Γ_2 .

If we now inspect the character table $D_3(32)$ found in Table A.12 (and reproduced below in Table 4.2), we find that these basis functions are listed in this character table. The basis functions labeled R_α represent the angular momentum component around axis α (e.g., $R_x = y p_z - z p_y$). For the two dimensional irreducible representations both partners of the basis functions are listed, for example (xz, yz) and $(x^2 - y^2, xy)$, etc. The reason why (x, y, z) and (R_x, R_y, R_z) often transform as different irreducible representations (not the case for the group $D_3(32)$) is that x, y, z transforms as a radial vector (such as coordinate, momentum) while R_x, R_y, R_z transforms as an axial vector (such as angular momentum $\mathbf{r} \times \mathbf{p}$).

Table 4.2. Character Table for Group D_3 (rhombohedral)

| $D_3(32)$ | | | E | $2C_3$ | $3C'_2$ |
|-------------------|--------------|-------|-----|--------|---------|
| $x^2 + y^2, z^2$ | | A_1 | 1 | 1 | 1 |
| (xz, yz) | R_z, z | A_2 | 1 | 1 | -1 |
| $(x^2 - y^2, xy)$ | (x, y) | E | 2 | -1 | 0 |
| | (R_x, R_y) | | | | |

4.3 Projection Operators $\hat{P}_{kl}^{(\Gamma_n)}$

The previous discussion of basis vectors assumed that we already knew how to write down the basis vectors. In many cases, representative basis functions are tabulated in the character tables. However, suppose that we have to find basis functions for the following cases:

- (a) An irreducible representation for which no basis functions are listed in the character table; or
- (b) An arbitrary function.

In such cases the basis functions can often be found using *projection operators* \hat{P}_{kl} , not to be confused with the symmetry operators \hat{P}_R . We define the projection operator $\hat{P}_{kl}^{(\Gamma_n)}$ as transforming one basis vector $|\Gamma_n \ell\rangle$ into another basis vector $|\Gamma_n k\rangle$ of the same irreducible representation Γ_n :

$$\hat{P}_{kl}^{(\Gamma_n)} |\Gamma_n \ell\rangle \equiv |\Gamma_n k\rangle . \quad (4.22)$$

The utility of projection operators is mainly to project out basis functions for a given partner of a given irreducible representation from an arbitrary function. The discussion of this topic focuses on the following issues:

- (a) The relation of the projection operator to symmetry operators of the group and to the matrix representation of these symmetry operators for an irreducible representation (see Sect. 4.4).
- (b) The effect of projection operators on an arbitrary function (see Sect. 4.5).

As an example, we illustrate in Sect. 4.6 how to find basis functions from an arbitrary function for the case of the group of the equilateral triangle (see Sect. 4.2).

4.4 Derivation of an Explicit Expression for $\hat{P}_{kl}^{(\Gamma_n)}$

In this section we find an explicit expression for the projection operators $\hat{P}_{kl}^{(\Gamma_n)}$ by considering the relation of the projection operator to symmetry operators of the group. We will find that the coefficients of this expression give the matrix representations of each of the symmetry elements.

Let the projection operator $\hat{P}_{kl}^{(\Gamma_n)}$ be written as a linear combination of the symmetry operators \hat{P}_R :

$$\hat{P}_{kl}^{(\Gamma_n)} = \sum_R A_{kl}(R) \hat{P}_R , \quad (4.23)$$

where the $A_{kl}(R)$ are arbitrary expansion coefficients to be determined. Substitution of (4.23) into (4.22) yields

$$\hat{P}_{k\ell}^{(\Gamma_n)}|\Gamma_n\ell\rangle \equiv |\Gamma_n k\rangle = \sum_R A_{k\ell}(R) \hat{P}_R |\Gamma_n\ell\rangle . \quad (4.24)$$

Multiply (4.24) on the left by $\langle \Gamma_n k |$ to yield

$$\langle \Gamma_n k | \Gamma_n k \rangle = 1 = \sum_R A_{k\ell}(R) \underbrace{\langle \Gamma_n k | \hat{P}_R | \Gamma_n \ell \rangle}_{D^{(\Gamma_n)}(R)_{k\ell}} . \quad (4.25)$$

But the Wonderful Orthogonality Theorem (2.51) specifies that

$$\sum_R D^{(\Gamma_n)}(R)_{k\ell}^* D^{(\Gamma_n)}(R)_{k\ell} = \frac{h}{\ell_n} , \quad (4.26)$$

where h is the number of symmetry operators in the group and ℓ_n is the dimensionality of the irreducible representation Γ_n , so that we can identify $A_{k\ell}(R)$ with the matrix element of the representation for the symmetry element R :

$$A_{k\ell}(R) = \frac{\ell_n}{h} D^{(\Gamma_n)}(R)_{k\ell}^* . \quad (4.27)$$

Thus the projection operator is explicitly given in terms of the symmetry operators of the group by the relation:

$$\hat{P}_{k\ell}^{(\Gamma_n)} = \frac{\ell_n}{h} \sum_R D^{(\Gamma_n)}(R)_{k\ell}^* \hat{P}_R . \quad (4.28)$$

From the explicit form for $\hat{P}_{k\ell}^{(\Gamma_n)}$ in (4.28) and from (4.22) we see how to find the partners of an irreducible representation Γ_n from any single known basis vector, provided that the matrix representation for all the symmetry operators $D^{(\Gamma_n)}(R)$ is known.

As a special case, the projection operator $\hat{P}_{kk}^{(\Gamma_n)}$ transforms $|\Gamma_n k\rangle$ into itself and can be used to check that $|\Gamma_n k\rangle$ is indeed a basis function. We note that the relation of $\hat{P}_{kk}^{(\Gamma_n)}$ to the symmetry operators \hat{P}_R involves only the *diagonal elements of the matrix representations* (though not the trace):

$$\hat{P}_{kk}^{(\Gamma_n)} = \frac{\ell_n}{h} \sum_R D^{(\Gamma_n)}(R)_{kk}^* \hat{P}_R , \quad (4.29)$$

where

$$\hat{P}_{kk}^{(\Gamma_n)}|\Gamma_n k\rangle \equiv |\Gamma_n k\rangle . \quad (4.30)$$

4.5 The Effect of Projection Operations on an Arbitrary Function

The projection operators $\hat{P}_{kk}^{(\Gamma_n)}$ defined in (4.30) are of special importance because they can project the k th partner of irreducible representation Γ_n

from an arbitrary function. Any arbitrary function F can be written as a linear combination of a complete set of basis functions $|\Gamma_{n'}j'\rangle$:

$$F = \sum_{\Gamma_{n'}} \sum_{j'} f_{j'}^{(\Gamma_{n'})} |\Gamma_{n'}j'\rangle . \quad (4.31)$$

We can then write from (4.29):

$$\hat{P}_{kk}^{(\Gamma_n)} F = \frac{\ell_n}{h} \sum_R D^{(\Gamma_n)}(R)_{kk}^* \hat{P}_R F \quad (4.32)$$

and substitution of (4.31) into (4.32) then yields

$$\hat{P}_{kk}^{(\Gamma_n)} F = \frac{\ell_n}{h} \sum_R \sum_{\Gamma_{n'}} \sum_{j'} f_{j'}^{(\Gamma_{n'})} D^{(\Gamma_n)}(R)_{kk}^* \hat{P}_R |\Gamma_{n'}j'\rangle . \quad (4.33)$$

But substitution of (4.1) into (4.33) and use of the Wonderful Orthogonality Theorem (2.51):

$$\sum_R D^{(\Gamma_{n'})}(R)_{jj'} D^{(\Gamma_n)}(R)_{kk}^* = \frac{h}{\ell_n} \delta_{\Gamma_n \Gamma_{n'}} \delta_{jk} \delta_{j'k} \quad (4.34)$$

yields

$$\hat{P}_{kk}^{(\Gamma_n)} F = f_k^{(\Gamma_n)} |\Gamma_n k\rangle , \quad (4.35)$$

where

$$\hat{P}_{kk}^{(\Gamma_n)} = \frac{\ell_n}{h} \sum_R D^{(\Gamma_n)}(R)_{kk}^* \hat{P}_R . \quad (4.36)$$

We note that the projection operator does not yield normalized basis functions. One strategy to find basis functions is to start with an arbitrary function F .

- (a) We then use $\hat{P}_{kk}^{(\Gamma_n)}$ to project out one basis function $|\Gamma_n k\rangle$.
- (b) We can then use the projection operator $\hat{P}_{k\ell}^{(\Gamma_n)}$ to project out all other partners $|\Gamma_n \ell\rangle$ orthogonal to $|\Gamma_n k\rangle$ in irreducible representation Γ_n . Or alternatively we can use $\hat{P}_{\ell\ell}^{(\Gamma_n)}$ to project out each of the partners ℓ of the representation, whichever method works most easily in a given case.

If we do not know the explicit representations $D_{k\ell}^{(\Gamma_n)}(R)^*$, but only know the characters, then we can still project out basis functions which transform according to the irreducible representations (using the argument given in the next paragraph), though we cannot in this case project out specific partners but only linear combinations of the partners of these irreducible representations.

If we only know the characters of an irreducible representation Γ_n , we define the projection operator for this irreducible representation as $\hat{P}^{(\Gamma_n)}$:

$$\hat{P}^{(\Gamma_n)} \equiv \sum_k \hat{P}_{kk}^{(\Gamma_n)} = \frac{\ell_n}{h} \sum_R \sum_k D^{(\Gamma_n)}(R)_{kk}^* \hat{P}_R , \quad (4.37)$$

so that

$$\hat{P}^{(\Gamma_n)} = \frac{\ell_n}{h} \sum_R \chi^{(\Gamma_n)}(R)^* \hat{P}_R \quad (4.38)$$

and using (4.35) we then obtain

$$\hat{P}^{(\Gamma_n)} F = \sum_k \hat{P}_{kk}^{(\Gamma_n)} F = \sum_k f_k^{(\Gamma_n)} |\Gamma_n k\rangle , \quad (4.39)$$

which projects out a function transforming as Γ_n but not a specific partner of Γ_n .

In dealing with physical problems it is useful to use physical insight in guessing at an appropriate “arbitrary function” to initiate this process for finding the basis functions and matrix representations for specific problems. This is the strategy to pursue when you do not know either the matrix representations or the basis functions *a priori*.

4.6 Linear Combinations of Atomic Orbitals for Three Equivalent Atoms at the Corners of an Equilateral Triangle

As an example of finding basis functions from an arbitrary function, we here consider forming linear combinations of atomic orbitals which transform as irreducible representations of the symmetry group.

In many of the applications that we will be making of group theory to solid-state physics, we will have equivalent atoms at different sites. We use the symmetry operations of the group to show which irreducible representations result when the equivalent atoms transform into each other under the symmetry operations of the group. The discussion of projection operators of an arbitrary function applies to this very important case.

As an example of this application, suppose that we have three equivalent atoms at the three corners of an equilateral triangle (see Fig. 4.2) and that each atom is in the same spherically symmetric ground state described by a wave function $\psi_0(\mathbf{r}_i)$, where the subscript i is a site index, which can apply to any of the three sites. As a short-hand notation for $\psi_0(\mathbf{r}_a)$, $\psi_0(\mathbf{r}_b)$, $\psi_0(\mathbf{r}_c)$ we will here use a, b, c .

We now want to combine these atomic orbitals to make a molecular orbital that transforms according to the irreducible representations of the group. We will see that only the Γ_1 and Γ_2 irreducible representations are contained in the linear combination of atomic orbitals for a, b, c . This makes sense since we have

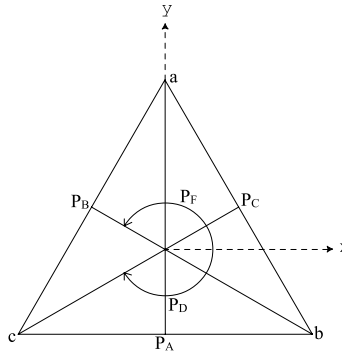


Fig. 4.2. Equilateral triangle and arbitrary functions a, b, c for atomic orbitals at corners of an equilateral triangle, defining the notation used in Sect. 4.6

three atomic orbitals which split into a nondegenerate and a two-dimensional representation in trigonal symmetry through the symmetry operations \hat{P}_R on the equivalent site functions a, b, c .

To generate the proper linear combination of atomic orbitals that transform as irreducible representations of the symmetry group, we use the results on the projection operator to find out which irreducible representations are contained in the function F . According to the above discussion, we can project out a basis function for representation Γ_n by considering the action of $\hat{P}_{kk}^{(\Gamma_n)}$ on one of the atomic orbitals, as for example orbital $F = a$:

$$\hat{P}_{kk}^{(\Gamma_n)} a = \frac{\ell_n}{h} \sum_R D^{(\Gamma_n)}(R)_{kk}^* \hat{P}_R a = f_k^{(\Gamma_n)} |\Gamma_n k\rangle , \quad (4.40)$$

in which we have used the definition for $\hat{P}_{kk}^{(\Gamma_n)}$ given by (4.35) and the expression for $\hat{P}_{kk}^{(\Gamma_n)}$ given by (4.36). If the representation Γ_n is one-dimensional, then we can obtain $D^{(\Gamma_n)}(R)$ directly from the character table, and (4.40) then becomes

$$\hat{P}^{(\Gamma_n)} a = \frac{\ell_n}{h} \sum_R \chi^{(\Gamma_n)}(R)^* \hat{P}_R a = f^{(\Gamma_n)} |\Gamma_n\rangle . \quad (4.41)$$

For the appropriate symmetry operators for this problem we refer to Sect. 1.2 where we have defined: $E \equiv$ identity; $(A, B, C) \equiv \pi$ rotations about twofold axes in the plane of triangle; $(D, F) \equiv 2\pi/3$ rotations about the threefold axis \perp to the plane of the triangle. These symmetry operations are also indicated in Fig. 4.2.

For the identity representation Γ_1 the characters and matrix representations are all unity so that

$$\begin{aligned}
\hat{P}^{(\Gamma_1)}a &= \frac{1}{6}(\hat{P}_Ea + \hat{P}_Aa + \hat{P}_Ba + \hat{P}_Ca + \hat{P}_Da + \hat{P}_Fa) \\
&= \frac{1}{6}(a + a + c + b + b + c) \\
&= \frac{1}{3}(a + b + c) ,
\end{aligned} \tag{4.42}$$

a result which is intuitively obvious. Each atom site must contribute equally to the perfectly symmetrical molecular representation Γ_1 . This example illustrates how starting with an arbitrary function a (or $\psi(\mathbf{r}_a)$) we have found a linear combination that transforms as Γ_1 . Likewise, we obtain the same result by selecting b or c as the arbitrary function

$$\hat{P}^{(\Gamma_1)}b = \hat{P}^{(\Gamma_1)}c = \frac{1}{3}(a + b + c) . \tag{4.43}$$

We now apply a similar analysis for representation $\Gamma_{1'}$ to illustrate another important point. In this case the matrix representations and characters are +1 for (E, D, F) , and -1 for (A, B, C) . Thus

$$\begin{aligned}
\hat{P}^{(\Gamma_{1'})}a &= \frac{1}{6}(\hat{P}_Ea - \hat{P}_Aa - \hat{P}_Ba - \hat{P}_Ca + \hat{P}_Da + \hat{P}_Fa) \\
&= \frac{1}{6}(a - a - c - b + b + c) = 0 ,
\end{aligned} \tag{4.44}$$

which states that no molecular orbital with $\Gamma_{1'}$ symmetry can be made by taking a linear combination of the a, b, c orbitals. This is verified by considering

$$\hat{P}^{(\Gamma_{1'})}b = \hat{P}^{(\Gamma_{1'})}c = 0 . \tag{4.45}$$

The same approach can be used to obtain the two-dimensional irreducible representations, but it does not result in a simple set of linear combinations of atomic orbitals with a set of unitary matrices for the representation of the symmetry operations of the group (see Problem 4.6).

To obtain a symmetrical set of basis functions for higher dimensional representations it is useful to start with an arbitrary function that takes account of the dominant symmetry operations of the group (e.g., a threefold rotation \hat{P}_D)

$$|\Gamma_2\alpha\rangle = a + \omega b + \omega^2 c , \tag{4.46}$$

where $\omega = e^{2\pi i/3}$ and we note here from symmetry that $\hat{P}_D|\Gamma_2\alpha\rangle = \omega^2|\Gamma_2\alpha\rangle$ and $\hat{P}_F|\Gamma_2\alpha\rangle = \omega|\Gamma_2\alpha\rangle$.

Thus $|\Gamma_2\alpha\rangle$ is already a basis function. Clearly the partner of $|\Gamma_2\alpha\rangle$ is $|\Gamma_2\alpha\rangle^*$ since $\hat{P}_D|\Gamma_2\alpha\rangle^* = \hat{P}_D(a + \omega^2 b + \omega c) = \omega(a + \omega^2 b + \omega c) = \omega|\Gamma_2\beta\rangle$, where we have used the notation (α, β) to denote the two partners of the Γ_2 representation:

$$|\Gamma_2\alpha\rangle = a + \omega b + \omega^2 c , \quad |\Gamma_2\beta\rangle = a + \omega^2 b + \omega c . \tag{4.47}$$

The two partners in (4.47) are complex conjugates of each other. Corresponding to these basis functions, the matrix representation for each of the group elements is simple and symmetrical

$$\begin{aligned} E &= \begin{pmatrix} 1 & 0 \\ 0 & 1 \end{pmatrix} & A &= \begin{pmatrix} 0 & 1 \\ 1 & 0 \end{pmatrix} & B &= \begin{pmatrix} 0 & \omega^2 \\ \omega & 0 \end{pmatrix} \\ C &= \begin{pmatrix} 0 & \omega \\ \omega^2 & 0 \end{pmatrix} & D &= \begin{pmatrix} \omega^2 & 0 \\ 0 & \omega \end{pmatrix} & F &= \begin{pmatrix} \omega & 0 \\ 0 & \omega^2 \end{pmatrix}. \end{aligned} \quad (4.48)$$

By inspection, the representation given by (4.48) is *unitary*.

4.7 The Application of Group Theory to Quantum Mechanics

Suppose E_n is a k -fold degenerate level of the group of Schrödinger's equation (see Sect. 1.8). Then any linear combination of the eigenfunctions $\psi_{n1}, \psi_{n2}, \dots, \psi_{nk}$ is also a solution of Schrödinger's equation. We can write the operation $\hat{P}_R \psi_{n\alpha}$ on one of these eigenfunctions as

$$\hat{P}_R \psi_{n\alpha} = \sum_j D^{(n)}(R)_{j\alpha} \psi_{nj}, \quad (4.49)$$

where $D^{(n)}(R)_{j\alpha}$ is an irreducible matrix which defines the linear combination, n labels the energy index, α labels the degeneracy index.

Equation (4.49) is identical with the more general equation for a basis function (4.1) where the states $|\Gamma_n \alpha\rangle$ and $|\Gamma_n j\rangle$ are written symbolically rather than explicitly as they are in (4.49).

We show here that the matrices $D^{(n)}(R)$ form an ℓ_n dimensional irreducible representation of the group of Schrödinger's equation where ℓ_n denotes the degeneracy of the energy eigenvalue E_n . Let R and S be two symmetry operations which commute with the Hamiltonian and let RS be their product. Then from (4.49) we can write

$$\begin{aligned} \hat{P}_{RS} \psi_{n\alpha} &= \hat{P}_R \hat{P}_S \psi_{n\alpha} = \hat{P}_R \sum_j D^{(n)}(S)_{j\alpha} \psi_{nj} \\ &= \sum_{jk} D^{(n)}(R)_{kj} D^{(n)}(S)_{j\alpha} \psi_{nk} = \sum_k \left[D^{(n)}(R) D^{(n)}(S) \right]_{k\alpha} \psi_{nk} \end{aligned} \quad (4.50)$$

after carrying out the indicated matrix multiplication. But by definition, the product operator RS can be written as

$$\hat{P}_{RS} \psi_{n\alpha} = \sum_k D^{(n)}(RS)_{k\alpha} \psi_{nk}, \quad (4.51)$$

so that

$$D^{(n)}(RS) = D^{(n)}(R)D^{(n)}(S) \quad (4.52)$$

and the matrices $D^{(n)}(R)$ form a representation for the group. We label quantum mechanical states typically by a state vector (basis vector) $|\alpha, \Gamma_n, j\rangle$ where Γ_n labels the irreducible representation, j the component or partner of the irreducible representation, and α labels the other quantum numbers that do not involve the symmetry of the \hat{P}_R operators.

The dimension of the irreducible representation is equal to the degeneracy of the eigenvalue E_n . The representation $D^{(n)}(R)$ generated by $\hat{P}_R \psi_{n\alpha}$ is an irreducible representation if all the ψ_{nk} correspond to a single eigenvalue E_n . For otherwise it would be possible to form linear combinations of the type

$$\underbrace{\psi'_{n1}, \psi'_{n2}, \dots, \psi'_{ns}}_{\text{subset 1}} \underbrace{\psi'_{n,s+1}, \dots, \psi'_{nk}}_{\text{subset 2}}, \quad (4.53)$$

whereby the linear combinations within the subsets would transform amongst themselves. But if this happened, then the eigenvalues for the two subsets would be different, except for the rare case of accidental degeneracy. Thus, the transformation matrices for the symmetry operations form an *irreducible* representation for the group of Schrödinger's equation.

The rest of the book discusses several applications of the group theory introduced up to this point to problems of solid state physics. It is convenient at this point to classify the ways that group theory is used to solve quantum mechanical problems. Group theory is used both to obtain exact results and in applications of perturbation theory. In the category of exact results, we have as examples:

- (a) Irreducible representations of the symmetry group of Schrödinger's equation *label the states and specify their degeneracies* (e.g., an atom in a crystal field).
- (b) Group theory is useful in following the changes in the degeneracies of the energy levels as the *symmetry* is lowered. This case can be thought of in terms of a Hamiltonian

$$\mathcal{H} = \mathcal{H}_0 + \mathcal{H}', \quad (4.54)$$

where \mathcal{H}_0 has high symmetry corresponding to the group G , and \mathcal{H}' is a perturbation having lower symmetry and corresponding to a group G' of lower order (fewer symmetry elements). Normally group G' is a subgroup of group G . Here we find first which symmetry operations of G are contained in G' ; the irreducible representations of G' label the states of the lower symmetry situation exactly. In going to lower symmetry we want to know what happens to the degeneracy of the various states in the initial higher symmetry situation (see Fig. 4.3). We say that in general the irreducible representation of the *higher symmetry group forms reducible representations for the lower symmetry group*.

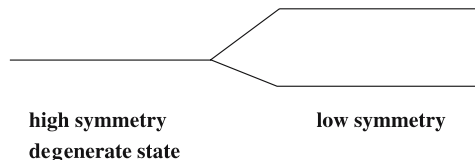


Fig. 4.3. The effect of lowering the symmetry often results in a lowering of the degeneracy of degenerate energy states

The degeneracy of states may either be lowered as the symmetry is lowered or the degeneracy may be unchanged. Group theory tells us exactly what happens to these degeneracies. We are also interested in finding the basis functions for the lower symmetry group G' . For those states where the degeneracy is unchanged, the basis functions are generally unchanged. When the degeneracy is reduced, then by proper choice of the form of the partners, the basis functions for the degenerate state will also be basis functions for the states in the lower symmetry situation.

An example of going from higher to lower symmetry is the following: If (x, y, z) are basis functions for a three-dimensional representation in the cubic group, then lowering the symmetry to tetragonal with z as the main symmetry direction will give a two-dimensional representation with basis functions (x, y) and a one-dimensional representation with basis function z . However, if the symmetry is lowered to tetragonal along a z' direction (different from z), then linear combinations of (x, y, z) must be taken to obtain a vector along z' and two others that are mutually orthogonal. The lowering of degeneracy is a very general topic and will enter the discussion of many applications of group theory (see Chap. 5).

- (c) Group theory is helpful in finding the correct *linear combination of wavefunctions* that is needed to diagonalize the Hamiltonian. This procedure involves the concept of equivalence which applies to situations where equivalent atoms sit at symmetrically equivalent sites (see Chap. 7).

Selected Problems

- 4.1. (a) What are the matrix representations for $(2xy, x^2 - y^2)$ and (R_x, R_y) in the point group D_3 ?
- (b) Using the results in (a), find the unitary transformation which transforms the matrices for the representation corresponding to the basis functions $(xy, x^2 - y^2)$ into the representation corresponding to the basis functions (x, y) .
- (c) Using projection operators, check that xy forms a proper basis function of the two-dimensional irreducible representation Γ_2 in point group D_3 . Using the matrix representation found in (a) and projection operators, find the partner of xy .

- (d) Using the basis functions in the character table for D_{3h} , write a set of (2×2) matrices for the two two-dimensional representations E' and E'' . Give some examples of molecular clusters that require D_{3h} symmetry.

- 4.2.** (a) Explain the Hermann–Mangun notation $T_d(\bar{4}3\ m)$.
 (b) What are the irreducible representations and partners of the following basis functions in T_d symmetry? (i) $\omega x^2 + \omega^2 y^2 + z^2$, where $\omega = \exp(2\pi i/3)$; (ii) xyz ; and (iii) x^2yz .
 (c) Using the results of (b) and the basis functions in the character table for the point group T_d , give one set of basis functions for each irreducible representation of T_d .
 (d) Using the basis function $\omega x^2 + \omega^2 y^2 + z^2$ and its partner (or partners), find the matrix for an S_4 rotation about the x -axis in this irreducible representation.

- 4.3.** Consider the cubic group O_h . Find the basis functions for all the symmetric combinations of cubic forms (x, y, z) and give their irreducible representations for the point group O_h .

- 4.4.** Consider the hypothetical molecule CH_4 (Fig. 4.4) where the four H atoms are at the corners of a square $(\pm a, 0, 0)$ and $(0, \pm a, 0)$ while the C atom is at $(0, 0, z)$, where $z < a$. What are the symmetry elements?

- (a) Identify the appropriate character table.
 (b) Using the basis functions in the character table, write down a set of (2×2) matrices which provide a representation for the two-dimensional irreducible representation of this group.
 (c) Find the four linear combinations of the four H orbitals (assume identical s-functions at each H site) that transform as the irreducible representations of the group. What are their symmetry types?
 (d) What are the basis functions that generate the irreducible representations.
 (e) Check that xz forms a proper basis function for the two-dimensional representation of this point group and find its partner.
 (f) What are the irreducible representations and partners of the following basis functions in the point group (assuming that the four hydrogens lie in the xy plane): (i) xyz , (ii) x^2y , (iii) x^2z , (iv) $x + iy$.
 (g) What additional symmetry operations result in the limit that all H atoms are coplanar with atom C? What is now the appropriate group and character table? (The stereograms in Figure 3.2 may be useful.)

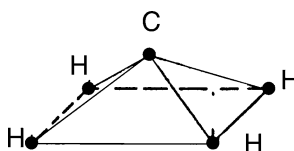
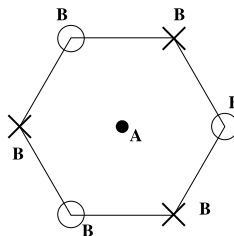


Fig. 4.4. Molecule CH_4

**Fig. 4.5.** Molecule AB_6

4.5. Consider a molecule AB_6 (Fig. 4.5) where the A atom lies in the central plane and three B atoms indicated by “○” lie in a plane at a distance c above the central plane and the B atoms indicated by “ \times ” lie in a plane below the central plane at a distance $-c'$. When projected onto the central plane, all B atoms occupy the corners of a hexagon.

- Find the symmetry elements and classes.
- Construct the character table. To which point group (Chap. 3) does this molecule correspond? How many irreducible representations are there? How many are one-dimensional and how many are of higher dimensionality?
- Using the basis functions in the character table for this point group, find a set of matrices for each irreducible representation of the group.
- Find the linear combinations of the six s-orbitals of the B atoms that transform as the irreducible representations of the group.
- What additional symmetry operations result in the limit that all B atoms are coplanar with A? What is now the appropriate group and character table for this more symmetric molecule?
- Indicate which stereograms in Fig. 3.2 are appropriate for the case where the B atoms are not coplanar with A and the case where they are coplanar.

4.6. Consider the linear combinations of atomic orbitals on an equilateral triangle (Sect. 4.6).

- Generate the basis functions $|\Gamma_2 1\rangle$ and $|\Gamma_2 2\rangle$ for the linear combination of atomic orbitals for the Γ_2 irreducible representation obtained by using the projection operator acting on one of the atomic orbitals $\hat{P}_{11}^{(\Gamma_2)} a$ and $\hat{P}_{22}^{(\Gamma_2)} a$.
- Show that the resulting basis functions $|\Gamma_2 1\rangle$ and $|\Gamma_2 2\rangle$ lead to matrix representations that are not unitary.
- Show that the $|\Gamma_2 1\rangle$ and $|\Gamma_2 2\rangle$ thus obtained can be expressed in terms of the basis functions $|\Gamma_2 \alpha\rangle$ and $|\Gamma_2 \beta\rangle$ given in (4.47).

4.7. The aim of this problem is to give the reader experience in going from a group with higher symmetry to a group with lower symmetry and to give

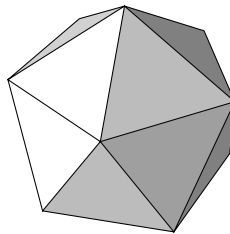


Fig. 4.6. Hypothetical XH_{12} molecule where the atom X is at the center of a regular dodecahedron

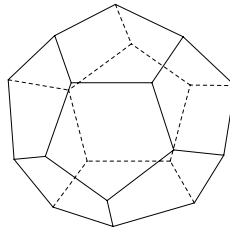


Fig. 4.7. Hypothetical XH_{12} molecule where the atom X is at the center of a regular truncated icosahedron

some experience in working with groups with icosahedral and fivefold symmetry. Consider the hypothetical XH_{12} molecule (see Fig. 4.6) which has I_h icosahedral symmetry, and the X atom is at the center. The lines connecting the X and H atoms are fivefold axes.

- Suppose that we stretch the XH_{12} molecule along one of the fivefold axes. What are the resulting symmetry elements of the stretched molecule?
- What is the appropriate point group for the stretched molecule?
- Consider the G_u and H_g irreducible representations of group I_h as a reducible representation of the lower symmetry group. Find the symmetries of the lower symmetry group that were contained in a fourfold energy level that transforms as G_u and in a fivefold level that transforms as H_g in the I_h group. Assuming the basis functions given in the character table for the I_h point group, give the corresponding basis functions for each of the levels in the multiplets for the stretched molecule.
- Suppose that the symmetry of the XH_{12} molecule is described in terms of hydrogen atoms placed at the center of each pentagon of a regular dodecahedron (see Fig. 4.7). A regular dodecahedron has 12 regular pentagonal faces, 20 vertices and 30 edges. What are the symmetry classes for the regular dodecahedron. Suppose that the XH_{12} molecule is stretched along one of its fivefold axes as in (a). What are the symmetry elements of the stretched XH_{12} molecule when viewed from the point of view of a distortion from dodecahedral symmetry?

Part II

Introductory Application to Quantum Systems

Splitting of Atomic Orbitals in a Crystal Potential

This is the first of several chapters aimed at presenting some *general applications* of group theory while further developing theoretical concepts and amplifying on those given in the first four chapters. The first application of group theory is made to the splitting of atomic energy levels when the atom is placed in a crystal potential, because of the relative simplicity of this application and because it provides a good example of going from higher to lower symmetry, a procedure used very frequently in applications of group theory to solid state physics. In this chapter we also consider irreducible representations of the full rotation group.

5.1 Introduction

The study of crystal field theory is relevant for physics and engineering applications in situations where it is desirable to exploit the sharp, discrete energy levels that are characteristic of atomic systems together with the larger atomic densities that are typical of solids. As an example, consider the variety of powerful lasers whose operation is based on the population inversion of impurity levels of rare earth ions in a transparent host crystal. The energy levels of an electron moving in the field of an ion embedded in such a solid are approximately the same as for an electron moving in the field of a free ion. Thus the interaction between the ion and the host crystal can be treated in perturbation theory. Group theory plays a major role in finding the degeneracy and the symmetry types of the electronic levels in the crystalline field. The topic of crystal field splittings has found many important applications such as in the use of erbium-doped silica-based optical glass fiber amplifiers in optical communications systems. Such applications provide motivation for understanding the splitting of the energy levels of an impurity ion in a crystal field.

In this chapter the point group symmetry of an impurity ion in a crystal is presented. The crystal potential V_{xtal} determines the point group symmetry.

Following the discussion on the form of the crystal potential, some properties of the full rotation group are given, most importantly the characters $\chi^{(\ell)}(\alpha)$ for rotations through an angle α and $\chi^{(\ell)}(i)$ for inversions. Irreducible representations of the full

rotation group are generally found to be reducible representations of a point group of lower symmetry which is a subgroup of the higher symmetry group. If the representation is reducible, then crystal field splittings of the energy levels occur. If, however, the representation is irreducible, then no crystal field splittings occur. Examples of each type of representation are presented. We focus explicitly on giving examples of going from higher to lower symmetry. In so doing, we consider the

- (a) Splitting of the energy levels,
- (b) Symmetry types of the split levels,
- (c) Choice of basis functions to bring the Hamiltonian \mathcal{H} into block diagonal form. Spherical symmetry results in spherical harmonics $Y_{\ell m}(\theta, \phi)$ for basis functions. Proper linear combinations of the spherical harmonics $Y_{\ell m}(\theta, \phi)$ are taken to make appropriate basis functions for the point group of lower symmetry.

In crystal field theory we write down the Hamiltonian for the impurity ion in a crystalline solid as

$$\mathcal{H} = \sum_i \left\{ \frac{p_i^2}{2m} - \frac{Ze^2}{r_{i\mu}} + \sum_j \frac{e^2}{r_{ij}} + \sum_j \xi_{ij} \boldsymbol{\ell}_i \cdot \boldsymbol{s}_j + \gamma_{i\mu} \boldsymbol{j}_i \cdot \boldsymbol{I}_\mu \right\} + V_{\text{xtal}}, \quad (5.1)$$

where the first term is the kinetic energy of the electrons associated with the ion, the second term represents the Coulomb attraction of the electrons of the ion to their nucleus, the third term represents the mutual Coulomb repulsion of the electrons associated with the impurity ion, and the sum on j denotes a sum on pairs of electrons. These three quantities are denoted by \mathcal{H}_0 the electronic Hamiltonian of the free atom without spin-orbit interaction. \mathcal{H}_0 is the dominant term in the total Hamiltonian \mathcal{H} . The remaining terms are treated in perturbation theory in some order. Here $\xi_{ij} \boldsymbol{\ell}_i \cdot \boldsymbol{s}_j$ is the spin-orbit interaction of electrons on the impurity ion and $\gamma_{i\mu} \boldsymbol{j}_i \cdot \boldsymbol{I}_\mu$ is the hyperfine interaction between the electrons on the ion and the nuclear spin. The perturbing crystal potential V_{xtal} of the host ions acts on the impurity ion and lowers its spherical symmetry.

Because of the various perturbation terms appearing in (5.1), it is important to distinguish the two limiting cases of weak and strong crystal fields.

- (a) *Weak field case.* In this case, the perturbing crystal field V_{xtal} is considered to be small compared with the spin-orbit interaction. In this limit, we find the energy levels of the free impurity ion with spin-orbit interaction and at this point we consider the crystal field as an additional perturbation. These approximations are appropriate to rare earth ions in ionic host

crystals. We will deal with the group theoretical aspects of this case in Chap. 14, after we have learned how to deal with the spin on the electron in the context of group theory.

- (b) *Strong field case.* In this case, the perturbing crystal field V_{xtal} is strong compared with the spin-orbit interaction. We now consider V_{xtal} as the major perturbation on the energy levels of \mathcal{H}_0 . Examples of the strong crystal field case are transition metal ions (Fe, Ni, Co, Cr, etc.) in a host crystal. It is this limit that we will consider first, and is the focus of this chapter.

We note that the crystal potential V_{xtal} lowers the full rotational symmetry of the free atom to cause level splittings relative to those of the free atom.

We now consider in Sect. 5.2 some of the fundamental properties of the full rotation group. These results are liberally used in later chapters.

5.2 Characters for the Full Rotation Group

The free atom has full rotational symmetry and the number of symmetry operations which commute with the Hamiltonian is infinite. That is, all C_ϕ rotations about any axis are symmetry operations of the full rotation group. We are not going to discuss infinite or continuous groups in any detail, but we will adopt results that we use frequently in quantum mechanics without rigorous proofs.

Let us then recall the form of the spherical harmonics $Y_{\ell m}(\theta, \phi)$ which are the basis functions for the full rotation group:

$$Y_{\ell m}(\theta, \phi) = \left[\frac{2\ell + 1}{4\pi} \frac{(\ell - |m|)!}{(\ell + |m|)!} \right]^{1/2} P_\ell^m(\cos \theta) e^{im\phi}, \quad (5.2)$$

in which

$$Y_{\ell, -m}(\theta, \phi) = (-1)^m Y_{\ell, m}(\theta, \phi)^*, \quad (5.3)$$

and the symbol $*$ denotes the complex conjugate. The associated Legendre polynomial in (5.2) is written as

$$P_\ell^m(x) = (1 - x^2)^{1/2|m|} \frac{d^{|m|}}{dx^{|m|}} P_\ell(x), \quad (5.4)$$

in which $x = \cos \theta$, while

$$P_\ell^{-m}(x) = [(-1)^m (\ell - m)! / (\ell + m)!] P_\ell^m(x),$$

and the Legendre polynomial $P_\ell(x)$ is generated by

$$1/\sqrt{1 - 2sx + s^2} = \sum_{\ell=0}^{\infty} P_\ell(x) s^\ell. \quad (5.5)$$

It is shown above that the spherical harmonics (angular momentum eigenfunctions) can be written in the form

$$Y_{\ell,m}(\theta, \phi) = C P_{\ell}^m(\theta) e^{im\phi}, \quad (5.6)$$

where C is a normalization constant and $P_{\ell}^m(\theta)$ is an associated Legendre polynomial given explicitly in (5.4). The coordinate system used to define the polar and azimuthal angles is shown in Fig. 5.1. The $Y_{\ell,m}(\theta, \phi)$ spherical harmonics generate odd-dimensional representations of the rotation group and these representations are irreducible representations. For $\ell = 0$, we have a one-dimensional representation; $\ell = 1$ ($m = 1, 0, -1$) gives a three-dimensional irreducible representation; $\ell = 2$ ($m = 2, 1, 0, -1, -2$) gives a five-dimensional representation, etc. So for each value of the angular momentum, the spherical harmonics provide us with a representation of the proper $2\ell+1$ dimensionality.

These irreducible representations are found from the so-called *addition theorem for spherical harmonics* which tells us that if we change the polar axis (i.e., the axis of quantization), then the “old” spherical harmonics $Y_{\ell,m}(\theta, \phi)$ and the “new” $Y_{\ell',m'}(\theta', \phi')$ are related by a *linear transformation* of basis functions when $\ell' = \ell$:

$$\hat{P}_R Y_{\ell,m}(\theta', \phi') = \sum_{m'} D^{(\ell)}(R)_{m'm} Y_{\ell,m'}(\theta, \phi), \quad (5.7)$$

where \hat{P}_R denotes a rotation operator that changes the polar axis, and the matrix $D^{(\ell)}(R)_{m'm}$ provides an ℓ -dimensional matrix representation of element R in the full rotation group. Let us assume that the reader has previously

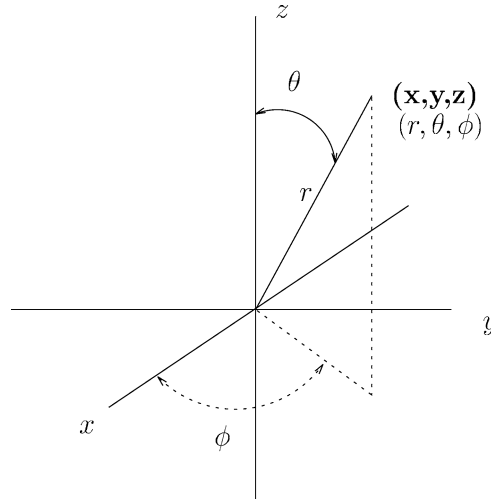


Fig. 5.1. Polar coordinate system defining the polar angle θ and the azimuthal angle ϕ

seen this expansion for spherical harmonics which is a major point in the development of the irreducible representations of the rotation group. From the similarity between (5.7) and (4.1), the reader can see the connection between the group theory mathematical background given in Chap. 4 and the application discussed here.

In any system with full rotational symmetry, the choice of the z -axis is arbitrary. We thus choose the z -axis as the axis about which the operator \hat{P}_α makes the rotation α . Because of the form of the spherical harmonics $Y_{\ell,m}(\theta, \phi)$ [see (5.6)] and the choice of the z -axis, the action of \hat{P}_α on the $Y_{\ell,m}(\theta, \phi)$ basis functions only affects the ϕ dependence of the spherical harmonic (not the θ dependence). The effect of this rotation on the function $Y_{\ell,m}(\theta, \phi)$ is equivalent to a rotation of the axes in the opposite sense by the angle $-\alpha$

$$\hat{P}_\alpha Y_{\ell,m}(\theta, \phi) = Y_{\ell,m}(\theta, \phi - \alpha) = e^{-im\alpha} Y_{\ell,m}(\theta, \phi), \quad (5.8)$$

in which the second equality results from the explicit form of $Y_{\ell,m}(\theta, \phi)$. But (5.8) gives the linear transformation of $Y_{\ell,m}(\theta, \phi)$ resulting from the action by the operator \hat{P}_α . Thus by comparing (5.7) and (5.8), we see that the matrix $D^{(\ell)}(\alpha)_{m'm}$ is diagonal in m so that we can write $D^{(\ell)}(\alpha)_{m'm} = e^{-im\alpha} \delta_{m'm}$, where $-\ell \leq m \leq \ell$, yielding

$$D^{(\ell)}(\alpha) = \begin{pmatrix} e^{-i\ell\alpha} & & & \mathcal{O} \\ & e^{-i(\ell-1)\alpha} & & \\ & & \ddots & \\ \mathcal{O} & & & e^{i\ell\alpha} \end{pmatrix}, \quad (5.9)$$

where \mathcal{O} represents all the zero entries in the off-diagonal positions. The character of the rotations C_α is thus given by the geometric series

$$\begin{aligned} \chi^{(\ell)}(\alpha) &= \text{trace } D^{(\ell)}(\alpha) = e^{-i\ell\alpha} + \cdots + e^{i\ell\alpha} \\ &= e^{-i\ell\alpha} [1 + e^{i\alpha} + \cdots + e^{2i\ell\alpha}] \\ &= e^{-i\ell\alpha} \sum_{k=0}^{2\ell} (e^{ik\alpha}) \\ &= e^{-i\ell\alpha} \left[\frac{e^{i(2\ell+1)\alpha} - 1}{e^{i\alpha} - 1} \right] \\ &= \frac{e^{i(\ell+1/2)\alpha} - e^{-i(\ell+1/2)\alpha}}{e^{i\alpha/2} - e^{-i\alpha/2}} = \frac{\sin[(\ell + \frac{1}{2})\alpha]}{\sin[(\frac{1}{2})\alpha]}. \end{aligned} \quad (5.10)$$

Thus we show that the character for rotations α about the z -axis is

$$\chi^{(\ell)}(\alpha) = \frac{\sin[(\ell + \frac{1}{2})\alpha]}{\sin[\alpha/2]}. \quad (5.11)$$

To obtain the character for the inversion operator i , we have

$$iY_{\ell m}(\theta, \phi) = Y_{\ell m}(\pi - \theta, \pi + \phi) = (-1)^\ell Y_{\ell m}(\theta, \phi) \quad (5.12)$$

and therefore

$$\chi^{(\ell)}(i) = \sum_{m=-\ell}^{m=\ell} (-1)^\ell = (-1)^\ell (2\ell + 1), \quad (5.13)$$

where $Y_{\ell m}(\theta, \phi)$ are the spherical harmonics, while ℓ and m denote the total and z -component angular momentum quantum numbers, respectively.

The dimensionalities of the representations for $\ell = 0, 1, 2, \dots$ are $1, 3, 5, \dots$. In dealing with the symmetry operations of the full rotation group, the inversion operation frequently occurs. This operation also occurs in the lower symmetry point groups either as a separate operation i or in conjunction with other compound operations (e.g., $S_6 = i \otimes C_3^{-1}$). A compound operation (like an improper rotation or a mirror plane) can be represented as a product of a proper rotation followed by inversion. The character for the inversion operation is $+(2\ell + 1)$ for *even* angular momentum states ($\ell = \text{even}$ in $Y_{\ell m}(\theta, \phi)$) and $-(2\ell + 1)$ for *odd* angular momentum states (see (5.13)). This idea of compound operations will become clearer after we have discussed in Chap. 6 the direct product groups and direct product representations.

We now give a general result for an improper rotation defined by

$$S_n = C_n \otimes \sigma_h \quad (5.14)$$

and $S_3 = C_3 \otimes \sigma_h$ is an example of (5.14) (for an odd integer n). Also S_n can be written as a product of $C_{n/2} \otimes i$, as for example, $S_6 = C_3 \otimes i$, for n an even integer, where \otimes denotes the direct product of the two symmetry operations appearing at the left and right of the symbol \otimes , which is discussed in Chap. 6. If we now apply (5.11) and (5.12), we obtain

$$\chi^{(\ell)}(S_n) = \chi^{(\ell)}(C_{n/2} \otimes i) = (-1)^\ell \frac{\sin[(\ell + \frac{1}{2})\alpha]}{\sin[\alpha/2]}. \quad (5.15)$$

In the case of mirror planes, such as σ_h , σ_d , or σ_v we can make use of relations such as

$$\sigma_h = C_2 \otimes i \quad (5.16)$$

to obtain the character for mirror planes in the full rotation group.

Now we are going to place our free ion into a crystal field which does not have full rotational symmetry operations, but rather has the symmetry operations of a crystal which may include rotations about finite angles, inversions and a finite number of reflections. The *full rotation group contains all these symmetry operations*. Therefore, the representation $D^{(\ell)}(\alpha)$ given above is a representation of the crystal point group if α is a symmetry operation in that point group. But $D^{(\ell)}(\alpha)$ is, in general, a *reducible* representation of the lower

symmetry group. Therefore the $(2\ell + 1)$ -fold degeneracy of each level will in general be partially lifted.

We can find out how the degeneracy of each level is lifted by asking what are the irreducible representations contained in $D^{(\ell)}(\alpha)$ in terms of the group of lower symmetry for the crystal. The actual calculation of the crystal field splittings depends on setting up a suitable Hamiltonian and solving it, usually in some approximation scheme. But the energy level *degeneracy* does not depend on the detailed Hamiltonian, but only on its symmetry. Thus, the decomposition of the level degeneracies in a crystal field is a consequence of the symmetry of the crystal field.

5.3 Cubic Crystal Field Environment for a Paramagnetic Transition Metal Ion

As an example of a crystal field environment, suppose that we place our

paramagnetic ion (e.g., an iron impurity) in a cubic host crystal. Assume further that this impurity goes into a substitutional lattice site, and is surrounded by a regular octahedron of negative ions (see Fig. 5.2). A regular octahedron has O_h symmetry, but since we have not yet discussed the inversion operation and direct product groups (see Chap. 6), we will simplify the symmetry operations and work with the point group O . The character table for O is shown in Table 5.1 (see also Table A.30). From all possible rotations on a sphere, only 24 symmetry operations of the full rotation group remain in the group O .

Reviewing the *notation* in Table 5.1, the Γ notations for the irreducible representations are the usual ones used in solid-state physics and are due to Bouckaert, Smoluchowski and Wigner [1].

The second column in Table 5.1 follows the notation usually found in molecular physics and chemistry applications, which are two research fields that also make lots of use of symmetry and group theory. The key

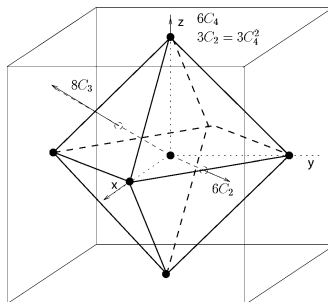


Fig. 5.2. A regular octahedron inscribed in a cube, illustrating the symmetry operations of group O

Table 5.1. Character table for O and decomposition of the angular momenta representations into the irreducible representations of group O

| | O | E | $8C_3$ | $3C_2 = 3C_4^2$ | $6C_2'$ | $6C_4$ |
|-------------------|-----------------------|-----|--------|-----------------|---------|--------|
| Γ_1 | A_1 | | 1 | 1 | 1 | 1 |
| Γ_2 | A_2 | | 1 | 1 | -1 | -1 |
| Γ_{12} | E | | 2 | -1 | 2 | 0 |
| $\Gamma_{15'}$ | T_1 | | 3 | 0 | -1 | -1 |
| $\Gamma_{25'}$ | T_2 | | 3 | 0 | -1 | 1 |
| $\Gamma_{\ell=0}$ | A_1 | | 1 | 1 | 1 | 1 |
| $\Gamma_{\ell=1}$ | T_1 | | 3 | 0 | -1 | 1 |
| $\Gamma_{\ell=2}$ | $E + T_2$ | | 5 | -1 | 1 | -1 |
| $\Gamma_{\ell=3}$ | $A_2 + T_1 + T_2$ | | 7 | 1 | -1 | -1 |
| $\Gamma_{\ell=4}$ | $A_1 + E + T_1 + T_2$ | | 9 | 0 | 1 | 1 |
| $\Gamma_{\ell=5}$ | $E + 2T_1 + T_2$ | | 11 | -1 | -1 | -1 |

to the notation is that A denotes one-dimensional representations, E denotes two-dimensional representations, and T denotes three-dimensional representations. Papers on lattice dynamics of solids often use the A, E, T symmetry notation to make contact with the molecular analog. The subscripts in Table 5.1 refer to the conventional indexing of the representations of the group O (see Table A.30). The pertinent symmetry operations can be found from Fig. 5.2, and the classes associated with these symmetry operations label the various columns where the characters in Table 5.1 appear.

The various types of rotational symmetry operations are listed as

- the $8C_3$ rotations are about the axes through the triangular face centroids of the octahedron,
- the $6C_4$ rotations are about the corners of the octahedron,
- the $3C_2$ rotations are also about the corners of the octahedron, with $C_2 = C_4^2$,
- the $6C_2'$ rotations are twofold rotations about a (110) axis passing through the midpoint of the edges (along the 110 directions of the cube).

To be specific, suppose that we have a magnetic impurity atom with angular momentum $\ell = 2$. We first find the characters for all the symmetry operations which occur in the O group for an irreducible representation of the full rotation group. The representation of the full rotation group will be a representation of group O , but in general this representation will be *reducible*.

Since the character for a general rotation α in the full rotation group is found using (5.11), the identity class (or $\alpha = 0$) yields the characters

$$\chi^{(\ell)}(0) = \frac{\ell + \frac{1}{2}}{1/2} = 2\ell + 1. \quad (5.17)$$

Table 5.2. Classes and characters for the group O

| class | α | $\chi^{(2)}(\alpha)$ |
|-------------------|----------|---|
| $8C_3$ | $2\pi/3$ | $\frac{\sin(5/2) \cdot (2\pi/3)}{\sin((2\pi)/(2 \cdot 3))} = (-\sqrt{3}/2)/(\sqrt{3}/2) = -1$ |
| $6C_4$ | $2\pi/4$ | $\frac{\sin(5/2) \cdot (\pi/2)}{\sin(\pi/4)} = (-1/\sqrt{2})/(1/\sqrt{2}) = -1$ |
| $3C_2$ and $6C_2$ | $2\pi/2$ | $\frac{\sin(5/2)\pi}{\sin(\pi/2)} = 1$ |

Table 5.3. Characters found in Table 5.2 for the $\Gamma_{\text{rot}}^{(2)}$ of the full rotation group ($\ell = 2$)

| | E | $8C_3$ | $3C_2$ | $6C'_2$ | $6C_4$ |
|-----------------------------|-----|--------|--------|---------|--------|
| $\Gamma_{\text{rot}}^{(2)}$ | 5 | -1 | 1 | 1 | -1 |

For our case $\ell = 2$ ($\chi^{(2)}(E) = 5$), and by applying (5.11) to the symmetry operations in each class we obtain the results summarized in Table 5.2. To compare with the character table for group O (Table 5.1), we list in Table 5.3 the characters found in Table 5.2 for the $\Gamma_{\text{rot}}^{(2)}$ of the full rotation group ($\ell = 2$) according to the classes listed in the character table for group O (see Tables 5.1 and A.30).

We note that $\Gamma_{\text{rot}}^{(2)}$ is a reducible representation of group O because group O has no irreducible representations with dimensions $\ell_n > 3$. To find the irreducible representations contained in $\Gamma_{\text{rot}}^{(2)}$ we use the decomposition formula for reducible representations (3.20):

$$a_j = \frac{1}{h} \sum_k N_k \chi^{(\Gamma_j)}(\mathcal{C}_k)^* \chi^{\text{reducible}}(\mathcal{C}_k), \quad (5.18)$$

where we have used (3.16)

$$\chi^{\text{reducible}}(\mathcal{C}_k) = \sum_{\Gamma_j} a_j \chi^{(\Gamma_j)}(\mathcal{C}_k), \quad (5.19)$$

in which $\chi^{(\Gamma_j)}$ is an irreducible representation and the characters for the reducible representation $\Gamma_{\text{rot}}^{(2)}$ are written as $\chi^{\text{reducible}}(\mathcal{C}_k) \equiv \chi^{\Gamma_{\text{rot}}^{(2)}}(\mathcal{C}_k)$. We now ask how many times is A_1 contained in $\Gamma_{\text{rot}}^{(2)}$? Using (5.18) we obtain

$$a_{A_1} = \frac{1}{24} [5 - 8 + 3 + 6 - 6] = 0, \quad (5.20)$$

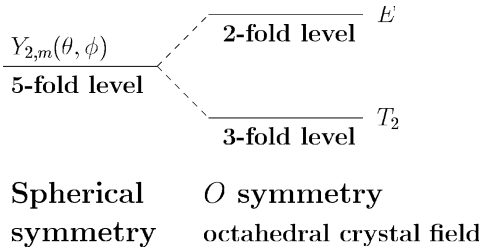


Fig. 5.3. The splitting of the d -Levels (fivefold) in an octahedral crystal field

which shows that the irreducible representation A_1 is not contained in $\Gamma_{\text{rot}}^{(2)}$. We then apply (5.18) to the other irreducible representations of group O :

$$\begin{aligned} A_2 : \quad a_{A_2} &= \frac{1}{24}[5 - 8 + 3 - 6 + 6] = 0 \\ E : \quad a_E &= \frac{1}{24}[10 + 8 + 6 + 0 - 0] = 1 \\ T_1 : \quad a_{T_1} &= \frac{1}{24}[15 + 0 - 3 - 6 - 6] = 0 \\ T_2 : \quad a_{T_2} &= \frac{1}{24}[15 + 0 - 3 + 6 + 6] = 1, \end{aligned}$$

so that finally we write

$$\Gamma_{\text{rot}}^{(2)} = E + T_2,$$

which means that the reducible representation $\Gamma_{\text{rot}}^{(2)}$ breaks into the irreducible representations E and T_2 in cubic symmetry. In other words, an atomic d -level in a cubic O crystal field splits into an E and a T_2 level. Similarly, an atomic d -level in a cubic O_h crystal field splits into an E_g and a T_{2g} level, where the g denotes evenness under inversion. Group theory does not provide any information about the ordering of the levels (see Fig. 5.3). For general utility, we have included in Table 5.1 the characters for the angular momentum states $\ell = 0, 1, 2, 3, 4, 5$ for the full rotation group expressed as reducible representations of the group O . The splittings of these angular momentum states in cubic group O symmetry are also included in Table 5.1.

We can now carry out the passage from higher to lower symmetry by going one step further. Suppose that the presence of the impurity strains the crystal. Let us further imagine (for the sake of argument) that the new local symmetry of the impurity site is D_4 (see Table 5.4 and Table A.18), which is a proper subgroup of the full rotation group. Then the levels E and T_2 given above may be split further in D_4 (tetragonal) symmetry (for example by stretching the molecule along the fourfold axis). We now apply the same technique to investigate this tetragonal field splitting. We start again by writing the character table for the group D_4 which is of order 8. We then consider the representations E and T_2 of the group O as reducible representations of group D_4 .

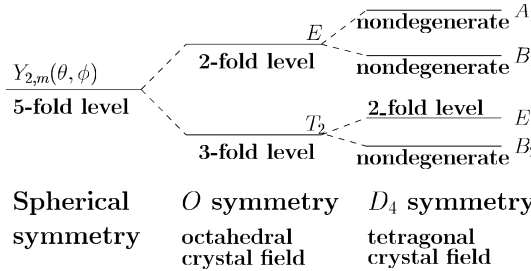


Fig. 5.4. d -Level splitting in octahedral and D_4 crystal fields

Table 5.4. Character table for D_4 and the decomposition of the irreducible representations of group O into representations for group D_4

| character table for D_4 | | E | $C_2 = C_4^2$ | $2C_4$ | $2C'_2$ | $2C''_2$ |
|---------------------------|-------|-----|---------------|--------|---------|----------|
| Γ_1 | A_1 | 1 | 1 | 1 | 1 | 1 |
| $\Gamma_{1'}$ | A_2 | 1 | 1 | 1 | -1 | -1 |
| Γ_2 | B_1 | 1 | 1 | -1 | 1 | -1 |
| $\Gamma_{2'}$ | B_2 | 1 | 1 | -1 | -1 | 1 |
| Γ_3 | E | 2 | -2 | 0 | 0 | 0 |

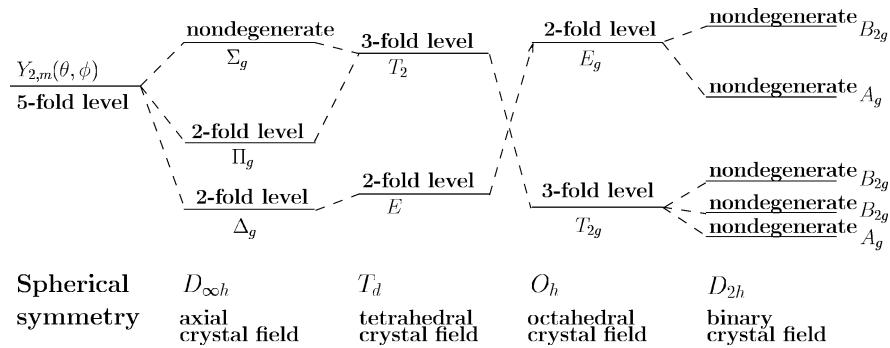
| reducible representations from O group | | | | | | |
|--|--|---|----|----|----|----------------------|
| E | | 2 | 2 | 0 | 2 | 0 $\equiv A_1 + B_1$ |
| T_2 | | 3 | -1 | -1 | -1 | 1 $\equiv E + B_2$ |

Table 5.5. Decomposition of the $\ell = 2$ angular momentum level into the irreducible representations of group D_4

| | E | C_2 | $2C_4$ | $2C'_2$ | $2C''_2$ | |
|-----------------------------|-----|-------|--------|---------|----------|-----------------------|
| $\Gamma_{\text{rot}}^{(2)}$ | 5 | 1 | -1 | 1 | 1 | $A_1 + B_1 + B_2 + E$ |

and write down the characters for the E , C_2 , C_4^2 , C'_2 and C''_2 operations from the character table for O given above, noting that the C''_2 in the group D_4 refers to three of the (110) axes $6C'_2$ of the cubic group O (Table 5.4). Using the decomposition theorem, (3.20), we find that E splits into the irreducible representations $A_1 + B_1$ in the group D_4 while T_2 splits into the irreducible representations $E + B_2$ in the group D_4 , as summarized in Fig. 5.4.

We note that the C_2 operations in D_4 is a π rotation about the z -axis and the $2C'_2$ are π rotations about the x - and y -axes. The C_2 and the $2C'_2$ come from the $3C_2 = 3C_4^2$ in group O . The $2C''_2$ are π rotations about (110) axes and come from the $6C'_2$ in group O . To check the decomposition of the $\ell = 2$ level in D_4 symmetry, we add up the characters for $A_1 + B_1 + B_2 + E$ for group D_4 (see Table 5.5), which are the characters for the spherical harmonics considered as a reducible representation of group D_4 , so that this result checks.

Fig. 5.5. *d*-Level splitting in various crystal fields

Suppose now that instead of applying a stress along a (001) direction, we apply a stress along a (110) direction (see Problem 5.4). You will see that the crystal field pattern is somewhat altered, so that the crystal field pattern provides symmetry information about the crystal field. Figure 5.5 shows the splitting of the $\ell = 2$ level in going from full rotational symmetry to various lower symmetries, including $D_{\infty h}$, T_d , O_h , and D_{2h} , showing in agreement with the above discussion, the lifting of all the degeneracy of the $\ell = 2$ level in D_{2h} symmetry.

5.4 Comments on Basis Functions

Although group theory tells us how the impurity ion energy levels are split by the crystal field, it does not tell us the ordering of these levels. Often a simple physical argument can be given to decide which levels ought to lie lower. Consider the case of a *d*-electron in a cubic field, where the host ions are at $x = \pm a$, $y = \pm a$, $z = \pm a$. Assume that the impurity ion enters the lattice substitutionally, so that it is replacing one of the cations. Then the nearest neighbor host ions are all anions. The charge distributions for the *d*-states are shown in Fig. 5.6. Referring to the basis functions for O , which can be obtained from Table A.30, we see that for the irreducible representation E we have basis functions $(x^2 - y^2, 3z^2 - r^2)$ and for T_2 we have basis functions (xy, yz, zx) . For the basis functions which transform as the T_2 representation, the charge distributions do not point to the host ion sites and hence the crystal field interaction is relatively weak.

However, for the *d*-functions which transform as E , the interaction will be stronger since the charge distributions now *do* point to the host ion sites. If, however, the interaction is repulsive, then the E level will lie higher than the T_2 level. A more quantitative way to determine the ordering of the levels is to solve the eigenvalue problem explicitly. In carrying out this solution it is con-

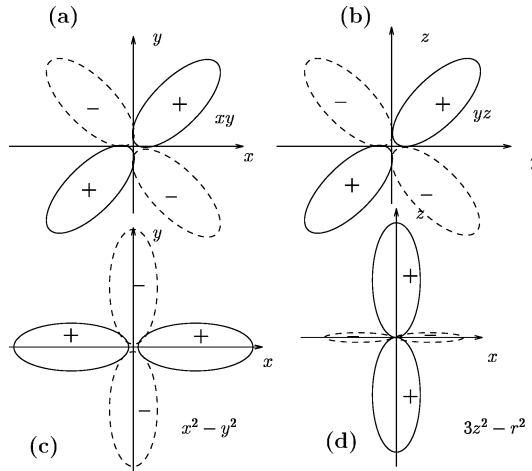


Fig. 5.6. The angular parts of d -wave functions in cubic crystals are shown as labeled by the basis functions for the partners of their irreducible representations. (a) $xy/r^2 \Rightarrow (T_2)$, (b) $yz/r^2 \Rightarrow (T_2)$, (c) $(x^2 - y^2)/r^2 \Rightarrow (E)$, (d) $(3z^2 - r^2)/r^2 \Rightarrow (E)$

venient to use basis functions that transform as the irreducible representations of the crystal field group.

We now look at the basis functions which provide irreducible representations for these cases of lower symmetry. In going from the full rotation group to the cubic group O , we obtain the irreducible representations E and T_2 shown in Fig. 5.3, which can be expressed in terms of the basis functions for these irreducible representations. The basis functions for the twofold level are $(x^2 - y^2)$ and $(3z^2 - r^2)$, while the basis functions for the threefold level are (xy) , (yz) , and (zx) . We note that these basis functions bring the crystal field potential into block form, but need not completely diagonalize the Hamiltonian. There are various forms of the crystal field potential that have O_h symmetry (e.g., octahedral sites, cubic sites, etc.), and in each case the appropriate set of basis functions that transform as irreducible representations of the group will bring the secular equation into block form.

Upon lowering the symmetry further to D_4 symmetry, the T_2 and E levels split further according to $T_2 \rightarrow E + B_2$ and $E \rightarrow A_1 + B_1$ (see Fig. 5.4). The appropriate basis functions for these levels can be identified with the help of the character table for group D_4 in Table A.18:

$$E \begin{Bmatrix} yz \\ zx \end{Bmatrix}, \quad B_2\{xy\}, \quad B_1\{x^2 - y^2\}, \quad A_1\{z^2\}. \quad (5.21)$$

In Sects. 5.3 and 5.4 we consider the spherical harmonics for $\ell = 2$ as reducible representations of the point groups O_h , O , and D_4 . In this connection, Table 5.6 gives the decomposition of the various spherical harmonics for angular

Table 5.6. Splitting of angular momentum in cubic symmetry O_h

| ℓ | A_{1g} | A_{2g} | E_g | T_{1g} | T_{2g} | A_{1u} | A_{2u} | E_u | T_{1u} | T_{2u} |
|--------|----------|----------|-------|----------|----------|----------|----------|-------|----------|----------|
| 0 | 1 | | | | | | | | | |
| 1 | | | | | | | | | 1 | |
| 2 | | | 1 | | 1 | | | | | |
| 3 | | | | | | | 1 | | 1 | 1 |
| 4 | 1 | | | 1 | 1 | 1 | | | | |
| 5 | | | | | | | | 1 | 2 | 1 |
| 6 | 1 | 1 | 1 | 1 | 2 | | | | | |
| 7 | | | | | | | 1 | 1 | 2 | 2 |
| 8 | 1 | | 2 | 2 | 2 | | | | | |
| 9 | | | | | | 1 | 1 | 1 | 3 | 2 |
| 10 | 1 | 1 | 2 | 2 | 3 | | | | 1 | 2 |
| 11 | | | | | | | 1 | 2 | 3 | 3 |
| 12 | 2 | 1 | 2 | 3 | 3 | | | | | |
| 13 | | | | | | 1 | 1 | 2 | 4 | 3 |
| 14 | 1 | 1 | 3 | 3 | 4 | | | 1 | 2 | 4 |
| 15 | | | | | | 1 | 2 | 2 | 4 | 4 |

momentum $\ell \leq 15$ into irreducible representations of the full cubic group O_h , which will be further discussed in Chap. 6 when direct product groups are discussed.

5.5 Comments on the Form of Crystal Fields

Any function (e.g., any arbitrary V_{xtal}) can be written in terms of a complete set of basis functions, such as the spherical harmonics. In the case of the crystal field problem, group theory can greatly simplify the search for the spherical harmonics $Y_{\ell,m}(\theta, \phi)$ pertaining to V_{xtal} . Consider, for example, V_{cubic} and Table 5.6. The spherical harmonics in V_{xtal} must exhibit all the symmetry operations of the physical system. We note that the lowest angular momentum state to contain the totally symmetric A_{1g} irreducible representation of O_h is $\ell = 4$, and must, therefore be the lowest angular momentum state in the crystal field for a cubic crystal V_{cubic} when written in terms of spherical harmonics.

We can check the predictions from group theory by obtaining the crystal field analytically. To construct the crystal field, we consider the electrostatic interaction of the neighboring host ions at the impurity site. To illustrate how this is done, consider the highly symmetric case of an impurity ion in a cubic environment provided by ions at $x = \pm a$, $y = \pm a$, $z = \pm a$. The contribution from an ion at $x = -a$ at the field point \mathbf{r} denoted by (x, y, z) is

$$V_{x=-a} = \frac{e}{|\mathbf{r}|} = \frac{e}{a\sqrt{(1+x/a)^2 + (y/a)^2 + (z/a)^2}} = \frac{e}{a\sqrt{1+\varepsilon}}, \quad (5.22)$$

where e is the charge on the electron and ε is a small dimensionless quantity if considering (x, y, z) in the neighborhood of the origin 0. Then using the binomial expansion:

$$(1 + \varepsilon)^{-1/2} = 1 - \frac{1}{2}\varepsilon + \frac{3}{8}\varepsilon^2 - \frac{5}{16}\varepsilon^3 + \frac{35}{128}\varepsilon^4 + \dots, \quad (5.23)$$

we obtain the contribution to the potential for charges e at $x = a$ and $x = -a$:

$$\begin{aligned} V_{x=-a} + V_{x=a} &= \frac{2e}{a} \left[1 - \frac{1}{2}(r^2/a^2) + \frac{3}{2}(x^2/a^2) + \frac{3}{8}(r^4/a^4) \right. \\ &\quad \left. - \frac{15}{4}(x^2/a^2)(r^2/a^2) + \frac{35}{8}(x^4/a^4) + \dots \right]. \end{aligned} \quad (5.24)$$

For a cubic field with charges e at $x = \pm a$, $y = \pm a$, $z = \pm a$ we get for $V_{\text{total}} = V_{\text{xtal}}$:

$$V_{\text{total}} = \frac{2e}{a} \left[3 + \frac{35}{8a^4}(x^4 + y^4 + z^4) - \frac{21}{8}(r^4/a^4) + \dots \right], \quad (5.25)$$

so that the perturbation that will lift the degeneracy of the free atom is of the form

$$V_{\text{cubic}} = \frac{35e}{4a^5} \left[(x^4 + y^4 + z^4) - \frac{3}{5}r^4 \right]. \quad (5.26)$$

From these expressions it also follows that for an orthorhombic field where the charges are at $x = \pm a$, $y = \pm b$, $z = \pm c$ (and $a \neq b \neq c$). The crystal potential becomes

$$\begin{aligned} V_{\text{total}} &= \frac{2e}{a} + \frac{2e}{b} + \frac{2e}{c} + ex^2 \left[\frac{2}{a^3} - \frac{1}{b^3} - \frac{1}{c^3} \right] \\ &\quad + ey^2 \left[\frac{2}{b^3} - \frac{1}{a^3} - \frac{1}{c^3} \right] + ez^2 \left[\frac{2}{c^3} - \frac{1}{a^3} - \frac{1}{b^3} \right], \end{aligned} \quad (5.27)$$

so that the orthorhombic perturbation V_{ortho} that will lift the degeneracy of the free atom is of the form

$$V_{\text{ortho}} = Ax^2 + By^2 - (A + B)z^2, \quad (5.28)$$

where the values for the coefficients A and B can be found from (5.27).

We note that V_{cubic} contains no terms of order x^2 , whereas V_{ortho} does. Let us now express the crystal field potential in terms of spherical harmonics since the unperturbed states for the free impurity ion are expressed in that way. Here we make use of the fact that the crystal field potential is generated by a collection of point sources and in the intervening space we are “outside” the field sources so that the potential must satisfy the Laplace equation $\nabla^2 V = 0$.

Solutions to Laplace's equation [5] are of the form $r^\ell Y_{\ell m}(\theta, \phi)$. From the definitions for the spherical harmonics (5.2) it is clear that for a cubic field (5.26), the only spherical harmonics that will enter V_{cubic} are $Y_{4,0}$, $Y_{4,4}$ and $Y_{4,-4}$ since $(z/4)^4$ involves only $Y_{4,0}$ while $[(x/4)^4 + (y/4)^4]$ involves only $Y_{4,4}$ and $Y_{4,-4}$.

The crystal field potential V_{xtal} can therefore be written in terms of spherical harmonics, the basis functions normally used to describe the potential of the free ion which has full spherical symmetry. One important role of group theory in the solution of quantum mechanical problems is to determine the degeneracy of the eigenvalues and which choice of basis functions yields the eigenvalues most directly. This information is available without the explicit diagonalization of the Hamiltonian. In the case of the crystal field problem, we determine V_{xtal} for a specific crystal symmetry using the appropriate basis functions for the relevant point group.

Selected Problems

5.1. Consider the hydrogen atom, described by the Schrödinger equation

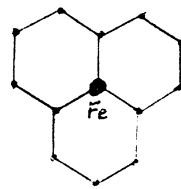
$$\mathcal{H}\Psi_{n\ell m} = \left\{ -\frac{\hbar^2}{2m} \nabla_r^2 - \frac{L^2}{r^2} + V(r) \right\} \Psi_{n\ell m} = E_{n\ell} \Psi_{n\ell m}.$$

- (a) Does \mathcal{H} commute with any arbitrary rotation about the origin? Explain your answer.
 (b) If the electron is in a d -orbital ($\ell = 2$) described by the eigenfunction

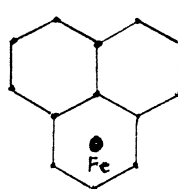
$$\Psi_{n2m}(r, \theta, \phi) = R_n(r)Y_{2,m}(\theta, \phi),$$

where $Y_{2,m}(\theta, \phi)$ is a spherical harmonic for $\ell = 2$, what is the effect on $\Psi_{n2m}(r, \theta, \phi)$ of rotating the coordinate system by a polar angle α . Is the new wave function still an eigenfunction of the Hamiltonian with the same eigenvalue? Explain.

5.2. Suppose that an iron (Fe) impurity is introduced into a two-dimensional honeycomb lattice of an insulating host material. A honeycomb lattice is a hexagonal lattice with atoms at the hexagon corners but not at the center. Suppose that the Fe impurity is placed first in a substitutional location and second in an interstitial location at the center of the hexagon.



substitutional



interstitial

- (a) What is the difference in crystal potential (include only nearest neighbors) between the substitutional and interstitial locations?
- (b) For the interstitial case, express your result in part (a) in terms of spherical harmonics for the lowest order terms with angular dependencies.
- (c) What is the proper point group symmetry and character table in each case?
- (d) Give the crystal field splitting of the fivefold d -levels of the Fe impurity in the crystal fields for the two locations of the Fe ion in part (a).
- (e) Identify the basis functions associated with each of the levels in part (d).
- (f) Since the bonding orbitals lie lower in energy than the antibonding orbitals, indicate how the ordering of the levels might indicate whether the Fe impurity is located substitutionally or interstitially in the honeycomb lattice.

5.3. Show (by finding the characters of the rotation group) that the d -level for a transition metal impurity in a metal cluster with I_h point symmetry is not split by the icosahedral crystal field.

5.4. Suppose that a stress is applied along a (110) axis of a cubic crystal, thereby lowering its symmetry from O to D_2 .

- (a) What are the symmetry operations of D_2 ? Identify each symmetry axis of D_2 with a particular (xyz) direction of the high symmetry group O .
- (b) Considering the irreducible representation $\Gamma_{\text{rot}}^{(2)}$ for the full rotation group as a reducible representation of D_2 , find the irreducible representations of D_2 contained in $\Gamma_{\text{rot}}^{(2)}$.
- (c) How do the T_2 and E levels corresponding to $\Gamma_{\text{rot}}^{(2)}$ in the cubic group split by the application of a force along the (110) direction, giving the irreducible representations of the group D_2 contained in the T_2 and E levels.
- (d) What is the physical interpretation of the occurrence of a particular irreducible representation Γ_j of group D_2 more than once when the fivefold degeneracy of $\Gamma_{\text{rot}}^{(2)}$ is lifted by applying a force in the (110) direction?

5.5. What is the form of the crystal field of a hexagonal semiconductor like ZnO? Which are the lowest order $Y_{\ell,m}(\theta, \phi)$ spherical harmonics that describe the crystal field potential?

Application to Selection Rules and Direct Products

Our second general application of group theory to physical problems will be to selection rules. In considering selection rules we always involve some interaction Hamiltonian matrix \mathcal{H}' that couples two states ψ_α and ψ_β . Group theory is often invoked to decide whether or not these states are indeed coupled and this is done by testing whether or not the matrix element $(\psi_\alpha, \mathcal{H}'\psi_\beta)$ vanishes by symmetry. The simplest case to consider is the one where the perturbation \mathcal{H}' does not destroy the symmetry operations and is invariant under all the symmetry operations of the group of the Schrödinger equation. Since these matrix elements transform as scalars (numbers), then $(\psi_\alpha, \mathcal{H}'\psi_\beta)$ must exhibit the full group symmetry, and must therefore transform as the fully symmetric representation Γ_1 . Thus, if $(\psi_\alpha, \mathcal{H}'\psi_\beta)$ does *not transform as a number, it vanishes*. To exploit these symmetry properties, we thus choose the wave functions ψ_α^* and ψ_β to be eigenfunctions for the unperturbed Hamiltonian, which are basis functions for irreducible representations of the group of Schrödinger's equation. Here $\mathcal{H}'\psi_\beta$ transforms according to an irreducible representation of the group of Schrödinger's equation. This product involves the direct product of two representations and the theory behind the direct product of two representations will be given in this chapter. If $\mathcal{H}'\psi_\beta$ is orthogonal to ψ_α , then the matrix element $(\psi_\alpha, \mathcal{H}'\psi_\beta)$ vanishes by symmetry; otherwise the matrix element need not vanish, and a transition between state ψ_α and ψ_β may occur.

6.1 The Electromagnetic Interaction as a Perturbation

In considering various selection rules that arise in physical problems, we often have to consider matrix elements of a perturbation Hamiltonian which lowers the symmetry of the unperturbed problem. For example, the Hamiltonian in the presence of electromagnetic fields can be written as

$$\mathcal{H} = \frac{1}{2m} \left(\mathbf{p} - \frac{e}{c} \mathbf{A} \right)^2 + V. \quad (6.1)$$

Then the proper form of the Hamiltonian for an electron in a solid in the presence of an electromagnetic field is

$$\mathcal{H} = \frac{(\mathbf{p} - e/c\mathbf{A})^2}{2m} + V(\mathbf{r}) = \frac{p^2}{2m} + V(\mathbf{r}) - \frac{e}{mc}\mathbf{p} \cdot \mathbf{A} + \frac{e^2 A^2}{2mc^2}, \quad (6.2)$$

in which \mathbf{A} is the vector potential due to the electromagnetic fields and $V(\mathbf{r})$ is the periodic potential. Thus, the one-electron Hamiltonian without electromagnetic fields is

$$\mathcal{H}_0 = \frac{p^2}{2m} + V(\mathbf{r}), \quad (6.3)$$

and the electromagnetic perturbation terms \mathcal{H}'_{em} are

$$\mathcal{H}'_{\text{em}} = -\frac{e}{mc}\mathbf{p} \cdot \mathbf{A} + \frac{e^2 A^2}{2mc^2}, \quad (6.4)$$

which is usually approximated by the leading term for the electromagnetic perturbation Hamiltonian

$$\mathcal{H}'_{\text{em}} \cong -\frac{e}{mc}\mathbf{p} \cdot \mathbf{A}. \quad (6.5)$$

Such a perturbation Hamiltonian is generally *not* invariant under the symmetry operations of the group of Schrödinger's equation which are determined by the symmetry of the unperturbed Hamiltonian \mathcal{H}_0 . Therefore, we must consider the transformation properties of $\mathcal{H}'\psi_\beta$ where the eigenfunction ψ_β is chosen to transform as one of the partners $\psi_j^{(\Gamma_i)}$ (denoted by $|\Gamma_i j\rangle$ in Chap. 4) of an irreducible representation Γ_i of the unperturbed Hamiltonian \mathcal{H}_0 . In general, the action of \mathcal{H}' on $\psi_j^{(\Gamma_i)}$ will mix all other partners of the representation Γ_i since any arbitrary function can be expanded in terms of a complete set of functions $\psi_j^{(\Gamma_i)}$. In group theory, the transformation properties of $\mathcal{H}'\psi_j^{(\Gamma_i)}$ are handled through what is called the *direct product*. When \mathcal{H}' does not transform as the totally symmetric representation (e.g., \mathcal{H}'_{em} transforms as a vector x, y, z), then the matrix element $(\psi_k^{(\Gamma_i)}, \mathcal{H}'\psi_j^{(\Gamma_i)})$ will not in general vanish.

The discussion of selection rules in this chapter is organized around the following topics:

- summary of important symmetry rules for basis functions,
- theory of the Direct Product of Groups and Representations,
- the Selection Rule concept in Group Theoretical Terms,
- example of Selection Rules for electric dipole transitions in a system with full cubic point group symmetry.

6.2 Orthogonality of Basis Functions

The basis functions $\psi_\alpha^{(i)}$ where we here use the superscript i as an abbreviated notation for the superscript Γ_i for a given irreducible representation i are defined by (see (4.1))

$$\hat{P}_R \psi_\alpha^{(i)} = \sum_{j=1}^{\ell_i} D^{(i)}(R)_{j\alpha} \psi_j^{(i)}, \quad (6.6)$$

where \hat{P}_R is the symmetry operator, $\psi_\alpha^{(i)}$ denotes the basis functions for an ℓ_i -dimensional irreducible representation (i) and $D^{(i)}(R)_{j\alpha}$ is the matrix representation for symmetry element R in irreducible representation (i) . To exploit the symmetry properties of a given problem, we want to find eigenfunctions which form basis functions for the irreducible representations of the group of Schrödinger's equation. We can find such eigenfunctions using the symmetry operator and projection operator techniques discussed in Chap. 4. In this chapter, we will then assume that the eigenfunctions have been chosen to transform as irreducible representations of the group of Schrödinger's equation for \mathcal{H}_0 . The application of group theory to selection rules then depends on the following orthogonality theorem. This orthogonality theorem can be considered as the selection rule for the identity operator.

Theorem. *Two basis functions which belong either to different irreducible representations or to different columns (rows) of the same representation are orthogonal.*

Proof. Let $\phi_\alpha^{(i)}$ and $\psi_{\alpha'}^{(i')}$ be two basis functions belonging, respectively, to irreducible representations (i) and (i') and corresponding to columns α and α' of their respective representations. By definition:

$$\begin{aligned} \hat{P}_R \phi_\alpha^{(i)} &= \sum_{j=1}^{\ell_i} D^{(i)}(R)_{\alpha j} \phi_j^{(i)}, \\ \hat{P}_R \psi_{\alpha'}^{(i')} &= \sum_{j'=1}^{\ell_{i'}} D^{(i')}(R)_{\alpha' j'} \psi_{j'}^{(i')}. \end{aligned} \quad (6.7)$$

Because the scalar product (or the matrix element of unity taken between the two states) is independent of the coordinate system, we can write the scalar product as

$$\begin{aligned} \left(\phi_\alpha^{(i)}, \psi_{\alpha'}^{(i')} \right) &= \left(\hat{P}_R \phi_\alpha^{(i)}, \hat{P}_R \psi_{\alpha'}^{(i')} \right) \\ &= \sum_{j,j'} D^{(i)}(R)_{\alpha j}^* D^{(i')}(R)_{\alpha' j'} \left(\phi_j^{(i)}, \psi_{j'}^{(i')} \right) \\ &= \frac{1}{h} \sum_{j,j'} \sum_R D^{(i)}(R)_{\alpha j}^* D^{(i')}(R)_{\alpha' j'} \left(\phi_j^{(i)}, \psi_{j'}^{(i')} \right), \end{aligned} \quad (6.8)$$

since the left-hand side of (6.8) is independent of R , and h is the order of the group. Now apply the Wonderful Orthogonality Theorem (Eq. 2.52)

$$\frac{1}{h} \sum_R D^{(i)}(R)_{\alpha j}^* D^{(i')}(R)_{\alpha' j'} = \frac{1}{\ell_i} \delta_{ii'} \delta_{jj'} \delta_{\alpha\alpha'} \quad (6.9)$$

to (6.8), which yields:

$$\left(\phi_{\alpha}^{(i)}, \psi_{\alpha'}^{(i')} \right) = \frac{1}{\ell_i} \delta_{i,i'} \delta_{\alpha,\alpha'} \sum_{j=1}^{\ell_i} \left(\phi_j^{(i)}, \psi_j^{(i')} \right). \quad (6.10)$$

Thus, according to (6.10), if the basis functions $\phi_{\alpha}^{(i)}$ and $\psi_{\alpha'}^{(i')}$ correspond to two different irreducible representations $i \neq i'$ they are orthogonal. If they correspond to the same representation ($i = i'$), they are still orthogonal if they correspond to different columns (or rows) of the matrix – i.e., if they correspond to different partners of representation i . We further note that the right-hand side of (6.10) is independent of α so that the *scalar product is the same for all components* α , thereby completing the proof of the orthogonality theorem. \square

In the context of selection rules, the orthogonality theorem discussed above applies directly to the identity operator. Clearly, if a symmetry operator is invariant under all of the symmetry operations of the group of Schrödinger's equation then it transforms like the identity operator. For example, if

$$\mathcal{H}_0 \psi_{\alpha'}^{(i')} = E_{\alpha'}^{(i')} \psi_{\alpha'}^{(i')} \quad (6.11)$$

then $E_{\alpha'}^{(i')}$ is a number (or eigenvalues) which is independent of any coordinate system.

If $\psi_{\alpha'}^{(i')}$ and $\phi_{\alpha}^{(i)}$ are both eigenfunctions of the Hamiltonian \mathcal{H}_0 and are also basis functions for irreducible representations (i') and (i) , then the *matrix element* $(\phi_{\alpha}^{(i)}, \mathcal{H}_0 \psi_{\alpha'}^{(i')})$ vanishes unless $i = i'$ and $\alpha = \alpha'$, which is a result familiar to us from quantum mechanics.

In general, selection rules deal with the matrix elements of an operator different from the identity operator. In the more general case when we have a perturbation \mathcal{H}' , the perturbation need not have the full symmetry of \mathcal{H}_0 . In general $\mathcal{H}'\psi$ transforms differently from ψ .

6.3 Direct Product of Two Groups

We now define the *direct product of two groups*. Let $G_A = E, A_2, \dots, A_{h_a}$ and $G_B = E, B_2, \dots, B_{h_b}$ be two groups such that all operators A_R commute with all operators B_S . Then the direct product group is

$$G_A \otimes G_B = E, A_2, \dots, A_{h_a}, B_2, A_2 B_2, \dots, A_{h_a} B_2, \dots, A_{h_a} B_{h_b} \quad (6.12)$$

and has $(h_a \times h_b)$ elements. It is easily shown that if G_A and G_B are groups, then the direct product group $G_A \otimes G_B$ is a group. Examples of direct product groups that are frequently encountered involve products of groups with the group of inversions (group $C_i(S_2)$ with two elements E, i) and the group of reflections (group $C_\sigma(C_{1h})$ with two elements E, σ_h). For example, we can make a direct product group D_{3d} from the group D_3 by compounding all the operations of D_3 with (E, i) (to obtain $D_{3d} = D_3 \otimes C_i$), where i is the inversion operation (see Table A.13). An example of the group D_{3d} is a triangle with finite thickness. In general, we simply write the direct product group

$$D_{3d} = D_3 \otimes i, \quad (6.13)$$

when compounding the initial group D_3 with the inversion operation or with the mirror reflection in a horizontal plane (see Table A.14):

$$D_{3h} = D_3 \otimes \sigma_h. \quad (6.14)$$

Likewise, the full cubic group O_h is a direct product group of $O \otimes i$.

6.4 Direct Product of Two Irreducible Representations

In addition to *direct product groups* we have the *direct product of two representations* which is conveniently defined in terms of the direct product of two matrices. From algebra, we have the definition of the direct product of two matrices $A \otimes B = C$, whereby every element of A is multiplied by every element of B . Thus, the direct product matrix C has a double set of indices

$$A_{ij} B_{k\ell} = C_{ik,j\ell}. \quad (6.15)$$

Thus, if A is a (2×2) matrix and B is a (3×3) matrix, then C is a (6×6) matrix.

Theorem. *The direct product of the representations of the groups A and B forms a representation of the direct product group.*

Proof. We need to prove that

$$D_{ij}^{(a)}(A_i) D_{pq}^{(b)}(B_j) = (D^{(a \otimes b)}(A_i B_j))_{ip,jq}. \quad (6.16)$$

To prove this theorem we need to show that

$$D^{(a \otimes b)}(A_k B_\ell) D^{(a \otimes b)}(A_{k'} B_{\ell'}) = D^{(a \otimes b)}(A_i B_j), \quad (6.17)$$

where

$$A_i = A_k A_{k'}, \quad B_j = B_\ell B_{\ell'}. \quad (6.18)$$

Since the elements of group A commute with those of group B by the definition of the direct product group, the multiplication property of elements in the direct product group is

$$A_k B_\ell A_{k'} B_{\ell'} = A_k A_{k'} B_\ell B_{\ell'} = A_i B_j, \quad (6.19)$$

where $A_k B_\ell$ is a typical element of the direct product group. We must now show that the representations reproduce this multiplication property. By definition:

$$\begin{aligned} & D^{(a \otimes b)}(A_k B_\ell) D^{(a \otimes b)}(A_{k'} B_{\ell'}) \\ &= [D^{(a)}(A_k) \otimes D^{(b)}(B_\ell)][D^{(a)}(A_{k'}) \otimes D^{(b)}(B_{\ell'})]. \end{aligned} \quad (6.20)$$

To proceed with the proof, we write (6.20) in terms of components and carry out the matrix multiplication:

$$\begin{aligned} & \left[D^{(a \otimes b)}(A_k B_\ell) D^{(a \otimes b)}(A_{k'} B_{\ell'}) \right]_{ip,jq} \\ &= \sum_{sr} (D^{(a)}(A_k) \otimes D^{(b)}(B_\ell))_{ip,sr} (D^{(a)}(A_{k'}) \otimes D^{(b)}(B_{\ell'}))_{sr,jq} \\ &= \sum_s D_{is}^{(a)}(A_k) D_{sj}^{(a)}(A_{k'}) \sum_r D_{pr}^{(b)}(B_\ell) D_{rq}^{(b)}(B_{\ell'}) \\ &= D_{ij}^{(a)}(A_i) D_{pq}^{(b)}(B_j) = (D^{(a \otimes b)}(A_i B_j))_{ip,jq}. \end{aligned} \quad (6.21)$$

This completes the proof. \square

It can be further shown that the direct product of two *irreducible* representations of groups G_A and G_B yields an *irreducible* representation of the direct product group so that all irreducible representations of the direct product group can be generated from the irreducible representations of the original groups before they are joined. We can also take direct products between two representations of the same group. Essentially the same proof as given in this section shows that the direct product of two representations of the same group is also a representation of that group, though in general, it is a reducible representation. The proof proceeds by showing

$$\left[D^{(\ell_1 \otimes \ell_2)}(A) D^{(\ell_1 \otimes \ell_2)}(B) \right]_{ip,jq} = D^{(\ell_1 \otimes \ell_2)}(AB)_{ip,jq}, \quad (6.22)$$

where we use the short-hand notation ℓ_1 and ℓ_2 to denote irreducible representations with the corresponding dimensionalities. The direct product representation $D^{(\ell_1 \otimes \ell_2)}(R)$ will in general be reducible even though the representations ℓ_1 and ℓ_2 are irreducible.

6.5 Characters for the Direct Product

In this section we find the characters for the direct product of groups and for the direct product of representations of the same group.

Theorem. *The simplest imaginable formulas are assumed by the characters in direct product groups or in taking the direct product of two representations:*

(a) *If the direct product occurs between two groups, then the characters for the irreducible representations in the direct product group are obtained by multiplication of the characters of the irreducible representations of the original groups according to*

$$\chi^{(a \otimes b)}(A_k B_\ell) = \chi^{(a)}(A_k) \chi^{(b)}(B_\ell). \quad (6.23)$$

(b) *If the direct product is taken between two representations of the same group, then the character for the direct product representation is written as*

$$\chi^{(\ell_1 \otimes \ell_2)}(R) = \chi^{(\ell_1)}(R) \chi^{(\ell_2)}(R). \quad (6.24)$$

Proof. Consider the diagonal matrix element of an element in the direct product group. From the definition of the direct product of two groups, we write

$$D^{(a \otimes b)}(A_k B_\ell)_{ip, iq} = D_{ij}^{(a)}(A_k) D_{pq}^{(b)}(B_\ell). \quad (6.25)$$

Taking the diagonal matrix elements of (6.25) and summing over these matrix elements, we obtain

$$\sum_{ip} D^{(a \otimes b)}(A_k B_\ell)_{ip, ip} = \sum_i D_{ii}^{(a)}(A_k) \sum_p D_{pp}^{(b)}(B_\ell), \quad (6.26)$$

which can be written in terms of the traces:

$$\chi^{(a \otimes b)}(A_k B_\ell) = \chi^{(a)}(A_k) \chi^{(b)}(B_\ell). \quad (6.27)$$

This completes the proof of the theorem for the direct product of two groups. \square

The result of (6.27) holds equally well for classes (i.e., $R \rightarrow \mathcal{C}$), and thus can be used to find the character tables for direct product groups as is explained below.

Exactly the same proof as given above can be applied to find the character for the direct product of two representations of the same group

$$\chi^{(\ell_1 \otimes \ell_2)}(R) = \chi^{(\ell_1)}(R) \chi^{(\ell_2)}(R) \quad (6.28)$$

for each symmetry element R . The direct product representation is irreducible only if $\chi^{(\ell_1 \otimes \ell_2)}(R)$ for all R is identical to the corresponding characters for one of the irreducible representations of the group $\ell_1 \otimes \ell_2$.

In general, if we take the direct product between two irreducible representations of a group, then the resulting direct product representation will be reducible. If it is reducible, the character for the direct product can then be written as a linear combination of the characters for irreducible representations of the group (see Sect. 3.4):

$$\chi^{(\lambda)}(R)\chi^{(\mu)}(R) = \sum_{\nu} a_{\lambda\mu\nu} \chi^{(\nu)}(R), \quad (6.29)$$

where from (3.20) we can write the coefficients $a_{\lambda\mu\nu}$ as

$$a_{\lambda\mu\nu} = \frac{1}{h} \sum_{C_{\alpha}} N_{C_{\alpha}} \chi^{(\nu)}(C_{\alpha})^* \left[\chi^{(\lambda)}(C_{\alpha}) \chi^{(\mu)}(C_{\alpha}) \right], \quad (6.30)$$

where C_{α} denotes classes and $N_{C_{\alpha}}$ denotes the number of elements in class C_{α} . In applications of group theory to selection rules, constant use is made of (6.29) and (6.30).

Finally, we use the result of (6.27) to show how the character tables for the original groups G_A and G_B are used to form the character table for the direct product group. First, we form the elements and classes of the direct product group and then we use the character tables of G_A and G_B to form the character table for $G_A \otimes G_B$. In many important cases, one of the groups (e.g., G_B) has only two elements (such as the group C_i with elements E, i) and two irreducible representations Γ_1 with characters $(1,1)$ and Γ_1' with characters $(1, -1)$. We illustrate such a case below for the direct product group $C_{4h} = C_4 \otimes i$, a table that is not listed explicitly in Chap. 3 or in Appendix A. In the character table for group C_{4h} (Table 6.1) we use the notation g to denote representations that are even (German, *gerade*) under inversion, and u to denote representations that are odd (German, *ungerade*) under inversion.

We note that the upper left-hand quadrant of Table 6.1 contains the character table for the group C_4 . The four classes obtained by multiplication of

Table 6.1. Character table for point group C_{4h}

| | $C_{4h} \equiv C_4 \otimes i$ | | | | $(4/m)$ | | | | |
|-------|--|--|--|--|--|--|--|--|-------------------|
| | E | C_2 | C_4 | C_4^3 | i | iC_2 | iC_4 | iC_4^3 | |
| A_g | 1 | 1 | 1 | 1 | 1 | 1 | 1 | 1 | |
| B_g | 1 | 1 | -1 | -1 | 1 | 1 | -1 | -1 | even under |
| E_g | $\begin{cases} 1 & -1 \\ 1 & -1 \end{cases}$ | $\begin{cases} i & -i \\ -i & i \end{cases}$ | $\begin{cases} 1 & -1 \\ 1 & -1 \end{cases}$ | $\begin{cases} i & -i \\ -i & i \end{cases}$ | $\begin{cases} 1 & -1 \\ 1 & -1 \end{cases}$ | $\begin{cases} i & -i \\ -i & i \end{cases}$ | $\begin{cases} 1 & -1 \\ -1 & 1 \end{cases}$ | $\begin{cases} i & -i \\ -i & i \end{cases}$ | inversion (g) |
| A_u | 1 | 1 | 1 | 1 | -1 | -1 | -1 | -1 | |
| B_u | 1 | 1 | -1 | -1 | -1 | -1 | 1 | 1 | odd under |
| E_u | $\begin{cases} 1 & -1 \\ 1 & -1 \end{cases}$ | $\begin{cases} i & -i \\ -i & i \end{cases}$ | $\begin{cases} -1 & 1 \\ 1 & -1 \end{cases}$ | $\begin{cases} i & -i \\ -i & i \end{cases}$ | $\begin{cases} -1 & 1 \\ 1 & -1 \end{cases}$ | $\begin{cases} i & -i \\ -i & i \end{cases}$ | $\begin{cases} 1 & -1 \\ -1 & 1 \end{cases}$ | $\begin{cases} i & -i \\ -i & i \end{cases}$ | inversion (u) |

the classes of C_4 by i are listed on top of the upper right columns. The characters in the upper right-hand and lower left-hand quadrants are the same as in the upper left hand quadrant, while the characters in the lower right-hand quadrant are all multiplied by (-1) to produce the odd (ungerade) irreducible representations of group C_{4h} .

6.6 Selection Rule Concept in Group Theoretical Terms

Having considered the background for taking direct products, we are now ready to consider the selection rules for the matrix element

$$(\psi_{\alpha}^{(i)}, \mathcal{H}' \phi_{\alpha'}^{(i')}). \quad (6.31)$$

This matrix element can be computed by integrating the indicated scalar product over all space. Group theory then tells us that when any or all the symmetry operations of the group are applied, this *matrix element must transform as a constant*. Conversely, if the matrix element is not invariant under the symmetry operations which form the group of Schrödinger's equation, then the matrix element must vanish. We will now express the same physical concepts in terms of the direct product formalism.

Let the wave functions $\phi_{\alpha}^{(i)}$ and $\psi_{\alpha'}^{(i')}$ transform, respectively, as partners α and α' of irreducible representations Γ_i and $\Gamma_{i'}$, and let \mathcal{H}' transform as representation Γ_j . Then if the direct product $\Gamma_j \otimes \Gamma_{i'}$ is orthogonal to Γ_i , the matrix element vanishes, or equivalently if $\Gamma_i \otimes \Gamma_j \otimes \Gamma_{i'}$ does not contain the fully symmetrical representation Γ_1 , the matrix element vanishes. In particular, if \mathcal{H}' transforms as Γ_1 (i.e., the perturbation does not lower the symmetry of the system), then, because of the orthogonality theorem for basis functions, either $\phi_{\alpha}^{(i')}$ and $\psi_{\alpha'}^{(i)}$ must correspond to the same irreducible representation and to the same partners of that representation or they are orthogonal to one another.

To illustrate the meaning of these statements for a more general case, we will apply these selection rule concepts to the case of electric dipole transitions in Sect. 6.7 below. First, we express the perturbation \mathcal{H}' (in this case due to the electromagnetic field) in terms of the irreducible representations that \mathcal{H}' contains in the group of Schrödinger's equation:

$$\mathcal{H}' = \sum_{j, \beta} f_{\beta}^{(j)} \mathcal{H}_{\beta}^{(j)}, \quad (6.32)$$

where j denotes the irreducible representations Γ_j of the Hamiltonian \mathcal{H}' , and β denotes the partners of Γ_j . Then $\mathcal{H}' \phi_{\alpha}^{(i)}$, where (i) denotes irreducible representation Γ_i , transforms as the direct product representation formed by taking the direct product $\mathcal{H}_{\beta}^{(j)} \otimes \phi_{\alpha}^{(i)}$ which in symmetry notation is $\Gamma_{j, \beta} \otimes \Gamma_{i, \alpha}$. The matrix element $(\psi_{\alpha'}^{(i')}, \mathcal{H}' \phi_{\alpha}^{(i)})$ vanishes if and only if $\psi_{\alpha'}^{(i')}$ is orthogonal to all

the basis functions that occur in the decomposition of $\mathcal{H}'\phi_{\alpha}^{(i)}$ into irreducible representations. An equivalent expression of the same concept is obtained by considering the triple direct product $\psi_{\alpha'}^{(i')}\otimes\mathcal{H}_{\beta}^{(j)}\otimes\phi_{\alpha}^{(i)}$. In order for the matrix element in (6.31) to be nonzero, this triple direct product must contain a term that transforms as a scalar or a constant number, or according to the irreducible representation Γ_1 .

6.7 Example of Selection Rules

We now illustrate the group theory of Sect. 6.6 by considering electric dipole transitions in a system with O_h symmetry. The electromagnetic interaction giving rise to electric dipole transitions is

$$\mathcal{H}'_{\text{em}} = -\frac{e}{mc}\mathbf{p} \cdot \mathbf{A}, \quad (6.33)$$

in which \mathbf{p} is the momentum of the electron and \mathbf{A} is the vector potential of an external electromagnetic field. The momentum operator is part of the physical electronic “system” under consideration, while the vector \mathbf{A} for the electromagnetic field acts like an external system or like a “bath” or “reservoir” in a thermodynamic sense. Thus \mathbf{p} acts like an operator with respect to the group of Schrödinger’s equation but \mathbf{A} is invariant and does not transform under the symmetry operations of the group of Schrödinger’s equation. Therefore, in terms of group theory, \mathcal{H}'_{em} for the electromagnetic interaction transforms like a vector, just as p transforms as a vector, in the context of the group of Schrödinger’s equation for the unperturbed system $\mathcal{H}_0\psi = E\psi$. If we have unpolarized radiation, we must then consider all three components of the vector \mathbf{p} (i.e., p_x, p_y, p_z). In cubic symmetry, all three components of the vector transform as the same irreducible representation. If instead, we had a system which exhibits tetragonal symmetry, then p_x and p_y would transform as one of the two-dimensional irreducible representations and p_z would transform as one of the one-dimensional irreducible representations.

To find the particular irreducible representations that are involved in cubic symmetry, we consult the character table for $O_h = O \otimes i$ (see Table A.30). In the cubic group O_h the vector (x, y, z) transforms according to the irreducible representation T_{1u} and so does (p_x, p_y, p_z) , because both are radial vectors and both are odd under inversion. We note that the character table for O_h (Table A.30) gives the irreducible representation for vectors, and the same is true for most of the other character tables in Appendix A. To obtain the character table for the direct product group $O_h = O \otimes i$ we note that each symmetry operation in O is also compounded with the symmetry operations E and i of group $C_i = S_2$ (see Table A.2) to yield 48 symmetry operations and ten classes.

Table 6.2. Characters for the direct product of the characters for the T_{1u} and T_{2g} irreducible representations of group O_h

| E | $8C_3$ | $3C_2$ | $6C_2$ | $6C_4$ | i | $8iC_3$ | $3iC_2$ | $6iC_2$ | $6iC_4$ |
|-----|--------|--------|--------|--------|-----|---------|---------|---------|---------|
| 9 | 0 | 1 | -1 | -1 | -9 | 0 | -1 | 1 | 1 |

For the O_h group there will then be ten irreducible representations, five of which are even and five are odd. For the even irreducible representations, the same characters are obtained for class \mathcal{C} and class $i\mathcal{C}$. For the odd representations, the characters for classes \mathcal{C} and $i\mathcal{C}$ have opposite signs. Even representations are denoted by the subscript g (gerade) and odd representations by the subscript u (ungerade). The radial vector \mathbf{p} transforms as an odd irreducible representation T_{1u} since \mathbf{p} goes into $-\mathbf{p}$ under inversion.

To find selection rules, we must also specify the initial and final states. For example, if the system is initially in a state with symmetry T_{2g} then the direct product $\mathcal{H}'_{\text{em}} \otimes \psi_{T_{2g}}$ contains the irreducible representations found by taking the direct product $\chi_{T_{1u}} \otimes \chi_{T_{2g}}$. The characters for $\chi_{T_{1u}} \otimes \chi_{T_{2g}}$ are given in Table 6.2, and the direct product $\chi_{T_{1u}} \otimes \chi_{T_{2g}}$ is a reducible representation of the group O_h . Then using the decomposition formula (6.30) we obtain:

$$T_{1u} \otimes T_{2g} = A_{2u} + E_u + T_{1u} + T_{2u}. \quad (6.34)$$

Thus we obtain the selection rules that electric dipole transitions from a state T_{2g} can only be made to states with A_{2u} , E_u , T_{1u} , and T_{2u} symmetry. Furthermore, since \mathcal{H}'_{em} is an odd function, electric dipole transitions will couple only states with opposite parity. The same arguments as given above can be used to find selection rules between any initial and final states for the case of cubic symmetry. For example, from Table A.30, we can write the following direct products as

$$\left. \begin{aligned} E_g \otimes T_{1u} &= T_{1u} + T_{2u} \\ T_{1u} \otimes T_{1u} &= A_{1g} + E_g + T_{1g} + T_{2g} \end{aligned} \right\}.$$

Suppose that we now consider the situation where we lower the symmetry from O_h to D_{4h} . Referring to the character table for D_4 in Tables A.18 and 6.3, we can form the direct product group D_{4h} by taking the direct product between groups $D_{4h} = D_4 \otimes i$ where i here refers to group $S_2 = C_i$ (Table A.2).

We note here the important result that the vector in $D_{4h} = D_4 \otimes i$ symmetry does not transform as a single irreducible representation but rather as the irreducible representations:

$$\left. \begin{aligned} z &\rightarrow A_{2u} \\ (x, y) &\rightarrow E_u \end{aligned} \right\},$$

so that T_{1u} in O_h symmetry goes into: $A_{2u} + E_u$ in D_{4h} symmetry.

Table 6.3. Character table for the pint group D_4 (422)

| D_4 (422) | | | E | $C_2 = C_4^2$ | $2C_4$ | $2C'_2$ | $2C''_2$ |
|------------------|--------------------------|-------|-----|---------------|--------|---------|----------|
| $x^2 + y^2, z^2$ | R_z, z | A_1 | 1 | 1 | 1 | 1 | 1 |
| | | A_2 | 1 | 1 | 1 | -1 | -1 |
| | | B_1 | 1 | 1 | -1 | 1 | -1 |
| | | B_2 | 1 | 1 | -1 | -1 | 1 |
| (xz, yz) | (x, y) (R_x, R_y) | E | 2 | -2 | 0 | 0 | 0 |

Table 6.4. Initial and final states of group D_{4h} that are connected by a perturbation Hamiltonian which transform like z

| initial state | final state |
|---------------|-------------|
| A_{1g} | A_{2u} |
| A_{2g} | A_{1u} |
| B_{1g} | B_{2u} |
| B_{2g} | B_{1u} |
| E_g | E_u |
| A_{1u} | A_{2g} |
| A_{2u} | A_{1g} |
| B_{1u} | B_{2g} |
| B_{2u} | B_{1g} |
| E_u | E_g |

Furthermore a state with symmetry T_{2g} in the O_h group goes into states with $E_g + B_{2g}$ symmetries in D_{4h} (see discussion in Sect. 5.3). Thus for the case of the D_{4h} group, electric dipole transitions will only couple an A_{1g} state to states with E_u and A_{2u} symmetries. For a state with E_g symmetry according to group D_{4h} the direct product with the vector yields

$$E_g \otimes (A_{2u} + E_u) = E_g \otimes A_{2u} + E_g \otimes E_u = E_u + (A_{1u} + A_{2u} + B_{1u} + B_{2u}), \quad (6.35)$$

so that for the D_{4h} group, electric dipole transitions from an E_g state can be made to any odd parity state. This analysis points out that as we reduce the amount of symmetry, the selection rules are less restrictive, and more transitions become allowed.

Polarization effects also are significant when considering selection rules. For example, if the electromagnetic radiation is polarized along the z -direction in the case of the D_{4h} group, then the electromagnetic interaction involves only p_z which transforms according to A_{2u} . With the p_z polarization, the states listed in Table 6.4 are coupled by electric dipole radiation (i.e., by matrix elements of p_z).

If, on the other hand, the radiation is polarized in the x -direction, then the basis function is a single partner x of the E_u representation. Then if the

initial state has A_{1g} symmetry, the electric dipole transition will be to a state which transforms as the x partner of the E_u representation. If the initial state has A_{2u} symmetry (transforms as z), then the general selection rule gives $A_{2u} \otimes E_u = E_g$ while polarization considerations indicate that the transition couples the A_{2u} level with the xz partner of the E_g representation. If the initial state has E_u symmetry, the general selection rule gives

$$(E_u \otimes E_u) = A_{1g} + A_{2g} + B_{1g} + B_{2g}. \quad (6.36)$$

The polarization x couples the partner E_u^x to $A_{1g}^{x^2+y^2}$ and $B_{1g}^{x^2-y^2}$ while the partner E_u^y couples to A_{2g}^{xy-yx} and B_{2g}^{xy} . We note that in the character table for group D_{4h} the quantity $xy-yx$ transforms as the axial vector R_z or the irreducible representation A_{2u} and xy transforms as the irreducible representation B_{2g} . Thus polarization effects further restrict the states that are coupled in electric dipole transitions. If the polarization direction is not along one of the (x, y, z) directions, \mathcal{H}'_{em} will transform as a linear combination of the irreducible representations $A_{2u} + E_u$ even though the incident radiation is polarized.

Selection rules can be applied to a variety of perturbations \mathcal{H}' other than the electric dipole interactions, such as uniaxial stress, hydrostatic pressure and the magnetic dipole interaction. In these cases, the special symmetry of \mathcal{H}' in the group of Schrödinger's equation must be considered.

Selected Problems

6.1. Find the 4×4 matrix A that is the direct product $A = B \otimes C$ of the (2×2) matrices B and C given by

$$B = \begin{pmatrix} b_{11} & b_{12} \\ b_{21} & b_{22} \end{pmatrix} \quad \text{and} \quad C = \begin{pmatrix} c_{11} & c_{12} \\ c_{21} & c_{22} \end{pmatrix}.$$

6.2. (a) Show that if G_A with elements E, A_2, \dots, A_{h_a} and G_B with elements E, B_2, \dots, B_{h_b} are groups, then the direct product group $G_A \otimes G_B$ is also a group. Use the notation $B_{ij}C_{kl} = (B \otimes C)_{ik,jl}$ to label the rows and columns of the direct product matrix.

(b) In going from higher to lower symmetry, if the inversion operation is preserved, show that even representations remain even and odd representations remain odd.

6.3. (a) Consider electric dipole transitions in full cubic O_h symmetry for transitions between an initial state with A_{1g} symmetry (s -state in quantum mechanics notation) and a final state with T_{1u} symmetry (p -state in quantum mechanics notation). [Note that one of these electric dipole matrix elements is proportional to a term $(1|p_x|x)$, where $|1\rangle$ denotes the

s-state and $|x\rangle$ denotes the *x* partner of the *p*-state.] Of the nine possible matrix elements that can be formed, how many are nonvanishing? Of those that are nonvanishing, how many are equivalent, meaning partners of the same irreducible representation?

- (b) If the initial state has E_g symmetry (rather than A_{1g} symmetry), repeat part (a). In this case, there are more than nine possible matrix elements. In solving this problem you will find it convenient to use as basis functions for the E_g level the two partners $x^2 + \omega y^2 + \omega^2 z^2$ and $x^2 + \omega^2 y^2 + \omega z^2$, where $\omega = \exp(2\pi i/3)$.
- (c) Repeat part (a) for the case of electric dipole transitions from an *s*-state to a *p*-state in tetragonal D_{4h} symmetry. Consider the light polarized first along the *z*-direction and then in the *x*-*y* plane. Note that as the symmetry is lowered, the selection rules become less stringent.

- 6.4.** (a) Consider the character table for group C_{4h} (see Sect. 6.5). Note that the irreducible representations for group C_4 correspond to the fourth roots of unity. Note that the two one-dimensional representations labeled *E* are complex conjugates of each other. Why must they be considered as one-dimensional irreducible representations?
- (b) Even though the character table of the direct product of the groups $C_4 \otimes C_i$ is written out in Sect. 6.5, the notations C_{4h} and $(4/m)$ are used to label the direct product group. Clarify the meaning of C_{4h} and $(4/m)$.
 - (c) Relate the elements of the direct product groups $C_4 \otimes C_i$ and $C_4 \otimes C_{1h}$ (see Table A.3) and use this result to clarify why the notation C_{4h} and $(4/m)$ is used to denote the group $C_4 \otimes i$ in Sect. 6.5. How do groups $C_4 \otimes i$ and $C_4 \otimes \sigma_h$ differ?

- 6.5.** Suppose that a molecule with full cubic symmetry is initially in a T_{2g} state and is then exposed to a perturbation \mathcal{H}' inducing a magnetic dipole transition.

- (a) Since \mathcal{H}' in this case transforms as an axial vector (with the same point symmetry as angular momentum), what are the symmetries of the final states to which magnetic dipole transitions can be made?
- (b) If the molecule is exposed to stress along a (111) direction, what is the new symmetry group? What is the splitting under (111) stress of the T_{2g} state in O_h symmetry? Use the irreducible representations of the lower symmetry group to denote these states. Which final states in the lower symmetry group would then be reached by magnetic dipole transitions?
- (c) What are the polarization effects for polarization along the highest symmetry axes in the case of O_h symmetry and for the lower symmetry group?

- 6.6.** Show that the factor group of the invariant subgroup (E, σ_h) of group C_{3h} is isomorphic to the group C_3 . This is an example of how the C_3 group properties can be recovered from the $C_{3h} = C_3 \otimes \sigma_h$ group by factoring out the (E, σ_h) group.

Part III

Molecular Systems

Electronic States of Molecules and Directed Valence

This chapter considers the electronic states of molecules, the formation of molecular bonds and the simplifications that are introduced through the use of group theory. We organize our discussion in this chapter in terms of a general discussion of molecular energy levels; the general concept of equivalence; the concept of directed valence bonding; the application of the directed valence bond concept to various molecules, including bond strengths in directed valence bonds; and finally σ and π bonding.

7.1 Introduction

The energy levels of molecules are basically more complicated than those of atoms because there are several centers of positive charge which serve to attract a given electron, and because these centers are themselves in relative motion. Since the nuclei are very massive relative to the electrons, we can utilize the Born–Oppenheimer approximation which separates out the electronic motion from the nuclear or ionic motion. In this approximation, the electrons move in a potential generated by the equilibrium positions of the nuclei. We are thus left with three kinds of molecular motion, the electronic motion which is most energetic, the vibrational motion which is less energetic, and the rotational motion which is least energetic. If these motions are independent they can be decoupled (but this is not always the case). In this chapter we consider the electronic energy levels of some typical molecules considering the Born–Oppenheimer approximation, and in Chap. 8 we consider the vibrational and rotational levels of molecules.

The effective one-electron potential $V(\mathbf{r})$ for an electron in a molecule must be invariant under all symmetry operations which leave the molecule invariant. If we did not exploit the symmetry explicitly through group theory, we would then solve the Schrödinger equation to find the energy eigenvalues

and the corresponding eigenfunctions of the molecule taking into account all the valence electrons for all the atoms in the molecule. This would require solution of a large secular equation of the form:

$$|\langle \psi_i | \mathcal{H} | \psi_j \rangle - E \delta_{ij}| = 0. \quad (7.1)$$

Utilization of symmetry (as for example using group theoretical methods) allows us to choose our basis functions wisely, so that many of the matrix elements in the secular equation vanish through symmetry arguments and the secular equation breaks up into block diagonal form. Thus by using symmetry, we have to solve much smaller secular equations, and only those states which transform according to the same irreducible representations will couple to each other according to group theory arguments. Group theory is used in yet another way for solving the electronic problem. Many molecules contain more than one *equivalent* atom. Symmetry is used to simplify the secular equation by forming linear combinations of atomic orbitals that transform according to the irreducible representations of the group of Schrödinger's equation. Using such linear combinations of atomic orbitals, the secular equation can more readily be brought into block diagonal form. In this chapter we show how to form linear combinations of atomic orbitals that transform as irreducible representations of the appropriate symmetry group, and we will show how the *equivalence* concept is used in forming these linear combinations.

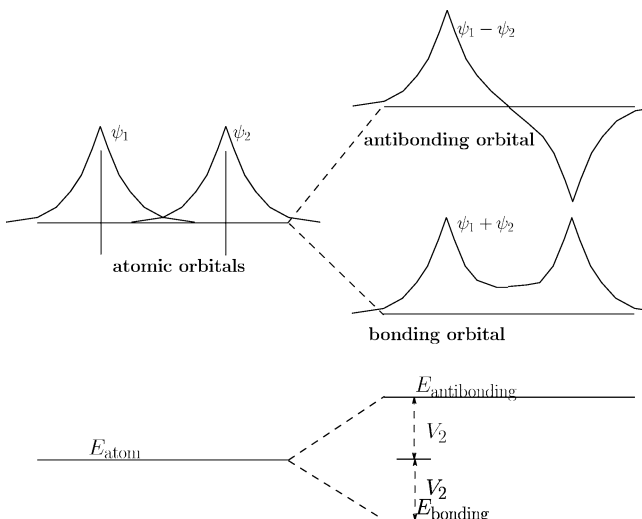


Fig. 7.1. Electronic wave functions for a diatomic molecule. On the *left* the free atomic orbitals are shown for two similar atoms on different sites. On the *right*, the formation of bonding and antibonding states is indicated. To find the energy splitting between the bonding and antibonding states (indicated schematically), the solution of Schrödinger's equation is necessary

In the free atom, the electronic orbitals display the symmetry of a $(1/r)$ potential, and therefore the free-atom orbitals are eigenfunctions which transform according to irreducible representations of the *full rotation group*. In a molecule or in a solid, the electrons tend to spend more time between the ion cores in the bonding state and the increased probability of finding the electron between two nuclei (see Fig. 7.1) is called a chemical bond. These bonds display the known symmetry of the molecule (or the solid). For this reason, the wavefunctions for the electrons in the molecule (or the solid) transform as irreducible representations of the appropriate symmetry group, which in general will be of lower symmetry than the full rotation group. From elementary considerations, we know that molecular bonds arise from the *exchange interaction* whose magnitude depends on the extent of the overlap of the charge clouds between neighboring atoms. Because these orbitals concentrate the charge along preferred directions, the bonding is called *directed valence bonding*, and these directed valence bonds exhibit the symmetry of the molecule (or of the solid). We use the directed valence bonding concepts to identify the kinds of symmetries needed to make the desired orbitals.

Symmetry enters the electronic problem of molecules in yet another way, namely through the Pauli principle and the effect of the permutation of the electrons on the electron wavefunctions. This topic is discussed in Chap. 17 for many-electron states.

7.2 General Concept of Equivalence

Equivalent bonding orbitals for a molecule are required to transform into one another under all the symmetry operations of the point group with no more change than a possible change of phase. The equivalence transformation, which takes one *equivalent function* into another, generates a representation for the point group called the equivalence representation. The equivalence representation will in general be reducible. We denote the representation that generates the transformation between equivalent atom sites by $\Gamma^{\text{a.s.}}$ and its characters by $\chi^{\text{a.s.}}$ where a.s. \equiv atomic sites. In this section we present the equivalence concept, show how to find the irreducible representations contained in the equivalence representation and then give a few examples.

The matrices $D^{\text{a.s.}}(R)_{ji}$ for the equivalence representation $\Gamma^{\text{a.s.}}$ are found from the general definition in (4.1)

$$\hat{P}_R \psi_i = \sum_j D^{\text{a.s.}}(R)_{ji} \psi_j \quad (7.2)$$

or written in matrix form from (4.5)

$$D^{\text{a.s.}}(R)_{ji} = \langle \psi_j | \hat{P}_R | \psi_i \rangle. \quad (7.3)$$

Explicitly, the $D^{\text{a.s.}}(R)_{ji}$ matrices are found by entering unity into the j, i position in the matrix if $\hat{P}(R)$ takes site i into an equivalent site j and zero

otherwise. From this argument we readily see that the characters for the equivalence representation can be found by counting the number of points which are left unaffected by the symmetry operation, because it is only those points that will give a contribution to the matrix on diagonal positions and will thus contribute to the character for that symmetry operator. To obtain the characters for the equivalence representation $\chi^{\text{a.s.}}$, we take a representative member of each class and consider the number of points that are left unchanged under action of the representative symmetry operator.

The representation $\Gamma^{\text{a.s.}}$ is in general reducible. The pertinent symmetry types for the problem are then found by decomposing $\Gamma^{\text{a.s.}}$ into its irreducible representations. To illustrate this concept, consider the example of three identical atoms at the corners of an equilateral triangle as for example the three hydrogen atoms in the NH_3 molecule. The symmetry group is C_{3v} , and the character table for group C_{3v} is given in Table A.10. Referring to Fig. 4.2, where the three equivalent sites are labeled by (a, b, c) we obtain $D^{\text{a.s.}}(R)$ for some typical symmetry operators:

$$D^{\text{(a.s.)}}(E) = \begin{pmatrix} 1 & 0 & 0 \\ 0 & 1 & 0 \\ 0 & 0 & 1 \end{pmatrix}, \quad (7.4)$$

$$D^{\text{(a.s.)}}(C_3) = \begin{pmatrix} 0 & 0 & 1 \\ 1 & 0 & 0 \\ 0 & 1 & 0 \end{pmatrix}, \quad (7.5)$$

$$D^{\text{(a.s.)}}(\sigma_v) = \begin{pmatrix} 1 & 0 & 0 \\ 0 & 0 & 1 \\ 0 & 1 & 0 \end{pmatrix}, \quad (7.6)$$

in which the rows and columns correspond to the sequence of atoms (a, b, c) and the symmetry operations selected are E , D , and A following Fig. 4.2. From these matrices we can compute the characters for each of the classes for the $\Gamma^{\text{a.s.}}$ representation in group $C_{3v}(3m)$. The character $\chi^{\text{a.s.}}(R)$ is always the number of sites that are left unchanged by the operation \hat{P}_R so that for each of the three classes $\chi^{\text{a.s.}}(E) = 3$, $\chi^{\text{a.s.}}(C_3) = 0$, and $\chi^{\text{a.s.}}(\sigma_v) = 1$. These results are summarized in Table 7.1. From Table A.10 we see immediately that $\chi^{\text{a.s.}} = \chi^{\Gamma_1} + \chi^{\Gamma_2}$ for every class, since $\Gamma^{\text{a.s.}} = \Gamma_1 + \Gamma_2$, in agreement with results obtained in Sect. 4.6. The orbitals on the nitrogen atom are then chosen so that they bond to the atomic orbitals of the three hydrogen atoms, as discussed in Sect. 7.5.1.

Table 7.1. $\chi^{\text{a.s.}}$ for the group C_{3v}

| | E | $2C_3$ | $3\sigma_v$ | |
|----------------------|-----|--------|-------------|---|
| $\chi^{\text{a.s.}}$ | 3 | 0 | 1 | $\Rightarrow \Gamma_1 + \Gamma_2 = A_1 + E$ |

7.3 Directed Valence Bonding

For diatomic molecules we know immediately, without recourse to group theory, how to make a bonding orbital out of the free atomic orbitals. In this case, we need simply to take the symmetrical combination $(\psi_a + \psi_b)$ to pile up charge in the directed valence bond (see Fig. 7.1).

For the case of the homopolar diatomic molecule, we thus form an occupied bonding state $(\psi_a + \psi_b)$ and an unoccupied antibonding state of higher energy $(\psi_a - \psi_b)$. Suppose that this diatomic molecule only has two symmetry operations, the identity E and the mirror plane reflections σ_h or m . These are the two symmetry elements of the group C_{1h} (see Table 7.2). (In Sect. 7.4 we will consider the semi-infinite groups $D_{\infty h}$ and $C_{\infty v}$ which give the full symmetry of typical homogeneous and heterogeneous diatomic molecules.) Taking ψ_a as an arbitrary function, and noting that $\hat{P}_m \psi_a = \psi_b$, for the mirror plane operations, the projection operator for one-dimensional irreducible representations (see (4.38)) can be written as

$$\hat{P}^{(\Gamma_n)} = \frac{\ell_n}{h} \sum_R \chi^{(\Gamma_n)}(R)^* \hat{P}_R. \quad (7.7)$$

The basic formula (7.7) for finding linear combinations of atomic orbitals when acting on the wave function ψ_a yields (see Table 7.2):

$$\begin{aligned} \hat{P}^{(\Gamma_1)} \psi_a &= \frac{1}{2} [(1) \hat{P}_E \psi_a + (1) \hat{P}_m \psi_a] = \frac{1}{2} [\psi_a + \psi_b] \quad \text{bonding} \\ \hat{P}^{(\Gamma'_1)} \psi_a &= \frac{1}{2} [(1) \hat{P}_E \psi_a + (-1) \hat{P}_m \psi_a] = \frac{1}{2} [\psi_a - \psi_b] \quad \text{antibonding} \end{aligned} \quad (7.8)$$

for the bonding and antibonding states, so that the bonding orbitals will have Γ_1 symmetry and the antibonding orbitals will have Γ'_1 symmetry. Since there are only two initial wave functions ψ_a and ψ_b , the combinations in (7.8) are all the independent linear combinations that can be formed, and except for a normalization factor of $\sqrt{2}$, these functions are proper bonding and antibonding orbitals.

Our discussion of the use of projection operators (see Sects. 4.5 and 4.6) illustrates how linear combinations of atomic orbitals could be found such that the resulting orbitals transform according to irreducible representations of the

Table 7.2. Character table for the group C_{1h}

| $C_{1h}(m)$ | | | E | σ_h |
|----------------------|---------------|-------------------|-----|--|
| x^2, y^2, z^2, xy | R_z, x, y | $A' (\Gamma_1)$ | 1 | 1 |
| xz, yz | R_x, R_y, z | $A'' (\Gamma'_1)$ | 1 | -1 |
| $\chi^{\text{a.s.}}$ | | | 2 | $0 \Rightarrow \Gamma_1 + \Gamma'_1 \equiv A' + A''$ |

point group. Here we used the C_{1h} group that has only two one-dimensional irreducible representations, and we found the two related electronic states. However, most of the symmetry groups have many irreducible representations with different dimensionalities. To find the right symmetries for the electronic states, one would have to apply the projectors to all of them. This process is largely simplified by using the *directed valence representation* $\Gamma_{D.V.}$ which introduces two kinds of simplifications:

- $\Gamma_{D.V.}$ gives all the *irreducible representations* for the molecular orbitals before the molecular orbitals are found explicitly. This saves time because the projection operator $\hat{P}^{(\Gamma_n)}$ need not then be applied to irrelevant representations, but only to those irreducible representations contained in $\Gamma_{D.V.}$.
- If we are only interested in finding the number of distinct eigenvalues and their degeneracies, this follows directly from the characters $\chi_{D.V.}$ of the representation $\Gamma_{D.V.}$. To obtain this kind of information, it is not necessary to solve Schrödinger's equation or even to find the linear combination of molecular orbitals as in Sect. 4.6.

The directed valence representation $\Gamma_{D.V.}$ uses the equivalence transformation to determine the characters of $\Gamma^{a.s.}$. In Sect. 7.4 we discuss the directed valence representation for diatomic molecules and in Sect. 7.5, we extend the concept to multiaatomic molecules with more complicated symmetries.

7.4 Diatomic Molecules

In this section we introduce the semi-infinite groups $D_{\infty h}$ and $C_{\infty v}$ and we illustrate the use of the equivalence transformation to form symmetrized linear combinations of atomic orbitals. We then develop the directed valence representation for the simplest case of diatomic molecules. Both homonuclear molecules (like H_2) and heteronuclear molecules (like CO) are considered.

7.4.1 Homonuclear Diatomic Molecules

The simplest molecules are the homonuclear diatomic molecules. For homonuclear molecules (such as H_2) the appropriate symmetry group is $D_{\infty h}$ and the character table for $D_{\infty h}$ is shown in Table 7.3 (see also Table A.34). We now summarize the main points about this character table. C_ϕ denotes an arbitrary rotation about the linear molecular axis (z -axis) and C'_2 is a twofold axis \perp to C_ϕ . In the group $D_{\infty h}$, each of the operations E , C_ϕ , and C'_2 is also combined with inversion. We further note that σ_v is a mirror plane through the molecular axis, so that $\sigma_v = iC'_2$. The subscripts g and u refer to the evenness and oddness of functions under the inversion operation, while the superscripts $+$ and $-$ refer to the evenness and oddness of functions under reflection in a mirror plane. The characters for σ_v in the $D_{\infty h}$ group are found

Table 7.3. Character table for the semi-infinite group $D_{\infty h}$ (∞/mn)

| $D_{\infty h}$ (∞/mm) | | | E | $2C_\phi$ | C'_2 | i | $2iC_\phi$ | iC'_2 |
|--------------------------------|------------|----------------------|----------|----------------|----------|----------|-----------------|----------|
| $x^2 + y^2, z^2$ | R_z | $A_{1g}(\Sigma_g^+)$ | 1 | 1 | 1 | 1 | 1 | 1 |
| | | $A_{1u}(\Sigma_u^-)$ | 1 | 1 | 1 | -1 | -1 | -1 |
| | | $A_{2g}(\Sigma_g^-)$ | 1 | 1 | -1 | 1 | 1 | -1 |
| | | $A_{2u}(\Sigma_u^+)$ | 1 | 1 | -1 | -1 | -1 | 1 |
| | (xz, yz) | $E_{1g}(\Pi_g)$ | 2 | $2 \cos \phi$ | 0 | 2 | $2 \cos \phi$ | 0 |
| | | $E_{1u}(\Pi_u)$ | 2 | $2 \cos \phi$ | 0 | -2 | $-2 \cos \phi$ | 0 |
| | (x, y) | $E_{2g}(\Delta_g)$ | 2 | $2 \cos 2\phi$ | 0 | 2 | $2 \cos 2\phi$ | 0 |
| | | $E_{2u}(\Delta_u)$ | 2 | $2 \cos 2\phi$ | 0 | -2 | $-2 \cos 2\phi$ | 0 |
| | | | \vdots | \vdots | \vdots | \vdots | \vdots | \vdots |

Table 7.4. $\chi^{\text{a.s.}}$ for the group $D_{\infty h}$

| E | $2C_\phi$ | $C'_2 = i\sigma_v$ | i | $2iC_\phi$ | $iC'_2 = \sigma_v$ | |
|----------------------|-----------|--------------------|-----|------------|--------------------|---|
| $\chi^{\text{a.s.}}$ | 2 | 2 | 0 | 0 | 0 | 2 |

$\Rightarrow A_{1g} + A_{2u}$
 $\Rightarrow \Sigma_g^+ + \Sigma_u^+$

most conveniently by considering the effect of the operation σ_v on the basis functions which correspond to a given irreducible representation. For example, the symmetry operation σ_v changes (x, y) into $(-x, y)$ yielding a transformation matrix

$$D(\sigma_v) = \begin{pmatrix} -1 & 0 \\ 0 & 1 \end{pmatrix} \quad (7.9)$$

and the corresponding character for σ_v is $\chi(\sigma_v) = 0$ which from the character table is associated with the E_{1u} irreducible representation.

For a homogeneous diatomic molecule (such as H_2) use of the equivalence transformation on the two sites of the homogeneous diatomic molecule, as shown in Table 7.4 yields the characters for the equivalence transformation. When forming a linear combination of atomic orbitals (LCAOs) from s functions on the two equivalent atomic sites (see Sect. 7.3), the normalized bonding orbital $\psi_S = (\psi_a + \psi_b)/\sqrt{2}$ is symmetric and has Σ_g^+ or A_{1g} symmetry and the normalized antibonding orbital $\psi_A = (\psi_a - \psi_b)/\sqrt{2}$ is antisymmetric and has Σ_u^+ or A_{2u} symmetry. These two LCAOs correspond to directed valence orbitals because they result in a rearrangement of the charge on the individual atomic sites. The bonding LCAO is a directed valence orbital corresponding to a pile up of charge between the two atoms to produce a lower energy state. By using the equivalence concept in Sect. 7.2, we have constructed a linear combination of atomic orbitals which transform as irreducible representations of the group of Schrödinger's equation. Thus ψ_S and ψ_A form such basis functions and the Hamiltonian for the homogeneous diatomic molecule will not couple states ψ_S and ψ_A to each other. This follows from the argument that the product $(\mathcal{H}\psi_S)$ transforms as A_{1g} , since \mathcal{H} transforms as A_{1g} and so does

ψ_S . Also ψ_A transforms as A_{2u} . The selection rules thus tell us that the matrix element $(\psi_A | \mathcal{H} | \psi_S)$ must vanish. Thus to bring the secular equation into block diagonal form, we have to make a unitary transformation on the atomic basis functions (ψ_a, ψ_b) to bring them into the form (ψ_S, ψ_A) :

$$\begin{pmatrix} \psi_S \\ \psi_A \end{pmatrix} = \underbrace{U}_{\text{unitary matrix}} \begin{pmatrix} \psi_a \\ \psi_b \end{pmatrix} = \begin{pmatrix} \frac{1}{\sqrt{2}} & \frac{1}{\sqrt{2}} \\ \frac{1}{\sqrt{2}} & -\frac{1}{\sqrt{2}} \end{pmatrix} \begin{pmatrix} \psi_a \\ \psi_b \end{pmatrix}. \quad (7.10)$$

Applying the unitary transformation $U\mathcal{H}U^\dagger$ to the original matrix (written in terms of the original ψ_a and ψ_b) will bring the secular matrix into block diagonal form. Bringing the secular equation into block diagonal form greatly simplifies the solution of the secular equation. In this simple case, the equivalence transformation and group theoretical arguments took a coupled (2×2) secular equation and decomposed it into two decoupled (1×1) secular equations. The bonding or directed valence state will be the state of lowest energy.

As an example of homonuclear diatomic molecule we discuss the hydrogen molecule H_2 . In this case we can put each electron in a $(\sigma_g 1s)$ orbital and construct bonding and antibonding orbitals. For H_2 , the bonding orbital σ_g is occupied with electrons having opposite spin states and the antibonding σ_u orbital is unoccupied. The $(\sigma_g 1s)$ state is symmetric under both inversion i and reflection σ_v . Hence the symmetry for each of the separated atoms is Σ_g^+ so that the symmetry for the molecule is $\Sigma_g^+ \otimes \Sigma_g^+ = \Sigma_g^+$. We write this state as ${}^1\Sigma_g^+$ where the superscript 1 denotes a singlet ($s = 0$) with a total spin degeneracy of $(2s + 1) = 1$. By making spatial bonding orbitals that are symmetric under exchange of the electrons, the Pauli principle tells us that the spin state for the directed valence bonding orbital must be antisymmetric:

$$\frac{1}{\sqrt{2}} [\alpha(1)\beta(2) - \alpha(2)\beta(1)], \quad (7.11)$$

where (α, β) give the spin state (up, down), and 1,2 number the electrons (group theory aspects for spin are treated in Chaps. 14 and 15). In Problem 7.1 we extend the concepts of Sect. 7.4.1 to the hypothetical He_2 molecule and the H_2^- ion.

7.4.2 Heterogeneous Diatomic Molecules

We next illustrate the case of a linear heterogeneous diatomic molecule with the CO molecule. Since the electronic wave functions on each site are not equivalent (see Fig. 7.2), there is no inversion symmetry. The appropriate symmetry group for CO is $C_{\infty v}$ which has the Character Table 7.5 (see also Table A.33). The symmetry operations of $C_{\infty v}$ have already been covered when discussing the symmetry operations of $D_{\infty h}$ (see Sect. 7.4.1). Using the equivalence operation on the carbon and oxygen atoms in CO, we have the result $\Gamma^{\text{a.s.}} = 2A_1$ (see also $\chi^{\text{a.s.}}(E, 2C_\phi, \sigma_v)$ for H_2 with $D_{\infty h}$ symmetry in

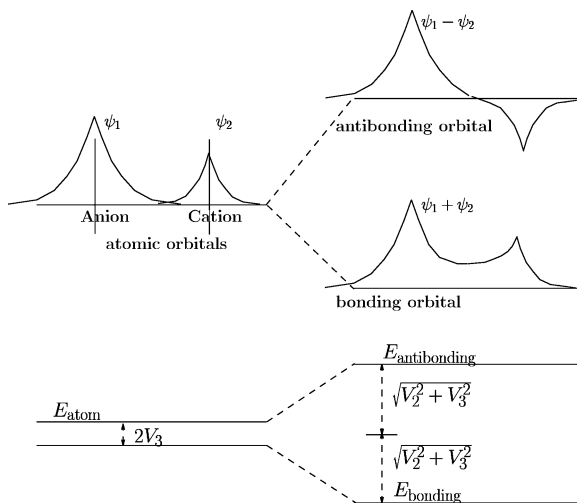


Fig. 7.2. The wave functions for a heteropolar diatomic molecule and their formation of bonding and antibonding states. If $2V_3$ is the energy separation between the anion and cation for large interatomic distance, the splitting resulting from an interaction energy $2V_2$ is shown

Table 7.5. Character Table for Group $C_{\infty v}$

| $C_{\infty v} (\infty m)$ | | | E | $2C_\phi$ | σ_v |
|---------------------------|--------------------------------|-----------------|----------|----------------|------------|
| $(x^2 + y^2, z^2)$ | z | $A_1(\Sigma^+)$ | 1 | 1 | 1 |
| | R_z | $A_2(\Sigma^-)$ | 1 | 1 | -1 |
| (xz, yz) | (x, y) $\{ (R_x, R_y) \}$ | $E_1(\Pi)$ | 2 | $2 \cos \phi$ | 0 |
| $(x^2 - y^2, xy)$ | | $E_2(\Delta)$ | 2 | $2 \cos 2\phi$ | 0 |
| | | \vdots | \vdots | \vdots | \vdots |

Sect. 7.4.1). Now the C atom in CO has the electronic configuration $2s^22p^2$ while O has the configuration $2s^22p^4$. We will then make bonding and antibonding molecular orbitals from $2s$, $2p_z$, and $2p_{x,y}$ atomic orbitals. From the basis functions given in the character table for group $C_{\infty v}$ we see that the irreducible representations for these atomic orbitals are

$$2s \rightarrow A_1$$

$$2p_z \rightarrow A_1$$

$$2p_{x,y} \rightarrow E_1 .$$

To find the direct products using the character table for $C_{\infty v}$ we note that

$$\cos^2 \phi = \left(\frac{1}{2} \right) (1 + \cos 2\phi) ,$$

which allows us to evaluate the direct product $E_1 \otimes E_1$ to obtain

$$E_1 \otimes E_1 = A_1 + A_2 + E_2.$$

state is symmetric, the spin state is antisymmetric by the Pauli principle (a singlet spin configuration). However, an antisymmetric spatial state (such as the A_2 state) is accompanied by a symmetric spin state (a triplet spin configuration) and therefore would have a molecular orbital notation $^3\Sigma^-$ (see character table for $D_{\infty h}$ in Sect. 7.4.1). The secular equation implied by the interactions in Fig. 7.2 (see caption) is

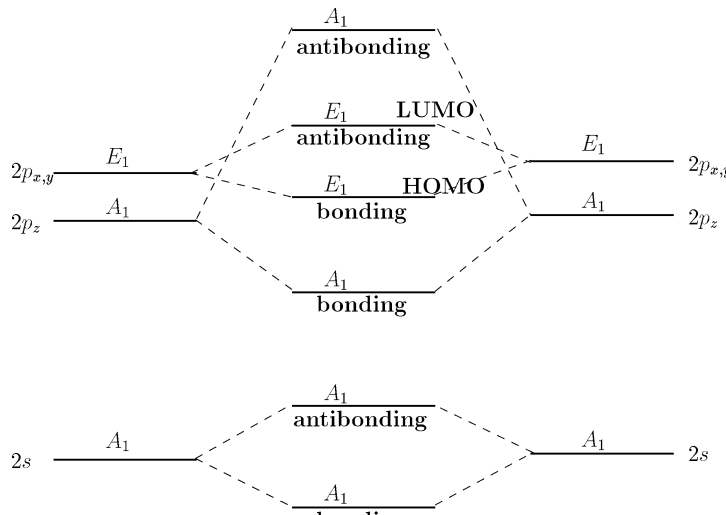
$$\begin{vmatrix} V_3 - E & V_2 \\ V_2 & -V_3 - E \end{vmatrix} = 0, \quad (7.12)$$

whose solution gives the splitting between the bonding and antibonding states of heteropolar diatomic molecules

$$E = \pm \sqrt{V_2^2 + V_3^2} \quad (7.13)$$

as shown in Fig. 7.2.

Referring to Fig. 7.3 the number of electrons which form bonds in CO are four from carbon and six from oxygen to give a total of ten electrons. We note from Fig. 7.3 that the occupied levels include the 2s A_1 bonding



C: $2s^22p^2$

CO molecule

O: $2s^22p^4$

Fig. 7.3. Bonding and antibonding molecular levels for the CO molecule

and antibonding orbitals and the 2p A_1 and E_1 bonding orbitals. The 2p A_1 and E_1 antibonding orbitals will remain unoccupied. Since the p_z orbitals are directed along the molecular axis, the bonding–antibonding interaction (and level splitting) will be largest for the p_z orbitals, as shown in Fig. 7.3.

The symmetry of the s-function orbitals for a diatomic molecule are found directly from the transformation properties of $\chi^{\text{a.s.}}$. However, since p electrons have angular momentum $l = 1$, they transform like the vector (basis functions x, y, z), so that for p-function orbitals we must take the direct product of the transformation of the equivalent sites with the transformation properties of a vector at each site written as $\chi^{\text{a.s.}} \otimes \chi^{\text{vector}}$. For the case of the heterogeneous CO molecule with $C_{\infty v}$ symmetry $\chi^{\text{a.s.}} = 2A_1 = 2\Sigma^+$ and $\chi^{\text{vector}} = A_1 + E_1 = \Sigma^+ + \Pi$. With regard to the p_z orbital, both the bonding and antibonding orbitals (see Fig. 7.3) have A_1 or Σ^+ symmetry. For the bonding p_z orbital, there is a maximum of the charge accumulation between the C and O atoms which results in the large separation in energy between the bonding and antibonding orbitals. For the (p_x, p_y) orbitals, the bonding and antibonding levels both have E_1 or Π symmetry. The character table for group $C_{\infty v}$ (Table 7.5) relates the notation for the irreducible representations

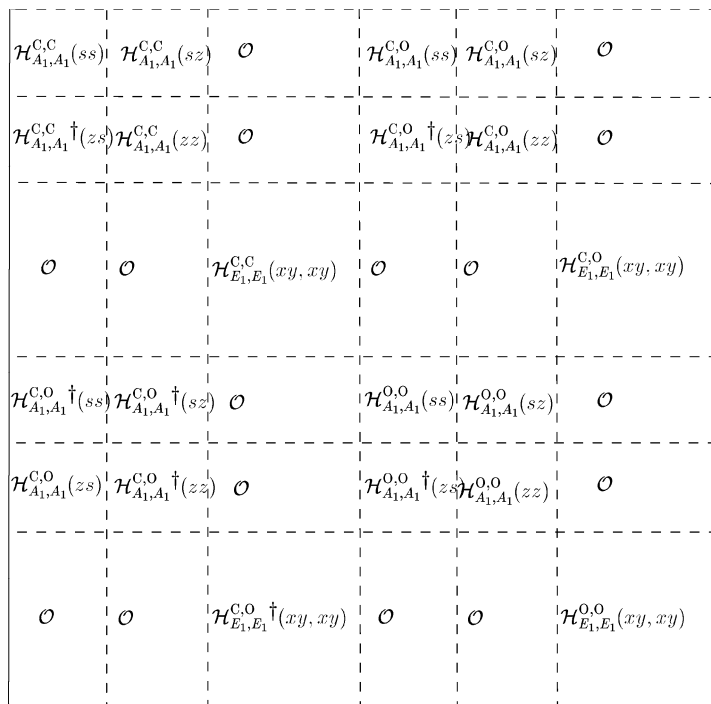


Fig. 7.4. Schematic diagram of the block structure of the matrix Hamiltonian for molecular orbitals for the CO molecule arising from the symmetry of the orbitals

with angular momenta states. The directed valence bonding is along the z -axis and involves only bonding levels.

The symmetry types of each of the molecular orbitals determines the form of the secular equation, as shown in Fig. 7.4. The minimum basis for describing the bonding states is eight, including the $2s$, $2p_x$, $2p_y$, and $2p_z$ orbitals for each atom, since the $1s$ level is too low in energy to be of importance. The terms on the diagonals represent the self energy of the electronic orbitals, and the terms in the off-diagonal positions are the coupling terms. Only electronic states belonging to the same irreducible representation can couple, and the block structure of the matrix Hamiltonian of the secular equation then assumes the form shown in Fig. 7.4.

7.5 Electronic Orbitals for Multiaatomic Molecules

In this section, we consider the electronic levels for several multiaatomic molecules, each selected for particular pedagogic purposes.

7.5.1 The NH_3 Molecule

To bond to the H atoms, the N atom must make orbitals directed to the three hydrogens (see Fig. 7.5). We refer to this as the directed valence bonds of the nitrogen atoms. The directed valence bonds $\Gamma_{\text{D.V.}}$ for the nitrogen must therefore exhibit the same symmetry as does the LCAO (linear combination of atomic orbitals) for the hydrogens which transform as $\Gamma^{\text{a.s.}}$. We have already seen in Sect. 4.6 how to construct LCAOs for the three equivalent atoms at the

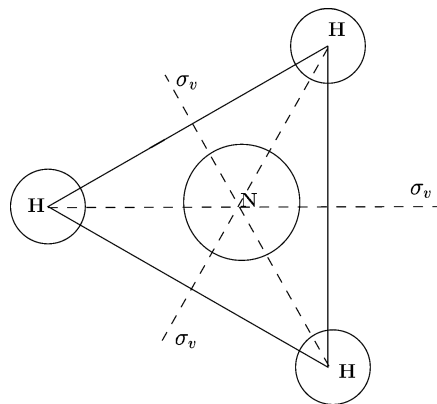


Fig. 7.5. Schematic diagram of the symmetry operations for an NH_3 molecule (group C_{3v}) where the three hydrogen atoms are at the corners of an equilateral triangle and the N atom is along the normal through the midpoint of this triangle but not coplanar with the hydrogens

corners of an equilateral triangle (e.g., the hydrogen atoms in NH_3). In this case we use group C_{3v} (see Fig. 7.5) and obtain the irreducible representations $A_1 + E$ for the linear combination of atomic orbitals for the three hydrogen atoms discussed in Sects. 4.6 and 7.2. To bond to the nitrogen atom, it is necessary for the directed valence representation $\Gamma_{\text{D.V.}}$ for the nitrogen atom to have the same symmetries as $\Gamma^{\text{a.s.}}$ so that $\Gamma_{\text{D.V.}} = \Gamma_1 + \Gamma_2 = A_1 + E$.

We now explore the orbitals that can be made at the nitrogen site. Nitrogen has the electronic configuration $1s^2 2s^2 2p^3$. The $1s$ and $2s$ electrons will lie low in energy, and bonding orbitals to the hydrogens will be made with the three $2p$ electrons [40]. The p electrons transform like the vectors (x, y, z) and the character table for C_{3v} shows that the p_x and p_y functions will transform as $E(\Gamma_2)$ and the p_z as $A_1(\Gamma_1)$. The nitrogen atom thus bonds to the linear combination of atomic orbitals of the three hydrogen atoms with the same symmetries $A_1 + E$ that comes from $\Gamma^{\text{a.s.}}$. Thus the nitrogen has three p electrons for bonding and the H_3 likewise has three electrons for bonding. The A_1 bonding states will hold two electrons and the E bonding state will hold four electrons. These bonding states can then accommodate all six valence electrons, with three coming from the hydrogen atoms and three from the nitrogen atom. All the antibonding states will be unoccupied. See reference [40] for a detailed analysis of the molecular orbitals of NH_3 and other molecules discussed in this chapter from a group theory standpoint.

7.5.2 The CH_4 Molecule

In this example we consider generally how carbon atoms can form tetrahedral bonds. One example of such tetrahedral bonds for carbon is in the diamond structure. The tetrahedral carbon bonds in diamond have the same point group symmetry as the directed valence bond of carbon in the CH_4 methane molecule. The methane molecule forms a regular tetrahedron (see Fig. 3.3), where the carbon atom is at the center of the tetrahedron, and the four H atoms are at the tetrahedral vertices; this structure has T_d point symmetry (see Table A.32).

The bonding of the CH_4 molecule is produced by a directed valence bond from the carbon atom to the four hydrogen atoms at the corners of a tetrahedron. The ground state of the carbon atom is $1s^2 2s^2 2p^2$. We will see below that the carbon atom must be promoted to a $1s^2 2s^1 2p^3$ configuration to make the directed valence bonds. The four equivalent hydrogen atoms form LCAOs to make the bonds from the four points labeled a, b, c, d in Fig. 3.3 (where the four hydrogens are located) to the center of the tetrahedron where the carbon atom is located.

Let us start with the symmetry of the linear combination of atomic orbitals of the four hydrogen atoms at the corner of a regular tetrahedron which has T_d symmetry (see Table A.32 and Table 7.6). The 24 symmetry operations of T_d are described in Sect. 3.11 and in Fig. 3.3. If we now consider each of the symmetry operations the group T_d acting on the points a, b, c, d (see Fig. 3.3)

Table 7.6. Character Table for group $T_d(43m)$

| $T_d(43m)$ | | E | $8C_3$ | $3C_2$ | $6\sigma_d$ | $6S_4$ | |
|-------------------|------------------------|-----|--------|--------|-------------|--------|-------------------------|
| (R_x, R_y, R_z) | A_1 | 1 | 1 | 1 | 1 | 1 | |
| | A_2 | 1 | 1 | 1 | -1 | -1 | |
| | E | 2 | -1 | 2 | 0 | 0 | |
| | T_1 | 3 | 0 | -1 | -1 | 1 | |
| | T_2 | 3 | 0 | -1 | 1 | -1 | |
| | $\Gamma^{\text{a.s.}}$ | 4 | 1 | 0 | 2 | 0 | $\Rightarrow A_1 + T_2$ |

where the four hydrogens are located, we obtain the equivalence representation for the hydrogen orbitals $\Gamma^{\text{a.s.}}$. Some typical matrices for the symmetry operations of T_d in the equivalence representation $\Gamma^{\text{a.s.}}$ for the four hydrogen atoms are

$$D^{\text{a.s.}}(E) = \begin{pmatrix} 1 & 0 & 0 & 0 \\ 0 & 1 & 0 & 0 \\ 0 & 0 & 1 & 0 \\ 0 & 0 & 0 & 1 \end{pmatrix}, \quad (7.14)$$

$$D^{\text{a.s.}}(C_3) = \begin{pmatrix} 1 & 0 & 0 & 0 \\ 0 & 0 & 1 & 0 \\ 0 & 0 & 0 & 1 \\ 0 & 1 & 0 & 0 \end{pmatrix}, \quad (7.15)$$

etc., where the rows and columns relate to the array $(a \ b \ c \ d)$ of Fig. 3.3. To find the characters for each class we use the equivalence transformation principle to find how many sites go into themselves under the symmetry operations of each class of T_d . The results for the characters of the equivalence representation $\Gamma^{\text{a.s.}}$ formed from transforming the atom sites (a.s.) according to the symmetry operations of group T_d are summarized just under the character table for T_d (see Table 7.6). Using the decomposition theorem (3.20) we then find the irreducible representations of T_d that are contained in $\Gamma^{\text{a.s.}}$ (see Table 7.6). Thus $\Gamma^{\text{a.s.}}$ gives the symmetries for the LCAOs for the equivalence transformation showing that these orbitals are made of an s-function transforming as A_1 and a p-function transforming as T_2 .

The linear combination of the atomic orbitals of the four hydrogen atoms transforming as A_1 is clearly the symmetric sum of the atomic orbitals.

$$\psi(A_1) = \frac{1}{2}(\psi_a + \psi_b + \psi_c + \psi_d) \quad (7.16)$$

and the three degenerate partners of the T_2 representation are

Table 7.7. Characters and symmetries for the angular momentum states in T_d symmetry

| | E | $8C_3$ | $3C_2$ | $6\sigma_d$ | $6S_4$ | | |
|-----------------|---|--------|--------|-------------|--------|-----------|---------------------------|
| $\chi_{\ell=0}$ | 1 | 1 | 1 | 1 | 1 | A_1 | $A_1 \rightarrow s$ state |
| $\chi_{\ell=1}$ | 3 | 0 | -1 | 1 | -1 | T_2 | $T_2 \rightarrow p$ state |
| $\chi_{\ell=2}$ | 5 | -1 | 1 | 1 | -1 | $E + T_2$ | |

$$\begin{aligned}\psi_1(T_2) &= \frac{1}{2}(\psi_a + \psi_b - \psi_c - \psi_d) \\ \psi_2(T_2) &= \frac{1}{2}(\psi_a - \psi_b + \psi_c - \psi_d) \\ \psi_3(T_2) &= \frac{1}{2}(\psi_a - \psi_b - \psi_c + \psi_d).\end{aligned}\quad (7.17)$$

The T_2 orbitals must be orthogonal to the A_1 orbitals and to each other and must transform as irreducible representation T_2 under symmetry operations of the group (see Problem 7.6).

The symmetries for the directed valence orbitals for the carbon atom can be related conveniently to angular momentum states using the full rotation group and the characters for rotations and inversions (see (5.11) and (5.13)). To make a directed valence bond from the central carbon atom to the four hydrogen atoms at locations a, b, c, d in Fig. 3.3, the carbon atom must have wave functions with the same symmetries for its four valence electrons as the four LCAOs for the hydrogen atoms (see (7.16) and (7.17)). This tells us that the electronic states for the carbon directed valence state must have a $2s^12p^3$ configuration and $A_1 + T_2$ symmetries for the carbon valence electrons. The symmetries for the angular momentum states are found from

$$\begin{aligned}\chi(\alpha) &= \frac{\sin[(\ell + \frac{1}{2})\alpha]}{\sin(\alpha/2)} \quad \text{for pure rotations} \\ \chi(i\alpha) &= (-1)^\ell \frac{\sin[(\ell + \frac{1}{2})\alpha]}{\sin(\alpha/2)} \quad \text{for improper rotations}.\end{aligned}$$

We thus obtain the characters for the angular momentum states in the T_d group and list them in Table 7.7, where we have made use of the fact that

$$\begin{cases} \sigma_d = iC'_2 \\ S_4 = iC_4, \end{cases}$$

in which the C'_2 is a (110) twofold axis. We note that the C'_2 operation together with the inversion operation take one of the a, b, c, d vertices in Fig. 3.3 into a vertex occupied by a hydrogen atom. The joint operation $iC_4 = S_4$ transforms the a, b, c, d vertices another themselves.

Table 7.8. Relation between angular momentum states and basis functions for group T_d

| basis functions | | |
|-----------------|------------|---|
| $\ell = 0$ | s -state | 1 |
| $\ell = 1$ | p -state | (x, y, z) |
| $\ell = 2$ | d -state | $\underbrace{(xy, yz, zx)}_{T_2}, \underbrace{x^2 - y^2, 3z^2 - r^2}_{E}$ |

The results in Table 7.7 could equally well have been obtained by looking at the character table for group T_d (see Table A.32) and making the identifications as displayed in Table 7.8, and by associating the various basis functions of the angular momentum states with the appropriate irreducible representations for the T_d group.

If we now apply this discussion to the CH_4 molecule we see that the directed valence orbitals for the carbon contain one $2s$ (A_1) state and three $2p$ (T_2) states to bond to the four hydrogen atoms. These A_1 and T_2 states can accommodate all eight valence electrons for the CH_4 molecule. A linear combination of s and p_x, p_y, p_z functions which transforms at A_1 and T_2 for the directed valence orbitals of the carbon atom along the four diagonal directions of the cube (see Fig. 3.3) is

$$\begin{aligned}\Psi(1, 1, 1) &= \frac{1}{2}(\psi_s + \psi_{p_x} + \psi_{p_y} + \psi_{p_z}) \\ \Psi(1, -1, -1) &= \frac{1}{2}(\psi_s + \psi_{p_x} - \psi_{p_y} - \psi_{p_z}) \\ \Psi(-1, 1, -1) &= \frac{1}{2}(\psi_s - \psi_{p_x} + \psi_{p_y} - \psi_{p_z}) \\ \Psi(-1, -1, 1) &= \frac{1}{2}(\psi_s - \psi_{p_x} - \psi_{p_y} + \psi_{p_z}).\end{aligned}\quad (7.18)$$

The linear combination with all “+” signs $\Psi(1, 1, 1)$ transforms as the A_1 irreducible representation. The other three functions with two “+” and two “-” signs transform as the three partners of the T_2 irreducible representation as can be seen by applying the symmetry operations of group T_d to these directed valence wave functions. Thus (7.18) gives a set of orthonormal wave functions for the four electrons of the carbon atom.

Bonding states are made between the A_1 carbon orbital and the A_1 orbital of the four hydrogens and between the corresponding T_2 carbon and hydrogen orbitals following the same type of block diagonal form as is shown in Fig. 7.4 for the CO molecule. Although the carbon electrons must be promoted to the excited sp^3 configuration to satisfy the bonding orbitals in the molecule, the attractive bonding energy due to the CH_4 bonds more than

compensates for the electronic excitation to form the sp^3 excited state for the carbon atom. It is of interest that the orbitals in (7.18) also represent normalized functions for tetrahedral bonding orbitals in common semiconductors.

Finally we consider the bond strengths along a directed valence orbital to show that the bond strength is a maximum along the directed valence orbital. To illustrate bond strengths, consider the $(1, 1, 1)$ directed valence bond $\frac{1}{2}(\psi_s + \psi_{p_x} + \psi_{p_y} + \psi_{p_z})$ with A_1 symmetry for CH_4 (see (7.18)). We express each of the terms of this equation in terms of spherical harmonics, using polar coordinates. For angular momentum $\ell = 0$ and $\ell = 1$ the spherical harmonics yield

$$\begin{aligned}\psi_s &= 1, & \psi_{p_y} &= \sqrt{3} \sin \theta \sin \phi, \\ \psi_{p_x} &= \sqrt{3} \sin \theta \cos \phi, & \psi_{p_z} &= \sqrt{3} \cos \theta.\end{aligned}\quad (7.19)$$

We can thus write the angular dependence of the directed valence bond along (111) as

$$\Psi(1, 1, 1)|_{(\theta, \phi)} = \frac{f(r)}{2} \left[1 + \sqrt{3} \sin \theta (\cos \phi + \sin \phi) + \sqrt{3} \cos \theta \right]. \quad (7.20)$$

Differentiation with respect to θ and ϕ determines the values of θ and ϕ which give a maximum bond strength. It is found that this wavefunction is a maximum along the (111) direction, but not along another one of the diagonal axes (see Problem 7.6).

7.5.3 The Hypothetical SH_6 Molecule

As another illustrative example, consider a hypothetical molecule SH_6 where the six identical H atoms are arranged on a regular hexagon (e.g., the benzene ring has this basic symmetry) and the sulfur is at the center. For the hydrogens, we have six distinct atomic orbitals. To simplify the secular equation we use group theory to make appropriate linear combinations of atomic orbitals:

$$\begin{pmatrix} \psi_a \\ \psi_b \\ \psi_c \\ \psi_d \\ \psi_e \\ \psi_f \end{pmatrix}, \quad (7.21)$$

so that the transformed linear combinations are proper basis functions for irreducible representations of the point symmetry group D_{6h} which applies to this problem. We see that the largest dimension for an irreducible representation in D_{6h} is $n = 2$. We show below that the use of symmetry will result in

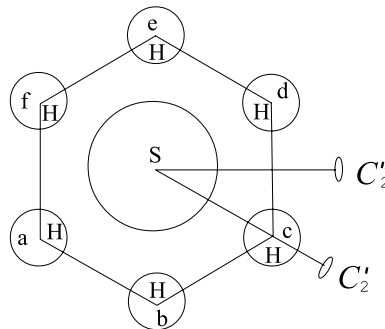


Fig. 7.6. Geometry of the hypothetical SH_6 planar molecule with six hydrogens at the corners of a hexagon and the sulfur atom at the center (D_{6h} symmetry)

a secular equation with block diagonal form, having blocks with dimensions no greater than (2×2) .

To find the proper linear combination of atomic orbitals, we find the characters for the equivalence transformation $\Gamma^{\text{a.s.}}(R)$ for the six hydrogen atoms in D_{6h} symmetry (see Fig. 7.6) by considering how many atom sites go into each other under the various symmetry operations of the group. The results for $\Gamma^{\text{a.s.}}$ for each class are given at the bottom of the Character Table 7.9 for D_6 where $D_{6h} = D_6 \otimes \text{i}$. We now set up the appropriate linear combinations of atomic orbitals for the six hydrogen atoms. This can be done most easily by utilizing the correspondence of this problem with the sixth roots of unity. We will denote the sixth roots of unity by $1, \Omega, \omega, -1, \omega^2, \Omega^5$, where $\omega = e^{2\pi i/3}$ and $\Omega = e^{2\pi i/6}$. For simplicity we will denote the atomic orbitals at a site α by ψ_α and use the abbreviated notation α . In terms of the site notation (a, b, c, d, e, f) , the sixth orthogonal linear combinations formed by taking the sixth roots of unity are

$$\begin{aligned}
 \psi_1 \quad & a + b + c + d + e + f \quad \text{transforms as } \Gamma_1, \\
 \psi_2 \quad & a + \Omega b + \omega c - d + \omega^2 e + \Omega^5 f, \\
 \psi_3 \quad & a + \omega b + \omega^2 c + d + \omega e + \omega^2 f, \\
 \psi_4 \quad & a - b + c - d + e - f \quad \text{transforms as } \Gamma_3, \\
 \psi_5 \quad & a + \omega^2 b + \omega c + d + \omega^2 e + \omega f, \\
 \psi_6 \quad & a + \Omega^5 b + \omega^2 c - d + \omega e + \Omega f.
 \end{aligned}$$

To obtain the symmetries of the functions ψ_1, \dots, ψ_6 we examine $\hat{P}_R \psi_i$ where \hat{P}_R is a symmetry operation in group D_6 . Clearly ψ_2 and ψ_6 are partners since $\psi_2^* = \psi_6$, and similarly ψ_3 and ψ_5 are partners since $\psi_3^* = \psi_5$, so these provide good candidates for representing the Γ_5 and Γ_6 irreducible

Table 7.9. Character table for point group D_6

| D_6 | | E | C_2 | $2C_3$ | $2C_6$ | $3C'_2$ | $3C''_2$ | |
|------------------------|-----------------|-----|-------|--------|--------|---------|----------|---|
| $x^2 + y^2, z^2$ | $\Gamma_1(A_1)$ | 1 | 1 | 1 | 1 | 1 | 1 | |
| z | $\Gamma_2(A_2)$ | 1 | 1 | 1 | 1 | -1 | -1 | |
| | $\Gamma_3(B_1)$ | 1 | -1 | 1 | -1 | 1 | -1 | |
| | $\Gamma_4(B_2)$ | 1 | -1 | 1 | -1 | -1 | 1 | |
| $(x^2 - y^2, xy)$ | $\Gamma_5(E_2)$ | 2 | 2 | -1 | -1 | 0 | 0 | |
| $(xz, yz), (x, y)$ | $\Gamma_6(E_1)$ | 2 | -2 | -1 | 1 | 0 | 0 | |
| $\Gamma^{\text{a.s.}}$ | | 6 | 0 | 0 | 0 | 2 | 0 | $\Rightarrow \Gamma_1 + \Gamma_3 + \Gamma_5 + \Gamma_6$ |

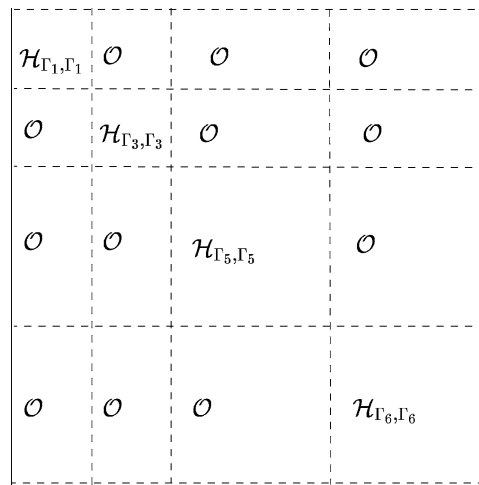


Fig. 7.7. Schematic of the secular equation for six hydrogen orbitals at the corners of a regular hexagon. Outside of the block structure, all entries are zeros. The Γ_1 and Γ_3 are one-dimensional representations and the Γ_5 and Γ_6 are two-dimensional representations

representations. By inspection, ψ_1 is invariant under all the symmetry operations of the group and thus ψ_1 transforms as Γ_1 . As for ψ_4 , application of $C_6(\psi_4) = -\psi_4$, and $C_3\psi_4 = \psi_4$, etc. verifies that ψ_4 transforms as Γ_3 . Inspection of the character table shows differences between Γ_5 and Γ_6 under the operations in classes C_2 and $2C_6$. It is clear that the basis formed by ψ_2 and ψ_6 transforms under C_6 as

$$C_6(\psi_2, \psi_6) = \begin{pmatrix} \Omega^5 & 0 \\ 0 & \Omega \end{pmatrix} \begin{pmatrix} \psi_2 \\ \psi_6 \end{pmatrix} \quad (7.22)$$

since $a \rightarrow b, b \rightarrow c, c \rightarrow d$, etc. Thus the trace of the matrix is

$$\Omega + \Omega^5 = e^{2\pi i/6} + e^{-2\pi i/6} = 2 \cos \frac{2\pi}{6} = 1, \quad (7.23)$$

which is the proper character for Γ_6 . As a check, we see that $C_2(\psi_2, \psi_6)$ results in a trace $= \Omega^3 + \Omega^{15} = \Omega^3 + \Omega^3 = 2 \cos \pi = -2$, and this also checks. Similarly we see that the transformation matrix for

$$C_6(\psi_3, \psi_5) = D^{\Gamma_5}(C_6) \begin{pmatrix} \psi_3 \\ \psi_5 \end{pmatrix}$$

again sends $a \rightarrow b, b \rightarrow c, c \rightarrow d$, etc. and yields a trace of $\omega + \omega^2 = -1$ while $C_2(\psi_3, \psi_5)$ yields a trace of $\omega^3 + \omega^6 = 2$. The unitary transformation U which takes the original basis a, b, c, d, e, f into a basis that exhibits D_6 symmetry

$$U \begin{pmatrix} a \\ b \\ c \\ d \\ e \\ f \end{pmatrix} = \begin{pmatrix} \psi_1 \\ \psi_4 \\ \psi_2 \\ \psi_6 \\ \psi_3 \\ \psi_5 \end{pmatrix} \quad (7.24)$$

brings the one-electron molecular secular matrix into the block diagonal form shown in Fig. 7.7, and zeros in all the off-diagonal positions coupling these blocks.

Just as we used some intuition to write down the appropriate basis functions, we can use physical arguments to suggest the ordering of the energy levels. The fully symmetric state yields a maximum charge density *between* the atom sites and therefore results in maximum bonding. On the other hand, the totally antisymmetric state yields a minimum bonding and therefore should be the highest energy state. The doubly degenerate levels have an intermediate amount of wave function overlap.

The six symmetric orbitals that we make can be populated by 12 electrons. But we only have six electrons at our disposal and these will go into the lowest energy states. Figure 7.8 shows a schematic view of the pile up of charge for

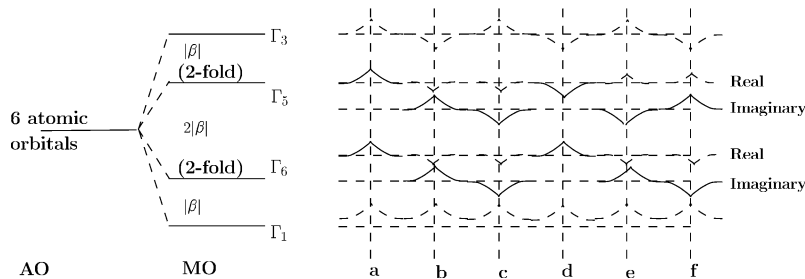


Fig. 7.8. Energies of the LCAOs formed by six hydrogen atoms at the corners of a hexagon. Also shown is a schematic summary of the wave functions for the various orbitals

the states of various symmetry. The Γ_1 state has the strongest bonding and the Γ_6 state has the next strongest binding, and therefore we can expect the six electrons to populate these states preferentially. For this reason, the molecular bonding produces a lower energy state than the free atoms.

Let us now consider making directed valence orbitals from the S atom at the center of the hexagon to the six hydrogens. An isolated S atom is in a $1s^2 2s^2 2p^6 3s^2 3p^4$ configuration. Thus to bond to the hydrogen atoms in the six LCAOs, given by ψ_1, \dots, ψ_6 , would require all the bonding states and all the antibonding states to be occupied. This implies that the sulfur atom would have to be promoted to a high energy state to bond in a planar configuration (see Problem 7.3). The sulfur atom in the ground state configuration would only bond to the Γ_1 and Γ_6 blocks of the secular equation for SH_6 in Fig. 7.7.

7.5.4 The Octahedral SF_6 Molecule

We next give an example of SF_6 with a molecular configuration that involves octahedral bonding (see Fig. 7.9). The octahedral configuration is very common in solid state physics.

If we now use the symmetry operations of O_h (Table A.30) we get the characters for the equivalence representation $\Gamma^{\text{a.s.}}$ for the six atoms which sit at the corners of the octahedron (see Fig. 7.9 and Table 7.10). The decomposition of the reducible representation $\Gamma^{\text{a.s.}}$ for the six equivalent fluorine atoms gives

$$\Gamma^{\text{a.s.}} = A_{1g} + E_g + T_{1u} . \quad (7.25)$$

If we (hypothetically) were to put s-functions on each of the six fluorine sites, then $\Gamma^{\text{a.s.}}$ given by (7.25) would be appropriate to make the linear combination of atomic orbitals for the six fluorine atoms. However, if we put

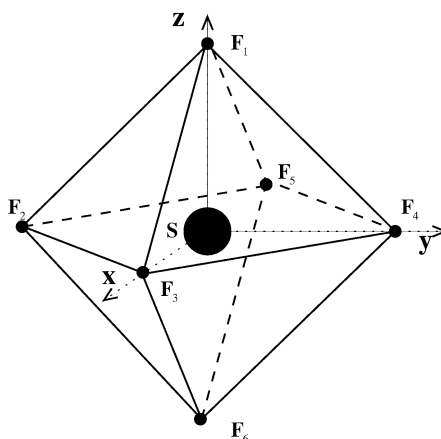


Fig. 7.9. Schematic diagram of the SF_6 molecule which exhibits octahedral bonding

p-functions on each fluorine site then the appropriate equivalence transformation for p-electrons would be $\Gamma^{\text{a.s.}} \otimes \Gamma^{(T_{1u})}$, where we note that for O_h symmetry the vector transforms as T_{1u} . This general concept of taking the direct product of the transformation of the atom sites with the symmetry of the orbital on each site is frequently used in applications of the equivalence principle.

Let us now look at the orbitals for electrons on the sulfur site to make the directed valence bonds as shown in Fig. 7.9. Bonding orbitals are found by setting the directed valence representation equal to the symmetries found from the equivalence transformation for the fluorine electrons bonding to the sulfur. For simplicity let us assume that $\Gamma^{\text{a.s.}} = \Gamma_{\text{D.V.}}$ to fully exploit the bonding of the cation and anions. We then need to identify the irreducible representations contained in $\chi_{\text{D.V.}}$ with angular momentum states. The characters for the angular momentum states in O_h symmetry are then found from

$$\chi(\alpha) = \frac{\sin(\ell + \frac{1}{2})\alpha}{\sin(\alpha/2)} \quad (7.26)$$

and using the character table for O_h (see Table A.30). The results for the angular momentum states are tabulated in Table 7.11. As an example, let us suppose for simplicity that we have s functions on each of the six fluorine sites. Then to produce $\Gamma_{\text{D.V.}} = A_{1g} + E_g + T_{1u}$ as in (7.25) we can use an s state $\ell = 0$ for the A_{1g} symmetry, a p state ($\ell = 1$) for the T_{1u} symmetry, and a d state ($\ell = 2$) for the E_g symmetry in (7.25). Thus sp^3d^2 orbitals are required for the directed valence of the sulfur ion, which ordinarily has an atomic ground state configuration $3s^23p^4$. Thus to make the necessary bonding, we must promote the S atom to an excited state, namely to a $3s^13p^33d^2$ state. This type of excitation is called *configuration mixing*. In Problem 7.2, a more realistic version of the octahedral SF_6 molecule is considered, with p -function wave functions for each of the six fluorine sites.

7.6 σ - and π -Bonds

We now discuss the difference between σ - and π -bonds which are defined in the diagram in Fig. 7.10. The situation which we have considered until now is bonding by s -functions or by p -functions in the direction of the bond and this is denoted by σ -bonding, as shown in Fig. 7.10. Because of their asymmetry, the

Table 7.10. Characters for the 6 atoms sitting at the corners of an octahedron, e.g., for the F sites of the SF_6 molecule

| | E | $8C_3$ | $3C_2$ | $6C'_2$ | $6C_4$ | i | $8iC_3$ | $3iC_2$ | $6iC'_2$ | $6iC_4$ |
|------------------------|-----|--------|--------|---------|--------|-----|---------|---------|----------|---------|
| $\Gamma^{\text{a.s.}}$ | 6 | 0 | 2 | 0 | 2 | 0 | 0 | 4 | 2 | 0 |

Table 7.11. Characters for angular momentum states and their irreducible representations in O_h symmetry

| | E | $8C_3$ | $3C_2$ | $6C'_2$ | $6C_4$ | i | $8iC_3$ | $3iC_2$ | $6iC'_2$ | $6iC_4$ | |
|------------|-----|--------|--------|---------|--------|-----|---------|---------|----------|---------|--|
| $\ell = 0$ | 1 | 1 | 1 | 1 | 1 | 1 | 1 | 1 | 1 | 1 | $\Rightarrow A_{1g}$ |
| $\ell = 1$ | 3 | 0 | -1 | -1 | 1 | -3 | 0 | 1 | 1 | -1 | $\Rightarrow T_{1u}$ |
| $\ell = 2$ | 5 | -1 | 1 | 1 | -1 | 5 | -1 | 1 | 1 | -1 | $\Rightarrow E_g + T_{2g}$ |
| $\ell = 3$ | 7 | 1 | -1 | -1 | -1 | -7 | -1 | 1 | 1 | 1 | $\Rightarrow A_{2u} + T_{1u} + T_{2u}$ |
| $\ell = 4$ | 9 | 0 | 1 | 1 | 1 | -9 | 0 | -1 | -1 | -1 | $\Rightarrow A_{1g} + E_g + T_{1g} + T_{2g}$ |

σ bonds with p -functions ($V_{pp\sigma}$ in Fig. 7.10) play an important role in making directed valence bonding orbitals. We can also obtain some degree of bonding by directing our p -functions \perp to the bond direction, as also shown in Fig. 7.10, and this is called π -bonding. We note that there are two equivalent mutually perpendicular directions that are involved in π -bonding. From considerations of overlapping wavefunctions, we would expect π -bonding to be much weaker than σ -bonding.

Just as group theory tells us which LCAOs are needed to form σ -bonds, group theory also provides the corresponding information about the linear combination of atomic orbitals that form π -bonds. We now describe in this section a procedure for finding the symmetry for both σ -bonds and π -bonds.

Let us first review the situation for the σ -bonds. To find a σ -bond, we consider the atomic wave function at each equivalent site to be degenerate with the corresponding wave functions on the other sites and we find the transformation matrices that transform equivalent sites into one another according to the symmetry operations of the group. To find out if an entry in this matrix is 1 or 0 we ask the question whether or not a site goes into itself under a particular symmetry operation. If it goes into itself we produce a 1 on the diagonal, otherwise a 0. Therefore by asking how many sites go into themselves, we obtain the character for each symmetry operation. This is the procedure we have used throughout the chapter to find $\Gamma^{\text{a.s.}}$ which denotes the equivalence transformation. This gives the symmetry designations for $V_{ss\sigma}$ bonds.

To find the characters for a π -bond, we have to consider how many vectors normal to the bond direction remain invariant under the symmetry operations of the group. The simplest way to obtain the characters for the σ -bonds and π -bonds is to consider the transformation as the product of two operations: the transformation of one equivalent site into another, followed by the transformation of the vector on a site. Thus we write

$$\begin{aligned} \Gamma^{\text{(a.s.)}} \otimes \Gamma_{\text{general vector}} &= \Gamma^{\text{(a.s.)}} \otimes \Gamma_{\text{vector } \perp \text{ to } \sigma\text{-bonds}} \\ &\quad + \Gamma^{\text{(a.s.)}} \otimes \Gamma_{\text{vector } \parallel \text{ to } \sigma\text{-bonds}}. \end{aligned} \quad (7.27)$$

But

$$\Gamma_{\text{D.V. } \sigma\text{-bonds}} \equiv \Gamma^{\text{(a.s.)}} \otimes \Gamma_{\text{(vector } \parallel \text{ to } \sigma\text{-bonds)}}.$$

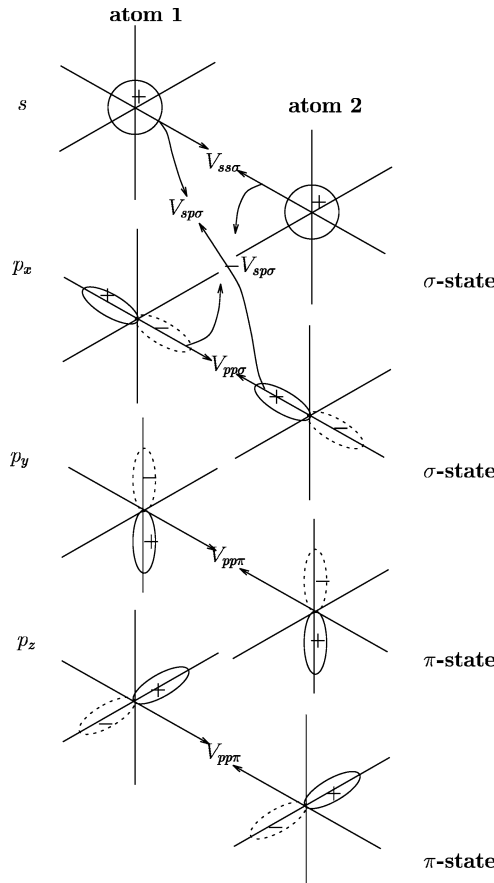


Fig. 7.10. Schematic diagram of: σ -bonding ($V_{ss\sigma}$) by s -functions and ($V_{pp\sigma}$) by longitudinally oriented p -functions. Directed valence $V_{sp\sigma}$ are also indicated. π -bonding ($V_{pp\pi}$) with transverse p -functions shown for two orientations

Thus

$$\Gamma_{\text{D.V. } \pi\text{-bonds}} = \Gamma^{(\text{a.s.})} \otimes \Gamma_{\text{general vector}} - \Gamma_{\text{D.V. } \sigma\text{-bonds}}, \quad (7.28)$$

and we thus obtain the desired result

$$\Gamma_{\text{D.V. } \pi\text{-bonds}} = \Gamma^{(\text{a.s.})} \otimes \Gamma_{\text{vector } \perp \text{ to } \sigma\text{-bonds}}. \quad (7.29)$$

As an example of σ -bonds and π -bonds let us consider the problem of *trigonal bonding* of a hypothetical C_4 cluster, where one carbon atom is at the center of an equilateral triangle and the other three carbon atoms are at the corners of the triangle, as shown in Fig. 7.11. The pertinent character table is D_{3h} which is given in Table 7.12. For this group σ_h denotes an $x-y$ reflection plane and σ_v denotes a reflection plane containing the threefold axis and one

of the twofold axes. Consider the linear combination of atomic orbitals made out of the three carbon atoms at the corners of the equilateral triangle. From the equivalence transformation for these three carbons, we obtain $\Gamma^{(\text{a.s.})}$ (see Table 7.13). Clearly if each of the orbitals at the corners of the equilateral triangle were s -functions, then the appropriate linear combination of atomic orbitals would transform as $A'_1 + E'$

$$A'_1 : \psi_1 + \psi_2 + \psi_3, \quad (7.30)$$

$$E' : \begin{cases} \psi_1 + \omega\psi_2 + \omega^2\psi_3 \\ \psi_1 + \omega^2\psi_2 + \omega\psi_3 \end{cases}, \quad (7.31)$$

where

$$\omega = \exp\left(\frac{2\pi i}{3}\right). \quad (7.32)$$

In transforming wavefunctions corresponding to higher angular momentum states, we must include the transformation of a tensor (vector) on each of the equivalent sites. This is done formally by considering the direct product of $\Gamma^{(\text{a.s.})}$ with Γ_{tensor} , where Γ_{tensor} gives the transformation properties of the orbital: a scalar for s -functions, a vector for p -functions, a tensor for d -functions, etc.

We now illustrate the construction of LCAOs from s - and p -functions, noting that from the character table for the group D_{3h} , s -functions transform

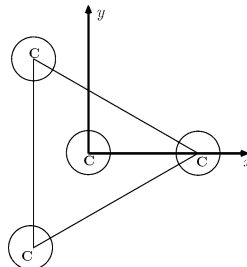


Fig. 7.11. Schematic diagram of a carbon atom forming bonds to three other carbon atoms at the corners of an equilateral triangle

Table 7.12. Character Table for Group $D_{3h}(6m2)$

| $D_{3h}(6m2) \equiv D_3 \otimes \sigma_h$ | | | E | σ_h | $2C_3$ | $2S_3$ | $3C'_2$ | $3\sigma_v$ |
|---|--------------|---------|-----|------------|--------|--------|---------|-------------|
| $x^2 + y^2, z^2$ | R_z | A'_1 | 1 | 1 | 1 | 1 | 1 | 1 |
| | | A'_2 | 1 | 1 | 1 | 1 | -1 | -1 |
| | | A''_1 | 1 | -1 | 1 | -1 | 1 | -1 |
| $(x^2 - y^2, xy)$ | z | A''_2 | 1 | -1 | 1 | -1 | -1 | 1 |
| | (x, y) | E' | 2 | 2 | -1 | -1 | 0 | 0 |
| (xz, yz) | (R_x, R_y) | E'' | 2 | -2 | -1 | 1 | 0 | 0 |

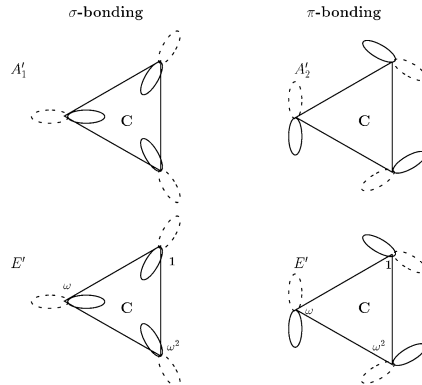


Fig. 7.12. Schematic diagram for the σ -bonds and the in-plane π -bonds for carbon atoms at the corners of a triangle to a carbon atom at the center of the triangle

as A'_1 , p_z functions as A''_2 and (p_x, p_y) functions as E' . We thus obtain for the transformation properties of the three s -functions at the corners of an equilateral triangle as

$$\Gamma^{\text{a.s.}} \otimes \Gamma_s = (A'_1 + E') \otimes A'_1 = A'_1 + E'. \quad (7.33)$$

For the p_z functions which transform as A''_2 we have for the direct product:

$$\Gamma^{\text{a.s.}} \otimes \Gamma_{p_z} = (A'_1 + E') \otimes A''_2 = A''_2 + E''. \quad (7.34)$$

Finally for the $p_{x,y}$ functions which transform as E' we obtain

$$\Gamma^{\text{a.s.}} \otimes \Gamma_{p_x, p_y} = (A'_1 + E') \otimes E' = A'_1 + A'_2 + 2E'. \quad (7.35)$$

We will see below that the $A'_1 + E'$ symmetries correspond to σ -bonds and the remaining $(A'_2 + E') + (A''_2 + E'')$ correspond to π -bonds, as shown in Fig. 7.12.

For the carbon atom at the center of the equilateral triangle (see Fig. 7.11) we make directed valence orbitals to the carbon atoms at sites (1), (2), and (3) from states with A'_1 and E' symmetry (see Sect. 7.5.1), which in accordance with the character table for D_{3h} , transform as the ψ_s and ψ_{p_x}, ψ_{p_y} wave functions. The directed orbitals from the central carbon atom are thus

Table 7.13. Characters for the $\Gamma^{\text{a.s.}}$ representation of three carbon atoms sitting at the corners of an equilateral triangle (D_{3h} symmetry)

| | E | σ_h | $2C_3$ | $2S_3$ | $3C'_2$ | $3\sigma_v$ | |
|--------------------------|-----|------------|--------|--------|---------|-------------|-------------------------|
| $\Gamma^{\text{(a.s.)}}$ | 3 | 3 | 0 | 0 | 1 | 1 | $\Rightarrow A'_1 + E'$ |

$$\begin{aligned}\psi_1 &= \alpha\psi_s + \beta\psi_{p_x} \\ \psi_2 &= \alpha\psi_s + \beta \left[-\frac{1}{2}\psi_{p_x} + \frac{\sqrt{3}}{2}\psi_{p_y} \right] \\ \psi_3 &= \alpha\psi_s + \beta \left[-\frac{1}{2}\psi_{p_x} - \frac{\sqrt{3}}{2}\psi_{p_y} \right].\end{aligned}\quad (7.36)$$

The orthonormality condition on the three waves functions in (7.36), gives

$$\alpha^2 + \beta^2 = 1, \quad \beta^2 = 2\alpha^2, \quad (7.37)$$

or

$$\alpha = \frac{1}{\sqrt{3}}, \quad \beta = \sqrt{\frac{2}{3}}, \quad (7.38)$$

so that

$$\begin{aligned}\psi_1 &= \sqrt{\frac{1}{3}}\psi_s + \sqrt{\frac{2}{3}}\psi_{p_x} \\ \psi_2 &= \sqrt{\frac{1}{3}}\psi_s - \sqrt{\frac{1}{6}}\psi_{p_x} + \sqrt{\frac{1}{2}}\psi_{p_y} \\ \psi_3 &= \sqrt{\frac{1}{3}}\psi_s - \sqrt{\frac{1}{6}}\psi_{p_x} - \sqrt{\frac{1}{2}}\psi_{p_y}.\end{aligned}\quad (7.39)$$

Using the basis functions in the character table for D_{3h} and the classification of angular momentum states in Table 7.14, we can make σ -bonding orbitals with the following orbitals for the central carbon atom, neglecting for the moment the energetic constraints on the problem:

$$\begin{aligned}2s2p^2 &\quad s + (p_x, p_y) \\ 2s3d^2 &\quad s + (d_{xy}, d_{x^2-y^2}) \\ 3d2p^2 &\quad d_{3z^2-r^2} + (p_x, p_y) \\ 3d^3 &\quad d_{3z^2-r^2} + (d_{xy}, d_{x^2-y^2}).\end{aligned}$$

It is clear from Table 7.14 that the lowest energy σ -bond is made with the $2s2p^2$ configuration. The carbon atom has four valence electrons, three of which make the in-plane trigonal σ -bonds. The fourth electron is free to bond in the z -direction. This electron is involved in π -bonds, frequently discussed in organic chemistry.

To obtain π -bonds from the central carbon atom to the atoms at the corners of the triangle, we look at the character table to see how the vector (x, y, z) transforms:

$$\Gamma_{\text{vector}} = E' + A_2''. \quad (7.40)$$

Table 7.14. Characters for the angular momentum states and their irreducible representations for the group D_{3h} ^(a)

| | E | σ_h | $2C_3$ | $2S_3$ | $3C'_2$ | $3\sigma_v$ | |
|------------|-----|------------|--------|--------|---------|-------------|----------------------------------|
| $\ell = 0$ | 1 | 1 | 1 | 1 | 1 | 1 | A'_1 |
| $\ell = 1$ | 3 | 1 | 0 | -2 | -1 | 1 | $A''_2 + E'$ |
| $\ell = 2$ | 5 | 1 | -1 | 1 | 1 | 1 | $A'_1 + E' + E''$ |
| $\ell = 3$ | 7 | 1 | 1 | 1 | -1 | 1 | $A'_1 + A'_2 + A''_2 + E' + E''$ |

^(a) In this character table, the characters for the various entries are found using the relations $\sigma_h = iC_2$, $2S_3 = 2iC_6$ and $3\sigma_v = 3iC_2$

We then take the direct product:

$$\begin{aligned}
 \Gamma^{\text{a.s.}} \otimes \Gamma_{\text{vector}} &= \overbrace{(A'_1 + E')}^{\Gamma^{\text{a.s.}}} \otimes \underbrace{(E' + A''_2)}_{\chi_{\text{vector}}} \\
 &= (A'_1 \otimes E') + (A'_1 \otimes A''_2) + (E' \otimes E') + (E' \otimes A''_2) \\
 &= (E') + (A''_2) + (E' + A'_1 + A'_2) + (E'') \\
 &= (A'_1 + E') + (E' + A''_2 + A'_2 + E''). \tag{7.41}
 \end{aligned}$$

Since the irreducible representations for the σ -bonds are A'_1 and E' , we have the desired result that the irreducible representations for the π -bonds are

$$E' + A''_2 + A'_2 + E''.$$

We can now go one step further by considering the polarization of the π -bonds in terms of the irreducible representations that are even and odd under the horizontal mirror plane operation σ_h :

$$\chi_{\text{D.V. } \pi\text{-bonds}} = \underbrace{A'_2 + E'}_{\substack{\text{Even under } \sigma_h \\ \text{Odd under } \sigma_h}} + \underbrace{A''_2 + E''}_{\substack{\text{Odd under } \sigma_h}}. \tag{7.42}$$

This polarization analysis identifies the bonds in (7.33)–(7.35).

To find the irreducible representations contained in the directed valence π -bonds, we have to go to rather high angular momentum states: $\ell = 2$ for an E'' state and $\ell = 3$ for an A'_2 state. Such high angular momentum states correspond to much higher energy. Therefore π -bonding will be much weaker than σ -bonding. The irreducible representations $A''_2 + E''$ correspond to π -bonding in the z -direction while the $A'_2 + E'$ representations correspond to π -bonding in the plane of the triangle, but \perp to the σ -bonding directions. We further note that the symmetries $A''_2 + E''$ correspond to p_z and d_{xz}, d_{yz} orbitals for angular momentum 1 and 2, respectively. On the other hand, the

symmetries $A'_2 + E'$ require $\ell = 3$ states, and therefore correspond to higher energies than the $A''_2 + E''$ orbitals. A diagram showing the orbitals for the σ -bonds and π -bonds for the various carbon atoms is given in Fig. 7.12.

7.7 Jahn–Teller Effect

The Jahn–Teller (JT) effect was discovered in 1937 [42] and it represents one of the earliest applications of group theory to solid-state physics [9]. The Jahn–Teller Theorem states that “any nonlinear molecular system in a degenerate electronic state will be unstable and will undergo a distortion to form a system of lower symmetry and lower energy, thereby removing the degeneracy.” The spontaneous geometrical distortion in an electronically excited state results in a lowering of the symmetry and a splitting of energy levels.

Both static and dynamic JT effects must be considered. In the static JT effect, a structural distortion lowers the symmetry of the system and lifts the degeneracy of the state. For a partially filled band, such a distortion thus leads to a lowering of the total energy of the system as the lower energy states of the multiplet are occupied and the higher-lying states remain empty.

The dynamic JT effect [44] can occur when there is more than one possible distortion that could lead to a lowering of the symmetry (and consequently also the lowering of the energy) of the system. If the potential minima of the adiabatic potential are degenerate for some symmetry-lowered states of a molecule, the electrons will jump from one potential minimum to another, utilizing their vibrational energy, and if this hopping occurs on the same time scale as atomic or molecular vibrations, then no static distortion will be observed by most experimental probes. Those vibrational modes which induce the dynamic JT effect contribute strongly to the electron–phonon coupling.

The Jahn–Teller effect applies to some simple polyatomic molecules, such as H_3 , and to complex organic molecules including carbon nanotubes as well as defect centers. The effect has also been discussed for different symmetry structures, such as cubic, tetrahedral, tetragonal, trigonal [60], and even icosahedral systems, such as C_{60} [32].

For nonlinear molecules in a geometry described by a point symmetry group possessing degenerate irreducible representations there always exists at least one nontotally symmetric vibration that makes such electronically degenerate states unstable. Under this symmetry-lowering vibration, the nuclei are displaced to new equilibrium positions of lower symmetry causing a splitting of the originally degenerate state. The Jahn–Teller effect describes the geometrical distortion of the electron cloud in the nonlinear molecule under certain situations. Consider a molecule that is in a degenerate state $\Psi_{\mu}^{\Gamma_i}$, belonging to the irreducible representation Γ_i , with partners μ . Then the complex conjugate wave function $K\Psi_{\nu}^{\Gamma_i}$ is necessarily a state with the same energy

where K is the complex conjugation operator (see Chapter 16). If the nuclear coordinates are displaced from the high-symmetry configuration by a normal mode vibration $Q_r^{\Gamma_j}$, the electronic potential deviates from its equilibrium situation. The electronic potential can, therefore, be expanded in terms of the vibrational symmetry coordinates:

$$V(\mathbf{r}, Q) = V_0 + \sum_{\Gamma_j, r} V_r^{\Gamma_j} Q_r^{\Gamma_j} + \sum_{\Gamma_j, k, r, s} V_{rs}^{\Gamma_j \Gamma_k} Q_r^{\Gamma_j} Q_s^{\Gamma_k} + \dots \quad (7.43)$$

For small displacements only the first sum can be considered, and we have the “linear” Jahn–Teller effect. A first-order perturbation approach to the electronic levels involves the matrix elements:

$$M = \langle \Psi_{\mu}^{\Gamma_i} | V(\mathbf{r}, Q) | \Psi_{\nu}^{\Gamma_i} \rangle. \quad (7.44)$$

The argument of Jahn and Teller is that, since M reverses its sign if Q is replaced by $-Q$, each perturbation ΔE of an electronic energy level should also reverse its sign. Consequently, if $M \neq 0$ due to any term related to a Q^{Γ_i} belonging to $\Gamma_i \neq \Gamma_1$, i.e., the lattice mode vibration does not belong to the totally symmetric representation, the symmetry of the unperturbed molecular configuration also becomes unstable.

An interesting and instructive example of the Jahn–Teller effect occurs in the C_{60} molecule which has 60 carbon atoms at the 60 vertices of a truncated regular icosahedron. Although each carbon atom is in an equivalent site to every other carbon atom on the icosahedron, two of the nearest neighbor C–C bonds are single bonds while one is a double bond to satisfy the valence requirements of the carbon atom which is in column IV of the periodic table. Since the length of the double bond (0.140 nm) is shorter than that of the single bond (0.146 nm), the icosahedron becomes slightly distorted. This distortion does not affect the energy of the neutral atom in the ground state (HOMO), but does affect the filling of the excited states as charge is added to the fullerene [32]. The Jahn–Teller effect often involves spins and time reversal symmetry (see Chap. 16), as illustrated in Fig. 16.5 and the associated text.

We also comment on the Renner–Teller effect, that is a splitting on the vibrational levels of molecules due to even terms in the vibronic perturbation expansion (7.43). This effect is usually smaller than the linear Jahn–Teller effect, which is due to the odd terms in the expansion in (7.43), but it becomes important for linear diatomic molecules where the Jahn–Teller effect is absent. More details about the Jahn–Teller effect can be found in the literature, for example in [60].

Selected Problems

7.1. This problem is on diatomic molecules and considers the helium molecule He_2 and the hydrogen molecular ion with an extra electron H_2^- .

- (a) Suppose that we could make a bound diatomic molecule containing four electrons out of two helium atoms. What would you expect the ground state electronic configuration to be, what would its symmetry state be, and what would be its total electronic spin? Since the He_2 molecule is not formed under ordinary circumstances we know that the antibonding state lies too high in energy to form a bound state.
- (b) H_2^- however involves occupation of an antibonding state and does indeed form a bound state. What is the symmetry configuration of the three electrons in H_2^- ? Why is it possible for H_2^- to form a stable bound state but not for He_2 ? Group Theory gives us the symmetry designation for each molecular electronic state, but does not by itself give definitive information as to whether or not a bound state is formed.

7.2. Consider a hypothetical SF_6 molecule with octahedral symmetry (see Sect. 7.5.4 and Fig. 7.9).

- (a) Using $\Gamma^{\text{a.s.}}$, construct the linear combination of atomic orbitals for the six holes on the six fluorine atoms which transform according to the three irreducible representations $A_{1g} + E_g + T_{1u}$ contained in $\Gamma^{\text{a.s.}}$, assuming that wave functions with p symmetry ($\ell = 1$) are used to describe the valence states for the fluorine wave functions. Note that it is easier to consider a single hole rather than all the electrons in the nearly filled shell of the fluorine atom.
- (b) What are the angular momentum states required to bond the sulfur to the six fluorine atoms in p states.
- (c) What are the irreducible representations corresponding to σ -bonds and π -bonds for the central sulfur atom to the six fluorine atoms? Sketch the orientation of these bonding orbitals.

7.3. Why would the octahedral configuration of Fig. 7.9 be more stable for a hypothetical SH_6 molecule than the planar configuration in Fig. 7.6? Consider the angular momentum states required for the S atom to make the appropriate directed valence bonds to the six hydrogens in the planar SH_6 hypothetical molecule.

7.4. C_2H_4 (ethylene) is a planar molecule which has the configuration shown in Fig. 7.13.

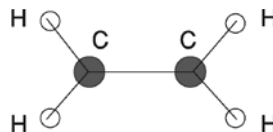


Fig. 7.13. Symmetry of the ethylene C_2H_4 molecule

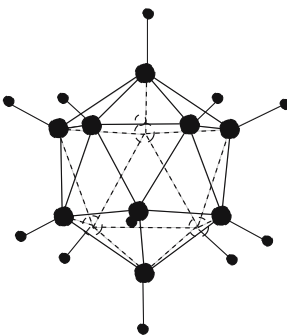


Fig. 7.14. Symmetry of the $\text{B}_{12}\text{H}_{12}$ icosahedral molecule

- Identify the appropriate point group for C_2H_4 .
- Find the equivalence representation $\Gamma^{\text{a.s.}}$ for the two carbon atoms and for the four hydrogen atoms in the C_2H_4 molecule.
- Considering the directed valence orbitals, how do the carbon atoms satisfy their bonding requirements? Which angular momentum states are needed to form bonding orbitals from each carbon atom?
- Give the block diagonal structure for the secular equation for the electronic energy levels of ethylene.

7.5. Consider the $\text{B}_{12}\text{H}_{12}$ molecule shown in Fig. 7.14 where the 12 hydrogen atoms (small balls) and the 12 boron atoms (large balls) are at vertices of a regular icosahedron.

- What are the symmetry operations associated with the ten classes of the full icosahedral group I_h (see Table A.28).
- What are the symmetries and degeneracies of the 12 linear combinations of atomic orbitals (LCAOs) associated with the 12 equivalent hydrogen atoms?
- Write the linear combinations of the 12 atomic orbitals (LCAOs) for the 12 hydrogen atoms in $\text{B}_{12}\text{H}_{12}$ in I_h symmetry.
- What are the angular momentum states involved with each of the directed valence σ orbitals from a boron atom to a hydrogen atom?

7.6. This problem further develops the symmetry properties of the CH_4 molecule introduced in Sect. 7.5.2.

- Using one symmetry operation from each class of the point group T_d , show that the linear combination of atomic orbitals $\psi_1(T_2)$ in (7.17) transforms as one of the partners of the irreducible representation T_2 .
- Using the symmetrized linear combination of atomic orbitals for the four hydrogen atoms in (7.16) and (7.17) and the wave functions for the four valence electrons for the carbon atom, construct the matrix Hamiltonian for the secular equation for the CH_4 molecule in block form showing the

nonzero entries and their symmetries, analogous to the corresponding matrix Hamiltonian for finding the electronic states for the CO molecule in Fig. 7.4.

- (c) Show that the directed valence bond wave function for CH_4 given by (7.20) has its maximum value along the (111) direction. What is the value of this bond along a $(\bar{1}\bar{1}\bar{1})$ direction? Along what direction does this bond have its minimum value?
- (d) What are the symmetries for the two lowest energy antibonding levels for the four hydrogen atoms and the four electrons on the carbon atom yielding the antibonding excited states of the CH_4 molecule? Why do you expect these excited states to have higher energies than the bonding states discussed in Sect. 7.5.2?

Molecular Vibrations, Infrared, and Raman Activity

In this chapter we review molecular vibrations and present the use of group theory to identify the symmetry and degeneracy of the normal modes. Selection rules for infrared and Raman activity are also discussed and are illustrated for a variety of molecules selected for pedagogic purposes.

8.1 Molecular Vibrations: Background

In this section we briefly indicate how group theory helps to simplify the solution of the dynamical matrix for molecular vibrations to obtain the symmetries and degeneracies of the normal modes and their characteristic displacements more quickly and directly. A molecule having its atoms at their equilibrium sites is in an energy minimum. If the atoms are displaced from their equilibrium positions, a restoring force will be exerted which will tend to bring the atoms back to equilibrium. If the displacement is small, the restoring forces and molecular motion will be harmonic. The harmonic nature of the force implies that the system can be in a quantum mechanical eigenstate, or normal mode of vibration.

Suppose that a molecule contains N atoms (depending on whether a net charge can be assigned to a specific atomic site) and suppose further that the potential function describing the forces, such as bond bending and bond stretching forces, can be expressed in terms of the $3N$ coordinates for the N atoms, as $V(\mathbf{R}_1, \dots, \mathbf{R}_N)$. We are particularly interested in $V(\mathbf{R}_1, \dots, \mathbf{R}_N)$ about its equilibrium coordinates at $\mathbf{R}_1^\circ, \dots, \mathbf{R}_N^\circ$, and we expand V about these equilibrium coordinates, utilizing the fact that a minimum in energy implies the vanishing of the first derivative of the potential. We can then conveniently take our zero of energy at the potential minimum and obtain a Hamiltonian for

molecular vibrations in terms of the small displacements from equilibrium:

$$\mathcal{H} = \underbrace{\sum_k \frac{1}{2} m_k \dot{\xi}_k^2}_{\text{kinetic energy}} + \underbrace{\sum_{k,\ell} \frac{1}{2} \frac{\partial^2 V}{\partial \xi_k \partial \xi_\ell} \xi_k \xi_\ell}_{\text{potential energy}}, \quad (8.1)$$

where m_k denotes the mass of the k th ion, ξ_k denotes its displacement coordinate, and the potential energy depends on the second derivative of $V(\mathbf{R}_1, \dots, \mathbf{R}_N)$. The Hamiltonian in (8.1) gives rise to a $(3N \times 3N)$ secular equation. The roots of this secular equation are the eigenfrequencies ω_K^2 and the eigenvectors denote the normal modes of the system.

The usual procedure for finding the normal modes involves two transformations, the first being used to eliminate the mass term in the kinetic energy:

$$q_k = \sqrt{m_k} \xi_k, \quad (8.2)$$

and a second transformation is used to express q_k in terms of the normal mode coordinates Q_K :

$$q_k = \sum_K a_{kK} Q_K, \quad (8.3)$$

where a_{kK} denotes the amplitude of each normal mode Q_K that is contained in q_k .

Thus, by a proper choice of the a_{kK} amplitudes, we can use (8.2) and (8.3) to reduce the potential energy V to a sum of squares of the form $\omega_K^2 Q_K^2 / 2$. These transformations yield for the potential function in (8.1):

$$V = \frac{1}{2} \sum_{\substack{k, \ell \\ K, L}} \left(\frac{\partial^2 V}{\partial q_k \partial q_\ell} \right) a_{kK} a_{\ell L} Q_K Q_L = \frac{1}{2} \sum_K \omega_K^2 Q_K^2, \quad (8.4)$$

where the coefficients a_{kK} are chosen to form a unitary matrix satisfying (8.4). Thus we obtain the relations $a_{Kk}^\dagger = a_{Kk}^{-1} = a_{kK}$ if the matrix elements of a_{kK} are real. The a_{kK} coefficients are thus chosen to solve the eigenvalue problem defined in (8.4). To achieve the diagonalization of the $V_{k\ell}$ matrix implied by (8.4) we must solve the secular equation

$$\sum_{k, \ell} a_{Kk}^{-1} \left(\frac{\partial^2 V}{\partial q_k \partial q_\ell} \right) a_{\ell L} = \omega_K^2 \delta_{KL}. \quad (8.5)$$

Solution of the secular equation (8.5) yields the eigenvalues or normal mode frequencies ω_K^2 and the eigenfunctions or normal mode amplitudes a_{kK} for

Table 8.1. Correspondence between important quantities in the electronic problem (see Sect. 7.1) and the molecular vibration problem

| quantity | electronic | molecular vibration |
|----------------------------|-------------|---|
| matrix element | $H_{k\ell}$ | $\frac{\partial^2 V}{\partial q_k \partial q_\ell} = V_{k\ell}$ |
| eigenvalue | E_n | ω_K^2 |
| eigenfunction ^a | $\psi_n(r)$ | a_{kK} |

For the molecular vibration problem, it is the normal mode amplitude a_{kK} which describes the physical nature of the small amplitude vibrations and is analogous to the wave function $\psi_n(r)$ for the electronic problem. The eigenvalues and eigenfunctions are found by diagonalizing $H_{k\ell}$ (electronic problem) or $V_{k\ell}$ (vibrational problem)

$K = 1, \dots, 3N$. From the form of the secular equation we can immediately see the correspondence between the electronic problem and the molecular vibration problem shown in Table 8.1.

The transformation defined by (8.2)–(8.5) leads to a simpler form for the Hamiltonian

$$\mathcal{H} = \sum_K P_K^2 / 2m_K + \omega_K^2 Q_K^2 / 2, \quad (8.6)$$

which is a sum of harmonic oscillators, where Q_K^2 is the normal coordinate.

The Hamiltonian in (8.6) can become quite complicated, but group theory can greatly simplify the required work by finding the normal modes that directly put \mathcal{H} into block diagonal form. As an example, one can compare the analytical solution for the “oscillator formed by three equal masses at the corners of an equilateral triangle”, as developed by Nussbaum [56], with the group theory analysis of this same pedagogic molecule to be developed in Problem 8.1.

8.2 Application of Group Theory to Molecular Vibrations

In an actual solution to a molecular vibration problem, group theory helps us to diagonalize the $V_{k\ell}$ matrix, to classify the normal modes and to find out which modes are coupled when electromagnetic radiation interacts with the molecule, either through electric dipole transitions (infrared activity) or in inelastic light scattering (the Raman effect). We discuss all of these issues in this chapter.

We make use of the symmetry of the molecule by noting that the molecule remains invariant under a symmetry operation of the group of the Schrödinger equation. Therefore, application of a symmetry operation \hat{P}_R to an eigenfunction of a normal mode f_K just produces a linear combination of other normal

modes of the same frequency ω_K . That is, f_K forms a basis for a representation for the symmetry operators \hat{P}_R of the molecule

$$\hat{P}_R f_K^{(i,\alpha)} = \sum_{K'} D^{(i)}(R)_{K'K} f_{K'}^{(i,\alpha)}, \quad (8.7)$$

where $D^{(i)}(R)_{K'K}$ denotes the matrix elements of the matrix representation for symmetry operator R , and i denotes the irreducible representation which labels both the matrix and the basis function (normal mode coordinate in this case) and α denotes the partner of the basis function in representation i . Since the basis functions for different irreducible representations do not couple to each other, group theory helps to bring the normal mode matrix $V_{k\ell}$ into block diagonal form, with each eigenvalue and its corresponding normal mode labeled by an appropriate irreducible representation. This is similar in concept to the solution of the electronic eigenvalue problem discussed in Chap. 7, except that for the vibrational problem every atom (or ion) in the molecule has three degrees of freedom, and a vector must be assigned to each atomic site. Thus the molecular vibration problem is analogous to the electronic problem for p -functions, where the p -functions also transform as a vector.

Therefore, to find the normal modes for the vibration problem, we carry out the following steps:

- Identify the symmetry operations that define the point group G of the molecule in its equilibrium configuration.
- Find the characters for the equivalence representation, $\Gamma_{\text{equivalence}} = \Gamma^{\text{a.s.}}$ (a.s. stands for atom site). These characters represent the number of atoms that are invariant under the symmetry operations of the group. Since $\Gamma^{\text{a.s.}}$ is, in general, a reducible representation of the group G , we must decompose $\Gamma^{\text{a.s.}}$ into its irreducible representations.
- We next use the concept that a molecular vibration involves the transformation properties of a vector. In group theoretical terms, this means that the molecular vibrations are found by taking the direct product of $\Gamma^{\text{a.s.}}$ with the irreducible representations for a radial vector [such as (x, y, z)]. The representation for the molecular vibrations $\Gamma_{\text{mol.vib.}}$ are thus found according to the relation

$$\Gamma_{\text{mol.vib.}} = (\Gamma^{\text{a.s.}} \otimes \Gamma_{\text{vec}}) - \Gamma_{\text{trans}} - \Gamma_{\text{rot}}, \quad (8.8)$$

where Γ_{trans} and Γ_{rot} denote the representations for the simple translations and rotations of the molecule about its center of mass. The characters found from (8.8), in general, correspond to a reducible representation of group G . We therefore express $\Gamma_{\text{mol.vib.}}$ in terms of the *irreducible* representations of group G to obtain the normal modes. Each eigen-mode is labeled by one of these irreducible representations, and the degeneracy of each eigen-frequency is the dimensionality of the corresponding irreducible representation. The characters for Γ_{trans} are found by identifying

the irreducible representations of the group G corresponding to the basis functions (x, y, z) for the radial vector \mathbf{r} . The characters for Γ_{rot} are found by identifying the irreducible representations corresponding to the basis functions (R_x, R_y, R_z) for the axial vector (e.g., angular momentum which for example corresponds to $\mathbf{r} \times \mathbf{p}$). Since the radial vector \mathbf{r} (x, y, z) and the axial vector $\mathbf{r} \times \mathbf{p}$ denoted symbolically by (R_x, R_y, R_z) transform differently under the symmetry operations of group G , every standard point group character table (see Appendix A) normally lists the irreducible representations for the six basis functions for (x, y, z) and (R_x, R_y, R_z) .

- (d) From the characters for the irreducible representations for the molecular vibrations, we find the normal modes, as discussed in the next section. The normal modes for a molecule as defined by (8.8) are constrained to contain only internal degrees of freedom, and *no translations or rotations* of the full molecule. Furthermore, the normal modes must be orthogonal to each other.
- (e) We use the techniques for selection rules (see Sect. 6.6 in Chap. 6) to find out whether or not each of the normal modes is infrared active (can be excited by electromagnetic radiation, see Sect. 8.6) or Raman-active (see Sect. 8.7).

It is important to recall that $\Gamma_{\text{vec}}(R)$ is obtained by summing the irreducible representations to which the x , y , and z basis functions belong. If (x, y, z) are the partners of a three-dimensional irreducible representation T , then $\Gamma_{\text{vec}}(R) = \Gamma^T(R)$. If, instead, x , y , and z belong to the same one-dimensional irreducible representation A , then $\Gamma_{\text{vec}}(R) = 3\Gamma^A(R)$. If the x , y , and z basis functions are not given in the character table, $\Gamma_{\text{vec}}(R)$ can be found directly from the trace of the matrix representation for each rotation R . All the point group operations are rotations or combination of rotations with inversion. For proper rotations, $\chi_{\text{vec}}(R) = 1 + 2 \cos \theta$, so that the trace for the rotation matrix can be always be found directly from

$$\begin{pmatrix} \cos(\theta) & \sin(\theta) & 0 \\ -\sin(\theta) & \cos(\theta) & 0 \\ 0 & 0 & 1 \end{pmatrix}. \quad (8.9)$$

Improper rotations consist of a rotation followed by a reflection in a horizontal plane resulting in the character $-1 + 2 \cos \theta$ where the $+1$ for the proper rotation goes into -1 for an improper rotation, since z goes into $-z$ upon reflection. Table 8.2 shows characters for Γ_{vec} for several selected point group operations. For C_5 , we need to consider $\cos 72^\circ = 0.30901\dots$ and the corresponding character becomes $\chi_{\text{vec}}(C_5) = 1.61803\dots$

To illustrate the procedure for finding molecular vibrations, we consider in the next sections the molecular vibrations of several different molecules to illustrate the methods discussed above and to provide more practice in using the various point groups. However, before going to specific molecules,

Table 8.2. Characters χ_{vec} for the vector for selected point group operations

| E | C_2 | C_3 | C_4 | C_6 | i | σ | S_6 | S_4 | S_3 |
|-----|-------|-------|-------|-------|-----|----------|-------|-------|-------|
| 3 | -1 | 0 | 1 | 2 | -3 | 1 | 0 | -1 | -2 |

we present the general procedure used to find the eigenvectors for the normal modes associated with a specific irreducible representation of a group.

8.3 Finding the Vibrational Normal Modes

In searching for the vectors which describe the normal mode displacements, we identify the point group of the molecule, thus providing us with the symmetry operations and the character table. Therefore, to find the normal mode eigenvector associated with an irreducible representation, we apply the projection operator algebra (see Chap. 4) to a chosen elementary motion of the atoms in the molecule (see (4.38))

$$\hat{P}(\Gamma_n) = \frac{\ell_n}{h} \sum_R \chi^{(\Gamma_n)}(R)^* \hat{P}_R. \quad (8.10)$$

This operation, however, projects out a function transforming as Γ_n but not a specific partner of Γ_n . While this is not a problem in dealing with 1D irreducible representations, for the case of multidimensional irreducible representations, physical insights are usually needed for finding physically meaningful partners of Γ_n quickly. The projection operators can also be used to check if the normal modes that are found are a combination of partners or not, and to find the other partners orthogonal to the first partner (see Chap. 4). Furthermore, a given set of partners is not unique, but the partners can be transformed among each other to get another orthonormal set. As an example, we can find the eigenfunction (normal mode) for a tetrahedral molecule (e.g., CH_4 , point group T_d) belonging, for example, to the totally symmetric A_1 irreducible representation. Since the four H atoms in CH_4 are equivalent (can be brought one into another by any of the symmetry operations of the group), the initial mode displacements of the atoms (denoted by ψ_0) can be chosen so that only one of the H atoms and the C atom are moving in an arbitrary direction, as shown in Fig. 8.1a. The identity operator applied to ψ_0 keeps it unchanged. The operation $(E + C_2)\psi_0$ gives the result shown in Fig. 8.1b, where the chosen axis for C_2 is displayed. By applying the complete set $\hat{P}^{(A_1)}\psi_0$ and summing up all the vectors, we find the A_1 mode, as shown in Fig. 8.1c, where the C atom does not move.

Through this example, we show how physical insight helps to find the eigenvectors. The mode in Fig. 8.1c is the stretching of the C–H bonds (the

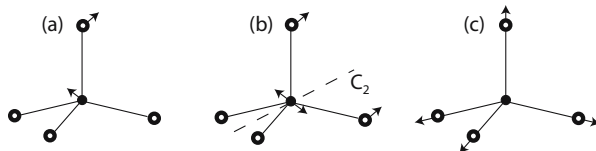


Fig. 8.1. Schematic for obtaining the totally symmetric normal mode of a tetrahedral (T_d point group) molecule. (a) The initial chosen arbitrary motion ψ_0 of two nonequivalent atoms; (b) the result of applying the operations E and C_2 on ψ_0 ; and (c) the normal mode displacements for the A_1 symmetry mode of CH_4 obtained from the projection operator $\hat{P}^{(A_1)}\psi_0$ after summing up all the vectors

so-called breathing mode) that keeps the tetrahedral symmetry unchanged, as it should, since it belongs to the totally symmetric A_1 irreducible representation. Therefore, this normal mode could be visualized without doing any of the procedures shown in Fig. 8.1a,b. In other cases, the final normal mode vector may not be so obvious, but still the use of physical insights are useful. For example, for finding the normal modes belonging to other irreducible representations of the tetrahedron, it is interesting to start with atomic motions that are not the ones found for the A_1 eigenvector, so that you increase the likelihood of finding displacements that may be orthogonal to the partners belonging to the normal modes that you already have. More about the normal modes of the tetrahedron will be discussed in Sect. 8.8.3.

Finding the normal vibrational modes is not a difficult procedure, but it gets more and more complicated as the number of atoms in the molecule increases. For dealing with a large molecule composed of N atoms, we can calculate

$$Q^{\Gamma_n} = \hat{P}^{(\Gamma_n)} \otimes \zeta. \quad (8.11)$$

Here ζ is a vector of dimensions $3N$ with the coordinates of an arbitrary initial motion of the atoms, and $\hat{P}^{(\Gamma_n)}$ is a $3N \times 3N$ matrix having all the atomic coordinates for the N atoms in their equilibrium positions, and describing the symmetry operations of the molecule. The Q^{Γ_n} is another $3N$ -dimensional vector giving the normal mode belonging to Γ_n , or a combination of normal modes if Γ_n is not a one-dimensional irreducible representation. In this way the partners can be found by using a less arbitrary initial vector ζ .

In the next sections we start to illustrate the procedure for finding molecular vibrations for specific and simple molecules. In doing so, we can better illustrate the physical insights for finding the normal modes, rather than using the formal procedure discussed above. We start by considering the molecular vibrations of an isolated H_2O molecule to illustrate finding the normal modes. Then we introduce additional theoretical issues associated with the observation of combination modes as well as infrared active and Raman active modes before returning to additional examples of molecular vibrations, for which we also include a discussion of their infrared and Raman activity.

8.4 Molecular Vibrations in H_2O

We start by considering the vibrations of an isolated H_2O molecule. This molecule is chosen because it is a simple molecule, has two different chemical species and involves a point group $C_{2v}(2mm)$ (Table A.5) we have not discussed previously. The four symmetry operations for the H_2O molecule (see Fig. 8.2) include E the identity operation, a 180° rotation C_2 around the z -axis, a reflection plane σ_v in the plane of molecule and a σ'_v reflection perpendicular to the plane of the molecule. The σ_v plane is a vertical reflection plane since the xz plane contains the highest symmetry axis C_2 . The reflection plane σ'_v which goes through C_2 is \perp to the plane of the molecule. In labeling the axes, the plane of the H_2O molecule is denoted by xz , with the x -axis parallel to a line going through the two hydrogens, and the perpendicular y -axis goes through the oxygen atom. The appropriate point group for the H_2O molecule is the group C_{2v} and the character table is given in Table 8.3 and Table A.5.

Next we find $\Gamma^{\text{a.s.}}$. For H_2O we have to consider the transformation of three atoms under the symmetry operations of the group. In writing down $\Gamma^{\text{a.s.}}$, we recall that for each site that is invariant under a symmetry operation,

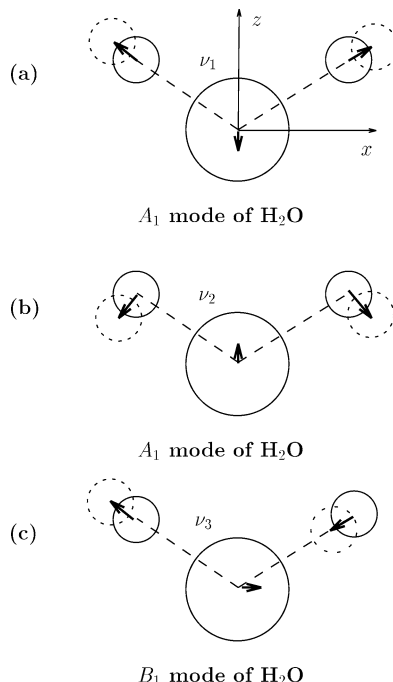


Fig. 8.2. Normal modes for the H_2O molecule with three vibrational degrees of freedom. (a) The breathing mode with symmetry A_1 , which changes only bond lengths. (b) The symmetric stretch mode of H_2O with A_1 symmetry, which changes bond angles. (c) The antisymmetric stretch mode with B_1 symmetry

a contribution of +1 is made to the character of that operation; otherwise the contribution is zero. Thus, we obtain for the characters for $\chi^{\text{a.s.}}(\text{H}_2\text{O})$ for all three atoms in the H₂O molecule as given in Table 8.4.

From the character table for group $C_{2v}(2mm)$ we see that the radial or polar vector transforms as

$$\Gamma_{\text{vec}} = A_1 + B_1 + B_2,$$

where z, x, y , respectively, transform as A_1, B_1 and B_2 . Likewise the irreducible representations for the rotations $\Gamma_{\text{rot.}}$ are $A_2 + B_1 + B_2$, corresponding to the rotations R_z, R_y , and R_x , respectively. We then calculate the irreducible representations $\Gamma_{\text{mol.vib.}}$ contained in the molecular vibrations:

$$\begin{aligned}\Gamma_{\text{mol.vib.}} &= \Gamma^{\text{a.s.}} \otimes \Gamma_{\text{vec}} - \Gamma_{\text{translations}} - \Gamma_{\text{rot}} \\ &= (2A_1 + B_1) \otimes (A_1 + B_1 + B_2) - (A_1 + B_1 + B_2) - (A_2 + B_1 + B_2) \\ &= [3A_1 + 3B_1 + 2B_2 + A_2] - (A_1 + B_1 + B_2) - (A_2 + B_1 + B_2) \\ \Gamma_{\text{mol.vib.}} &= 2A_1 + B_1.\end{aligned}\tag{8.12}$$

The three modes in $\Gamma_{\text{mol.vib.}}$ are all one-dimensional irreducible representations and therefore have nondegenerate or distinct vibrational frequencies.

We must now find the normal modes corresponding to each eigenfrequency. It is easy to use physical insights in such a simple symmetry. The two normal modes with A_1 symmetry must leave the symmetry undisturbed and this can be accomplished by the stretching of bonds and flexing of bond angles. These modes are the breathing and symmetric stretch modes (see Fig. 8.2). All molecules have a “breathing” mode which leaves the symmetry unchanged. To get the eigenvectors for the breathing mode of the H₂O molecule, assume that one of the hydrogen atoms is displaced in some way. With A_1 symmetry, this implies (under operation C_2) that the other H

Table 8.3. Character Table for Group $C_{2v}(2mm)$

| $C_{2v}(2mm)$ | | | E | C_2 | σ_v | σ'_v |
|-----------------|----------|-------|-----|-------|------------|-------------|
| x^2, y^2, z^2 | z | A_1 | 1 | 1 | 1 | 1 |
| xy | R_z | A_2 | 1 | 1 | -1 | -1 |
| xz | R_y, x | B_1 | 1 | -1 | 1 | -1 |
| yz | R_x, y | B_2 | 1 | -1 | -1 | 1 |

Table 8.4. Characters for the Atomic Site Transformation for H₂O

| | E | C_2 | σ_v | σ'_v | |
|--|-----|-------|------------|-------------|--------------------------|
| $\Gamma^{\text{a.s.}}(\text{H}_2\text{O})$ | 3 | 1 | 3 | 1 | $\Rightarrow 2A_1 + B_1$ |

atom must be correspondingly displaced (see Fig. 8.2(a)). To prevent translations and rotations of the molecule, O must be displaced as shown in Fig. 8.2(a). (The actual vibration amplitude for each atom is constrained to avoid translation and rotation of the molecule.)

The same arguments can be applied to obtain the A_1 symmetric stretch mode shown in Fig. 8.2(b). Application of the symmetry operations of group $C_{2v}(2mm)$ (Table A.5) confirms that this mode has A_1 symmetry. The H atom motion is taken so that the two A_1 modes are orthogonal. Since the breathing mode and symmetric stretch mode have the same symmetry they can mix (or couple to each other) and for this reason the directions of the H atom motion for each of the modes in Fig. 8.2(a), (b) are not uniquely specified.

To obtain the normal mode for B_1 symmetry, we observe that the character for the C_2 operation is -1 , so that the two hydrogen atoms must move in opposite directions relative to the O atom. Likewise, the motion of the O atom must be odd under C_2 . These arguments determine the normal B_1 mode shown in Fig. 8.2(c).

As mentioned above, all molecules have a breathing mode which transforms as A_1 and preserves the molecular symmetry. As a practical matter in checking whether or not the calculated normal modes are proper normal modes, it is useful to verify that the normal mode motion does not involve motion of the center of mass or rotation about the center of mass, and that all normal modes are orthogonal to each other.

8.5 Overtones and Combination Modes

In addition to the first-order molecular vibrations discussed above, harmonics (or multiples of the fundamental mode frequency such as 2ω , 3ω , etc.) and combination modes (which refer to the sum and differences of the mode frequencies, such as $\omega_1 \pm \omega_2$) are observed. The observation of these modes usually involves a perturbation to excite these modes, but this perturbation will also perturb their frequencies somewhat. We consider in this section the group theory of harmonics and combination modes in the limit of small perturbations so that the perturbation to the mode frequencies is minimal.

Since the two phonon state is a product of the normal modes, the mode frequency for the lowest overtone mode (or second harmonic) is at $\sim 2\omega_{\Gamma_i}$ and the symmetry of the harmonic is given by the direct product $\Gamma_i \otimes \Gamma_i$ and the irreducible representations combined therein. Similarly, the combination modes are at frequencies $\simeq (\omega_{\Gamma_i} + \omega_{\Gamma_j})$ in the limit of a very weak perturbation and have symmetries given by $\Gamma_i \otimes \Gamma_j$. In Sect. 8.8.3 where we consider the overtones (harmonics) and combination modes of the methane molecule, we can see which modes are activated in the infrared and Raman spectra for a real molecule and we can see the frequency shifts produced by the perturbation exciting these higher order molecular vibrations. Some of these modes for the

Table 8.5. Observed vibrational frequencies for the methane molecule^a

| assignment | symmetry | mode | frequency (cm ⁻¹) |
|-----------------|-------------------------|-----------------------|-------------------------------|
| $\nu_1(A_1)$ | A_1 | fundamental | 2914.2 |
| $\nu_2(E)$ | E | fundamental | 1526 |
| $\nu_3(T_2)$ | T_2 | fundamental | 3020.3 |
| $\nu_4(T_2)$ | T_2 | fundamental | 1306.2 |
| $2\nu_2$ | $A_1 + A_2 + E$ | overtone ^b | 3067.0 |
| $2\nu_3$ | $(A_1 + E) + T_1 + T_2$ | overtone ^b | 6006 |
| $3\nu_3$ | $(A_1 + T_1) + 2T_2$ | overtone ^c | 9047 |
| $2\nu_4$ | $(A_1 + E) + T_1 + T_2$ | overtone ^b | 2600 |
| $\nu_4 - \nu_3$ | $(A_1 + E) + T_1 + T_2$ | combination | 1720 |
| $\nu_2 + \nu_4$ | $T_1 + T_2$ | combination | 2823 |

^aHerzberg, "Infrared and Raman Spectra of Polyatomic Molecules", "Molecular Spectra and Molecular Structure II", 1949, "Van Nostrand Reinhold", "New York" [40]

^bFor overtones, only the symmetric combinations of basis functions are Raman allowed

^cFor $3\nu_3$ the symmetric combinations correspond to the angular momentum states $L = 1$ which transforms as T_2 and $L = 3$ which transforms as $A_1 + T_1 + T_2$

methane molecule CH₄ are given in Table 8.5 and are further discussed in Sect. 8.8.3.

8.6 Infrared Activity

If electromagnetic radiation is incident on a molecule in its ground state, then the radiation will excite those vibrational modes which give rise to a dipole moment. In the ground state, the molecule is in a zero phonon state and therefore has A_1 symmetry. We can use group theory to decide whether or not an electromagnetic transition will occur, i.e., if a given excited mode can be connected by the electromagnetic wave to the ground state A_1 (or more generally to the initial state of a highly excited molecule). The perturbation Hamiltonian for the interaction of the molecule with the electromagnetic (infrared) interaction is

$$\mathcal{H}'_{\text{infrared}} = -\mathbf{E} \cdot \mathbf{u}, \quad (8.13)$$

where \mathbf{E} is the incident oscillating electric field and \mathbf{u} is the induced dipole moment arising from atomic displacements. In this interaction, \mathbf{u} transforms like a vector. To find out whether the incident photon will excite a particular vibrational mode, we must examine the selection rules for the process. This means that we must see whether or not the matrix element for the excitation ($\psi_f | \mathbf{u} | \psi_i$) vanishes, where ψ_f denotes the normal mode which we are

trying to excite and \mathbf{u} is the vector giving the transformation properties of $\mathcal{H}'_{\text{infrared}}$, while ψ_i denotes the initial state of the molecule, which for most cases is the ground state. The ground state has no vibrations and is represented by the totally symmetric state A_1 of the unperturbed molecule, while $\mathcal{H}'_{\text{infrared}}$ transforms like a vector, since the applied field is external to the molecule.

To determine whether or not a molecule is infrared active, we use the usual methods for finding out whether or not a matrix element vanishes. That is, we ask whether the direct product $\Gamma_{\text{vec}} \otimes \Gamma_i$ contains the representation Γ_f ; if $(\Gamma_{\text{vec}} \otimes \Gamma_i)$ does not contain Γ_f , or equivalently if $\Gamma_f \otimes \Gamma_{\text{vec}} \otimes \Gamma_i$ does not contain A_1 , then the matrix element $\equiv 0$. Since molecular vibrations are typically excited at infrared frequencies, we say that a molecule is *infrared active* if any molecular vibrations can be excited by the absorption of electromagnetic radiation. The particular modes that are excited are called *infrared-active modes*. Correspondingly, the modes that cannot be optically excited are called *infrared inactive*. Considering infrared excitation from the vibrational ground state (no phonon), we write $\Gamma_{\text{vec}} \otimes A_1 = \Gamma_{\text{vec}}$. The infrared active modes thus transform as the irreducible representations for the basis vector x, y , and z (usually given in the character tables), and the specific basis vector indicates the polarization of the light needed to excite that specific mode.

As applied to the H_2O molecule (see Sect. 8.4) we have the following identification of terms in the electromagnetic matrix element. Suppose that the initial state has A_1 symmetry for the unexcited molecule and that the vector \mathbf{u} transforms as

$$\mathbf{u} \rightarrow A_1 + B_1 + B_2$$

corresponding to the transformation properties of z, x, y , respectively. The case of the H_2O molecule shows that the components of the vector may transform according to different irreducible representations of the point group for the molecule. Thus, we obtain for the direct product between the vector and the initial state:

$$(A_1 + B_1 + B_2) \otimes (A_1) = A_1 + B_1 + B_2 \quad (8.14)$$

showing the irreducible representations that are infrared active.

Therefore the two A_1 modes and the B_1 mode of water are all infrared-active. Each of the three vibrations corresponds to an oscillating dipole moment. As far as polarization selection rules are concerned, we can excite either of the two A_1 modes with an optical electric field in the z -direction, the twofold axis of the molecule. To excite the B_1 mode, the optical electric field must be along the x -direction, the direction of a line connecting the two hydrogen atoms. An electric field in the y direction (perpendicular to the plane of the molecule) does not excite any vibrational modes. Since all vibrational modes of the water molecule can be excited by an arbitrarily directed \mathbf{E} field, all the vibrational modes of the water molecule are infrared-active. It

is not always the case that *all* vibrational modes of a molecule are infrared-active. It can also happen that for some molecules only a few of the modes are infrared-active. This situation occurs in molecules having a great deal of symmetry.

To observe infrared activity in the second-order infrared spectra, we require that the combination of two vibrational modes be infrared-active. From a group theoretical standpoint, the symmetry of the combination mode arising from constituent modes of symmetries Γ_i and Γ_j is given by the direct product $\Gamma_i \otimes \Gamma_j$. Since groups containing inversion symmetry have only odd parity infrared-active modes, such symmetry groups have no overtones in the second-order infrared spectrum.

8.7 Raman Effect

In the Raman effect the inelastically scattered light from a system is detected. The *induced* dipole moment is

$$\mathbf{u} = \overleftrightarrow{\alpha} \cdot \mathbf{E}_i \cos \omega t, \quad (8.15)$$

where $\overleftrightarrow{\alpha}$ is the Raman polarizability tensor, a second rank symmetric tensor. Because the inelastic scattering of the incident light \mathbf{E}_i can excite molecular vibrations, the polarizability tensor has frequency dependent contributions at the molecular vibration frequencies ω_v

$$\overleftrightarrow{\alpha} = \overleftrightarrow{\alpha}_0 + \Delta \overleftrightarrow{\alpha} \cos \omega_v t, \quad (8.16)$$

so that

$$\begin{aligned} \mathbf{u} &= \left(\overleftrightarrow{\alpha}_0 + \Delta \overleftrightarrow{\alpha} \cos \omega_v t \right) \cdot \mathbf{E}_i \cos \omega t \\ &= \overleftrightarrow{\alpha}_0 \cdot \mathbf{E}_i \cos \omega t + \frac{\Delta \overleftrightarrow{\alpha}}{2} [\cos(\omega - \omega_v)t + \cos(\omega + \omega_v)t] \cdot \mathbf{E}_i, \end{aligned} \quad (8.17)$$

where the first term in (8.16 and 8.17) is the Rayleigh component at incident frequency ω , the second term is the Stokes component at frequency $(\omega - \omega_v)$, and the third term is the anti-Stokes component at frequency $(\omega + \omega_v)$. In observing the first-order Raman effect,¹ the scattered light is examined for the presence of Stokes components at frequencies $(\omega - \omega_v)$ and of anti-Stokes components at frequencies $(\omega + \omega_v)$. Not all normal modes of the molecule will yield scattered light at $(\omega \pm \omega_v)$, although if the Stokes component is excited, symmetry requires the anti-Stokes component to be present also, though its intensity may be small.

¹The first-order Raman process is the interaction of light with one vibrational mode. The second-, third-, ... n th-order Raman effect is related to combination or overtones involving two, three, ... n th vibrational modes.

To find whether or not a vibrational mode is Raman active, we ask whether or not the matrix element for the Raman perturbation vanishes. The Raman perturbation is of the $-\mathbf{u} \cdot \mathbf{E}$ form and using (8.15), $\mathcal{H}'_{\text{Raman}}$ is written as

$$\mathcal{H}'_{\text{Raman}} = -\frac{\Delta \overset{\leftrightarrow}{\alpha}}{2} \mathbf{E}_i \mathbf{E}_s \cos(\omega \pm \omega_v) t. \quad (8.18)$$

The transformation properties of $\mathcal{H}'_{\text{Raman}}$ are those of a second rank symmetric tensor $\Delta\alpha_{ij}$ (where $i, j = x, y, z$). The vectors \mathbf{E}_i and \mathbf{E}_s for the incident and scattered light are external to the molecular system and it is only the symmetry of the polarizability tensor $\Delta\alpha_{ij}$ that pertains to the molecule. To find out whether a particular normal mode is Raman-active we need only consider the matrix element:

$$(\psi_f | \mathcal{H}'_{\text{Raman}} | \psi_i), \quad (8.19)$$

where ψ_f is the final state corresponding to a normal mode we are trying to excite, $\mathcal{H}'_{\text{Raman}}$ is the Raman perturbation which has the transformation properties of a symmetric second rank tensor, and ψ_i is the initial state generally taken as the ground state which has the full symmetry of the group of Schrödinger's equation. A vibrational mode is Raman active if the direct product ($\Gamma_i \otimes \Gamma_{\mathcal{H}'_{\text{Raman}}}$, where $\mathcal{H}'_{\text{Raman}}$ transforms as a second rank symmetric tensor) contains the irreducible representation for the final state Γ_f . This is the basic selection rule for Raman activity. The group theory associated with tensors is discussed in more detail in Chap. 18.

Since the Raman process is a second-order process, it involves an intermediate state. The process involves an electron–photon interaction to produce an excited state where an electron–phonon scattering event occurs creating (Stokes process) or absorbing (anti-Stokes process) a phonon, and finally the scattered photon is emitted in an electron–photon interaction. In terms of the spectroscopy of molecular systems with inversion symmetry, the Raman effect is especially important because it is a *complementary technique to infrared spectroscopy*. Since the infrared excitation is a first-order process and the dipole operator transforms as a vector, selection rules for a vector interaction couple states with opposite parity. On the other hand, the Raman process, being a symmetric second-order process, is characterized by an interaction $\mathcal{H}'_{\text{Raman}}$ which transforms as a tensor that is even under inversion and therefore couples an initial and final state of similar parity. Thus for molecules with inversion symmetry infrared spectroscopy probes molecular vibrations with odd parity, while Raman spectroscopy probes modes with even parity.

If the molecule does not have inversion symmetry, some vibrational modes are both Raman and infrared active, and others can be neither Raman nor infrared-active. The latter symmetry modes are called silent modes.

The use of *polarized light* plays a major role in the assignment of experimentally observed Raman lines to specific Raman-active modes. In Raman experiments with polarized light, it is customary to use the notation:

$\mathbf{k}_i(\mathbf{E}_i\mathbf{E}_s)\mathbf{k}_s$ to denote the incident propagation direction \mathbf{k}_i , the incident and scattered polarization directions $(\mathbf{E}_i\mathbf{E}_s)$ and the scattered propagation direction \mathbf{k}_s . From (8.18) we see that the Raman tensor $\mathcal{H}'_{\text{Raman}}$ depends on both \mathbf{E}_i and \mathbf{E}_s and on the change in the polarizability tensor $\Delta \overset{\leftrightarrow}{\alpha}$, where \mathbf{E}_i and \mathbf{E}_s are, respectively, the incident and the scattered electric fields. It is customary to designate the scattered light as having *diagonal* Raman components ($\mathbf{E}_i \parallel \mathbf{E}_s$), or *off-diagonal* Raman components ($\mathbf{E}_i \perp \mathbf{E}_s$).

To find the selection rules for the Raman effect, we observe that the polarizability $\Delta \overset{\leftrightarrow}{\alpha}$ in (8.15) is a *second rank symmetric tensor* (see Chap. 18) and has the same transformation properties as a general quadratic form (e.g., $x^2, y^2, z^2, xy, yz, zx$). The transformation properties of these basis functions are usually found in the table of characters for the point groups, indicating the irreducible representations to which the Raman-active vibrational modes belong. The polarization selection rules for specific modes according to their incident and scattered polarization is also obtained from the basis functions. We note here that the symmetric off-diagonal components correspond to combinations $(xy + yx)/2$ and the corresponding terms for yz and zx . The anti-symmetric terms for a second rank tensor correspond to $(xy - yx)/2$ and its partners, which transform as the axial vectors (R_x, R_y, R_z) , and are so listed in the character tables. In a second-order Raman spectrum, a combination mode or overtone will be observable if $\Gamma_i \otimes \Gamma_j$ contains irreducible representations that are themselves Raman-active, since the $\mathcal{H}'_{\text{Raman}}$ matrix element in this case will couple a no-phonon ground state to a combination mode excited state (see (8.19)). Since $x^2 + y^2 + z^2$ transforms as the identity transformation and the direct product $\Gamma_i \otimes \Gamma_i$ always contains the identity representation, all second harmonics at $2\omega_i$ are Raman-active modes. Thus, some silent modes that cannot be found in the first-order spectrum can thus be observed in the second-order spectrum.

In the following subsections we discuss molecular vibrations for specific molecules, and in so doing, we will also include comments about the infrared and the Raman activity of these molecules.

8.8 Vibrations for Specific Molecules

In this section we consider molecular vibrations for specific molecules, starting with linear molecules in Sect. 8.8.1 and then going to more complex multiaatomic molecules. We also discuss the infrared (Sect. 8.6) and Raman (Sect. 8.7) activity of the normal modes for each of the molecules that are considered.

8.8.1 The Linear Molecules

The procedure for dealing with the molecular vibrations of linear molecules such as CO or H₂ is special and is slightly different from what has been de-

scribed in Sect. 8.2. We now present a method for handling the linear molecules and give some examples. For a linear molecule, the irreducible representations for the rotations just involves the rotations R_x and R_y , assuming the molecular axis to be along \hat{z} . Thus for the linear molecule, only two degrees of freedom are removed by Γ_{rot} , since rotations along the axis of the molecule correspond to the identity operation, considering the atoms as homogeneous balls without any internal degrees of freedom. First we consider the heterogeneous CO linear molecule (group $C_{\infty v}$ in Table A.33) followed by the homogeneous H₂ linear molecule (group $D_{\infty h}$ in Table A.34). With these simple molecules, we illustrate both molecular vibrations of linear molecules and the use of the semi-infinite point groups $C_{\infty v}$ and $D_{\infty v}$ in this context.

The appropriate symmetry group for CO is $C_{\infty v}$ (see Sect. 7.4.2). The symmetry operations $2C_\phi$ denote rotations about the \hat{z} axis in clockwise and counter-clockwise senses by an arbitrary angle ϕ . Thus C_ϕ is a class with an ∞ number of symmetry operations. The symmetry plane σ_v is a vertical plane through the molecular axis at an angle ϕ with respect to an arbitrary direction denoted by $\phi = 0$. Since the $2C_\phi$ and σ_v classes are of infinite order, the number of irreducible representations is also infinite.

The first step in finding $\Gamma_{\text{mol.vib.}}$ for a linear molecule is to compute $\Gamma^{\text{a.s.}}$. For the CO molecule shown in Fig. 8.3, the equivalence transformation yields $\Gamma^{\text{a.s.}}$ (see Table 8.6), from which we find the irreducible representations for the molecular vibrations of CO, remembering that Γ_{rot} only contains rotations in the xy plane normal to the rotation axis of the molecule, and therefore Γ_{rot} transform as E_1 while Γ_{vec} transform as $A_1 + E_1$:

$$\Gamma_{\text{mol.vib.}} = \Gamma^{\text{a.s.}} \otimes \Gamma_{\text{vec}} - \Gamma_{\text{trans}} - \Gamma_{\text{rot}},$$

$$\Gamma_{\text{mol.vib.}} = (2A_1) \otimes (A_1 + E_1) - (A_1 + E_1) - E_1 = A_1.$$

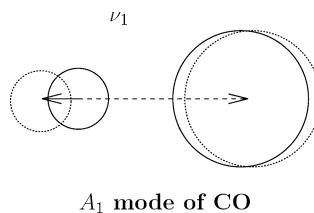


Fig. 8.3. CO molecule only has an A_1 breathing mode. The lighter mass of the C atom results in a larger displacement to maintain the center of mass

Table 8.6. Characters for the Atomic Site Transformation for the CO molecule

| | E | $2C_\phi$ | σ_v | |
|------------------------|-----|-----------|------------|--------------------|
| $\Gamma^{\text{a.s.}}$ | 2 | 2 | 2 | $\Rightarrow 2A_1$ |

The A_1 mode is the breathing mode for the CO molecule (see Fig. 8.3). Since the C and the O atoms are distinct, this molecule has a dipole moment along the z direction so that CO is infrared active. From the character table for $C_{\infty v}$ we see that the components of the Raman tensor ($x^2 + y^2$) and z^2 transform as A_1 , so we conclude that CO is also Raman active.

If we now consider the O_2 molecule (see Fig. 8.4), we have a homo-nuclear molecule following the symmetry group $D_{\infty h}$ (see Character Table A.34). Here the displacements are now fully symmetric unlike the situation for the CO molecule where the center of mass of the molecule must be conserved so that the lighter atom has a larger vibrational amplitude. In the case of the O_2 molecule the characters for $\Gamma^{\text{a.s.}}$ are listed in Table 8.7. Thus the irreducible representations for the molecular vibrations of O_2 become:

$$\begin{aligned}\Gamma_{\text{mol.vib.}} &= \Gamma^{\text{a.s.}} \otimes \Gamma_{\text{vec}} - \Gamma_{\text{trans}} - \Gamma_{\text{rot}} \\ \Gamma_{\text{mol.vib.}} &= (A_{1g} + A_{2u}) \otimes (A_{2u} + E_{1u}) - (A_{2u} + E_{1u}) - E_{1g} \quad (8.20) \\ &= A_{1g},\end{aligned}$$

where $\Gamma_{\text{rot}} = E_{1g}$ for the rotations R_x, R_y . Because of the inversion symmetry of the O_2 molecule, all the normal modes have either even (gerade) or odd (ungerade) symmetries. Thus for O_2 the breathing mode (see Fig. 8.4) has A_{1g} symmetry and is infrared-inactive. From simple physical considerations the breathing mode for O_2 has no oscillating dipole moment nor can a dipole moment be induced. Hence O_2 does not couple to an electromagnetic field through an electric dipole interaction, in agreement with our group theoretical result, so O_2 is not infrared active. The A_{1g} mode of the O_2 molecule is however Raman active, as is also the CO molecular vibrational mode mentioned above.

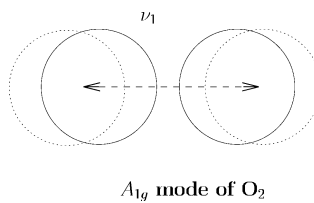


Fig. 8.4. The O_2 molecule only has an A_{1g} breathing mode with symmetric displacements of the atoms in the normal mode vibration

Table 8.7. Characters for the Atomic Site Transformation for the O_2 molecule

| | E | $2C_\phi$ | C'_2 | i | $2iC_\phi$ | iC'_2 | |
|------------------------|-----|-----------|--------|-----|------------|---------|-------------------------------|
| $\Gamma^{\text{a.s.}}$ | 2 | 2 | 0 | 0 | 0 | 2 | $\Rightarrow A_{1g} + A_{2u}$ |

Table 8.8. Characters for the Atomic Site Transformation for the CO_2 molecule

| | E | $2C_\phi$ | C'_2 | i | $2iC_\phi$ | iC'_2 |
|------------------------|-----|-----------|--------|-----|------------|---------|
| $\Gamma^{\text{a.s.}}$ | 3 | 3 | 1 | 1 | 1 | 3 |

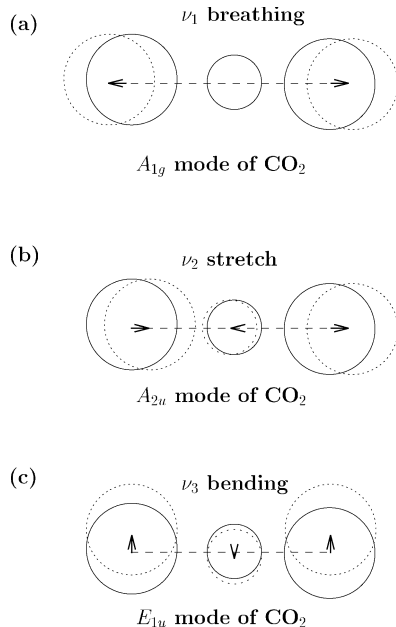


Fig. 8.5. The three vibrational normal modes of CO_2 : (a) the breathing mode with A_{1g} symmetry, (b) the antisymmetric stretch mode with A_{2u} symmetry, and (c) the doubly degenerate E_{1u} mode where the mode displacements for the two partners are orthogonal (i.e., \parallel and \perp to the page)

The CO_2 molecule is chosen for discussion to show the various types of modes that can be expected for linear molecules involving three or more atoms. Below we consider another molecule (C_2H_2) described by the same symmetry group $D_{\infty h}$ but having slightly more complexity.

For the case of CO_2 (see Fig. 8.5), we again have a linear molecule with $D_{\infty h}$ symmetry and now $\Gamma^{\text{a.s.}}$ corresponds to a three-dimensional representation (see Table 8.8), so that $\Gamma^{\text{a.s.}} = 2A_{1g} + A_{2u}$.

$$\begin{aligned}
 \Gamma_{\text{mol.vib.}} &= \Gamma^{\text{a.s.}} \otimes \Gamma_{\text{vec}} - \Gamma_{\text{trans}} - \Gamma_{\text{rot}} \\
 \Gamma_{\text{mol.vib.}} &= (2A_{1g} + A_{2u}) \otimes (A_{2u} + E_{1u}) - (A_{2u} + E_{1u}) - E_{1g} \quad (8.21) \\
 &= A_{1g} + A_{2u} + E_{1u}.
 \end{aligned}$$

The normal modes for CO_2 are easily found with the help of the character table, and are shown in Fig. 8.5. The A_{1g} mode is the breathing mode, the

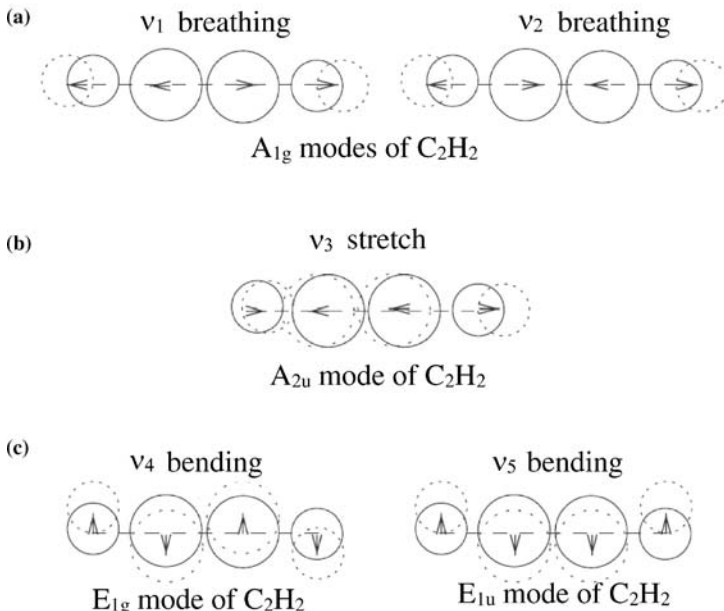


Fig. 8.6. Schematic diagram of the normal modes of the linear C_2H_2 molecule: (a) two breathing modes of A_{1g} symmetry, (b) an antisymmetric stretch mode of A_{2u} symmetry, and (c) and (d) two doubly-degenerate bending modes of E_{1g} and E_{1u} symmetries

A_{2u} mode is the antisymmetric stretch mode and the E_{1u} mode is a doubly degenerate bending mode where the displacements of the carbon and the two oxygens are normal to the molecular axis for each partner of the E_{1u} bending mode. Of these modes only the A_{1g} mode is Raman active. In this case, the A_{2u} and E_{1u} modes are infrared-active while the symmetric A_{1g} mode is infrared-inactive as can be seen from the character table for $D_{\infty h}$ (Table A.34).

For the case of the linear C_2H_2 molecule, $H-C\equiv C-H$, also following group $D_{\infty h}$ symmetry, we obtain

$$\Gamma^{\text{a.s.}} = 2A_{1g} + 2A_{2u} \quad (8.22)$$

using the result for O_2 . Thus $\Gamma_{\text{mol.vib.}}$ for the C_2H_2 molecule becomes

$$\Gamma_{\text{mol.vib.}} = (2A_{1g} + 2A_{2u}) \otimes (A_{2u} + E_{1u}) - (A_{2u} + E_{1u}) - E_{1g}$$

$$\Gamma_{\text{mol.vib.}} = 2A_{1g} + A_{2u} + E_{1u} + E_{1g}.$$

The five normal modes for the molecular vibrations of C_2H_2 are shown in Fig. 8.6, again illustrating the breathing, antisymmetric stretch and bending modes corresponding to five different vibrational frequencies. These concepts can of course be generalized to give normal modes for more complex linear

molecules. For the C_2H_2 molecule, the two A_{1g} modes correspond to basis functions (z^2 and x^2+y^2) while the E_{1g} modes correspond to the (zx, zy) basis functions. These two different symmetry modes can be distinguished using optical polarization experiments whereby the A_{1g} modes will be observable when the incident and scattered light are polarized parallel to each other, but the E_{1g} mode will be observed when the polarization of the incident beam is along the molecular axis but the scattered beam is perpendicular to the molecular axis.

In Problem 8.3 it is shown that $\Gamma_{\text{mol.vib.}}$ and the normal modes of the C_2H_2 linear molecule can be easily found by considering the C_2H_2 molecule as being composed of two C–H blocks or of the two hydrogen atoms and the two carbon atoms as two other blocks, each with internal degrees of freedom vibrating against each other. Such considerations help in providing intuition about obtaining the internal vibrational modes of complex molecules.

We now illustrate how symmetry is used to assist in the solution of molecular vibration problems for several 3D molecules of pedagogic interest.

8.8.2 Vibrations of the NH_3 Molecule

The NH_3 molecule is one of two molecules selected for illustrating normal mode properties of three-dimensional molecular vibrations. To illustrate some features of degenerate normal modes, let us consider the NH_3 molecule (see Fig. 8.7). The hydrogen atoms in NH_3 are at the corners of an equilateral triangle and the nitrogen atom is either above or below the center of the triangle. If the molecule were planar, it would have D_{3h} symmetry, but because the N atom is not coplanar with the three hydrogen atoms, the appropriate symmetry group is C_{3v} (see Table A.10). We note that $\Gamma^{\text{a.s.}}$ for the three hydrogen atoms at the corners of a triangle transforms as $A_1 + E$ and we further note that $\Gamma^{\text{a.s.}}$ for the nitrogen atom transforms as A_1 under all the symmetry operations of the group. The results are written in Table 8.9 first for all four atoms. We can also consider the three hydrogen atoms separately and build up $\Gamma_{\text{mol.vib.}}$ from the N atom plus the three hydrogen LCAOs as two building blocks (see Problem 8.1).

$$\begin{aligned}\Gamma_{\text{mol.vib.}} &= \Gamma^{\text{a.s.}} \otimes \Gamma_{\text{vec}} - \Gamma_{\text{trans}} - \Gamma_{\text{rot}} \\ \Gamma_{\text{mol.vib.}} &= (2A_1 + E) \otimes (A_1 + E) - (A_1 + E) - (A_2 + E) \\ &= 2A_1 + 2E.\end{aligned}\tag{8.23}$$

Table 8.9. Characters for the Atomic Site Transformation for the NH_3 molecule

| | E | $2C_3$ | $3\sigma_v$ | |
|---------------------------------------|-----|--------|-------------|------------------------|
| $\Gamma_{\text{total}}^{\text{a.s.}}$ | 4 | 1 | 2 | $\Rightarrow 2A_1 + E$ |
| $\Gamma_{\text{H}}^{\text{a.s.}}$ | 3 | 0 | 1 | $\Rightarrow A_1 + E$ |

- One mode of the NH_3 molecule with A_1 symmetry is the breathing mode, where the nitrogen atom is at rest and the equilateral triangle expands and contracts (see Fig. 8.7(a)).
- For the A_1 out-of-plane breathing mode, the H atoms move in the $+z$ direction while the N atom moves in the $-z$ direction, such that no translation of the center of mass occurs (see Fig. 8.7(b)).
- One of the E modes is a doubly-degenerate in-plane mode. One eigenvector is made from the linear combination of hydrogen atom motions ($H_1 + \omega H_2 + \omega^2 H_3$) where the motion of each H atom bears a phase relation of $\omega = e^{2\pi i/3}$ relative to the next H atom. The second eigenvector is

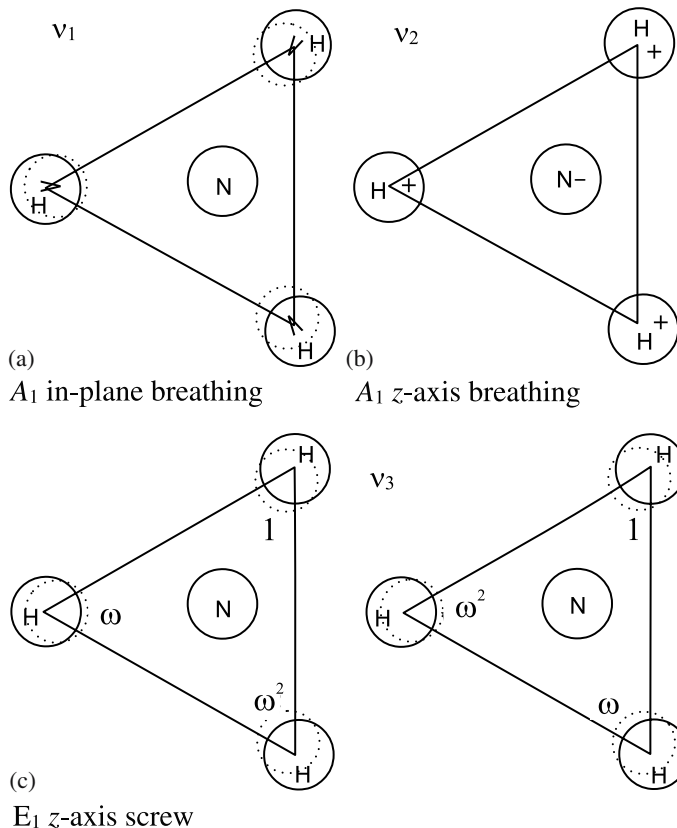


Fig. 8.7. Normal modes for the NH_3 molecule: (a) the in-plane breathing mode, (b) the out-of-plane (z -axis) breathing mode for which $+$ and $-$ refer to above and below the plane, respectively, and (c) the two partners of the in-plane mode of E symmetry which are complex conjugates of each other. The phase factor ω is $\exp(2\pi/3)$. There is also another doubly-degenerate E mode for z -axis (out-of-plane) motion that is not shown

$H_1 + \omega^2 H_2 + \omega H_3$ which is orthogonal to the first. The nitrogen atom moves in the xy plane in such a way as to prevent translation of the center of mass and rotation of the molecule (see Fig. 8.7(c)).

- For the second doubly degenerate E mode, the hydrogen atoms move in the out-of-plane direction with a phase difference between adjacent hydrogen atoms. For one partner, the three hydrogen atoms have phase factors of 1, ω and ω^2 while the second partner has motions with phases for its three hydrogen atoms that are the complex conjugates of the phases of the first partner $\omega = e^{2\pi i/3}$ for one partner and $\omega^2 = e^{4\pi i/3}$ for the other partner. The nitrogen atom again moves in such a way as to prevent translations or rotations of the molecule (not shown in Fig. 8.7(c)).

The molecular vibrations for the NH_3 molecule illustrate the concept of phase relations between the motions of various atoms in executing a normal mode. Though it should be emphasized that in the case of degenerate modes, the normal mode (basis function) picture is not unique, and therefore linear combinations of modes of the same symmetry are also possible. Since the normal modes for the NH_3 molecules have A_1 and E symmetries and since $\Gamma_{\text{vec}} = A_1 + E$, all the vibrational modes for NH_3 are infrared-active, with one of the two A_1 modes excited by polarization $\mathbf{E} \parallel \hat{z}$, the other being excited by polarization $\mathbf{E} \perp \hat{z}$. The same is true for the two E modes. The connection of the normal modes of NH_3 to the normal modes of three atoms at the vertices of a triangle is considered in Problem 8.1. For the case of the NH_3 molecule which has C_{3v} symmetry, the two Raman-active modes with A_1 symmetries have normal mode displacements $x^2 + y^2$ and z^2 and the two modes with E symmetries have normal mode displacements $(x^2 - y^2, xy)$ and (xz, yz) , so that all the normal modes for the NH_3 molecule ($2A_1 + 2E$) are Raman-active. Polarization selection rules imply that the A_1 modes are diagonal (i.e., scattering occurs when the incident and scattered polarizations are parallel $\mathbf{E}_i \parallel \mathbf{E}_s$), while the E modes are off-diagonal (i.e., scattering occurs when $\mathbf{E}_i \perp \mathbf{E}_s$).

8.8.3 Vibrations of the CH_4 Molecule

The CH_4 molecule is chosen to illustrate the vibrational modes of a five atom molecule with high symmetry and to give more practice with the T_d point group symmetry (Table A.32) because of the importance of this point group symmetry to semiconductor physics.

The equivalence transformation for the four hydrogen atoms of the CH_4 molecule yields $\Gamma_{4\text{H}}^{\text{a.s.}} = A_1 + T_2$ (see Sect. 7.5.2) while for the carbon atom $\Gamma_{\text{C}}^{\text{a.s.}} = A_1$ since the carbon atom is at the center of the regular tetrahedron. Thus for the whole CH_4 molecule with T_d symmetry we have $\Gamma^{\text{a.s.}} = 2A_1 + T_2$. In T_d symmetry, the radial vector transforms as T_2 while the angular momentum (or axial vector for rotations) transforms as T_1 . We thus get the following result for $\Gamma_{\text{mol.vib.}}$ for the CH_4 molecule.

For the symmetry types in the molecular vibrations $\Gamma_{\text{mol.vib.}}$ (see Fig. 8.8):

$$\begin{aligned}\Gamma_{\text{mol.vib.}} &= \Gamma^{\text{a.s.}} \otimes \Gamma_{\text{vec}} - \Gamma_{\text{trans}} - \Gamma_{\text{rot}} \\ \Gamma_{\text{mol.vib.}} &= [(2A_1 + T_2) \otimes (T_2)] - \underbrace{T_2}_{\text{translations}} - \overbrace{T_1}^{\text{rot}} \\ &= 2T_2 + (T_1 + T_2 + E + A_1) - T_2 - T_1 \\ &= A_1 + E + 2T_2.\end{aligned}$$

For many molecules of interest, the normal modes are given in [40]. We give in Fig. 8.8 the normal modes adapted from this reference. For the CH_4 molecule only the modes with T_2 symmetry are infrared active. The modes with A_1 , E , and T_2 symmetries are Raman active, where (xy, yz, zx) transforms as T_2 and

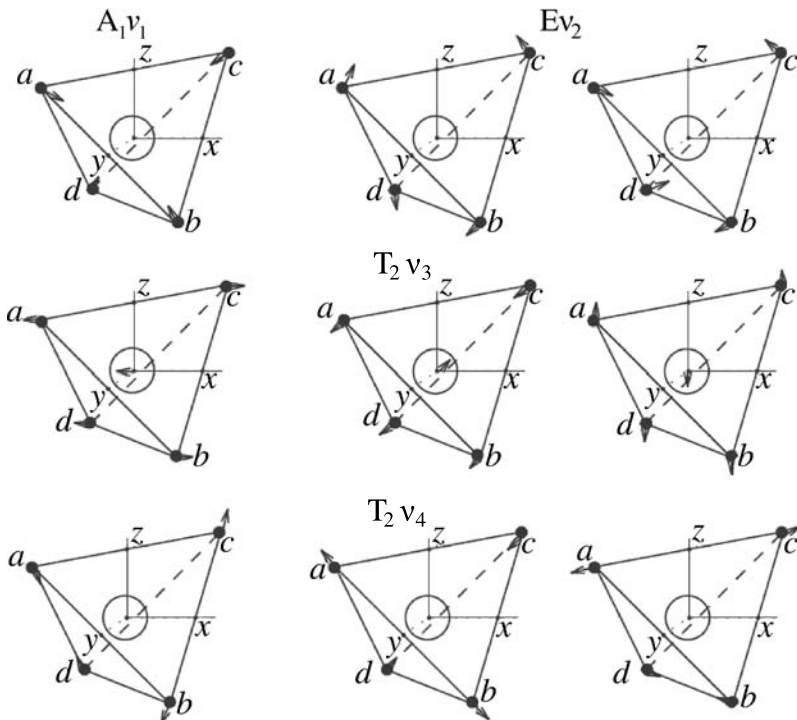


Fig. 8.8. Normal vibrations of a tetrahedral CH_4 molecule [40]. The three twofold axes (dot-dash lines) are chosen as the x -, y -, and z -axes. The exact directions of the H atom displacements depend on the nature of the C-H bond strength and the masses of H and C. Although CH_4 and CCl_4 have, of course, the same symmetry modes, the H and Cl atom displacement directions will differ. This issue was also discussed in Sect. 8.4 for the modes of H_2O (see Fig. 8.2)

the basis functions $x^2 - y^2$, and $3z^2 - r^2$ transform as E , while r^2 transforms as A_1 (see Table A.32).

We now give an example of harmonics and combination modes that can be observed in the second-order Raman and infrared spectra in terms of the CH_4 molecule. In Table 8.5 the frequencies of the four fundamental modes in the Raman spectra are given along with some of the overtones and combination modes. The symmetries of the overtones (harmonics) and combination modes are found by taking the direct product $\Gamma_i \otimes \Gamma_j$ between these modes. We see that the mode frequencies can deviate significantly from $\omega_i \pm \omega_j$ and the reason for this is that the perturbation which excites the harmonics and combination modes also perturbs the harmonic oscillator potential for the molecule with some combination mode frequencies being increased and others being decreased. We note that the T_2 modes are observed in the first-order infrared spectrum for CH_4 . Some of the direct products of importance in interpreting the second-order spectra are

$$E \otimes E = A_1 + A_2 + E$$

and

$$T_2 \otimes T_2 = A_1 + E + T_1 + T_2.$$

8.9 Rotational Energy Levels

In practice all molecules have rotational levels (labeled by quantum number j). In the approximation that we can discuss the rotational motion as distinct from the vibrational motion, the rotational motion of molecules should be much lower in frequency than the vibrational motion, and of course *very* much lower in frequency than the electronic motion. Typical rotational energies are of the order of $\sim 1 \text{ meV}$ and occur at far-infrared frequencies. The vibrational modes are observed in the mid-IR range, typically in the range 20–200 meV.

In Sect. 8.9.1 we discuss rotational energy levels of a molecule in terms of the rigid rotator as a simple example. Then in Sect. 8.9.2 we state the Wigner–Eckart theorem which gives in succinct form the selection rules for IR and Raman activity for rotational energy levels. Finally in Sect. 8.9.3 we introduce the coupling between the vibrational and rotational levels, giving some examples of rotational energy levels for a few simple molecules.

8.9.1 The Rigid Rotator

To illustrate molecular vibrations, we consider the simple case of the rigid rotator neglecting the effect of the molecular vibrations. The Hamiltonian for

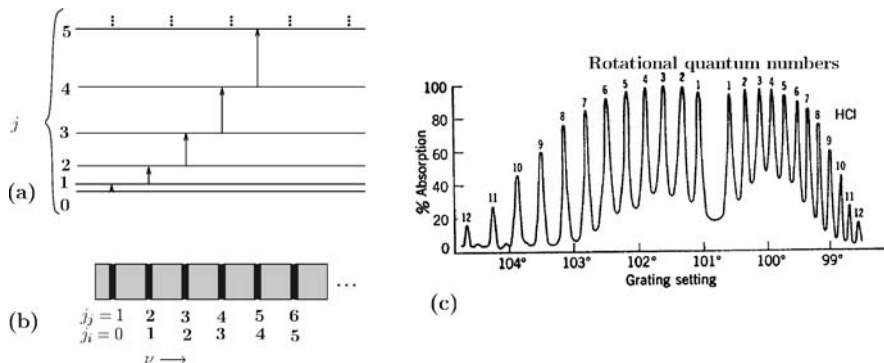


Fig. 8.9. (a) Rotational levels of a diatomic molecule. (b) Energy separation between sequential rotational levels. (c) The rotational absorption spectrum for gaseous HCl

rotational motion is written as

$$\mathcal{H}_{\text{rot}} = \frac{J_x^2}{2I_x} + \frac{J_y^2}{2I_y} + \frac{J_z^2}{2I_z}, \quad (8.24)$$

where I_x, I_y, I_z are the principal moments of inertia and J_x, J_y, J_z are the angular momentum operators. The coordinates x, y, z are chosen so that the z axis is along the main symmetry axis of the molecule. If we have a diatomic molecule, one principal moment of inertia vanishes $I_z = 0$, while the other two become equal $I_x = I_y$. In this case the Hamiltonian is simply

$$\mathcal{H}_{\text{rot}} = \frac{J^2}{2I}, \quad (8.25)$$

and has eigenvalues

$$E_j = \hbar^2 j(j+1)/2I.$$

Unlike the vibrational energy levels which are all equally spaced with a level separation $\hbar\omega_v$, the rotational energy levels are unequally spaced:

$$E_{j+1} - E_j = \mathcal{C}[(j+1)(j+2) - j(j+1)] = 2\mathcal{C}(j+1) \quad (8.26)$$

with $\mathcal{C} = \hbar^2/2I$ and the level spacing depends on the quantum number j (see Fig. 8.9(a)). If the molecule contains a permanent electric dipole moment, then it is possible to excite the molecule into higher rotational energy states by electric dipole transitions. The selection rules for transitions between rotational energy levels follow from the Wigner–Eckart theorem (Sect. 8.9.2).

According to this theorem, for light polarized along the principal axis of rotation of the HCl molecule, the selection rule for electric dipole transitions

is $\Delta j = 0$ while for light polarized in the plane \perp to this axis, the selection rule is $\Delta j = \pm 1$. If there is no vibrational–rotational interaction, $\Delta j = 0$ does not give rise to optical absorption.

Thus, the first rotational transition will require a photon energy $2C$, the second $4C$, the third $6C$, etc. This pattern is indicated in Fig. 8.9(a) for the HCl molecule and in Fig. 8.9(b) we see that $(E_j + 1 - E_j)$ increases proportional to (j_1) with a constant coefficient of $2C$. The actual spectrum for HCl is shown in Fig 8.9(c). It is clear that diatomic molecules like H_2 have a *center of inversion* and hence *no permanent dipole moment*. Thus, molecules of this type do not exhibit any pure rotational infrared spectra. On the other hand, heterogeneous diatomic molecules like CO and HCl can exhibit rotational infrared spectra.

8.9.2 Wigner–Eckart Theorem

The Wigner–Eckart theorem, based on the full rotation group, gives the selection rules for transitions between rotational levels observed for molecules in IR and Raman spectroscopy and their polarization effects.

For proof of the Wigner–Eckart theorem, see Tinkham, p. 131–132 [70]. This theorem deals with the matrix elements of a tensor T_μ^ω where ω is the rank of the tensor and μ is a component index, to be discussed further below. The theorem is discussed for angular momentum states which correspond (through the group of Schrödinger’s equation) to the full rotation group.

The full rotation group has only odd-dimensional representations:

$$\begin{aligned} \text{One-dimensional} & \quad \ell = 0 \text{ } s\text{-states} \\ \text{Three-dimensional} & \quad \ell = 1 \text{ } p\text{-states} \\ \text{Five-dimensional} & \quad \ell = 2 \text{ } d\text{-states}. \end{aligned}$$

Thus, a scalar ($\ell = 0$) corresponds to a tensor with $\omega = 0$ and $\mu = 0$. A vector corresponds to a tensor with $\omega = 1$, $\ell = 1$, and $\mu = \pm 1, 0$, which denote the three m_ℓ values for $\ell = 1$. A general second rank tensor can be considered as the direct product

$$\Gamma^{\ell=1} \otimes \Gamma^{\ell=1} = \Gamma^{\ell=0} + \Gamma^{\ell=1} + \Gamma^{\ell=2} \quad (8.27)$$

having dimensions $3 \times 3 = 1 + 3 + 5 = 9$. Thus the second rank tensor will have a part which transforms as $\omega = 0$ and $\mu = 0$, another part which transforms as $\omega = 1$, $\mu = \pm 1, 0$ and a third part which transforms as $\omega = 2$, $\mu = \pm 2, 1, 0$, thereby accounting for all nine components of the second rank tensor. The parts that transform as $\omega = 0$ and $\omega = 2$ constitute the symmetric components and correspond to the Raman tensor. The parts that transform as $\omega = 1$ constitute the antisymmetric components of a second rank tensor and correspond to the angular momentum components.

Because of the form of the Wigner–Eckart Theorem given by

$$(N'j'm' | T_\mu^\omega | Nj) = A_{m\mu}^{j\omega j'} \delta_{m',m+\mu} (Nj' || T^\omega || Nj) , \quad (8.28)$$

the selection rules for a tensor operator T_μ^ω between states having full rotational symmetry can be obtained quickly. Here j' lies in the range

$$|j - \omega| \leq j' \leq (j + \omega) , \quad (8.29)$$

which is related to the properties of the addition of angular momentum vectors. In (8.28), N and N' are principal quantum numbers, j and j' are quantum numbers for the total angular momentum, while m and m' are quantum numbers for the z component of the angular momentum. The coefficients $A_{m\mu}^{j\omega j'}$ are called Wigner coefficients [2] and are tabulated in group theory texts (see for example, Tinkham) [70]. The reduced matrix element $(Nj' || T^\omega || Nj)$ in (8.28) is independent of μ, m , and m' and can therefore be found for the simplest case $\mu = m' = m = 0$. This generality makes the Wigner–Eckart theorem so powerful. The selection rules on both j and m are obtained by rewriting the restrictions implied by (8.28) and (8.29), yielding

$$\begin{aligned} |\Delta j| &= |j - j'| \leq \omega \\ |\Delta m| &= |m' - m| = \mu \leq \omega . \end{aligned} \quad (8.30)$$

We now write down some special cases of (8.30).

For electric dipole transitions, we have $\omega = 1$ and the selection rules

$$\begin{aligned} \Delta j &= 0, \pm 1 \\ \Delta m &= 0 \quad \text{for } \mathbf{E} \parallel \hat{z} \\ \Delta m &= \pm 1 \quad \text{for } \mathbf{E} \perp \hat{z} , \end{aligned} \quad (8.31)$$

where $\mathbf{E} \parallel \hat{z}$ refers to linear polarization along the quantization axis and $\mathbf{E} \perp \hat{z}$ refers to circular polarization about the quantization axis.

For Raman transitions (where $\mathcal{H}'_{\text{Raman}}$ transforms as a second rank symmetric tensor), we have either $\omega = 0$ or $\omega = 2$ and the corresponding selection rules

$$\begin{aligned} \omega = 0 : \quad \Delta j &= 0 , \quad \Delta m = 0 , \\ \omega = 2 : \quad \Delta j &= 0, \pm 1, \pm 2 , \quad \Delta m = 0, \pm 1, \pm 2 . \end{aligned} \quad (8.32)$$

In specific geometries, not all of these transitions are possible.

In applying the Wigner–Eckart theorem to the *rotational selection rules* for a *linear diatomic molecule*, we know that the dipole moment must be along the molecular z -axis, so that only $\mu = 0$ applies. In this case the *Wigner–Eckart Theorem* gives the selection rules

$$\begin{aligned} \Delta j &= 0, \pm 1 ; \quad \Delta m = 0 \quad \text{for I.R. activity} \\ \Delta j &= 0, \pm 2 ; \quad \Delta m = 0 \quad \text{for Raman activity} . \end{aligned} \quad (8.33)$$

8.9.3 Vibrational–Rotational Interaction

Since the nuclei of a molecule are actually in vibrational motion, there is consequently an interaction between the vibrational and rotational motions. These interactions become important when the energy of a rotational energy level becomes comparable to a vibrational energy level. Let us illustrate this coupling in terms of a diatomic molecule, where we write for the Hamiltonian

$$\mathcal{H} = \frac{p^2}{2\mu} + \frac{J^2}{2\mu R^2} + a_2\xi^2 + a_3\xi^3, \quad (8.34)$$

in which the first term is the kinetic energy (and μ is the reduced mass of the molecule). The second term denotes the rotational energy of the molecule, while $a_2\xi^2$ is the harmonic restoring force for the vibrational energy, and $a_3\xi^3$ is an anharmonic restoring term arising in the vibrational problem. The distance between the nuclei is now modified by the vibrational displacements from equilibrium

$$\frac{R - R_{\text{eq}}}{R_{\text{eq}}} = \xi \quad \text{where} \quad R = R_{\text{eq}}(1 + \xi). \quad (8.35)$$

We therefore write

$$\frac{1}{R^2} = \frac{1}{R_{\text{eq}}^2(1 + \xi)^2} = \frac{1}{R_{\text{eq}}^2} [1 - 2\xi + 3\xi^2 + \dots] \quad (8.36)$$

so that we can express the Hamiltonian in terms of an unperturbed term \mathcal{H}_0 and a perturbation term \mathcal{H}' :

$$\mathcal{H} = \mathcal{H}_0 + \mathcal{H}', \quad (8.37)$$

where

$$\mathcal{H}_0 = \frac{p^2}{2\mu} + B_{\text{eq}}J^2 + a_2\xi^2 \quad (8.38)$$

and

$$B_{\text{eq}} = \frac{1}{2\mu R_{\text{eq}}^2}. \quad (8.39)$$

The first term in (8.38) denotes the kinetic energy and the second term defines the rotational energy when the molecule is in its equilibrium configuration, while the third term denotes the vibrational potential energy for the harmonic restoring forces. Thus \mathcal{H}_0 gives the energies for the vibrational and rotational motion in the limit where the vibrational and rotational motions are decoupled. For the \mathcal{H}_0 limit the selection rules are the same as if the vibrations and rotations occurred independently. The perturbation Hamiltonian then becomes

$$\mathcal{H}' = a_3\xi^3 - 2B_{\text{eq}}\xi J^2 + 3B_{\text{eq}}\xi^2 J^2, \quad (8.40)$$

where the first term is an anharmonic term that gives rise to overtones and combination modes in the vibrational spectrum. The second and third terms in (8.40) are associated with coupling between rotational and vibrational levels and give corrections to the rotational levels. The term in ξJ^2 makes a contribution in second-order perturbation theory, while the term in $\xi^2 J^2$ makes a contribution in first-order perturbation theory which is proportional to

$$\left(n + \frac{1}{2} \right) \hbar \omega_v j(j+1).$$

Thus, the application of perturbation theory results in energy levels for the vibrational-rotational problem:

$$E_{n,j} = \underbrace{\hbar \omega_v \left(n + \frac{1}{2} \right)}_{\text{pure vibrational}} + \underbrace{\mathcal{A}_1 j(j+1)}_{\text{pure rotational}} + \underbrace{\mathcal{A}_2 \hbar \omega_v \left(n + \frac{1}{2} \right) j(j+1) + \dots}_{\text{interaction terms}} \quad (8.41)$$

in which \mathcal{A}_1 and \mathcal{A}_2 are constants. For the diatomic molecule $\mathcal{A}_1 = (\hbar/2I)$ in accordance with (8.25). From a group theoretical point of view, the interaction terms modify the selection rules and new features in the IR and Raman spectra can be seen. In general, the symmetry of an interacting vibrational and rotational level is given by the direct product $\Gamma_{\text{vib}} \otimes \Gamma_{\text{rot}}$.

In making rotational transitions on absorption between different vibrational levels, we not only can have $\Delta j = 1$ (*the R-branch*) but we also can have $\Delta j = -1$ (*the P-branch*). This is illustrated in the vibrational-rotational spectrum shown in Fig. 8.10 for the HCl molecule. We note here that the spectral lines in the R-branch (upshifted in frequency) are not symmetrically spaced with respect to the down-shifted P-branch. The *Q-branch* ($\Delta j = 0$) occurs very close to the central frequency ν_0 , and would in fact be coincident with ν_0 if the moment of inertia would be independent of the vibrational state. Study of the *Q-branch* requires high resolution laser spectroscopy.

If there were no vibrational-rotational interaction, the spacing of all spectral lines (shown in the top portion of Fig. 8.10) would be the same for all vibrational levels n . For the case of diatomic molecules and for the polarization where \mathbf{E} is along the molecular axis, then the selection rules $\Delta n = +1$ and $\Delta j = 0$ determine the vibrational-rotational spectrum, while for \mathbf{E} perpendicular to the main symmetry axis of the molecule, the selection rules are $\Delta n = 0$ and $\Delta j = +1$.

Rotational Raman Spectra are also observed. Here the transitions with $\Delta j = 2$ are excited for the pure rotational transitions, $\Delta n = 0$ (see Figs. 8.9 and 8.10). This series is called the *S-branch*. When vibrational-rotational Raman spectra are excited, transitions with $\Delta j = 0$ and $\Delta j = -2$ are also possible and these are called the *O-branches*. Because of the anharmonic terms in the Hamiltonian, there are vibrational-rotational spectra which occur between vibrational states separated by $\Delta n = 2, 3, \dots$, etc. These anharmonic transitions would be expected to have lower intensity.

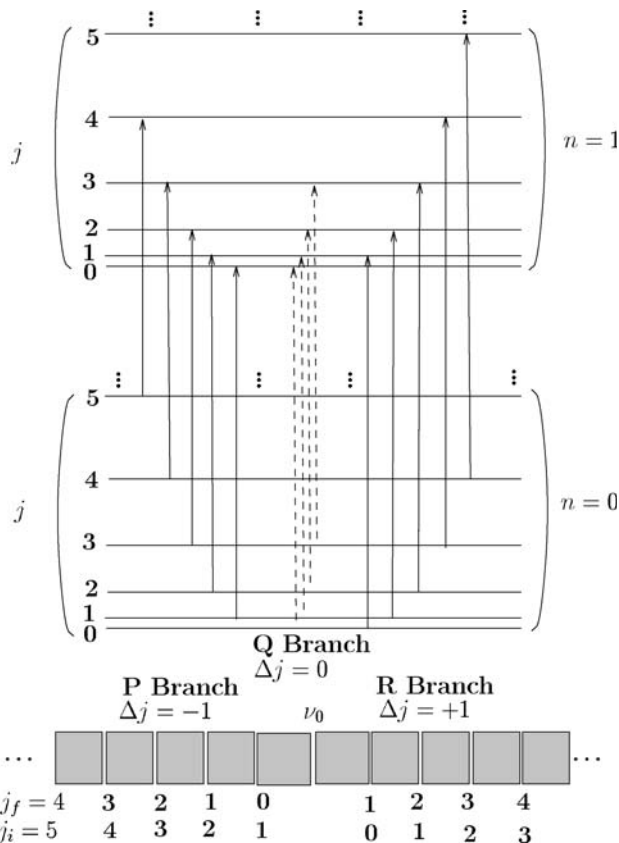


Fig. 8.10. P ($\Delta j = -1$), R ($\Delta j = +1$) and Q ($\Delta j = 0$) branches of the rotational structure of the HCl vibrational-rotational band near $2,885 \text{ cm}^{-1}$ shown schematically

The above discussion focused on the vibrational degrees of freedom. There are in addition the electronic levels which generally are separated by much greater energies than are the vibrational and rotational levels. There is however some interaction also between the vibrational and rotational states and the electronic levels. *Interactions between the electronic and rotational levels* give rise to “*Λ-doubling*” of the rotational levels, and *coupling between the electronic and vibrational levels* gives rise to *vibronic levels*.

Selected Problems

8.1. This problem relates to the interrelation of fundamental group theory concepts from small molecular clusters to the molecular vibrations of actual molecules of interest. We illustrate this approach using the normal

modes for three equal masses at the corners of an equilibrium triangular (see Sect. 8.1).

- Find the normal modes for a triangular cluster containing three hydrogen atoms at the corners of an equilateral triangle. Indicate which modes are IR active and which are Raman active.
- Find the normal modes for a hypothetical planar NH_3 molecule where the N atom is at the centroid of the triangle and coplanar with the three hydrogens. Which point group describes this molecule? Which modes are infrared active and which are Raman active?
- Relate the results in (a) and (b) to the normal modes, and to the IR and Raman activity for the NH_3 molecule with C_{3v} group symmetry.
- Relate the normal modes of the water molecule (Sect. 8.4) to the normal modes of the triangular cluster in (a). Account for the similarities and differences between the two cases.

8.2. Both CO_2 and N_2O are linear molecules, but have different equilibrium arrangements giving rise to different symmetry groups (see Fig. 8.11).

- What are the appropriate point groups for CO_2 and N_2O ?
- What symmetries are involved for the bonding and antibonding electronic orbitals for these molecules?
- What are the differences in the symmetries of the normal modes for these two molecules?
- Show schematically the atomic displacements for the normal modes of each molecule.
- What are the expected differences in their IR spectra? Raman spectra?
- What are the expected differences in the rotational spectra of these two molecules?
- Which of these rotational modes can be excited by infrared or Raman spectroscopy?

8.3. Consider the linear C_2H_2 molecule ($\text{H}-\text{C}=\text{C}-\text{H}$) as being composed of either two C–H blocks or of another configuration with the two hydrogen atoms vibrating against the two carbon atoms as another block, each with internal degrees of freedom. Such block grouping approaches help in providing intuition about the internal vibrations of complex molecules.

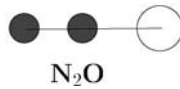
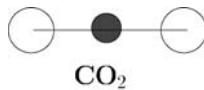


Fig. 8.11. Configurations for the linear molecules CO_2 and N_2O

- (a) Show that the same results for $\Gamma_{\text{mol.vib.}}$ are obtained for C_2H_2 by taking the direct product of the $\Gamma_{\text{mol.vib.}}$ for the constituent C–H blocks considered above.
- (b) By applying appropriate symmetry operations on the basis functions, show that the bending and stretching modes as given in Fig. 8.6 belong to the E_{1g} and E_{1u} irreducible representations.

8.4. C_2H_4 (ethylene) is a planar molecule which has the configuration shown on Fig. 8.12.

- (a) Using the point group and $\Gamma^{\text{a.s.}}$ found in Problem 7.4, find the symmetries of the allowed molecular vibrations for the C_2H_4 molecule.
- (b) Sketch the normal mode displacements for each of the allowed molecular vibrations in (a).
- (c) Which modes are infrared-active? Which are Raman-active? What are the polarization selection rules?

8.5. This problem is designed to show that group theory becomes increasingly important for treating molecular vibrations for high symmetry molecules

- (a) Find the molecular vibrations for the hypothetical molecule XH_{12} where the 12 hydrogen atoms are at the vertices of a regular icosahedron and the atom X is at the center of the icosahedron. Find $\Gamma^{\text{a.s.}}$ for XH_{12} for the icosahedral group I_h .
- (b) What are the symmetries for the normal modes? Which are infrared-active? Raman active?
- (c) What are the polarization selection rules for observing the infrared modes? for the Raman modes?

8.6. Consider the methane molecule CH_4 .

- (a) What is the group symmetry and to which irreducible representations do the R_x , R_y , and R_z basis functions belong (see Sect. 7.5.2 and Sect. 8.8.3)?
- (b) Describe the symmetries and eigenvectors for the rotational levels.
- (c) What are the symmetries for the vibrational–rotational interactions?
- (d) Describe the infrared and Raman spectra of methane including rotational, vibrational modes, and the interaction between them. Consider also the combination modes (see Table A.32).
- (e) What are the expected polarization effects in these spectra?

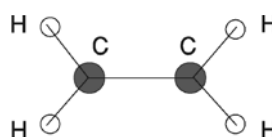


Fig. 8.12. Configurations of the C_2H_4 ethylene molecule

Part IV

Application to Periodic Lattices

Space Groups in Real Space

According to the one-electron Hamiltonian for the electronic energy band structure for solids, we write Schrödinger's equation as

$$\mathcal{H}\psi(\mathbf{r}) = \left[-\frac{\hbar^2}{2m} \nabla^2 + V(\mathbf{r}) \right] \psi(\mathbf{r}) = E\psi(\mathbf{r}), \quad (9.1)$$

where $V(\mathbf{r})$ is a periodic potential. The symmetry group of the one-electron Hamiltonian and of the periodic potential in (9.1) is the *space group* of the crystal lattice, which consists of both *translational* symmetry operations and *point group* symmetry operations. Both the translational and point group symmetry operations leave the Hamiltonian invariant, and consequently all these symmetry operators will commute with the Hamiltonian, and provide quantum numbers for labeling the energy eigenvalues and eigenfunctions.

In this chapter we introduce the basic background for space group operations (Sect. 9.1) and show how these operations form space groups (Sect. 9.2). In addition to the point group and translation operations, we consider the compound symmetry operations of glide planes and screw axes (Sect. 9.1.2) and the nonsymmorphic space groups associated with these compound symmetry operations (Sect. 9.2.3). An introduction to a few kinds of 3D space groups is given in Sect. 9.2. However, for pedagogic purposes we discuss all 17 two-dimensional (2D) space groups in some detail in Sect. 9.3 to familiarize the reader with the notation and the symmetry operations occurring in both *symmorphic* and *nonsymmorphic* 2D-space groups. A brief introduction to line groups, describing the properties of systems exhibiting translational properties in one dimension, is given in Sect. 9.4. Finally we discuss the determination of the crystal structure and space groups in Sect. 9.5, and the use of standard reference texts, [58, 76] such as the *Crystal Structures*, by R.W.G. Wyckoff, and the *International Tables for X-Ray Crystallography*.

9.1 Mathematical Background for Space Groups

9.1.1 Space Groups Symmetry Operations

Definition 18. *The point group and translation symmetry operations which carry the crystal into itself form a group called the space group.*

A common notation for space group operators is

$$\{R_\alpha|\tau\} , \quad (9.2)$$

where R_α denotes point group operations such as rotations, reflections, improper rotations and inversions, while τ denotes translation operations. Pure rotations and pure translations are special cases of space group operations:

$$\{\varepsilon|0\} = \text{identity}$$

$$\{\alpha|0\} = \text{pure rotations or more generally point group operations}$$

$$\{\varepsilon|\tau\} = \text{pure translations by vector } \tau .$$

We can relate the operator $\{\alpha|\tau\}$ for the space group to a coordinate transformation

$$\{\alpha|\tau\}r = r' = \vec{\alpha} \cdot r + \tau , \quad (9.3)$$

where $\vec{\alpha}$ denotes the transformation matrix for rotations and τ denotes a translational transformation.

Definition 19. *The result for the multiplication of two space group operators is*

$$\{\beta|\tau'\} \{\alpha|\tau\} = \{\beta\alpha|\beta\tau + \tau'\} , \quad (9.4)$$

where $\{\alpha|\tau\}$ is the first space group operator and $\{\beta|\tau'\}$ is the second.

Proof. Multiplication of two space group operators proceeds from this identification:

$$\begin{aligned} \{\beta|\tau'\} \{\alpha|\tau\} &= \vec{\beta} \cdot [\vec{\alpha} \cdot r + \tau] + \tau' \\ &= \vec{\beta} \cdot \vec{\alpha} \cdot r + \vec{\beta} \cdot \tau + \tau' \\ &= \{\beta\alpha|\beta\tau + \tau'\} . \end{aligned}$$

Using the results of this definition of the multiplication of two space group operations we can write

$$\{\alpha|\tau\} \{\beta|\tau'\} = \vec{\alpha} \cdot \vec{\beta} \cdot r + \vec{\alpha} \cdot \vec{\beta} \cdot \tau + \tau \quad (9.5)$$

so that commutation of these two space group operators requires that

$$\overleftrightarrow{\alpha} \cdot \overleftrightarrow{\beta} = \overleftrightarrow{\beta} \cdot \overleftrightarrow{\alpha} \quad \text{and} \quad \overleftrightarrow{\beta} \cdot \overleftrightarrow{\tau} + \overleftrightarrow{\tau}' = \overleftrightarrow{\alpha} \cdot \overleftrightarrow{\tau}' + \overleftrightarrow{\tau} \quad (9.6)$$

which is not generally valid. Thus we conclude that although simple translations commute with each other, general space group operations do not commute. \square

Definition 20. *The inverse of $\{\alpha|\tau\}$ is given by*

$$\{\alpha|\tau\}^{-1} = \{\alpha^{-1}|-\alpha^{-1}\tau\}. \quad (9.7)$$

Proof. Using the proposed definition of $\{\alpha|\tau\}^{-1}$ we carry out the following multiplication of two space group symmetry elements to obtain

$$\{\alpha|\tau\}\{\alpha|\tau\}^{-1} = \{\alpha\alpha^{-1}|\alpha(-\alpha^{-1}\tau) + \tau\} = \{\varepsilon|0\} \quad (9.8)$$

which verifies the definition for $\{\alpha|\tau\}^{-1}$. \square

Having specified the identity operation $\{\varepsilon|0\}$, the rules for multiplication, and the rules for specifying the inverse operation, and noting that the associative law applies, we see that the elements $\{\alpha|\tau\}$ form a space group.

Definition 21. *The matrix representation for the space group operator is*

$$\{\alpha|\tau\} = \begin{pmatrix} 1 & 0 \\ \tau & \overleftrightarrow{\alpha} \end{pmatrix}, \quad (9.9)$$

where 1 is a number, 0 denotes a row of three zeros, τ is a column vector, and $\overleftrightarrow{\alpha}$ is a (3×3) rotation matrix. Introducing the basis

$$\begin{pmatrix} 1 \\ \mathbf{r} \end{pmatrix},$$

where 1 is a number and \mathbf{r} is a column vector consisting for example of

$$\begin{pmatrix} x \\ y \\ z \end{pmatrix},$$

the action of the space group operation on the coordinate system then is written as

$$\begin{pmatrix} 1 & 0 \\ \tau & \overleftrightarrow{\alpha} \end{pmatrix} \begin{pmatrix} 1 \\ \mathbf{r} \end{pmatrix} = \begin{pmatrix} 1 \\ \tau + \overleftrightarrow{\alpha} \cdot \mathbf{r} \end{pmatrix} = \begin{pmatrix} 1 \\ \mathbf{r}' \end{pmatrix}. \quad (9.10)$$

Theorem. *The matrix*

$$\begin{pmatrix} 1 & 0 \\ \tau & \overleftrightarrow{\alpha} \end{pmatrix}$$

forms a representation for the space group operator $\{\alpha|\tau\}$.

Proof. To prove that the matrix of (9.9) is a representation for the space group operator $\{\alpha|\tau\}$, we write down the multiplication and inverse transformations. Multiplication of two matrices yields

$$\begin{pmatrix} 1 & 0 \\ \tau' & \overset{\leftrightarrow}{\beta} \end{pmatrix} \begin{pmatrix} 1 & 0 \\ \tau & \overset{\leftrightarrow}{\alpha} \end{pmatrix} = \begin{pmatrix} 1 & 0 \\ \tau' + \overset{\leftrightarrow}{\beta} \cdot \tau & \overset{\leftrightarrow}{\beta} \cdot \overset{\leftrightarrow}{\alpha} \end{pmatrix}, \quad (9.11)$$

which yields another symmetry operation of the space group

$$\{\beta|\tau'\}\{\alpha|\tau\} = \{\beta\alpha|\beta\tau + \tau'\}. \quad (9.12)$$

Using (9.11) we can write the product of the matrix representation of $\{\alpha|\tau\}$ with that of its inverse operator $\{\alpha|\tau\}^{-1}$ to obtain

$$\begin{pmatrix} 1 & 0 \\ -\overset{\leftrightarrow}{\alpha}^{-1} \cdot \tau & \overset{\leftrightarrow}{\alpha}^{-1} \end{pmatrix} \begin{pmatrix} 1 & 0 \\ \tau & \overset{\leftrightarrow}{\alpha} \end{pmatrix} = \begin{pmatrix} 1 & 0 \\ 0 & \varepsilon \end{pmatrix}, \quad (9.13)$$

thereby showing that

$$\{\alpha|\tau\}^{-1}\{\alpha|\tau\} = \{\varepsilon|0\}. \quad (9.14)$$

□

9.1.2 Compound Space Group Operations

In space groups we may find instead of simple translation operations, compound symmetry operations that combine translations and point group operations. The two types of compound symmetry operations are the glide planes and the screw axes.

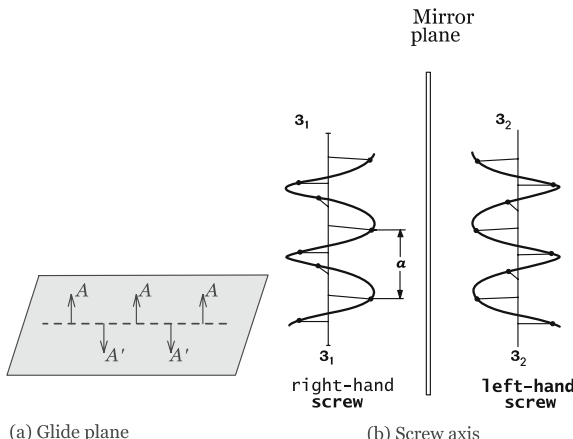


Fig. 9.1. (a) The glide plane operation that takes A into A' . (b) Right- and left-hand screw axes (belong to closely related but different space groups)

A *glide plane* consists of a translation parallel to a given plane followed by a reflection in that plane (see Fig. 9.1(a)). There are in fact three different types of glide planes that are identified: the *axial glide* along a symmetry axis (\mathbf{a} , \mathbf{b} , or \mathbf{c}), the *diagonal glide* or *n-glide* in two or three directions (e.g., $(\mathbf{a} + \mathbf{b})/2$ or $(\mathbf{a} + \mathbf{b} + \mathbf{c})/2$) and finally the *diamond glide* corresponding to $(\mathbf{a} + \mathbf{b})/4$ or $(\mathbf{a} + \mathbf{b} + \mathbf{c})/4$.

A *screw axis* is a translation along an axis about which a rotation is simultaneously occurring. In Fig. 9.1(b) we show a threefold screw axis, where a is the lattice constant. The tellurium and selenium structures have threefold screw axes similar to those shown in Fig. 9.1b. A summary of the various possible screw axes and the crystallographic notation for each is given in Fig. 9.2. The screw axes shown in Fig. 9.2 are from top to bottom: the first row shows twofold screw axes, followed by a row of threefold and fourfold screw axes and the last two rows show sixfold screw axes. An n -fold screw axis has a trans-

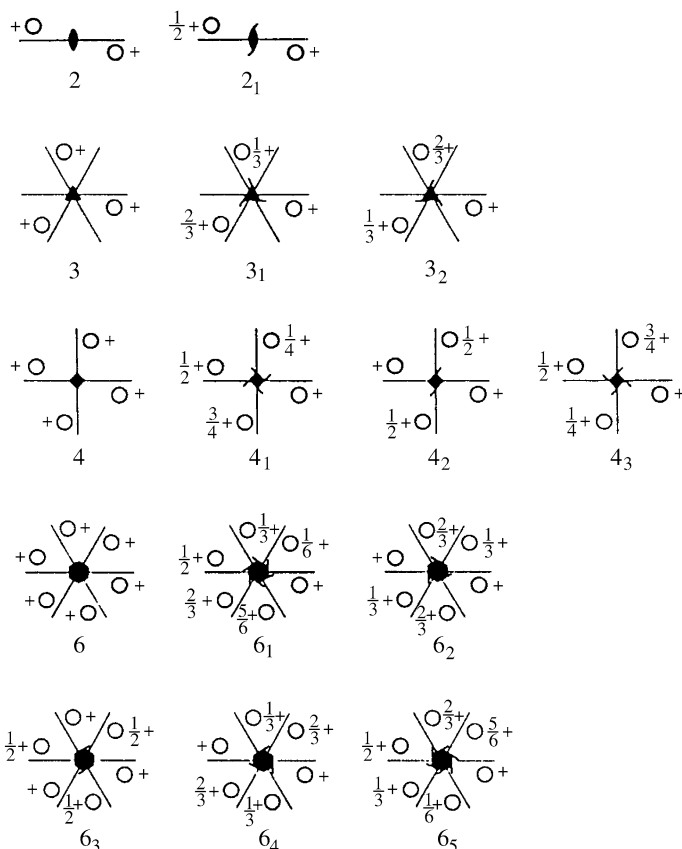


Fig. 9.2. A summary of all possible screw axes, including twofold, threefold, fourfold and sixfold screw axes (see text)

lation of $p\tau_0/n$ where τ_0 is a unit cell translation of the translation group, p is an integer $p = 1, \dots, n$, and the rotation that goes with the translation is $2\pi p/n$. Thus for the threefold row, the first entry is a 2π or zero rotation every time there is a translation of $\tau_0/3$, while the second entry has a rotation of $2\pi/3$, for each $\tau_0/3$ translation and the last entry has a rotation of $4\pi/3$ or $(-2\pi/3)$, for each $\tau_0/3$ translation.

9.1.3 Translation Subgroup

Theorem. *All the elements of the space group G that are of the form $\{\varepsilon|\tau\}$ constitute the translation group T . Here T is a subgroup of G and defines the Bravais lattice.*

Proof. Symmetry elements of the group T are defined by the translation vectors \mathbf{R}_n which leave the Bravais lattice invariant $\mathbf{R}_n = \sum n_i \mathbf{a}_i$, and \mathbf{a}_i is the primitive vector of the Bravais lattice. The *translation* group is a *self-conjugate* or invariant or normal subgroup of G since

$$\begin{aligned} \{R_\alpha|\tau\}\{\varepsilon|t\}\{R_\alpha|\tau\}^{-1} &= \{R_\alpha|\tau\}\{\varepsilon|t\}\{R_\alpha^{-1}| - R_\alpha^{-1}\tau\} \\ &= \{R_\alpha|\tau\}\{R_\alpha^{-1}| - R_\alpha^{-1}\tau + t\} \\ &= \{\varepsilon| - R_\alpha R_\alpha^{-1}\tau + R_\alpha t + \tau\} \\ &= \{\varepsilon|R_\alpha t\}. \end{aligned} \quad (9.15)$$

But $R_\alpha t$ is just another translation vector in group T and therefore the operation $\{\varepsilon|R_\alpha t\}$ is a symmetry operation of group T , and we have shown that $\{\varepsilon|\tau\}$ forms the translation subgroup of G . \square

Although the translation group T is an invariant subgroup of G , we cannot generally say that the space group G is a direct product of a translation group with a point group, as discussed in Sect. 9.1.4. It should be noted that since the individual elements $\{\varepsilon|\tau'\}$ and $\{R_\alpha|\tau\}$ do not commute, as we show below:

$$\begin{aligned} \{\varepsilon|\tau'\}\{R_\alpha|\tau\} &= \{R_\alpha|\tau' + \tau\} \\ \{R_\alpha|\tau\}\{\varepsilon|\tau'\} &= \{R_\alpha|R_\alpha\tau' + \tau\}. \end{aligned} \quad (9.16)$$

However, since the translation group is an invariant subgroup of G , it is of interest to study the cosets of the factor group which it defines. A right coset of the translation group considered as a subgroup of G is then

$$C_\alpha = [\{\varepsilon|\tau'\}\{R_\alpha|\tau\}] = [\{R_\alpha|\tau''\}], \quad (9.17)$$

where the bracket in (9.17) denotes all the terms in the coset that can be formed using all possible values of τ' . Although each element $\{R_\alpha|\tau\}$ does not commute with $\{\varepsilon|\tau'\}$ as seen in (9.16), all $\{R_\alpha|\tau''\}$ are contained in the right coset. Using the same argument as used above for the right coset, we can show that C_α is also a left coset of the translation group from which we conclude that T is a self-conjugate (or normal) subgroup of G .

Theorem. *The cosets C_α form a factor group of the space group G .*

Proof. Consider the multiplication rule for the cosets:

$$C_\alpha C_\beta = [\{R_\alpha|\tau_1\}\{R_\beta|\tau_2\}] = [\{R_\alpha R_\beta|R_\alpha\tau_2 + \tau_1\}] = [\{R_\gamma|\tau_3\}] = C_\gamma, \quad (9.18)$$

where $R_\alpha R_\beta = R_\gamma$ defines the group property in the point group and $\tau_3 = R_\alpha\tau_2 + \tau_1$ is a translation of the lattice. Since τ_1 and τ_2 range over all possible translation vectors, the vector τ_3 also spans all possible translations, and C_γ satisfies the multiplication rule. \square

The factor group G/T will be very important in applications of group theory to space groups, since it factors out the pure translational properties of the space groups, being isomorphic with the point group which makes up the rotational parts of the operators of the space groups. For a summary of cosets and factor group properties, see Sect. 1.5–1.7.

9.1.4 Symmorphic and Nonsymmorphic Space Groups

The space group G consists of all operations $\{R_\alpha|\tau\}$ which leave a given lattice invariant. We can write the space group operations in the form

$$\{R_\alpha|\tau\} = \{R_\alpha|R_n + \tau_\alpha\} = \{\varepsilon|R_n\}\{R_\alpha|\tau_\alpha\}, \quad (9.19)$$

where R_n is a general vector of the Bravais lattice and the vector τ_α (associated with each of the point group operators R_α) is either zero or a translation that is not a primitive translation of the Bravais lattice. The $\{R_\alpha|\tau_\alpha\}$ for which $R_n = 0$ are either simple point group operations, when $\tau_\alpha = 0$, or one of the compound operations (glide plane or screw axis discussed in Sect 9.1.2) when $\tau_\alpha \neq 0$.

Definition 22. *If, with a suitable choice of origin in the direct lattice, we find that all the elements of G are in the form $\{R_\alpha|\tau\} = \{R_\alpha|R_n\} = \{\varepsilon|R_n\}\{R_\alpha|0\}$ ($\tau_\alpha = 0$ for all symmetry operations), then the space group G is called a simple or symmorphic group. If, with any suitable choice of origin in the direct lattice, $\tau_\alpha \neq 0$ for at least one $\{R_\alpha|\tau_\alpha\}$ operation, then G is called a nonsymmorphic group.*

Symmorphic space groups, therefore, contain an entire point group as a subgroup. The point group g is obtained from the space group G by placing $\tau = R_n = 0$ for all $\{R_\alpha|\tau\}$ elements in G . The space group is said to be a *semi-direct* product of the translation and point groups, where *semi* is used since a *direct* product would give $\{R_\alpha|R_n\} \otimes \{\varepsilon|R_n\} = \{R_\alpha|R_n + R_{n'}\}$. We will see in the next chapters that, once the wavevector k of the wavefunctions under study is chosen, we can work the space group problem by considering the rotational aspects, which reduce the work to a point group g_k problem. We then have h symmetry elements rather than $\mathcal{N}h$, where $\mathcal{N} \sim 10^{23}$.

For nonsymmorphic groups, τ_α is not zero for at least one R_α . By multiplying two space group elements of the type $\{R_\alpha|\tau_\alpha\}$ ($R_n = 0$) we get

$$\{R_\alpha|\tau_\alpha\}\{R_\beta|\tau_\beta\} = \{R_\gamma|\tau_\gamma + R_n\} \quad (9.20)$$

and R_n may or may not be zero. Therefore, the entire set of space group elements $\{R_\alpha|\tau_\alpha\}$ may fail to form a group if the lattice vector $R_n \neq 0$. Furthermore, the entire point group g of the crystal, obtained by setting all translations (including the nonprimitive ones) in G equal to zero is a subgroup of its Bravais lattice point group (called the *holohedral* group, which is defined as the group of the Bravais lattice), but it is not a subgroup of G . In this case, to work with the rotational aspects of the nonsymmorphic space group, a procedure to remove the translational effect is needed. Two alternative procedures are available: (1) One approach is to form the factor group G/T of G with respect to the translation group T (Sect. 9.1.3). The G/T factor group will be isomorphic with the point group which makes up the rotational parts of the operators in the space group. (2) The G/T factor group representation can be obtained by means of the *multiplier algebra*, where all members of a given coset are represented by a single element, and we work with the *multiplier groups* or *multiplier representation*. These concepts will be discussed briefly in Sect. 10.4.

To fully describe a space group G , it is sufficient to list the elements $\{R_\alpha|\tau_\alpha\}$ representing the cosets of G/T and the \mathbf{a}_i primitive vectors of the Bravais lattice. It is clear that the applications of group theory to symmorphic space groups are simpler when compared to applications to nonsymmorphic space groups. The operations R_α apply to the translation vectors in accordance with the definition of the space group operations, and the symmetry operations of the factor group G/T for symmorphic space groups are isomorphic with the point group g . Thus irreducible representations of the factor group G/T are also irreducible representations of g and are likewise irreducible representations of G . It can be shown that all irreducible representations of G can be compounded from irreducible representations of g and T , even though G is not a direct product group of g and T [47]. The development of representations for the space groups will be discussed in Chap. 10.

9.2 Bravais Lattices and Space Groups

Now that we have introduced the mathematical background for working with space groups, we can introduce the 14 Bravais lattices which denote the possible crystallographic lattices that can form three-dimensional structures, and the 230 space groups (73 symmorphic and 157 nonsymmorphic) that can be formed by placing different atomic structures in the Bravais lattice sites.

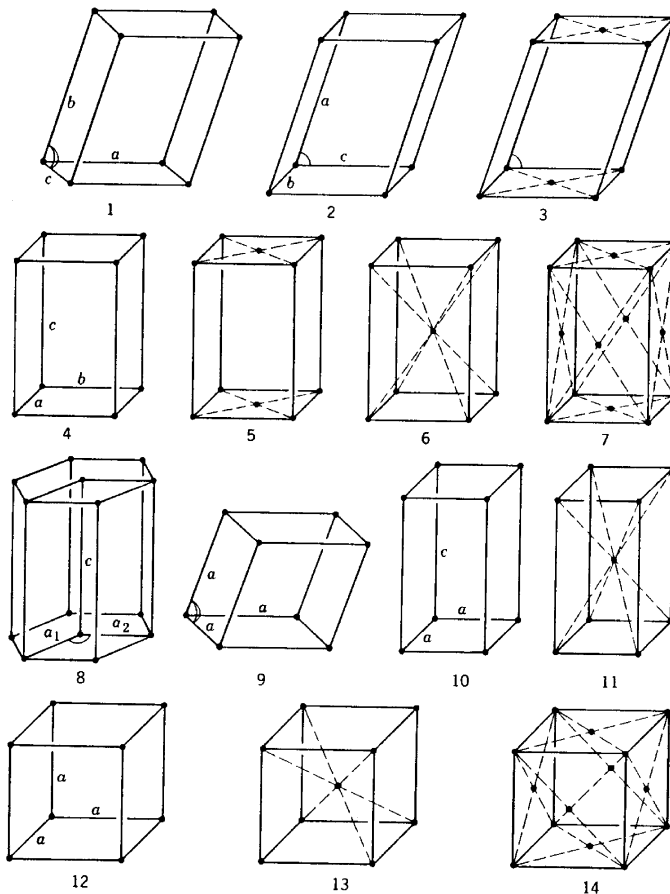


Fig. 9.3. The fourteen Bravais space lattices illustrated by a unit cell of each: (1) triclinic, simple; (2) monoclinic, simple; (3) monoclinic, base centered; (4) orthorhombic, simple; (5) orthorhombic, base centered; (6) orthorhombic, body centered; (7) orthorhombic, face centered; (8) hexagonal; (9) rhombohedral; (10) tetragonal, simple; (11) tetragonal, body centered; (12) cubic, simple; (13) cubic, body centered; and (14) cubic, face centered

The requirements of translational symmetry limit the possible rotation angles of a Bravais lattice and in particular restrict the possible rotation axes to onefold, twofold, threefold, fourfold and sixfold. Fivefold axes or axes greater than six do not occur in crystalline materials because these axes are not compatible with translational symmetry [7]¹ as shown in Problem 9.5. When rotational symmetry does occur in crystals, then severe restrictions on the rotation angle are imposed by the simultaneous occurrence of the repetition of the unit cells through rotations and translations. The 14 Bravais lattices

¹See [47], pp. 14 and 178.

which form 3D space groups are shown in Fig. 9.3. They are also discussed in solid state physics texts [45] and in crystallography texts [58, 68].

9.2.1 Examples of Symmorphic Space Groups

If all the operations of the space group are simply point group operations on to which we add translation operations from the Bravais lattice, we have a simple or *symmorphic* space group. The 73 symmorphic space groups are listed in Table 9.1, and they can be found in the “International Crystallographic Tables”. Symbols that are used for 3D space groups (see Table 9.1) include *A* or *B* for monoclinic groups, and *C*, *A* or *B*, *I*, *F* for orthorhombic groups, and these are defined in Table 9.1. In the case of rectangular lattices,

Table 9.1. The 73 symmorphic space groups

| crystal system | Bravais lattice | space group |
|----------------|-----------------------------------|--|
| triclinic | <i>P</i> | <i>P</i> 1, <i>P</i> 1̄ |
| monoclinic | <i>P</i> | <i>P</i> 2, <i>P</i> m, <i>P</i> 2/ <i>m</i> |
| | <i>B</i> or <i>A</i> | <i>B</i> 2, <i>B</i> m, <i>B</i> 2/ <i>m</i> |
| orthorhombic | <i>P</i> | <i>P</i> 222, <i>P</i> m <i>m</i> 2, <i>P</i> <i>m</i> <i>m</i> |
| | <i>C</i> , <i>A</i> , or <i>B</i> | <i>C</i> 222, <i>C</i> <i>m</i> <i>m</i> 2, <i>A</i> <i>m</i> <i>m</i> 2 ^a , <i>C</i> <i>m</i> <i>m</i> |
| | <i>I</i> | <i>I</i> 222, <i>I</i> <i>m</i> <i>m</i> 2, <i>I</i> <i>m</i> <i>m</i> |
| | <i>F</i> | <i>F</i> 222, <i>F</i> <i>m</i> <i>m</i> 2, <i>F</i> <i>m</i> <i>m</i> |
| tetragonal | <i>P</i> | <i>P</i> 4, <i>P</i> 4̄, <i>P</i> 4/ <i>m</i> , <i>P</i> 422, <i>P</i> 4 <i>m</i> |
| | | <i>P</i> 42 <i>m</i> , <i>P</i> 4̄ <i>m</i> 2 ^a , <i>P</i> 4/ <i>m</i> <i>m</i> |
| | <i>I</i> | <i>I</i> 4, <i>I</i> 4̄, <i>I</i> 4/ <i>m</i> , <i>I</i> 422, <i>I</i> 4 <i>m</i> |
| | | <i>I</i> 42 <i>m</i> , <i>I</i> 4̄ <i>m</i> 2 ^a , <i>I</i> 4/ <i>m</i> <i>m</i> |
| cubic | <i>P</i> | <i>P</i> 23, <i>P</i> <i>m</i> 3, <i>P</i> 432, <i>P</i> 4̄3 <i>m</i> , <i>P</i> <i>m</i> 3 <i>m</i> |
| | <i>I</i> | <i>I</i> 23, <i>I</i> <i>m</i> 3, <i>I</i> 432, <i>I</i> 4̄3 <i>m</i> , <i>I</i> <i>m</i> 3 <i>m</i> |
| | <i>F</i> | <i>F</i> 23, <i>F</i> <i>m</i> 3, <i>F</i> 432, <i>F</i> 4̄3 <i>m</i> , <i>F</i> <i>m</i> 3 <i>m</i> |
| trigonal | <i>P</i> ^b | <i>P</i> 3, <i>P</i> 3̄, <i>P</i> 312, <i>P</i> 321 ^a , <i>P</i> 3 <i>m</i> 1 |
| | | <i>P</i> 31 <i>m</i> ^a , <i>P</i> 3̄1 <i>m</i> , <i>P</i> 3̄3 <i>m</i> ^a |
| (rhombohedral) | <i>R</i> | <i>R</i> 3, <i>R</i> 3̄, <i>R</i> 32, <i>R</i> 3 <i>m</i> , <i>R</i> 3̄ <i>m</i> |
| hexagonal | <i>P</i> ^b | <i>P</i> 6, <i>P</i> 6̄, <i>P</i> 6/ <i>m</i> , <i>P</i> 622, <i>P</i> 6 <i>m</i> |
| | | <i>P</i> 6̄ <i>m</i> 2, <i>P</i> 6̄ <i>m</i> 2 ^a , <i>P</i> 6/ <i>m</i> <i>m</i> |

[*P*, *I*, *F* (*A*, *B* or *C*) and *R*, respectively, denote primitive, body centered, face centered, base centered (along the *a*, *b* or *c* crystallographic axis) and rhombohedral Bravais lattices (see Fig. 9.3)]

^a The seven additional space groups that are generated when the orientations of the point group operations are taken into account with respect to the Bravais unit cell

^b Primitive hexagonal and trigonal crystal systems have the same hexagonal Bravais lattice

the inequivalent axes are parallel to the sides of the conventional rectangular unit cell. In the case of square lattices, the first set of axes is parallel to the sides and the second set is along the diagonals. In the case of hexagonal lattices, one axis is 30° away from a translation vector.

We now illustrate the idea of symmorphic space groups using an example based on the D_{2d} point group (see character Table A.8) embedded in a tetragonal Bravais lattice (no. 11 in Fig. 9.3). Suppose that we have a molecule with atoms arranged in a D_{2d} point group configuration as shown in Fig. 9.4. We see that the D_{2d} point group has classes E , C_2 rotations about the z -axis, $2S_4$ improper rotations about the z -axis, $2\sigma_d$ passing through the z axis and through the center of each of the dumbbell axes, and $2C'_2$ axes in (110) directions in the median plane. The top view of this molecule is shown in Fig. 9.4(b).

We could put such X_4 molecules into a solid in many ways and still retain the point group symmetry of the molecule. To illustrate how different space

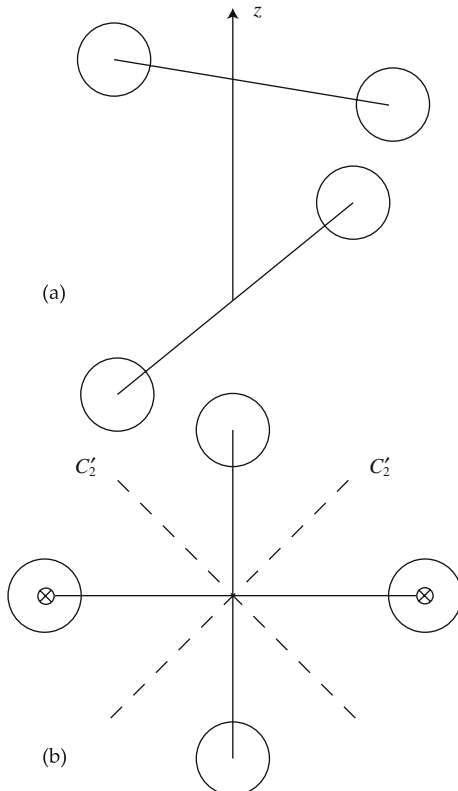


Fig. 9.4. (a) Schematic diagram of an X_4 molecule with point group D_{2d} ($\bar{4}2m$) symmetry. (b) Top view of a molecule X_4 with D_{2d} symmetry. The symmetry axes are indicated

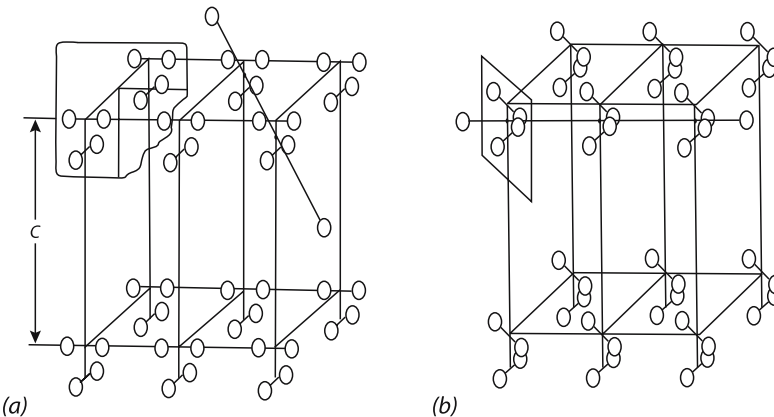


Fig. 9.5. Tetragonal Bravais lattice with two possible orientations of a molecule with D_{2d} symmetry resulting in two different three-dimensional space groups. The maximum symmetry that the tetragonal Bravais lattice can support is $D_{4h} = D_4 \otimes i$ ($4/mmm$)

groups can be produced with a single molecular configuration, we will put the X_4 molecule with D_{2d} symmetry into two different symmorphic space groups, as shown in Fig. 9.5.

We note that with either of the placements of the molecule in Fig. 9.5, *all the point group operations of the molecule are also operations of the space lattice*. However, if the symmetry axes of the molecule do not coincide with the symmetry axes of the lattice in which they are embedded, the combined space group symmetry is lowered. Particular point group operations are appropriate to specific Bravais lattices, but the connection is homomorphic rather than isomorphic. For example, the point group operations T , T_d , T_h , O and O_h leave each of the simple cubic, face-centered cubic and body-centered cubic Bravais lattices invariant. Even though a given Bravais lattice is capable of supporting a high symmetry point group (e.g., the FCC structure), if we have a lower symmetry structure at each of the lattice sites (e.g., the structure in Fig. 9.4), then the point symmetry is lowered to correspond to that structure. On the other hand, the highest point group symmetry that is possible in a crystal lattice is that which has all the symmetry operations of the Bravais lattice, so that the group O_h will be the appropriate point group for an FCC structure with spherical balls at each lattice site (see Problem 9.1).

9.2.2 Cubic Space Groups and the Equivalence Transformation

We now introduce the cubic groups that will be frequently discussed for illustrative purposes in subsequent chapters. The use of the equivalence transformation to obtain the characters $\chi^{a.s.}$ for this transformation is also discussed. Figure 9.6 illustrates several different kinds of cubic space groups com-

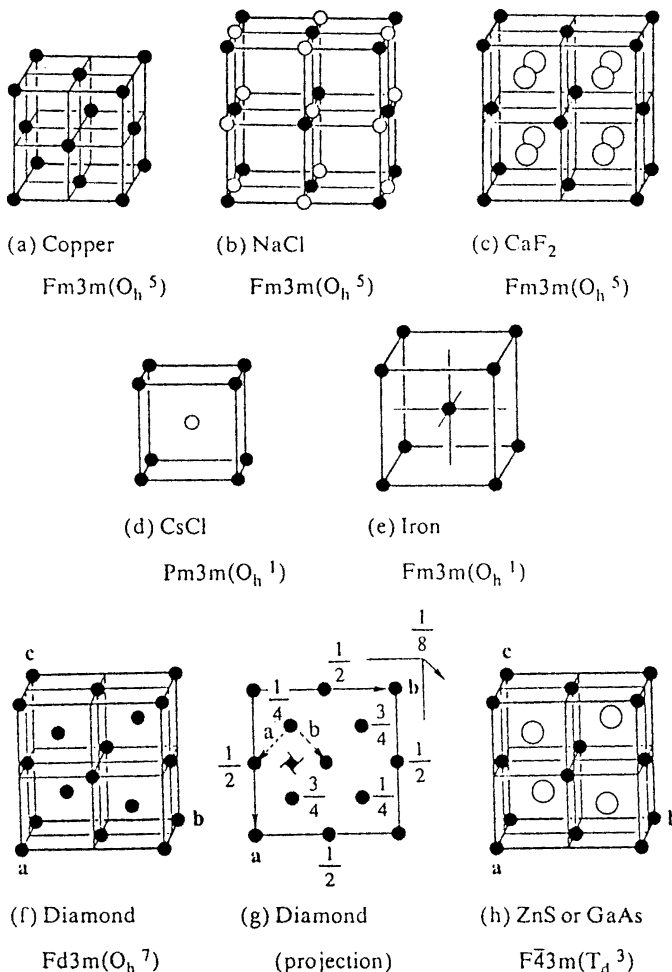


Fig. 9.6. Example of cubic lattices. Here (a), (b), (c) pertain to space group #225; (d) pertains to #221 and (e) to #229; while (f) and (g) are for #227; and (h) is for #223

monly occurring in solid state physics, including FCC, BCC, diamond and zinc blende structures. The diamond structure is nonsymmorphic and will be discussed in Sect. 9.2.3. First we show that a given space can support several different crystal structures. We illustrate this with Fig. 9.7 which shows three different crystal structures all having the same space group symmetry operations of $O_h^1(Pm3m)$. This space group will support full O_h point symmetry. The different crystal structures are obtained by occupying different sites as listed in the “International Crystallographic Tables” (see Table C.2). The space group is specified in terms of an origin at the center which has the full

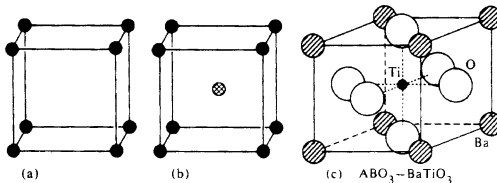


Fig. 9.7. Example of three cubic lattices with the space group #221 O_h^1 ($Pm3m$) (see Table C.2). (a) Simple cubic (SC), (b) body centered cubic (BCC), and (c) perovskite structure

symmetry of the Bravais lattice ($P4/m(\bar{3})2/m$). Inspection of space group 221 yields the structure shown in Fig. 9.7(a) where only site b is occupied, while Fig. 9.7(b) has site occupation of both sites a and b , each having site symmetry $m3m$ (see Table C.2). For the perovskite structure in Fig. 9.7(c) we have occupation of Ba atoms on b sites, Ti atoms on a sites and three oxygens on c sites. We note in Table C.2 that the site symmetry $4/mmm$ is different on the c sites than for the a or b sites which have $m3m$ site symmetries.

Important for many applications of group theory is the number of atoms within the primitive cell (for example for calculation of $\chi^{a.s.}$). For example, in Fig. 9.7(a) there is one atom per unit cell. This can be obtained from Fig. 9.7(a) by considering that only one eighth of each of the eight atoms shown in the figure is inside the cubic primitive cell. In Fig. 9.7(b) there are two distinct atoms per unit cell but for each $\Gamma^{a.s.} = \Gamma_1$ to give a total $\Gamma^{a.s.} = 2\Gamma_1$. In Fig. 9.7(c), there are one Ti, six half O, and eight 1/8 parts of Ba inside the primitive cell, giving altogether five atoms, i.e., one unit of BaTiO_3 per unit cell. Here $\Gamma^{a.s.}$ for each of the Ba and Ti sublattices we have $\Gamma^{a.s.} = \Gamma_1$ but for the three oxygens $\Gamma^{a.s.} = \Gamma_1 + \Gamma_{12}$ to give a total of $\Gamma^{a.s.} = 3\Gamma_1 + \Gamma_{12}$ for the whole BaTiO_3 molecule (see Sect. 11.3.2).

Concerning more general cubic groups, the structures for Fig. 9.6(a–c) are all group #225 based on a FCC Bravais lattice, while (d) has the CsCl structure (group #221) as in Fig. 9.7(b) which has two atoms per unit cell. The structure for iron (group #229) is based on the full BCC Bravais lattice where the central atom and the corner atoms are the same. Figures 9.6(f) and (g) are for the nonsymmorphic diamond lattice, discussed in detail in Sect. 9.2.3, which has two atoms/unit cell. The zinc blende structure shown in Fig. 9.6(h) is similar to that of Fig. 9.6(f) except that the atoms on the two sublattices are of a different species and therefore the zinc blende structure has a different symmetry group #203, and this group is a symmorphic group.

9.2.3 Examples of Nonsymmorphic Space Groups

A familiar example of a *non-symmorphic space group* is the *diamond* structure shown in Fig. 9.6(f), where we note that there are two atoms per unit cell

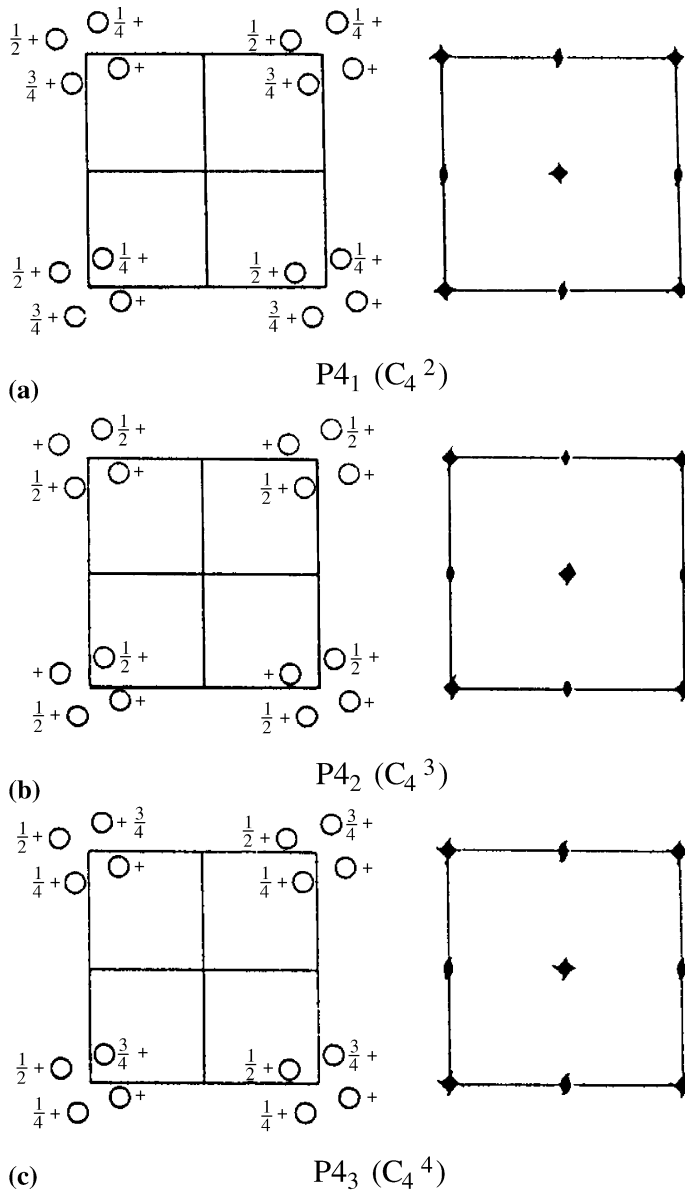


Fig. 9.8. Examples of space groups with screw axes. The three examples are (a) $P4_1 (C_4^2)$ #76, (b) $P4_2 (C_4^3)$ #77 and (c) $P4_3 (C_4^4)$ #78. See Sect. 9.1.2 and Fig. 9.2 for notation

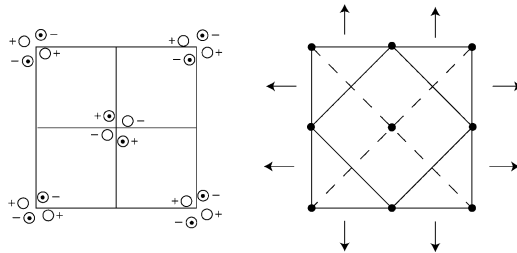


Fig. 9.9. Example of a space group with a screw axis in the plane of the figure: $P\bar{4}2_1m$ (D_{2d}^3) (#113)

(the atoms on the cube corner positions and those in the centered positions). The symmetry operations of T_d represent all the point group operations that take one type of atom into another. In addition, each of the operations of T_d can be compounded with a translation along $(a/4)(111)$ which takes one inequivalent atom into another. Because of these additional symmetry operations, which are not point group operations of T_d , the diamond structure is not a Bravais lattice and is nonsymmorphic. The screw axis pertinent to the diamond structure is shown in Fig. 9.6(g).

Another example of space groups with screw axes is given in Fig. 9.8 for space groups $P4_1$ (C_4^2) #76, $P4_2$ (C_4^3) #77 and $P4_3$ (C_4^4) #78. The space group $P4$ #75 is a symmorphic space group with a similar arrangement of the four atom cluster but without a screw axis. The group numbers #75 to #78 come from the International Tables of X-ray Crystallography [58] (see Appendix C for a few examples of such tables). Each space group in Fig. 9.8 has point group C_4 symmetry, but has a different fourfold screw axis $(4_1, 4_2, 4_3)$. The atom locations are given in the left hand diagrams and the symmetry operations which include screw axes are shown in the right hand diagrams. Some twofold screw axes are also present.

Screw axes may also occur normal to the c -axis, as is shown in Fig. 9.9 for space group $P\bar{4}2_1m$ (D_{2d}^3) #113. Diamond glide planes along $\langle 110 \rangle$ directions also occur for this space group. The D_{2d} operations result in the occurrence of equivalent sites (x, y, z) , $(-y, x, -z)$, $(-x, -y, z)$ and $(y, -x, -z)$.

Three-dimensional space groups will be discussed further in the next chapters. The reader is referred to texts such as Burns and Glazer [16] who give a detailed treatment of space group symmetries. In the next section we discuss the 2D space groups in more depth, first because they are simpler, and because they provide an instructive pedagogic introduction to space groups.

9.3 Two-Dimensional Space Groups

In this section we use the 17 two-dimensional space groups to illustrate in some detail the concepts introduced in this chapter from a pedagogic standpoint.

Table 9.2. Summary of the 17 two-dimensional space groups, their properties and notations

| point group | lattice type | international ^a table number | notation full | type | notation short |
|-------------|---|---|-----------------------|---------------|-----------------------|
| 1 | oblique | 1 | <i>p</i> 1 | symmorphic | <i>p</i> 1 |
| 2 | $a \neq b, \phi \neq 90^\circ$ | 2 | <i>p</i> 211 | symmorphic | <i>p</i> 2 |
| <i>m</i> | rectangular (<i>p</i> or <i>c</i>) | 3 | <i>p</i> 1 <i>m</i> 1 | symmorphic | <i>pm</i> |
| | $a \neq b, \phi = 90^\circ$ | 4 | <i>p</i> 1 <i>g</i> 1 | nonsymmorphic | <i>pg</i> |
| | | 5 | <i>c</i> 1 <i>m</i> 1 | symmorphic | <i>cm</i> |
| <i>2mm</i> | rectangular | 6 | <i>p</i> 2 <i>mm</i> | symmorphic | <i>pmm</i> |
| | $a \neq b, \phi = 90^\circ$ | 7 | <i>p</i> 2 <i>mg</i> | nonsymmorphic | <i>pmg</i> |
| | | 8 | <i>p</i> 2 <i>gg</i> | nonsymmorphic | <i>pgg</i> |
| | | 9 | <i>c</i> 2 <i>mm</i> | symmorphic | <i>cmm</i> |
| 4 | square <i>p</i> | 10 | <i>p</i> 4 | symmorphic | <i>p</i> 4 |
| <i>4mm</i> | $a = b, \phi = 90^\circ$ | 11 | <i>p</i> 4 <i>mm</i> | symmorphic | <i>p</i> 4 <i>m</i> |
| | | 12 | <i>p</i> 4 <i>gm</i> | nonsymmorphic | <i>p</i> 4 <i>g</i> |
| 3 | hexagonal | 13 | <i>p</i> 3 | symmorphic | <i>p</i> 3 |
| <i>3m</i> | $a = b, \phi = 120^\circ$ | 14 | <i>p</i> 3 <i>m</i> 1 | symmorphic | <i>p</i> 3 <i>m</i> 1 |
| | | 15 | <i>p</i> 3 <i>1m</i> | symmorphic | <i>p</i> 3 <i>1m</i> |
| 6 | | 16 | <i>p</i> 6 | symmorphic | <i>p</i> 6 |
| <i>6mm</i> | | 17 | <i>p</i> 6 <i>mm</i> | symmorphic | <i>p</i> 6 <i>m</i> |

^a International Tables for X-Ray Crystallography, published by the International Union of Crystallography, Kynoch Press, [58] Birmingham, England (1952). See also G. Burns and A.M. Glazer, [16] “Space Groups for Solid State Scientists”, Academic Press, Inc., 2nd Edition 1978

There are five distinct Bravais lattices in two-dimensions. If we consider \mathbf{a}, \mathbf{b} to be the two primitive translation vectors and ϕ to be the angle between \mathbf{a} and \mathbf{b} , then the five lattice types are summarized in Table 9.2, where the 17 two-dimensional space groups are listed.

If we add two-dimensional objects, e.g., a set of atoms, to each cell of a Bravais lattice, we can change the symmetry of the lattice. If the object, sometimes called a motif, lowers the symmetry to that of another group, then the resulting symmetry space group for the structure is identified with the lower symmetry space group.

We give in this table the symmetries of each of these space groups, classified in terms of the five Bravais lattices in two dimensions. Listings from the “International Tables for X-Ray Crystallography” are given in Tables B.2–B.17 of Appendix B [58].

The notation used to designate the two-dimensional space groups is illustrated by the example *p*4*gm* (see Table 9.2). The initial symbol (“*p*” in this example) indicates that the unit cell is either a primitive (*p*) unit cell or a cen-

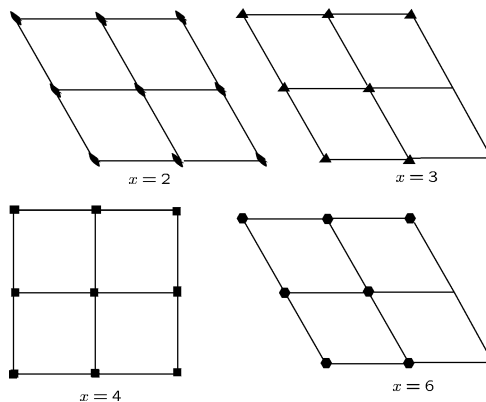


Fig. 9.10. Space group symbols used at lattice points for twofold (an American football), threefold (a triangle), fourfold (a square), and sixfold (a hexagon) rotations ($x = n$ to denote an n -fold rotation)

tered (c) unit cell. The next symbol “4” indicates rotational symmetry about an axis perpendicular to the plane of the two-dimensional crystal. The possible n -fold rotations for a space group are 1, 2, 3, 4, and 6, and the symbols used to denote such axes are shown in Fig. 9.10. The last two symbols in $p4gm$, when present, indicate either additional symmetries for the two inequivalent in-plane axes, or they refer to a glide plane (denoted by “ g ”) through the primary axis, or to a mirror plane denoted by “ m ” through the primary axis, and “1” indicates that there is no additional symmetry.

In the following sections we discuss the space groups associated with each of the five 2D Bravais lattices.

9.3.1 2D Oblique Space Groups

The symmetries of the two 2D oblique space groups are shown in Tables B.1 and B.2 of Appendix B. The lowest symmetry two-dimensional space group (#1) only has translational symmetry ($p1$) and no additional point group operations. We use the lower case notation $p1$ to denote 2D space groups and $P1$ with a capital letter to denote the corresponding 3D space groups. The diagram for $p1$ shows only one general point (x, y) with translations by lattice vectors $(1,0)$, $(0,1)$, and $(1,1)$. Open circles on the left hand diagram in Table B.1 are used to denote the three open circles obtained from the first open circle by these three translations.

However, by placing a motif with twofold rotational symmetry normal to the plane, the $p211$ space group (#2) is obtained, as shown in the symmetry diagram from the International Tables for X-Ray Crystallography. The twofold axis through the center of the rhombus (indicated by an American-football-shaped symbol on the right of Table B.2) denotes the symmetry operation that takes a general point (x, y) into $(-x, -y)$, shown

as point symmetry type e on the crystallographic table for space group #2($p211$). Points obtained by rotations are indicated by open circles in Table B.2. For the four special points $(1/2, 1/2)$, $(1/2, 0)$, $(0, 1/2)$, $(0, 0)$, labeled d, c, b, a , respectively, the twofold rotation takes the point into itself or into an equivalent point separated by a lattice vector. The site symmetry for these four special points is listed in the table for group $p2$ as having a twofold axis. A general point (such as e) under the action of the twofold axis and translation by $(1,0)$, $(0,1)$, and $(1,1)$ yields the eight open points in the figure for group $p2$, two of which are within the unit cell shown in Table B.2.

These special points d, c, b, a are examples of what is generally called *Wyckoff positions* [76]. The concept of *Wyckoff positions* and their site symmetries is fundamental for the determination and description of crystal structures, since it is important to establish the reference point for the symmetry operations of an overall consistent coordinate system. The group of all symmetry operations that leaves a point P invariant is called the *site-symmetry group*. A point P is called the *point of special position* with respect to the space group G if there is at least one symmetry operation of G , in addition to the identity, that leaves P invariant (otherwise, P is called a *point of general position*). A Wyckoff position consists of all points P for which the site-symmetry groups are conjugate subgroups of G , and each Wyckoff position of a space group is labeled by a letter which is called the *Wyckoff letter*, and the site symmetries are indicated in the International Crystallography Tables [58].

9.3.2 2D Rectangular Space Groups

Primitive lattices. Of the seven rectangular 2D space groups, five are primitive and two are centered (see Table 9.2). We consider these together as is done in the International Tables for X-Ray Crystallography [58]. Of the five primitive rectangular space groups only two are symmorphic, and three are nonsymmorphic. In general, the full rectangular point symmetry is $2mm$ (C_{2v}). The point group $2mm$ has elements E , C_{2z} , σ_x , σ_y : the identity; a twofold axis C_{2z} perpendicular to the plane; and mirror planes parallel to the x and y axes through C_{2z} . The corresponding space group listed as space group #6 is $p2mm$ (see Table B.6). When introducing a lower symmetry motif, the resulting group must be a subgroup of the original group. The lower symmetry rectangular space group $p1m1$ has point group operations (E, σ_x) and is listed as space group #3 (see Table B.4). We note that (E, σ_y) is equivalent to (E, σ_x) by an interchange of axes and each corresponds to point group m (C_{1h}).

The symbol \odot containing a comma inside the circle provides a sense of orientation that is preserved under translations. Under a mirror plane operation (see Table B.4), the symbols \odot and \bigcirc are interchanged; the mirror plane is represented on the right by a solid horizontal line. The three kinds of Wyckoff

positions [76] and site symmetries (the general point c and the points a and b on the mirror planes) are also listed in Table B.4 for space group #3.

So far we have dealt with space groups where the point group operations are separable from the translation group operations. Such groups are *symmorphic* space groups.

In the case of the rectangular primitive lattice, mirror operations can be replaced by glide reflections. The glide planes are denoted by dashed lines (see diagram for space group #4 ($p1g1$) in Table B.4). No distinct screw operations are possible in two-dimensions. A glide reflection symmetry operation is a compound operation consisting of a reflection combined with a fractional unit cell translation, not a primitive unit cell translation. The resulting space group is nonsymmorphic because of the glide plane operation. Replacing m by g in $p1m1$ (space group #3) gives $p1g1$ (space group #4) where the translation $\tau_1/2$ is compounded with the reflection operation; this translation can be followed by comparing the \odot symbols for space groups #3 and #4 (Tables B.3 and B.4).

For the case of space group #6 ($p2mm$), replacing one of the mirror planes by a glide plane gives the nonsymmorphic group $p2mg$ (#7) as shown in Table B.7. When both mirror planes of space group #6 are replaced by glide planes, we get space group #8 ($p2gg$) which has the fractional translation $(1/2)\tau_1 + (1/2)\tau_2$, but a mirror plane reflection σ_x or σ_y as shown in Table B.8. The compound mirror plane translation operations can be denoted by $\{\sigma_x|(1/2)\tau_1 + (1/2)\tau_2\}, \{\sigma_y|(1/2)\tau_1 + (1/2)\tau_2\}$.

Centered Rectangular Lattices. The centered rectangular lattice with the full centered rectangular symmetry (see Table B.9) is the space group $c2mm$ (#9) which is a centering of space group #6 ($p2mm$). The lower symmetry centered rectangular subgroup, related to space group #3 ($p1m1$) is space group #5 ($c1m1$) (shown in Table B.5). We note that the centering is equivalent to introducing a $(1/2)\tau_1 + (1/2)\tau_2$ translation as indicated in Table B.5 for space group $c1m1$ (#5). All the centered rectangular lattices are considered to be *symmorphic* even though they have the translation $(1/2)\tau_1 + (1/2)\tau_2$ to do the centering operation. As a more interesting example of a centered rectangular space group, let us look at space group #9 which is denoted by $c2mm$ (Table B.9). This space group has two equivalent positions $(0,0)$ and $(1/2, 1/2)$. The symmetry operations include a twofold axis along the z -direction and two sets of intersecting mirror planes. Four of the symmetry operations shown in Table B.9 are connected with the $2mm$ operations, and the other four symmetry operations are related to compounding these point group operations with the simple translation $(1/2)\tau_1 + (1/2)\tau_2$ taking $(0,0)$ to $(1/2, 1/2)$. The table shows that $c2mm$ can be realized through six different kinds of Wyckoff positions and their corresponding site symmetries. It should be noted that the various 2D space group tables provide special relations for the crystallographic h and k Miller indices that are used to distinguish diffraction patterns associated with each of the space groups.

9.3.3 2D Square Space Group

There are three 2D square space groups. The square lattice space with the full $4mm$ point group symmetry is $p4mm$ (space group #11), which is shown in Table B.11. The point group symmetry elements are E , C_{4z}^+ , C_{4z}^- , C_{2z} , σ_y , σ_x , σ_{da} , σ_{db} corresponding to C_{4v} . The only distinct subgroup of C_{4v} is C_4 which has symmetry elements E , C_{4z}^+ , C_{4z}^- , C_{2z} . In this case, the space group is $p4$ (space group #10 in International Tables for X-Ray Crystallography). The fourfold axis is clearly seen on the left hand diagram in Table B.10. The \odot points in space group #11 are obtained by adding mirror planes to space group #10. In the diagram on the right we see lattice locations with fourfold and with twofold axes, a feature found in all three 2D square lattices (see Tables B.10–B.12).

By combining the translation $(1/2)\tau_1 + (1/2)\tau_2$, where $1/2\tau_1$ and $(1/2)\tau_2$ are translation vectors, with the mirror planes $\sigma_x, \sigma_y, \sigma_{da}, \sigma_{db}$ we obtain the glide reflections $\{\sigma_x|(1/2)\tau_1 + (1/2)\tau_2\}$, $\{\sigma_y|(1/2)\tau_1 + (1/2)\tau_2\}$, $\{\sigma_{da}|(1/2)\tau_1 + (1/2)\tau_2\}$, $\{\sigma_{db}|(1/2)\tau_1 + (1/2)\tau_2\}$. These glide reflections are used to form the nonsymmorphic square lattice of space group #12 ($p4gm$). We note there are mirror planes along the square diagonals and also mirror planes through the x - and y -axes. Space group #12 ($p4gm$) is obtained from space group #11 ($p4mm$) by translation of the comma points by $(1/2)\tau_1 + (1/2)\tau_2$, taking the open points into comma points.

9.3.4 2D Hexagonal Space Groups

There are five 2D hexagonal space groups, and all are symmorphic. The \rightarrow hexagonal space group #17 with the full hexagonal point group symmetry is $p6mm$. The point group symmetry elements are E , C_6^+ , C_6^- , C_3^+ , C_3^- , C_2 , $\sigma_{d1}, \sigma_{d2}, \sigma_{d3}, \sigma_{v1}, \sigma_{v2}, \sigma_{v3}$. The diagram for $p6mm$ (#17) is shown in Table B.17.

The four subgroups of C_{6v} are C_6 , C_{3v} , C_{3d} , C_3 , giving rise, respectively, to space groups $p6$ (#16), $p3m1$ (#14), $p31m$ (#15), and $p3$ (#13), as summarized in Table 9.3. The symmetry diagrams for the five 2D hexagonal space groups are shown in Tables B.13–B.17.

Table 9.3. Summary of the symmetry operations of two-dimensional hexagonal space groups that are subgroups of #17 ($p6mm$)

| space group | point group elements |
|-------------|--|
| $p3$ | E, C_3^+, C_3^- |
| $p3m1$ | $E, C_3^+, C_3^-, \sigma_{v1}, \sigma_{v2}, \sigma_{v3}$ |
| $p31m$ | $E, C_3^+, C_3^-, \sigma_{d1}, \sigma_{d2}, \sigma_{d3}$ |
| $p6$ | $E, C_6^+, C_6^-, C_3^+, C_3^-, C_2$ |

9.4 Line Groups

Line groups describe the symmetry of systems exhibiting translational periodicity in one dimension [71]. Examples of quasi-one-dimensional systems, are stereoregular polymers and carbon nanotubes. In addition, some three-dimensional crystals can be highly anisotropic, as for example chain-type crystals which have line groups as subgroups of their space group. Whenever only one direction is relevant for some physical properties of a three-dimensional system, one can expect to derive useful information by applying suitable line group approaches. The advantage of using line groups is their simplicity.

Generally, quasi-1D systems exhibit, besides translational symmetry, point group and compound operations. As explained further below, line groups generally involve a *generalized* translation group Z and an *axial* point group P giving the internal symmetries [22]. By a *generalized* translation group we mean that Z denotes an infinite cyclic group composed of general translational operations along the line axis, that may include screw axes or glide planes. The line group symmetry elements are represented by $\{C_n^r|\alpha\}$, where C_n^r is a rotation of $2\pi r/n$, and n and r are non-negative integers and where $r < n$, and $0 < \alpha < 1$ represent a translation along the line axis by αa , where a is the translational period of the system. For a given choice for r , any multiple of q/n , where q is a divisor of n , may be added to r with no effect on the resulting line group L , so that the minimum value of r is used to avoid nonuniqueness. There are three different types of generalized translation groups:

- Those formed by simple translations, $T = \{E|\alpha\}$ and the translational period is αa ;
- Those with the occurrence of a screw axis, $T_n^r = \{C_n^r|\alpha\}$ and in this case the translational period is $n\alpha a$;
- Those with the occurrence of a glide plane, $T_c = \{\sigma_v|\alpha\}$ and in this case the translational period is $2\alpha a$.

The *axial* point groups P are: C_n , S_{2n} , C_{nh} , C_{nv} , D_n , D_{nh} and D_{nd} , where $n = 1, 2, 3, \dots$ is the order of the principal rotational axis.

The line groups are formed by taking the weak direct product $L = Z \cdot P$. The product between Z and P must be a weak direct product² (indicated here by “.”) because all elements of Z , except for the identity, have a nonzero translational part, while no point group element on P has translations. The intersection between groups Z and P is, therefore, only the identity operation. However, the product $Z \cdot P$ forms a group only if Z and P commute (this is

²The general concept of a weak direct product is defined in the following way: A Group G is said to be the weak direct product of its subgroups H and K when (i) the identity element is the only intersection of H and K and (ii) each element of G is the product of one element in H with one element in K . Semi-direct and direct products are special cases of the weak-direct product. When H and K are invariant subgroups, the result is a direct product. When only H is an invariant subgroup, the result is a semidirect product.

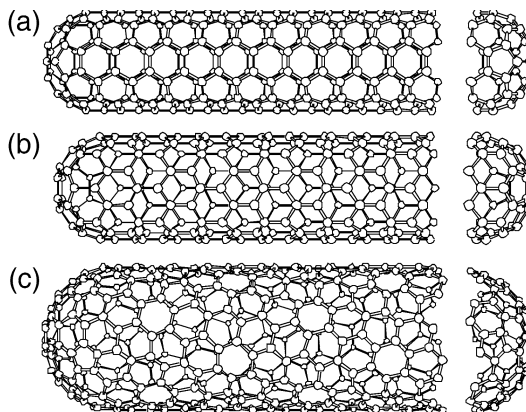


Fig. 9.11. Schematic theoretical model for the three different types of single-wall carbon nanotubes: (a) the “armchair” nanotube, (b) the “zigzag” nanotube, and (c) the “chiral” nanotube [63]

always the case only for $Z = T$). Furthermore, some products with different factors are identical. There are an infinite number of line groups, and they are classified into 13 families [22]. In Problem 9.7 we use carbon nanotubes to exemplify the use of line groups.

Carbon nanotubes can be viewed as a graphene sheet (a single layer from a 3D graphite crystal) rolled up into a cylinder, one atomic layer in thickness. Their physical properties depend on how the graphene sheet is rolled up, and from a symmetry point of view, two types of tubes can be formed, namely the achiral tubes, as shown in Fig. 9.11(a) and (b), or the chiral tubes, illustrated in Fig. 9.11(c). Because of the small diameter of a carbon nanotube ($\sim 10 \text{ \AA}$) and the large length-to-diameter ratio ($> 10^4$), a carbon nanotube from a symmetry standpoint is a one-dimensional crystal with a translation vector \mathbf{T} along the cylinder axis and a small number of carbon hexagons associated with the circumferential direction. For this reason, this structure is a very appropriate system to study line groups. The relation between carbon atoms on a carbon nanotube and the symmetry operations on the respective line groups is one-to-one, and nanotubes are, therefore, a prototype system for illustrating line groups [23, 24].

9.5 The Determination of Crystal Structure and Space Group

In many research situations, the researcher must first identify the crystal structure and the space group, as summarized below.

9.5.1 Determination of the Crystal Structure

The standard determinations of crystal structures are carried out using diffraction techniques, either X-ray or neutron diffraction. The elastically scattered beams give rise to a series of diffraction peaks which can be indexed according to the points in reciprocal lattice. The results of many such structural determinations for specific materials are listed in the series of books by Wyckoff [76].

We illustrate the use of Wyckoff's books to find the crystal structure of a particular material in Problem 9.6. The information to be extracted from Wyckoff's book concerns the number of allotropic structures of a given chemical species, the Wyckoff positions of the atoms within the unit cell, the site symmetries of the atoms in each of the structures and the space group designations. Such information is also available from websites [58]. Appendix C shows some illustrative crystal structures.

9.5.2 Determination of the Space Group

The International Tables for X-Ray Crystallography [58] helps with the determination of the space group and the symmetry operations of the space group³ [58]. These volumes deal with space groups in general but do not refer to specific materials, which is the central theme of Wyckoff's books. In some cases Wyckoff's books give the space group designation, and then the listing of the Wyckoff positions needs to match up with the proper Wyckoff positions in the International Tables for X-Ray Crystallography under the appropriate space group. If the space group is not given explicitly in Wyckoff's books [76], then the space group must be found from the Crystallographic information and the Wyckoff positions. The procedure that is used to find the space group is to first find the Wyckoff positions and site symmetries as illustrated in Problems 9.4 and 9.6. Information about space groups is also available from websites [54, 58, 76].

Selected Problems

- 9.1. (a) For the crystal structure shown in Fig. 9.5(a) list the symmetry elements and identify the space group and give the space group number and symmetry designations for this space group (see Table 9.1).
 (b) Find the Wyckoff positions for the four atoms per unit cell and find the site symmetries for the structure shown in Fig. 9.5(a).
 (c) Find χ^{equiv} for the space group in Fig. 9.5(a) and find the irreducible representations contained in Γ^{equiv} .
 (d) Repeat (a), (b) and (c) for the space group in Fig. 9.5(b).

³International Tables for X-ray Crystallography.

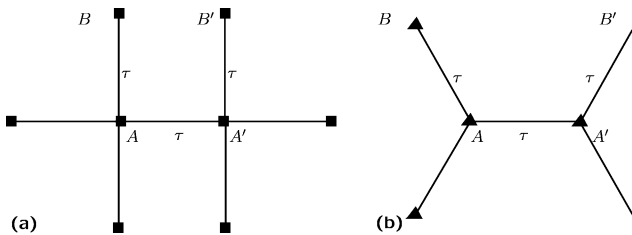


Fig. 9.12. Translation-rotation symmetry for a fourfold axis (a), and a threefold axis (b)

9.2. (a) List the real space symmetry operations of the nonsymmorphic two-dimensional square space group $p4gm$ (#12).

- (b) Explain all the open and filled points, and the solid and dashed lines in the diagram for the 2D space group $p4gm$ (#12). Explain the point symmetry entries for each of the site symmetries a, b, c, d on the table for space group #12 ($p4gm$) in Table B.12 in Appendix B which was taken from the International Crystallography Tables.
- (c) Explain the differences in the symmetry operations between the 2D space group #12 and the 2D space group #11. Why does the figure for group #11 have dashed lines? Why is group #12 not classified as a centered space group? Why are there no centered square 2D space groups?

9.3. Show that in the diamond structure, the product of two symmetry operations involving translations τ yields a symmetry element with no translations

$$\{\alpha|\tau\}\{\beta|\tau\} = \{\gamma|0\},$$

where $\tau = (1, 1, 1)a/4$. What is the physical significance of this result?

9.4. Consulting Wyckoff's book "Crystal Structures" 2nd edn., Krieger (1981) for the crystal structure of Nb_3Sn , a prototype superconductor with the A-15 (or β -W) structure used for high field superconducting magnet applications:

- (a) List the site locations of each atom within the unit cell of Nb_3Sn as obtained from Wyckoff's book or from another source.
- (b) Identify the proper space group for Nb_3Sn and give the Wyckoff positions for each atom and its site symmetry.

9.5. To understand why fivefold symmetry does not form a Bravais lattice, consider the interplay of a fourfold or threefold axes and their translations, shown in Fig. 9.12. In general, the only acceptable values of α are those that cause BB' in Fig. 9.12 to be an integer multiple of the original translation, τ (that is we require $BB' = m\tau$, where m is an integer).

- (a) By relating BB' to τ and α , show that the only values of α satisfying the restriction $BB' = m\tau$ are $0, \pi/3, \pi/2, 2\pi/3$ and π .

- (b) Show schematically that in the case of fivefold symmetry, BB' gives rise to a new translation τ' in the same direction as τ , but inconsistent with the original lattice vectors coming from A . This inconsistency can also be expressed by stating that BB' violates the initial hypothesis that τ is the shortest translation in the direction BB' .

9.6. This problem provides experience with finding the Wyckoff positions for 3D graphite in the hexagonal crystal structure (see Fig. C.1 in Appendix C) and in the rhombohedral crystal structure (see Fig. C.2)

- (a) From the crystal structure model, find the coordinates for the four distinct atoms per unit cell in 3D graphite and give their site symmetries.
- (b) Using space group #194 (Table C.3 in Appendix C) find the Wyckoff positions and their symmetries.
- (c) Explain the diagrams appearing at the top of Table C.3, especially the notation. Why are space groups #191, #192, and #193 not appropriate for describing the structure for 3D graphite (Fig. C.1)?
- (d) Repeat (a) for rhombohedral graphite (Table C.4) with 6 atoms/unit cell in the hexagonal system and two atoms/unit cell in the rhombohedral system (space group #166).

9.7. Consider single wall carbon nanotubes, as presented in Sect. 9.4 and discussed in Appendix E.

- (a) Find the space groups with the appropriate symmetries for the semiconducting (6,5) and the metallic (6,6) carbon nanotubes.
- (b) The physical properties of carbon nanotubes can be obtained from those of a graphene sheet by the zone-folding procedure. Using the linear-helical construction (see Appendix E), show how the allowed k vectors of a carbon nanotube can be mapped into the Brillouin zone of two-dimensional graphite, and discuss the conservation of the linear and helical quantum numbers. The diagram on the cover to this book can be very helpful for solving this problem.
- (c) Find the appropriate line groups for chiral and achiral carbon nanotubes.

Space Groups in Reciprocal Space and Representations

When moving from molecules to crystals, the physical properties will be described by dispersion relations in reciprocal space, rather than by energy levels. One of the most important applications of group theory to solid state physics relates to the symmetries and degeneracies of the dispersion relations, especially at high symmetry points in the Brillouin zone. As discussed for the Bravais lattices in Sect. 9.2, the number of possible types of Brillouin zones is limited. The reciprocal space for Bravais lattices is discussed in Sect. 10.1 and this topic is also discussed in solid state physics courses [6, 45].

The classification of the symmetry properties in reciprocal space involves the *group of the wave vector*, which is the subject of this chapter. The group of the wave vector is important because it is the way in which both the *point group symmetry* and the *translational symmetry* of the crystal lattice are incorporated into the formalism that describes the dispersion relations of elementary excitations in a solid. Suppose that we have a symmetry operator $\hat{P}_{\{R_\alpha|\tau\}}$ based on the space group element $\{R_\alpha|\tau\}$ that leaves the periodic potential $V(\mathbf{r})$ invariant,

$$\hat{P}_{\{R_\alpha|\tau\}} V(\mathbf{r}) = V(\mathbf{r}). \quad (10.1)$$

The invariance relation of (10.1) has important implications on the form of the wave function $\psi(\mathbf{r})$. In particular if we consider only the translation operator $\hat{P}_{\{\varepsilon|\tau\}}$ based on the translation group elements $\{\varepsilon|\tau\}$, we have the result

$$\hat{P}_{\{\varepsilon|\tau\}} \psi(\mathbf{r}) = \psi(\mathbf{r} + \boldsymbol{\tau}). \quad (10.2)$$

Within this framework, we can prove *Bloch's theorem* in Sect. 10.2.2, and then we go on in Sect. 10.3 to determine the symmetry of the wave vector. We then discuss representations for symmorphic and nonsymmorphic space groups and illustrate the group of the wave vector. In Sect. 10.6 we consider the group of the wave vector in some detail for the simple cubic lattice and then we make a few comments to extend these results for the simple cubic lattice to the face centered and body centered cubic structures. The compatibility relations

leading to the formation of branches in the dispersion relations are discussed (Sect. 10.7), illustrated by the same three cubic space groups as in Sect. 10.6. Finally, the group of the wave vector is considered for the nonsymmorphic diamond lattice in Sect. 10.8.

10.1 Reciprocal Space

Definition 23. *The set of all wave vectors \mathbf{K}_m that yield plane waves with the periodicity of a given Bravais lattice defines its reciprocal lattice, and the \mathbf{K}_m are called reciprocal lattice vectors.*

The relation

$$e^{i\mathbf{K}_m \cdot (\mathbf{r} + \mathbf{R}_n)} = e^{i\mathbf{K}_m \cdot \mathbf{r}} \quad (10.3)$$

holds for any \mathbf{r} , and for all \mathbf{R}_n and \mathbf{K}_m defining the Bravais lattice in real space and reciprocal space, respectively, where the reciprocal lattice is characterized by the set of wavevectors \mathbf{K}_m satisfying

$$e^{i\mathbf{K}_m \cdot \mathbf{R}_n} = 1. \quad (10.4)$$

Considering $\mathbf{R}_n = \sum n_i \mathbf{a}_i$ and $\mathbf{K}_m = \sum m_j \mathbf{b}_j$ ($i, j = 1, 2, 3$), where \mathbf{a}_i and \mathbf{b}_j are, respectively, the primitive translation vector and the primitive reciprocal lattice vector for the unit cells of a space lattice, then

$$\mathbf{b}_j \cdot \mathbf{a}_i = 2\pi\delta_{ij} \quad (10.5)$$

defines the orthonormality relation satisfying (10.4).

The more general *ortho*-normality relation for a general lattice vector \mathbf{R}_n and a general reciprocal lattice vector \mathbf{K}_m will be given by

$$\mathbf{R}_n \cdot \mathbf{K}_m = 2\pi N_{nm} = 2\pi N_1, \quad (10.6)$$

where $N_{nm} = N_1$ is an integer depending on n, m .

Table 10.1. Summary of the real and reciprocal lattice vectors for the five two-dimensional Bravais lattices (see Sect. 9.3)

| type | translation vectors | | reciprocal lattice vectors | |
|------------------|---------------------|-------------------------------|------------------------------|-----------------------------|
| | \mathbf{a}_1 | \mathbf{a}_2 | \mathbf{b}_1 | \mathbf{b}_2 |
| oblique, p | $(a_1, 0)$ | $a_2(\cos\theta, \sin\theta)$ | $(2\pi/a_1)(1, -\cot\theta)$ | $(2\pi/a_2)(0, \csc\theta)$ |
| rectangular, p | $(a_1, 0)$ | $(0, a_2)$ | $(2\pi/a_1)(1, 0)$ | $(2\pi/a_2)(0, 1)$ |
| rectangular, c | $(a_1/2, a_2/2)$ | $(-a_1/2, a_2/2)$ | $2\pi(1/a_1, 1/a_2)$ | $2\pi(-1/a_1, 1/a_2)$ |
| square, p | $(a, 0)$ | $(0, a)$ | $(2\pi/a)(1, 0)$ | $(2\pi/a)(0, 1)$ |
| hexagonal, p | $(0, -a)$ | $a(\sqrt{3}/2, 1/2)$ | $(2\pi/a)(1/\sqrt{3}, -1)$ | $(2\pi/a)(2/\sqrt{3}, 0)$ |

To illustrate the primitive translation vectors of the unit cells in real and reciprocal space for the Bravais lattices, we list in Table 10.1 the primitive translation vectors and the corresponding reciprocal lattice vectors for the five two-dimensional Bravais lattices based on (10.5). The vectors \mathbf{a}_1 and \mathbf{a}_2 for these 2D lattices are expressed in terms of unit vectors along appropriate directions of the five Bravais lattices, and a and b are lattice constants. For three-dimensional space groups, there are three unit vectors \mathbf{a}_i , and three unit vectors \mathbf{b}_j in k -space, using the space group notation. The Brillouin zones for several three-dimensional space groups can be found in Appendix C and in the literature [50].

10.2 Translation Subgroup

For the translation subgroup T which is a subgroup of the space group G , consider the translation operator $\hat{P}_{\{\varepsilon|\tau\}}$ based on the translation group elements $\{\varepsilon|\tau\}$, yielding the result

$$\hat{P}_{\{\varepsilon|\tau\}}\psi(\mathbf{r}) = \psi(\mathbf{r} + \tau), \quad (10.7)$$

but since the translation operations all commute with one another, the translations form an Abelian group.

Definition 24. *Since the translation operation τ can be written in terms of translations over the unit vectors \mathbf{a}_i*

$$\tau = \sum_{i=1}^3 n_i \mathbf{a}_i,$$

we can think of the translation operators in each of the \mathbf{a}_i directions as commuting operators:

$$\{\varepsilon|\tau\} = \{\varepsilon|\tau_1\}\{\varepsilon|\tau_2\}\{\varepsilon|\tau_3\}, \quad (10.8)$$

where $\tau_i = n_i \mathbf{a}_i$. The real space lattice vectors produced by the translation operator are denoted in Sect. 10.1 by \mathbf{R}_n .

10.2.1 Representations for the Translation Group

The commutativity of the $\{\varepsilon|\tau_i\}$ operations in (10.8) gives three commuting subgroups. It is convenient to use periodic boundary conditions and to relate the periodic boundary conditions to cyclic subgroups (see Sect. 1.3), so that $\{\varepsilon|\tau_1\}^{\mathcal{N}_1} = \{\varepsilon|\tau_2\}^{\mathcal{N}_2} = \{\varepsilon|\tau_3\}^{\mathcal{N}_3} = \{\varepsilon|0\}$, and \mathcal{N}_i is the number of unit cells along τ_i . In a cyclic subgroup, all symmetry elements commute with one another, and therefore the subgroup is Abelian and has only one-dimensional irreducible matrix representations. Furthermore, the number of irreducible representations of the cyclic subgroup is equal to the number of elements h

in the group, and each element is in a class by itself. Since $\{\varepsilon|\boldsymbol{\tau}_i\}^{\mathcal{N}_i} = \{\varepsilon|0\}$, the irreducible representation for the cyclic group can be written as a set of matrices which are phase factors or characters of the form $\exp(ik_i n_i a_i)$, and are the \mathcal{N}_i roots of unity. Here $k_i = 2\pi m_i / L_i$ (where m_i is an integer and L_i is the length of the crystal in direction \mathbf{a}_i) defines the irreducible representation, and there are $\mathcal{N}_1 \mathcal{N}_2 \mathcal{N}_3 \sim 10^{23}$ of such irreducible representations. In this context, the wave vector k serves as a quantum number for the translation operator.

10.2.2 Bloch's Theorem and the Basis Functions of the Translational Group

Theorem. *If an eigenfunction ψ_k transforms under the translation group according to the irreducible representation labeled by k , then $\psi_k(\mathbf{r})$ obeys the relation*

$$\hat{P}_{\{\varepsilon|\boldsymbol{\tau}\}} \psi_k(\mathbf{r}) = \psi_k(\mathbf{r} + \boldsymbol{\tau}) = e^{i\mathbf{k}\cdot\boldsymbol{\tau}} \psi_k(\mathbf{r}) \quad (10.9)$$

and $\psi_k(\mathbf{r})$ can be written in the form

$$\psi_k(\mathbf{r}) = e^{i\mathbf{k}\cdot\mathbf{r}} u_k(\mathbf{r}), \quad (10.10)$$

where $u_k(\mathbf{r} + \boldsymbol{\tau}) = u_k(\mathbf{r})$ has the full translational symmetry of the crystal.

Proof. Since the translation group is Abelian, all the elements of the group commute and all the irreducible representations are one-dimensional. The requirement of the *periodic boundary condition* can be written as

$$\{\varepsilon|\boldsymbol{\tau}_1 + NL_1\} = \{\varepsilon|\boldsymbol{\tau}_1\}, \quad (10.11)$$

where N is an integer and L_1 is the length of the crystal along basis vector \mathbf{a}_1 . This results in the one-dimensional matrix representation for the translation operator $\boldsymbol{\tau}_i = n_i \mathbf{a}_i$

$$D^{k_1}(n_1 a_1) = e^{ik_1 n_1 a_1} = e^{ik_1 \boldsymbol{\tau}_1} \quad (10.12)$$

since

$$\hat{P}_R \psi_k(\mathbf{r}) = D^k(R) \psi_k(\mathbf{r}), \quad (10.13)$$

where R denotes a symmetry element $k_1 = 2\pi m_1 / L_1$ corresponds to the m_1 th irreducible representation and $m_1 = 1, 2, \dots, (L_1/a_1)$. For each m_1 , there is a unique k_1 , so that each irreducible representation is labeled by either m_1 or k_1 , as indicated above.

We now extend these arguments to three dimensions. For a general translation

$$\boldsymbol{\tau} = \sum_{i=1}^3 n_i \mathbf{a}_i, \quad (10.14)$$

the matrix representation or character for the $(m_1 m_2 m_3)$ th irreducible representation is

$$D^{k_1}(n_1 a_1) D^{k_2}(n_2 a_2) D^{k_3}(n_3 a_3) = e^{ik_1 n_1 a_1} e^{ik_2 n_2 a_2} e^{ik_3 n_3 a_3} = e^{i\mathbf{k} \cdot \boldsymbol{\tau}}, \quad (10.15)$$

since

$$\{\varepsilon|\boldsymbol{\tau}\} = \{\varepsilon|\boldsymbol{\tau}_1\} \{\varepsilon|\boldsymbol{\tau}_2\} \{\varepsilon|\boldsymbol{\tau}_3\}. \quad (10.16)$$

Thus our basic formula $\hat{P}_R \psi_j = \sum_{\alpha} \psi_{\alpha} D(R)_{\alpha j}$ yields

$$\hat{P}_{\{\varepsilon|\boldsymbol{\tau}\}} \psi(\mathbf{r}) = \psi(\mathbf{r}) e^{i\mathbf{k} \cdot \boldsymbol{\tau}} = e^{i\mathbf{k} \cdot \boldsymbol{\tau}} \psi(\mathbf{r}) = \psi(\mathbf{r} + \boldsymbol{\tau}), \quad (10.17)$$

since the representations are all one-dimensional. This result is Bloch's theorem where we often write $\boldsymbol{\tau} = \mathbf{R}_n$ in terms of the lattice vector \mathbf{R}_n . This derivation shows that the phase factor $e^{i\mathbf{k} \cdot \boldsymbol{\tau}}$ is the eigenvalue of the translation operator $\hat{P}_{\{\varepsilon|\boldsymbol{\tau}\}}$. \square

Because of Bloch's theorem, the wave function $\psi(\mathbf{r})$ can be written in the form

$$\psi_k(\mathbf{r}) = e^{i\mathbf{k} \cdot \mathbf{r}} u_k(\mathbf{r}), \quad (10.18)$$

where $u_k(\mathbf{r})$ exhibits the full translational symmetry of the crystal. This result follows from:

$$\psi_k(\mathbf{r} + \mathbf{R}_n) = e^{i\mathbf{k} \cdot (\mathbf{r} + \mathbf{R}_n)} u_k(\mathbf{r} + \mathbf{R}_n) = e^{i\mathbf{k} \cdot \mathbf{R}_n} [e^{i\mathbf{k} \cdot \mathbf{r}} u_k(\mathbf{r})], \quad (10.19)$$

where the first equality in (10.19) is obtained simply by substitution in (10.18) and the second equality follows from Bloch's theorem. In these terms, Bloch's theorem is simply a statement of the translational symmetry of a crystal.

The Bloch functions are the basis functions for the translation group T . The wave vector \mathbf{k} has a special significance as the *quantum number of translation* and provides a label for the irreducible representations of the translation group. If the crystal has a length L_i on a side so that n_0 different lattice translations can be made for each direction \mathbf{a}_i , then the number of \mathbf{k} vectors must be limited to

$$k_x, k_y, k_z = 0, \pm \frac{2\pi}{n_0 a}, \pm \frac{4\pi}{n_0 a}, \dots, \pm \frac{\pi}{a} \quad (10.20)$$

in order to insure that the number of irreducible representations is equal to the number of classes. Since the translation group is Abelian, every group element is in a class by itself, so that the *number of irreducible representations must equal the number of possible translations*. Since the number of translation operators for bulk crystals is very large ($\sim 10^{23}$), the quantum numbers for translations are discrete, but very closely spaced, and form a quasi-continuum of points in reciprocal space. For nanostructures, the number of translation operations can be quite small (less than 100) and some unusual quantum size effects can then be observed.

We note that all of these \mathbf{k} -vectors are contained within the first Brillouin zone. Thus, if we consider a vector in the extended Brillouin zone $\mathbf{k} + \mathbf{K}_m$, where \mathbf{K}_m is a reciprocal lattice vector, the appropriate phase factor in Bloch's theorem is

$$e^{i(\mathbf{k} + \mathbf{K}_m) \cdot \mathbf{R}_n} = e^{i\mathbf{k} \cdot \mathbf{R}_n}, \quad (10.21)$$

since $\mathbf{K}_m \cdot \mathbf{R}_n = 2\pi N$ where N is an integer.

10.3 Symmetry of k Vectors and the Group of the Wave Vector

When we choose a given eigenstate $\psi_k(\mathbf{r})$ of the crystal potential, except for eigenstates at the Γ point ($k = 0$), the basis function will exhibit a modulation described by the wavevector k , and this modulation will decrease the crystal symmetry. In this case, we work with the *group of the wave vector*, that is a subgroup of the space group G . To introduce this concept, we consider in Sect. 10.3.1 the action of a point group symmetry operator on a lattice vector and on a reciprocal lattice vector. Next we discuss the group of the wave vector and the *star of a wave vector*, including an example of these concepts in terms of the two-dimensional square lattice (Sect. 10.3.2). Finally in Sect. 10.3.3 we consider the effect of translations and point group operations on Bloch functions, thereby clarifying the degeneracies introduced by the point group symmetries of crystal lattices.

10.3.1 Point Group Operation in r -space and k -space

The effect of a symmetry operator \hat{P}_α on a lattice vector \mathbf{R}_n and on a reciprocal lattice vector \mathbf{K}_m subject to the orthogonality relation (10.6) is considered in this section.

Let \hat{P}_α denote a symmetry operator of the point group of the crystal, then $\hat{P}_\alpha \mathbf{R}_n$ leaves the crystal invariant. If \mathbf{R}_n is a translation operator, then $\hat{P}_\alpha \mathbf{R}_n$ is also a translation operator (lattice vector), since the full symmetry of the lattice is preserved. Likewise $\hat{P}_\alpha \mathbf{K}_m$ is a translation operator in reciprocal space. Since $\hat{P}_\alpha \mathbf{R}_n$ is a lattice vector, we can write

$$(\hat{P}_\alpha \mathbf{R}_n) \cdot \mathbf{K}_m = 2\pi N_2, \quad (10.22)$$

where N_2 is an integer, not necessarily the same integer as N_1 in (10.6). Since α^{-1} is also a symmetry operator of the group, we have

$$(\hat{P}_\alpha^{-1} \mathbf{R}_n) \cdot \mathbf{K}_m = 2\pi N_3, \quad (10.23)$$

and again N_3 is not necessarily the same integer as N_1 or N_2 . Furthermore, any scalar product (being a constant) must be invariant under any point symmetry operator. Thus if we perform the same symmetry operation on each member of the scalar product in (10.23), then the scalar product remains invariant

$$\hat{P}_\alpha(\hat{P}_\alpha^{-1} \mathbf{R}_n) \cdot (\hat{P}_\alpha \mathbf{K}_m) = 2\pi N_3 = \mathbf{R}_n \cdot (\hat{P}_\alpha \mathbf{K}_m). \quad (10.24)$$

Equations (10.22)–(10.24) lead to several results: If \hat{P}_α is a symmetry operator of a point group of a crystal, and \mathbf{R}_n and \mathbf{K}_m are, respectively, lattice and reciprocal lattice vectors, then $\hat{P}_\alpha^{-1} \mathbf{R}_n$ and $\hat{P}_\alpha \mathbf{K}_m$ also are, respectively, a lattice vector and a reciprocal lattice vector. Thus the *effect of an operator \hat{P}_α on a direct lattice vector \mathbf{R}_n is equivalent to the effect of operator \hat{P}_α^{-1} on the corresponding reciprocal lattice vector \mathbf{K}_m* .

10.3.2 The Group of the Wave Vector \mathbf{G}_k and the Star of \mathbf{k}

Definition 25. *The group of the wave vector is formed by the set of space group operations which transform \mathbf{k} into itself, or into an equivalent $\mathbf{k} = \mathbf{k} + \mathbf{K}_m$ vector, where \mathbf{K}_m is a vector of the reciprocal lattice.*

The addition of \mathbf{K}_m does not change the energy of the system since $e^{i\mathbf{k}\cdot\mathbf{R}_n} = e^{i(\mathbf{k}+\mathbf{K}_m)\cdot\mathbf{R}_n}$, i.e., both \mathbf{k} and $(\mathbf{k} + \mathbf{K}_m)$ belong to the same translational irreducible representation (see Sect. 10.2.2). Clearly, all the symmetry operations of the space group take the point $\mathbf{k} = 0$ into itself so that the space group itself forms the group of the wave vector at $\mathbf{k} = 0$. Furthermore, the group of the wave vector for nonzone center \mathbf{k} -vectors ($\mathbf{k} \neq 0$) remains a subgroup of the space group for $\mathbf{k} = 0$.

Let us now consider the action of the point group operations on a general vector \mathbf{k} in reciprocal space, not necessarily a reciprocal lattice vector. The set of wave vectors \mathbf{k}' which are obtained by carrying out all the point group operations on \mathbf{k} is called the *star of \mathbf{k}* . If \mathbf{k} is a general point in the Brillouin zone, there will be only one symmetry element, namely the identity, which takes \mathbf{k} into itself and in this case the wave functions describing electron states only see the translational symmetry $\{\varepsilon|\tau\}$ of the space group. On the other hand, if the \mathbf{k} -vector under consideration lies on a symmetry axis or is at a high symmetry point in the Brillouin zone, then perhaps several of the point group operations will transform \mathbf{k} into itself or into an equivalent \mathbf{k} -vector $\mathbf{k} + \mathbf{K}_m$.

An informative example for the formation of the group of the wave vector for various \mathbf{k} -vectors is provided by the two-dimensional square lattice. Here the point group is D_4 and the symmetry operations are E , $C_2 = 2C_4^2$, $2C_4$, $2C_2'$, $2C_2''$ (diagonals). The various \mathbf{k} -vectors in the star of \mathbf{k} are indicated in the diagrams in Fig. 10.1 for the two-dimensional square lattice. The group elements for the group of the wave vector in each case are indicated within the parenthesis. The top three diagrams are for \mathbf{k} -vectors to interior points within the first Brillouin zone and the lower set of three diagrams are for \mathbf{k} -vectors to the Brillouin zone boundary. Thus the star of \mathbf{k} shown in Fig. 10.1 is formed by consideration of $\hat{P}_\alpha \mathbf{k}$ for all operators \hat{P}_α for the point group. The group of the wave vector is formed by those \hat{P}_α for which $\hat{P}_\alpha \mathbf{k} = \mathbf{k} + \mathbf{K}_m$, where \mathbf{K}_m is a reciprocal lattice vector (including $\mathbf{K}_m = 0$). The concepts presented in Fig. 10.1, are reinforced in Problem 10.2 for the hexagonal lattice with point group D_6 .

10.3.3 Effect of Translations and Point Group Operations on Bloch Functions

We will now consider the effect of the symmetry operations on \mathbf{k} with regard to the eigenfunctions of Schrödinger's equation. We already know from

Bloch's theorem that the action of any pure translation operator $\hat{P}_{\{\varepsilon|\tau\}}$ on wave function $\psi_k(r)$ (where $\tau = \mathbf{R}_n$) yields a wave function $e^{i\mathbf{k}\cdot\mathbf{R}_n}\psi_k(r)$

$$\hat{P}_{\{\varepsilon|\tau\}}\psi_k(r) = e^{i\mathbf{k}\cdot\tau}\psi_k(r). \quad (10.25)$$

There will be as many wave functions of this functional form as there are translation vectors, each corresponding to the energy $E(\mathbf{k})$. These Bloch functions provide basis functions for irreducible representations for the group of the wave vector. If \mathbf{k} is a general point in the Brillouin zone, then the star of \mathbf{k} contains wave vectors which are all equivalent to \mathbf{k} from a physical standpoint. The space group for a general wave vector \mathbf{k} will however contain only the symmetry elements $\{\varepsilon|\mathbf{R}_n\}$, since in this case all the \mathbf{k} -vectors are distinct. For a wave vector with higher symmetry, where the operations $\hat{P}_\beta \mathbf{k} = \mathbf{k} + \mathbf{K}_m$ transform \mathbf{k} into an equivalent wave vector, the space group of the wave vector contains the symmetry element $\{\beta|\mathbf{R}_n\}$ and the energy at equivalent \mathbf{k} points must be equal. If the point group of the wave vector contains irreducible representations that have more than one dimension, then a degeneracy in the energy bands will occur. Thus bands tend to "stick together" along high symmetry axes and at high symmetry points.

The effect of a point group operation on this eigenfunction is

$$\hat{P}_{\{R_\alpha|0\}}\psi_k(r) = \hat{P}_{\{R_\alpha|0\}}e^{i\mathbf{k}\cdot\mathbf{r}}u_k(r), \quad (10.26)$$

in which we have written the eigenfunction in the Bloch form. Since the effect of a point group operation on a function is equivalent to preserving the form of the function and rotating the coordinate system in the opposite sense, to maintain invariance of scalar products we require

$$\mathbf{k} \cdot R_\alpha^{-1}\mathbf{r} = R_\alpha \mathbf{k} \cdot \mathbf{r}. \quad (10.27)$$

If we now define $u_{R_\alpha k}(r) \equiv u_k(R_\alpha^{-1}\mathbf{r})$ for the periodic part of the Bloch function and denote the transformed wave vector by $\mathbf{k}' \equiv R_\alpha \mathbf{k}$, then we have

$$\hat{P}_{\{R_\alpha|0\}}\psi_k(r) = e^{iR_\alpha \mathbf{k} \cdot \mathbf{r}}u_{R_\alpha k}(r) \equiv \psi_{R_\alpha k}(r), \quad (10.28)$$

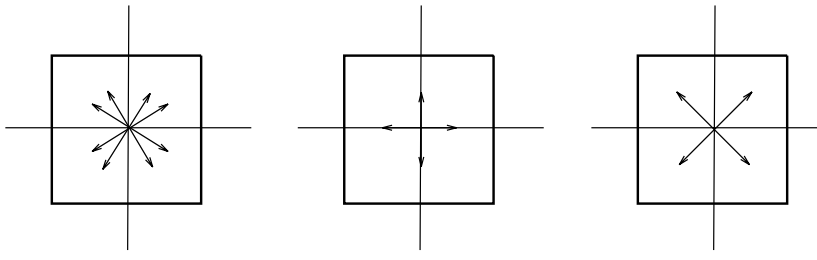
which we will now show to be of the Bloch form by operating with the translation operator on $\psi_{R_\alpha k}(r)$

$$\begin{aligned} \hat{P}_{\{\varepsilon|\tau\}}\psi_{R_\alpha k}(r) &= \hat{P}_{\{\varepsilon|\tau\}}[e^{iR_\alpha \mathbf{k} \cdot \mathbf{r}}u_k(R_\alpha^{-1}\mathbf{r})] \\ &= e^{iR_\alpha \mathbf{k} \cdot (\mathbf{r} + \tau)}u_k(R_\alpha^{-1}\mathbf{r} + R_\alpha^{-1}\tau). \end{aligned} \quad (10.29)$$

Because of the periodicity of $u_k(r)$ we have

$$u_{R_\alpha k}(\mathbf{r} + \tau) = u_k(R_\alpha^{-1}\mathbf{r} + R_\alpha^{-1}\tau) = u_k(R_\alpha^{-1}\mathbf{r}) \equiv u_{R_\alpha k}(r), \quad (10.30)$$

\vec{k} to an interior point in the Brillouin zone

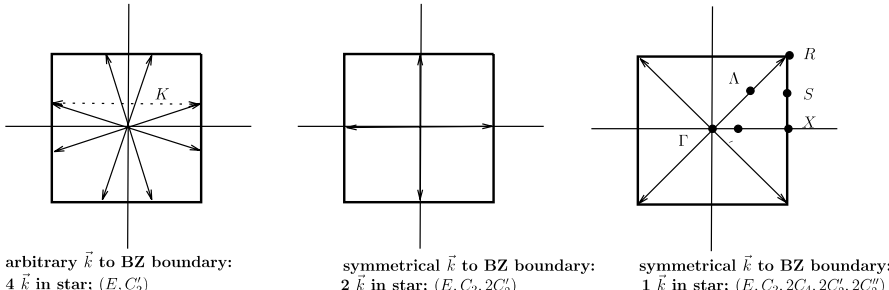


arbitrary \vec{k} to BZ interior:
8 \vec{k} in star; (E)

symmetrical \vec{k} to BZ interior:
4 \vec{k} in star; (E, C_2')

symmetrical \vec{k} to BZ interior:
4 \vec{k} in star; (E, C_2'')

\vec{k} to a point on the Brillouin zone boundary



arbitrary \vec{k} to BZ boundary:
4 \vec{k} in star; (E, C_2')

symmetrical \vec{k} to BZ boundary:
2 \vec{k} in star; $(E, C_2, 2C_2')$

symmetrical \vec{k} to BZ boundary:
1 \vec{k} in star; $(E, C_2, 2C_4, 2C_2', 2C_2'')$

Fig. 10.1. Illustration of the star of \mathbf{k} for various wave vectors in the Brillouin zone of a simple 2D square lattice. The top three diagrams are for \mathbf{k} -vectors to an interior point in the Brillouin zone, while the bottom three diagrams are for wave vectors extending to the Brillouin zone boundary. In each case the point group elements for the group of the wave vector are given in parentheses

and noting the orthonormality relation (10.6) for the plane wave factor, we get

$$\hat{P}_{\{\varepsilon|\tau\}} \psi_{R_\alpha k}(\mathbf{r}) = e^{iR_\alpha \mathbf{k} \cdot \tau} \psi_{R_\alpha k}(\mathbf{r}), \quad (10.31)$$

where $u_{R_\alpha k}(\mathbf{r})$ is periodic in the direct lattice. The *eigenfunctions* $\psi_{R_\alpha k}(\mathbf{r})$ thus forms *basis functions* for the R_α th *irreducible representation* of the translation group T . As we saw in Sect. 10.3.2, the set of distinct wave vectors in \mathbf{k} -space which can be generated by operating on one \mathbf{k} vector by all the symmetry elements of the point group g is called the “star of \mathbf{k} ” (see Fig. 10.1).

Considering the above arguments on symmorphic groups for simplicity, where the point group g is isomorphic to G/T and $\{R_\alpha|\tau\} = \{\varepsilon|\tau\} \hat{P}_{\{R_\alpha|0\}}$, we have

$$\begin{aligned} \hat{P}_{\{R_\alpha|\tau\}} \psi_k(\mathbf{r}) &= \hat{P}_{\{\varepsilon|\tau\}} \hat{P}_{\{R_\alpha|0\}} \psi_k(\mathbf{r}) \\ &= \hat{P}_{\{\varepsilon|\tau\}} \psi_{R_\alpha k}(\mathbf{r}) \\ &= e^{iR_\alpha \mathbf{k} \cdot \tau} \psi_{R_\alpha k}(\mathbf{r}). \end{aligned} \quad (10.32)$$

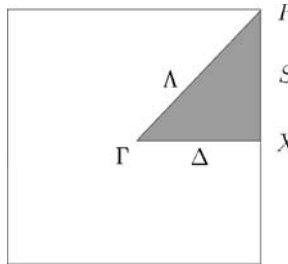


Fig. 10.2. The shaded triangle $\Gamma\Lambda RSX\Delta\Gamma$ which constitutes 1/8 of the Brillouin zone for the 2D square lattice and contains the basic wave vectors and high symmetry points

Similarly we obtain

$$\hat{P}_{\{R_\beta|\tau'\}}\psi_{R_\alpha k}(\mathbf{r}) = e^{iR_\beta R_\alpha \mathbf{k} \cdot \tau'} \psi_{R_\beta R_\alpha k}(\mathbf{r}). \quad (10.33)$$

Thus the set of eigenfunctions $\{\psi_{R_\alpha k}(\mathbf{r})\}$ obtained by taking the star of \mathbf{k} spans the invariant subspace of the point group g since the product operation $R_\beta R_\alpha$ is contained in g . If h is the order of the group g , there are h functions in the set $\{\psi_{R_\alpha k}(\mathbf{r})\}$. All of these representations are completely specified by \mathbf{k} , but they are equally well specified by any of the \mathbf{k} vectors in the star of \mathbf{k} . Although all the functions in the set $\{\psi_{R_\alpha k}(\mathbf{r})\}$ correspond to the same energy, we do *not* say that the functions $\psi_k(\mathbf{r})$ and $\psi_{R_\alpha k}(\mathbf{r})$ are degenerate. Instead we write $\{\psi_k(\mathbf{r})\}$ for all the functions in the set $\{\psi_{R_\alpha k}(\mathbf{r})\}$ and consider the extra point group symmetry to yield the relation $E(\mathbf{k}) = E(R_\alpha \mathbf{k})$ for all R_α . In this way, we guarantee that the energy $E(\mathbf{k})$ will show the full point group symmetry of the reciprocal lattice. Thus for the two-dimensional square lattice, it is only necessary to calculate $E(\mathbf{k})$ explicitly for \mathbf{k} points in 1/8 of the Brillouin zone contained within the sector $\Gamma\Lambda RSX\Delta\Gamma$ (see Fig. 10.2). These statements are generally valid for nonsymmorphic groups as well.

We use the term “degeneracy” to describe states with exactly the same energy *and* the same wave vector. Such degeneracies do in fact occur because of symmetry restrictions at special high symmetry points in the Brillouin zone and such degeneracies are called “*essential*” degeneracies. “Essential” degeneracies occur only at high symmetry or special \mathbf{k} points, while accidental (“nonessential”) degeneracies occur at arbitrary \mathbf{k} points. “Special” high symmetry points in the Brillouin zone are those for which

$$R_\alpha \mathbf{k} = \mathbf{k} + \mathbf{K}_m, \quad (10.34)$$

where \mathbf{K}_m is the reciprocal lattice vector including $\mathbf{K}_m = 0$. In the cases where the symmetry operation yields $R_\alpha \mathbf{k} = \mathbf{k} + \mathbf{K}_m$, then the eigenfunctions have essential degeneracies because we now can have degenerate eigenfunctions with the same energy eigenvalue at the same \mathbf{k} vector. These essential band degeneracies are lifted as we move away from the high symmetry points

to a general point in the Brillouin zone. The rules governing the lifting of these degeneracies are called *compatibility relations*, discussed in Sect. 10.7.

10.4 Space Group Representations

We start by saying that tables for the group of the wave vector for each unique \mathbf{k} vector for each of the 230 space groups have been established and are available in different references, as reviewed in Sect. 10.9. For each wavevector \mathbf{k} , the spacial group representations are constructed from the analysis of the group of wavevector and of the star of \mathbf{k} , and the use of the *multiplier algebra*, that we briefly discuss below. The representations will be square matrices with dimension $(\ell q) \times (\ell q)$, i.e., $\ell \times \ell$ blocks of $q \times q$ matrices, where ℓ is the number of \mathbf{k} vectors in the star, and q is defined by the representations in the group of the wavevector. Each line (or column) in the matrix will have only one $q \times q$ nonzero entry and the remaining entries are filled with null $q \times q$ matrices. The $\ell \times \ell$ block arrangement describes the symmetries relating the different vectors in the star of \mathbf{k} , and the nonzero $q \times q$ matrix describes the symmetry with respect to the specific \mathbf{k} and its group of the wavevector.

The rotational aspects of the group of the wave vector are described by the $q \times q$ matrices related to the factor group G_k/T_k . The T_k group can be represented by a linear combination of the three lattice vectors, and the symmetry elements usually shown in the character tables are related to a $\{R_\alpha|\tau_\alpha\}/T_k$ coset. The subgroups of the group of the wave vector \mathbf{k} occurring at points in the Brillouin zone with fewer symmetry operations are called the *small representations*, in contrast to the full point group symmetry for $k = 0$ which is called the *large representation*. The Bloch functions with wavevectors \mathbf{k} form the basis, and each symmetry element is a coset formed by several elements, but is represented by a typical element, a “representative coset.”

10.4.1 Symmorphic Group Representations

The representation theory for symmorphic groups is relatively simple. Since there are no compound operations, the factor group G_k/T_k is symmorphic to the point group g_k .

Small Representation. The small representations for the group of the wave vector of \mathbf{k} are given by

$$D_k^{\Gamma_i}(\{R_\alpha|\mathbf{R}_n\}) = e^{i\mathbf{k} \cdot \mathbf{R}_n} D^{\Gamma_i}(R_\alpha), \quad (10.35)$$

where $\{R_\alpha|\mathbf{R}_n\}$ belongs to G_k , and $e^{i\mathbf{k} \cdot \mathbf{R}_n}$ comes from T , with \mathbf{R}_n being a lattice vector or a primitive translation, and Γ_i is an irreducible representation coming from one of the 32 crystallographic point groups (see Chap. 3), whose character tables are given in Appendix A. Here $D^{\Gamma_i}(R_\alpha)$ refers only to the point group.

Characters for Small Representation. The characters for the irreducible representations are given by

$$\chi_k^{\Gamma_i}(\{R_\alpha | \mathbf{R}_n\}) = e^{i\mathbf{k} \cdot \mathbf{R}_n} \chi^{\Gamma_i}(R_\alpha). \quad (10.36)$$

where $\chi^{\Gamma_i}(R_\alpha)$ only refers to the point group.

Large Representation. For the Γ point we have $k = 0$ and $e^{i\mathbf{k} \cdot \mathbf{R}_n} = 1$. Also, if we consider the factor group of G_k with respect to the translations, then also $\mathbf{R}_n = 0$ and again $e^{i\mathbf{k} \cdot \mathbf{R}_n} = 1$. In both cases, both representations and characters are identical to those from the point groups.

10.4.2 Nonsymmorphic Group Representations and the Multiplier Algebra

As for the symmorphic groups, we denote the group of the wave vector \mathbf{k} by G_k . For symmetry operations $\{R|\boldsymbol{\tau}\}$ that involve translations $\boldsymbol{\tau}$ smaller than the smallest Bravais lattice vector, the translations introduce a phase factor $\exp[i\mathbf{k} \cdot \boldsymbol{\tau}]$. However, as discussed in Sect. 9.1.4, the entire set of space group elements $\{R_\alpha | \boldsymbol{\tau}_\alpha\}$ may fail to form a group, and the point group g of the crystal is not a subgroup of G . In this case, to work with the rotational aspects of the nonsymmorphic space group, procedures to remove the translational effect are needed. Furthermore, the factor group G_k/T_k contain cosets formed only by pure translations, giving rise to *irrelevant representations*. The *relevant representations*, describing the rotational aspects of the group of the wavevector, can be directly obtained by using the *multiplier algebra*.

Multiplier Groups. If the representations are written in terms of a Bloch wave basis, the translational group is diagonalized and the multiplier groups are defined by

$$\{R_\alpha | \boldsymbol{\tau}_\alpha\} \{R_\beta | \boldsymbol{\tau}_\beta\} = e^{-i\mathbf{k} \cdot [\boldsymbol{\tau}_\alpha + R_\alpha \boldsymbol{\tau}_\beta - \boldsymbol{\tau}_{\alpha\beta}]} \{R_\alpha R_\beta | \boldsymbol{\tau}_{\alpha\beta}\}, \quad (10.37)$$

where the $[\boldsymbol{\tau}_\alpha + R_\alpha \boldsymbol{\tau}_\beta - \boldsymbol{\tau}_{\alpha\beta}]$ represents a lattice vector translation resulting from the product of the elements in the group of the wave vector. Any element $\{R_\gamma | \boldsymbol{\tau}_\gamma + R_n\}$ thus generated can be represented by a single element

$$M(\gamma) = e^{-i\mathbf{k} \cdot [\boldsymbol{\tau}_\gamma + R_n]} \{R_\gamma | \boldsymbol{\tau}_\gamma + R_n\} \quad (10.38)$$

in the multiplier group, obeying the algebra

$$M(\alpha)M(\alpha') = e^{i\mathbf{K}_\alpha \cdot \boldsymbol{\tau}_{\alpha'}} M(\alpha\alpha'), \quad (10.39)$$

the exponential factor being 1 except for points at the Brillouin zone boundary, where $R_\alpha \mathbf{k} = \mathbf{k} + \mathbf{K}_\alpha$, and \mathbf{K}_α is a reciprocal lattice translation. The factor group G_k/T_k will, therefore, be isomorphic to a point group from which the rotational aspects of the group of the wave vector can be treated.

Small and Large Representations. In general the representations are obtained from the irreducible representations of the multiplier group. From (10.38) and (10.39) it can be shown that the small representations are obtained from ordinary point group representations when the point group operation leaves \mathbf{k} invariant, since in that case $\mathbf{K}_\alpha = 0$ in (10.39). The same applies to the large representation, where $\mathbf{K}_\alpha = 0$ always. Note that the multiplier algebra also applies to symmorphic groups. In this case $\boldsymbol{\tau}_\alpha = \boldsymbol{\tau}_{\alpha'} = \boldsymbol{\tau}_\beta = 0$ in (10.38) and (10.39), and the representations are also obtained from ordinary point group representations, as discussed above.

Characters for Small and Large Representations. At the zone center, the characters for the group of the wave vector are the same as the isomorphic point group, because the phase factor $\exp[i\mathbf{k} \cdot \boldsymbol{\tau}]$ reduces to unity when $k = 0$. For each symmetry axis leading away from $\mathbf{k} = 0$, the character tables for those \mathbf{k} points can be obtained by selecting the

appropriate point group character table and by multiplying the character for the symmetry operations that contain a translation $\boldsymbol{\tau}$ by a phase factor $\exp[i\mathbf{k} \cdot \boldsymbol{\tau}]$.

More detailed discussions of the space group representations and *multiplier groups* are available elsewhere [50, 53].

10.5 Characters for the Equivalence Representation

We now discuss the computation of the characters $\chi^{\text{equiv.}}$ for the equivalence representation in space groups, and its decomposition into the irreducible representations of the group. For a specific wavevector \mathbf{k} , the general formulation for $\chi_k^{\text{equiv.}}$ related to a specific class of symmetry space group operators $\{R_\alpha | \mathbf{R}_n + \boldsymbol{\tau}_\alpha\}$ is given by

$$\chi^{\text{equiv.}}(\{R_\alpha | \mathbf{R}_n + \boldsymbol{\tau}_\alpha\}) = e^{i\mathbf{k} \cdot (\mathbf{R}_n + \boldsymbol{\tau}_\alpha)} \sum_j \delta_{\{R_\alpha | \mathbf{R}_n + \boldsymbol{\tau}_\alpha\} \mathbf{r}_j, \mathbf{r}_j} e^{i\mathbf{K}_m \cdot \mathbf{r}_j}, \quad (10.40)$$

where the first exponential factor is related to the phase factor for translation $\mathbf{R}_n + \boldsymbol{\tau}_\alpha$. The delta function basically gives 1 for atoms remaining in their position under the space group symmetry operation $\{R_\alpha | \mathbf{R}_n + \boldsymbol{\tau}_\alpha\}$ or is 0 otherwise. For space groups, however, equivalent atoms on different unit cells must be considered as equivalent. Here \mathbf{r}_j is the position in the j th atom with respect to the origin of the point group, and $\delta_{\{R_\alpha | \mathbf{R}_n + \boldsymbol{\tau}_\alpha\} \mathbf{r}_j, \mathbf{r}_j} = 1$ if $\{R_\alpha | \mathbf{R}_n + \boldsymbol{\tau}_\alpha\} \mathbf{r}_j$ and \mathbf{r}_j refer to equivalent atomic positions, occurring when $(R_\alpha \mathbf{r}_j = \mathbf{r}_j + \mathbf{R}_n)$. It is clear that the delta function is always zero when $\boldsymbol{\tau}_\alpha \neq 0$.

The decomposition of the equivalence transformation into the irreducible representations of the space group is made by using the procedure discussed in Sect. 3.4. The first exponential factor in (10.40) turns out not to be important

for this decomposition process, since $\chi^{\text{equiv.}}$ will then be multiplied by $[\chi^{(\Gamma_i)}]^*$ (see (3.20)), which carries the complex conjugate of the exponential factor.

Equation (10.40) gives the general rule for the equivalence transformation in crystalline structures. The last exponential term in (10.40) appears for specific \mathbf{k} points at the zone boundary, for which $R_\alpha^{-1}\mathbf{k} = \mathbf{k} + \mathbf{K}_m$ where \mathbf{K}_m is a reciprocal lattice vector. At most of the \mathbf{k} points, including the Γ point, $R_\alpha^{-1}\mathbf{k} = \mathbf{k}$ and $\mathbf{K}_m = 0$ so that $e^{i\mathbf{K}_m \cdot \mathbf{r}_j} = 1$, and we just work with the general concept of $\chi^{\text{a.s.}} = 0$ or 1.

10.6 Common Cubic Lattices: Symmorphic Space Groups

In this section we limit our discussion to symmorphic space groups, where the group of the wave vector for arbitrary \mathbf{k} is a subgroup of the group of the wave vector $\mathbf{k} = 0$, which displays the full point group symmetry of the crystal (see Sect. 10.4.1). This situation applies to all crystal lattices, whether they are cubic, hexagonal, etc. We discuss here the group of the wave vector for the three-dimensional simple cubic lattice $Pm3m$ (O_h^1) #221 (see Fig. 10.3) in

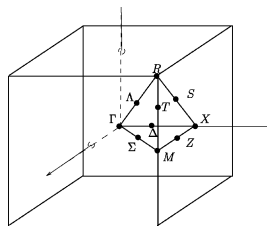


Fig. 10.3. The Brillouin zone for the simple cubic lattice (space group #221) showing the high symmetry points and axes

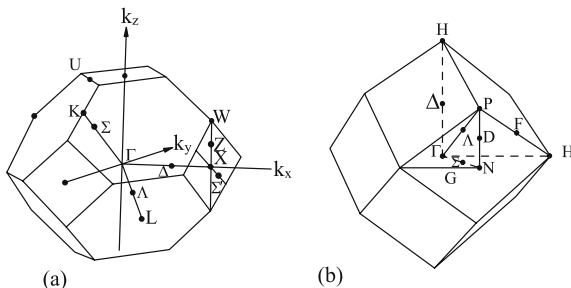


Fig. 10.4. Brillouin zones for the (a) face-centered (space group #225) and (b) body-centered (space group #229) cubic lattices showing the points and lines of high symmetry in (a). The point Z on the line between X and W is also called V in the literature and point Q is between L and W

some detail, and we refer also to the group of the wave vector for the B.C.C. (space group $Im3m$ (O_h^9) #229) and for the F.C.C. (space group $Fm3m$ (O_h^5) #225) structures (see Fig. 10.4).

Figure 10.3 shows the Brillouin zone for the simple cubic lattice. The high symmetry points and axes in these figures are labeled using the standard notation found in the crystallography literature, the group theory literature, and in the solid state physics literature.

10.6.1 The Γ Point

The symmetry operations of the group of the wave vector at the Γ point ($k = 0$) are the symmetry operations of the O_h group indicated in Fig. 3.4 compounded with full inversion symmetry, $O_h = O \otimes i$. The character table for O_h along with the basis functions for all the irreducible representations is given in Table 10.2. The form of the basis functions is helpful in identifying s (Γ_1), p (Γ_{15}) and d ($\Gamma_{12}, \Gamma'_{25}$) electronic states of the O_h cubic crystal where the symmetries of the corresponding irreducible representations are shown.

The notation used in Table 10.2 is that traditionally used in the solid state physics literature [1] and dates back to the 1930s. Here Γ_1 and Γ_2 denote

Table 10.2. Character table for the cubic group O_h corresponding to the group of the wave vector at $k = 0$ for the three cubic space groups #221 (SC), #225 (FCC), and #229 (BCC)[†]

| repr. | basis functions | E | $3C_4^2$ | $6C_4$ | $6C'_2$ | $8C_3$ | i | $3iC_4^2$ | $6iC_4$ | $6iC'_2$ | $8iC_3$ |
|-------------------------------|---|-----|----------|--------|---------|--------|-----|-----------|---------|----------|---------|
| $\Gamma_1(\Gamma_1^+)$ | 1 | | 1 | 1 | 1 | 1 | 1 | 1 | 1 | 1 | 1 |
| $\Gamma_2(\Gamma_2^+)$ | $\begin{cases} x^4(y^2 - z^2) + \\ y^4(z^2 - x^2) + \\ z^4(x^2 - y^2) \end{cases}$ | | 1 | 1 | -1 | -1 | 1 | 1 | 1 | -1 | -1 |
| $\Gamma_{12}(\Gamma_{12}^+)$ | $\begin{cases} x^2 - y^2 \\ 2z^2 - x^2 - y^2 \end{cases}$ | | 2 | 2 | 0 | 0 | -1 | 2 | 2 | 0 | 0 |
| $\Gamma_{15}(\Gamma_{15}^-)$ | x, y, z | | 3 | -1 | 1 | -1 | 0 | -3 | 1 | -1 | 1 |
| $\Gamma_{25}(\Gamma_{25}^-)$ | $z(x^2 - y^2) \dots$ | | 3 | -1 | -1 | 1 | 0 | -3 | 1 | 1 | -1 |
| $\Gamma'_1(\Gamma_1^-)$ | $\begin{cases} xyz[x^4(y^2 - z^2) + \\ y^4(z^2 - x^2) + \\ z^4(x^2 - y^2)] \end{cases}$ | | 1 | 1 | 1 | 1 | 1 | -1 | -1 | -1 | -1 |
| $\Gamma'_2(\Gamma_2^-)$ | xyz | | 1 | 1 | -1 | -1 | 1 | -1 | -1 | 1 | -1 |
| $\Gamma'_{12}(\Gamma_{12}^-)$ | $xyz(x^2 - y^2) \dots$ | | 2 | 2 | 0 | 0 | -1 | -2 | -2 | 0 | 0 |
| $\Gamma'_{15}(\Gamma_{15}^+)$ | $xy(x^2 - y^2) \dots$ | | 3 | -1 | 1 | -1 | 0 | 3 | -1 | 1 | -1 |
| $\Gamma'_{25}(\Gamma_{25}^+)$ | xy, yz, zx | | 3 | -1 | -1 | 1 | 0 | 3 | -1 | -1 | 1 |

[†] The basis functions for Γ_{25}^- are $z(x^2 - y^2)$, $x(y^2 - z^2)$, $y(z^2 - x^2)$, for Γ_{12}^- are $xyz(x^2 - y^2)$, $xyz(3z^2 - r^2)$ and for Γ_{15}^+ are $xy(x^2 - y^2)$, $yz(y^2 - z^2)$, $zx(z^2 - x^2)$

Table 10.3. Character table C_{4v} for the group of the wave vector at a Δ point^a

| representation | basis functions | E | C_4^2 | $2C_4$ | $2iC_4^2$ | $2iC_2'$ |
|----------------|--------------------------|-----|---------|--------|-----------|----------|
| Δ_1 | $1, x, 2x^2 - y^2 - z^2$ | 1 | 1 | 1 | 1 | 1 |
| Δ_2 | $y^2 - z^2$ | 1 | 1 | -1 | 1 | -1 |
| Δ'_2 | yz | 1 | 1 | -1 | -1 | 1 |
| Δ'_1 | $yz(y^2 - z^2)$ | 1 | 1 | 1 | -1 | -1 |
| Δ_5 | $y, z; xy, xz$ | 2 | -2 | 0 | 0 | 0 |

^a $\Delta = \frac{2\pi}{a}(x, 0, 0)$ (SC, FCC, BCC); $T = \frac{2\pi}{a}(1, 1, z)$ (SC)

1D irreducible representations, Γ_{12} denotes the 2D irreducible representation, while Γ_{15} and Γ_{25} denote the two 3D irreducible representations and the notations used are historical.¹ In this notation, Γ_{15} and Γ_{25} are odd while Γ'_{15} and Γ'_{25} are even under inversion (as can be seen from the basis functions in Table 10.2). To get around this apparent nonuniformity of notation with regard to even and odd functions, we often use Γ_i^\pm (e.g., Γ_{15}^\pm) to emphasize the parity (even or odd property) of a wavefunction for the cubic groups. We notice that to obtain basis functions for all the irreducible representations of the group O_h in Table 10.2 we need to include up to sixth-order polynomials.

10.6.2 Points with $k \neq 0$

In Table C.6 in Appendix C we see that the special point R in Fig. 10.3 for the simple cubic lattice that also has full O_h symmetry. Special care must be given to operations taking k into $k + K_m$, since they also add exponential factors to the computation of χ^{equiv} , for example, as discussed in Sect. 10.5.

We next consider the group of the wave vector at lower symmetry points. First we consider the group of the wave vector for a point along the Δ axis (see Fig. 10.3) which has fewer symmetry operations than the group of the wave vector at $\mathbf{k} = 0$. The group of the wave vector at Δ is an example of a *small representation*. The symmetry operations for a point along the Δ axis for the simple cubic lattice are those of a square, rather than those of a cube and are the symmetry operations of point group C_{4v} . Group C_{4v} is a subgroup of the full cubic group O_h . The multiplication table for the elements of the point group C_{4v} which is appropriate for a reciprocal lattice point Δ along the \hat{x} axis is given in Table C.9. Multiplication tables like this can be compiled for all the groups of the wave vectors for all high symmetry points in the Brillouin zone for all the space groups.

The character table (including basis functions) for the group of the wave vector for Δ , where $\Delta = (\Delta, 0, 0)$ is along \hat{x} , is given in Table 10.3 and Table C.8. Since the Δ point occurs in space groups #221 (SC), #225 (FCC)

¹The numbers contained in the subscripts denote how the Γ point levels split in the Δ axis direction, as discussed in Sect. 10.7.

Table 10.4. Character table for the group of the wave vector Λ

| character table for the Λ axis | | | |
|--|-----|--------|---------|
| $\Lambda = C_{3v}$ | E | $2C_3$ | $3iC_2$ |
| A_1 | 1 | 1 | 1 |
| A_2 | 1 | 1 | -1 |
| A_3 | 2 | -1 | 0 |

and #229 (BCC), the character table and basis functions in Table 10.3 are applicable for all these space groups. In Table 10.3 for the Δ point, the C_4 rotation operation is along \hat{x} , the $2iC_4^2$ are along \hat{y}, \hat{z} , and the $2iC_2'$ are along $\{011\}$. The basis functions in the character table can be found from inspection by taking linear combinations of (x^ℓ, y^m, z^n) following the discussion in Chap. 4. The process of going from higher to the lower symmetry defines the *compatibility relations* (Sect. 10.7) between irreducible representations of O_h and those of C_{4v} showing the path from the higher group O_h to the lower symmetry C_{4v} . The basis functions for the lower symmetry groups (such as the group of Δ) are related to those of O_h by considering the basis functions of the point group O_h as reducible representations of the subgroup Δ , and decomposing these reducible representations into irreducible representations of the group Δ . For example Γ'_{25} (or using Γ_{25}^+ to show its parity) of point group O_h is a reducible representation of C_{4v} , and reduction of Γ'_{25} (or Γ_{25}^+) into irreducible representations of C_{4v} yields the compatibility relation (see Sect. 10.7)

$$[\Gamma'_{25}]_{O_h} \equiv [\Gamma_{25}^+]_{O_h} \rightarrow [\Delta_{2'} + \Delta_5]_{C_{4v}},$$

showing the origin of the Γ'_{25} notation. We note that yz is the longitudinal partner for $\Delta = (\Delta, 0, 0)$ and corresponds to the irreducible representation Δ'_2 , while xy, xz are the transverse partners corresponding to Δ_5 . What is different here from the discussion in Sect. 5.3 is that the dispersion relations also go from lower to higher symmetry. For example, the Δ point goes into the X point for space groups # 221 and # 225 and into the H point for # 229 (BCC) all having more symmetry operations than at the Δ point. We also note that the group of the wave vector for point T for the simple cubic lattice (see Fig. 10.3) also has C_{4v} symmetry (see Tables C.6 and C.8). In considering the group of the wave vector for point T , remember that any reciprocal lattice point separated by a reciprocal lattice vector from T is an equally good T point. The character Table 10.3 also serves for the T -point, but the symmetry operations and basis functions would need proper modification. Character tables for all the high symmetry points for \mathbf{k} vectors in the simple cubic lattice are discussed in this section. For example, the symmetry group for a wave vector along the (111) axis or Λ axis is C_{3v} (see Fig. 10.3), which is given in Table 10.4. For a Λ point along the (111) direction, the $2C_3$ are

along $\{111\}$, and the $3iC_2$ are along $(\bar{1}\bar{1}0)$, $(10\bar{1})$, and $(0\bar{1}1)$ directions. For the Λ point we can do threefold rotations in both \pm senses about ΓR for group #221, about ΓL for #225 and about ΓP for #229 (see Fig. 10.4). Whereas the Λ point follows the same point group C_{3v} , the end points R , L , and P for the three space groups have different point group symmetries. We can also do 180° rotations about twofold axes ΓM followed by inversion (see Fig. 10.3). By $\Gamma M'$ we mean the wave vector to the center of an adjacent cube edge, and we here note that a rotation by π about $\Gamma M'$ in group #221 followed by inversion does not leave Λ invariant. Only three of the “ $\Gamma M'$ ” axes are symmetry operations of the group; the other three such axes (like ΓM in the diagram) are not symmetry operations. Therefore instead of the symmetry operations $6iC_2$ which hold for the Γ and R points, the class $3iC_2$ for the group of the Λ point only has three symmetry elements. Table C.10 in Appendix C gives the basis functions for each irreducible representation of the group of the wave vector at a Λ point and shows that point F for the BCC structure also has C_{3v} symmetry, but the symmetry operations and basis functions need to be appropriately modified.

The final high symmetry point along one of the three main symmetry axes is the Σ point along the $\{110\}$ axes. The group of the wave vector for the Σ point is C_{2v} and the character table is shown in Table C.11 in Appendix C. This character table applies to the Σ point for the simple cubic, FCC and BCC lattices (see Fig. 10.4). All the irreducible representations are one-dimensional. Table C.6 identifies high symmetry points in other space groups which have high symmetry points with C_{2v} symmetry. Table C.11 in Appendix C also shows that the group of the wave vector for high symmetry points Z and S for the simple cubic lattice, points U , Z , and K for the FCC lattice, and points G and D for the BCC lattice all belong to group C_{2v} .

Table 10.5. Character tables for the group of the wave vector (group D_{4h}) for points M and X for space group #221

| M | E | $2C_4^2$ | $C_{4\perp}^2$ | $2C_{4\perp}$ | $2C_2$ | i | $2iC_4^2$ | $iC_{4\perp}^2$ | $2iC_{4\perp}$ | $2iC_4$ | $2iC_2$ |
|--------------|-----|-----------------|--------------------|-------------------|--------|-----|------------------|---------------------|--------------------|---------|---------|
| X | E | $2C_{4\perp}^2$ | $C_{4\parallel}^2$ | $2C_{4\parallel}$ | $2C_2$ | i | $2iC_{4\perp}^2$ | $iC_{4\parallel}^2$ | $2iC_{4\parallel}$ | $2iC_4$ | $2iC_2$ |
| M_1, X_1 | 1 | 1 | 1 | 1 | 1 | 1 | 1 | 1 | 1 | 1 | 1 |
| M_2, X_2 | 1 | 1 | 1 | -1 | -1 | 1 | 1 | 1 | -1 | -1 | -1 |
| M_3, X_3 | 1 | -1 | 1 | -1 | 1 | 1 | -1 | 1 | -1 | 1 | |
| M_4, X_4 | 1 | -1 | 1 | 1 | -1 | 1 | -1 | 1 | 1 | 1 | -1 |
| M'_1, X'_1 | 1 | 1 | 1 | 1 | 1 | -1 | -1 | -1 | -1 | -1 | -1 |
| M'_2, X'_2 | 1 | 1 | 1 | -1 | -1 | -1 | -1 | -1 | 1 | 1 | |
| M'_3, X'_3 | 1 | -1 | 1 | -1 | 1 | -1 | 1 | -1 | 1 | -1 | |
| M'_4, X'_4 | 1 | -1 | 1 | 1 | -1 | -1 | 1 | -1 | -1 | 1 | |
| M_5, X_5 | 2 | 0 | -2 | 0 | 0 | 2 | 0 | -2 | 0 | 0 | 0 |
| M'_5, X'_5 | 2 | 0 | -2 | 0 | 0 | -2 | 0 | 2 | 0 | 0 | 0 |

It can also happen that two high symmetry points such as M and X for the simple cubic lattice belong to the same point group D_{4h} , but the symmetry operations for the two groups of the wave vector can refer to different axes of rotation, as shown in Table 10.5. The notation $C_{4\parallel}^2$ in Table 10.5 refers to a twofold axis ΓX , while $2C_{4\perp}^2$ refers to the two twofold axes \perp to ΓX . These are in different classes because in one case X is left invariant, while in the other case X goes into an equivalent X point separated by a reciprocal lattice vector. To put it in more physical terms, if the X point would not exactly be on the zone boundary but were instead at a Δ point arbitrarily close, the $C_{4\parallel}^2$ operation would still hold, while the $2C_{4\perp}^2$ operations would not. When we list multiple high symmetry points with a given character table in Appendix C, we do not generally distinguish between the symmetry operations for the individual classes (compare for example Table 10.5 and Table C.15). Character tables for all the high symmetry points in the Brillouin zone for the simple cubic lattice (#221) (see Fig. 10.3) and for the FCC and BCC lattices (see Fig. 10.4) are given in Appendix C, since we use these groups frequently for illustrative purposes in this book.

10.7 Compatibility Relations

As stated above, compatibility relations relate the basis functions (wave functions) in going from one wave vector to another belonging to a different symmetry group. Such a situation, for example, occurs when going from $k = 0$ (Γ point with full O_h symmetry) to an interior k point such as a Δ point with C_{4v} symmetry and then in going from the Δ point to the X point with D_{4h} symmetry.

To study these compatibility relations, let us follow some particular energy band around the Brillouin zone and see how its symmetry type and hence how its degeneracy changes. The problem of connectivity (connecting energy bands as we move from one \mathbf{k} point to a neighboring \mathbf{k} point with a different group of the wave vector) is exactly the same type of problem as that occurring in crystal field splittings (Sect. 5.3) as we go from a high symmetry crystal field to a perturbed crystal field of lower symmetry.

As an illustration of compatibility relations, consider a simple cubic lattice as we move along a (111) direction from $\Gamma \rightarrow \Lambda \rightarrow R$ from the center of the Brillouin zone to the zone corner (see Fig. 10.3). At the Γ point ($\mathbf{k} = 0$) we have the full point group symmetry O_h . As we now go from a higher point group symmetry O_h at Γ to a \mathbf{k} vector along Λ , we go to a point group of lower symmetry C_{3v} . Since there are no three-dimensional representations in C_{3v} , we know that the degeneracy of the threefold degenerate levels in O_h symmetry, i.e., $\Gamma_{15}^-, \Gamma_{25}^-, \Gamma_{15}^+, \Gamma_{25}^+$ levels, will be at least partially lifted. We proceed as before to write down the character table for the Λ point, and below it we will write down the representations of the Γ point group, which we now treat as reducible representations of the Λ point group. We then reduce out

Table 10.6. Compatibility relations along Λ in the simple cubic BZ

| Λ | E | $2C_3$ | $3iC_2$ | irreducible representations |
|--------------------------------|-----|--------|---------|-----------------------------|
| Λ_1 | 1 | 1 | 1 | |
| Λ_2 | 1 | 1 | -1 | |
| Λ_3 | 2 | -1 | 0 | |
| $\Gamma_1 (\Gamma_1^+)$ | 1 | 1 | 1 | A_1 |
| $\Gamma_2 (\Gamma_2^+)$ | 1 | 1 | -1 | A_2 |
| $\Gamma_{12} (\Gamma_{12}^+)$ | 2 | -1 | 0 | A_3 |
| $\Gamma'_{15} (\Gamma_{15}^+)$ | 3 | 0 | -1 | $A_2 + A_3$ |
| $\Gamma'_{25} (\Gamma_{25}^+)$ | 3 | 0 | 1 | $A_1 + A_3$ |
| $\Gamma'_1 (\Gamma_1^-)$ | 1 | 1 | -1 | A_2 |
| $\Gamma'_2 (\Gamma_2^-)$ | 1 | 1 | 1 | A_1 |
| $\Gamma'_{12} (\Gamma_{12}^-)$ | 2 | -1 | 0 | A_3 |
| $\Gamma_{15} (\Gamma_{15}^-)$ | 3 | 0 | 1 | $A_1 + A_3$ |
| $\Gamma_{25} (\Gamma_{25}^-)$ | 3 | 0 | -1 | $A_2 + A_3$ |

the irreducible representations of the Λ point symmetry group. This process is indicated in Table 10.6, below where we list the ten irreducible representations of O_h and indicate the irreducible representations of C_{3v} therein contained. This procedure gives a set of compatibility conditions. In a similar way, the compatibility relations for a simple cubic lattice along the Δ and Σ axes follow the progression from Γ to Δ to X and also from Γ to Σ to M as can be seen from Fig. 10.3. In going from $\Delta \rightarrow X$ we go from C_{4v} symmetry to D_{4h} symmetry, since at the Brillouin zone boundary, translation by a reciprocal lattice vector introduces additional symmetries associated with a mirror plane. Similarly, in going from $\Sigma \rightarrow M$ we get four equivalent M points so that the symmetry group goes from C_{2v} to D_{4h} . Compatibility relations for the simple cubic lattice are summarized in Table 10.7 for illustrative purposes.

Tables of compatibility relations for all space groups are compiled in the literature, e.g. Miller and Love's book [54] (see Sect. 10.9).

As an example of using these compatibility relations, let us consider what happens as we move away from the Γ point $\mathbf{k} = 0$ on a threefold level, such as Γ'_{25} (or Γ_{25}^+) in Table 10.7. There are many possibilities, as indicated below:

$$\Gamma'_{25} \rightarrow \Delta_{2'} + \Delta_5 \rightarrow X_3 + X_5, \quad (10.41)$$

$$\Gamma'_{25} \rightarrow A_1 + A_3 \rightarrow R_{15}, \quad (10.42)$$

$$\Gamma'_{25} \rightarrow \Sigma_1 + \Sigma_2 + \Sigma_3 \rightarrow M_1 + M_5. \quad (10.43)$$

Suppose that we want to find a set of compatible symmetries in going around a circuit using the Brillouin zone shown in Fig. 10.3.

$$\Gamma \rightarrow \Sigma \rightarrow M \rightarrow Z \rightarrow X \rightarrow \Delta \rightarrow \Gamma. \quad (10.44)$$

Table 10.7. Compatibility relations for the high symmetry points in the simple cubic lattice

| compatibility relations between Γ and Δ, Λ, Σ | | | | | | | | | |
|--|--------------|--------------|--------------------|----------------------------|----------------------------|---------------|---------------|--------------------------|----------------------------|
| (100) | Γ_1^+ | Γ_2^+ | Γ_{12}^+ | Γ_{15}^- | Γ_{25}^+ | Γ_1^- | Γ_2^- | Γ_{12}^- | Γ_{15}^+ |
| (111) | Δ_1 | Δ_2 | $\Delta_1\Delta_2$ | $\Delta_1\Delta_5$ | $\Delta_{2'}\Delta_5$ | $\Delta_{1'}$ | $\Delta_{2'}$ | $\Delta_{1'}\Delta_{2'}$ | $\Delta_{1'}\Delta_5$ |
| (110) | Λ_1 | Λ_2 | Λ_3 | $\Lambda_1\Lambda_3$ | $\Lambda_1\Lambda_3$ | Λ_2 | Λ_1 | Λ_3 | $\Lambda_2\Lambda_3$ |
| | Σ_1 | Σ_4 | $\Sigma_1\Sigma_4$ | $\Sigma_1\Sigma_3\Sigma_4$ | $\Sigma_1\Sigma_2\Sigma_3$ | Σ_2 | Σ_3 | $\Sigma_2\Sigma_3$ | $\Sigma_2\Sigma_3\Sigma_4$ |
| compatibility relations between X and Δ, Z, S | | | | | | | | | |
| | X_1 | X_2 | X_3 | X_4 | X_5 | $X_{1'}$ | $X_{2'}$ | $X_{3'}$ | $X_{4'}$ |
| | Δ_1 | Δ_2 | $\Delta_{2'}$ | $\Delta_{1'}$ | Δ_5 | $\Delta_{1'}$ | $\Delta_{2'}$ | Δ_2 | Δ_1 |
| | Z_1 | Z_1 | Z_4 | Z_4 | Z_3Z_2 | Z_2 | Z_2 | Z_3 | Z_1Z_4 |
| | S_1 | S_4 | S_1 | S_4 | S_2S_3 | S_2 | S_3 | S_2 | S_1S_4 |
| compatibility relations between M and Σ, Z, T | | | | | | | | | |
| | M_1 | M_2 | M_3 | M_4 | $M_{1'}$ | $M_{2'}$ | $M_{3'}$ | $M_{4'}$ | M_5 |
| | Σ_1 | Σ_4 | Σ_1 | Σ_4 | Σ_2 | Σ_3 | Σ_2 | Σ_3 | $\Sigma_1\Sigma_4$ |
| | Z_1 | Z_1 | Z_3 | Z_3 | Z_2 | Z_2 | Z_4 | Z_4 | Z_1Z_3 |
| | T_1 | T_2 | $T_{2'}$ | $T_{1'}$ | $T_{1'}$ | $T_{2'}$ | T_2 | T_1 | T_5 |

Then we must verify that when we arrive back at Γ we have the same symmetry type as we started with. A set of such compatible symmetries designates a whole band.

To go around one of these circuits, basis functions prove very useful and the tight binding wave functions are often used to keep track of the symmetry. We know that s -functions transform like the identity representation so that a possible circuit would be $\Gamma_1 \rightarrow \Lambda_1 \rightarrow R_1 \rightarrow S_1 \rightarrow X_1 \rightarrow \Delta_1 \rightarrow \Gamma_1$ (see Fig. 10.3). If we have p -functions, the basis functions are (x, y, z) and we can join up representations corresponding to these basis functions. Likewise for the five d -functions in cubic symmetry, we have three that transform as (xy, xz, yz) with Γ_{25}^+ symmetry and two that transform as $(x^2 + \omega y^2 + \omega^2 z^2)$ and $(x^2 + \omega^2 y^2 + \omega z^2)$ corresponding to Γ_{12}^+ symmetry, where $\omega = \exp(2\pi i/3)$.

As an example of how compatibility relations are used in the *labeling* of energy bands, we show the energy dispersion relation $E(\mathbf{k})$ in Fig. 10.5 for the high symmetry directions \mathbf{k}_{100} and \mathbf{k}_{111} for the simple cubic structure. For the band with lower energy, we have the compatibility relations $\Gamma_1 \rightarrow \Delta_1 \rightarrow X_1$ and $\Gamma_1 \rightarrow \Lambda_1 \rightarrow R_1$. For the upper band, we see a splitting of a p -band as we move away from $k = 0$, and a consistent set of compatibility relations is

$$\begin{aligned} \Gamma_{25}^+ &\rightarrow \Delta_{2'} + \Delta_5, \quad \Delta_{2'} \rightarrow X_2 \quad \text{and} \quad \Delta_5 \rightarrow X_5 \\ \Gamma_{25}^+ &\rightarrow \Lambda_1 + \Lambda_3, \quad \Lambda_1 \rightarrow R_1^+ \quad \text{and} \quad \Lambda_3 \rightarrow R_{12}^+. \end{aligned}$$

In applying the compatibility relations as we approach the R point from the Λ direction, we note that the R point has the same group of the wave vector as $\mathbf{k} = 0$ and the same subscript notation can be used to label the R point, namely R_1, R_2, R_{12}, R_{15} and R_{25} .

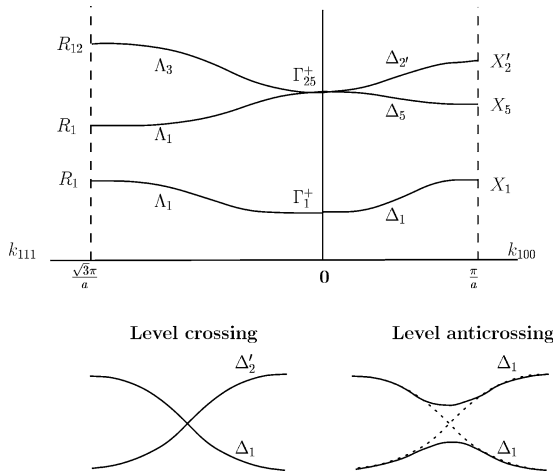


Fig. 10.5. Schematic diagram of energy bands illustrating compatibility relations. The diagrams below show both level crossings between bands of the same symmetries and level anticrossings between bands of different symmetries where interactions occur

When levels of different symmetry approach one another, they can simply cross as indicated in Fig. 10.5 for the Δ_1 and Δ'_2 levels, and this is simply referred to as a *level crossing*, where the two bands retain their original symmetry after the crossing. However, when two levels of the same symmetry approach one another, there is an interaction between them and this case is also illustrated in Fig. 10.5 for two energy levels of Δ_1 symmetry. The effect in this case is called *level anticrossing* because the levels do not actually cross in this case, though their wave functions become admixed in an appropriate linear combination.

10.8 The Diamond Structure: Nonsymmorphic Space Group

In this section we extend our discussion to nonsymmorphic space groups, where the symmetry operations can be a combination of point group and translation operations. In this case, to work with the rotational aspects of the nonsymmorphic space group, procedures to remove the translational effect are needed, and they are discussed in Sect. 10.4.

To illustrate the symmetry of a nonsymmorphic space group we use the diamond lattice (space group #227, O_h^7) which is shown in Fig. 10.6 as a specific example. Not only C, but also Si and Ge crystallize in the diamond structure, that is described by a nonsymmorphic space group with two atoms/primitive unit cell. Figure 10.6 is equivalent to Fig. 9.6(f), except that Fig. 10.6 explicitly shows the two distinct atoms per unit cell, indicated as light atoms and

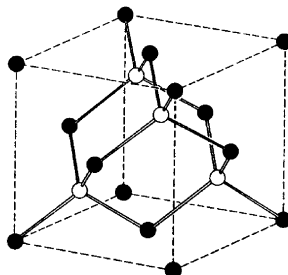


Fig. 10.6. The zinc blende structure with T_d symmetry illustrating the two dissimilar lattice sites. With identical atoms at the two sites, the diamond structure results. The space group for the diamond lattice is $Fd\bar{3}m$ or #227 (O_h^7). The space group for the zinc blende structure is #216 [$F\bar{4}3m$]

dark atoms. We will take the “primitive unit cell” for the diamond structure to be the FCC primitive unit cell formed by the four dark atoms in Fig. 10.6 surrounding one light atom (see Fig. 9.6(b) for the NaCl structure which consists of inter-penetrating FCC structures for Na and for Cl). The dark atoms in Fig. 10.6 are on sites for one FCC lattice, and the light inequivalent atoms of the same species are on another FCC lattice displaced from the first FCC lattice by $a(1/4, 1/4, 1/4)$, as shown in Fig. 10.6. A screw axis indicated in Fig. 9.6(g) takes the dark atoms on the first sublattice in Fig. 10.6 into the light atoms on the second sublattice and vice versa.

10.8.1 Factor Group and the Γ Point

The factor group G/T for diamond is isomorphic to the point group O_h . The set of operations \hat{P}_R that are relevant for the diamond structure are, therefore, the 48 operations of the O_h point group. Each of the 24 symmetry operators \hat{P}_R of group T_d will leave each distinct atom on the same sublattice. However, the operations in O_h that are not in T_d when combined with a translation $\tau_d = a/4(111)$ for the diamond structure take each atom on one sublattice into the other sublattice. This space group is nonsymmorphic because half of the symmetry operations of the group of the wave vector at $\mathbf{k} = 0$ contain translations $\tau_d = a/4(111)$. The 48 symmetry operations and ten classes for the diamond structure at $\mathbf{k} = 0$ are given in Table 10.8, showing 24 operations of the form $\{R_\alpha | \varepsilon\}$ and 24 operations of the form $\{R_\alpha | \tau_d\}$. At the Γ point $\mathbf{k} = 0$, we have $\exp[i\mathbf{k} \cdot \boldsymbol{\tau}] = 1$ so that the phase factor does not matter, and the group of the wave vector is given by the O_h group, compare Tables 10.2 and C.17.

In computing the characters χ^{equiv} for the equivalence transformation T^{equiv} , we take into account the two kinds of lattice sites, one on each of the two FCC sublattices. Thus an atom is considered “to go into itself” if it remains on its own sublattice and “not to go into itself” if it switches sublattices under a symmetry operation \hat{P}_R . Using this criterion, the results for

Table 10.8. Classes and characters for the equivalence transformation for the diamond lattice

| | $\{E 0\}$ | $8\{C_3 0\}$ | $3\{C_2 0\}$ | $6\{C'_2 \tau_d\}$ | $6\{C_4 \tau_d\}$ |
|-------------------------|----------------|--------------------|--------------------|--------------------|-------------------|
| Γ^{equiv} | 2 | 2 | 2 | 0 | 0 |
| | $\{i \tau_d\}$ | $8\{iC_3 \tau_d\}$ | $3\{iC_2 \tau_d\}$ | $6\{iC'_2 0\}$ | $6\{iC_4 0\}$ |
| Γ^{equiv} | 0 | 0 | 0 | 2 | 2 |

χ^{equiv} for the diamond structure are given in Table 10.8. Note that, although we can count eight C atoms inside the full cubic unit cell, $\chi^{\text{equiv}}(E) = 2$ for the identity operation. One must keep in mind that the primitive unit cell has only 2 atoms/cell while the full cubic unit cell is four times larger. We emphasize that χ^{equiv} must be computed on the basis of the number of atoms in the *primitive* unit cell.

Decomposition of Γ^{equiv} in Table 10.8 into irreducible representations of O_h (see Table 10.2) leads to $\Gamma^{\text{equiv}} = \Gamma_1 + \Gamma'_2$ or $\Gamma_1^+ + \Gamma_2^-$. Here Γ_1^+ is even under inversion and Γ_2^- is odd under inversion, using the usual notation for irreducible representations for solids. We also note that the operation $\{i|\tau_d\}$ interchanges sublattices $1 \leftrightarrow 2$. We make use of this result for Γ^{equiv} in subsequent chapters in discussing the electronic energy band structure and phonon dispersion relations of solids crystallizing in the diamond structure. The character table for the group of the wave vector for the Γ point for the diamond structure is given in Table C.17, utilizing the classes given in Table 10.8 and utilizing the character table for the O_h group in Table 10.2.

10.8.2 Points with $k \neq 0$

We next consider the group of the wave vector for the high symmetry points with $k \neq 0$ in the Brillouin zone for the diamond structure, and we use the FCC Brillouin zone in Fig. 10.4(a) to delineate those high symmetry points.

At the Δ point, which is an interior point in the Brillouin zone, the five classes for group C_{4v} for the Δ point for the symmorphic FCC group in Table 10.3, go into $\{E|0\}$, $\{C_4^2|0\}$, $2\{C_4|\tau_d\}$, $2\{iC_4^2|\tau_d\}$, $\{2iC'_2|0\}$ for the diamond lattice. The characters for the classes with a translation τ_d will include phase factors $T_\Delta = \exp[i\mathbf{k} \cdot \tau_d]$ for all k points along the Δ axis where $\mathbf{k} \cdot \tau_d = (2\pi/a)(\kappa, 0, 0) \cdot (a/4)(1, 1, 1) = \pi\kappa/2$, and where $\kappa \rightarrow 0$ as $k \rightarrow 0$, and $\kappa \rightarrow 1$ as k approaches the X point. Thus κ denotes the fractional length of the k vector along the Δ axis. The corresponding character table then is derived from Table 10.3 by multiplying the characters in classes $2\{C_4|\tau_d\}$ and $2\{iC_4^2|\tau_d\}$ by the phase factor T_Δ to yield Table 10.9.

For interior k points along the Σ direction, the phase factor $\exp[i\mathbf{k} \cdot \tau_d]$ enters in a similar way and here the classes and characters for the irreducible

Table 10.9. Character table C_{4v} for the group of the wave-vector at a Δ point for the nonsymmorphic diamond structure^a

| representation | $\{E 0\}$ | $\{C_4^2 0\}$ | $2\{C_4 \tau_d\}$ | $2\{iC_4^2 \tau_d\}$ | $2\{iC_2' 0\}$ |
|----------------|-----------|---------------|---------------------|----------------------|----------------|
| Δ_1 | 1 | 1 | $1 \cdot T_\Delta$ | $1 \cdot T_\Delta$ | 1 |
| Δ_2 | 1 | 1 | $-1 \cdot T_\Delta$ | $1 \cdot T_\Delta$ | -1 |
| $\Delta_{2'}$ | 1 | 1 | $-1 \cdot T_\Delta$ | $-1 \cdot T_\Delta$ | 1 |
| $\Delta_{1'}$ | 1 | 1 | $1 \cdot T_\Delta$ | $-1 \cdot T_\Delta$ | -1 |
| Δ_5 | 2 | -2 | 0 | 0 | 0 |

^a $\Delta = 2\pi/a(\kappa, 0, 0)$ (diamond). Phase factor $T_\Delta = \exp[i\frac{\pi}{2}\kappa]$

Table 10.10. Character table C_{2v} for the group of the wave-vector at a Σ point for the nonsymmorphic diamond lattice^a

| representation | $\{E 0\}$ | $\{C_2' \tau_d\}$ | $2\{iC_4^2 \tau_d\}$ | $\{iC_2' 0\}$ |
|----------------|-----------|---------------------|----------------------|---------------|
| Σ_1 | 1 | $1 \cdot T_\Sigma$ | $1 \cdot T_\Sigma$ | 1 |
| Σ_2 | 1 | $1 \cdot T_\Sigma$ | $-1 \cdot T_\Sigma$ | -1 |
| Σ_3 | 1 | $-1 \cdot T_\Sigma$ | $-1 \cdot T_\Sigma$ | 1 |
| Σ_4 | 1 | $-1 \cdot T_\Sigma$ | $1 \cdot T_\Sigma$ | -1 |

^a $\Sigma = 2\pi/a(\kappa, \kappa, 0)$ (diamond). Phase factor $T_\Sigma = \exp[i\pi\kappa]$

Table 10.11. Character table C_{3v} for the group of the wave-vector at a Λ point for the nonsymmorphic diamond structure^a

| representation | $\{E 0\}$ | $2\{C_3 0\}$ | $3\{iC_2' 0\}$ |
|----------------|-----------|--------------|----------------|
| Λ_1 | 1 | 1 | 1 |
| Λ_2 | 1 | 1 | -1 |
| Λ_3 | 2 | -1 | 0 |

^a $\Lambda = 2\pi/a(\kappa, \kappa, \kappa)$ (diamond)

representations for the group of the wave vector are given in Table 10.10, where the phase factor T_Σ is $\exp[i\pi\kappa]$. As $\kappa \rightarrow 0$ the Σ point approaches the Γ point (group O_h) and as $\kappa \rightarrow 3/4$ the K point (see Fig. 10.4(a)) is reached. The corresponding compatibility relations are found by relating Table 10.10 to Table C.17 in the limit $\kappa \rightarrow 0$ and to a modified form of Table 10.10 in the limit $\kappa \rightarrow 3/4$.

Along the Λ direction the symmetry operations do not involve the translation τ_d and therefore no phase factors appear in the character table for the group of the wave vector along the Λ axis (Table 10.11), nor do phase factors enter the character table for the end points of the Λ axis either at the Γ point (0,0,0) or at the L point $(\pi/a)(1, 1, 1)$ which has symmetry D_{3d} (see Table C.18).

Table 10.12. Character table for the group of the wave-vector at a X point for the nonsymmorphic diamond structure^a

| representation | $\{E 0\}$ | $\{C_2 0\}$ | $2\{C_2 \tau_d\}$ | $2\{iC_2 0\}$ |
|----------------|-----------|-------------|-------------------|---------------|
| X_1 | 2 | 2 | 0 | 2 |
| X_2 | 2 | 2 | 0 | -2 |
| X_3 | 2 | -2 | -2 | 0 |
| X_4 | 2 | -2 | 2 | 0 |

^a $X = (2\pi/a)(1, 0, 0)$

The point X at $\mathbf{k} = (2\pi/a)(1, 0, 0)$ is a special point. The primitive translations can be written as

$$\mathbf{a}_1 = (a/2)(1, 1, 0), \quad \mathbf{a}_2 = (a/2)(0, 1, 1), \quad \mathbf{a}_3 = (a/2)(1, 0, 1). \quad (10.45)$$

The translation group T_k is formed by elements $\{\varepsilon|\mathbf{R}_n\}$, where $\mathbf{R}_n = n_1\mathbf{a}_1 + n_2\mathbf{a}_2 + n_3\mathbf{a}_3$, and where n_1, n_2, n_3 are integers. Using the Bloch wave functions as a basis, the phase factors are represented by $e^{i\mathbf{K}_X \cdot \mathbf{R}_n} = (-1)^{(n_2+n_3)}$ considering the X point at the zone boundary along the Δ -axis.

The factor group G_X/T_X has 14 classes. However, Table 10.12 shows only four classes and four relevant irreducible representations. Six of the 14 classes corresponding to translations have only 0 entries for all the characters, and the remaining four classes can be obtained from Table 10.12 by adding a τ_d translation and multiplying the characters by -1. Because of the irrelevant representations, the compatibility relations between high symmetry points in nonsymmorphic groups are sometimes not evident. For example, $\Delta_1 + \Delta'_2$ go into X_1 and Δ_5 goes into X_4 . This is easily seen for the first $\{E|0\}$, second $\{C_2^2|0\}$ and fifth $\{2iC_2'|0\}$ classes in Table 10.9, while the two remaining classes in the Δ group, namely $\{2C_4|\tau_d\}$ and $\{2iC_4^2|\tau_d\}$, go into two classes of the X point that are not listed in Table 10.12 and have all entries for their characters equals zero.

In summary, for some of the high symmetry points of the diamond structure, the group of the wave vector is found in a similar way as for a symmorphic FCC structure, while for other high symmetry points (e.g., along the Δ and Σ axes) the group of the wave vector behaves differently. The high symmetry points where phase factors are introduced are $\Delta, \Sigma, W, S(Z)$ and those without phase factors are Γ, A, L, Q . The point X is a special point at which the structure factor vanishes and there is no Bragg reflection, nor are there phase factors, but the behavior of the X point in the diamond structure is different from that of the X point in the FCC structure which is a true Bragg reflection point. The group of the wave vector for all the high symmetry points on the square face, for example W and $S(Z)$, of the Brillouin zone for the diamond structure are also twofold degenerate. This degeneracy reflects the fact that the structure factor for the Bragg reflection for that whole face is

identically zero and hence there is no physical reason for the electronic or phonon dispersion curves to be split by that particular wave vector.

10.9 Finding Character Tables for all Groups of the Wave Vectors

Fortunately, tables for the group of the wave vector for each unique \mathbf{k} vector for each of the 230 space groups have been established and are available in various references [49, 54]. These listings contain character tables for all groups of the wave vectors for every space group. These references do not refer to specific materials – they only refer to the space group which describes specific materials.

Appendix C gives the character tables for the group of the wave vector for all the high symmetry points for the simple cubic lattice space group #221. Familiarity with the use of character tables for the group of the wave vector can be gained through the problems at the end of this chapter (Sect. 10.9).

Selected Problems

10.1. Sketch the primitive translation vectors for the unit cells in r -space and k -space for the five 2D Bravais lattices given in Table 10.1. What is the angle between \mathbf{b}_1 and \mathbf{b}_2 ?

10.2. (a) Construct the star and group of the wave vector for a simple 2D hexagonal space group (#17), as discussed in Sect. 10.3.2. Show how the group of the wave vector for $\mathbf{k} = \mathbf{b}_2/2$ is a subgroup of the group of the wavevector at $\mathbf{k} = 0$.
 (b) Now construct the star and group of the wave vector for the 2D hexagonal space group #14 and contrast your results with those in (a).

10.3. The Brillouin zone and the high symmetry points of the tetragonal structure shown in Fig. 10.7 on the right applies to the space group of the structure shown on the left. See Problem 9.1 for the real space symmetry of this 3D structure.

- (a) Find the star of the wave vector for this space group.
- (b) Find the group of the wave vector for the Γ point ($\mathbf{k} = 0$).
- (c) Now find the group of the wave vector along the Δ , Λ and Σ directions and give the compatibility relations relating the irreducible representations at $\mathbf{k} = 0$ to those along these high symmetry axes when we move away from the Γ point.

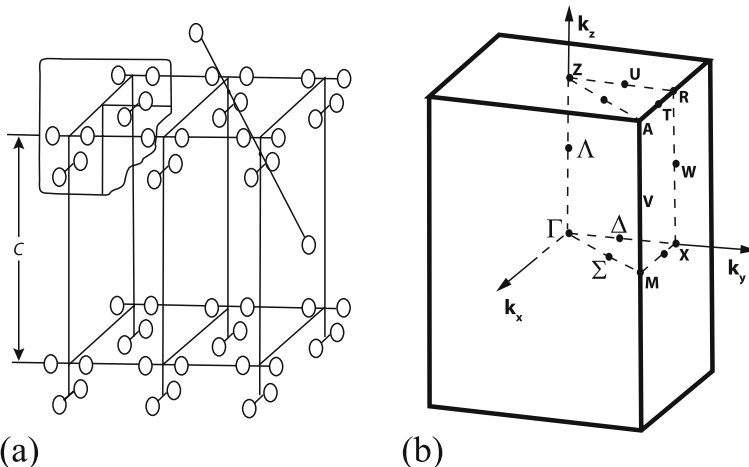


Fig. 10.7. (a) 3D crystal structure composed of a tetragonal Bravais lattice with a molecule with D_{2d} symmetry. (b) The tetragonal Brillouin zone with the high symmetry points

- 10.4.** (a) Show that for the diamond structure (Sect. 10.8) the product of two symmetry operations involving translations τ yields a symmetry element with no translations

$$\{\alpha|\tau\}\{\beta|\tau\} = \{\gamma|0\},$$

- where $\tau = (1, 1, 1)a/4$. What is the physical significance of this result?
- (b) What is the result of the product of the two symmetry elements $\{\alpha|\tau\}\{\beta|0\}$? Is this product the same as $\{\beta|0\}\{\alpha|\tau\}$? If not what is the difference?
- (c) What are the symmetry operations and the group of the wave vector for the diamond structure at the L point? at the K point? at the W point?
- (d) Find the characters χ^{equiv} for one symmetry operation in each class of the diamond structure, space group #227.

- 10.5.** (a) List the real space symmetry operations of the nonsymmorphic two-dimensional square space group $p4gm$ (#12).
- (b) Explain the symmetry diagrams and the point symmetry notations for space group #12 ($p4gm$) in Table B.12 (Appendix B) which was taken from the International Crystallography Tables.
- (c) Find the group of the wave vector for the high symmetry points in the space group $p4gm$ and compare your results with those for the symmorphic group $p4mm$ [Table B.11 (Appendix B)].
- (d) What is the difference between the 2D space group #11 ($p4mm$) and the 3D group $P4mm$? What would be the difference in the equivalence transformation Γ^{equiv} for the two cases (you can instead give the characters χ^{equiv} for this transformation)?

10.6. The electronic energy band structure of graphite near the Fermi level has become especially interesting after the discovery of single wall carbon nanotubes in 1993. (The crystal structure of 3D graphite is shown in Fig. C.1 in Appendix C and problem 9.6 relates to the space group crystal structures.)

- (a) Find Γ^{equiv} at the Γ -point for the four atoms in the unit cell of graphite (see Fig. C.1 in Appendix C). Give the Γ point irreducible representations contained in Γ^{equiv} .
- (b) Explain the symmetry operations for the group of the wave vector at $k = 0$ for group #194 that combine point group operations with translations. Compare your results to Table C.24 in Appendix C.

10.7. This problem makes use of carbon nanotubes (see Problem 9.7) to discuss space groups and line groups. Appendix E provides information of use to solve this problem (see also reference [8]).

- (a) Find the lattice vectors in reciprocal space and describe the one-dimensional Brillouin zone of carbon nanotubes. Compare your results to Appendix E.
- (b) Find the factor groups G_k/T for the group of the wave vectors at the Γ point ($k = 0$) for chiral and achiral carbon nanotubes, and the character tables for the isomorphic point groups. Then apply your result explicitly to a metallic (6,6) and a semiconducting (6,5) nanotube.
- (c) Find the line groups for chiral and achiral carbon nanotubes and their respective character tables. By factoring out the effect of translations from line groups, find the resulting point groups (called isogonal point groups), with the same order of the principal rotation axis, where rotations include a screw-axis. Also give explicit results for the (6,6) and (6,5) nanotubes.
- (d) Repeat (a), (b) and (c) for $k \neq 0$.
- (e) Discuss the different dimensionalities for the irreducible representations in space groups compared with line groups, for both $k = 0$ and $k \neq 0$.

10.8. Consider the carbon nanotubes presented in Sect. 9.4 and discussed in Appendix E.

- (a) Show that the Γ^{equiv} for zigzag SWNTs at $k = 0$ is

$$\Gamma_{\text{zigzag}}^{\text{equiv}} = A_{1g} + B_{2g} + A_{2u} + B_{1u} + \sum_{j=1}^{n-1} (E_{jg} + E_{ju}), \quad (10.46)$$

- (b) Find the compatibility relations along the one-dimensional Brillouin zone for both chiral and achiral carbon nanotubes.

Part V

Electron and Phonon Dispersion Relation

11

Applications to Lattice Vibrations

Our first application of the space groups to excitations in periodic solids is in the area of lattice modes. Group theoretical techniques are important for lattice dynamics in formulating the normal mode secular determinant in block diagonal form, and symmetry is also important in determining the selection rules for optical processes involving lattice modes such as infrared and Raman activity. Transitions to lower symmetry through either phase transitions or *strain-induced* effects may lead to mode splittings. These mode splittings can be predicted using group theoretical techniques and the changes in the infrared and Raman spectra can be predicted. Another aim of this chapter is to consolidate some of the space group concepts of Chap. 9 on r space and Chap. 10 on \mathbf{k} space with additional developments on both the fundamentals and applications of space groups.

11.1 Introduction

The atoms in a solid are in constant motion and give rise to lattice vibrations which are very similar to the molecular vibrations which we have discussed in Chap. 8. We discuss in this section and in Sect. 11.2 the similarities and differences between lattice modes and molecular vibrations.

Suppose that we have a solid with N atoms which crystallize into a simple Bravais lattice with 1 atom/unit cell. For this system there are $3N$ degrees of freedom corresponding to three degrees of freedom/atom for the molecular system or three degrees of freedom/primitive unit cell for simple crystalline solids. There are N allowed wave vector states in the Brillouin zone which implies that there are three branches for the phonon dispersion curves of a simple monatomic solid, each branch containing solutions for N \mathbf{k} -vectors. For the case of molecules, we subtract three degrees of freedom corresponding to the uniform translation of the molecule. In the crystalline solid, these uniform translational modes correspond to the acoustic modes at $\mathbf{k} = 0$, which are subject to the constraint that

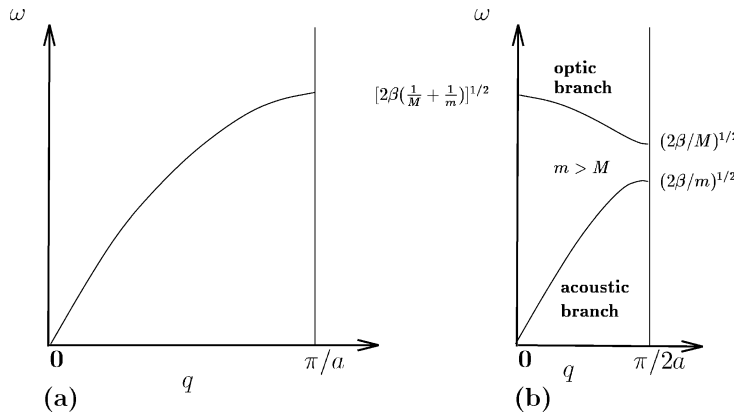


Fig. 11.1. Phonon dispersion curves for a one-dimensional line of atoms with (a) a single mass and (b) two different masses m and M

$\omega_{\text{acoustic}}^2 \equiv 0$ as $k \rightarrow 0$. The three modes corresponding to the rotations of the solid about the *center* of mass are not specifically considered here.

We have found in Chap. 10 that the translational symmetry of a crystal is conveniently handled by *labeling* the N irreducible representations of the translation group by the N \mathbf{k} vectors which are accommodated in the 1st Brillouin zone. So if we have a primitive unit cell with 1 atom/unit cell, there are three vibrational modes for each \mathbf{k} value and together these three modes constitute the acoustic branches. In particular, there are three acoustic vibrational modes for the $\mathbf{k} = 0$ wave vector, which exhibits the full point group symmetry of the crystal; these three acoustic modes correspond to the pure *translational modes* which have zero frequency and zero restoring force.

We review here the phonon dispersion relations in a one-dimensional crystal with 1 atom/unit cell (see Fig. 11.1(a)) and with 2 atoms/unit cell (see Fig. 11.1(b)) having masses m and M where $m < M$, and a is the distance between adjacent atoms. For the acoustic branch at $\mathbf{k} = 0$, all atoms vibrate in phase with identical displacements u along the direction of the atomic chain, thus corresponding to a pure translation of the chain. The wave vector \mathbf{k} distinguishes each normal mode of the system by introducing a phase factor $e^{i\mathbf{k}a}$ between the displacements on adjacent sites. For the case of one atom/unit cell, the lattice mode at the zone boundary corresponds to atoms moving 90° out of phase with respect to their neighbors. For the case of 2 atoms/unit cell, the size of the unit cell is twice as large, so that the size of the corresponding Brillouin zone (B.Z.) is reduced by a factor of 2. The dispersion relations and lattice modes in this case relate to those for one atom/unit cell by a zone folding of the dispersion relation shown in Fig. 11.1(a), thus leading to Fig. 11.1(b). Thus the optical mode at $\mathbf{k} = 0$ has *neighboring* atoms moving out of phase with respect to each other. The normal mode at the new B.Z.

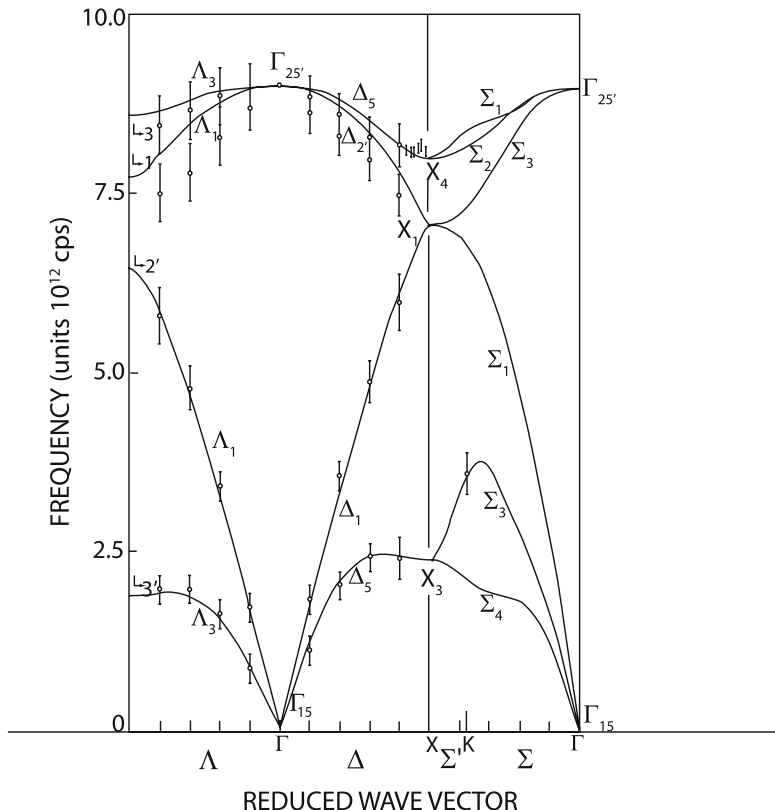


Fig. 11.2. Phonon dispersion curves for Ge along certain high symmetry axes in the Brillouin zone. The data at the Γ point are from Raman scattering measurements and the data elsewhere in the zone are from neutron scattering experiments [28]

boundary $k = \pi/2a$ thus corresponds to a mode where one atom is at rest, while its neighbor is in motion.

In three-dimensions, the phonon dispersion relations for Ge with the diamond structure (with 2 atoms/unit cell) are plotted along high symmetry directions in Fig. 11.2 and the dispersion relations are *labeled* by the appropriate irreducible representations by giving the symmetry of the corresponding normal mode (see Chap. 10 for the notation used in Fig. 11.2). The phonon dispersion relations for *germanium* are determined from inelastic neutron scattering measurements and are plotted as points in Fig. 11.2. At a general point k in the B.Z. for the diamond structure, there are three acoustic branches and three optical branches. However, at certain high symmetry points and along certain high symmetry directions, mode degeneracies occur as, for example, along ΓL and ΓX . Group theory allows us to identify the high symmetry points in the B.Z. where degeneracies occur, which branches stick together,

which branches show simple mode crossings, and which modes show anticrossings, [12–14, 28, 30] (see Fig. 10.5), to be discussed further in this chapter.

The symmetry aspects of the lattice mode problem at $\mathbf{k} = 0$ for simple structures with 1 atom/unit cell are simply the uniform translation of the solid. However, group theory is needed to deal with lattice modes away from $\mathbf{k} = 0$. Furthermore, the lattice modes that are of interest in the current literature often involve complicated crystal structures with many atoms/unit cell or systems with reduced dimensionality; for such problems, group theory is a powerful tool for lattice mode classification and for the determination of selection rules for infrared and Raman spectroscopy and for phonon-assisted optical transitions more generally.

The *general outline* for procedures that utilize group theory to solve for the lattice modes in solids is as follows:

1. Find the symmetry operations for the group of the wave vector $\mathbf{k} = 0$, the appropriate character table and irreducible representations.
2. Find the irreducible representations using $\Gamma_{\text{lat. mod.}} = \Gamma^{\text{equiv.}} \otimes \Gamma_{\text{vector.}}$ The meaning of this relation is discussed below (item (c) in Sect. 11.2). We will use $\Gamma_{\text{lat. mod.}}$ to denote $\Gamma_{\text{lattice modes.}}$
3. Find the irreducible representations of $\Gamma_{\text{lat. mod.}}$. The characters for the lattice mode representation express the symmetry types and degeneracies of the lattice modes.
4. Find the normal mode patterns.
5. Which modes are IR-active? Which modes are Raman-active? Are there any polarization effects?
6. Repeat items 1–4 for other points in the Brillouin zone and find the lattice for $\mathbf{k} \neq 0$.
7. Using the compatibility relations, connect up the lattice modes at neighboring \mathbf{k} points to form a phonon branch.

11.2 Lattice Modes and Molecular Vibrations

There are several aspects of the lattice mode problem in the crystalline phase that differ from simple molecular vibrations (see Sect. 8.2):

- (a) *The eigenvectors and normal modes.* In the lattice mode problem, we consider normal modes for the atoms in a unit cell rather than for a molecule, and in either case the lattice mode is one form of a basis vector or eigenvector (see Chap. 4). Since the symmetry is different for the various types of \mathbf{k} -vectors in the Brillouin zone, we must solve the lattice mode problem for each distinct type of \mathbf{k} -vector. On the other hand, for many experimental studies of the lattice modes, we use light as our probe. Usually the main interest is in lattice modes at or near $\mathbf{k} = 0$ (the Γ point) because the wavelength of light is long ($\lambda \approx 500$ nm) compared to lattice constants a , and the magnitude of the corresponding \mathbf{k} wavevector ($k = 2\pi/\lambda$) is very

small compared with Brillouin zone dimensions ($2\pi/a$, $a \sim 0.1\text{--}1.0\text{ nm}$). Most of our simple examples, therefore emphasize the lattice modes for $\mathbf{k} = 0$.

- (b) *Equivalence.* To find the equivalence transformation $\Gamma^{\text{equiv.}}$ for molecules, we consider the action of a symmetry operator \hat{P}_R on an atomic site and examine the transformation matrix to see whether or not the site is transformed into itself under the point symmetry operation \hat{P}_{R_α} . In the case of a crystal, however, we consider all points separated by a lattice vector \mathbf{R}_n as identical when considering Γ point ($k = 0$) phonons. Thus $\mathbf{r} \rightarrow \mathbf{r} + \mathbf{R}_n$ is an *identity transformation* for all \mathbf{R}_n , and therefore we denote the equivalence transformation in crystalline solids by $\Gamma^{\text{equiv.}}$ and the corresponding characters of this representation by $\chi^{\text{equiv.}}$. Compound operations in nonsymmorphic groups always give $\chi^{\text{equiv.}} = 0$ since the translation τ_α is not a lattice vector. When considering lattice modes away from the Γ point, we must consider the group of the wavevector G_k and phase factors related to translations. Modes away from $k = 0$ are discussed in Sect. 11.4.
- (c) *Degrees of freedom and phonon branches.* For the case of molecular vibrations, we have

$$\Gamma_{\text{mol. vib.}} = \Gamma^{\text{equiv.}} \otimes \Gamma_{\text{vec}} - \Gamma_{\text{trans}} - \Gamma_{\text{rot}}, \quad (11.1)$$

whereas for lattice modes (lat. mod.), we simply write

$$\Gamma_{\text{lat. mod.}} = \Gamma^{\text{equiv.}} \otimes \Gamma_{\text{vec}}. \quad (11.2)$$

That is, we do not subtract $\Gamma_{\text{trans.}}$ and $\Gamma_{\text{rot.}}$ in (11.2) for the lattice modes for the following reasons. Each atom/unit cell has three degrees of freedom, yielding a normal mode for each wave vector \mathbf{k} in the Brillouin zone. The collection of normal modes for a given degree of freedom for all \mathbf{k} vectors forms a *phonon branch*. Thus for a structure with one atom/unit cell there are three phonon branches, the acoustic branches. If there is more than 1 atom/unit cell, then

$$\text{no. of branches} = (\text{no. of atoms/unit cell}) \times 3 \quad (11.3)$$

of which three are acoustic branches and the remainder are optical branches. The translational degrees of freedom correspond to the trivial $\mathbf{k} = 0$ solution for the three acoustic branches which occur at $\omega = 0$ and are smoothly connected with nontrivial solutions as we move away from the Γ point. Since the atoms in the solid are fixed in space, there are no rotational degrees of freedom to be subtracted.

We will now illustrate the application of group theory to the solution of the lattice mode problem for several illustrative structures. First we consider simple symmorphic structures in Sect. 11.3. Then we consider some simple nonsymmorphic structures (see Sect. 11.3.3). Our initial examples will be for the $\mathbf{k} = 0$ modes. This will be followed by a discussion of modes elsewhere in the Brillouin zone.

11.3 Zone Center Phonon Modes

In this section we consider the symmetries of zone center phonon modes for some illustrative cases. The examples selected in this section are chosen to demonstrate some important aspect of the lattice mode problem and to gain some experience in using simple space groups.

11.3.1 The NaCl Structure

The NaCl structure is shown in Fig. 9.6(b). This very simple example is selected to illustrate how the symmetries of the lattice modes are found. We take our “basic unit cell” to be the primitive rhombohedral unit cell of either one of the inter-penetrating FCC structures (space group #225 ($Fm\bar{3}m$) O_h^5), so that each primitive unit cell will contain an Na atom and a Cl atom. The larger cubic unit cell (Fig. 9.6(b)) contains four primitive unit cells with four Na and four Cl atoms (ions). The space group O_h^5 for the NaCl structure is a symmorphic structure, and the group of the wave vector at $\mathbf{k} = 0$ for the NaCl structure is O_h . Since the details of the translations do not enter into the considerations of phonons at $\mathbf{k} = 0$ for symmorphic space groups, we need to consider only point group operations for O_h as given in Table 10.2. Under all symmetry operations of O_h each Na and Cl atom site is transformed either into itself or into an equivalent atom site separated by a lattice vector \mathbf{R}_m . Thus,

$$\Gamma^{\text{equiv.}} = 2\Gamma_1. \quad (11.4)$$

For O_h symmetry, $\Gamma_{\text{vec.}} = \Gamma_{15}$, so that at $\mathbf{k} = 0$

$$\Gamma_{\text{lat. mod.}} = 2\Gamma_1 \otimes \Gamma_{15} = 2\Gamma_{15}, \quad (11.5)$$

where the basis functions for Γ_{15} are (x, y, z) . Thus both the acoustic branch and the optic branch at $\mathbf{k} = 0$ have Γ_{15} (or Γ_{15}^-) symmetry. The normal modes for the acoustic branches of the NaCl structure have both the Na and Cl atoms moving in phase in the x , y , and z directions, while for normal

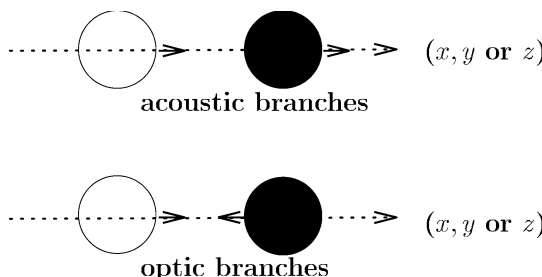


Fig. 11.3. In-phase (acoustic) and out-of-phase (optic) normal modes at $\mathbf{k} = 0$ for NaCl

modes in the optic branches, the two atoms move out of phase in the x , y , and z directions (see Fig. 11.3). Since the electromagnetic interaction transforms as the vector (Γ_{15}), the optic branch is infrared-active. The acoustic branch is not optically excited because $\omega = 0$ at $\mathbf{k} = 0$. Since the optic branch for the NaCl structure has odd parity, it is not Raman-active. As we move away from the Γ point ($\mathbf{k} = 0$), the appropriate symmetries can be found by compatibility relations. For example along the (100) directions $\Gamma_{15} \rightarrow \Delta_1 + \Delta_5$ in which Δ_1 is the symmetry of the longitudinal mode and Δ_5 is that for the doubly degenerate transverse modes. We will now give several other examples of zone center modes in other structures and then return in Sect. 11.4 to the discussion of nonzone-center modes for simple structures.

11.3.2 The Perovskite Structure

Let us now consider lattice modes in BaTiO_3 (see Fig. 9.7(c)), an example of a cubic crystal structure with slightly more complexity, but still corresponding to a symmorphic space group. The focus of this section is to illustrate the identification of the normal modes. For the perovskite structure shown in Fig. 9.7(c), there are 5 atoms/unit cell and therefore there are 15 degrees of freedom, giving rise to three acoustic branches and twelve optical branches. The point group of symmetry at $\mathbf{k} = 0$ is O_h . Consider the unit cell shown in Fig. 11.4. The Ba^{2+} ions at the cube corners are shared by eight neighboring unit cells, so that one Ba^{2+} ion is considered to be associated with the unit cell shown. Likewise the O^{2-} ions in the face centers are shared by two unit cells, so that 3O^{2-} ions are treated in the unit cell shown. The Ti^{4+} ion at the cube center is of course fully contained in the unit cell shown in Fig. 11.4.

Using the diagram in Fig. 11.4, we thus obtain Character Table 11.1 for Γ^{equiv} . From the character table for O_h (see Table A.31) we see that

$$\Gamma^{\text{equiv.}} = 3\Gamma_1^+ + \Gamma_{12}^+. \quad (11.6)$$

We note that the Ba^{2+} and Ti^{4+} ions each transform as Γ_1^+ with the three oxygens transforming as $\Gamma_1 + \Gamma_{12}$. In O_h symmetry

$$\Gamma_{\text{vec.}} = \Gamma_{15}^-, \quad (11.7)$$

so that

$$\Gamma_{\text{lat.mod.}} = (3\Gamma_1^+ + \Gamma_{12}^+) \otimes \Gamma_{15}^- = 3\Gamma_{15}^- + (\Gamma_{12}^+ \otimes \Gamma_{15}^-) \quad (11.8)$$

$$= 4\Gamma_{15}^- + \Gamma_{25}^- = 4\Gamma_{15}^- + \Gamma_{25}^-. \quad (11.9)$$

Table 11.1. Characters for Γ_{equiv} for perovskite. The atoms that remain unchanged under each symmetry operation are indicated

| | E | $8C_3$ | $3C_4^2$ | $6C'_2$ | $6C_4$ | i | $8iC_3$ | $3iC_4^2$ | $6iC'_2$ | $6iC_4$ |
|--------------------------|-----|--------|----------|---------|--------|-----|---------|-----------|----------|---------|
| $\Gamma^{\text{equiv.}}$ | 5 | 2 | 5 | 3 | 3 | 5 | 2 | 5 | 3 | 3 |
| | all | Ba,Ti | all | Ba,Ti | Ba,Ti | all | Ba,Ti | all | Ba,Ti | Ba,Ti |
| | | | one O | one O | | | | | one O | one O |

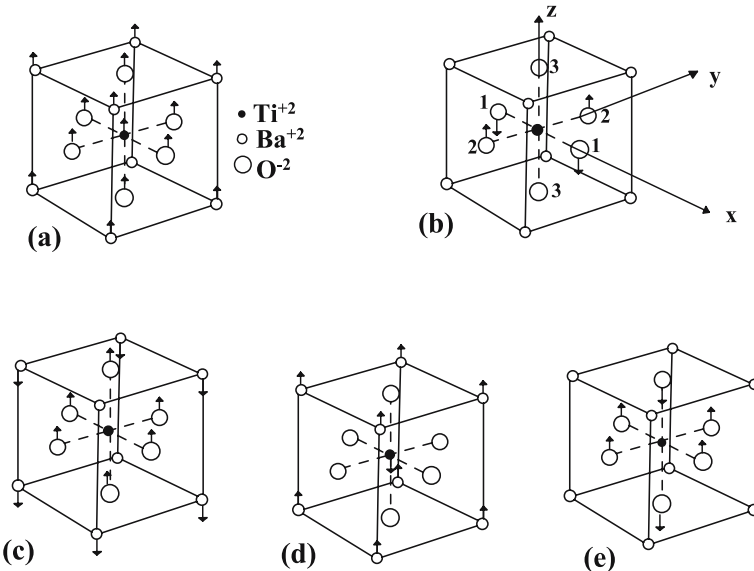


Fig. 11.4. Schematic diagram of the z -component lattice modes at $\mathbf{k} = 0$ for the BaTiO_3 perovskite structure. (a) Γ_{15} acoustic mode; (b) Γ_{25} mode where only two of the three distinct oxygens move; (c) Γ_{15} mode with the Ti^{4+} and Ba^{2+} vibrating against the oxygens. (d) Γ_{15} mode with the Ti^{4+} vibrating against the Ba^{2+} and longitudinal oxygens. (e) Γ_{15} breathing mode of the transverse oxygens vibrating against the longitudinal oxygens, while the Ti^{4+} and Ba^{2+} are at rest

where we note that both Γ_{15}^- and Γ_{25}^- have odd parity. Thus at $\mathbf{k} = 0$ there are five distinct normal mode frequencies, including the acoustic branch with Γ_{15} symmetry and $\omega = 0$. Since the atom sites for the Ba^{2+} and Ti^{4+} ions transform as Γ_1^+ , we know that the Γ_{25} mode requires motion of the oxygens. In the following we illustrate how the normal mode patterns shown in Fig. 11.4 are obtained. Note the numbers assigned to the oxygens in Fig. 11.4(b).

The search for the eigenvectors at the Γ point is similar to the procedure used for finding the normal modes of molecular vibration (see Sect. 8.3). Since $\mathbf{k} = 0$, the phase factors for the translational symmetries are all $e^{i\mathbf{k}\cdot\boldsymbol{\tau}} = 1$. One just needs to consider the unit cell as the “molecule”, find the normal

modes, and the eigenvectors will be a repetition of the normal modes in all the unit cells in the lattice.

From the character table for O_h we note that the characters for C_4^z are different for the Γ_{15} and Γ_{25} modes, and for this reason C_4^z is a useful symmetry operation for finding the normal mode displacements. First we consider the effect of C_4^z on each of the three inequivalent oxygen sites and on each of the three components of the vector; this consideration is independent of the symmetry of the vibrational mode:

$$C_4^z \begin{pmatrix} 1 \\ 2 \\ 3 \end{pmatrix} = \begin{pmatrix} 2 \\ 1 \\ 3 \end{pmatrix}, \quad C_4^z \begin{pmatrix} x \\ y \\ z \end{pmatrix} = \begin{pmatrix} -y \\ -x \\ z \end{pmatrix}. \quad (11.10)$$

Finding the normal mode for the acoustic translational branch is trivial (see Fig. 11.4a). The operations of (11.10) are now applied to find the normal modes in Fig. 11.4b and e. For the Γ_{25} displacements, Fig. 11.4b shows the motions for the z component of the mode. The partners are found by cyclic operations on (x, y, z) and atom sites (1, 2, 3), as given in (11.11). Then operation by C_4^z yields

$$C_4^z \begin{pmatrix} -x_2 + x_3 \\ y_1 - y_3 \\ -z_1 + z_2 \end{pmatrix} = \begin{pmatrix} -y_1 + y_3 \\ -x_2 + x_3 \\ -z_2 + z_1 \end{pmatrix} = \begin{pmatrix} 0 & -1 & 0 \\ 1 & 0 & 0 \\ 0 & 0 & -1 \end{pmatrix} \begin{pmatrix} -x_2 + x_3 \\ y_1 - y_3 \\ -z_1 + z_2 \end{pmatrix} \quad (11.11)$$

giving a character of -1 for C_4^z in the Γ_{25} representation. Performing representative operations on this normal mode will show that it provides a proper basis function for the Γ_{25} irreducible representation in the point group O_h .

Now consider the Γ_{15} normal mode given in Fig. 11.4e. The displacements shown in the diagram are for the z component of the mode. To achieve no motion of the center of mass, the actual displacements must be $-z_1 - z_2 + 2z_3$ for the three oxygens at positions 1, 2 and 3. Using cyclic permutations we obtain the three components of the mode given in (11.12). Then action of C_4^z yields

$$\begin{aligned} C_4^z \begin{pmatrix} 2x_1 - x_2 - x_3 \\ -y_1 + 2y_2 - y_3 \\ -z_1 - z_2 + 2z_3 \end{pmatrix} &= \begin{pmatrix} 2y_2 - y_1 - y_3 \\ x_2 - 2x_1 + x_3 \\ -z_2 - z_1 + 2z_3 \end{pmatrix} \\ &= \begin{pmatrix} 0 & 1 & 0 \\ -1 & 0 & 0 \\ 0 & 0 & 1 \end{pmatrix} \begin{pmatrix} 2x_1 - x_2 - x_3 \\ -y_1 + 2y_2 - y_3 \\ -z_1 - z_2 + 2z_3 \end{pmatrix}, \end{aligned} \quad (11.12)$$

so that the character for this Γ_{15} mode is $+1$, in agreement with the character for the C_4^z operation in the $\Gamma_{15,z}$ irreducible representation (see the character table for O_h). Operation with typical elements in each class shows this mode provides a proper basis function for Γ_{15} .

Clearly all the modes shown in Fig. 11.4 have partners x, y and z , so that collectively they are all the normal modes for BaTiO_3 . Since all modes for

BaTiO_3 at $\mathbf{k} = 0$ have odd parity, none are Raman-active, noting that for the O_h point group, Raman-active modes have A_g , E_g and T_{2g} (or Γ_1 , Γ_{12} and $\Gamma_{25'}$) symmetries. However, the $3\Gamma_{15}$ or $3\Gamma_{15}^-$ modes are *infrared-active*, and can be excited when the \mathbf{E} vector for the light is polarized in the direction of the oscillating dipole moment, as indicated in Fig. 11.4.

11.3.3 Phonons in the Nonsymmorphic Diamond Structure

We now illustrate the mode symmetries at the Γ point for a nonsymmorphic space group with 2 atoms/unit cell (specifically we illustrate the lattice modes of Ge or Si, which both crystallize in the diamond structure). Most of the symmetry properties, including the calculation of $\chi^{\text{equiv.}}$ and the decomposition of $\Gamma^{\text{equiv.}}$ into irreducible representations of O_h ($\Gamma^{\text{equiv.}} = \Gamma_1 + \Gamma_{2'}$), were discussed in Sect. 10.8. We now make use of this result for $\Gamma^{\text{equiv.}}$ in discussing the Γ point phonons.

To get the characters for the lattice vibrations, we then take $\Gamma_{\text{vec.}} = \Gamma_{15}$ which is odd under the inversion operation:

$$\Gamma_{\text{lat. mod.}} = \Gamma^{\text{equiv.}} \otimes \Gamma_{\text{vec.}} = (\Gamma_1 + \Gamma_{2'}) \otimes \Gamma_{15} = \Gamma_{15} + \Gamma_{25'}, \quad (11.13)$$

where $\Gamma_{25'}$ and $\Gamma_{2'}$ are respectively, even and odd under the inversion operation.

For each \mathbf{k} value, there are six vibrational degrees of freedom with 2 atoms/unit cell. These break up into two triply degenerate modes at $\mathbf{k} = 0$, one of which is even, the other odd under inversion. The odd mode Γ_{15} is the acoustic mode, which at $\mathbf{k} = 0$ is the pure translational mode. The other mode is a $\Gamma_{25'}$ mode, which is symmetric under inversion and represents a breathing or optic mode. The optic mode is Raman-active but not infrared-active. Furthermore, the Raman-active mode is observed only with *off-diagonal polarization* $\mathbf{E}_i \perp \mathbf{E}_s$ for the incident and scattered light.

Let us now illustrate a screw axis operation in the diamond structure (see Fig. 9.6(g)) and see how this operation is used in finding the normal modes in a nonsymmorphic crystal. Denoting the dark atoms in Fig. 10.6 by 1 and the light atoms by 2, consider the effect of $\{C_4^z|\boldsymbol{\tau}\}$ on atom sites $\begin{pmatrix} 1 \\ 2 \end{pmatrix}$ and on the

vector $\begin{pmatrix} x \\ y \\ z \end{pmatrix}$

$$\{C_4^z|\boldsymbol{\tau}\} \begin{pmatrix} 1 \\ 2 \end{pmatrix} = \begin{pmatrix} 2 \\ 1 \end{pmatrix}, \quad \{C_4^z|\boldsymbol{\tau}\} \begin{pmatrix} x \\ y \\ z \end{pmatrix} = \begin{pmatrix} y \\ -x \\ z \end{pmatrix}. \quad (11.14)$$

Using these results we can then obtain the characters for the displacements $(\mathbf{R}_1 + \mathbf{R}_2)$ which has Γ_{15} symmetry and is identified with the basic vibration of an FCC sublattice:

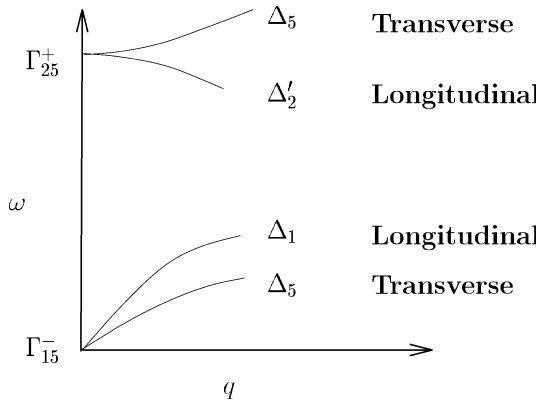


Fig. 11.5. Lattice modes along the Δ -axis for the diamond structure, showing the compatibility relations as we move away from the center of the cubic Brillouin zone

$$\{C_4^z|\tau\} \begin{pmatrix} x_1 + x_2 \\ y_1 + y_2 \\ z_1 + z_2 \end{pmatrix} = \begin{pmatrix} y_2 + y_1 \\ -x_2 - x_1 \\ z_2 + z_1 \end{pmatrix} = \begin{pmatrix} 0 & 1 & 0 \\ -1 & 0 & 0 \\ 0 & 0 & 1 \end{pmatrix} \begin{pmatrix} x_1 + x_2 \\ y_1 + y_2 \\ z_1 + z_2 \end{pmatrix} \quad (11.15)$$

yielding a character of +1 for $\{C_4^z|\tau\}$, in agreement with the character for $\{C_4^z|\tau\}$ in the Γ_{15} irreducible representation for the acoustic mode translational branches of point group O_h . If all the symmetry operations are then carried out, it is verified that $\mathbf{R}_1 + \mathbf{R}_2$ provides basis functions for the Γ_{15} irreducible representation of O_h .

When the two FCC sublattices vibrate out of phase, their parity is reversed and a mode with even parity (the $\Gamma_{25'}$ mode) is obtained

$$\{C_4^z|\tau\} \begin{pmatrix} x_1 - x_2 \\ y_1 - y_2 \\ z_1 - z_2 \end{pmatrix} = \begin{pmatrix} y_2 - y_1 \\ -x_2 + x_1 \\ z_2 - z_1 \end{pmatrix} = \begin{pmatrix} 0 & -1 & 0 \\ 1 & 0 & 0 \\ 0 & 0 & -1 \end{pmatrix} \begin{pmatrix} x_1 - x_2 \\ y_1 - y_2 \\ z_1 - z_2 \end{pmatrix} \quad (11.16)$$

yielding a character of -1. This checks with the character for $\{C_4^z|\tau\}$ in the irreducible representation $\Gamma_{25'}$ for the point group O_h .

As we move away from $\mathbf{k} = 0$ along the Δ axis or the Λ axis, the triply degenerate modes break up into longitudinal and transverse branches. The symmetries for these branches can be found from the compatibility relations (see Sect. 10.7). For example, as we move away from $\mathbf{k} = 0$ along the Δ axis toward the X point (see Fig. 11.5), we have the compatibility relations

$$\begin{aligned} \Gamma_{15} &\rightarrow \Delta_1 + \Delta_5 \\ \Gamma_{25'} &\rightarrow \Delta_{2'} + \Delta_5. \end{aligned} \quad (11.17)$$

Group theory gives no information on the relative frequencies of the Γ_{15} and $\Gamma_{25'}$ modes.

We finally note that in general the Raman tensor has modes which transform as a second rank symmetric tensor (see Table 10.2). The Raman-active modes would include modes for the O_h group of the wave vector with symmetries $\Gamma_1 + \Gamma_{12} + \Gamma_{25'}$. Since the optic mode for the diamond structure at $k = 0$ has $\Gamma_{25'}$ symmetry, this mode is Raman-active. Table 10.2 also tells us that the $\Gamma_{25'}$ symmetry mode has basis functions of the form xy, yz, zx , indicating that the Raman tensor for the diamond structure is of the functional form $E_x^i E_y^s; \alpha_{xy}(\Gamma_{25'})$ plus cyclic permutations of x, y, z . Thus, observation of this Raman-active mode requires the use of cross-polarized light or (\parallel, \perp) settings of the incident and scattered polarizations, respectively.

11.3.4 Phonons in the Zinc Blende Structure

Closely related to the diamond structure is the zinc blende structure (space group $F\bar{4}3m$ #216, T_d^3) where the two FCC sublattices in Fig. 10.6 are chemically distinct. This space group is symmorphic. This is the crystal structure for III-V semiconductor compounds, such as GaAs. For this case, the Ga atoms (ions) would be on one FCC sublattice and the As ions on the other FCC sublattice. If it happens that a Ga atom is on the wrong lattice, this is called an antisite location, and is considered a defect in the lattice.

Since the sublattices are chemically distinct, the group of the \mathbf{k} -vector at $\mathbf{k} = 0$ for the zinc blende structure has only the 24 operations of the point group T_d . It is a symmorphic structure and the factor group G_k/T_k is therefore isomorphic to its point group T_d (Sect. 9.1.4). In calculating $\Gamma_{\text{lat.mod.}}$, we note that the vector in group T_d transforms as the irreducible representation Γ_{15} . Thus from the irreducible representations contained in $\Gamma^{\text{equiv.}}$, we obtain

$$\Gamma^{\text{equiv.}} = 2A_1 = 2\Gamma_1,$$

so that when we take the direct product of $\Gamma^{\text{equiv.}}$ with $\Gamma_{\text{vec.}}$ we obtain

$$\Gamma_{\text{lat.mod.}} = 2A_1 \otimes T_2 = 2T_2 = 2\Gamma_{15}. \quad (11.18)$$

For the zinc blende structure, the optic mode is both infrared-active and Raman-active since the irreducible representation Γ_{15} for point group T_d corresponds to both Γ_{15} and $\Gamma_{25'}$ of the point group O_h . This correspondence is apparent from comparing the character tables for T_d and O_h (see Table 10.2).

The well known LO-TO splitting of the optic phonon in ionic crystals is associated with an anticrossing of the optic phonon level and the photon propagation dispersion relation which occurs very close to the B.Z. center (see discussion in Sect. 10.7). Appropriate linear combinations of wave functions

will lead to two distinct levels that do not cross, each represented by the movement of one sublattice. Since GaAs is a polar crystal, in this case, the LO and TO modes will be split. The more polar the crystal, the larger the LO–TO splitting.

11.4 Lattice Modes Away from $\mathbf{k} = 0$

Modes at $\mathbf{k} \neq 0$ can be observed by optical spectroscopy when superlattice effects are present, giving rise to zone folding, or when defects are present, breaking down translational symmetry. Nonzone center modes can also be observed in second-order Raman spectra (comprising phonons with wave vectors $+\mathbf{k}$ and $-\mathbf{k}$). Lattice modes at $\mathbf{k} \neq 0$ are routinely observed by neutron, X-ray and electron inelastic scattering techniques.

To construct phonon branches for the entire range of \mathbf{k} vectors within the first Brillouin zone, we must consider the general procedure for finding the lattice modes at other high symmetry points in the B.Z., and we make use of compatibility relations to relate these solutions to related solutions at neighboring \mathbf{k} -points.

The procedure for finding lattice modes at $\mathbf{k} \neq 0$ is outlined below:

- Find the appropriate group of the wave vector at point \mathbf{k} .
- Find $\Gamma^{\text{equiv.}}$ and $\Gamma_{\text{vec.}}$ for this group of the wave vector. When considering lattice modes away from the Γ point, care must be taken with special \mathbf{k} points at the Brillouin zone boundary where $R_{\alpha}^{-1}\mathbf{k} = \mathbf{k} + \mathbf{K}_m$ (\mathbf{K}_m is a reciprocal lattice vector). One should not simply use $\chi^{\text{equiv.}} = 1$ or 0, as for the case of molecules, because the lattice vector translation for $\mathbf{k} \neq 0$ will add a phase factor (see Sect. 10.5). In this case we use for the characters for the equivalence transformation

$$\chi^{\text{equiv.}} = \sum_j \delta_{R_{\alpha}\mathbf{r}_j, \mathbf{r}_j} e^{i\mathbf{K}_m \cdot \mathbf{r}_j}, \quad (11.19)$$

where \mathbf{r}_j is the position of the j th atom with respect to the origin of the point group, and $\delta_{R_{\alpha}\mathbf{r}_j, \mathbf{r}_j} = 1$ if $R_{\alpha}\mathbf{r}_j$ and \mathbf{r}_j refer to equivalent atomic positions ($R_{\alpha}\mathbf{r}_j = \mathbf{r}_j + \mathbf{R}_n$).

- Within a unit cell

$$\Gamma_{\text{lat.mod.}} = \Gamma^{\text{equiv.}} \otimes \Gamma_{\text{vec.}} \quad (11.20)$$

find the symmetry types and mode degeneracies of $\Gamma_{\text{lat.mod.}}$.

- Introduce a phase factor relating unit cells with translation by $\boldsymbol{\tau}$:

$$P_{\{\varepsilon|\boldsymbol{\tau}\}} \Psi_k(\mathbf{r}) = e^{i\mathbf{k} \cdot \boldsymbol{\tau}} \Psi_k(\mathbf{r}) \quad \text{Bloch theorem.} \quad (11.21)$$

- Find lattice modes (including phase factor).

We illustrate these issues in terms of the NaCl structure which was previously considered with regard to its normal modes at $\mathbf{k} = 0$ (see Sect. 11.3.1).

11.4.1 Phonons in NaCl at the X Point $k = (\pi/a)(100)$

The group of the wave vector at the point X is given in the Table C.15 in Appendix C. We first identify the symmetry operations of point group D_{4h} and we then obtain $\Gamma^{\text{equiv.}}$ for these symmetry operations.

We first review the situation for the Γ point (O_h), see Table 11.2. Thus, we have $\Gamma^{\text{equiv.}}$ for the Na and Cl ions, and for $\Gamma_{\text{vec.}}$ at $k = 0$

$$\begin{aligned}\Gamma_{\text{Na}}^{\text{equiv.}} &= \Gamma_1 \\ \Gamma_{\text{Cl}}^{\text{equiv.}} &= \Gamma_1 \\ \Gamma_{\text{vec.}} &= \Gamma_{15} \end{aligned}$$

so that for $k = 0$ we have

$$\Gamma_{\text{lat.mod.}} = 2\Gamma_1 \otimes \Gamma_{15} = 2\Gamma_{15}.$$

Similarly for the X point, we first find $\Gamma^{\text{equiv.}}$ for each type of atom (see Table 11.3). Thus, we obtain $\Gamma^{\text{equiv.}}$, $\Gamma_{\text{vec.}}$, and $\Gamma_{\text{lat.mod.}}$ at the X point:

$$\begin{aligned}\Gamma_{\text{Na}}^{\text{equiv.}} &= X_1 \\ \Gamma_{\text{Cl}}^{\text{equiv.}} &= X_1 \\ \Gamma_{\text{vec.}} &= X'_4 + X'_5\end{aligned}$$

where X'_4 corresponds to x , and X'_5 corresponds to (y, z) . We thus obtain

$$\Gamma_{\text{lat.mod.}} = 2X_1 \otimes (X'_4 + X'_5) = 2X'_4 + 2X'_5$$

Compatibility relations give $\Gamma_{15} \rightarrow \Delta_1 + \Delta_5 \rightarrow X'_4 + X'_5$ for the phonon branch connecting Γ to X .

The action of the translation operator on a basis function (normal mode) yields

$$\hat{P}_{\{\varepsilon|\tau\}} u(\mathbf{r}) = e^{i\mathbf{k}\cdot\boldsymbol{\tau}} u(\mathbf{r}), \quad (11.22)$$

Table 11.2. Characters for $\Gamma^{\text{equiv.}}$ for NaCl at the Γ point

Table 11.3. Characters for $\Gamma^{\text{equiv.}}$ for NaCl at the X point

where $\mathbf{k} = (\pi/a)\hat{x}$ at the X point under consideration. For $\mathbf{R}_n = a\hat{x}$ we obtain $e^{i\mathbf{k}\cdot\mathbf{r}} = e^{i\pi} = -1$ so that there is a π phase difference between unit cells along \hat{x} . However, for $\mathbf{R}_n = a\hat{y}$ or $a\hat{z}$, we have $e^{i\mathbf{k}\cdot\mathbf{r}} = e^{i(0)} = 1$, and there is effectively no phase factor along \hat{y} and \hat{z} .

The phase factor of (11.22) refers to the relative phase in the vibration between atoms in adjacent unit cells. The relative motion between atoms within a unit cell was considered in Sect. 11.2. Thus the NaCl structure (space group #225) has a set of three acoustic branches and three optical branches each having X'_4 and X'_5 symmetries at the X point, where

$$\begin{aligned} X'_4 &\rightarrow x, \\ X'_5 &\rightarrow y, z. \end{aligned}$$

The normal modes for the three acoustic branches are shown in Fig. 11.6 in terms of the symmetry classifications X'_4 and X'_5 (twofold) for the longitudinal and transverse branches, respectively. The corresponding normal modes for the three optical branches are shown in Fig. 11.7.

For rows of atoms in unit cells along the y and z directions, even considering that the crystal is strictly not infinite, there will be essentially *zero* phase difference ($e^{i\delta a}$, with $\delta = \pi/N$, where $N \approx 10^7$) between molecules vibrating

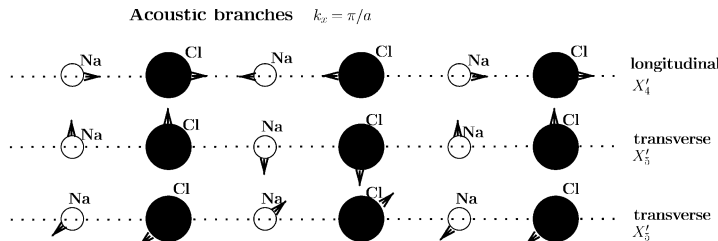


Fig. 11.6. Acoustic vibrational modes of NaCl showing longitudinal and transverse normal mode displacements at the X point ($k_x = \pi/a$) in the Brillouin zone for the X'_4 and X'_5 normal modes

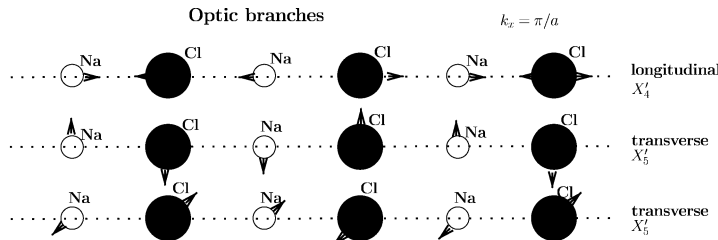


Fig. 11.7. Optic vibrational modes of NaCl showing longitudinal and transverse normal mode displacements at the X point ($k_x = \pi/a$) in the Brillouin zone for the X'_4 and X'_5 normal modes

in the acoustic mode as we move in the y and z directions. This is also true for the optical branches shown in Fig. 11.7.

11.4.2 Phonons in BaTiO_3 at the X Point

The modes in the case of BaTiO_3 (see Fig. 9.7(c)) involve more than one atom of the same species within the unit cell so that a few new aspects enter the lattice mode problem in this case. The character table for the group of the wave vector at the X point for BaTiO_3 is the same as for NaCl (Table C.15). At the X point, we compute $\Gamma^{\text{equiv.}}$ (see Table 11.4) using the symmetry operators for the group of the wave vector at the X point making use of the notation in Fig. 11.8.

$$\begin{aligned}\Gamma_{\text{Ba}}^{\text{equiv.}} &= X_1 \\ \Gamma_{\text{Ti}}^{\text{equiv.}} &= X_1 \\ \Gamma_{\text{O}_3}^{\text{equiv.}} &= 2X_1 + X_2 \\ \Gamma_{\text{vec.}} &= X'_4 + X'_5,\end{aligned}\quad (11.23)$$

where X'_4 corresponds to x , and X'_5 to (y, z) . The symmetries of the normal modes are found by taking the direct product of $\Gamma^{\text{equiv.}} \otimes \Gamma_{\text{vec.}}$.

$$\begin{aligned}\Gamma_{\text{lat.mod.}}^{\text{Ba}} &= X_1 \otimes (X'_4 + X'_5) = X'_4 + X'_5 \\ \Gamma_{\text{lat.mod.}}^{\text{Ti}} &= X_1 \otimes (X'_4 + X'_5) = X'_4 + X'_5.\end{aligned}$$

The Ba and Ti atoms form normal modes similar to NaCl with the Ba moving along x (X'_4 symmetry) or along y or z (X'_5 symmetry) with the Ti and O_3 at rest, and likewise for the Ti atoms moving along the x direction. The phase relations for atomic vibrations in adjacent unit cells in the x direction have a phase factor $e^{\pi i} = -1$, while rows of similar atoms in the y and z direction have no phase shift. For the oxygens,

$$\Gamma_{\text{lat.mod.}}^{\text{O}_3} = (2X_1 + X_2) \otimes (X'_4 + X'_5) = 2X'_4 + X'_3 + 3X'_5. \quad (11.24)$$

The mode patterns and basis functions at the X point for BaTiO_3 are given in Fig. 11.8 and Table 11.5.

Table 11.4. Characters for the equivalence transformation for the Ba, Ti and three oxygen ions in BaTiO_3 with O_h symmetry

| X point | E | $2C_{4\perp}^2$ | $C_{4\parallel}^2$ | $2C_{4\parallel}$ | $2C_2$ | i | $2iC_{4\perp}^2$ | $iC_{4\parallel}^2$ | $2iC_{4\parallel}$ | $2iC_2$ |
|---------------------------------------|-----|-----------------|--------------------|-------------------|--------|-----|------------------|---------------------|--------------------|---------|
| $\Gamma_{\text{Ba}}^{\text{equiv.}}$ | 1 | 1 | 1 | 1 | 1 | 1 | 1 | 1 | 1 | 1 |
| $\Gamma_{\text{Ti}}^{\text{equiv.}}$ | 1 | 1 | 1 | 1 | 1 | 1 | 1 | 1 | 1 | 1 |
| $\Gamma_{\text{O}_3}^{\text{equiv.}}$ | 3 | 3 | 3 | 1 | 1 | 3 | 3 | 3 | 1 | 1 |

The mode symmetry and the normal mode displacements are verified by the following considerations. Perusal of the X -point character table shows that the symmetry types are uniquely specified by the operations $C_{4\parallel}, C_2$ and i . The effect of these operations on the coordinates (x, y, z) and on the site locations are

$$C_{4\parallel} \begin{pmatrix} 1 \\ 2 \\ 3 \end{pmatrix} = \begin{pmatrix} 1 \\ 3 \\ 2 \end{pmatrix}, \quad C_{4\parallel} \begin{pmatrix} x \\ y \\ z \end{pmatrix} = \begin{pmatrix} x \\ -z \\ y \end{pmatrix},$$

$$C_2 \begin{pmatrix} 1 \\ 2 \\ 3 \end{pmatrix} = \begin{pmatrix} 1 \\ 3 \\ 2 \end{pmatrix}, \quad C_2 \begin{pmatrix} x \\ y \\ z \end{pmatrix} = \begin{pmatrix} -x \\ z \\ y \end{pmatrix},$$

$$i \begin{pmatrix} 1 \\ 2 \\ 3 \end{pmatrix} = \begin{pmatrix} 1 \\ 2 \\ 3 \end{pmatrix}, \quad i \begin{pmatrix} x \\ y \\ z \end{pmatrix} = \begin{pmatrix} -x \\ -y \\ -z \end{pmatrix}.$$

By carrying out the symmetry operations on the basis functions, we verify that the matrix representations for each of the symmetry operations have the correct characters for the X'_4 irreducible representation:

$$C_{4\parallel}(x_1 + x_2 + x_3) = (x_1 + x_3 + x_2), \quad \text{so that } \chi^{(C_{4\parallel})} = +1,$$

$$C_2(x_1 + x_2 + x_3) = -(x_1 + x_3 + x_2), \quad \text{so that } \chi^{(C_2)} = -1,$$

$$i(x_1 + x_2 + x_3) = -(x_1 + x_2 + x_3), \quad \text{so that } \chi^{(i)} = -1.$$

Applying the same approach to the normal mode displacements with X'_5 symmetry we have

$$C_{4\parallel} \begin{pmatrix} y_1 + y_2 + y_3 \\ z_1 + z_2 + z_3 \end{pmatrix} = \begin{pmatrix} -z_1 - z_3 - z_2 \\ y_1 + y_3 + y_2 \end{pmatrix} = \begin{pmatrix} 0 & -1 \\ 1 & 0 \end{pmatrix} \begin{pmatrix} y_1 + y_2 + y_3 \\ z_1 + z_2 + z_3 \end{pmatrix}$$

$$i \begin{pmatrix} y_1 + y_2 + y_3 \\ z_1 + z_2 + z_3 \end{pmatrix} = \begin{pmatrix} -1 & 0 \\ 0 & -1 \end{pmatrix} \begin{pmatrix} y_1 + y_2 + y_3 \\ z_1 + z_2 + z_3 \end{pmatrix},$$

so that $\chi(C_{4\parallel}) = 0$, and $\chi(i) = -2$, which are the correct characters for the X'_5 irreducible representation. Finally for the X'_3 modes

$$C_{4\parallel}(-x_2 + x_3) = (-x_3 + x_2) = -(-x_2 + x_3) \rightarrow \chi(C_{4\parallel}) = -1$$

$$C_2(-x_2 + x_3) = x_3 - x_2 = (-x_2 + x_3) \rightarrow \chi(C_2) = +1$$

$$i(-x_2 + x_3) = -(-x_2 + x_3) \rightarrow \chi(i) = -1.$$

These same calculations can be applied to the basis functions in Fig. 11.8 and their irreducible representations and the results are listed in Table 11.5.

The phase factors for oxygens separated by a lattice vector $a\hat{x}$ are $e^{\pi i} = -1$ while the oxygens separated by a lattice vector $a\hat{y}$ or $a\hat{z}$ have no phase difference (i.e., phase factor $\equiv 1$).

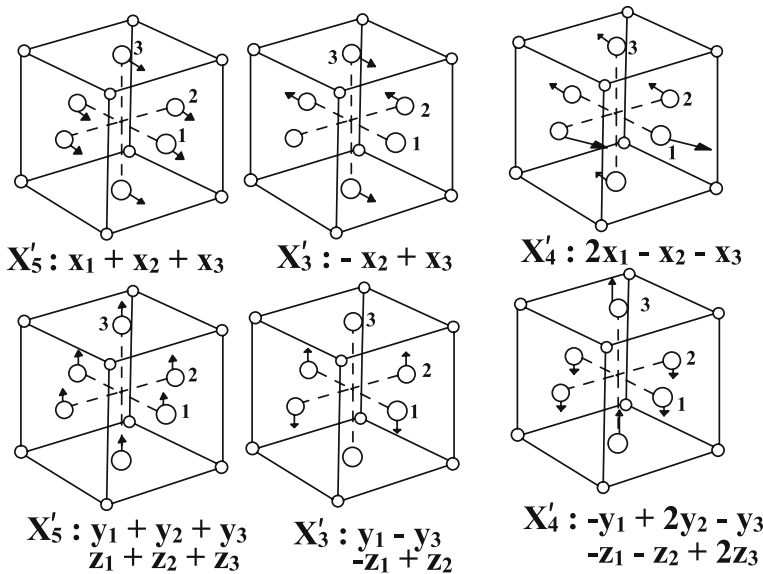


Fig. 11.8. Mode pattern models for the X point modes in BaTiO_3 . The basis functions for each normal mode are indicated

Table 11.5. Basis functions for the various irreducible representations entering the lattice modes in BaTiO_3

| basis functions | irreducible representation |
|---|----------------------------|
| $x_3 - x_2$ | X'_3 |
| $\left. \begin{array}{l} y_1 - y_3 \\ -z_1 + z_2 \end{array} \right\}$ | X'_5 |
| $\left. \begin{array}{l} 2x_1 - x_2 - x_3 \\ -y_1 + 2y_2 - y_3 \\ -z_1 - z_2 + 2z_3 \end{array} \right\}$ | X'_4 X'_5 |
| $x_1 + x_2 + x_3$ | X'_4 |
| $\left. \begin{array}{l} y_1 + y_2 + y_3 \\ z_1 + z_2 + z_3 \end{array} \right\}$ | X'_5 |

11.4.3 Phonons at the K Point in Two-Dimensional Graphite

Two-dimensional graphite, called a graphene sheet, belongs to the nonsymmorphic hexagonal space group #191 of the International Tables of Crystallography [58] and has the symmetry designations D_{6h}^1 in accord with the Schoenflies notation, and $P6/mmm$ in the Hermann–Mauguin notation. Three-dimensional graphite is described by the nonsymmorphic space group #194

and symmetry designation D_{6h}^4 as is discussed further in Problem 11.1. Although a single graphene sheet is two-dimensional, we need to consider a three-dimensional space group to account for the out-of-plane phonons. The rotational aspects for real space and for the group of the wave vector at $k = 0$ in reciprocal space are described by the point group D_{6h} (see Fig. 11.9) and Table A.21. The direct lattice vectors are given by

$$\begin{aligned}\mathbf{a}_1 &= \frac{a}{2} \left(\sqrt{3} \hat{x} + \hat{y} \right) \\ \mathbf{a}_2 &= \frac{a}{2} \left(-\sqrt{3} \hat{x} + \hat{y} \right),\end{aligned}\quad (11.25)$$

where $a = 2.456 \text{ \AA}$ is the lattice parameter denoting the nearest neighbor distance between crystallographically equivalent atoms. The dotted line in Fig. 11.9a defines the rhombus for the real space unit cell containing two inequivalent carbon atoms, *labeled* 1 and 2. The associated Wyckoff positions for atoms 1 and 2 are

$$\begin{aligned}1 &= (2/3, 1/3) \\ 2 &= (1/3, 2/3).\end{aligned}\quad (11.26)$$

Figure 11.9b shows the hexagonal Brillouin zone of 2D graphite. The reciprocal lattice vectors are given by

$$\begin{aligned}\mathbf{b}_1 &= \frac{2\pi}{a} \left(\frac{\sqrt{3}}{3} \hat{k}_x + \hat{k}_y \right) \\ \mathbf{b}_2 &= \frac{2\pi}{a} \left(-\frac{\sqrt{3}}{3} \hat{k}_x + \hat{k}_y \right).\end{aligned}\quad (11.27)$$

The letters Γ , \mathbf{M} and \mathbf{K} are the high symmetry points while Σ , T , and λ denote arbitrary points along high symmetry lines, and u represents a general point inside the two-dimensional Brillouin zone. The K point is a special symmetry point where the electronic valence and conduction bands cross in a single point through which the Fermi level passes. Before developing the group theory for the K point phonons, however, it is interesting to point out that, for the hexagonal Bravais lattice, the real and reciprocal lattice are rotated by 90° with respect to each other (see Fig. 11.9), and this is reflected in the definition of the symmetry axes (Fig. 11.10).

The appropriate group of the wave vector at the K point is the D_{3h} (see Table A.14). The $\Gamma_{\text{vec.}}$ transforms as A_2'' for light polarized along the z -axis, and as E' for light polarized in the (x, y) plane. The $\chi^{\text{equiv.}}$ and $\Gamma^{\text{equiv.}}$ are given in Table 11.6. The characters for $\chi^{\text{equiv.}}$ in Table 11.6 are given by the number of atoms in the unit cell that remain unchanged under a symmetry operation for each class, except for $\chi^{\text{equiv.}}(C_3)$, since the C_3 operation takes the $\mathbf{k} = \mathbf{K}$ vector into an equivalent point, i.e., $C_3^{-1} \mathbf{K} = \mathbf{K} + \mathbf{K}_m$, where

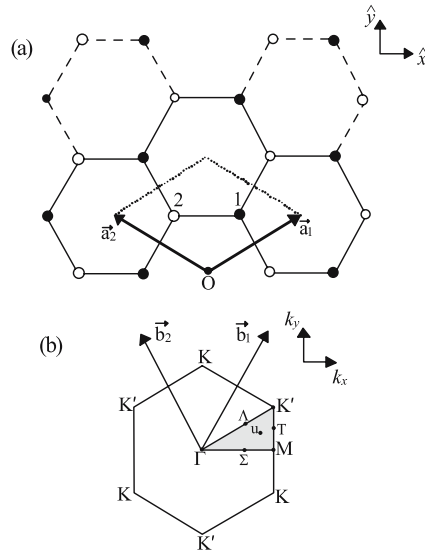


Fig. 11.9. Real (a) and reciprocal (b) lattices for a two-dimensional graphene sheet. The lattice vectors for real and reciprocal space are indicated and the two nonequivalent atoms with the real space unit cell are indicated in (a)

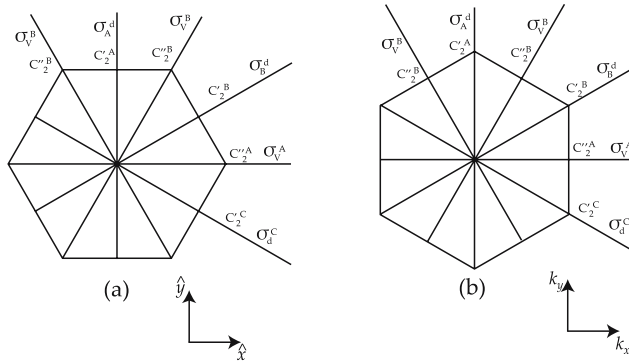


Fig. 11.10. (a) Directions of some symmetry operations of 2D graphite in the direct space. (b) Directions of some symmetry operations of 2D graphite in the reciprocal space

Table 11.6. $\Gamma^{\text{equiv.}}$ for the K point in graphite (D_{3h})

| D_{3h} | E | $2C_3$ | $3C_2$ | σ_h | $2S_3$ | $3\sigma_v$ | |
|--------------------------|-----|--------|--------|------------|--------|-------------|---------------------------------|
| $\chi_K^{\text{equiv.}}$ | 2 | -1 | 0 | 2 | -1 | 0 | $\Gamma_K^{\text{equiv.}} = E'$ |

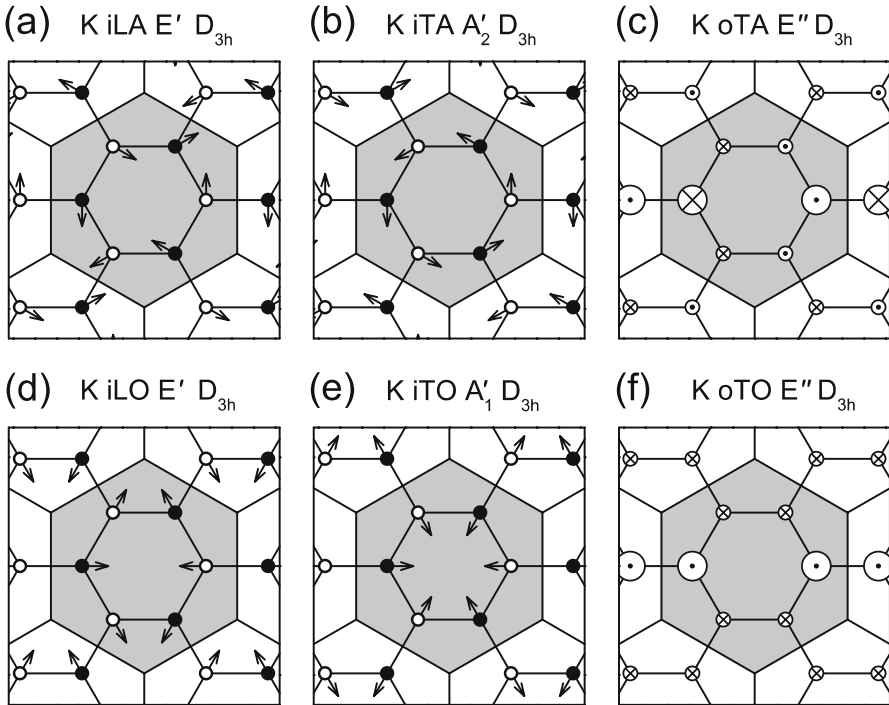


Fig. 11.11. A single graphene sheet. The solid and open dots indicate the A and B sublattices, respectively. The arrows show directions of the atomic displacements for the six stationary phonon modes of the graphene sheet at the K point. The labels of the phonon modes are identified in the text. The dotted and crossed points in (c) and (f) represent the vectors pointing in and out of the image plane. The large and small points indicate the magnitudes of the vectors equal to $\sqrt{2}$ and $1/\sqrt{2}$, respectively

\mathbf{K}_m is a reciprocal lattice vector. The equivalence transformation is therefore given by (11.19), where $j = 1, 2$, and $\mathbf{r}_1 = (a/2)[(\sqrt{3}/3)\hat{x} + \hat{y}]$ and $\mathbf{r}_2 = (a/2)[(-\sqrt{3}/3)\hat{x} + \hat{y}]$. Considering the K point at $\mathbf{K} = (\mathbf{b}_1 + \mathbf{b}_2)/3$, and considering $C_3^{-1}\mathbf{K} = \mathbf{K} - \mathbf{b}_1$ and from (11.19) we have for the equivalence representation (see Sect. 11.4)

$$\chi^{\text{equiv.}}(C_3) = e^{i\mathbf{b}_1 \cdot \mathbf{r}_1} + e^{i\mathbf{b}_2 \cdot \mathbf{r}_2} = e^{-i4\pi/3} + e^{-i2\pi/3} = 2 \cos 2\pi/3 = -1, \quad (11.28)$$

as shown in Table 11.6 and a similar result follows for $S_3^{-1}K$. Finally,

$$\Gamma_{\text{lat.mod.}} = \Gamma^{\text{equiv.}} \otimes \Gamma_{\text{vec.}} = E' \otimes (A_2'' + E') = A_1' + A_2' + E' + E''. \quad (11.29)$$

There are four eigenvalues at the K point; two are nondegenerate and two are doubly degenerate.

The eigenvectors can be found from the projector algebra (see Sect. 4.3) by introducing a phase factor relating unit cells with translations by $\mathbf{R}_n = n_1\mathbf{a}_1 + n_2\mathbf{a}_2$, according to (11.21).

Figure 11.11 shows the normal mode displacements in the graphene sheet at the K point. When considering the D_{3h} symmetry and introducing the K point phase factor, the K point wavefunction periodicity is described by a supercell of six carbon atoms, as shown in gray in Fig. 11.11 (the lattice distortions caused by the K point phonon mode is incommensurate with the two-atom unit cell). The A'_1 and A'_2 phonon modes shown in Figs. 11.11 (b) and (e) obey C_6 symmetry, while the E' and E'' phonon modes in Figs. 11.11 (a), (d), and (f) have the C_2 rotation axes perpendicular to the hexagonal plane. In contrast, the point group D_{3h} contains the C_3 rotation axis, but neither the C_6 nor C_2 rotation axes. This contradiction is resolved by considering that the complex travelling phonon modes at the K (K') point only have the C_3 rotation axes. Time-reversal symmetry mixes the complex travelling phonon modes at the K and K' points into real stationary phonon modes that obey D_{6h} symmetry. The stationary phonon modes shown in Figs. 11.11 thus preserve the C_6 and C_2 rotation axes.

11.5 Phonons in Te and α -Quartz Nonsymmorphic Structures

In this section we discuss phonon modes for tellurium (with 3 atoms/unit cell). We then show how the lattice modes for this nonsymmorphic structure can be used to obtain the lattice modes for α -quartz (with 9 atoms/unit cell) which has the same space group as Te.

11.5.1 Phonons in Tellurium

The structure for Te (space groups $P3_121'$, #152; $P3_221'$, #154) is a spiral nonsymmorphic space group as shown in Fig. 11.12. There are three Te atoms/unit cell and these Te atoms are at levels 0, $c/3$ and $2c/3$. The structure for right-handed Te shows a right-handed screw when viewed along $+\hat{z}$. When the atoms are arranged with the opposite screw orientation, we have

Table 11.7. Character Table for the D_3 Point Group

| D_3 (32) | | | E | $2C_3$ | $3C'_2$ |
|-------------------|--------------------------|-------|-----|--------|---------|
| $x^2 + y^2, z^2$ | | A_1 | 1 | 1 | 1 |
| (xz, yz) | R_z, z | A_2 | 1 | 1 | -1 |
| $(x^2 - y^2, xy)$ | (x, y) (R_x, R_y) | E | 2 | -1 | 0 |

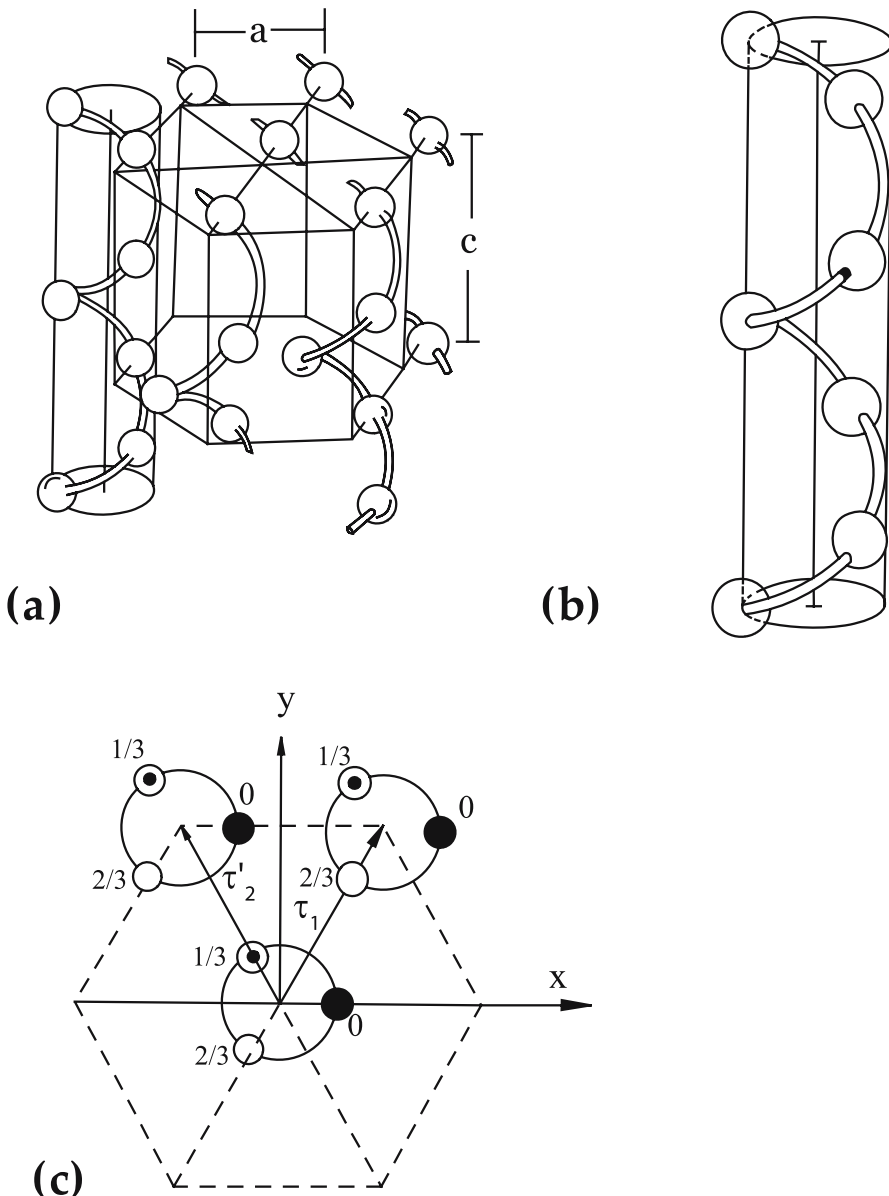


Fig. 11.12. (a) Model for the Te crystal structure showing the overall structure, (b) the structure of one chain from the side view, and (c) the top view of three adjacent chains Fix labels a, b, c on figure

Table 11.8. Characters for the Equivalence Transformation for the Group of the Wave Vector at $k = 0$ for Tellurium

| | $\{E 0\}$ | $2\{C_3 \tau\}$ | $3\{C_2 0\}$ | |
|------------------------|-----------|-----------------|--------------|------------------------------------|
| $\chi^{\text{equiv.}}$ | 3 | 0 | 1 | $\Gamma^{\text{equiv.}} = A_1 + E$ |

left-handed Te. For this structure threefold rotations about the c axis must be combined with a translation $\tau = (c/3)(001)$ to leave the crystal invariant. The three twofold symmetry axes normal to the threefold axis do not require translations. The appropriate point group at $\mathbf{k} = 0$ is D_3 and the character table is given in Table 11.7. Note that mirror planes are not symmetry operations.

Following the same procedure as was used for the nonsymmorphic diamond structure (see Sect. 11.3.3), we find $\Gamma^{\text{equiv.}}$ by considering the number of sites within the unit cell that remain invariant (or transform into the identical site in a neighboring unit cell, see Table 11.8). To find the lattice vibrations, we note that the vector transforms as $A_2 + E$. This allows us to separate out the lattice modes in the z -direction from those in the $x - y$ plane. For the z -direction

$$\Gamma^{\text{equiv.}} \otimes \Gamma_{\text{vec. } z} = (A_1 + E) \otimes A_2 = A_2 + E, \quad (11.30)$$

where the A_2 mode corresponds to pure translations in the z direction at $\mathbf{k} = 0$. The phonon dispersion curves for tellurium have been measured [61] by inelastic neutron scattering and the results along the high symmetry axes are shown in Fig. 11.13.

We show the normal modes with A_2 and E symmetry in Fig. 11.14. For the in-plane motion, the symmetries are obtained by computing:

$$\Gamma^{\text{equiv.}} \otimes \Gamma_{\text{vec. } (x,y)} = (A_1 + E) \otimes E = E + (A_1 + A_2 + E). \quad (11.31)$$

The translational mode in the x, y directions transforms as E . The in-plane modes at $\mathbf{k} = 0$ are shown in Fig. 11.15. The A_2 and E modes are IR active, and the A_1 and E modes are Raman-active.

Since the Te structure has a screw axis, right and left circularly polarized light are of importance for optical experiments. For linear polarization, we consider the \mathbf{E} vector for the light in terms of x, y, z components. For circular polarization we take the linear combinations $(x + iy)$ and $(x - iy)$. From the character table, we note that $(x + iy)(x - iy) = x^2 + y^2$ transforms as A_1 and the dipole moment \mathbf{u} is related to the polarizability tensor $\overleftrightarrow{\alpha}$ by

$$\begin{pmatrix} (u_x + iu_y)/\sqrt{2} \\ (u_x - iu_y)/\sqrt{2} \\ u_z \end{pmatrix} = \begin{pmatrix} \alpha_{11} & \alpha_{12} & \alpha_{13} \\ \alpha_{21} & \alpha_{22} & \alpha_{23} \\ \alpha_{31} & \alpha_{32} & \alpha_{33} \end{pmatrix} \begin{pmatrix} (E_x + iE_y)/\sqrt{2} \\ (E_x - iE_y)/\sqrt{2} \\ E_z \end{pmatrix}, \quad (11.32)$$

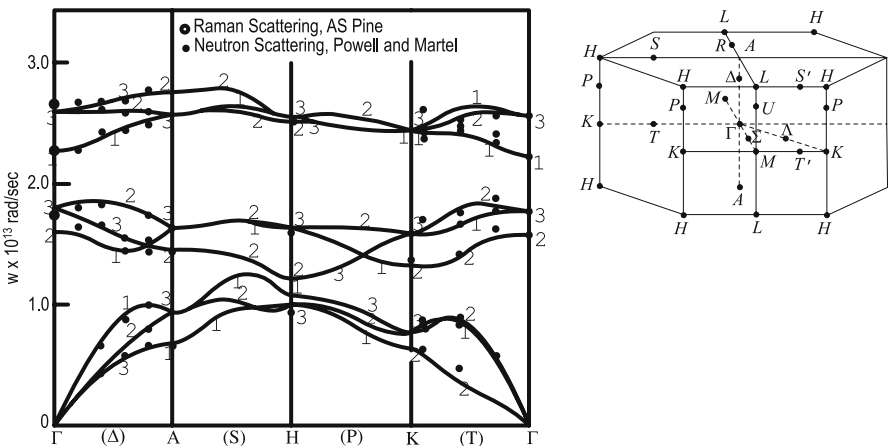


Fig. 11.13. Phonon modes for Te shown on the left along several high symmetry directions as indicated on the right (A.S. Pine and G. Dresselhaus, PRB Vol 4, p 356 (1971))

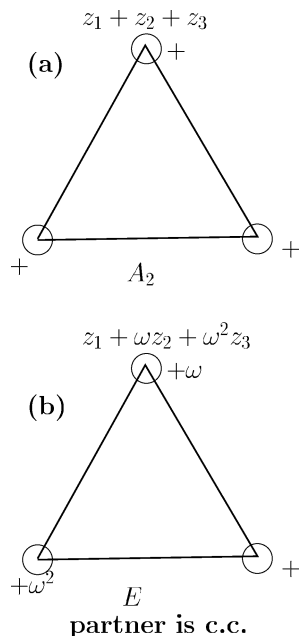


Fig. 11.14. Normal modes for Te for z -axis vibrations. The A_2 mode (a) is a pure translational mode along the z -axis. The E mode has displacements along z which have phase differences of $\omega = \exp(2\pi i/3)$ with respect to one another. One partner of the E mode is shown explicitly in (b). For the other partner, the displacements correspond to the interchange of $\omega \leftrightarrow \omega^2$, yielding the complex conjugate (c.c.) of the mode that is shown

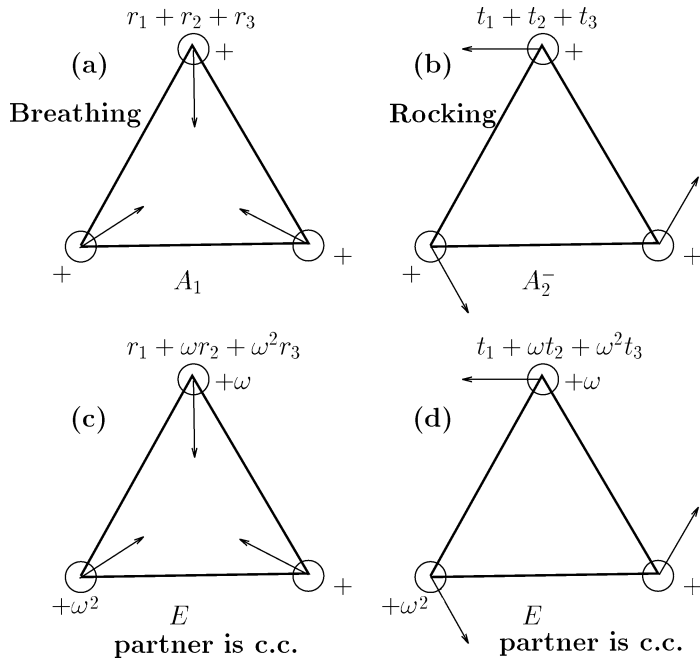


Fig. 11.15. In-plane normal modes for Te. The A_1 normal mode (a) is a breathing mode, while the A_2 mode (b) is a rocking mode corresponding to rotations of the three tellurium atoms for each half cycle of the vibration. The two E modes (c, d) can be described as a breathing and a rocking mode with phase relations $\omega = \exp(2\pi i/3)$ between each of the atoms as indicated (with the complex conjugate partner in each case obtained by the interchange of $\omega \leftrightarrow \omega^2$)

so that the polarizability tensor for A_1 modes will have the form

$$\overleftrightarrow{\alpha}_{A'_1} = \begin{pmatrix} a & 0 & 0 \\ 0 & a & 0 \\ 0 & 0 & 0 \end{pmatrix}$$

for in-plane motion with the Raman tensor having components $(E_+^i E_-^s + E_-^i E_+^s)\alpha(A_1)$. The polarizability tensor for the z -axis motion is

$$\overleftrightarrow{\alpha}_{A''_1} = \begin{pmatrix} 0 & 0 & 0 \\ 0 & 0 & 0 \\ 0 & 0 & b \end{pmatrix}$$

and has A_1 symmetry with the Raman tensor having components $E_z^i E_z^s \alpha(A_1)$. Finally for general A_1 motion, the polarizability tensor is written as

$$\overset{\leftrightarrow}{\alpha}_{A_1} = \begin{pmatrix} a & 0 & 0 \\ 0 & a & 0 \\ 0 & 0 & b \end{pmatrix}. \quad (11.33)$$

To find the energy for aligning the dipole moment in an electric field, we need to take the dot product of the dipole moment with the electric field

$$\mathbf{E}^* \cdot \mathbf{u} = \left([E_x - iE_y]/\sqrt{2}, (E_x + iE_y)/\sqrt{2}, E_z \right) \cdot \begin{pmatrix} (u_x + iu_y)/\sqrt{2} \\ (u_x - iu_y)/\sqrt{2} \\ u_z \end{pmatrix},$$

so that

$$\begin{aligned} \mathbf{E}^* \cdot \mathbf{u} &= (E_-, E_+, E_z) \cdot \begin{pmatrix} u_+ \\ u_- \\ u_z \end{pmatrix} \\ &= E_- u_+ + E_+ u_- + E_z u_z = E_x u_x + E_y u_y + E_z u_z = \text{real quantity}. \end{aligned}$$

For the electromagnetic (infrared) interaction, the pertinent symmetries are $E_+ u_-(E) + E_- u_+(E)$ for in-plane motion and $E_z u_z(A_2)$ for z -axis motion.

In considering the Raman effect, we find the energy of the Raman interaction in terms of $\mathbf{E}^* \cdot \overset{\leftrightarrow}{\alpha} \cdot \mathbf{E}$ which, when properly symmetrized becomes $1/2 [\mathbf{E}^* \cdot \overset{\leftrightarrow}{\alpha} \cdot \mathbf{E} + \mathbf{E} \cdot \overset{\leftrightarrow}{\alpha}^* \cdot \mathbf{E}^*]$. Thus for the Raman mode with A_1 symmetry, the induced dipole u_+ has the same sense of polarization as the incident electric field. However, the energy involves \mathbf{E}_i^* and \mathbf{E}_s or alternatively \mathbf{E}_s^* and \mathbf{E}_i to yield the combination $(1/2)(E_+^i E_-^s + E_-^i E_+^s)$ which transforms as $(x+iy)(x-iy) = x^2 + y^2$, as desired for a basis function with A_1 symmetry.

For Raman modes with E symmetry we can have a dipole moment u_z induced by E_+ , leading to the combination of electric fields $E_z^* E_+$. To have a symmetric polarizability tensor, we must also include the term $(E_z^* E_+)^* = E_- E_z$ since the energy must be unchanged upon interchange of electric fields $\mathbf{E} \leftrightarrow \mathbf{E}^*$. Thus the polarizability and Raman tensors must be of the form

$$\overset{\leftrightarrow}{\alpha}_{E,1} = \begin{pmatrix} 0 & 0 & 0 \\ 0 & 0 & r^* \\ r & 0 & 0 \end{pmatrix}, \quad \text{and} \quad \begin{cases} E_+^i E_z^s \alpha_-(E) + E_-^i E_z^s \alpha_+(E) \\ \text{or } E_z^s E_+^s \alpha_-(E) + E_z^i E_-^s \alpha_+(E). \end{cases} \quad (11.34)$$

The partner of this polarizability tensor with E symmetry will produce the displacement u_z from an electric field displacement E_- yielding

$$\overset{\leftrightarrow}{\alpha}_{E,2} = \begin{pmatrix} 0 & 0 & r \\ 0 & 0 & 0 \\ 0 & r^* & 0 \end{pmatrix}. \quad (11.35)$$

The other lattice mode for Te with E symmetry (denoted here by E') produces a dipole moment u_+ from an electric field E_- . This however involves $E_-(E_+)^* = E_-^2$ for the incident and scattered electric fields so that the polarizability tensor in this case is

$$\overleftrightarrow{\alpha}_{E',1} = \begin{pmatrix} 0 & s & 0 \\ 0 & 0 & 0 \\ 0 & 0 & 0 \end{pmatrix}; \quad \text{basis function } x_-^2 \quad (11.36)$$

and the corresponding partner is

$$\overleftrightarrow{\alpha}_{E',2} = \begin{pmatrix} 0 & 0 & 0 \\ s^* & 0 & 0 \\ 0 & 0 & 0 \end{pmatrix}; \quad \text{basis function } x_+^2. \quad (11.37)$$

The Raman tensor for the E' mode has the form $E_+^i E_+^s \alpha_+(E) + E_-^i E_-^s \alpha_-(E)$. We can relate these partners of the E' modes to the basis functions of the character table for D_3 by considering the basis functions for the partners

$$\begin{aligned} \text{Partner \#1: } & \frac{1}{2}(x - iy)^2 = x_-^2 \\ \text{Partner \#2: } & \frac{1}{2}(x + iy)^2 = x_+^2. \end{aligned} \quad (11.38)$$

By taking the sums and differences of these partners we obtain

$$\begin{aligned} x_+^2 + x_-^2 &= \frac{1}{2}(x + iy)^2 + \frac{1}{2}(x - iy)^2 = (x^2 - y^2) \\ x_+^2 - x_-^2 &= \frac{1}{2}(x + iy)^2 - \frac{1}{2}(x - iy)^2 = 2xy, \end{aligned} \quad (11.39)$$

which form a set of partners listed in the character table for D_3 .

11.5.2 Phonons in the α -Quartz Structure

We will now examine the lattice modes of α -quartz (space group D_3^4 , #152, $P3_121$ for the right-hand crystal or D_3^5 , #153, $P3_212$ for the left-hand crystal). We will use this example as a means for showing how lattice modes for crystals with several atoms per unit cell (such as α -quartz) can be built up from simpler units, in this case the tellurium structure discussed in Sect. 11.5.1. In Sect. 11.6 we discuss the effect of an applied axial compressive force upon lattice vibrations in α -quartz.

The spiral structure of α -quartz about the z -axis is shown in Fig. 11.16(a) where each solid ball represents a SiO_2 unit, and the diagram on the left is identical to that for tellurium (see Fig. 11.12(a)). The projection of the nine atoms in SiO_2 onto the basal plane is shown in Fig. 11.16(b). The Si

atoms (1, 4 and 7) occupy positions at levels 0, $c/3$, $2c/3$, respectively (as for tellurium). The oxygen atoms (9, 5, 3, 8, 6 and 2) occupy positions at levels $c/9$, $2c/9$, $4c/9$, $5c/9$, $7c/9$ and $8c/9$, respectively (these sites are of course not occupied in tellurium). Thus both Te and α -quartz are described by the same space group, but have different site symmetries. Figure 11.16 shows the right-handed tellurium structure.

There are three molecular SiO_2 units per unit cell giving rise to nine atoms per unit cell or 27 lattice branches of which 24 are optic modes. By examining the atom locations in Fig. 11.16(b), we can determine the point group symmetry of α -quartz. The z -axis is a threefold axis of rotation when combined with the translation $\tau = (c/3)(001)$. In addition there is a twofold axis from the center to each of the silicon atoms. The symmetry elements are the same as for tellurium discussed in Sect. 11.5.1. In order to determine the normal modes of vibration, we first find the characters for the transformation of the atomic sites. It is convenient to make use of the results for tellurium, noting that the silicon atoms in quartz occupy the same sites as in tellurium. In Table 11.9 we obtain the lattice modes in α -quartz at $\mathbf{k} = 0$.

The lattice modes for the silicon are identical with those found previously for Te, so that part of the problem is already finished. For the six oxygens we have

$$\Gamma_{\text{lat.mod.}, z} = (A_1 + A_2 + 2E) \otimes A_2; \quad \text{for } z \text{ motion}$$

$$\Gamma_{\text{lat.mod.}, x,y} = (A_1 + A_2 + 2E) \otimes E; \quad \text{for } x, y \text{ motion.}$$

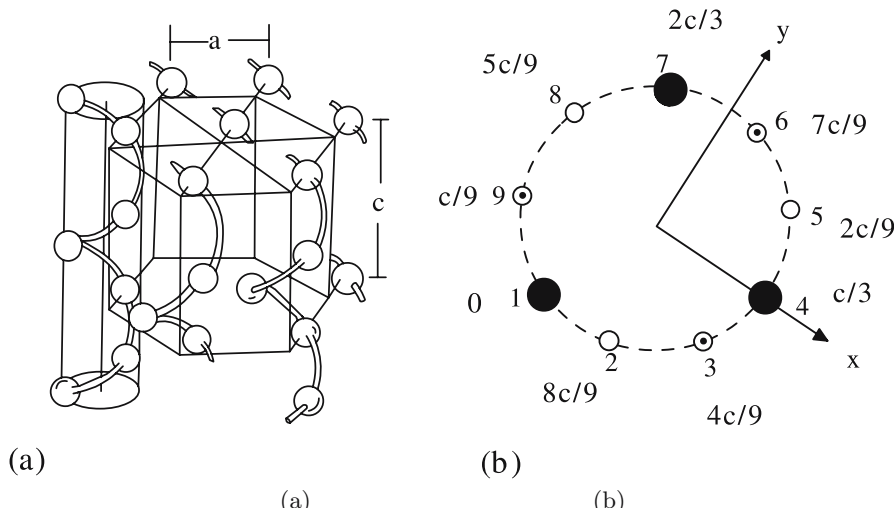


Fig. 11.16. Structure of (a) right-handed α -quartz and (b) the projection of the atoms on the basal plane of α -quartz. Atoms #1, 4, 7 denote Si and the other numbers denote oxygen atoms

Table 11.9. Characters for the Equivalence Transformation for α -quartz

| | $\{E 0\}$ | $2\{C_3 \tau\}$ | $3\{C'_2 0\}$ | |
|--|-----------|-----------------|---------------|--------------------|
| $\Gamma_{\text{Si}}^{\text{equiv.}}$ | 3 | 0 | 1 | $= A_1 + E$ |
| $\Gamma_{\text{oxygen}}^{\text{equiv.}}$ | 6 | 0 | 0 | $= A_1 + A_2 + 2E$ |

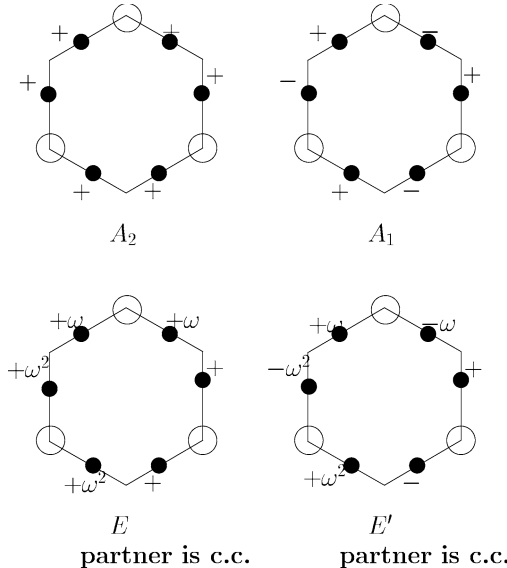


Fig. 11.17. Normal modes along the z -direction for the six oxygens in the α -quartz crystal. The A_2 mode is a uniform translation while the A_1 mode is a rocking of the oxygens around the Si. The E modes are related to the A_2 and A_1 modes by combining the $1, \omega, \omega^2$ phases with the translational and rocking motions

Carrying out the direct products we obtain

$$\begin{aligned}\Gamma_{\text{lat.mod.}, z} &= A_2 + A_1 + 2E; \quad \text{for } z \text{ motion} \\ \Gamma_{\text{lat.mod.}, x,y} &= 2A_1 + 2A_2 + 4E; \quad \text{for } x, y \text{ motion},\end{aligned}\quad (11.40)$$

where we note that for the D_3 point group $E \otimes E = A_1 + A_2 + E$.

The corresponding z -axis normal modes A_2 , A_1 , E and E' for the six oxygens are shown in Fig. 11.17. The normal mode A_2 is clearly a uniform translation of the six oxygens, while the A_1 mode is a rocking of the two oxygens on either side of a silicon atom (one going up, while the other goes down). The twofold E mode is derived from A_2 by introducing phases $1, \omega, \omega^2$ for each of the pairs of oxygens around a silicon atom; the complex conjugate E' mode is obtained from the one that is illustrated by the substitution $\omega \leftrightarrow \omega^2$. Finally the E' mode is obtained from the A_1 mode in a similar way as the

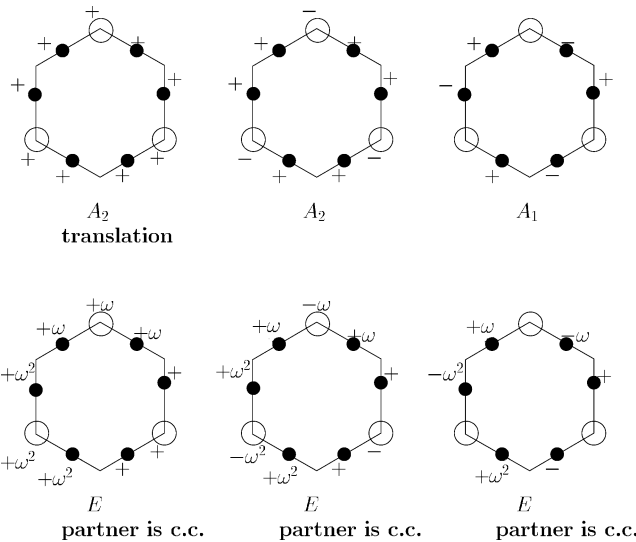


Fig. 11.18. Normal modes along the z -direction for the three SiO_2 groups in α -quartz. Here the motions of the Si atoms are combined with those of the oxygens

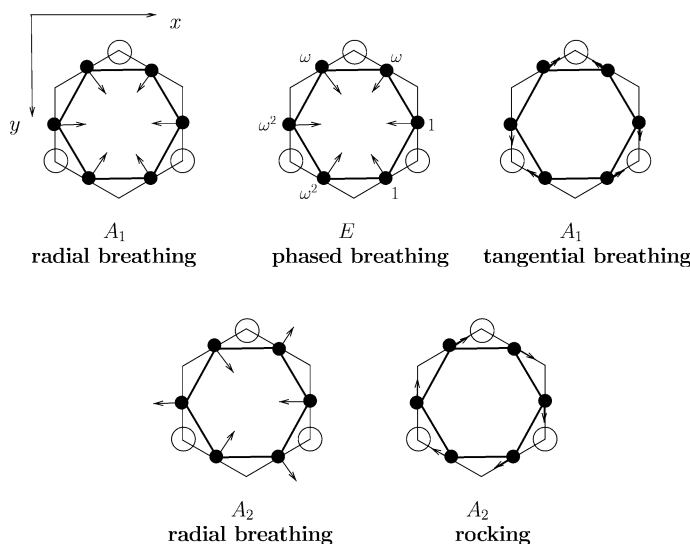


Fig. 11.19. Normal modes in the $x-y$ plane for the six oxygens in the α quartz crystal. In addition, the A_1 tangential breathing mode, the A_2 radial breathing mode, and the A_2 rocking mode have corresponding E modes, with phases $1, \omega, \omega^2$ for the three SiO_2 units, each having two partners related by $\omega \leftrightarrow \omega^2$. In the crystal, all modes with the same symmetry are coupled, so that the actual normal mode is an admixture of the modes pictured here

E mode is obtained from the A_2 mode. In identifying the symmetry type for these normal modes, we note the effect of symmetry operation C'_2 .

We now combine the z motion for the silicons (symmetries A_2+E) with the z motion for the oxygens (symmetries A_1+A_2+2E) to obtain A_1+2A_2+3E for SiO_2 . The resulting normal mode patterns are shown in Fig. 11.18. The z -axis translational mode for the six oxygens combine either in-phase or out of phase to form the two normal modes with A_2 symmetry. For the mode with A_1 symmetry, the silicon atoms remain stationary. Introducing the phases 1, ω , ω^2 for each SiO_2 group gives the three E normal modes along the z -direction in α -quartz.

For the xy motion, the six oxygens form lattice modes with symmetries $2A_1+2A_2+4E$ and the normal mode patterns are shown in Fig. 11.19.

The next step is to combine the motion of the silicon (A_1+A_2+2E) with that of the two oxygens ($2A_1+2A_2+4E$) for the in-plane modes, and this step is the focus of Problem 11.2.

11.6 Effect of Axial Stress on Phonons

In general, an external perturbation, when applied to a crystal, reduces the symmetry of the crystal. The fundamental principle used to deduce this lower symmetry is called the Curie principle which states that only those symmetry operations are allowed which are common to both the unperturbed system and to the perturbation itself. This condition restricts the new symmetry group to a subgroup common to the original group.

| Polarizability Tensors for the Raman-Active Modes of α -quartz with | | | |
|---|---|---|---------------------|
| $\vec{F} = 0$ or $\vec{F} \parallel z$ | (D_3) | $\vec{F} \parallel x$ or $\vec{F} \perp x$ | (C_2) |
| Basis Functions | D_3 | C_2 | Basis Functions |
| $x^2 + y^2, z^2$ | A'_1 $\begin{bmatrix} p & 0 & 0 \\ 0 & p & 0 \\ 0 & 0 & q \end{bmatrix}$ | A' $\begin{bmatrix} t & u & 0 \\ u & t & 0 \\ 0 & 0 & v \end{bmatrix}$ | x^2, y^2, z^2, xy |
| $x^2 - y^2, xy$ | E' $\begin{bmatrix} 0 & m & 0 \\ m^* & 0 & 0 \\ 0 & 0 & 0 \end{bmatrix}$ | | |
| xz, yz | A'_2 $\begin{bmatrix} 0 & 0 & r \\ 0 & 0 & r^* \\ r^* & r & 0 \end{bmatrix}$ | B' $\begin{bmatrix} 0 & 0 & m \\ 0 & 0 & n \\ m & n & 0 \end{bmatrix}$ | xz, yz |
| Raman inactive | | | |

Fig. 11.20. The symmetry of the Polarizability Tensors for Raman Active Modes of α -quartz, for stress applied along the threefold axis, and along a twofold axis perpendicular to the threefold axis

When a homogeneous axial compression is applied to a crystal, the resulting strain is described by a symmetric tensor of the second rank. The strain tensor can be represented by an ellipsoid which has at least D_{2h} point group symmetry; if two of its major axes are equal, the ellipsoid acquires rotational symmetry about the third axis, and the point group symmetry is $D_{\infty h}$, whereas, if all three axes are equal it becomes a sphere with three-dimensional continuous rotation and reflection symmetry. In order to determine the symmetry operations of the strained crystal it is necessary to know the orientation of the strain ellipsoid relative to the crystallographic axes. An alternative procedure is to treat the stress itself as the imposed condition and to find the symmetry elements common to the unstrained crystal and to the symmetry of the stress tensor.

Using the symmetry properties of the stress tensor is particularly simple when the external perturbation is an axial compression. In this case the stress ellipsoid has $D_{\infty h}$ point group symmetry and can be conveniently represented by a right circular cylinder with its center coinciding with the center of the crystal and its axis of revolution along the direction of the force. The symmetry operations common to the unstrained crystal and to the cylinder representing the stress can then be easily determined by inspection.

As an illustrative case, consider the point group D_3 , the point group of α -quartz (Sect. 11.5.2). The symmetry operations of D_3 are a threefold axis of rotation along the z -axis and three twofold axes perpendicular to the z -axis, one of which is taken to be the x -axis. If the force, \mathbf{F} , is applied along the z -direction, all of the operations of the group are common to the symmetry of the stress and hence the symmetry remains D_3 . If, however, the force is applied along the x direction, the only remaining symmetry operation is C_2 . Similarly, if the force is applied along the y -axis, the only remaining symmetry operation is again the twofold axis of rotation along the x -axis and the symmetry is reduced to the point group C_2 . If the force is in a direction other than along z or parallel or perpendicular to a two-fold axis, the crystal symmetry is reduced to C_1 .

Table 11.10. Character table for group C_2 pertinent to uniaxial deformation applied to D_3 symmetry group. The compatibility relations among their irreducible representations are also given

| C_2 (2) | | E | C_2 | |
|--------------------------|------------|-------|-------|---------|
| x^2, y^2, z^2, xy | R_z, z | A | 1 | 1 |
| | x, y | B | 1 | -1 |
| xz, yz | R_x, R_y | | | |
| representations of D_3 | | A_1 | 1 | 1 |
| | | A_2 | 1 | -1 |
| | | E | 2 | 0 |
| | | | | $A + B$ |

Once the reduced symmetry of the crystal in the presence of the external perturbation is determined, the correlation between the irreducible representations of the two groups can be obtained. From such a correlation, the removal of the degeneracy of a particular energy level can be immediately deduced as illustrated below for the force applied along the twofold axis.

This group theoretical analysis thus predicts that the Raman lines of E symmetry should split and the Raman inactive A_2 mode in D_3 symmetry should become Raman-active in C_2 symmetry. We note that the basis functions that are used for C_2 are x, y, z while for D_3 , the combinations $(x + iy, x - iy, z)$ are used. The form of the polarizability tensors for the Raman-active modes in D_3 and C_2 point group symmetries are given in Fig. 11.20, and are further considered in Problem 11.2.

Selected Problems

11.1. This problem involves the lattice modes of a three-dimensional graphite crystal (see Fig. C.1).

- What are the symmetry operations for 3D crystalline graphite, and how do they differ from those for 2D graphite (see Sect. 11.4.3)?
- Why is the space group #194 appropriate for 3D hexagonal graphite, rather than #191, or #192, or #193?
- Find the number of lattice modes for 3D graphite at $k = 0$. What are their symmetries and what are their mode degeneracies?
- What are the normal mode displacements for each of these lattice modes at $k = 0$?
- Find the mode symmetries and compatibility relations for the modes in the $\Gamma - T - K$ direction (see Fig. 11.13). Be aware that the K point is a special point where the relation $R_\alpha k = k + K_m$ occurs (see Table C.27).
- Which modes in (e) are IR active, Raman active? What are the polarizations of the Raman active modes?
- Find the eigenvectors at the K point for 3D graphite.
- Compare the results for two-dimensional and three-dimensional graphite and discuss the difference in behavior in terms of the connection between symmorphic and nonsymmorphic groups.

11.2. Use the results given in Sect. 11.5.2 for the lattice modes of crystalline SiO_2 to do this problem.

- Find the normal modes for the in-plane vibrations of crystalline SiO_2 obtained by combining the lattice modes for the three Si atoms and for the six oxygen atoms given in Sect. 11.5.2. How many have A_1 , A_2 and E symmetry? On the basis of your results explain the normal mode patterns given in Fig. 11.21 for the modes with A_1 and A_2 symmetry, and discuss the normal mode patterns for the E symmetry modes.

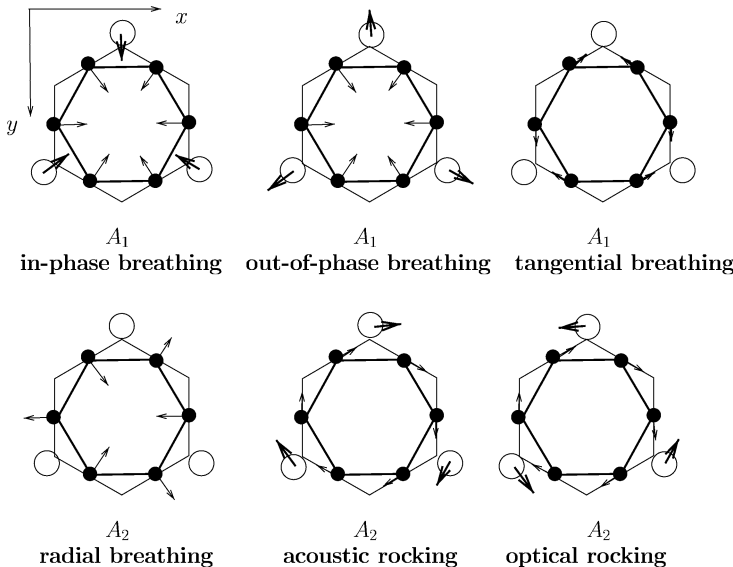


Fig. 11.21. The in-plane normal modes for α -quartz obtained by superposition of the normal modes for the oxygens and the silicons. Corresponding to each of the one-dimensional modes shown here are two-dimensional E modes with phases $1, \omega, \omega^2$ for the three SiO_2 units, with the two partners related by $\omega \leftrightarrow \omega^2$

- (b) Suppose that a stress is applied along the c -axis, what is the effect on the normal mode patterns? Now suppose that a stress is applied along a twofold axis going through a Si atom, what is the effect on the normal mode patterns?

11.3. Consider the crystal structure in the diagram for Nb_3Sn , a prototype superconductor with the A-15 (or β -W) structure used for high field superconducting magnet applications [54, 76].

- (a) How many lattice modes are there at $k = 0$, what are their symmetries and what are their degeneracies?
 (b) What are the normal mode displacements for each of these lattice modes?
 (c) Which modes are IR active, Raman active? What are the polarizations of the Raman-active modes?

11.4. Tin oxide (SnO_2 with space group #136) is an important electronic material [54, 76].

- (a) Find the Wyckoff positions from the site positions of the Sn and O atoms in the unit cell. Find $I^{\text{equiv.}}$ for the SnO_2 structure.
 (b) Find the lattice modes at $k = 0$, their symmetries, degeneracies and the normal mode patterns.
 (c) Indicate the IR-activity and Raman activity of these modes.

11.5. Bromine forms a molecular crystal [54, 76].

- (a) What is the appropriate space group? What are the Wyckoff positions for each of the distinct bromine atoms within the unit cell.
- (b) Find the lattice modes at $k = 0$, their symmetries, degeneracies and the normal mode patterns.
- (c) Indicate the IR-activity and Raman activity of these modes.

11.6. Carbon nanotubes are an interesting system where first-order Raman activity can be based on selection rules for the *electron–phonon* interaction [8]. The electronic states usually belong to two-dimensional irreducible representations (E_μ) and five types of allowed first-order resonance Raman scattering processes between $E_\mu^{(v)}$ and $E_{\mu'}^{(c)}$ can be obtained

$$\begin{aligned}
 \text{(I)} \quad & E_\mu^{(v)} \xrightarrow{Z} E_\mu^{(c)} \xrightarrow{A} E_\mu^{(c)} \xrightarrow{Z} E_\mu^{(v)}, \\
 \text{(II)} \quad & E_\mu^{(v)} \xrightarrow{X} E_{\mu \pm 1}^{(c)} \xrightarrow{A} E_{\mu \pm 1}^{(c)} \xrightarrow{X} E_\mu^{(v)}, \\
 \text{(III)} \quad & E_\mu^{(v)} \xrightarrow{Z} E_\mu^{(c)} \xrightarrow{E_1} E_{\mu \pm 1}^{(c)} \xrightarrow{X} E_\mu^{(v)}, \\
 \text{(IV)} \quad & E_\mu^{(v)} \xrightarrow{X} E_{\mu \pm 1}^{(c)} \xrightarrow{E_1} E_\mu^{(c)} \xrightarrow{Z} E_\mu^{(v)}, \\
 \text{(V)} \quad & E_\mu^{(v)} \xrightarrow{X} E_{\mu \pm 1}^{(c)} \xrightarrow{E_2} E_{\mu \mp 1}^{(c)} \xrightarrow{X} E_\mu^{(v)}, \tag{11.41}
 \end{aligned}$$

where A , E_1 , and E_2 denote phonon modes of different Γ -point symmetries of $\mu = 0$, $\mu = \pm 1$, and $\mu = \pm 2$, respectively. The XZ plane is parallel to the substrate on which the nanotubes lie, the Z axis is directed along the nanotube axis, and the Y -axis is directed along the light propagation direction, so that the Z and X in (11.41) stand for the light polarized parallel and perpendicular to the nanotube axis, respectively. The five processes of (11.41) result in different polarization configurations for different phonon modes: ZZ and XX for A , ZX and XZ for E_1 , and XX for E_2 .

- (a) Derive the selection rules in (11.41) explicitly.
- (b) The Raman active modes are those transforming like quadratic functions (XX, YY, ZZ, XY, YZ, ZX). The selection rules associated with the first and third arrows in (11.41) come basically from selection rules for the *electron–photon* interaction. Show that the selection rules for different polarizations obtained in (11.41) are in perfect agreement with the basis functions analysis.

11.7. Show that the Raman and infrared active modes in chiral and achiral carbon nanotubes are given by the following symmetries [8]:

$$\begin{aligned}\Gamma_{\text{zigzag}}^{\text{Raman}} &= 2A_{1g} + 3E_{1g} + 3E_{2g} \rightarrow 8 \text{ modes}, \\ \Gamma_{\text{zigzag}}^{\text{infrared}} &= A_{2u} + 2E_{1u} \rightarrow 3 \text{ modes}, \\ \Gamma_{\text{armchair}}^{\text{Raman}} &= 2A_{1g} + 2E_{1g} + 4E_{2g} \rightarrow 8 \text{ modes}, \\ \Gamma_{\text{armchair}}^{\text{infrared}} &= 3E_{1u} \rightarrow 3 \text{ modes}, \\ \Gamma_{\text{chiral}}^{\text{Raman}} &= 3A_1 + 5E_1 + 6E_2 \rightarrow 14 \text{ modes}, \\ \Gamma_{\text{chiral}}^{\text{infrared}} &= A_2 + 5E_1 \rightarrow 6 \text{ modes}.\end{aligned}\tag{11.42}$$

Electronic Energy Levels in a Cubic Crystal

In this chapter we apply space groups to determine the electronic dispersion relations in crystalline materials, and use as an illustration the symmetrized plane wave solutions of a cubic crystal.

12.1 Introduction

Suppose that we wish to calculate the electronic energy levels of a solid from a specified potential. There are many techniques available for this purpose. Some techniques are based on what is called first principles *ab initio* calculations and directly find solutions to Schrödinger's equation. Others are based on the symmetry-imposed form of the dispersion relations, which are used to fit experimental data. In all cases these techniques utilize the *spacial symmetry of the crystal*, and emphasize the electronic energy bands at high symmetry points and along high symmetry axes in the Brillouin zone.

To illustrate how group theory is utilized in these calculations, we will consider explicitly the energy bands of the nearly free electron model because of its pedagogic value. If there were no periodic potential, the energy eigenvalues would be the free electron energies

$$E(\mathbf{k}') = \frac{\hbar^2 k'^2}{2m}, \quad V(\mathbf{r}) = 0, \quad (12.1)$$

and the free electron eigenfunctions would be

$$\psi_{k'}(\mathbf{r}) = \frac{1}{\sqrt{\Omega}} e^{i\mathbf{k}' \cdot \mathbf{r}}, \quad (12.2)$$

where \mathbf{k}' is a wave vector in the extended Brillouin zone and Ω is the volume of the crystal. In the empty lattice model, the presence of a weak periodic potential imposes the symmetry of the crystal on the "empty lattice" electronic energy bands, but the potential $V(\mathbf{r})$ itself is considered in the limit

$V(\mathbf{r}) \rightarrow 0$. From a group theoretical point of view, the *free electron energy bands correspond to the symmetry of the full rotation group and the weak periodic potential serves to lower the symmetry* to that of the crystalline solid, as for example to O_h^1 (space group #221) symmetry for a simple cubic crystal. Thus, the introduction of a periodic potential results in symmetry-lowering, similar to the crystal field problem (Sect. 5.3) which we have by now encountered in several contexts. We consider the empty lattice energy bands in the reduced zone by writing the wave vector \mathbf{k}' in the extended zone scheme as

$$\mathbf{k}' = \mathbf{k} + \mathbf{K}_{n_i}, \quad (12.3)$$

where \mathbf{k} is a reduced wave vector in the first Brillouin zone and \mathbf{K}_{n_i} is a reciprocal lattice vector to obtain

$$E(\mathbf{k} + \mathbf{K}_{n_i}) = \frac{\hbar^2}{2m} (\mathbf{k} + \mathbf{K}_{n_i}) \cdot (\mathbf{k} + \mathbf{K}_{n_i}), \quad (12.4)$$

where

$$\mathbf{K}_{n_i} = \frac{2\pi}{a} (n_1, n_2, n_3), \quad \text{and} \quad n_i = \text{integer}, \quad i = 1, 2, 3. \quad (12.5)$$

We use the subscript \mathbf{K}_{n_i} on the energy eigenvalues E_{n_i} to denote the pertinent \mathbf{K}_{n_i} vector when using the wave vector \mathbf{k} within the first Brillouin zone. If we write \mathbf{k} in dimensionless units

$$\xi = \frac{\mathbf{k}a}{2\pi}, \quad (12.6)$$

we obtain

$$E_{\mathbf{K}_{n_i}}(\mathbf{k}) = \frac{\hbar^2}{2m} \left(\frac{2\pi}{a} \right)^2 \left[(\xi_1 + n_1)^2 + (\xi_2 + n_2)^2 + (\xi_3 + n_3)^2 \right]. \quad (12.7)$$

The empty lattice energy bands for the FCC cubic structure are shown in Fig. 12.1 at the high symmetry points and along the high symmetry directions indicated by the Brillouin zone for the FCC lattice (see Fig. C.5a in Appendix C). The energy bands are labeled by the symmetries of the irreducible representations appropriate to the group of the wave vector corresponding to the pertinent space group. Group theory provides us with the symmetry designations and with the level degeneracies. In Sect. 12.2, we treat the symmetry designations and mode degeneracies for the simple cubic lattice at $\mathbf{k} = 0$, and in Sects. 12.3 and 12.4 at other symmetry points in the Brillouin zone. In Sect. 12.5, the effect of screw axes and glide planes on the electronic energy band structure is considered.

In the reduced zone scheme, the wave functions for the plane wave solutions to the empty lattice model become the Bloch functions

$$\psi_{\mathbf{k}'}(\mathbf{r}) = \frac{1}{\sqrt{\Omega}} e^{i\mathbf{k}' \cdot \mathbf{r}} = \frac{1}{\sqrt{\Omega}} e^{i\mathbf{k} \cdot \mathbf{r}} e^{i\mathbf{K}_{n_i} \cdot \mathbf{r}}, \quad (12.8)$$

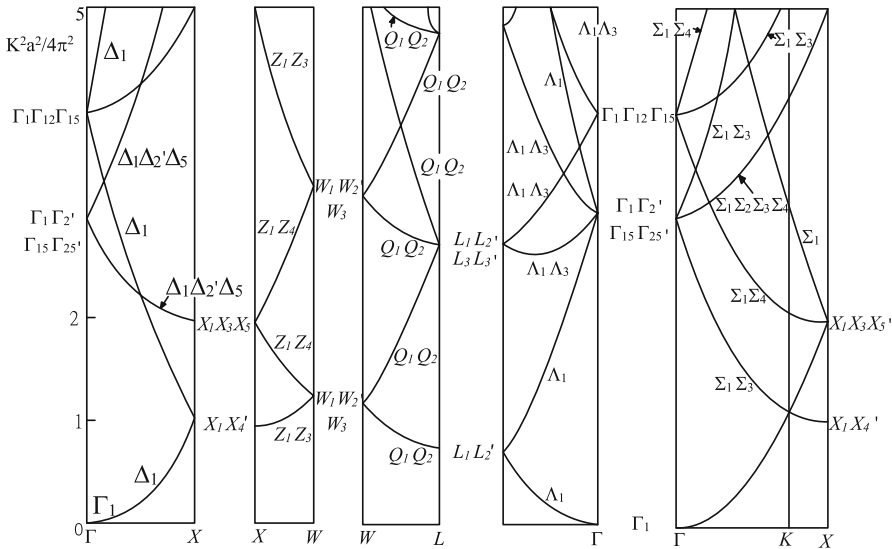


Fig. 12.1. Free-electron bands of the empty lattice in a face centered cubic structure. The labels of the high symmetry points in the FCC structure are given in Fig. C.5(a) of Appendix C. The band degeneracies can be obtained from the dimensions of the irreducible representations indicated on this diagram, and the energy is given in units of $(\hbar^2/2m)(2\pi/a)^2$

where the periodic part of the Bloch function is written as

$$u_{\mathbf{k}}(\mathbf{r}) = e^{i\mathbf{K}_{n_i} \cdot \mathbf{r}}. \quad (12.9)$$

According to Bloch's theorem, the effect of the lattice vector translation operator $\{\varepsilon|\mathbf{R}_n\}$ is to introduce a phase factor

$$\{\varepsilon|\mathbf{R}_n\}\psi_{\mathbf{k}}(\mathbf{r}) = e^{i\mathbf{k} \cdot \mathbf{R}_n} \psi_{\mathbf{k}}(\mathbf{r}), \quad (12.10)$$

$e^{i\mathbf{k} \cdot \mathbf{R}_n}$ involving the lattice vector \mathbf{R}_n .

In calculating the electronic energy bands in the empty lattice approximation, we recognize that the main effect of the periodic potential $V(\mathbf{r})$ in the limit $V(\mathbf{r}) \rightarrow 0$ limit is to lift the degeneracy of $E_{\mathbf{K}_{n_i}}(\mathbf{k})$. At certain high symmetry points or axes and at the Brillouin zone boundary, the degeneracy in many cases is not fully lifted in the $V(\mathbf{r}) \rightarrow 0$ limit and a finite periodic potential is needed to lift the degeneracy of the empty lattice dispersion relations. Group theory tells us the form of the interactions, the symmetry of the levels and their degeneracies. For each of the high symmetry points in the Brillouin zone, different symmetry operations will be applicable, depending on the appropriate group of the wave vector for the \mathbf{k} point under consideration, as illustrated below.

12.2 Plane Wave Solutions at $\mathbf{k} = 0$

The highest symmetry point in the Brillouin zone is of course the Γ point ($\mathbf{k} = 0$) and we will therefore first illustrate the application of group theoretical considerations to the energy bands at the Γ point first for a cubic crystal. Setting $\mathbf{k} = 0$ in (12.7), the energy eigenvalue $E_{\mathbf{K}_{n_i}}(\mathbf{k})$ becomes

$$E_{\mathbf{K}_{n_i}}(0) = \frac{\hbar^2}{2m} \left(\frac{2\pi}{a} \right)^2 [n_1^2 + n_2^2 + n_3^2] = \frac{\hbar^2}{2m} \left(\frac{2\pi}{a} \right)^2 N^2, \quad (12.11)$$

where

$$N^2 = n_1^2 + n_2^2 + n_3^2. \quad (12.12)$$

Corresponding to each reciprocal lattice vector \mathbf{K}_{n_i} , a value for $E_{\mathbf{K}_{n_i}}(0)$ is obtained. For most \mathbf{K}_{n_i} vectors, these energies are degenerate. We will now enumerate for illustrative purposes the degeneracy of the first few levels, starting with $\mathbf{K}_{n_i} = 0$ and $n_1 = n_2 = n_3 = 0$. We then find which irreducible representations for O_h are contained in each degenerate state. If then a periodic potential is applied, the degeneracy of some of these levels will be lifted. Group theory provides a powerful tool for specifying how these degeneracies are lifted. In Table 12.1 we give the energy, the degeneracy and the set of \mathbf{K}_{n_i} vectors that yield each of the five lowest energy eigenvalues $E_{\mathbf{K}_{n_i}}(0)$ in cubic symmetry. The example that we explicitly work out here is for the simple cubic lattice [space group #221 (O_h^1) or $Pm3m$], and many of the pertinent character tables are found in Appendix C.

At $\mathbf{K}_{n_i} = 0$ we have $\psi_{\mathbf{k}}(\mathbf{r}) = (1/\sqrt{\Omega})e^{i\mathbf{k}\cdot\mathbf{r}}$. For a general \mathbf{K}_{n_i} vector, (n_1, n_2, n_3) there will in general be a multiplicity of states with the same energy. We now show how to choose a properly symmetrized combination of plane waves which transform as irreducible representations of the group of the wave vector at $\mathbf{k} = 0$, and therefore bring the empty lattice Hamiltonian into block diagonal form. In the presence of a weak cubic periodic potential $V(\mathbf{r})$, the degeneracy of states which transform as different irreducible representations will be partially lifted.

By calculating the characters for the equivalence transformation, we obtain $\chi^{\text{equiv.}}$ which is used to project out the irreducible representations contained in $\Gamma^{\text{equiv.}}$. We can then specify which plane waves are transformed into one another by the elements of the group of the wave vector at the Γ point ($\mathbf{k} = 0$). From $\Gamma^{\text{equiv.}}$, we can find the irreducible representations of O_h which correspond to each empty lattice energy state and we can furthermore find the appropriate linear combination of plane wave states which correspond to a particular irreducible representation of O_h .

To calculate $\Gamma^{\text{equiv.}}$, we use the diagram in Fig. 12.2 which shows the cubic symmetry operations of point group O_h . The character table for O_h symmetry is given in Table 10.2 (see also Table A.30), where the column on the left gives the familiar solid state notation for the irreducible representations of O_h . In calculating $\chi^{\text{equiv.}}$ we consider that if a given plane wave goes into itself under

Table 12.1. Listing of the energy, degeneracy and the list of \mathbf{K}_{n_i} vectors for the five lowest energy levels for the simple cubic lattice at $\mathbf{k} = 0$

| (i) | $E_{\{000\}}(0) = 0$ | degeneracy=1 | $\mathbf{K}_{n_{\{000\}}} = 0$ | $(0,0,0)$ | $N^2 = 0$ |
|-------|---|---------------|---|--|-----------|
| (ii) | $E_{\{100\}}(0) = \frac{\hbar^2}{2m} \left(\frac{2\pi}{a}\right)^2$ | degeneracy=6 | $\mathbf{K}_{n_{\{100\}}} = \frac{2\pi}{a}$ | $(1, 0, 0)$ $(\bar{1}, 0, 0)$ $(0, 1, 0)$ $(0, \bar{1}, 0)$ $(0, 0, 1)$ $(0, 0, \bar{1})$ | $N^2 = 1$ |
| | Plane Wave States: $e^{\pm \frac{2\pi i x}{a}}, e^{\pm \frac{2\pi i y}{a}}, e^{\pm \frac{2\pi i z}{a}}$ | | | | |
| (iii) | $E_{\{110\}}(0) = 2 \frac{\hbar^2}{2m} \left(\frac{2\pi}{a}\right)^2$ | degeneracy=12 | $\mathbf{K}_{n_{\{110\}}} = \frac{2\sqrt{2}\pi}{a}$ | $(1, 1, 0)$ $(\bar{1}, 1, 0)$ $(1, 0, 1)$ $(\bar{1}, 0, 1)$ $(0, 1, 1)$ $(0, \bar{1}, 1)$ $(1, \bar{1}, 0)$ $(\bar{1}, \bar{1}, 0)$ $(1, 0, \bar{1})$ $(\bar{1}, 0, \bar{1})$ $(0, 1, \bar{1})$ $(0, \bar{1}, \bar{1})$ | $N^2 = 2$ |
| (iv) | $E_{\{111\}}(0) = 3 \frac{\hbar^2}{2m} \left(\frac{2\pi}{a}\right)^2$ | degeneracy=8 | $\mathbf{K}_{n_{\{111\}}} = \frac{2\sqrt{3}\pi}{a}$ | $(1, 1, 1)$ $(1, \bar{1}, 1)$ $(1, 1, \bar{1})$ $(\bar{1}, 1, 1)$ $(\bar{1}, \bar{1}, 1)$ $(1, \bar{1}, \bar{1})$ $(\bar{1}, 1, \bar{1})$ $(\bar{1}, \bar{1}, \bar{1})$ | $N^2 = 3$ |
| (v) | $E_{\{200\}}(0) = 4 \frac{\hbar^2}{2m} \left(\frac{2\pi}{a}\right)^2$ | degeneracy=6 | $\mathbf{K}_{n_{\{200\}}} = \frac{4\pi}{a}$ | $(2, 0, 0)$ $(\bar{2}, 0, 0)$ $(0, 2, 0)$ $(0, \bar{2}, 0)$ $(0, 0, 2)$ $(0, 0, \bar{2})$ | $N^2 = 4$ |

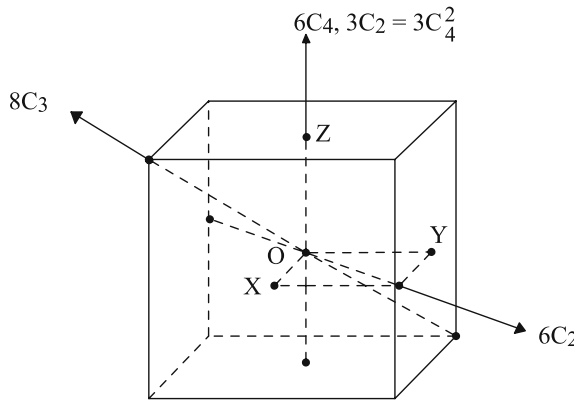


Fig. 12.2. Diagram of cubic symmetry operations

Table 12.2. Characters for the equivalence representation $\Gamma^{\text{equiv.}}$ for the five lowest energy levels of plane wave states labeled by $\{\mathbf{K}_{n_i}\}$ using the notation of Table 12.1

| \mathbf{K}_{n_i} | E | $3C_4^2$ | $6C_2$ | $8C_3$ | $6C_4$ | i | $3iC_4^2$ | $6iC_2$ | $8iC_3$ | $6iC_4$ | |
|--------------------|-----|----------|--------|--------|--------|-----|-----------|---------|---------|---------|---|
| {0,0,0} | 1 | 1 | 1 | 1 | 1 | 1 | 1 | 1 | 1 | 1 | Γ_1 |
| {1,0,0} | 6 | 2 | 0 | 0 | 2 | 0 | 4 | 2 | 0 | 0 | $\Gamma_1 + \Gamma_{12} + \Gamma_{15}$ |
| {1,1,0} | 12 | 0 | 2 | 0 | 0 | 0 | 4 | 2 | 0 | 0 | $\Gamma_1 + \Gamma_{12} + \Gamma_{15} + \Gamma_{25'} + \Gamma_{25}$ |
| {1,1,1} | 8 | 0 | 0 | 2 | 0 | 0 | 0 | 4 | 0 | 0 | $\Gamma_1 + \Gamma_2 + \Gamma_{15} + \Gamma_{25'}$ |
| {2,0,0} | 6 | 2 | 0 | 0 | 2 | 0 | 4 | 2 | 0 | 0 | $\Gamma_1 + \Gamma_{12} + \Gamma_{15}$ |

The irreducible representations for each energy level contained in $\Gamma^{\text{equiv.}}$ are listed in the right-hand column

the symmetry operations of O_h , a contribution of one is made to the character; otherwise a zero contribution is made. Using these definitions, we obtain the characters $\chi^{\text{equiv.}}$ and the characters for the various plane waves are given in Table 12.2, where the various plane wave states are denoted by one of the reciprocal lattice vectors which describe each of these states using the notation of Table 12.1. The reducible representations $\Gamma^{\text{equiv.}}$ for the various plane wave states in the simple cubic lattice are decomposed into irreducible representations of O_h and the results are given on the right-hand side of Table 12.2.

Once we know the irreducible representations of O_h that are contained in each of the degenerate levels of the simple cubic empty lattice, we can find appropriate linear combinations of these plane wave states which will then transform as the desired irreducible representations of O_h . When a cubic periodic potential is now applied, the degeneracy of these empty lattice states will be lifted in accordance with the decomposition of the reducible representations of $\Gamma^{\text{equiv.}}$ into the irreducible representations of O_h . Thus the proper linear combinations of the plane wave states will bring the secular equation of the nearly free electron model energy bands into block diagonal form. As an example of how this works, let us list the six appropriate linear combinations for

the $\{1, 0, 0\}$ set of reciprocal lattice vectors $\exp(\pm 2\pi i x/a)$, $\exp(\pm 2\pi i y/a)$, and $\exp(\pm 2\pi i z/a)$ which will bring the secular equation into block diagonal form:

$$\begin{aligned} \frac{1}{\sqrt{6}}[(1, 0, 0) + (\bar{1}, 0, 0) + (0, 1, 0) + (0, \bar{1}, 0) + (0, 0, 1) + (0, 0, \bar{1})] &\rightarrow \Gamma_1 \\ \left. \begin{aligned} \frac{1}{\sqrt{6}}[(1, 0, 0) + (\bar{1}, 0, 0) + \omega(0, 1, 0) + \omega(0, \bar{1}, 0) \\ + \omega^2(0, 0, 1) + \omega^2(0, 0, \bar{1})] \\ \frac{1}{\sqrt{6}}[(1, 0, 0) + (\bar{1}, 0, 0) + \omega^2(0, 1, 0) + \omega^2(0, \bar{1}, 0) \\ + \omega(0, 0, 1) + \omega(0, 0, \bar{1})] \end{aligned} \right\} &\rightarrow \Gamma_{12} \\ \left. \begin{aligned} \frac{1}{i\sqrt{2}}[(1, 0, 0) - (\bar{1}, 0, 0)] \\ \frac{1}{i\sqrt{2}}[(0, 1, 0) - (0, \bar{1}, 0)] \\ \frac{1}{i\sqrt{2}}[(0, 0, 1) - (0, 0, \bar{1})] \end{aligned} \right\} &\rightarrow \Gamma_{15}, \end{aligned} \tag{12.13}$$

in which we have used $(1, 0, 0)$ to denote $\exp(2\pi i x/a)$ and correspondingly for the other plane waves. Here $\omega = 2\pi i/3$ and we note that Γ_1 and Γ_{12} are even under inversion, but Γ_{15} is odd under inversion. Substituting

$$\begin{aligned} \frac{1}{2}[(1, 0, 0) + (\bar{1}, 0, 0)] &= \cos(2\pi x/a) \\ \frac{1}{2i}[(1, 0, 0) - (\bar{1}, 0, 0)] &= \sin(2\pi x/a), \end{aligned} \tag{12.14}$$

we obtain the following linear combinations of symmetrized plane waves from (12.13):

$$\begin{aligned} \frac{2}{\sqrt{6}} \left[\cos\left(\frac{2\pi x}{a}\right) + \cos\left(\frac{2\pi y}{a}\right) + \cos\left(\frac{2\pi z}{a}\right) \right] &\rightarrow \Gamma_1 \\ \left. \begin{aligned} \frac{2}{\sqrt{6}} \left[\cos\left(\frac{2\pi x}{a}\right) + \omega \cos\left(\frac{2\pi y}{a}\right) + \omega^2 \cos\left(\frac{2\pi z}{a}\right) \right] \\ \frac{2}{\sqrt{6}} \left[\cos\left(\frac{2\pi x}{a}\right) + \omega^2 \cos\left(\frac{2\pi y}{a}\right) + \omega \cos\left(\frac{2\pi z}{a}\right) \right] \end{aligned} \right\} &\rightarrow \Gamma_{12} \\ \left. \begin{aligned} \sqrt{2} \sin\left(\frac{2\pi x}{a}\right) \\ \sqrt{2} \sin\left(\frac{2\pi y}{a}\right) \\ \sqrt{2} \sin\left(\frac{2\pi z}{a}\right) \end{aligned} \right\} &\rightarrow \Gamma_{15}. \end{aligned} \tag{12.15}$$

The linear combinations of plane wave states given in (12.15) transform as irreducible representations of O_h , and bring the secular equation for $E(\mathbf{k} = 0)$ into block diagonal form. For example, using the six combinations of plane wave states given in (12.15), we bring the (6×6) secular equation for $\mathbf{K}_{n_i} = \{1, 0, 0\}$ into a (1×1) , a (2×2) and a (3×3) block, with no coupling between the blocks. Since there are three distinct energy levels, each corresponding to a different symmetry type, the introduction of a weak periodic potential will, in general, split the sixfold level into three levels with degeneracies 1 (Γ_1), 2 (Γ_{12}) and 3 (Γ_{15}). This procedure is used to simplify the evaluation of $E(\mathbf{k})$ and $\psi_k(\mathbf{r})$ in first-order degenerate perturbation theory. Referring to Table 12.1, (12.15) gives the symmetrized wave functions for the six $K_{\{1,0,0\}}$ vectors. The corresponding analysis can be done for the twelve $K_{\{110\}}$ vectors for the third lowest energy level, etc. The results for $E(\mathbf{k})$ for the empty lattice for the simple cubic group #221 are shown in Fig. 12.3 for the $\Gamma - X$ and $\Gamma - R$ axes.

The results obtained for the simple cubic lattice can be extended to other cubic lattices (see Appendix C). The space group numbers for common cubic crystals are as follows: simple cubic (#221), FCC (#225), diamond (#227), BCC (#229) (using standard references such as [54] and [58]). For the FCC lattice the (n_1, n_2, n_3) integers are all even or all odd so that the allowed \mathbf{K}_{n_i} vectors are $\{000\}$, $\{1, 1, 1\}$, $\{200\}$, etc. (see for example: [6] or [45]). For the BCC lattice, the integers $(n_1 + n_2 + n_3)$ must all sum to an even number, so that we can have reciprocal lattice \mathbf{K}_{n_i} vectors $\{000\}$, $\{1, 1, 0\}$, $\{200\}$, etc. Thus Table 12.1 can be used together with an analysis, such as given in this section, to obtain the proper linear combination of plane waves for the pertinent \mathbf{K}_{n_i} vectors for the various cubic groups. These issues are clarified in Problem 12.2. In this problem a weak periodic potential is considered. Then the character tables for the group of the wave vector in Appendix C will be of use.

To complete the discussion of the use of group theory for the solution of the electronic states of the empty lattice (or more generally the nearly free electron) model, we will next consider the construction of the symmetrized plane wave states $E(\mathbf{k})$ as we move away from $\mathbf{k} = 0$.

12.3 Symmetrized Plane Wave Solutions along the Δ -Axis

As an example of a nonzero \mathbf{k} vector, let us consider $E(\mathbf{k})$ as we move from $\Gamma(\mathbf{k} = 0)$ toward point $X[\mathbf{k} = \pi/a(1, 0, 0)]$ along the $(1, 0, 0)$ axis (labeled Δ in Figs. 10.3 and 12.4). The appropriate point group of the wave vector \mathbf{k} is C_{4v} , with the character table given in Table 10.3 (see also Table A.16).

In Table 12.3 are listed the characters for the three irreducible representations of $\mathbf{K}_{n_i} = \{1, 0, 0\}(2\pi/a)$ corresponding for the simple cubic empty lattice dispersion relations at $\mathbf{k} = 0$ and O_h symmetry. We consider these

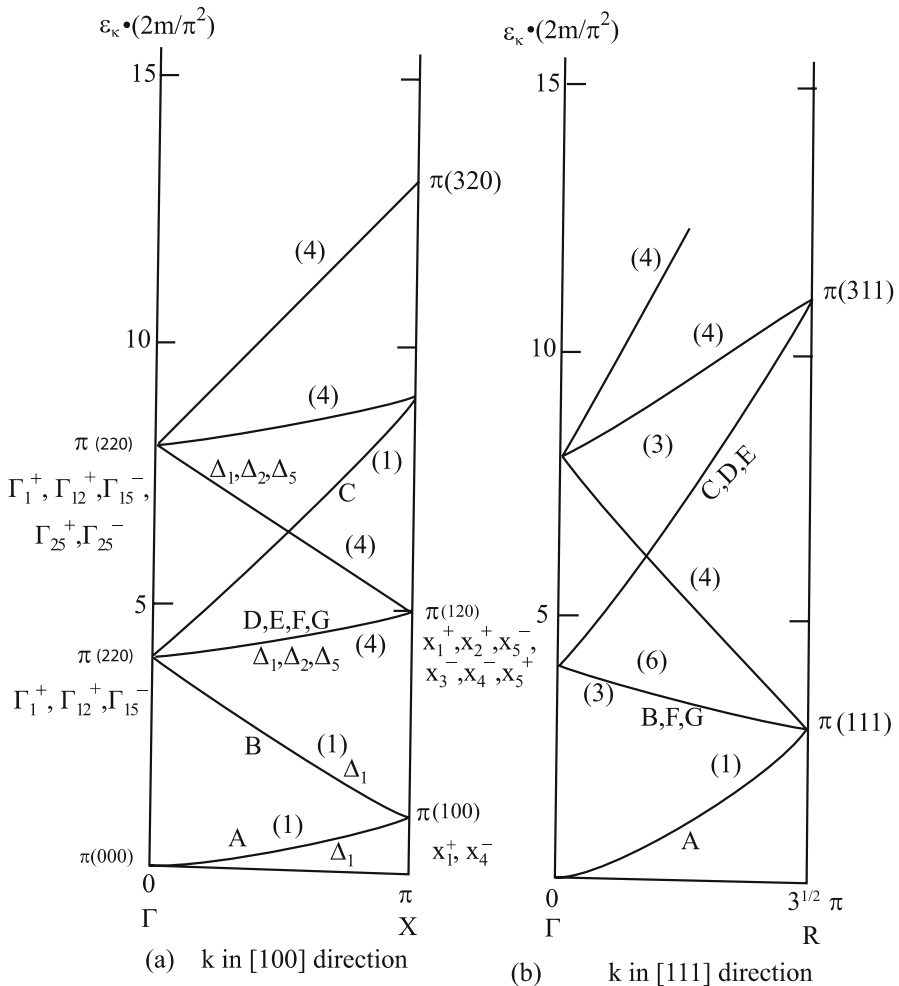


Fig. 12.3. Diagram of the empty lattice energy levels along (a) Γ -X and (b) Γ -R for the simple cubic lattice #221. See the text for the symmetries of the energy bands that are degenerate at the high symmetry points of the simple cubic empty lattice model

as reducible representations of point group C_{4v} . The decomposition of these three reducible representations in C_{4v} point group symmetry is indicated on the right of Table 12.3. This decomposition yields the compatibility relations (see Sect. 10.7):

$$\begin{aligned}
 \Gamma_1 &\rightarrow \Delta_1 \\
 \Gamma_{12} &\rightarrow \Delta_1 + \Delta_2 \\
 \Gamma_{15} &\rightarrow \Delta_1 + \Delta_5 .
 \end{aligned} \tag{12.16}$$

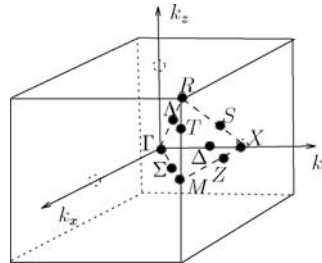


Fig. 12.4. Brillouin zone for a simple cubic lattice showing high symmetry points

Table 12.3. Characters for the three symmetrized plane waves (12.16) corresponding to the six plane waves $\mathbf{K}_{n_i} = (2\pi/a)(1, 0, 0)$ in Table 12.1^{a,b}

| C_{4v} (4mm) | E | C_2 | $2C_4$ | $2\sigma_v$ | $2\sigma_d$ |
|----------------|-----|-------|--------|-------------|-----------------------|
| Γ_1 | 1 | 1 | 1 | 1 | Δ_1 |
| Γ_{12} | 2 | 2 | 0 | 2 | $\Delta_1 + \Delta_2$ |
| Γ_{15} | 3 | -1 | 1 | 1 | $\Delta_1 + \Delta_5$ |

^a The characters for each symmetrized plane wave at $k = 0$ with O_h symmetry is considered as a reducible representation in the $C_{4v}(4mm)$ group which is appropriate for the wave vector \mathbf{k} along a cubic axis. The decomposition of the reducible representations into their irreducible components along the Δ axis are indicated using the notation of the character table for C_{4v}

^b The operation σ_v denotes iC_2^{010} and iC_2^{001} , while σ_d denotes iC_2^{011} and $iC_2^{01\bar{1}}$

In the character table (Table 12.3), the main symmetry axis is the x -axis, so that the basis functions that should be used (see Table A.16) require the transformation: $x \rightarrow y$, $y \rightarrow z$, $z \rightarrow x$. The symmetry axis $\sigma_v = iC_2^{010}$ denotes the mirror planes $y = 0$ and $z = 0$, while $\sigma_d = iC_2^{011}$ denotes the diagonal (011) planes, with all symmetry operations referring to reciprocal space, since we are considering the group of the wave vector at a point along the Δ axis. The results of (12.16) are of course in agreement with the compatibility relations given in Sect. 10.7 for the simple cubic structure. Compatibility relations of this type can be used to obtain the degeneracies and symmetries for all the levels at the Δ point, starting from the plane wave solution at $\mathbf{k} = 0$. A similar approach can be used to obtain the symmetries and degeneracies as we move away from $\mathbf{k} = 0$ in other directions. For an arbitrary crystal structure we have to use standard references or websites [54] to construct the compatibility relations using the tables for the group of the wave vector given in this reference. Some illustrative examples are given in Appendix C.

12.4 Plane Wave Solutions at the X Point

As we move in the Brillouin zone from a point of high symmetry to a point of lower symmetry, the solution using the compatibility relations discussed

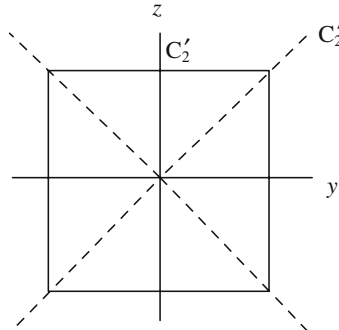


Fig. 12.5. Diagram of a square showing the twofold axes normal to the principal C_4 symmetry axis which are pertinent to point group D_{4h}

in Sect. 12.3 is unique. On the other hand, when going from a point of lower symmetry like a Δ point to one of higher symmetry, the solution from the compatibility relations is not unique, and we must then go back to consideration of the equivalence transformation. An example of this situation occurs when we go from the Δ point (see Table C.8) to the X -point (D_{4h} symmetry and Table C.15), which has higher symmetry than the Δ point (C_{4v} symmetry). The appropriate character table for the group of the wave vector at the X point (see Table C.15 in Appendix C) is $D_{4h} = D_4 \otimes i$ shown in Table A.18. At the X -point, the nearly free electron solutions for the simple cubic lattice given by (12.7) become:

$$E\left(\mathbf{k} = \frac{\pi}{a}\hat{x}\right) = \frac{\hbar^2}{2m} \left(\frac{2\pi}{a}\right)^2 \left[\left(\frac{1}{2} + n_1\right)^2 + n_2^2 + n_3^2 \right]. \quad (12.17)$$

The lowest energy level at the X -point is

$$E_1\left(\mathbf{k} = \frac{\pi}{a}\hat{x}\right) = \frac{\hbar^2}{2m} \left(\frac{2\pi}{a}\right)^2 \left(\frac{1}{4}\right). \quad (12.18)$$

The pertinent plane waves which contribute to the energy level E_1 in (12.18) correspond to \mathbf{K}_{n_i} vectors

$$\mathbf{K}_{n_i} = (0, 0, 0)$$

$$\mathbf{K}_{n_i} = \frac{2\pi}{a}(\bar{1}, 0, 0).$$

We will now find $\chi^{\text{equiv.}}$ for these plane waves, using the symmetry operations in Fig. 12.5 and in the character table for D_{4h} in which we use the transformation $x \rightarrow y$, $y \rightarrow z$, $z \rightarrow x$ to obtain the proper X -point (Table 12.4). We note that the plane wave labeled $\mathbf{K}_{n_i} = (0, 0, 0)$ in Table 12.1 yields a plane wave $e^{(\pi i/a)x}$ at the X -point while the plane wave labeled

Table 12.4. Character table for the point group D_4 , showing the solid state notation in the right-hand column

| D_4 (422) | | E | $C_2 = C_4^2$ | $2C_4$ | $2C_2'$ | $2C_2''$ | |
|------------------|------------------------|-------|---------------|--------|---------|----------|-------|
| $x^2 + y^2, z^2$ | | A_1 | 1 | 1 | 1 | 1 | X_1 |
| R_z, z | | A_2 | 1 | 1 | 1 | -1 | X_4 |
| $x^2 - y^2$ | | B_1 | 1 | 1 | -1 | 1 | X_2 |
| xy | | B_2 | 1 | 1 | -1 | -1 | X_3 |
| (xz, yz) | $(x, y) \\ (R_x, R_y)$ | E | 2 | -2 | 0 | 0 | X_5 |

With inversion $D_{4h} = D_4 \otimes i$

Table 12.5. Characters for the two plane waves with energy E_1 for the simple cubic empty lattice electron dispersion relations at the X point (D_{4h} symmetry)

| E | C_2 | $2C_4$ | $2C_2'$ | $2C_2''$ | i | iC_2 | $2iC_4$ | $2iC_2'$ | $2iC_2''$ | |
|---------------------|-------|--------|---------|----------|-----|--------|---------|----------|-----------|-------------------|
| $\exp(\pm\pi ix/a)$ | 2 | 2 | 2 | 0 | 0 | 0 | 0 | 0 | 2 | $A_{1g} + A_{2u}$ |

$\mathbf{K}_{n_i} = (2\pi/a)(\bar{1}, 0, 0)$ in Table 12.1 yields a plane wave $e^{(\frac{\pi}{a}ix - \frac{2\pi}{a}ix)} = e^{-\frac{\pi}{a}ix}$ and both have energies $E_1 = \hbar^2/2m(\frac{2\pi}{a})^2(1/4)$. The plane waves denoted by $\mathbf{K}_{n_i} = (0, 0, 0)$ and $\mathbf{K}_{n_i} = 2\pi/a(\bar{1}, 0, 0)$ form partners of a reducible representation, and the characters for these two plane waves in the equivalence transformation $\Gamma^{\text{equiv.}}$ are here shown to yield (Table 12.5):

$$\Gamma^{\text{equiv.}} = X_1^+ + X_4^- . \quad (12.19)$$

We thus obtain irreducible representations with X_1^+ and X_4^- symmetries for the lowest X -point level so that a periodic potential will split the degeneracy of these levels at the X -point. In this case the level separation becomes $2|V_{\mathbf{K}_{n_i}}|$ (see for example [6, 45]) where $\mathbf{K}_{n_i} = (2\pi/a)(\bar{1}, 0, 0)$. The appropriate linear combination of plane waves corresponding to the X_1^+ and X_4^- irreducible representations are

$$\begin{aligned} X_1^+ \text{ symmetry: } & (0, 0, 0) + (\bar{1}, 0, 0) \rightarrow 2 \cos \frac{\pi}{a} x \\ X_4^- \text{ symmetry: } & (0, 0, 0) - (\bar{1}, 0, 0) \rightarrow 2 \sin \frac{\pi}{a} x . \end{aligned} \quad (12.20)$$

and each of the X_1^+ and X_4^- levels is nondegenerate. Referring to (12.17), the next lowest energy level at the X point is

$$E_2 \left(\mathbf{k} = \frac{\pi}{a} \hat{x} \right) = \frac{\hbar^2}{2m} \left(\frac{2\pi}{a} \right)^2 \left(\frac{5}{4} \right) . \quad (12.21)$$

Table 12.6. Characters for the plane waves comprising state with energy E_2 at the X point (D_{4h} symmetry) for the simple cubic empty lattice electronic energy bands

| | E | C_2 | $2C_4$ | $2C'_2$ | $2C''_2$ | i | iC_2 | $2iC_4$ | $2iC'_2$ | $2iC''_2$ |
|-----------------------|-----|-------|--------|---------|----------|-----|--------|---------|----------|-----------|
| (12.22) | 8 | 0 | 0 | 0 | 0 | 0 | 0 | 0 | 4 | 0 |
| $\exp(\pm 2\pi iy/a)$ | 4 | 0 | 0 | 2 | 0 | 0 | 4 | 0 | 2 | 0 |
| $\exp(\pm 2\pi iz/a)$ | | | | | | | | | | |

The eight pertinent plane waves for this energy level correspond to the \mathbf{K}_{n_i} vectors

$$\begin{aligned}\mathbf{K}_{n_i} &= \frac{2\pi}{a}(0, 1, 0), \frac{2\pi}{a}(0, \bar{1}, 0), \frac{2\pi}{a}(0, 0, 1), \frac{2\pi}{a}(0, 0, \bar{1}) \\ \mathbf{K}_{n_i} &= \frac{2\pi}{a}(\bar{1}, 1, 0), \frac{2\pi}{a}(\bar{1}, \bar{1}, 0), \frac{2\pi}{a}(\bar{1}, 0, 1), \frac{2\pi}{a}(\bar{1}, 0, \bar{1})\end{aligned}$$

in Table 12.1. More explicitly, the eight plane waves corresponding to these \mathbf{K}_{n_i} vectors are

$$\begin{aligned}\exp\left\{\frac{\pi ix}{a} + \frac{2\pi iy}{a}\right\}, \quad &\exp\left\{\frac{\pi ix}{a} - \frac{2\pi iy}{a}\right\}, \\ \exp\left\{\frac{\pi ix}{a} + \frac{2\pi iz}{a}\right\}, \quad &\exp\left\{\frac{\pi ix}{a} - \frac{2\pi iz}{a}\right\}, \\ \exp\left\{-\frac{\pi ix}{a} + \frac{2\pi iy}{a}\right\}, \quad &\exp\left\{-\frac{\pi ix}{a} - \frac{2\pi iy}{a}\right\}, \\ \exp\left\{-\frac{\pi ix}{a} + \frac{2\pi iz}{a}\right\}, \quad &\exp\left\{-\frac{\pi ix}{a} - \frac{2\pi iz}{a}\right\}.\end{aligned}\quad (12.22)$$

To find the characters for the equivalence transformation for the eight plane waves of (12.22) we use the character table for D_{4h} and Fig. 12.5. The results for several pertinent plane wave combinations are given in Table 12.6. The reducible representation for the eight plane waves given by (12.22) yields the following X -point irreducible representations

$$X_1^+ + X_2^+ + X_5^- + X_4^- + X_3^- + X_5^+.\quad (12.23)$$

The same result can be obtained by considering the $e^{\pm\pi ix/a}$ functions as common factors of the $e^{\pm 2\pi iy/a}$ and $e^{\pm 2\pi iz/a}$ functions. The $\chi^{\text{equiv.}}$ for the four $e^{\pm 2\pi iy/a}$ and $e^{\pm 2\pi iz/a}$ plane waves is also tabulated in Table 12.6. The $e^{\pm\pi ix/a}$ functions transform as $X_1^+ + X_4^-$ (see (12.19)), and the four functions $e^{\pm 2\pi iy/a}$ and $e^{\pm 2\pi iz/a}$ transform as $X_1^+ + X_2^+ + X_5^-$. If we now take the direct product indicated in (12.24), we obtain

$$(X_1^+ + X_4^-) \otimes (X_1^+ + X_2^+ + X_5^-) = X_1^+ + X_2^+ + X_5^- + X_4^- + X_3^- + X_5^+ \quad (12.24)$$

in agreement with the result of (12.23). The proper linear combination of the eight plane waves which transform as irreducible representations of the D_{4h} point symmetry group for the second lowest X point level is found from the \mathbf{K}_{n_i} vectors given in (16.16):

$$\begin{aligned}
 X_1^+ : & (0, 1, 0) + (0, \bar{1}, 0) + (0, 0, 1) + (0, 0, \bar{1}) \\
 & + (\bar{1}, 1, 0) + (\bar{1}, \bar{1}, 0) + (\bar{1}, 0, 1) + (\bar{1}, 0, \bar{1}) \\
 X_4^- : & (0, 1, 0) + (0, \bar{1}, 0) + (0, 0, 1) + (0, 0, \bar{1}) \\
 & - (\bar{1}, 1, 0) - (\bar{1}, \bar{1}, 0) - (\bar{1}, 0, 1) - (\bar{1}, 0, \bar{1}) \\
 X_2^+ : & (0, 1, 0) - (0, 0, 1) + (0, \bar{1}, 0) - (0, 0, \bar{1}) \\
 & + (\bar{1}, 1, 0) - (\bar{1}, 0, 1) + (\bar{1}, \bar{1}, 0) - (\bar{1}, 0, \bar{1}) \\
 X_3^- : & (0, 1, 0) - (0, 0, 1) + (0, \bar{1}, 0) - (0, 0, \bar{1}) \\
 & - (\bar{1}, 1, 0) + (\bar{1}, 0, 1) - (\bar{1}, \bar{1}, 0) + (\bar{1}, 0, \bar{1}) \\
 X_5^- : & (0, 1, 0) - (0, \bar{1}, 0) + (\bar{1}, 1, 0) - (\bar{1}, \bar{1}, 0) \} \text{ two partners} \\
 & (0, 0, 1) - (0, 0, \bar{1}) + (\bar{1}, 0, 1) - (\bar{1}, 0, \bar{1}) \} \text{ two partners} \\
 X_5^+ : & (0, 1, 0) - (0, \bar{1}, 0) - (\bar{1}, 1, 0) + (\bar{1}, \bar{1}, 0) \} \text{ two partners}, \quad (12.25) \\
 & (0, 0, 1) - (0, 0, \bar{1}) - (\bar{1}, 0, 1) + (\bar{1}, 0, \bar{1}) \} \text{ two partners}
 \end{aligned}$$

in which the plane waves are denoted by their corresponding \mathbf{K}_{n_i} vectors. We note that the wave vector $\mathbf{K}_{n_i} = (2\pi/a)(0, 1, 0)$ gives rise to a plane wave $\exp[(\pi i x/a) + (2\pi i y/a)]$. Likewise the wave vector $\mathbf{K}_{n_i} = (2\pi/a)(\bar{1}, 1, 0)$ gives rise to a plane wave $\exp[(\pi i x/a) - (2\pi i x/a) + (\pi i y/a)]$. Using this notation we find that the appropriate combinations of plane waves corresponding to (12.25) are

$$\begin{aligned}
 X_1^+ : & \cos \frac{\pi x}{a} \left(\cos \frac{2\pi y}{a} + \cos \frac{2\pi z}{a} \right) \\
 X_4^- : & \sin \frac{\pi x}{a} \left(\cos \frac{2\pi y}{a} + \cos \frac{2\pi z}{a} \right) \\
 X_2^+ : & \cos \frac{\pi x}{a} \left(\cos \frac{2\pi y}{a} - \cos \frac{2\pi z}{a} \right) \\
 X_3^- : & \sin \frac{\pi x}{a} \left(\cos \frac{2\pi y}{a} - \cos \frac{2\pi z}{a} \right) \\
 X_5^- : & \begin{cases} \cos \frac{\pi x}{a} \sin \frac{2\pi y}{a} \\ \cos \frac{\pi x}{a} \sin \frac{2\pi z}{a} \end{cases} \} \text{ two partners} \\
 X_5^+ : & \begin{cases} \sin \frac{\pi x}{a} \sin \frac{2\pi y}{a} \\ \sin \frac{\pi x}{a} \sin \frac{2\pi z}{a} \end{cases} \} \text{ two partners}. \quad (12.26)
 \end{aligned}$$

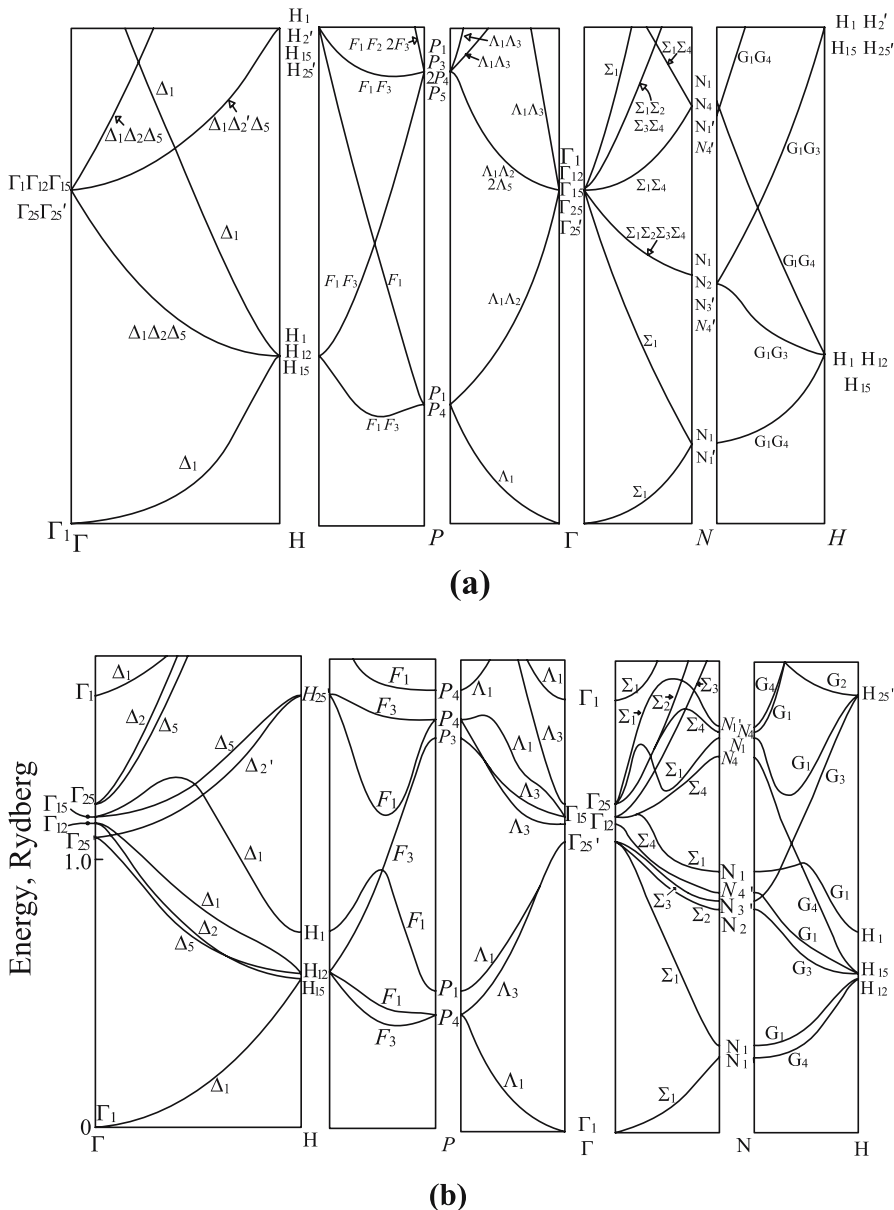


Fig. 12.6. (a) $E(\mathbf{k})$ for a BCC lattice in the empty lattice approximation, $V \equiv 0$. (b) $E(\mathbf{k})$ for sodium, showing the effect of a weak periodic potential in lifting accidental band degeneracies at $k = 0$ and at the zone boundaries (high symmetry points) in the Brillouin zone. Note that the splittings are quite different for the various bands and at different high symmetry points. The character tables in Appendix C for the group of the wave vector for the BCC lattice are useful for solving the problem of the electronic structure for a nearly free electron model for a BCC alkali metal

A summary of the energy levels and symmetries along $\Gamma - X$ for the simple cubic lattice is given in Fig. 12.3(a). A similar procedure is used to find the degeneracies and the symmetrized linear combination of plane waves for any of the energy levels at each of the high symmetry points in the Brillouin zone. We show for example results in Fig. 12.3(b) also for the empty lattice bands along $\Gamma - R$. The corresponding results can be obtained by this same procedure for the FCC and BCC lattices as well (see Figs. 12.1 and 12.6). Some elaboration of these concepts is found in Problems 12.2 and 12.6.

In the following section we will consider the effect of nonsymmorphic operations on plane waves.

12.5 Effect of Glide Planes and Screw Axes

Up to this point we have considered only symmorphic space groups where the symmetry operations of the group of the wave vectors are simply point group operations. The main effect of the glide planes and screw axes in nonsymmorphic space groups on the group of the wave vector is to cause energy bands to stick together along some of the high symmetry points and axes in the Brillouin zone. We first illustrate this phenomenon using the 2D space group $p2mg$ (#7) which has a twofold axis, mirror planes normal to the x -axis at $x = 1/4a$ and $x = 3/4a$, and a glide plane g parallel to the x -axis with a translation distance $a/2$. In addition, group $p2mg$ has inversion symmetry. Suppose that $X(x, y)$ is a solution to Schrödinger's equation at the X point $\mathbf{k}_X = \pi/a(1, 0)$ (see Fig. 12.7).

In the two-dimensional case for the space group $p2mg$, the mirror glide operation g implies

$$gX(x, y) = X\left(x + \frac{1}{2}a, -y\right), \quad (12.27)$$

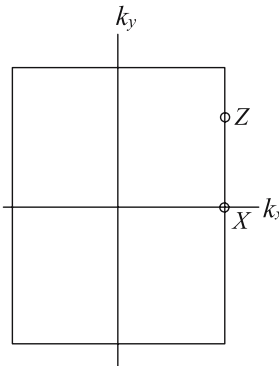


Fig. 12.7. Brillouin zone for a rectangular 2D lattice [such as $p2mg$ (#7)]

while inversion i implies

$$iX(x, y) = X(-x, -y). \quad (12.28)$$

The mirror plane m at $x = a/4$ implies

$$mX(x, y) = X\left(-x + \frac{1}{2}a, y\right), \quad (12.29)$$

so that

$$gX(x, y) = m iX(x, y), \quad (12.30)$$

where m denotes reflection in a mirror plane and i denotes inversion. Since $i^2X(x, y) = X(x, y)$ and $m^2X(x, y) = X(x, y)$, we would expect from (12.30) that

$$g^2X(x, y) = X(x, y). \quad (12.31)$$

But direct application of the glide operation twice yields for $k_x = \pi/a$,

$$g^2X(x, y) = X(x + a, y) = e^{ik_x a}X(x, y) = e^{\pi i}X(x, y) = -X(x, y), \quad (12.32)$$

which contradicts (12.31). This contradiction is resolved by having the solutions that $\pm X(x, y)$ stick together at the X point.

In fact, if we employ time reversal symmetry (to be discussed in Chap. 16), we can show that bands $\pm \Phi_Z(x, y)$ stick together along the entire Brillouin zone edge for all Z points, i.e., $(\pi/a, k_y)$ (see Fig. 12.7). Thus in addition to the degeneracies imposed by the group of the wave vector, other symmetry relations can in some cases cause energy bands to stick together at high symmetry points and axes.

The same situation also arises for 3D space groups. Some common examples where energy bands stick together are on the hexagonal face of the hexagonal close-packed structure (space group #194, see Brillouin zone in Fig. 12.8(a)), and the square face in the diamond structure (#227) for which the Brillouin zone is given in Fig. 12.8(b). For the case of the hexagonal close packed structure, there is only a single translation $\tau = (c/2)(0, 0, 1)$ connected with nonsymmorphic operations in space group #194. The character table for the group of the wave vector at the A point (see Table C.26) shows that the bands stick together, i.e., there are no nondegenerate levels at the A point. To illustrate this point, we give in Tables C.24 and C.26 the character tables for the Γ point and the A point, respectively, for space group #194.

For the case of the diamond structure (space group #227), Miller and Love [54] show that there are three different translation vectors $(a/4)(1, 1, 0)$, $(a/4)(0, 1, 1)$, and $(a/4)(1, 0, 1)$ can be used to describe the nonsymmorphic aspects of the diamond structure [54]. The reason why these translations differ from those used in this section (see Fig. 10.6) is the selection of a different origin for the unit cell. In Miller and Love [54] the origin is selected to lie

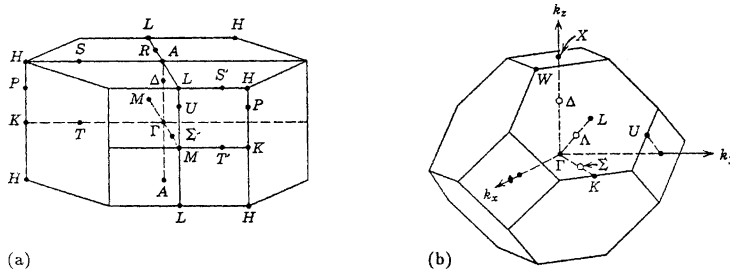


Fig. 12.8. Brillouin zone for (a) the hexagonal close packed structure, D_{6h} , #194 and (b) the FCC structure (e.g., diamond #227) in which the high symmetry axes are emphasized (see also Fig. C.5).

halfway between the two inequivalent lattice points, which is at $a/8(1, 1, 1)$ or at $a/8(\bar{1}, \bar{1}, \bar{1})$, so that the inversion operation takes the white sublattice into a black sublattice, and vice versa. In contrast, we have taken the origin in Sect. 10.8 to coincide with the origin of the white sublattice so that in this case the space group operation for inversion contains a translation by $\tau = (a/4)(1, 1, 1)$ and is denoted by $\{i|\tau\}$.

In Table C.17, we show the character tables for the group of the wave vector appropriate for the diamond structure at the Γ point. The behavior of $E(\mathbf{k})$ at $\mathbf{k} = 0$ for the diamond structure is similar to that for a symmorphic cubic like the FCC structure. Furthermore, at the L -point in the Brillouin zone, the structure factor does not vanish:

$$\sum_j e^{i\mathbf{K}_{nL} \cdot \mathbf{r}_j} = 1 + e^{i2\pi/a(1,1,1) \cdot a/4(1,1,1)} = 1 - i \neq 0, \quad (12.33)$$

and the behavior of $E(\mathbf{k})$ is expected to be similar to the behavior of a symmorphic cubic space group like that for the FCC structure, space group #225. Thus for the nonsymmorphic diamond structure, some high symmetry points behave normally (such as the L point), while for other points (such as the X point as we discuss below), the energy bands stick together.

Next we show that the nonsymmorphic nature of the diamond structure strongly affects the empty lattice energy band structure and is totally an effect of symmetry considerations. Application of the empty lattice plane wave energies for the first few lowest energy states at $k = 0$ (Γ point), the L -point, and the X -point are shown in Table 12.7, and the corresponding empty lattice $E(\mathbf{k})$ diagram is shown in Fig. 12.9. The twofold, fourfold and eightfold degenerate levels at the X -point are noted with the empty lattice nondegenerate bands coming into the X -point with equal and opposite slopes.

At the X point (Table 10.12) we see that there are no nondegenerate levels so that levels stick together (see Sect. 10.8). In the $E(\mathbf{k})$ diagram for the diamond structure (see Fig. 12.10 for $E(\mathbf{k})$ for Ge), we see that all the bands stick together at the X point, all being either twofold or fourfold degenerate,

Table 12.7. Classification of the empty lattice eigenvalues at the symmetry points Γ , L and X of the diamond structure (#227)

| | number of plane waves | empty lattice eigenvalues in units of $(\hbar^2/2m)(4\pi^2/a^2)$ | irreducible representations |
|---|--------------------------|--|---|
| point Γ | 1 | (0,0,0) | Γ_1 |
| $\mathbf{k} = (0, 0, 0)$ | 8 | (1,1,1) | $\Gamma_1 \quad \Gamma'_{25} \quad \Gamma_{15} \quad \Gamma'_2$ |
| | 6 | (2,0,0) | $\Gamma'_{25} \quad \Gamma'_{12} \quad \Gamma'_2$ |
| | 12 | (2,2,0) | $\Gamma_1 \quad \Gamma'_{25} \quad \Gamma_{15} \quad \Gamma_{12} \quad \Gamma_{25}$ |
| point L | 2 | $(\frac{1}{2}, \frac{1}{2}, \frac{1}{2})$ | $L_1 \quad L'_2$ |
| $\mathbf{k} = \frac{2\pi}{a} (\frac{1}{2}, \frac{1}{2}, \frac{1}{2})$ | 6 | $(\frac{3}{2}, \frac{1}{2}, \frac{1}{2})$ | $L_1 \quad L'_2 \quad L_3 \quad L'_3$ |
| | 6 | $(\frac{1}{2}, \frac{3}{2}, \frac{3}{2})$ | $L_1 \quad L'_2 \quad L_3 \quad L'_3$ |
| | 6 | $(\frac{5}{2}, \frac{1}{2}, \frac{1}{2})$ | $L_1 \quad L'_2 \quad L_3 \quad L'_3$ |
| | 2 | $(\frac{3}{2}, \frac{3}{2}, \frac{3}{2})$ | $L_1 \quad L'_2$ |
| point X | 2 | (1,0,0) | X_1 |
| $\mathbf{k} = \frac{2\pi}{a} (1, 0, 0)$ | 4 | (0,1,1) | $X_1 \quad X_4$ |
| | 8 | (1,2,0) | $X_1 \quad X_2 \quad X_3 \quad X_4$ |
| | 8 | (2,1,1) | $2X_1 \quad X_3 \quad X_4$ |

as seen in the character table for the X point in Table 10.12 and in the empty lattice model in Table 12.7. The plane wave basis functions for the irreducible representations X_1 , X_2 , X_3 and X_4 for the diamond structure are listed in Table 12.8 and are consistent with these symmetry requirements.

Because of the nonsymmorphic features of the diamond structure, the energy bands at the X point behave differently from the bands at high symmetry points where “essential” degeneracies occur. For the case of essential degeneracies, the energy bands $E(\mathbf{k})$ come into the Brillouin zone with zero slope. For the X point in the diamond structure, the $E(\mathbf{k})$ dispersion relations with X_1 and X_2 symmetry in general have a nonzero slope, but rather the slopes are equal and opposite for the two levels X_1 and X_2 that stick together. The physical reason for this behavior is that the X-ray structure factor for the Bragg reflection associated with the X point in the Brillouin zone for the diamond structure vanishes and thus no energy discontinuity in $E(\mathbf{k})$ is expected, nor is it observed upon small variation of k_x relative to the X point. Explicitly the structure factor [45] at the X point for the diamond structure is

$$\sum_j e^{i\mathbf{K}_{nX} \cdot \mathbf{r}_j} = 1 + e^{i4\pi/a(1,0,0) \cdot a/4(1,1,1)} = 1 - 1 \equiv 0, \quad (12.34)$$

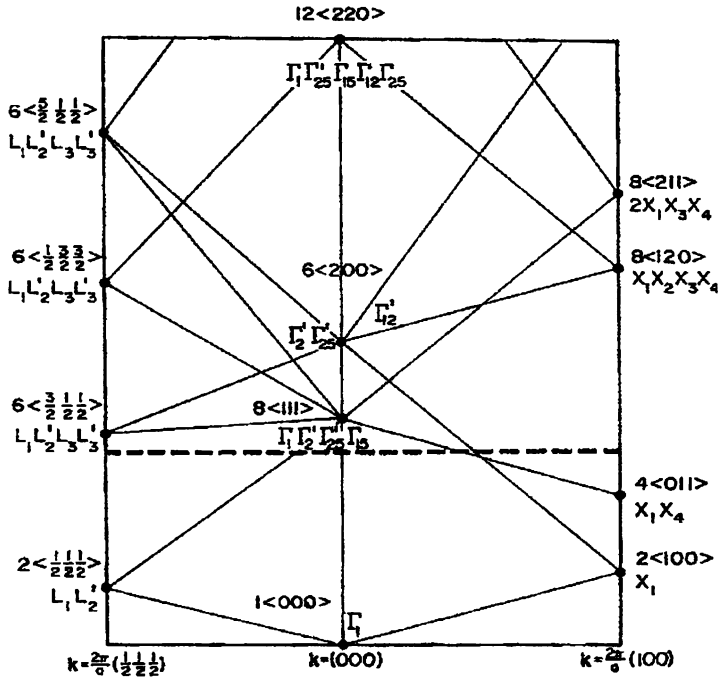


Fig. 12.9. Schematic diagram which indicates the symmetry types of the empty lattice energy levels along $\Gamma - L$ and $\Gamma - X$ for the diamond structure, space group #227 [10]. The dashed horizontal line indicates the Fermi level on the empty lattice model for four electrons per atom, indicating that the empty lattice model gives a semimetal for the diamond structure for group IV materials. We therefore conclude that the empty lattice model is not a good approximation for semiconductors crystallizing in the diamond structure

where $K_{n_X} = (2\pi/a)(1,0,0)$ for the FCC structure from Table 12.1 and the sum is over the two inequivalent atom sites in the unit cell [one is at the origin and the other is at $(a/4)(1,1,1)$]. The vanishing of this structure factor for the reciprocal lattice vector $\mathbf{K}_{n_X} = (4\pi/a)(1,0,0)$ associated with the X point implies that there is no Fourier component of the periodic potential to split the degeneracy caused by having two atoms of the same chemical species per unit cell and thus the energy bands at the X -point stick together. In fact, the structure factor in the diamond structure vanishes for all points on the square face of the FCC Brillouin zone (see Fig. 12.8(b)), and we have energy bands sticking together across the entire square face. A comparison between the empty lattice energy band symmetries for the X -point of the FCC lattice (Fig. 12.1) and for the diamond structure (Fig. 12.9) highlights the effect of the nonsymmorphic symmetry on the electronic structure near the X -point but not near the L -point.

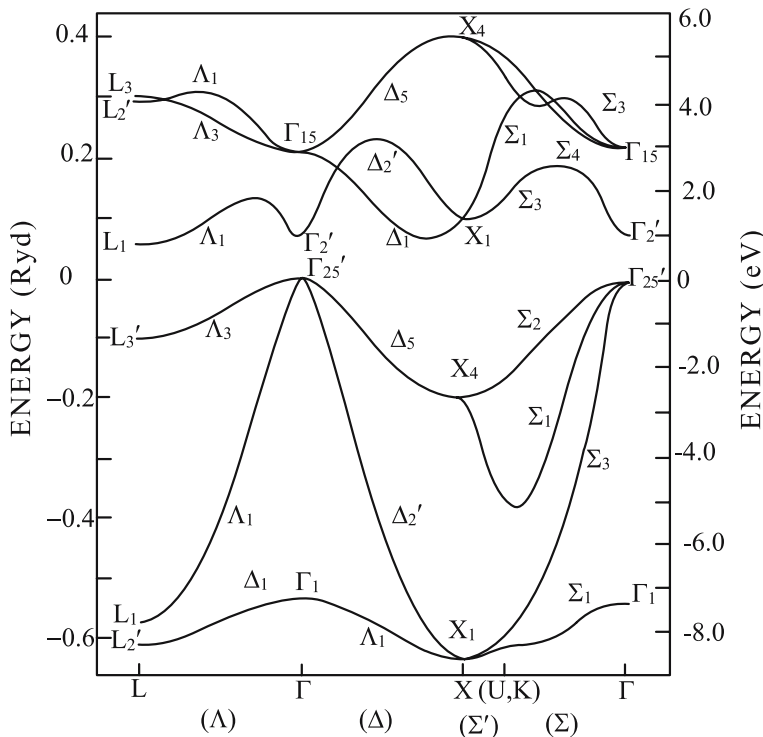


Fig. 12.10. Energy band structure for germanium as an example of a material which is described by a nonsymmorphic space group #227 for the diamond structure. Note that the energy bands stick together at the X point as predicted by group theory (see text). In this diagram the spin-orbit interaction is neglected (see the treatment of double groups in Chap. 14)

To get further insight into how the energy bands at the X -point stick together, consider the operations of the inversion symmetry operator $\{i|\boldsymbol{\tau}_d\}$ on the basis functions for the X -point listed in Table 12.8. To treat the effect of $\{i|\boldsymbol{\tau}_d\}$ on the various functions of (x, y, z) in Table 12.8, consider first the action of $\{i|\boldsymbol{\tau}_d\}$ on the coordinates:

$$\{i|\boldsymbol{\tau}_d\} \begin{pmatrix} x \\ y \\ z \end{pmatrix} = \begin{pmatrix} -x + (a/4) \\ -y + (a/4) \\ -z + (a/4) \end{pmatrix}. \quad (12.35)$$

Then using the trigonometric identity:

$$\begin{aligned} \cos(\alpha + \beta) &= \cos \alpha \cos \beta - \sin \alpha \sin \beta \\ \sin(\alpha + \beta) &= \sin \alpha \cos \beta + \cos \alpha \sin \beta, \end{aligned} \quad (12.36)$$

Table 12.8. Plane wave basis functions for the group of the wave vector for the X-point $[2\pi/a(1, 0, 0)]$ for the nonsymmorphic diamond structure

| representation | function |
|----------------|--|
| X_1 | $x_{11} = \cos \frac{2\pi}{a}x$ |
| | $x_{12} = \sin \frac{2\pi}{a}x$ |
| X_2 | $x_{21} = \cos \frac{2\pi}{a}x \left[\cos \frac{4\pi}{a}y - \cos \frac{4\pi}{a}z \right]$ |
| | $x_{22} = \sin \frac{2\pi}{a}x \left[\cos \frac{4\pi}{a}y - \cos \frac{4\pi}{a}z \right]$ |
| X_3 | $x_{31} = \sin \frac{4\pi}{a}(y+z) \left[\cos \frac{2\pi}{a}x + \sin \frac{2\pi}{a}x \right]$ |
| | $x_{32} = \sin \frac{4\pi}{a}(y-z) \left[\cos \frac{2\pi}{a}x - \sin \frac{2\pi}{a}x \right]$ |
| X_4 | $x_{41} = \sin \frac{4\pi}{a}(y-z) \left[\cos \frac{2\pi}{a}x + \sin \frac{2\pi}{a}x \right]$ |
| | $x_{42} = \sin \frac{4\pi}{a}(y+z) \left[\cos \frac{2\pi}{a}x - \sin \frac{2\pi}{a}x \right]$ |

we obtain for the effect of $\{i|\boldsymbol{\tau}_d\}$ on the various trigonometric functions in Table 12.8:

$$\begin{aligned}
 \{i|\boldsymbol{\tau}_d\} \cos\left(\frac{2\pi}{a}x\right) &= \cos\left(\frac{2\pi}{a}(-x) + \frac{\pi}{2}\right) = \sin\left(\frac{2\pi}{a}x\right) \\
 \{i|\boldsymbol{\tau}_d\} \sin\left(\frac{2\pi}{a}x\right) &= \sin\left(\frac{2\pi}{a}(-x) + \frac{\pi}{2}\right) = \cos\left(\frac{2\pi}{a}x\right) \\
 \{i|\boldsymbol{\tau}_d\} \cos\left(\frac{4\pi}{a}y\right) &= \cos\left(\frac{4\pi}{a}(-y) + \pi\right) = -\cos\left(\frac{4\pi}{a}y\right) \\
 \{i|\boldsymbol{\tau}_d\} \sin\left(\frac{4\pi}{a}y\right) &= \sin\left(\frac{4\pi}{a}(-y) + \pi\right) = \sin\left(\frac{4\pi}{a}y\right) \\
 \{i|\boldsymbol{\tau}_d\} \sin\left(\frac{4\pi}{a}(y+z)\right) &= \sin\left(\frac{4\pi}{a}(-y-z) + 2\pi\right) = -\sin\left(\frac{4\pi}{a}(y+z)\right) \\
 \{i|\boldsymbol{\tau}_d\} \sin\left(\frac{4\pi}{a}(y-z)\right) &= \sin\left(\frac{4\pi}{a}(-y+z)\right) = -\sin\left(\frac{4\pi}{a}(y-z)\right) \quad (12.37)
 \end{aligned}$$

Thus we obtain

$$\{i|\boldsymbol{\tau}_d\} \begin{pmatrix} x_{11} \\ x_{12} \end{pmatrix} = \begin{pmatrix} \cos\left(\frac{2\pi}{a}(-x) + \frac{\pi}{2}\right) \\ \sin\left(\frac{2\pi}{a}(-x) + \frac{\pi}{2}\right) \end{pmatrix} = \begin{pmatrix} \sin\left(\frac{2\pi}{a}x\right) \\ \cos\left(\frac{2\pi}{a}x\right) \end{pmatrix} = \begin{pmatrix} x_{12} \\ x_{11} \end{pmatrix}, \quad (12.38)$$

and we see that the effect of $\{i|\boldsymbol{\tau}_d\}$ is to interchange $x_{11} \leftrightarrow x_{12}$. Similarly the effect of $\{i|\boldsymbol{\tau}_d\}$ on x_{12} and x_{22} is

$$\{i|\tau_d\} \begin{pmatrix} x_{21} \\ x_{22} \end{pmatrix} = \begin{pmatrix} -\sin\left(\frac{2\pi}{a}(x)\right) [\cos\left(\frac{4\pi}{a}y\right) - \cos\left(\frac{4\pi}{a}z\right)] \\ -\cos\left(\frac{2\pi}{a}(x)\right) [\cos\left(\frac{4\pi}{a}y\right) - \cos\left(\frac{4\pi}{a}z\right)] \end{pmatrix} = \begin{pmatrix} -x_{22} \\ -x_{21} \end{pmatrix}, \quad (12.39)$$

so that $\{i|\tau_d\}$ in this case interchanges the functions and reverses their signs $x_{21} \leftrightarrow -x_{22}$. Similar results can be obtained by considering other operations that are in the point group O_h (and not in the group T_d), that is by considering symmetry operations involving the translation operation $\tau_d = (a/4)(1, 1, 1)$. Correspondingly, the other symmetry operations involving translation τ_d also interchange the basis functions for the X_1 and X_2 irreducible representations.

The physical meaning of this phenomenon is that the energy bands $E_{X_1}(\mathbf{k})$ and $E_{X_2}(\mathbf{k})$ go right through the X point without interruption in the extended zone scheme, except for an interchange in the symmetry designations of their basis functions in crossing the X point, consistent with the $E(\mathbf{k})$ diagram for Ge where bands with X_1 symmetry are seen.

In contrast, the effect of $\{i|\tau_d\}$ on the x_{31} and x_{32} basis functions:

$$\{i|\tau_d\} \begin{pmatrix} x_{31} \\ x_{32} \end{pmatrix} = \begin{pmatrix} -\sin\left(\frac{4\pi}{a}(y+z)\right) [\sin\left(\frac{2\pi}{a}x\right) + \cos\left(\frac{2\pi}{a}x\right)] \\ -\sin\left(\frac{4\pi}{a}(y-z)\right) [\sin\left(\frac{2\pi}{a}x\right) - \cos\left(\frac{2\pi}{a}x\right)] \end{pmatrix} = \begin{pmatrix} -x_{31} \\ x_{32} \end{pmatrix} \quad (12.40)$$

does not interchange x_{31} and x_{32} . Thus the X_3 level comes into the X point with zero slope. The behavior for the X_4 levels is similar

$$\{i|\tau_d\} \begin{pmatrix} x_{41} \\ x_{42} \end{pmatrix} = \begin{pmatrix} -\sin\left(\frac{4\pi}{a}(y-z)\right) [\sin\left(\frac{2\pi}{a}x\right) + \cos\left(\frac{2\pi}{a}x\right)] \\ -\sin\left(\frac{4\pi}{a}(y+z)\right) [\sin\left(\frac{2\pi}{a}x\right) - \cos\left(\frac{2\pi}{a}x\right)] \end{pmatrix} = \begin{pmatrix} -x_{41} \\ x_{42} \end{pmatrix} \quad (12.41)$$

so that the X_3 and X_4 levels behave like ordinary doubly degenerate levels. Equations (12.38)–(12.41) show that the character $\chi(\{i|\tau_d\})$ vanishes at the X point for the X_1 , X_2 , X_3 and X_4 levels, consistent with the character table for the diamond X -point given in Table 12.8 (see Problem 12.4). These results also explain the behavior of the energy bands for Ge at the X -point shown in Fig. 12.10. The nondegenerate Δ_1 and Δ_2' energy bands going into the X point stick together and interchange their symmetry designations on crossing the X point, while the doubly degenerate Δ_5 levels go into a doubly-degenerate X_4 level with zero slope at the Brillouin zone boundary. In Chap. 14 we will see that when the spin-orbit interaction is considered the doubly-degenerate X_5 levels are split by the spin-orbit interaction into Δ_6 and Δ_7 levels, and when the spin-orbit interaction is taken into account, all the levels at the X -point have X_5 symmetry and all show sticking-together properties.

Selected Problems

12.1. (a) For the simple cubic lattice find the proper linear combinations of plane waves for the twelve (1,1,0) plane wave states at $\mathbf{k} = 0$ which transform as irreducible representations of the O_h point group.

(b) As we move away from $\mathbf{k} = 0$, find the plane wave eigenfunctions which transform according to Δ_1 and Δ_5 and are compatible with the eigenfunctions for the Γ_{15}^- level at $k = 0$.

(c) Repeat part (b) for the case of $\Gamma_{12}^+ \rightarrow \Delta_1 + \Delta_2$.

12.2. Using the empty lattice, find the energy eigenvalues, degeneracies and symmetry types for the two electronic levels of lowest energy for the FCC lattice at the L point.

(a) Find the appropriate linear combinations of plane waves which provide basis functions for the two lowest FCC L -point electronic states.

(b) Which states of the lower and upper energy levels in (a) are coupled by optical dipole transitions?

(c) Repeat parts (a) and (b) for the two lowest X point energy levels for the FCC empty lattice (i.e., the X_1, X_4' and X_1, X_3, X_5' levels).

(d) Compare your results to those for the simple cubic lattice.

12.3. (a) Considering the empty lattice model for the 2D hexagonal lattice (space group #17 $p6mm$), find the symmetries of the two lowest energy states at the Γ point ($k = 0$).

(b) Find the linear combination of plane waves that transform according to the irreducible representations in part (a).

(c) Repeat (a) and (b) for the lowest energy state at the M point shown in the Fig. 12.11.

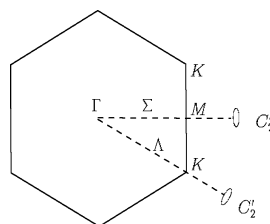


Fig. 12.11. Brillouin zone for the 2D triangular lattice

12.4. (a) Construct the character table for the group of the wave vector for the diamond structure at $k = 0$ using the classes given in Table 10.8 and check your results with Table C.17.

- (b) Consider the effect of the symmetry operation $\{C_4|\tau_d\}$ for the diamond structure on the x_{11} and x_{12} basis functions in Table 12.8 to show that these basis functions stick together at the X point.
- (c) Repeat (a) with the symmetry operation $\{C_4|\tau_d\}$ for the x_{31} and x_{32} basis functions in Table 12.8 to show that these basis functions come into the X point with zero slope.

12.5. Find the structure factor for the nonsymmorphic 3D graphite structure (see Problem 10.6) at a Δ point and at the A point in the Brillouin zone (see (12.34)) for the structure factor at the X point for diamond). Discuss the implication of your results on the electronic structure of 3D graphite.

12.6. Find the form of the $E(\mathbf{k})$ relation for the second level of the empty lattice for a BCC system and show how the degeneracy at $k = 0$ is lifted by application of a finite potential. What is the form of $E(\mathbf{k})$ for each of these cases, and compare your results to those for the $E(\mathbf{k})$ diagram for sodium (see Fig. 12.6(b)). To do this problem you will find Tables C.7 and C.8 of use.

Energy Band Models Based on Symmetry

Chapter 12 addressed the general application of space groups to the one-electron energy bands in a periodic solid in the limit of vanishing periodic potential [$V(\mathbf{r}) \rightarrow 0$]. This chapter deals with a model for which $V(\mathbf{r}) \neq 0$ is present and where extensive use is made of crystal symmetry, namely $\mathbf{k} \cdot \mathbf{p}$ perturbation theory. The Slater–Koster model, which also has a basic symmetry formalism, is discussed in Chap. 15, after the spin–orbit interaction is considered in Chap. 14.

13.1 Introduction

Just from the symmetry properties of a particular crystal, a good deal can be deduced concerning the form of the energy bands of that crystal. Our study of the group of the wave vector illustrates that some of the basic questions, such as band degeneracy and connectivity, are answered by group theory alone. It is not necessary to solve Schrödinger’s equations explicitly to find the *degeneracies* and the *connectivity* relations for $E_n(\mathbf{k})$. An interpolation or extrapolation technique for determining energy band dispersion relations based on symmetry often provides the functional form of $E_n(\mathbf{k})$ without actual solution of Schrödinger’s equation. Such an approach is useful as an interpolation scheme for experimental data or also for band calculations that are carried out with great care at a few high symmetry points in the Brillouin zone.

The interpolation/extrapolation method considered in this chapter is called $\mathbf{k} \cdot \mathbf{p}$ perturbation theory (extrapolation or a Taylor’s series expansion of $E(\mathbf{k})$). A related method called the Slater–Koster Fourier expansion [29] (an interpolation or Fourier series expansion of $E(\mathbf{k})$) is the basis for symmetry formalism in the tight-binding method, and it will be discussed in Chap. 15, after spin–orbit interaction is considered in Chap. 14. If the available experimental data are limited to one small region in the Brillouin zone

Table 13.1. Irreducible representations (IRs) of the cubic group O_h

| even | odd | | |
|-----------------|----------------|-----------------|----------------|
| Γ_1^+ | Γ_1 | Γ_1^- | $\Gamma_{1'}$ |
| Γ_2^+ | Γ_2 | Γ_2^- | $\Gamma_{2'}$ |
| Γ_{12}^+ | Γ_{12} | Γ_{12}^- | $\Gamma_{12'}$ |
| Γ_{15}^+ | $\Gamma_{15'}$ | Γ_{15}^- | Γ_{15} |
| Γ_{25}^+ | $\Gamma_{25'}$ | Γ_{25}^- | Γ_{25} |

and that is all that is known and under consideration, then $\mathbf{k} \cdot \mathbf{p}$ perturbation theory is the appropriate method to use for describing $E(\mathbf{k})$. This is often the case in practice for semiconductors. If, however, the available experimental data relate to several points or regions in the Brillouin zone, then the Slater–Koster approach is more appropriate. Although such experiments might seem to yield unrelated information about the energy bands, the Slater–Koster approach is useful for interrelating the results of such experiments.

The particular example used here to illustrate $\mathbf{k} \cdot \mathbf{p}$ perturbation theory is the electronic structure for a material with simple cubic symmetry. This discussion is readily extended to the electronic structure of semiconductors that crystallize in the diamond structure (e.g., silicon) or the zincblende structure (e.g., GaAs). The valence and conduction bands for these semiconductors are formed from hybridized s - and p -bands.

We first consider cubic electronic energy band structures with inversion symmetry. To emphasize inversion symmetry we will here use the notation Γ_i^\pm to denote irreducible representations that are even and odd under the inversion operator, when we write the irreducible representations of the cubic O_h group, see Table 13.1. For the nonsymmorphic diamond structure, the s - and p -functions at $\mathbf{k} = 0$ in the O_h point group (at $\mathbf{k} = 0$) transform as the Γ_1^+ and Γ_{15}^- irreducible representations, respectively (see Sect. 10.8). In the diamond structure there are 2 atoms per unit cell and Γ^{equiv} at $\mathbf{k} = 0$ transforms as $\Gamma_1^+ + \Gamma_2^-$ (see Table 10.8). Thus we must consider eight bands in discussing the valence and conduction bands formed by s - and p -bands for the diamond structure. These bands have symmetries

$$\begin{aligned} \Gamma^{\text{equiv}} \otimes \Gamma_{s\text{-functions}}(\Gamma_1^+ + \Gamma_2^-) \otimes \Gamma_1^+ &= \Gamma_1^+ + \Gamma_2^- \\ \Gamma^{\text{equiv}} \otimes \Gamma_{p\text{-functions}}(\Gamma_1^+ + \Gamma_2^-) \otimes \Gamma_{15}^- &= \Gamma_{15}^- + \Gamma_{25}^+. \end{aligned} \quad (13.1)$$

We identify the Γ_1^+ and Γ_{25}^+ bands as the bonding s - and p -bands and the Γ_2^- and Γ_{15}^- bands as antibonding s - and p -bands. The reason why the bonding p -band has Γ_{25}^+ symmetry follows from the direct product $\Gamma_2^- \otimes \Gamma_{15}^- = \Gamma_{25}^+$ in (13.1). So long as the discussion of $E_n(\mathbf{k})$ remains close to $\mathbf{k} = 0$, the nonsymmorphic nature of the energy bands is not important and the simple discussion presented here remains valid.

Our discussion starts with a brief review of $\mathbf{k} \cdot \mathbf{p}$ perturbation theory in general (Sect. 13.2). An example of $\mathbf{k} \cdot \mathbf{p}$ perturbation theory for a nondegenerate level is then given in Sect. 13.3. This is followed by an example of degenerate first-order perturbation theory and a two-band model (Sect. 13.4) which is then followed by degenerate second-order $\mathbf{k} \cdot \mathbf{p}$ perturbation theory which is appropriate for describing the p -bonding and antibonding levels in the diamond structure (Sect. 13.5). In all of these cases, group theory tells us which are the nonvanishing matrix elements, which bands couple to one another and which matrix elements are equal to each other. The application of $\mathbf{k} \cdot \mathbf{p}$ perturbation theory to the electronic energy bands at a Δ point is discussed in Sect. 13.6, and to the valley-orbit interaction in semiconductors is given in Sect. 13.8.

13.2 $\mathbf{k} \cdot \mathbf{p}$ Perturbation Theory

An electron in a periodic potential obeys the one-electron Hamiltonian:

$$\left[\frac{p^2}{2m} + V(\mathbf{r}) \right] \psi_{n,\mathbf{k}}(\mathbf{r}) = E_n(\mathbf{k}) \psi_{n,\mathbf{k}}(\mathbf{r}), \quad (13.2)$$

where the eigenfunctions of the Hamiltonian are the Bloch functions

$$\psi_{n,\mathbf{k}}(\mathbf{r}) = e^{i\mathbf{k} \cdot \mathbf{r}} u_{n,\mathbf{k}}(\mathbf{r}) \quad (13.3)$$

and n is the band index. Substitution of $\psi_{n,\mathbf{k}}(\mathbf{r})$ into Schrödinger's equation gives an equation for the periodic function $u_{n,\mathbf{k}}(\mathbf{r})$

$$\left[\frac{p^2}{2m} + V(\mathbf{r}) + \frac{\hbar \mathbf{k} \cdot \mathbf{p}}{m} + \frac{\hbar^2 k^2}{2m} \right] u_{n,\mathbf{k}}(\mathbf{r}) = E_n(\mathbf{k}) u_{n,\mathbf{k}}(\mathbf{r}). \quad (13.4)$$

In the spirit of the $(\mathbf{k} \cdot \mathbf{p})$ method, we assume that $E_n(\mathbf{k})$ is known at point $\mathbf{k} = \mathbf{k}_0$ either from experimental information or from direct solution of Schrödinger's equation for some model potential $V(\mathbf{r})$. Assume the band in question has symmetry Γ_i so that the function $u_{n,\mathbf{k}_0}(\mathbf{r})$ transforms as the irreducible representation Γ_i . Then we have

$$\mathcal{H}_{\mathbf{k}_0} u_{n,\mathbf{k}_0}^{(\Gamma_i)} = \varepsilon_n(\mathbf{k}_0) u_{n,\mathbf{k}_0}^{(\Gamma_i)}, \quad (13.5)$$

where

$$\mathcal{H}_{\mathbf{k}_0} = \frac{p^2}{2m} + V(\mathbf{r}) + \frac{\hbar \mathbf{k}_0 \cdot \mathbf{p}}{m} \quad (13.6)$$

and

$$\varepsilon_n(\mathbf{k}_0) = E_n(\mathbf{k}_0) - \frac{\hbar^2 \mathbf{k}_0^2}{2m}. \quad (13.7)$$

If $\varepsilon_n(\mathbf{k}_0)$ and $u_{n,\mathbf{k}_0}(\mathbf{r})$ are specified at \mathbf{k}_0 , the $\mathbf{k} \cdot \mathbf{p}$ method prescribes the development of the periodic $u_{n,\mathbf{k}_0}(\mathbf{r})$ functions under variation of \mathbf{k} . At point $\mathbf{k} = \mathbf{k}_0 + \boldsymbol{\kappa}$, the eigenvalue problem becomes

$$\begin{aligned}\mathcal{H}_{\mathbf{k}_0+\boldsymbol{\kappa}} u_{n,\mathbf{k}_0+\boldsymbol{\kappa}}(\mathbf{r}) &= \left(\mathcal{H}_{\mathbf{k}_0} + \frac{\hbar \boldsymbol{\kappa} \cdot \mathbf{p}}{m} \right) u_{n,\mathbf{k}_0+\boldsymbol{\kappa}}(\mathbf{r}) \\ &= \varepsilon_n(\mathbf{k}_0 + \boldsymbol{\kappa}) u_{n,\mathbf{k}_0+\boldsymbol{\kappa}}(\mathbf{r}).\end{aligned}\quad (13.8)$$

In the spirit of the usual $\mathbf{k} \cdot \mathbf{p}$ perturbation theory, $\boldsymbol{\kappa}$ is small so that the perturbation Hamiltonian is taken as $\mathcal{H}' = \hbar \boldsymbol{\kappa} \cdot \mathbf{p}/m$ and the energy eigenvalue at the displaced \mathbf{k} vector $\varepsilon_n(\mathbf{k}_0 + \boldsymbol{\kappa})$ is given by (13.7), and $E_n(\mathbf{k}_0)$ is given by (13.2). We will illustrate this method first for a nondegenerate band (a Γ_1^\pm band for the simple cubic lattice) and then in Sect. 13.5 for a degenerate band (a Γ_{15}^\pm band for the simple cubic lattice).

13.3 Example of $\mathbf{k} \cdot \mathbf{p}$ Perturbation Theory for a Nondegenerate Γ_1^+ Band

Suppose the energy of the Γ_1^\pm band at $\mathbf{k} = 0$ in a crystal with O_h point symmetry is established by the identification of an optical transition and measurement of its resonant photon energy. The unperturbed wave function at $\mathbf{k} = 0$ is $u_{n,0}^{\Gamma_1^+}(\mathbf{r})$ and its eigenvalue from (13.7) is $\varepsilon_n^{(\Gamma_1^+)}(0) = E_n^{(\Gamma_1^+)}(0)$ since $\mathbf{k}_0 = 0$. Away from $\mathbf{k}_0 = 0$, we use $\mathbf{k} \cdot \mathbf{p}$ perturbation theory [31, 45]:

$$\begin{aligned}\varepsilon_n^{(\Gamma_1^+)}(\boldsymbol{\kappa}) &= E_n^{(\Gamma_1^+)}(0) + \left(u_{n,0}^{\Gamma_1^+} | \mathcal{H}' | u_{n,0}^{\Gamma_1^+} \right) \\ &+ \sum_{n' \neq n} \frac{\left(u_{n,0}^{\Gamma_1^+} | \mathcal{H}' | u_{n',0}^{\Gamma_i} \right) \left(u_{n',0}^{\Gamma_i} | \mathcal{H}' | u_{n,0}^{\Gamma_1^+} \right)}{E_n^{(\Gamma_1^+)}(0) - E_{n'}^{(\Gamma_i)}(0)},\end{aligned}\quad (13.9)$$

where the sum is over states n' which have symmetries Γ_i .

Now $\mathcal{H}' = \hbar \boldsymbol{\kappa} \cdot \mathbf{p}/m$ transforms like a vector, since \mathcal{H}' is proportional to the vector \mathbf{p} , which pertains to the electronic system and $\boldsymbol{\kappa}$ is considered as an external variable not connected to the electronic system. If we expand the eigenfunctions and eigenvalues of (13.9) about the Γ point ($\mathbf{k} = 0$), then \mathcal{H}' which transforms according to the vector, will transform as the irreducible representation Γ_{15}^- in O_h symmetry. In the spirit of $\mathbf{k} \cdot \mathbf{p}$ perturbation theory, the vector \mathbf{k}_0 determines the point symmetry group that is used to classify the wave functions and eigenvalues for \mathcal{H}' .

For the $\mathbf{k} \cdot \mathbf{p}$ expansion about the Γ point, the linear term in k which arises in first order perturbation theory *vanishes* when $\mathbf{k}_0 = 0$ since $(u_{n,0}^{\Gamma_1^+} | \mathcal{H}' | u_{n,0}^{\Gamma_1^+})$ transforms according to the direct product $\Gamma_1^+ \otimes \Gamma_{15}^- \otimes \Gamma_1^+ = \Gamma_{15}^-$ which does not contain Γ_1^+ (see Sect. 6.7). The same result is obtained using arguments

relevant to the oddness and evenness of the functions which enter the matrix elements of (13.9). At other \mathbf{k} points in the Brillouin zone, the $\mathbf{k} \cdot \mathbf{p}$ expansion may contain linear \mathbf{k} terms since the group of the wave vector for that $\mathbf{k} \cdot \mathbf{p}$ expansion point may not contain the inversion operation.

Now let us look at the terms

$$\left(u_{n',0}^{\Gamma_i} | \mathcal{H}' | u_{n,0}^{\Gamma_1^+} \right)$$

that arise in second order perturbation theory. The product $\mathcal{H}' u_{n,0}^{\Gamma_1^+}$ transforms as $\Gamma_{15}^- \otimes \Gamma_1^+ = \Gamma_{15}^-$ so that Γ_i must be of Γ_{15}^- symmetry if a nonvanishing matrix element is to result. We thus obtain

$$\varepsilon_n^{\Gamma_1^+}(\boldsymbol{\kappa}) = E_n^{\Gamma_1^+}(0) + \sum_{n' \neq n} (\Gamma_{15}^-) \frac{\left(u_{n,0}^{\Gamma_1^+} | \mathcal{H}' | u_{n',0}^{\Gamma_{15}^-} \right) \left(u_{n',0}^{\Gamma_{15}^-} | \mathcal{H}' | u_{n,0}^{\Gamma_1^+} \right)}{E_n^{\Gamma_1^+}(0) - E_n^{\Gamma_{15}^-}(0)} + \dots \quad (13.10)$$

and a corresponding relation is obtained for the nondegenerate Γ_1^- and Γ_2^\pm levels. For a semiconductor that crystallizes in the diamond structure, the symmetry Γ_1^+ describes the valence band s -band bonding state, while symmetry Γ_2^- describes the conduction band s -band antibonding state (see Problem 13.1).

Thus we see that by using group theory, our $\mathbf{k} \cdot \mathbf{p}$ expansion is greatly simplified, since it is only the Γ_{15}^- levels that couple to the Γ_1^+ level by $\mathbf{k} \cdot \mathbf{p}$ perturbation theory in (13.10). These statements are completely independent of the explicit wave functions which enter the problem, but depend only on their *symmetry*. Further simplifications result from the observation that for cubic symmetry the matrix elements

$$\left(u_{n,0}^{\Gamma_1^+} | \mathcal{H}' | u_{n',0}^{\Gamma_{15}^-} \right)$$

can all be expressed in terms of a single matrix element, if $u_{n',0}^{\Gamma_{15}^-}$ is identified with specific basis functions, such as p -functions (denoted by x, y, z for brevity) and $u_{n,0}^{\Gamma_1^+}$ with an s -function (denoted by 1 for brevity). Thus for the O_h group, the selection rules (see Sect. 6.6) give

$$(1|p_x|x) = (1|p_y|y) = (1|p_z|z), \quad (13.11)$$

and all other cross terms of the form $(1|p_x|y)$ vanish. This result, that the matrix elements of \mathbf{p} in O_h symmetry have only one independent matrix element, also follows from the theory of permutation groups (see Chap. 17). Combining these results with

$$\varepsilon_n^{\Gamma_1^+}(\boldsymbol{\kappa}) = E_n^{\Gamma_1^+}(\boldsymbol{\kappa}) - \hbar^2 \kappa^2 / 2m$$

we get

$$E_n^{\Gamma_1^+}(\kappa) = E_n^{\Gamma_1^+}(0) + \frac{\hbar^2 \kappa^2}{2m} + \frac{\hbar^2 \kappa^2}{m^2} \sum_{n' \neq n} \frac{|(1|p_x|x)|^2}{E_n^{\Gamma_1^+}(0) - E_{n'}^{\Gamma_1^-}(0)}, \quad (13.12)$$

where the sum is over all states n' with Γ_1^- symmetry. A similar expansion formula is applicable to

$$E_n^{\Gamma_2^-}(\kappa),$$

which corresponds to the conduction antibonding s -band in the diamond structure. Equation (13.12) is sometimes written in the form

$$E_n^{\Gamma_1^+}(\kappa) = E_n^{\Gamma_1^+}(0) + \frac{\hbar^2 \kappa^2}{2m_n^*}, \quad (13.13)$$

where the effective mass parameter m_n^* is related to band couplings through the momentum matrix element:

$$\frac{m}{m_n^*} = 1 + \frac{2}{m} \sum_{n' \neq n} \frac{|(1|p_x|x)|^2}{E_n^{\Gamma_1^+}(0) - E_{n'}^{\Gamma_1^-}(0)}, \quad (13.14)$$

in which the sum over n' is restricted to states with Γ_1^- symmetry. Consistent with (13.12), the effective mass m_n^* is related to the band curvature by the relation

$$\frac{\partial^2 E_n^{\Gamma_1^+}(\kappa)}{\partial \kappa^2} = \frac{\hbar^2}{m_n^*}. \quad (13.15)$$

Thus m_n^* is proportional to the inverse of the band curvature. If the curvature is large, the effective mass is small and conversely, and if the bands are “flat” (essentially k -independent), the effective masses are large. Thus the $\mathbf{k} \cdot \mathbf{p}$ expansion for a nondegenerate band in a cubic crystal leads to an isotropic parabolic dependence of $E_n(\mathbf{k})$ on \mathbf{k} which looks just like the free electron dispersion relation except that the free electron mass m is replaced by m^* which reflects the effect of the crystalline potential on the motion of the electron.

For the case that the nondegenerate level with Γ_1^+ symmetry is predominantly coupled to a single degenerate band (such as one degenerate band with Γ_1^- symmetry which in this case relates to the p bonding state in the conduction band), the effective mass formula (13.14) becomes

$$\frac{m}{m_n^*} = 1 + \frac{2}{m} \frac{|(1|p_x|x)|^2}{\varepsilon_g}, \quad (13.16)$$

which is useful for estimating effective masses, provided that we know the magnitude of the matrix element and the band gap ε_g . On the other hand,

if m^* and ε_g are known experimentally, then (13.16) is useful for evaluating $| \langle 1 | p_x | x \rangle |^2$. This is, in fact, the most common use of (13.16). The words *matrix element* or *oscillator strength* typically refer to the momentum matrix element $\langle u_{n,\mathbf{k}} | p_x | u_{n',\mathbf{k}} \rangle$ when discussing the optical properties of solids.

The treatment given here for the nondegenerate bands is easily carried over to treating the $\mathbf{k} \cdot \mathbf{p}$ expansion about some other high symmetry point in the Brillouin zone for symmorphic structures. For arbitrary points in the Brillouin zone, the diagonal term arising from first order perturbation theory does not vanish. Also the matrix element

$$\left(u_{n,\mathbf{k}_0}^{\Gamma_i^\pm} | p_\alpha | u_{n,\mathbf{k}_0}^{\Gamma_j^\mp} \right)$$

need not be the same for each component $\alpha = x, y, z$, and for the most general case, six independent matrix elements would be expected. For example, along the Δ and Λ axes, the matrix element for momentum \parallel to the high symmetry axis is not equal to the components \perp to the axis, and there are two independent matrix elements along each of the Δ and Λ axes (see Sect. 13.6).

These two directions are called *longitudinal* (\parallel to the axis) and *transverse* (\perp to the axis), and lead to longitudinal and transverse effective mass components away from the Γ point. Furthermore, for the case of nonsymmorphic structures like the diamond structure, the nonsymmorphic symmetry elements involving translations must be considered in detail away from $k = 0$.

13.4 Two Band Model: Degenerate First-Order Perturbation Theory

One of the simplest applications of $\mathbf{k} \cdot \mathbf{p}$ perturbation theory is to two-band models for crystalline solids. These models are applicable to describe the energy dispersion $E(\mathbf{k})$ about a point \mathbf{k}_0 for one of two bands that are strongly coupled to each other and are weakly coupled to all other bands. The strongly coupled set is called the nearly degenerate set (NDS) and, if need be, the weakly coupled bands can always be treated in perturbation theory after the problem of the strongly interacting bands is solved. Simple extensions of the two-band model are made to handle three strongly coupled bands, such as the valence band of silicon, germanium and related semiconductors, or even to handle four strongly coupled bands as occur in graphite. We illustrate the procedure here for symmorphic systems, but for application to nonsymmorphic groups, care with handling phase factors becomes important (see Sect. 12.5).

The eigenvalue problem to be solved is

$$\left[\frac{p^2}{2m} + V(\mathbf{r}) + \frac{\hbar \mathbf{k}_0 \cdot \mathbf{p}}{m} + \frac{\hbar \boldsymbol{\kappa} \cdot \mathbf{p}}{m} \right] u_{n,\mathbf{k}_0+\boldsymbol{\kappa}}(\mathbf{r}) = \varepsilon_n(\mathbf{k}_0 + \boldsymbol{\kappa}) u_{n,\mathbf{k}_0+\boldsymbol{\kappa}}(\mathbf{r}), \quad (13.17)$$

in which $\varepsilon_n(\mathbf{k}_0)$ is related to the solution of Schrödinger's equation $E_n(\mathbf{k}_0)$ by (13.7).

Let $n = i, j$ be the two bands that are nearly degenerate. Using first-order degenerate perturbation theory, the secular equation is written as

$$i \begin{vmatrix} i & j \\ \langle i | \mathcal{H}_0 + \mathcal{H}' | i \rangle - \varepsilon & \langle i | \mathcal{H}_0 + \mathcal{H}' | j \rangle \\ \langle j | \mathcal{H}_0 + \mathcal{H}' | i \rangle & \langle j | \mathcal{H}_0 + \mathcal{H}' | j \rangle - \varepsilon \end{vmatrix} = 0, \quad (13.18)$$

in which we have explicitly written i and j to label the rows and columns.

Equation (13.18) is exact within the two-band model, i.e., all the coupling occurs between the nearly degenerate set and no coupling is made to bands outside this set. For many cases where the two-band model is applied (e.g., PbTe), the unperturbed wave functions $u_{n,\mathbf{k}_0}(\mathbf{r})$ are invariant under inversion. Then because of the oddness of $\mathcal{H}' = \hbar\boldsymbol{\kappa} \cdot \mathbf{p}/m$, the matrix elements vanish

$$\langle i | \mathcal{H}' | i \rangle = \langle j | \mathcal{H}' | j \rangle = 0. \quad (13.19)$$

Also since the “band edge” wave functions $u_{n,\mathbf{k}_0}(\mathbf{r})$ are constructed to diagonalize the Hamiltonian

$$\mathcal{H}_0 u_{n,\mathbf{k}_0}(\mathbf{r}) = \varepsilon_n(\mathbf{k}_0) u_{n,\mathbf{k}_0}(\mathbf{r}), \quad (13.20)$$

there are no off-diagonal matrix elements of \mathcal{H}_0 or

$$\langle i | \mathcal{H}_0 | j \rangle = 0, \quad \text{for } i \neq j. \quad (13.21)$$

We then write

$$\langle i | \mathcal{H}_0 | i \rangle = E_i^0 \quad \text{and} \quad \langle j | \mathcal{H}_0 | j \rangle = E_j^0, \quad (13.22)$$

where for $n = i, j$

$$E_n^0 = E_n(\mathbf{k}_0) - \frac{\hbar^2 k_0^2}{2m}. \quad (13.23)$$

In this notation the secular equation can be written as

$$\begin{vmatrix} E_i^0 - \varepsilon & (\hbar/m)\boldsymbol{\kappa} \cdot \langle i | \mathbf{p} | j \rangle \\ (\hbar/m)\boldsymbol{\kappa} \cdot \langle j | \mathbf{p} | i \rangle & E_j^0 - \varepsilon \end{vmatrix} = 0, \quad (13.24)$$

where $\langle i | \mathbf{p} | j \rangle \neq 0$ for the two-band model. The secular equation implied by (13.24) is equivalent to the quadratic equation

$$\varepsilon^2 - \varepsilon [E_i^0 + E_j^0] + E_i^0 E_j^0 - \frac{\hbar^2}{m^2} \boldsymbol{\kappa} \cdot \langle i | \mathbf{p} | j \rangle \langle j | \mathbf{p} | i \rangle \cdot \boldsymbol{\kappa} = 0. \quad (13.25)$$

We write the symmetric tensor p_{ij}^2 coupling the two bands as

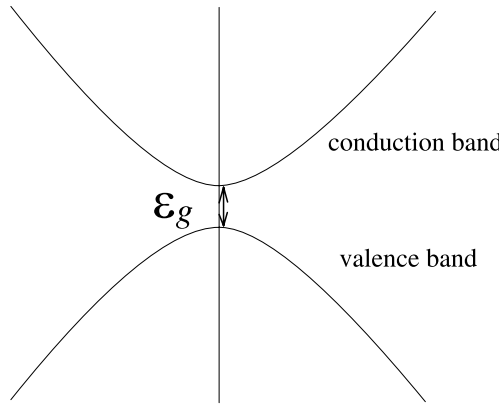


Fig. 13.1. Two strongly coupled mirror bands separated by an energy ε_g at the band extremum. This sketch is based on the concept that these two bands would be degenerate at the center of the band gap but a strong interaction splits this degeneracy at a high symmetry point and creates a band gap ε_g

$$\overset{\leftrightarrow}{p}_{ij}^2 = \langle i | \mathbf{p} | j \rangle \langle j | \mathbf{p} | i \rangle, \quad (13.26)$$

where i and j in the matrix elements refer to the band edge wave functions $u_{n,\mathbf{k}_0}(\mathbf{r})$ and $n = i, j$. The solution to the quadratic equation (13.25) yields

$$\varepsilon(\boldsymbol{\kappa}) = \frac{E_i^0 + E_j^0}{2} \pm \frac{1}{2} \sqrt{(E_i^0 - E_j^0)^2 + \frac{4\hbar^2}{m^2} \boldsymbol{\kappa} \cdot \overset{\leftrightarrow}{p}_{ij}^2 \cdot \boldsymbol{\kappa}}. \quad (13.27)$$

We choose our zero of energy symmetrically such that

$$E_i^0 = \varepsilon_g/2, \quad E_j^0 = -\varepsilon_g/2 \quad (13.28)$$

to obtain the two-band model result (see Fig. 13.1):

$$\varepsilon(\boldsymbol{\kappa}) = \pm \frac{1}{2} \sqrt{\varepsilon_g^2 + \frac{4\hbar^2}{m^2} \boldsymbol{\kappa} \cdot \overset{\leftrightarrow}{p}_{ij}^2 \cdot \boldsymbol{\kappa}}, \quad (13.29)$$

which at $\boldsymbol{\kappa} = 0$ reduces properly to $\varepsilon(0) = \pm 1/2\varepsilon_g$.

Equation (13.29) gives a *nonparabolic dependence of E upon $\boldsymbol{\kappa}$* . For strongly coupled bands, the two-band model is characterized by its non-parabolicity. In the approximation that there is no coupling to bands outside the nondegenerate set, these bands are strictly *mirror bands*, whereby one band is described by an $E(\boldsymbol{\kappa})$ relation given by the + sign; the other by the identical relation with the - sign. For cubic materials there is only one independent matrix element

$$\overset{\leftrightarrow}{p}_{ij}^2 = \langle i | p_\alpha | j \rangle \langle j | p_\alpha | i \rangle \equiv p_{ij}^2, \quad \alpha = x, y, z, \quad (13.30)$$

and the $\overset{\leftrightarrow}{p}_{ij}^2$ tensor assumes the form

$$\overset{\leftrightarrow}{p}_{ij}^2 = \begin{pmatrix} p_{ij}^2 & 0 & 0 \\ 0 & p_{ij}^2 & 0 \\ 0 & 0 & p_{ij}^2 \end{pmatrix}. \quad (13.31)$$

In applying the two-band model to cubic symmetry, the degeneracy of the Γ_{25}^+ valence bands or the Γ_{15}^- conduction bands is often ignored. The two-band model formula then becomes

$$\varepsilon(\boldsymbol{\kappa}) = \pm \frac{1}{2} \sqrt{\varepsilon_g^2 + \frac{4\hbar^2\kappa^2 p_{ij}^2}{m^2}}, \quad \text{where } \kappa^2 = \kappa_x^2 + \kappa_y^2 + \kappa_z^2. \quad (13.32)$$

In this form, (13.32) is called the Kane two-band model. The generalization of (13.32) to noncubic materials is usually called the Lax two-band model, and in the case of bismuth the $\overset{\leftrightarrow}{p}_{ij}^2$ tensor has the following form

$$\overset{\leftrightarrow}{p}_{ij}^2 = \begin{pmatrix} p_{xx}^2 & 0 & 0 \\ 0 & p_{yy}^2 & p_{yz}^2 \\ 0 & p_{yz}^2 & p_{zz}^2 \end{pmatrix}, \quad (13.33)$$

where the x axis is a binary axis \perp to the mirror plane in bismuth (space group $R\bar{3}m$, #166), and the matrix elements of (13.33) have four independent components.

We now show that for small κ we recover the parabolic $\varepsilon(\boldsymbol{\kappa})$ relations. For example, for the Kane two-band model, a Taylor's series expansion of (13.32) yields

$$\varepsilon(\boldsymbol{\kappa}) = \pm \frac{1}{2} \sqrt{\varepsilon_g^2 + \frac{4\hbar^2\kappa^2 p_{ij}^2}{m^2}} = \pm \frac{\varepsilon_g}{2} \left[1 + \frac{4\hbar^2\kappa^2 p_{ij}^2}{\varepsilon_g^2 m^2} \right]^{1/2}, \quad (13.34)$$

which to order κ^4 becomes

$$\varepsilon(\boldsymbol{\kappa}) = \pm \left[\frac{\varepsilon_g}{2} + \frac{\hbar^2\kappa^2 p_{ij}^2}{\varepsilon_g m^2} - \frac{\hbar^4\kappa^4 p_{ij}^4}{\varepsilon_g^3 m^4} + \dots \right], \quad (13.35)$$

where $\varepsilon(\boldsymbol{\kappa})$ is given by (13.7), the momentum matrix elements, which reflect group theoretical considerations, are given by

$$p_{ij}^2 = |(1|p_x|x)|^2, \quad (13.36)$$

and the bandgap at the band extrema is given by $E_n(\mathbf{k}_0) - E_{n'}(\mathbf{k}_0) = \pm \varepsilon_g$.

If the power series expansion in (13.35) is rapidly convergent (either because κ is small or the bands are not that strongly coupled – i.e., p_{ij}^2 is not

too large), then the expansion through terms in κ^4 is useful. We note that, within the two-band model, the square root formula of (13.34) is exact and is the one that is not restricted to small κ or small p_{ij}^2 . It is valid so long as the two-band model itself is valid.

Some interesting consequences arise from these nonparabolic features of the dispersion relations. For example, the effective mass (or band curvature) is energy or κ -dependent. Consider the expression which follows from (13.35):

$$E_n(\mathbf{k}_0 + \boldsymbol{\kappa}) \simeq \frac{\hbar^2 |\mathbf{k}_0 + \boldsymbol{\kappa}|^2}{2m} \pm \left[\frac{\varepsilon_g}{2} + \frac{\hbar^2 \kappa^2 p_{ij}^2}{\varepsilon_g m^2} - \frac{\hbar^4 \kappa^4 p_{ij}^4}{\varepsilon_g^3 m^4} \right]. \quad (13.37)$$

Take $\mathbf{k}_0 = 0$, so that

$$\frac{\partial^2 E}{\partial \kappa^2} = \frac{\hbar^2}{m} \pm \left[\frac{2\hbar^2 p_{ij}^2}{\varepsilon_g m^2} - \frac{12\kappa^2 \hbar^4 p_{ij}^4}{\varepsilon_g^3 m^4} \right] \equiv \frac{\hbar^2}{m^*}. \quad (13.38)$$

From this equation we see that the curvature $\partial^2 E / \partial \kappa^2$ is κ dependent. In fact as we move further from the band extrema, the band curvature decreases, the bands become more flat and the effective mass increases. This result is also seen from the definition of m^* (13.38)

$$\frac{m}{m^*} = 1 \pm \left[\frac{2}{m} \frac{p_{ij}^2}{\varepsilon_g} - \frac{12\hbar^2 \kappa^2 p_{ij}^4}{\varepsilon_g^3 m^3} \right]. \quad (13.39)$$

Another way to see that the masses become heavier as we move higher into the band (away from \mathbf{k}_0) is to work with the square root formula (13.34):

$$\varepsilon = \pm \frac{1}{2} \sqrt{\varepsilon_g^2 + \frac{4\hbar^2 \kappa^2 p_{ij}^2}{m^2}}. \quad (13.40)$$

Squaring (13.40) and rewriting this equation, we obtain

$$(2\varepsilon - \varepsilon_g)(2\varepsilon + \varepsilon_g) = \frac{4\hbar^2 \kappa^2 p_{ij}^2}{m^2}, \quad (13.41)$$

$$(2\varepsilon - \varepsilon_g) = \frac{4\hbar^2 \kappa^2 p_{ij}^2}{m^2(2\varepsilon + \varepsilon_g)}. \quad (13.42)$$

For $\kappa = 0$ we have $\varepsilon = \varepsilon_g/2$, and we then write an expression for $\varepsilon(\kappa)$:

$$\varepsilon(\kappa) = \frac{\varepsilon_g}{2} + \frac{2\hbar^2 \kappa^2 p_{ij}^2}{m^2(2\varepsilon + \varepsilon_g)} = \frac{\varepsilon_g}{2} + \frac{\hbar^2 \kappa^2 p_{ij}^2}{m^2(\varepsilon + \frac{\varepsilon_g}{2})}. \quad (13.43)$$

Therefore we obtain the nonparabolic two-band model relation

$$E(\boldsymbol{\kappa}) = \frac{\varepsilon_g}{2} + \frac{\hbar^2 \kappa^2}{2m} \left[1 + \frac{2p_{ij}^2}{m(\varepsilon + \frac{\varepsilon_g}{2})} \right], \quad (13.44)$$

which is to be compared with the result for simple nondegenerate bands (13.12):

$$E_i(\boldsymbol{\kappa}) = E_i(0) + \frac{\hbar^2 \kappa^2}{2m} \left[1 + \frac{2p_{ij}^2}{m\varepsilon_g} \right]. \quad (13.45)$$

Equation (13.44) shows that for the nonparabolic two-band model, the effective mass at the band edge is given by

$$\frac{m}{m^*} = \left[1 + \frac{2p_{ij}^2}{m\varepsilon_g} \right], \quad (13.46)$$

but the effective mass becomes heavier as we move away from \mathbf{k}_0 and as we move up into the band. The magnitude of the k or energy dependence of the effective mass is very important in narrow gap materials such as bismuth. At the band edge, the effective mass parameter for electrons in Bi is $\sim 0.001m_0$ whereas at the Fermi level $m^* \sim 0.008m_0$. The number of electron carriers in Bi is only 10^{17} cm^{-3} . Since the density of states for simple bands in a 3D crystal has a dependence $\sim m^{*3/2} E^{1/2}$, we can expect a large increase in the density of states with increasing energy in a nonparabolic band with a small effective mass at the band edge. Since bismuth has relatively low symmetry, the tensorial nature of the effective mass tensor must be considered and the dispersion relations for the coupled bands at the L point in bismuth are generally written as

$$\varepsilon(\boldsymbol{\kappa}) = \pm \frac{1}{2} \sqrt{\varepsilon_g^2 + 2\hbar^2 \varepsilon_g \frac{\boldsymbol{\kappa} \cdot \overleftrightarrow{\alpha} \cdot \boldsymbol{\kappa}}{m}}, \quad (13.47)$$

in which $\overleftrightarrow{\alpha}$ is a reciprocal effective mass tensor.

13.5 Degenerate second-order $\mathbf{k} \cdot \mathbf{p}$ Perturbation Theory

For many cubic crystals it is common to have triply degenerate energy bands arising from degenerate p states, with extrema at $\mathbf{k} = 0$. Such bands are of great importance in the transport properties of semiconductors such as silicon, germanium, and III-V compounds. The analysis of experiments such as cyclotron resonance in the valence band of semiconductors depends upon degenerate second-order $\mathbf{k} \cdot \mathbf{p}$ perturbation theory which is discussed in this section.

Second-order degenerate $\mathbf{k} \cdot \mathbf{p}$ perturbation theory becomes much more complicated than the simpler applications of perturbation theory discussed in Sect. 13.2–13.4. Group theory thus provides a valuable tool for the solution of practical problems. For example, we consider here how the degeneracy is lifted as we move away from $\mathbf{k} = 0$ for a Γ_{15}^- level for a crystal with O_h symmetry; a similar analysis applies for the Γ_{25}^+ level, which pertains to the degenerate p -band bonding states in the valence band in the diamond structure.

Suppose that we set up the secular equation for a Γ_{15}^- level using degenerate perturbation theory

$$\begin{array}{c|ccc} & x & y & z \\ x & (x|\mathcal{H}'|x) - \varepsilon & (x|\mathcal{H}'|y) & (x|\mathcal{H}'|z) \\ y & (y|\mathcal{H}'|x) & (y|\mathcal{H}'|y) - \varepsilon & (y|\mathcal{H}'|z) \\ z & (z|\mathcal{H}'|x) & (z|\mathcal{H}'|y) & (z|\mathcal{H}'|z) - \varepsilon \end{array} = 0, \quad (13.48)$$

where the x, y and z symbols denote the (x, y, z) partners of the basis functions in the Γ_{15}^- irreducible representation derived from atomic p -functions and the diagonal matrix elements for \mathcal{H}'_0 are set equal to zero at the band extremum, such as the top of the valence band. We notice that since $\mathcal{H}' = \hbar\mathbf{k} \cdot \mathbf{p}/m$, then \mathcal{H}' transforms like the Γ_{15}^- irreducible representation. Therefore we get $(\Gamma_{15}^-|\mathcal{H}'|\Gamma_{15}^-) = 0$, since

$$\Gamma_{15}^- \otimes \Gamma_{15}^- = \Gamma_1^+ + \Gamma_{12}^+ + \Gamma_{15}^+ + \Gamma_{25}^+, \quad (13.49)$$

or more simply, since \mathcal{H}' is odd under inversion, each matrix element in (13.48) vanishes because of parity considerations. Since each of the matrix elements of (13.48) vanishes, the degeneracy of the Γ_{15}^- level is not lifted in first-order degenerate perturbation theory; thus we must use *second-order* degenerate perturbation theory to lift this level degeneracy. We show below the derivation of the form of the matrix elements for the off-diagonal matrix elements in (13.48) showing that the vanishing \mathcal{H}'_{mn} is replaced by

$$\mathcal{H}'_{mn} \rightarrow \mathcal{H}'_{mn} + \sum_{\alpha} \frac{\mathcal{H}'_{m\alpha} \mathcal{H}'_{\alpha n}}{E_m^{(0)} - E_n^{(0)}}. \quad (13.50)$$

We will see below that the states with symmetries given in (13.49) will serve as the intermediate states α which arise in second-order perturbation theory. In applying second-order degenerate perturbation theory, we assume that we have a degenerate (or nearly degenerate) set of levels – abbreviated NDS. We assume that the states inside the NDS are strongly coupled and those outside the NDS are only weakly coupled to states within the NDS (see Fig. 13.2).

The wave function for a state is now written in terms of the unperturbed wave functions and the distinction is made as to whether we are dealing with

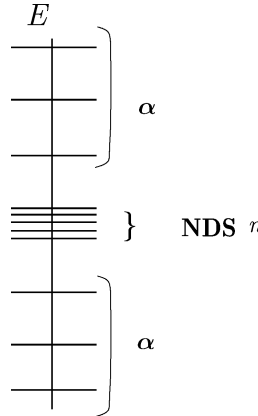


Fig. 13.2. NDS \equiv nearly degenerate set. We use Roman letter subscripts for levels within the NDS (such as n) and Greek indices for levels outside the NDS (such as α)

a state inside or outside of the NDS. If we now expand the wavefunction $\psi_{n'}$ in terms of the unperturbed band edge states, we obtain

$$\psi_{n'} = \sum_n a_n \psi_n^{(0)} + \sum_\alpha a_\alpha \psi_\alpha^{(0)}, \quad (13.51)$$

where $\psi_n^{(0)}$ and $\psi_\alpha^{(0)}$ are, respectively, the unperturbed wavefunctions inside (n) and outside (α) of the nearly degenerate set. Substitution into Schrödinger's equation yields

$$\mathcal{H}\psi_{n'} = E\psi_{n'} = \sum_n a_n (E_n^0 + \mathcal{H}') \psi_n^{(0)} + \sum_\alpha a_\alpha (E_\alpha^{(0)} + \mathcal{H}') \psi_\alpha^{(0)}. \quad (13.52)$$

We multiply the left-hand side of (13.52) by $\psi_{m_0}^{(0)*}$ and integrate over all space, making use of the orthogonality theorem $\int \psi_m^{(0)*} \psi_n^{(0)} d\mathbf{r} = \delta_{mn}$ to obtain the iterative relation between the expansion coefficients (Brillouin–Wigner Perturbation Theory)

$$[E - E_m^{(0)}] a_m = a_m \mathcal{H}'_{mm} + \sum_{n' \neq m} a_{n'} \mathcal{H}'_{mn'} + \sum_\alpha a_\alpha \mathcal{H}'_{m\alpha}, \quad (13.53)$$

where the sum over n' denotes coupling to states in the NDS and the sum over α denotes coupling to states outside the NDS (see Fig. 13.2). A similar procedure also leads to a similar equation for levels outside the NDS:

$$[E - E_\alpha^{(0)}] a_\alpha = a_\alpha \mathcal{H}'_{\alpha\alpha} + \sum_n a_n \mathcal{H}'_{\alpha n} + \sum_{\beta \neq \alpha} a_\beta \mathcal{H}'_{\alpha\beta}. \quad (13.54)$$

We now substitute (13.54) for the coefficients a_α outside the NDS in (13.53) to obtain

$$[E - E_m^{(0)}]a_m = a_m \mathcal{H}'_{mm} + \sum_{n' \neq m} a_{n'} \mathcal{H}'_{mn'} + \sum_{\alpha} \frac{\mathcal{H}'_{m\alpha}}{E - E_{\alpha}^{(0)}} \left\{ \sum_n a_n \mathcal{H}'_{\alpha n} + a_{\alpha} \mathcal{H}'_{\alpha\alpha} + \sum_{\beta} a_{\beta} \mathcal{H}'_{\alpha\beta} \right\}. \quad (13.55)$$

If we neglect terms in (13.56) which couple states outside the NDS to other states outside the NDS, we obtain

$$a_m(E_m^{(0)} - E) + \sum_n a_n \mathcal{H}'_{mn} + \sum_n a_n \sum_{\alpha} \frac{\mathcal{H}'_{m\alpha} \mathcal{H}'_{\alpha n}}{E_m^{(0)} - E_{\alpha}^{(0)}} = 0, \quad (13.56)$$

in which the first sum is over all n without restriction, and for E in the denominator of the second-order perturbation term in (13.56) we replace E by $E_m^{(0)}$ in the spirit of perturbation theory. Equation (13.56) then implies the secular equation

$$\sum_{n=1}^n a_n \left[(E_m^{(0)} - E) \delta_{mn} + \mathcal{H}'_{mn} + \sum_{\alpha} \frac{\mathcal{H}'_{m\alpha} \mathcal{H}'_{\alpha n}}{E_m^{(0)} - E_{\alpha}^{(0)}} \right] = 0, \quad (13.57)$$

which yields an $n \times n$ secular equation with each matrix element given by

$$\mathcal{H}'_{mn} + \sum_{\alpha} \frac{\mathcal{H}'_{m\alpha} \mathcal{H}'_{\alpha n}}{E_m^{(0)} - E_{\alpha}^{(0)}}, \quad (13.58)$$

as indicated in (13.50). In degenerate $\mathbf{k} \cdot \mathbf{p}$ perturbation theory, we found that $\mathcal{H}'_{mn} = 0$ for a Γ_{15}^- level, and it was for this precise reason that we had to go to degenerate *second*-order perturbation theory. In this case, each state in the NDS couples to other states in the NDS only through an intermediate state outside of the NDS.

In second-order degenerate perturbation theory (13.49) shows us that for a threefold Γ_{15}^- level $\mathbf{k} \cdot \mathbf{p}$ degenerate perturbation theory will involve only states of $\Gamma_1^+, \Gamma_{12}^+, \Gamma_{15}^+$, or Γ_{25}^+ symmetry as intermediate states. In our discussion of nondegenerate $\mathbf{k} \cdot \mathbf{p}$ perturbation theory (see Sect. 13.3), we found that there was only one independent matrix element of \mathbf{p} coupling a Γ_1^+ state to a Γ_{15}^- state. To facilitate the use of (13.48) and its more explicit form (13.58), we include in Table 13.2 a useful list of matrix elements of \mathbf{p} between states of different symmetries for Γ point levels in cubic crystals. These matrix elements are found using the basis functions for each of the irreducible representations of O_h given in Table 10.2 and appearing also in Tables C.17 and 10.9 for the Γ point and Δ point of the diamond structure. Table 13.2 lists the nonvanishing matrix elements appearing in the $\mathbf{k} \cdot \mathbf{p}$ perturbation theory for electronic energy bands with cubic O_h symmetry.

For the matrix element A_2 in Table 13.2 we note with the help of Table 10.2 that the pertinent basis functions are $\Gamma_2^- = xyz$ and $\Gamma_{25,x}^+ = yz$. For

Table 13.2. Matrix elements for $\mathcal{H}' = \hbar\mathbf{k} \cdot \mathbf{p}/m$ in cubic O_h symmetry, where \mathcal{H}' transforms as Γ_{15}^-

| | |
|--|---|
| $(\Gamma_1^\pm \mathcal{H}' \Gamma_{15,\alpha}^\mp) = A_1 \frac{\hbar}{m} k_\alpha$ | $A_1 = (\Gamma_1^\pm p_x \Gamma_{15,x}^\mp)$ |
| $(\Gamma_2^\pm \mathcal{H}' \Gamma_{25,\alpha}^\mp) = A_2 \frac{\hbar}{m} k_\alpha$ | $A_2 = (\Gamma_2^\pm p_x \Gamma_{25,x}^\mp)$ |
| $\left. \begin{cases} (\Gamma_{12,1}^\pm \mathcal{H}' \Gamma_{15,x}^\mp) = A_3 \frac{\hbar}{m} k_x \\ (\Gamma_{12,1}^\pm \mathcal{H}' \Gamma_{15,y}^\mp) = A_3 \frac{\hbar}{m} k_y \omega^2 \\ (\Gamma_{12,1}^\pm \mathcal{H}' \Gamma_{15,z}^\mp) = A_3 \frac{\hbar}{m} k_z \omega \end{cases} \right\}$ | $A_3 = (\Gamma_{12}^\pm p_x \Gamma_{15,x}^\mp)$ $f_1 = f_2^* = x^2 + \omega y^2 + \omega^2 z^2$ $\omega = \exp(2\pi i/3)$ |
| $(\Gamma_{12,2}^\pm \mathcal{H}' \Gamma_{15,x}^\mp) = A_3^* \frac{\hbar}{m} k_x$ | |
| $(\Gamma_{12,2}^\pm \mathcal{H}' \Gamma_{15,y}^\mp) = A_3^* \frac{\hbar}{m} k_y \omega$ | |
| $(\Gamma_{12,2}^\pm \mathcal{H}' \Gamma_{15,z}^\mp) = A_3^* \frac{\hbar}{m} k_z \omega^2$ | |
| $\left. \begin{cases} (\Gamma_{12,1}^\pm \mathcal{H}' \Gamma_{25,x}^\mp) = A_4 \frac{\hbar}{m} k_x \\ (\Gamma_{12,1}^\pm \mathcal{H}' \Gamma_{25,y}^\mp) = A_4 \frac{\hbar}{m} k_y \omega^2 \\ (\Gamma_{12,1}^\pm \mathcal{H}' \Gamma_{25,z}^\mp) = A_4 \frac{\hbar}{m} k_z \omega \end{cases} \right\}$ | $A_4 = (\Gamma_{12}^\pm p_x \Gamma_{25,x}^\mp)$ $f_1 = f_2^* = x^2 + \omega y^2 + \omega^2 z^2$ |
| $(\Gamma_{12,2}^\pm \mathcal{H}' \Gamma_{25,x}^\mp) = A_4^* \frac{\hbar}{m} k_x$ | |
| $(\Gamma_{12,2}^\pm \mathcal{H}' \Gamma_{25,y}^\mp) = A_4^* \frac{\hbar}{m} k_y \omega$ | |
| $(\Gamma_{12,2}^\pm \mathcal{H}' \Gamma_{25,z}^\mp) = A_4^* \frac{\hbar}{m} k_z \omega^2$ | |
| $\left. \begin{cases} (\Gamma_{15,x}^\pm \mathcal{H}' \Gamma_{15,x}^\mp) = 0 \\ (\Gamma_{15,x}^\pm \mathcal{H}' \Gamma_{15,y}^\mp) = -A_5 \frac{\hbar}{m} k_z \\ (\Gamma_{15,x}^\pm \mathcal{H}' \Gamma_{15,z}^\mp) = A_5 \frac{\hbar}{m} k_y \end{cases} \right\}$ | $A_5 = (\Gamma_{15,y}^\pm p_x \Gamma_{15,z}^\mp)$ |
| $(\Gamma_{15,y}^\pm \mathcal{H}' \Gamma_{15,x}^\mp) = A_5 \frac{\hbar}{m} k_z$ | |
| $(\Gamma_{15,y}^\pm \mathcal{H}' \Gamma_{15,y}^\mp) = 0$ | |
| $(\Gamma_{15,y}^\pm \mathcal{H}' \Gamma_{15,z}^\mp) = -A_5 \frac{\hbar}{m} k_x$ | |
| $\left. \begin{cases} (\Gamma_{15,z}^\pm \mathcal{H}' \Gamma_{15,x}^\mp) = -A_5 \frac{\hbar}{m} k_y \\ (\Gamma_{15,z}^\pm \mathcal{H}' \Gamma_{15,y}^\mp) = A_5 \frac{\hbar}{m} k_x \\ (\Gamma_{15,z}^\pm \mathcal{H}' \Gamma_{15,z}^\mp) = 0 \end{cases} \right\}$ | |
| $\left. \begin{cases} (\Gamma_{15,x}^\pm \mathcal{H}' \Gamma_{25,x}^\mp) = 0 \\ (\Gamma_{15,x}^\pm \mathcal{H}' \Gamma_{25,y}^\mp) = A_6 \frac{\hbar}{m} k_z \\ (\Gamma_{15,x}^\pm \mathcal{H}' \Gamma_{25,z}^\mp) = A_6 \frac{\hbar}{m} k_y \end{cases} \right\}$ | $A_6 = (\Gamma_{15,x}^\pm p_y \Gamma_{25,z}^\mp)$ |
| $(\Gamma_{15,y}^\pm \mathcal{H}' \Gamma_{25,x}^\mp) = A_6 \frac{\hbar}{m} k_z$ | |
| $(\Gamma_{15,y}^\pm \mathcal{H}' \Gamma_{25,y}^\mp) = 0$ | |
| $(\Gamma_{15,y}^\pm \mathcal{H}' \Gamma_{25,z}^\mp) = A_6 \frac{\hbar}{m} k_x$ | |
| $\left. \begin{cases} (\Gamma_{15,z}^\pm \mathcal{H}' \Gamma_{25,x}^\mp) = A_6 \frac{\hbar}{m} k_y \\ (\Gamma_{15,z}^\pm \mathcal{H}' \Gamma_{25,y}^\mp) = A_6 \frac{\hbar}{m} k_x \\ (\Gamma_{15,z}^\pm \mathcal{H}' \Gamma_{25,z}^\mp) = 0 \end{cases} \right\}$ | |
| $\left. \begin{cases} (\Gamma_{25,x}^\pm \mathcal{H}' \Gamma_{25,x}^\mp) = 0 \\ (\Gamma_{25,x}^\pm \mathcal{H}' \Gamma_{25,y}^\mp) = -A_7 \frac{\hbar}{m} k_z \\ (\Gamma_{25,x}^\pm \mathcal{H}' \Gamma_{25,z}^\mp) = A_7 \frac{\hbar}{m} k_y \end{cases} \right\}$ | $A_7 = (\Gamma_{25,x}^\pm p_y \Gamma_{25,z}^\mp)$ |
| $(\Gamma_{25,y}^\pm \mathcal{H}' \Gamma_{25,x}^\mp) = A_7 \frac{\hbar}{m} k_z$ | |
| $(\Gamma_{25,y}^\pm \mathcal{H}' \Gamma_{25,y}^\mp) = 0$ | |
| $(\Gamma_{25,y}^\pm \mathcal{H}' \Gamma_{25,z}^\mp) = -A_7 \frac{\hbar}{m} k_x$ | |
| $\left. \begin{cases} (\Gamma_{25,z}^\pm \mathcal{H}' \Gamma_{25,x}^\mp) = -A_7 \frac{\hbar}{m} k_y \\ (\Gamma_{25,z}^\pm \mathcal{H}' \Gamma_{25,y}^\mp) = A_7 \frac{\hbar}{m} k_x \\ (\Gamma_{25,z}^\pm \mathcal{H}' \Gamma_{25,z}^\mp) = 0 \end{cases} \right\}$ | |

+ denotes even and - denotes odd states under inversion,
except for $f_1 \equiv f_1^+$ and $f_2 \equiv f_2^-$.

See Table 10.2 for explicit forms for the basis functions for the O_h group

A_4 we note that the basis function $\Gamma_{25,z}^- = z(x^2 - y^2)$ gives $C_2 \Gamma_{25,z}^- = -\Gamma_{25,z}^-$ where C_2 denotes a rotation of π around the (011) axis. For A_5 we use as basis functions: $\Gamma_{15,x}^- = x$ and $\Gamma_{15,x}^+ = yz(z^2 - y^2)$ which is odd under the interchange $y \leftrightarrow z$. For A_6 we use as basis functions: $\Gamma_{25,x}^+ = yz$ and $\Gamma_{15,x}^- = x$, where $A_6 = (\Gamma_{15,x}^\pm | p_y | \Gamma_{25,z}^\mp)$. For A_7 we use as basis functions: $\Gamma_{25,x}^+ = yz$; $\Gamma_{25,x}^- = x(y^2 - z^2)$; $\Gamma_{25,z}^- = z(x^2 - y^2)$.

Let us make a few general comments about Table 13.2. Since \mathcal{H}' is odd, only states of opposite parity are coupled. For each of the seven symmetry type couplings given in the table, there is only one independent matrix element. For example, the coupling between the Γ_{12}^+ and Γ_{15}^- representations involve $2 \times 3 \times 3 = 18$ matrix elements, but there is only one *independent* matrix element:

$$(x|p_x|f_1) = (x|p_x|f_2) = \omega(y|p_y|f_1) = \omega^2(y|p_y|f_2) = \omega^2(z|p_z|f_1) = \omega(z|p_z|f_2)$$

and all others vanish. Here we write

$$\left. \begin{aligned} f_1 &= x^2 + \omega y^2 + \omega^2 z^2 \\ f_2 &= x^2 + \omega^2 y^2 + \omega z^2 \end{aligned} \right\} \quad (13.59)$$

as the basis functions for the Γ_{12}^+ representation. For Γ_{25}^+ symmetry we can take our basis functions as

$$\left. \begin{aligned} &yz \\ &zx \\ &xy \end{aligned} \right. \quad \text{which in the table are denoted by} \quad \left. \begin{aligned} &(\Gamma_{25,x}^+) \\ &(\Gamma_{25,y}^+) \\ &(\Gamma_{25,z}^+) \end{aligned} \right.$$

The three Γ_{25}^+ basis functions are derived from three of the five atomic d functions, the other two being Γ_{12}^+ functions. Using these results for the matrix elements, the secular equation (13.48) can be written as a function of k_x, k_y and k_z to yield the dispersion relations for the degenerate Γ_{15}^- bands as we move away from the Γ point $k = 0$ in the Brillouin zone.

Since $\Gamma_{15}^- \otimes \Gamma_{15}^- = \Gamma_1^+ + \Gamma_{12}^+ + \Gamma_{15}^+ + \Gamma_{25}^+$, and from (13.57), the secular equation (13.48) for the Γ_{15}^- levels involves the following sums:

$$\begin{aligned} F &= \frac{\hbar^2}{m^2} \sum_{\Gamma_1^+(n')} \frac{|(x|p_x|1)|^2}{E_n^{\Gamma_{15}^-}(0) - E_{n'}^{\Gamma_1^+}(0)}, \\ G &= \frac{\hbar^2}{m^2} \sum_{\Gamma_{12}^+(n')} \frac{|(x|p_x|f_1)|^2}{E_n^{\Gamma_{15}^-}(0) - E_{n'}^{\Gamma_{12}^+}(0)}, \\ H_1 &= \frac{\hbar^2}{m^2} \sum_{\Gamma_{25}^+(n)} \frac{|(x|p_y|xy)|^2}{E_n^{\Gamma_{15}^-}(0) - E_n^{\Gamma_{25}^+}(0)}, \\ H_2 &= \frac{\hbar^2}{m^2} \sum_{\Gamma_{15}^+(n)} \frac{|(x|p_y|xy(x^2 - y^2))|^2}{E_n^{\Gamma_{15}^-}(0) - E_n^{\Gamma_{15}^+}(0)}. \end{aligned} \quad (13.60)$$

We are now ready to solve the secular equation (13.48) using (13.57) to include the various terms which occur in second-order degenerate perturbation theory. Let us consider the diagonal entries first, as for example the xx entry. We can go from an initial $\Gamma_{15,x}^-$ state to the same final state through an intermediate Γ_1^+ state which brings down a k_x^2 term through the F term in (13.60). We can also couple the initial Γ_{15}^- state to itself through an intermediate $\Gamma_{12,1}^+$ or $\Gamma_{12,2}^+$ state, in either case bringing down a k_x^2 term through the G contribution – so far we have $Fk_x^2 + 2Gk_x^2$. We can also go from a $\Gamma_{15,x}^-$ state and back again through a $\Gamma_{25,y}^+$ or $\Gamma_{25,z}^+$ state to give a $(k_y^2 + k_z^2)H_1$ contribution and also through a $\Gamma_{15,y}^+$ or $\Gamma_{15,z}^+$ state to give a $(k_y^2 + k_z^2)H_2$ contribution. Therefore on the diagonal xx entry we get

$$Lk_x^2 + M(k_y^2 + k_z^2), \quad \text{where } L = F + 2G \quad \text{and} \quad M = H_1 + H_2. \quad (13.61)$$

Using similar arguments, we obtain the results for other diagonal entries yy and zz , using a cyclic permutation of indices.

Now let us consider an off-diagonal entry such as $(x|\mathcal{H}'|y)$, where we start with an initial $\Gamma_{15,x}^-$ state and go to a final $\Gamma_{15,y}^-$ state. This can be done through either of four intermediate states:

$$\begin{aligned} \text{Intermediate state } \Gamma_1^+ &\text{ gives } k_x k_y F \\ \text{Intermediate state } \Gamma_{12}^+ &\text{ gives } (\omega^2 + \omega) k_x k_y G = -k_x k_y G \\ \text{Intermediate state } \Gamma_{15}^+ &\text{ gives } -k_x k_y H_2 \\ \text{Intermediate state } \Gamma_{25}^+ &\text{ gives } k_x k_y H_1. \end{aligned}$$

Therefore we get $Nk_x k_y = (F - G + H_1 - H_2)k_x k_y$ for the total xy entry.

Using the same procedure we calculate the other four independent entries to the secular equation. Collecting terms we have the final result for the Taylor expansion of the secular equation for the Γ_{15}^- degenerate p -band:

$$\begin{vmatrix} Lk_x^2 + M(k_y^2 + k_z^2) & Nk_x k_y & Nk_x k_z \\ -\varepsilon(k) & & \\ Nk_x k_y & Lk_y^2 + M(k_z^2 + k_x^2) & Nk_y k_z \\ -\varepsilon(k) & & \\ Nk_x k_z & Nk_y k_z & Lk_z^2 + M(k_x^2 + k_y^2) \\ & & -\varepsilon(k) \end{vmatrix} = 0. \quad (13.62)$$

The secular equation (13.62) is greatly simplified along the high symmetry directions. For a [100] axis, $k_y = k_z = 0$, and $k_x = \kappa$, then (13.62) reduces to

$$\begin{vmatrix} L\kappa^2 - \varepsilon(\kappa) & 0 & 0 \\ 0 & M\kappa^2 - \varepsilon(\kappa) & 0 \\ 0 & 0 & M\kappa^2 - \varepsilon(\kappa) \end{vmatrix} = 0, \quad (13.63)$$

which has the roots

$$\begin{aligned}\varepsilon(\kappa) &= L\kappa^2 \\ \varepsilon(\kappa) &= M\kappa^2 \quad \text{twice.}\end{aligned}\quad (13.64)$$

The result in (13.64) must be consistent with the compatibility relations about the $\mathbf{k} = 0$ (Γ -point) whereby

$$\Gamma_{15}^+ \rightarrow \Delta_{1'} + \Delta_5, \quad (13.65)$$

in which the $\Delta_{1'}$ level is nondegenerate and the Δ_5 level is doubly degenerate.

Along a Λ [111] axis, $k_x = k_y = k_z = \kappa$ and the general secular equation of (13.62) simplifies into

$$\begin{vmatrix} (L + 2M)\kappa^2 - \varepsilon(\kappa) & N\kappa^2 & N\kappa^2 \\ N\kappa^2 & (L + 2M)\kappa^2 - \varepsilon(\kappa) & N\kappa^2 \\ N\kappa^2 & N\kappa^2 & (L + 2M)\kappa^2 - \varepsilon(\kappa) \end{vmatrix} = 0, \quad (13.66)$$

which can readily be diagonalized to give

$$\begin{aligned}\varepsilon(\kappa) &= \frac{L + 2M + 2N}{3}\kappa^2 \quad \text{once } (\Lambda_2 \text{ level}), \\ \varepsilon(\kappa) &= \frac{L + 2M - N}{3}\kappa^2 \quad \text{twice } (\Lambda_3 \text{ level}),\end{aligned}\quad (13.67)$$

where the Λ_2 level is nondegenerate and the Λ_3 level is doubly degenerate.

The secular equation for a general κ point is more difficult to solve, but it can still be done in closed form by solving a cubic equation. In practice, the problem is actually simplified by including the effects of the *electron spin* (see Chap. 15). For each partner of the Γ_{15}^- levels we get a spin up state and a spin down state so that the secular equation is now a (6×6) equation. However, we will see that spin-orbit interaction simplifies the problem somewhat and the secular equation can be solved analytically.

The band parameters L , M , and N , which enter the secular equation (13.62), express the strength of the coupling of the Γ_{15}^- levels to the various other levels. In practice, these quantities are determined from experimental data. The cyclotron resonance experiment carried out along various high symmetry directions provides accurate values [31] for the band curvatures and hence for the quantities L , M and N . In the spirit of the $\mathbf{k} \cdot \mathbf{p}$ perturbation theory, solution of the secular equation provides the most general form allowed by symmetry for $E(\mathbf{k})$ about $\mathbf{k} = 0$. The solution reduces to the proper form along the high symmetry directions, Δ , Λ and Σ . However, group theory cannot provide information about the magnitude of these coefficients. These magnitudes are most easily obtained from experimental data.

The $\mathbf{k} \cdot \mathbf{p}$ method has also been used to obtain the energy bands throughout the Brillouin zone for such semiconductors as silicon and germanium [17]. In the $\mathbf{k} \cdot \mathbf{p}$ approach of Cardona and Pollack, seven other bands outside this “nearly degenerate set” of eight ($\Gamma_1^+, \Gamma_2^-, \Gamma_{15}^-, \Gamma_{25}^+$) bands are allowed to couple to this nearly degenerate set of bands.

New features in the electronic energy band problem arise in going from points of lower symmetry to points of higher symmetry. For example, the $\mathbf{k} \cdot \mathbf{p}$ expansion can be used to connect a Λ point to an L point, along the Λ or (111) axis. The $\mathbf{k} \cdot \mathbf{p}$ method has been made to work well in this context, to parametrize theoretical calculations at high symmetry points and axes for use in regions of the Brillouin zone adjoining the locations for which the calculations were carried out. This use of $\mathbf{k} \cdot \mathbf{p}$ perturbation theory for a high symmetry point in the interior of the Brillouin zone is illustrated in the next section.

13.6 Nondegenerate $\mathbf{k} \cdot \mathbf{p}$ Perturbation Theory at a Δ Point

Figure 13.3 shows that important aspects of the electronic band structure for many cubic semiconductors occurs at \mathbf{k} points away from $\mathbf{k} = 0$ in the Brillouin zone, examples being the location of band extrema, of energy gaps and of carrier pockets for electrons and holes. In this section we illustrate how $\mathbf{k} \cdot \mathbf{p}$ perturbation theory is used both as an interpolation method and as an extrapolation method for the solution of the energy eigenvalues and eigenfunctions for an unperturbed crystal for \mathbf{k} points of high symmetry away from $\mathbf{k} = 0$. In Sect. 13.7 we will show how $\mathbf{k} \cdot \mathbf{p}$ perturbation theory is used to interpret experiments where a probe is used to interact with a sample to study the electronic structure of the perturbed electronic system (from a group theory standpoint, the procedure is quite similar).

Let us consider the use of $\mathbf{k} \cdot \mathbf{p}$ perturbation theory for the group of the wave vector for a Δ point rather than about a Γ point, which was considered in Sects. 13.3–13.5. The momentum operator \mathbf{p} in the $\mathbf{k} \cdot \mathbf{p}$ Hamiltonian transforms as a vector. For the group of the wave vector at a Δ point, the vector transforms as Δ_1 for the longitudinal component x and as Δ_5 for the transverse components y, z .

Typically for semiconductors the conduction bands are nondegenerate. In most cases the conduction band extrema are at $\mathbf{k} = 0$ but for silicon the conduction band extrema are located at the six equivalent $(\Delta, 0, 0)$ locations, where Δ is 85% of the distance from Γ to X . The nondegenerate level in the conduction band at $\mathbf{k} = 0$ has Γ_2^- symmetry, but has Δ_2' symmetry as we move away from $\mathbf{k} = 0$ in a (100) direction (see the compatibility relations for cubic groups in Sect. 10.7 and the character table for the group of the wave vector at a Δ point in Table 10.9 for the diamond structure).

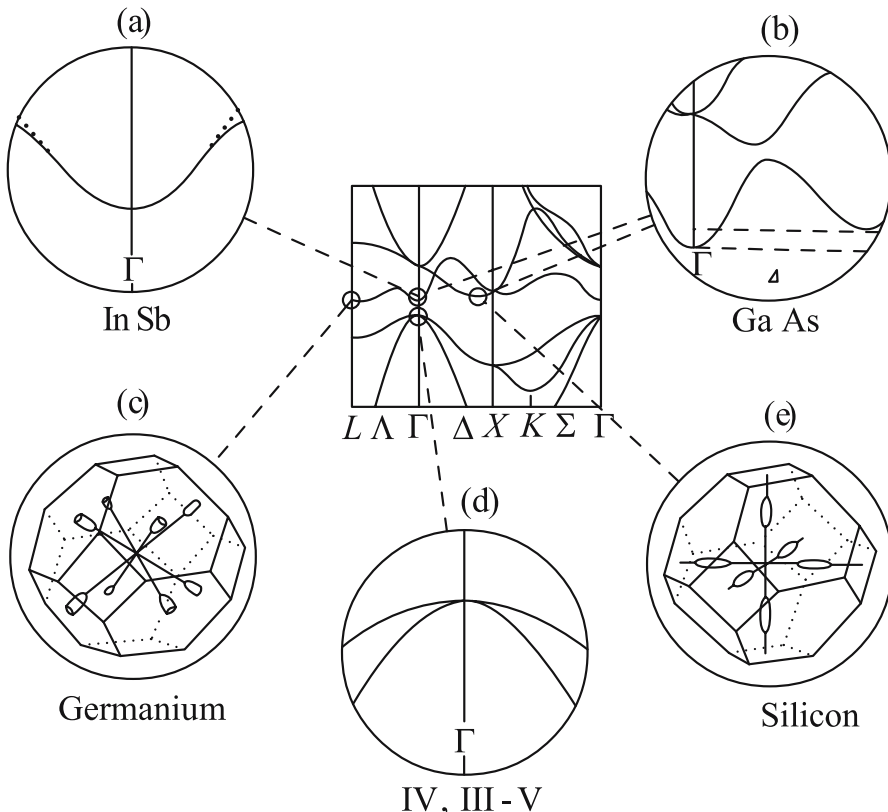


Fig. 13.3. Important details of the band structure of typical group IV and III-V semiconductors are found to occur both at $\mathbf{k} = 0$ and for \mathbf{k} points elsewhere in the Brillouin zone, including the location of conduction and valence band extrema and the location of carrier pockets

We now consider matrix elements of the form $(\Delta_{2'}|p_x|\Delta_{2'})$ which enter the expression for $E(\mathbf{k})$ about the Δ point. In first-order perturbation theory, we can have a nonvanishing contribution along k_x of the form $(\Delta_{2'}|p_x|\Delta_{2'})$ since $\Delta_1 \otimes \Delta_{2'} = \Delta_{2'}$. Thus, there is in general a linear \mathbf{k} term for $E(\mathbf{k})$ in the longitudinal direction. However, at the band extremum this matrix element vanishes (not by symmetry but because of the band extremum). We show below that the transverse matrix elements $(\Delta_{2'}|p_y|\Delta_{2'})$ and $(\Delta_{2'}|p_z|\Delta_{2'})$ vanish by symmetry along the Δ -axis. The second-order contributions to $E(\mathbf{k})$ are as follows:

$$E(\mathbf{k}) = E(\mathbf{k}_0) + \frac{\hbar^2 k_x^2}{2m_\ell^*} + \frac{\hbar^2 (k_y^2 + k_z^2)}{2m_t^*}. \quad (13.68)$$

The longitudinal terms $(\Delta_{2'}|\Delta_1|\Delta_j)$ require that the intermediate state Δ_j transforms as $\Delta_{2'}$ according to the compatibility relations, or else the matrix

element vanishes. States with $\Delta_{2'}$ symmetry at a Δ point arise by compatibility relations from Γ_{25}^+ , Γ_2^- , and Γ_{12}^- states at $\mathbf{k} = 0$ and all of these intermediate states make contributions to a quadratic term in k_x^2 in the dispersion relation given by (13.68). For the transverse k_y and k_z terms, the matrix element $(\Delta_{2'}|\Delta_5|\Delta_j)$ requires the intermediate state Δ_j to transform as Δ_5 . States with Δ_5 symmetry arise from Γ_{25}^\pm levels at $\mathbf{k} = 0$.

Since the basis function for $\Delta_{2'}$ is yz (see Table 10.3), the vector component $\Delta_{5,y}$ couples to the z component of the intermediate state with symmetry $\Delta_{5,z}$ while the vector component $\Delta_{5,z}$ couples to the y component of the intermediate state with symmetry $\Delta_{5,y}$. Therefore there cannot be any nonvanishing matrix elements of the form $(\Delta_{2'}|\Delta_5|\Delta_{2'})$ for either a $\Delta_{5,y}$ or a $\Delta_{5,z}$ component of the vector.

However, in second-order we can have nonvanishing matrix elements about band extremum at \mathbf{k}_0 of the form $(\Delta_{2'}|\Delta_{5,y}|\Delta_{5,z})$ and $(\Delta_{2'}|\Delta_{5,z}|\Delta_{5,y})$ and therefore $E(\mathbf{k})$ about the Δ point extremum must be of the form of (13.68), in agreement with the expression used in solid state physics textbooks. As we move away from the Δ point extremum along the (100) axis, a linear term k_x in the $E(\mathbf{k})$ relation develops, but this term (allowed by group theory) is generally too small to be of significance to the constant energy contours applicable to practical situations, even for high doping levels and carrier pockets of larger volumes in k space.

The ellipsoidal form of $E(\mathbf{k})$ given by (13.68) is very common in semiconductor physics as we move away from $k = 0$. The case of the conduction band of silicon was shown here as an illustration, but similar ellipsoidal constant energy surfaces occur for germanium at the zone boundary L point and for other common III-V semiconductors at the X -point. These arguments given above can then be extended to other points in the Brillouin zone, and to two-band and three-band models for materials with cubic symmetry (see Problems 13.3 and 13.4). The $\mathbf{k} \cdot \mathbf{p}$ perturbation theory approach can of course also be extended to crystals described by other space groups.

13.7 Use of $\mathbf{k} \cdot \mathbf{p}$ Perturbation Theory to Interpret Optical Experiments

To carry out experiments in solid state crystalline physics, a probe is normally used to interrogate the materials system under investigation. These probes interact weakly with the system, causing perturbations that we measure in some way to provide information about the electronic structure of the solid state system. In this section we show how $\mathbf{k} \cdot \mathbf{p}$ perturbation theory is used to study the perturbation imposed on a material by an electromagnetic field and how information is provided by studying this perturbation with an electromagnetic (optical) probe.

The Hamiltonian in the presence of electromagnetic is discussed in Sect. 6.1, and the optical perturbation terms $\mathcal{H}'_{\text{opt}}$ are

$$\mathcal{H}'_{\text{opt}} = -\frac{e}{mc} \mathbf{A} \cdot \mathbf{p} + \frac{e^2 A^2}{2mc^2}, \quad (13.69)$$

in which the lowest order term is

$$\mathcal{H}'_{\text{opt}} \cong -\frac{e}{mc} \mathbf{p} \cdot \mathbf{A}, \quad (13.70)$$

where the vector potential \mathbf{A} relates to the optical fields and is not strongly affected by the crystal, while \mathbf{p} relates directly to the momentum of electrons in the crystal and is strongly affected by the symmetry of the crystal. Therefore the momentum matrix elements $\langle v | \mathbf{p} | c \rangle$ coupling valence and conduction states mainly determine the strength of optical transitions in a low-loss (but finite loss) crystal. It is of interest that this same momentum matrix element governs $\mathbf{k} \cdot \mathbf{p}$ perturbation theory within a crystal and also governs the magnitudes of the effective mass components. With regard to the spatial dependence of the vector potential in (13.70) we can write

$$\mathbf{A} = \mathbf{A}_0 \exp[i(\mathbf{k}_{n_i} \cdot \mathbf{r} - \omega t)], \quad (13.71)$$

where for a loss-less medium described by a propagation constant $k_n = \tilde{n}\omega/c = 2\pi\tilde{n}/\lambda$ is a slowly varying function of \mathbf{r} , since $2\pi\tilde{n}/\lambda$ is much smaller than typical wave vectors in solids. Here \tilde{n} , ω , and λ are, respectively, the real part of the index of refraction, the optical frequency, and the wavelength of light. Thus, to the extent that we neglect the small spatial dependence of the optical propagation constant k_n , it is only the momentum matrix element $\langle v | \mathbf{p} | c \rangle$ coupling the valence and conduction bands that is important to lowest order perturbation theory. We note that electromagnetic interactions with a crystal involve the same matrix element that is connected with the effective mass components of the effective mass tensor for the unperturbed crystal. Group theory thus shows us that optical fields provide a very sensitive probe of the symmetry of a crystal by providing a way to measure this matrix element which is closely related to the effective mass tensor in the solid.

13.8 Application of Group Theory to Valley–Orbit Interactions in Semiconductors

In this section, we shall discuss the application of group theory to the impurity problem of a multivalley semiconductor, such as occurs in the donor carrier pockets in silicon and germanium. In the case of silicon, the lowest conduction bands occur at the six equivalent $(\Delta, 0, 0)$ points where $\Delta = 0.85$ on a scale where the Γ point is at the origin and the X point is at 1. In the

case of germanium, the conduction band minima occur at the L points so that the Fermi surface for electrons consists of eight equivalent half-ellipsoids of revolution (four full ellipsoids). Other cases where valley–orbit interactions are important are multivalley semiconductors, such as PbTe or Te, where the conduction and valence band extrema are both away from $\mathbf{k} = 0$.

Group theory tells us that the maximum degeneracy that energy levels or vibrational states can have with cubic symmetry is a threefold degeneracy. Cubic symmetry is imposed on the problem of donor doping of a semiconductor through the valley–orbit interaction which causes a partial lifting of the n -fold degeneracy of an n -valley semiconductor. In this section we show how group theory prescribes the partial lifting of this n -fold degeneracy. This effect is important in describing the ground state energy of a donor-doped n -valley semiconductor.

Our discussion of the application of group theory to the classification of the symmetries of the impurity levels in a degenerate semiconductor proceeds with the following outline:

- Review of the one-electron Hamiltonian and the effective mass Hamiltonian for a donor impurity in a semiconductor yielding hydrogenic impurity levels for a single-valley semiconductor.
- Discussion of the impurity states for multivalley semiconductors in the effective mass approximation.
- Discussion of the valley–orbit interaction. In this application we consider a situation where the lower symmetry group is not a subgroup of the higher symmetry group.

13.8.1 Background

In this section, we briefly review the one-electron Hamiltonian, effective mass approximation and the hydrogenic impurity problem for a single-valley semiconductor. We write the one-electron Hamiltonian for an electron in a crystal which experiences a perturbation potential $U(\mathbf{r})$ due to an impurity:

$$\left[\frac{p^2}{2m} + V(\mathbf{r}) + U(\mathbf{r}) \right] \Psi(\mathbf{r}) = E\Psi(\mathbf{r}), \quad (13.72)$$

in which $V(\mathbf{r})$ is the periodic potential. In the effective mass approximation, the perturbing potential due to an impurity is taken as $U(\mathbf{r}) = -e^2/(\varepsilon r)$ where ε is the dielectric constant and the origin of the coordinate system is placed at the impurity sites. This problem is usually solved in terms of the effective mass theorem to obtain

$$\left[\frac{p^2}{2m_{\alpha\beta}^*} + U(\mathbf{r}) \right] f_j(\mathbf{r}) = (E - E_j^0) f_j(\mathbf{r}), \quad (13.73)$$

where $m_{\alpha\beta}^*$ is the effective mass tensor for electrons in the conduction band about the band extremum at energy E_j^0 , and $f_j(\mathbf{r})$ is the effective mass wave

function. We thus note that by replacing the periodic potential $V(\mathbf{r})$ by an effective mass tensor, we have *lost most of the symmetry information* contained in the original periodic potential. This symmetry information is restored by introducing the valley–orbit interaction, as in Sects. 13.8.2 and 13.8.3.

The simplest case for an impurity in a semiconductor is that for a shallow substitutional impurity level described by hydrogenic impurity states in a nondegenerate conduction band, as for example a Si atom substituted for a Ga atom in GaAs, a direct gap semiconductor with the conduction band extremum at the Γ point ($k = 0$). To satisfy the bonding requirements in this case, one electron becomes available for conduction and a donor state is formed. The effective mass equation in this case becomes

$$\left[\frac{p^2}{2m^*} - \frac{e^2}{\varepsilon r} \right] f(\mathbf{r}) = (E - E_j^0) f(\mathbf{r}), \quad (13.74)$$

where $U(\mathbf{r}) = -e^2/(\varepsilon r)$ is the screened Coulomb potential for the donor electron, ε is the low frequency dielectric constant, and the donor energies are measured from the band edge E_j^0 . This screened Coulomb potential is expected to be a good approximation for \mathbf{r} at a sufficiently *large distance from the impurity site*, so that ε is taken to be independent of r . The solutions to this hydrogenic problem are the hydrogenic levels

$$E_n - E_j^0 = -\frac{e^2}{2\varepsilon a_0^* n^2} \quad n = 1, 2, \dots, \quad (13.75)$$

where the effective Bohr radius is

$$a_0^* = \frac{\varepsilon \hbar^2}{m^* e^2}. \quad (13.76)$$

Since $(E_n - E_j^0) \sim m^*/\varepsilon^2$, we have *shallow* donor levels located below the band extrema, because of the large value of ε and the small value of m^* in many semiconductors of interest.

Group theoretical considerations enter in the following way. For many III–V compound semiconductors, the valence and conduction band extrema are at $\mathbf{k} = 0$ so that the effective mass Hamiltonian has full rotational symmetry. Since the hydrogenic impurity is embedded in a crystal with a periodic potential, the crystal symmetry (i.e., T_d point group symmetry) will perturb the hydrogenic levels and cause a splitting of various degenerate levels:

$$\begin{aligned} s \text{ levels} &\rightarrow \Gamma_1 \quad (\text{no splitting}), \\ p \text{ levels} &\rightarrow \Gamma_{15} \quad (\text{no splitting}), \\ d \text{ levels} &\rightarrow \Gamma_{12} + \Gamma_{15} \quad (\text{splitting occurs}), \\ f \text{ levels} &\rightarrow \Gamma_2 + \Gamma_{15} + \Gamma_{25} \quad (\text{splitting occurs}). \end{aligned}$$

In principle, if a multiplet has the same symmetry as an s or p level, then an interaction can occur giving rise to an admixture of states of similar symmetries. In practice, the splittings are very small in magnitude and the effects of

the crystal field are generally unimportant for shallow donor levels in single valley semiconductors.

13.8.2 Impurities in Multivalley Semiconductors

Group theory plays a more important role in the determination of impurity states in multivalley semiconductors than for the simple hydrogenic case described in Sect. 13.8.1. A common example of a multivalley impurity state is an As impurity in Si (or in Ge). In Si there are six equivalent valleys for the carrier pockets while for Ge there are four equivalent valleys. The multivalley aspect of the problem results in two departures from the simple hydrogenic series.

The first is associated with the fact that the constant energy surfaces are ellipsoids rather than spheres. We then write Schrödinger's equation for a single valley in the effective mass approximation as

$$\left[\frac{p_x^2 + p_y^2}{2m_t} + \frac{p_z^2}{2m_l} - \frac{e^2}{\varepsilon r} \right] = E f(\mathbf{r}), \quad (13.77)$$

in which m_t is the transverse mass component, m_l is the longitudinal mass component, and the energy E is measured from the energy band extremum. The appropriate symmetry group for the effective mass equation given by (13.77) is $D_{\infty h}$ rather than the full rotation group which applies to the hydrogenic impurity levels. This form for the effective mass Hamiltonian follows from the fact that the constant energy surfaces are ellipsoids of revolution, which in turn is a consequence of the selection rules for the $\mathbf{k} \cdot \mathbf{p}$ Hamiltonian at a Δ point (group of the wave vector C_{4v}) in the case of Si, and at an L point (group of the wave vector D_{3d}) in the case of Ge. The anisotropy of the kinetic energy terms corresponds to the anisotropy of the effective mass tensor. For example in the case of silicon $m_l/m_0 = 0.98$ (heavy mass), $m_t/m_0 = 0.19$ (light mass). This anisotropy in the kinetic energy terms results in a splitting of the impurity levels with angular momentum greater than 1, in accordance with the irreducible representations of $D_{\infty h}$. For example, in $D_{\infty h}$ symmetry we have the following correspondence with angular momentum states:

$$\begin{aligned} s \text{ states} &\rightarrow \Sigma_g^+ = A_{1g}, \\ p \text{ states} &\rightarrow \Sigma_u^+ + \pi_u = A_{2u} + E_{1u}, \\ d \text{ states} &\rightarrow \Delta_g + \pi_g + \Sigma_g^+ = A_{1g} + E_{1g} + E_{2g}. \end{aligned}$$

We note that s and d states are even (g) and p states are odd (u) under inversion in accordance with the character table for $D_{\infty h}$ (see Table A.34.). Thus a $2p$ level with an angular momentum of one splits into a twofold $2p^{\pm 1}$ level and a nondegenerate $2p^0$ level in which the superscripts denote

the n_l component of the angular momentum. Furthermore in $D_{\infty h}$ symmetry, the splitting of d -levels gives rise to the same irreducible representation (Σ_g^+) that describes the s -levels, and consequently a mixing of these levels occurs.

Referring back to (13.77), we note that the effective mass equation cannot be solved exactly if $m_l \neq m_t$. Thus, the donor impurity levels in these indirect gap semiconductors must be deduced from some approximate technique such as a variational calculation or using perturbation theory. The effective mass approximation itself works very well for these p -states because $|\psi_p|^2$ for p states vanishes for $\mathbf{r} = 0$; consequently, for \mathbf{r} values small enough for central cell corrections to be significant, the wave function has a small amplitude and thus small \mathbf{r} values do not contribute significantly to the expectation value of the energy for p -states.

13.8.3 The Valley–Orbit Interaction

The second departure from the hydrogenic series in a multivalley semiconductor is one that relates closely to group theory. This effect is most important for s -states, particularly for the $1s$ hydrogenic state.

For s -states, a sizable contribution to the expectation value for the energy is made by the perturbing potential for small \mathbf{r} . The physical picture of a spherically symmetric potential $U(\mathbf{r})$ for small \mathbf{r} cannot fully apply because the tetrahedral bonding must become important for $|\mathbf{r}| \leq a$. This tetrahedral crystal field which is important within the central cell lifts the spherical symmetry of an isolated atom. Thus we need to consider corrections to the effective mass equation due to the tetrahedral crystal field. This tetrahedral crystal field term is called the valley–orbit effective Hamiltonian, $\mathcal{H}'_{\text{valley–orbit}}$, which couples equivalent conduction band extrema in the various conduction band valleys.

To find the wave functions for the donor states in a multivalley semiconductor, we must find linear combinations of wave functions from each of the conduction band valleys that transform as irreducible representations of the crystal field about the impurity ion. For example, in silicon, the symmetrized linear combination of valley wave functions is in the form

$$\psi^\gamma(\mathbf{r}) = \sum_{j=1}^6 A_j^\gamma f_j(\mathbf{r}) u_{j,k_0^j}(\mathbf{r}) e^{i\mathbf{k}_0^j \cdot \mathbf{r}}, \quad (13.78)$$

in which $\psi^\gamma(\mathbf{r})$ denotes one of six possible linear combinations of the wave functions for the six carrier pockets denoted by γ . The index j is the valley index and $f_j(\mathbf{r})$ is the envelope effective mass wave function, while $u_{j,k_0^j}(\mathbf{r})$ is the periodic part of the Bloch function in which k_0^j is the wave vector to the band minimum of valley j . The six equivalent valleys along the (100) axes for the conduction band of silicon are shown in Fig. 13.4(a). The indices j which label the various ellipsoids or valleys in Fig. 13.4(a) correspond to the

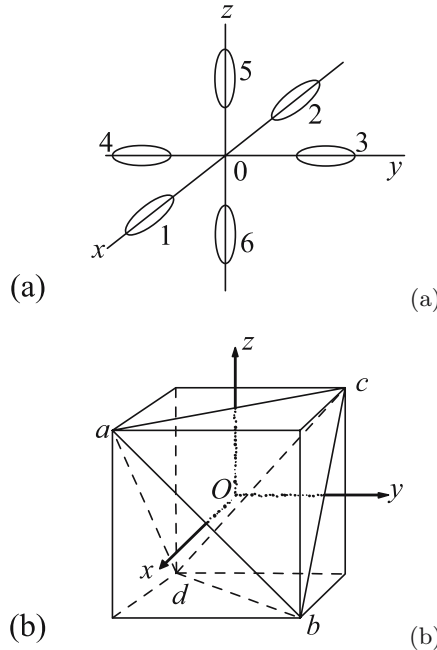


Fig. 13.4. (a) Constant energy ellipsoids of the conduction-band minima of silicon along $\{100\}$ directions in reciprocal space. (b) The regular tetrahedron inscribed inside a cube, useful for seeing the symmetry operations of the six valleys in (a)

Table 13.3. Irreducible representations contained in Γ_{valley} sites of Si

| | E | $8C_3$ | $3C_2$ | $6\sigma_d$ | $6S_4$ | |
|------------------------------|-----|--------|--------|-------------|--------|--|
| $\chi_{\text{valley sites}}$ | 6 | 0 | 2 | 2 | 0 | $= \Gamma_1 + \Gamma_{12} + \Gamma_{15}$ |

indices j of (13.78). The local symmetry close to the impurity center is T_d , reflecting the tetrahedral bonding at the impurity site. The character table for the T_d point group is shown in Table A.32. The diagram which is useful for finding which valleys are invariant under the symmetry operations of T_d is given in Fig. 13.4(b). To get the equivalence transformation for the valley sites, we ask for the number of valleys which remain invariant under the various symmetry operations of T_d . This is equivalent to finding Γ^{equiv} or $\Gamma_{\text{valley sites}}$, which forms a *reducible* representation of point group T_d . From Fig. 13.4(b), we immediately see that the characters for the reducible representation $\Gamma_{\text{valley sites}}$ are (see Table 13.3), and that the irreducible representations contained in $\Gamma_{\text{valley sites}}$ are the $\Gamma_1 + \Gamma_{12} + \Gamma_{15}$ irreducible representations of the point group T_d . To find the splitting of a level we must take the direct product

of the symmetry of the level with $\Gamma_{\text{valley sites}}$, *provided that the level itself transforms as an irreducible representation of group T_d :*

$$\Gamma_{\text{level}} \otimes \Gamma_{\text{valley sites}}. \quad (13.79)$$

Since Γ_{level} for s -states transforms as Γ_1 , the level splitting for s -states is just $\Gamma_{\text{valley sites}} = \Gamma_1 + \Gamma_{12} + \Gamma_{15}$:

$$\begin{aligned} &-\Gamma_{15} \\ &-\Gamma_{12} \\ &-\Gamma_1. \end{aligned}$$

The appropriate linear combination of valley functions corresponding to each of these irreducible representations is (using the notation from (13.78)):

$$\begin{aligned} A_j^{(\Gamma_1)} &= \frac{1}{\sqrt{6}}(1, 1, 1, 1, 1, 1), \\ A_j^{(\Gamma_{12,1})} &= \frac{1}{\sqrt{6}}(1, 1, \omega, \omega, \omega^2, \omega^2) \\ A_j^{(\Gamma_{12,2})} &= \frac{1}{\sqrt{6}}(1, 1, \omega^2, \omega^2, \omega, \omega) \end{aligned} \left. \right\}, \quad (13.80)$$

$$\begin{aligned} A_j^{(\Gamma_{15,1})} &= \frac{1}{\sqrt{2}}(1, -1, 0, 0, 0, 0) \\ A_j^{(\Gamma_{15,2})} &= \frac{1}{\sqrt{2}}(0, 0, 1, -1, 0, 0) \\ A_j^{(\Gamma_{15,3})} &= \frac{1}{\sqrt{2}}(0, 0, 0, 0, 1, -1) \end{aligned} \left. \right\},$$

in which each of the six components of the coefficients A_j^γ refers to one of the valleys. The totally symmetric linear combination Γ_1 is a nondegenerate level, while the Γ_{12} basis functions have two partners which are given by $f_1 = x^2 + \omega y^2 + \omega^2 z^2$ and $f_2 = f_1^*$ and the Γ_{15} basis functions have three partners (x, y, z) .

The analysis for the p -levels is more complicated because the p -levels in $D_{\infty h}$ do not transform as irreducible representations of group T_d . The p -level in group $D_{\infty h}$ transforms as a vector, with A_{2u} and E_{1u} symmetries for the longitudinal and transverse components, respectively. Since T_d does not form a subgroup of $D_{\infty h}$ we write the vector for group T_d as a sum over its longitudinal and transverse components

$$\Gamma_{\text{vec.}} = \Gamma_{\text{longitudinal}} + \Gamma_{\text{transverse}}, \quad (13.81)$$

where $\Gamma_{\text{vec.}} = \Gamma_{15}$. We treat the longitudinal component of the vector as forming a σ -bond and the transverse component as forming a π -bond so that $\Gamma_{\text{longitudinal}} = \Gamma_1$ and $\Gamma_{\text{transverse}} = \Gamma_{15} - \Gamma_1$, where we note that

$$\Gamma_{15} \otimes (\Gamma_1 + \Gamma_{12} + \Gamma_{15}) = \Gamma_{15} + (\Gamma_{15} + \Gamma_{25}) + (\Gamma_1 + \Gamma_{12} + \Gamma_{15} + \Gamma_{25}). \quad (13.82)$$

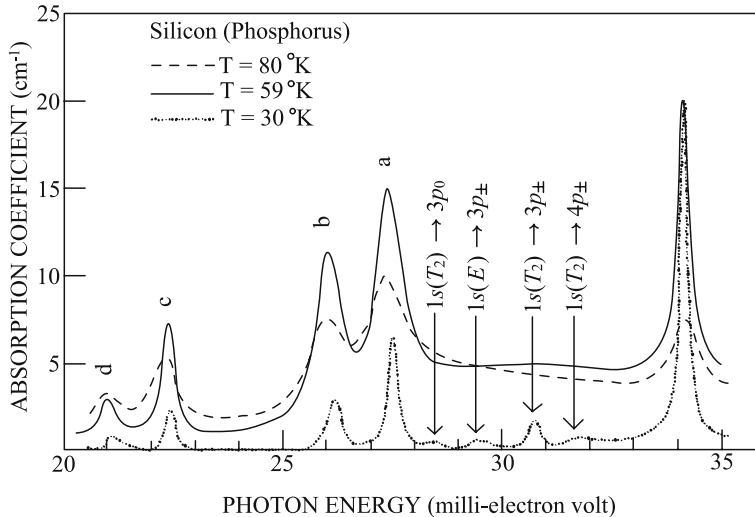


Fig. 13.5. Excitation spectrum of phosphorus donors in silicon. The donor concentration is $N_D \sim 5 \times 10^{15} \text{ cm}^{-3}$. Various donor level transitions to valley-orbit split levels are indicated. The labels for the final state of the optical transitions are in accordance with the symmetries of point group T_d

We thus obtain for the longitudinal (Γ^{2p_0}) and transverse ($\Gamma^{2p_{\pm}}$) levels:

$$\Gamma^{2p_0} = \Gamma_{\text{valley sites}} \otimes \Gamma_1 = \Gamma_1 + \Gamma_{12} + \Gamma_{15} \quad \text{for } m_{\ell} = 0 \quad (13.83)$$

$$\Gamma^{2p_{\pm}} = \Gamma_{\text{valley sites}} \otimes (\Gamma_{15} - \Gamma_1) = 2\Gamma_{15} + 2\Gamma_{25} \quad \text{for } m_{\ell} = \pm 1 \quad (13.84)$$

for group T_d . If we perform high resolution spectroscopy experiments for the donor impurity levels, we would expect to observe transitions between the various $1s$ multiplets to the various $2p$ -multiplets, as allowed by symmetry selection rules [46]. Experimental evidence for the splitting of the degeneracy of the $1s$ donor levels in silicon is provided by infrared absorption studies [4, 67]. An experimental trace for the excitation spectrum of phosphorus impurities in silicon is shown in Fig. 13.5 for several sample temperatures. The interpretation of this spectrum follows from the energy level diagram in Fig 13.6 [46].

It is of interest that the valley orbit splitting effect is only important for the $1s$ levels. For the higher levels, the tetrahedral site location of the impurity atom becomes less important since the Bohr orbit for the impurity level increases as n^2 which qualitatively follows from

$$a_{\text{Bohr}}^* = \frac{\varepsilon \hbar^2}{m^* e^2} n^2 \quad (13.85)$$

where n is the principal quantum number for the donor impurity level.

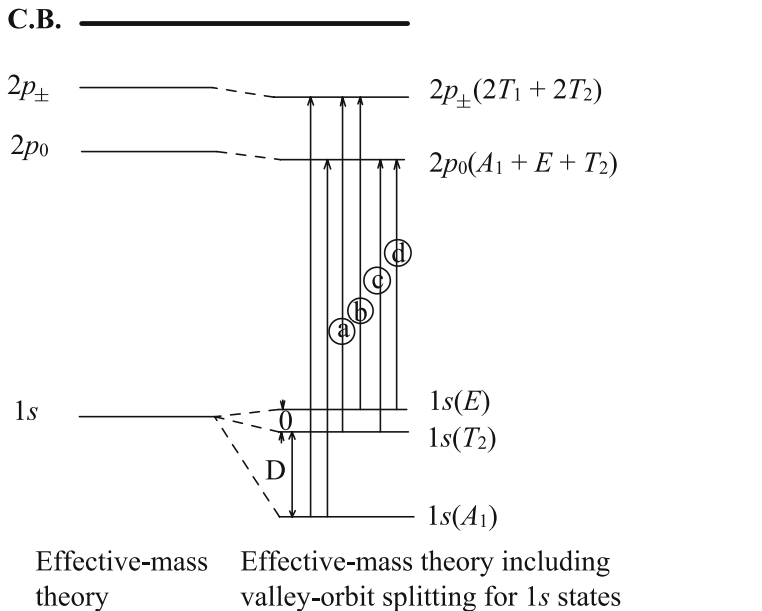


Fig. 13.6. Energy-level scheme for transitions from the valley–orbit split $1s$ multiplet of states to the $2p_0$, $2p_{\pm}$ levels. The irreducible representations for the various valley–orbit split levels in T_d symmetry are indicated. The conduction band edge (C.B.) is also indicated schematically as are the splittings between the three constituents of the valley-orbit split $1s$ level, showing a separation of D between the A_1 and T_2 levels and a separation of O between the T_2 and E levels

In addition to spectroscopic studies of impurity states, these donor states for multivalley semiconductors have been studied by the ENDOR technique [35]. Here the nuclear resonance of the ^{29}Si atoms is observed. The random distribution of the ^{29}Si sites with respect to the donor impurity sites is used to study the spatial dependence of the donor wavefunction, and to determine the location in \mathbf{k} -space of the conduction band extrema.

Selected Problems

- 13.1.** (a) Using $\mathbf{k} \cdot \mathbf{p}$ perturbation theory, find the dispersion relation $E(\mathbf{k})$ for the nondegenerate Γ_2^- (or Γ_2') band around the conduction band extremum near $\mathbf{k} = 0$ for a simple cubic solid.
- (b) The conduction band for germanium which crystallizes in the diamond structure has Γ_2^- (or Γ_2') symmetry. Explain how your result in (a) can be used to describe $E(\mathbf{k})$ about $\mathbf{k} = 0$ for the conduction band of germanium. What modifications occur to (13.12) and (13.14)?

13.2. In this problem, use $\mathbf{k} \cdot \mathbf{p}$ perturbation theory to find the form of the secular equation for the valence band of Si with Γ_{25}^+ symmetry, neglecting the spin-orbit interaction

- (a) Which intermediate states couple to the Γ_{25}^+ valence band states in second-order $\mathbf{k} \cdot \mathbf{p}$ perturbation theory?
- (b) Which matrix elements (listed in Table 13.2) enter the secular equation in (a)?
- (c) Write the secular equation for the Γ_{25}^+ valence bands that is analogous to (13.62) for the Γ_{15}^- band?
- (d) Using the general result in (a), find the special form of the secular equation for the Γ_{25}^+ valence band that is obtained along a Λ (111) axis?

13.3. (a) Using $\mathbf{k} \cdot \mathbf{p}$ perturbation theory, find the form of the $E(\mathbf{k})$ relation near the L -point in the Brillouin zone for a face centered cubic lattice arising from the lowest energy levels. In the free electron model these levels are doubly degenerate and have L_1 and L'_2 symmetry. Which of the nonvanishing $\mathbf{k} \cdot \mathbf{p}$ matrix elements at the L -point are equal to each other by symmetry?
 (b) Using $\mathbf{k} \cdot \mathbf{p}$ perturbation theory, find the form of $E(\mathbf{k})$ for a nondegenerate band with W_1 symmetry about the W point in the FCC lattice (see Table C.12).

13.4. The form of the $E(\mathbf{k})$ relation for the second level of the empty lattice for a BCC system was discussed in Problem 12.6 for both the empty lattice and in the presence of a small periodic potential

- (a) Now consider the lowest energy levels at the H point where the Δ axis along (100) meets the Brillouin zone boundary (see Fig. 12.6 and Tables C.15 and C.8). Find the form of the dispersion relations near the H point using $\mathbf{k} \cdot \mathbf{p}$ perturbation theory and compare your results with the dispersion relations for Na shown in Fig. 12.6(b).
- (b) Using symmetry arguments, why is the splitting between H_1 and H_{15} so much larger than between H_{12} and H_{15} ?

13.5. Find the symmetries and appropriate linear combination of valley functions for the 1s and 2p donor levels for germanium (conduction band minima at the L -point in the Brillouin zone), including the effect of valley-orbit interaction. Indicate the transitions expected in the far infrared spectra for these low temperature donor level states.

Spin–Orbit Interaction in Solids and Double Groups

The discussion of angular momentum and the rotation group has thus far been limited to integral values of the angular momentum (see Chap. 5). The inclusion of half integral angular momentum states requires the introduction of the spin–orbit interaction and “double groups”, which are the focus of this chapter.

14.1 Introduction

The spin angular momentum of an electron is half integral or $S_z = \hbar/2$. Furthermore, associated with each electron is a magnetic moment $\mu_B = -|e|\hbar/(2mc) = 0.927 \times 10^{-20}$ erg/gauss. The magnetic moment and spin angular momentum for the free electron are related by

$$\boldsymbol{\mu} = -\frac{|e|}{mc} \boldsymbol{S} = -\frac{|e|}{mc} \frac{\hbar}{2} \frac{\boldsymbol{S}}{|\boldsymbol{S}|} \quad (14.1)$$

and $\boldsymbol{\mu}$ and \boldsymbol{S} are oppositely directed because of the negative charge on electrons. This relation between the spin angular momentum and the magnetic moment gives rise to an interaction, called the spin–orbit interaction, which is important in describing the electronic structure of crystalline materials. In this section we briefly review this interaction and then in the following sections of this Chapter, we consider the group theoretical consequences of the half-integral spin and the spin–orbit interaction.

An electron in an atom sees a magnetic field because of its own orbital motion and consequently gives rise to the spin–orbit interaction whereby this internal magnetic field tends to line up its magnetic moment along the magnetic field: $\mathcal{H}_{SO} = -\boldsymbol{\mu} \cdot \boldsymbol{H}$. Substitution for $\boldsymbol{H} = -(\mathbf{v}/c) \times \boldsymbol{E}$ and $\boldsymbol{\mu} = -[|e|/(mc)]\boldsymbol{S}$ together with a factor of 1/2 to make the result correct relativistically yields

$$\mathcal{H}'_{SO} = \frac{1}{2m^2c^2} (\boldsymbol{\nabla}V \times \boldsymbol{p}) \cdot \boldsymbol{S}. \quad (14.2)$$

For an atom the corresponding expression is written as

$$\mathcal{H}'_{\text{SO atom}} = \xi(r) \mathbf{L} \cdot \mathbf{S} \quad (14.3)$$

since $\nabla V \sim \mathbf{r}/r^3$ and where \mathbf{L} is the orbital angular momentum. A detailed discussion of the spin–orbit interaction is found in standard quantum mechanics text books.

This spin–orbit interaction gives rise to a spin–orbit splitting of atomic levels which are labeled by their total angular momentum quantum numbers, as discussed below. As an example, consider an atomic p state ($\ell = 1$). Writing the total angular momentum

$$\mathbf{J} = \mathbf{L} + \mathbf{S}, \quad (14.4)$$

where \mathbf{L} and \mathbf{S} are, respectively, the orbital angular momentum operator and the spin angular momentum operator, we obtain for the dot product

$$\mathbf{J} \cdot \mathbf{J} = (\mathbf{L} + \mathbf{S}) \cdot (\mathbf{L} + \mathbf{S}) = \mathbf{L} \cdot \mathbf{L} + \mathbf{S} \cdot \mathbf{S} + (\mathbf{L} \cdot \mathbf{S} + \mathbf{S} \cdot \mathbf{L}), \quad (14.5)$$

in which the operators \mathbf{L} and \mathbf{S} commute since they operate in different coordinate spaces. Since \mathbf{L} and \mathbf{S} are coupled through the spin–orbit interaction, m_ℓ and m_s are no longer good quantum numbers since they are coupled by \mathcal{H}'_{SO} , though ℓ and s remain good quantum numbers. To find the magnitude of the spin–orbit interaction in (14.2), we need to take the matrix elements of \mathcal{H}'_{SO} in the $|j, \ell, s, m_j\rangle$ representation. Using (14.5) for the operators \mathbf{J} , \mathbf{L} and \mathbf{S} , we obtain for the diagonal matrix element of $\mathbf{J} \cdot \mathbf{J}$

$$j(j+1) = \ell(\ell+1) + s(s+1) + 2\langle \mathbf{L} \cdot \mathbf{S} \rangle / \hbar^2, \quad (14.6)$$

so that the expectation value of $\mathbf{L} \cdot \mathbf{S}$ in the $|j, \ell, s, m_j\rangle$ representation becomes

$$\langle \mathbf{L} \cdot \mathbf{S} \rangle = \frac{\hbar^2}{2} [j(j+1) - \ell(\ell+1) - s(s+1)]. \quad (14.7)$$

For p states with spin–orbit interaction, we have $\ell = 1$, and $s = 1/2$ so that $j = 3/2$ or $1/2$

$$\begin{aligned} \langle \mathbf{L} \cdot \mathbf{S} \rangle &= \hbar^2/2 \quad \text{for } j = 3/2 \\ \langle \mathbf{L} \cdot \mathbf{S} \rangle &= -\hbar^2 \quad \text{for } j = 1/2. \end{aligned} \quad (14.8)$$

Thus the spin–orbit interaction introduces a splitting between the $j = 3/2$ and $j = 1/2$ angular momentum states of the p -levels.

From the expression for the expectation value of $\langle \mathbf{L} \cdot \mathbf{S} \rangle$, we note that the degeneracy of an s -state is unaffected by the spin–orbit interaction, and remains two denoting a spin up and spin down state. On the other hand, a d -state is split up into a $D_{5/2}$ (sixfold degenerate) and a $D_{3/2}$ (fourfold degenerate) state. Thus, the spin–orbit interaction does not lift all the degeneracy of atomic states. To lift the remaining degeneracy, it is necessary to

Table 14.1. Spin-orbit interaction energies for some important cubic semiconductors (for the valence band at $k = 0$) [38, 55]

| semiconductor | atomic number | Γ -point splitting |
|---------------|---------------|---------------------------|
| diamond | $Z = 6$ | $\Delta E = 0.006$ eV |
| silicon | $Z = 14$ | $\Delta E = 0.044$ eV |
| germanium | $Z = 32$ | $\Delta E = 0.29$ eV |
| InSb | $Z = 49$ | $\Delta E = 0.9$ eV |
| | $Z = 51$ | |

lower the symmetry further, for example, by the application of a magnetic field. The magnitude of the spin-orbit interaction in atomic physics depends also on the expectation value of $\xi(r)$. For example,

$$\begin{aligned} \langle n, j, \ell, s, m_j | \mathcal{H}'_{\text{SO}} | n, j, \ell, s, m_j \rangle &= \langle j, \ell, s, m_j | \mathbf{L} \cdot \mathbf{S} | j, \ell, s, m_j \rangle \\ &\times \int_0^\infty R_{n\ell}^* \xi(r) R_{n\ell} dr, \end{aligned} \quad (14.9)$$

where $R_{n\ell}$ (the radial part of the wave function) has an r dependence. The magnitude of the integral in (14.9) increases rapidly with increasing atomic number Z , approximately as Z^3 or Z^4 . The physical reason behind the strong Z dependence of $\langle \mathcal{H}'_{\text{SO}} \rangle$ is that atoms with high Z have more electrons to generate larger internal H fields and more electrons with magnetic moments to experience the interaction with these magnetic fields.

For most atomic species that are important in semiconducting materials, the spin-orbit interaction plays a significant role. Some typical values for the spin-orbit splitting energies ΔE for common cubic semiconductors are shown in Table 14.1, where the ΔE listing gives the Γ -point valence band splittings. We will see that in crystalline solids the spin-orbit splittings are \mathbf{k} -dependent. For example, at the L -point for cubic materials, the spin-orbit splittings are typically about 2/3 of the Γ -point value.

The one-electron Hamiltonian for a solid including spin-orbit interaction is

$$\mathcal{H} = \underbrace{\frac{p^2}{2m} + V(\mathbf{r})}_{\mathcal{H}_0} + \underbrace{\frac{1}{2m^2c^2}(\nabla V \times \mathbf{p}) \cdot \mathbf{S}}_{\mathcal{H}'_{\text{SO}}}. \quad (14.10)$$

When the spin-orbit interaction is included, the wave functions consist of a spatial part and a spin part. This means that the irreducible representations that classify the states in a solid must depend on the spin angular momentum. To show the effect of the \mathbf{k} -dependence of the spin-orbit interaction on the energy bands of a semiconductor, consider the energy bands for germanium shown in Fig. 14.1(a) along the $\Delta(100)$ axis, $\Lambda(111)$ axis and $\Sigma(110)$ axes

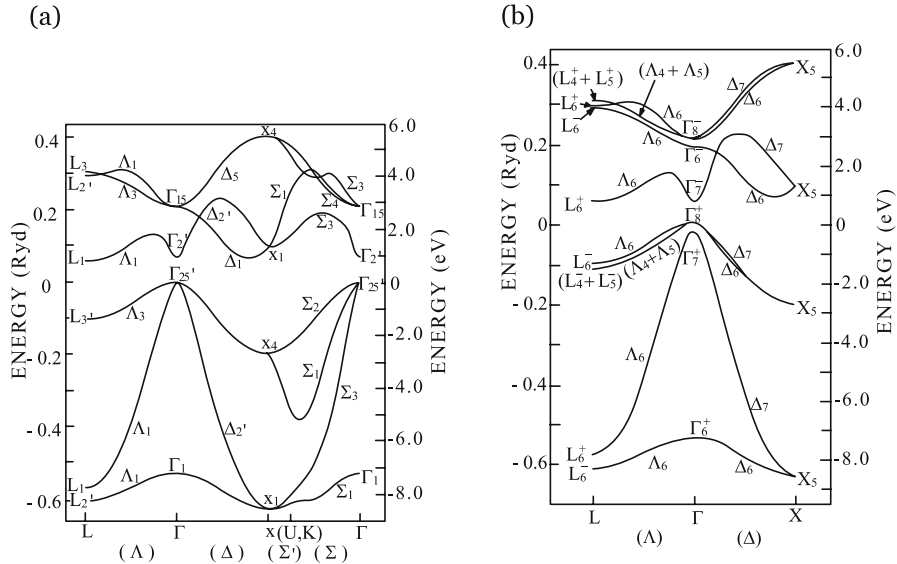


Fig. 14.1. Energy versus dimensionless wave vector for a few high-symmetry directions in germanium using standard notation. (a) The spin–orbit interaction has been neglected. (b) The spin–orbit interaction has been included and the bands are labeled by the double group representations

for no spin–orbit interaction. Here we show the four bonding and the four antibonding s - and p -bands. This picture is to be compared with the energy bands for Ge including the spin–orbit interaction shown in Fig. 14.1(b). The treatment of spin–orbit interaction in crystals that lack inversion symmetry (e.g., such as III–V compounds which have T_d symmetry) gives rise to the “Dresselhaus spin–orbit” term [25] which is often referred to in the spintronics literature. This topic is further discussed in Chap. 16 in connection with time reversal symmetry.

We note that the Fermi level is between the top of the highest valence band (the $\Gamma_{25'}$ band) and the bottom of the lowest conduction band (the L_1 band). The energy band extrema for the more common semiconductors usually occur at high symmetry points. The inclusion of the spin–orbit interaction has two major effects on the energy band structure affecting both the level degeneracies and the labeling of the energy bands. Note that the $(L_4^\pm + L_5^\pm)$ and $(A_4 + A_5)$ are Kramers-degenerate doublet states, which means that these bands stick together at high symmetry points and along high symmetry directions, because of time reversal symmetry to be discussed in Chap. 16. The Γ_7^+ band which lies below the Γ_8^+ valence band in Fig. 14.1(b) is called the *split-off band*, and the separation between the Γ_7^+ and the Γ_8^+ bands is the Γ -point spin–orbit splitting energy ΔE given in Table 14.1 for Ge.

14.2 Crystal Double Groups

Figure 14.1(b) shows energy bands that are labeled by the irreducible representations of the *double group* for the diamond structure. Double groups come into play when we are dealing with the electron spin, whereby half-integral angular momentum states are introduced. In this section we discuss the double group irreducible representations which arise when the electron spin is introduced.

The character tables for states of half-integral angular momentum are constructed from the same basic formula as we used in Chap. 5 for finding the characters for a rotation by an angle α in the full rotation group:

$$\chi_j(\alpha) = \frac{\sin(j + 1/2)\alpha}{\sin(\alpha/2)}. \quad (14.11)$$

Not only is (14.11) valid for integral j (as we have discussed in Chap. 5) but the formula is also valid for j equal to half-integral angular momentum states. We will now discuss the special issues that must be considered for the case of half-integral spin.

Firstly we note that (14.11) behaves differently under the transformation $\alpha \rightarrow (\alpha + 2\pi)$ depending on whether j is an integral or half-integral angular momentum state. This difference in behavior is responsible for the name of *double groups* when j is allowed to assume half-integral values. Let us consider how rotation by $\alpha + 2\pi$ is related to a rotation by α :

$$\chi_j(\alpha + 2\pi) = \frac{\sin(j + 1/2)(\alpha + 2\pi)}{\sin(\frac{\alpha+2\pi}{2})} = \frac{\sin(j + 1/2)\alpha \cdot \cos(j + 1/2)2\pi}{\sin(\alpha/2) \cdot \cos\pi}, \quad (14.12)$$

since $\sin(j + 1/2)2\pi = 0$ whether j is an integer or a half-integer. For integral values of j , $\cos(j + 1/2)2\pi = -1$ while for half-integral values of j , $\cos(j + 1/2)2\pi = +1$. Therefore we have the important relation

$$\chi_j(\alpha + 2\pi) = \chi_j(\alpha)(-1)^{2j}, \quad (14.13)$$

which implies that for integral j , a rotation by $\alpha, \alpha \pm 2\pi, \alpha \pm 4\pi$, etc. yields identical characters (integral values of j correspond to odd-dimensional representations of the full rotation group), the dimensionality being given by $2j + 1$. For half-integral values of j , corresponding to the even-dimensional representations of the rotation group, we have

$$\begin{aligned} \chi_j(\alpha \pm 2\pi) &= -\chi_j(\alpha) \\ \chi_j(\alpha \pm 4\pi) &= +\chi_j(\alpha), \end{aligned} \quad (14.14)$$

so that rotation by 4π is needed to yield the same character for $\chi_j(\alpha)$. The need to rotate by 4π (rather than by 2π) to generate the identity operation leads to the concept of double groups which is the main theme of this chapter.

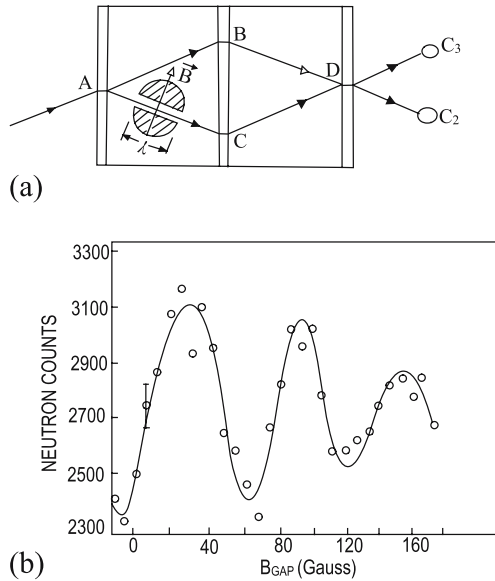


Fig. 14.2. (a) A schematic diagram of the neutron interferometer used to establish the phase of the electron wave function along the path AC along which the neutrons are in a magnetic field B (500 G) for a distance ℓ (2 cm), while the path AB has no magnetic field [72]. (b) The periodic interference pattern as a function of magnetic field, implying a periodicity of 4π

Although the concept of double groups goes back to 1929 [11] experimental evidence that wave functions for Fermions are periodic in 4π and not 2π was not available until 1975 [72] when an ingenious experiment was carried out to measure the phase shift of a neutron due to its precession in a magnetic field. The experiment utilizes a neutron interferometer and determines the phase shift of the neutron as it travels along path AC, where it sees a magnetic field B_{gap} as opposed to path AB where there is no magnetic field, as shown in Fig. 14.2(a). The phase shift measured by counters C_2 and C_3 shows an interference pattern that is periodic, as shown in Fig. 14.2(b), implying a magnetic field precession with a periodicity of 4π . To account for this behavior of the wave function, it is convenient to *introduce a new group element* (rotation by 2π) in dealing with symmetry properties of crystals for which half-integral values of the angular momentum arise as, for example, through the introduction of the electron spin.

Let \mathcal{R} denote a rotation by 2π , and now let us assume that $\mathcal{R} = \pm E$ or equivalently $\mathcal{R}^2 = E$, since the rotation by 4π leaves the characters for the full rotation group invariant for both integral and half-integral j values. Suppose that the elements of the symmetry group without the electron spin are E, A_2, A_3, \dots, A_h . Then, with spin, we have twice as many group elements. That is, we now have the same h elements of the type A_i that we had before

the spin on the electron was considered, plus h new elements of the form $\mathcal{R}A_i$. Just as the matrix representation for the identity operator E is the unit matrix $\hat{1}$ and for $\mathcal{R}E$ it is $\pm\hat{1}$, the matrix representation for A_i is $D^{(\Gamma_j)}(A_i)$ and for $\mathcal{R}A_i$ it is $\pm D^{(\Gamma_j)}(A_i)$, depending upon whether the representation Γ_j is related by compatibility relations to even- or odd-dimensional representations of the full rotation group. The introduction of this symmetry element \mathcal{R} leads to no difficulties with the quantum mechanical description of the problem, since the wave functions ψ and $-\psi$ describe the same physical problem and the matrices $\pm D^{(\Gamma_j)}(A_i)$ each produce the same linear combination of the basis functions.

Because of the introduction of the symmetry element \mathcal{R} , the point groups of the crystal have twice as many elements as before. These point groups also have more classes, but not exactly twice as many classes because some of the elements $\mathcal{R}A_i$ are in the same classes as other elements A_k . For example, according to (14.11), when j assumes *half-integral values*, then we have for a C_2 operation

$$\chi_j(\pi) = \frac{\sin(j + 1/2)\pi}{\sin(\pi/2)} = 0 \quad (14.15)$$

and

$$\chi_j(\pi \pm 2\pi) = \frac{\sin(j + 1/2)(\pi \pm 2\pi)}{\sin(\frac{\pi \pm 2\pi}{2})} = \frac{0}{-1} = 0. \quad (14.16)$$

As presented in Sect. 14.3, for some classes of twofold axes, the elements $\mathcal{R}C_2$ and C_2 are, in fact, in the same class.

14.3 Double Group Properties

We will now state some properties of the even-dimensional representations of the full rotation group and of double groups corresponding to the half-integral angular momentum states. These properties are given here without proof. More complete treatments can be found, for example, in Heine's book on group theory [37]. We list below four important rules for the properties of double groups.

- If a set of symmetry operations $\{A_k\}$ forms a class in the original point group, then $\{A_k\}$ and the corresponding symmetry operations for the double group $\{\mathcal{R}A_k\}$ form two different classes in the double group, except in the case noted below under heading (b).
- The exceptions to property (a) are classes of rotations by π , if, and only if, there is in addition to the operation C_2 another twofold axis \perp to the twofold axis C_2 for all members of the class. In this case only, C_2 and $\mathcal{R}C_2$ are in the same class.
- Any irreducible representation of the original group is also an irreducible representation of the double group, with the same set of characters $[\chi(\mathcal{R}C_k) = \chi(C_k)]$.

- (d) In addition to the irreducible representations described in property (c), there must be additional double group representations, so that we have as many irreducible representations as there are classes. For these additional irreducible representations, the characters for the class \mathcal{RC}_k are found from the characters of class \mathcal{C}_k according to the relation $\chi(\mathcal{RC}_k) = -\chi(\mathcal{C}_k)$. The relation $\chi(\mathcal{C}_k) = -\chi(\mathcal{RC}_k)$ follows because the signs of the wavefunctions change as a result of the symmetry operation \mathcal{RC}_k . In the special case where property (b) applies and $\{A_k\}$ and $\{\mathcal{RA}_k\}$ are in the same class, then

$$\chi(\mathcal{C}_k) = +\chi(\mathcal{RC}_k) = -\chi(\mathcal{RC}_k) = 0, \quad (14.17)$$

since both types of symmetry operations are in same class. Therefore, for classes obeying property (b), it is always the case that $\mathcal{C}_k = C_2$ where $\chi(C_2) = 0$.

We can now write down the characters for double group representations and relate these results to the spin–orbit interaction. In a solid, without spin–orbit coupling

$$\mathcal{H}_0 = \frac{p^2}{2m} + V(\mathbf{r}). \quad (14.18)$$

Now if we include the electron spin, but still neglect the spin–orbit interaction, the Bloch functions in the simplest case can be written as

$$\begin{aligned} \psi_{nk}^+ &= e^{i\mathbf{k}\cdot\mathbf{r}} u_{nk}(\mathbf{r})\alpha \\ \psi_{nk}^- &= e^{i\mathbf{k}\cdot\mathbf{r}} u_{nk}(\mathbf{r})\beta, \end{aligned} \quad (14.19)$$

where α, β are the spin up and spin down eigenfunctions for spin $1/2$, and n, k denote the band index and wave number, respectively, and for a single electron with $S_z = \pm 1/2$. Without spin–orbit coupling, each state is doubly degenerate and is an eigenstate of S_z . If the spin–orbit interaction is included, then the states are no longer eigenstates of S_z and the wave function becomes some linear combination of the states given by (14.19)

$$\psi_{nk} = a\psi_{nk}^+ + b\psi_{nk}^-. \quad (14.20)$$

The group theoretical way to describe these states is in terms of the direct product $\Gamma_i \otimes D_{1/2}$ of the irreducible representation of the spatial wave functions Γ_i with the irreducible representation of the spin function of an electron which we will denote by $D_{1/2}$ and is called the Spinor.

To illustrate how we write the characters for $D_{1/2}$, let us consider cubic crystals with an O symmetry point group. (The results for O_h are immediately obtained from O by taking the direct product $O_h = O \otimes i$.) From the rules given above, the classes of the double group for O are $E, \mathcal{R}, (3C_4^2 +$

Table 14.2. Character for rotations by α for the full rotational symmetry group and the $j = 1/2$ Spinor irreducible representation $D_{1/2}$

| α | $\chi_{1/2}(\alpha)$ | $\chi_{1/2}(\mathcal{R}\alpha)$ |
|-----------------|--|---------------------------------|
| 0 | $\frac{\alpha}{\alpha/2} = 2$ | -2 |
| π | 0 | 0 |
| $\frac{\pi}{2}$ | $\frac{\sin \frac{\pi}{2}}{\sin \frac{\pi}{4}} = \frac{1}{\frac{1}{\sqrt{2}}} = \sqrt{2}$ | $-\sqrt{2}$ |
| $\frac{\pi}{3}$ | $\frac{\sin \frac{2\pi}{3}}{\sin \frac{\pi}{3}} = \frac{\frac{\sqrt{3}}{2}}{\frac{\sqrt{3}}{2}} = 1$ | -1 |

$3\mathcal{RC}_4^2), 6C_4, 6\mathcal{RC}_4, (6C_2 + 6\mathcal{RC}_2), 8C_3, 8\mathcal{RC}_3$. Having listed the classes (eight in this case), we can now find the characters for $D_{1/2}$ by the formula

$$\chi_j(\alpha) = \frac{\sin(j + 1/2)\alpha}{\sin(\alpha/2)} = \frac{\sin \alpha}{\sin(\alpha/2)}, \quad (14.21)$$

since $j = 1/2$. For the Full Rotational Symmetry group, the characters for a rotation by α for the double point group O are found using (14.21) and the results are given in Table 14.2. This procedure for finding the characters for the spinor $D_{1/2}$ is general and can be done for any point group.

Now we will write down the complete character table for the double group O . In O itself, there are 24 elements, and therefore in the double group derived from O there are $24 \times 2 = 48$ elements. There are eight classes in the double group O and therefore eight irreducible representations. We already have five of these irreducible representations (see Table 14.3 for group O). These five irreducible representations are all even representations of the group O_h (see Table D.1 for the corresponding basis functions). Using rule (b) in Sect. 14.3 for the character tables of double group representations, we have the following condition for the dimensionality of the three additional double group representations ($\Gamma_6, \Gamma_7, \Gamma_8$) that are not present in the original group O

$$\sum_i \ell_i^2 = h \quad (14.22)$$

$$1^2 + 1^2 + 2^2 + 3^2 + 3^2 + \ell_6^2 + \ell_7^2 + \ell_8^2 = 48, \quad (14.23)$$

yielding the following restriction on the dimensionalities of the double group irreducible representations:

$$\ell_6^2 + \ell_7^2 + \ell_8^2 = 24. \quad (14.24)$$

Table 14.3. Worksheet for the double group characters for the group O

| | E | \mathcal{R} | $3C_4^2 + 3\mathcal{R}C_4^2$ | $6C_4$ | $6\mathcal{R}C_4$ | $6C_2' + 6\mathcal{R}C_2''$ | $8C_3$ | $8\mathcal{R}C_3$ |
|----------------|-----|---------------|------------------------------|------------|-------------------|-----------------------------|--------|-------------------|
| Γ_1 | 1 | 1 | 1 | 1 | 1 | 1 | 1 | 1 |
| Γ_2 | 1 | 1 | 1 | -1 | -1 | -1 | 1 | 1 |
| Γ_{12} | 2 | 2 | 2 | 0 | 0 | 0 | -1 | -1 |
| $\Gamma_{15'}$ | 3 | 3 | -1 | 1 | 1 | -1 | 0 | 0 |
| $\Gamma_{25'}$ | 3 | 3 | -1 | -1 | -1 | 1 | 0 | 0 |
| Γ_6 | 2 | -2 | 0 | $\sqrt{2}$ | $-\sqrt{2}$ | 0 | 1 | -1 |
| Γ_7 | 2 | -2 | 0 | | | 0 | | |
| Γ_8 | 4 | -4 | 0 | | | 0 | | |

Table 14.4. Characters used to find entries x and y for representation Γ_7

| | E | $8C_3$ | $6C_4$ |
|------------|-----|--------|------------|
| Γ_6 | 2 | 1 | $\sqrt{2}$ |
| Γ_7 | 2 | x | y |

Table 14.5. Characters used to find entries x' and y' for representation Γ_8

| | E | $8C_3$ | $6C_4$ |
|------------|-----|--------|-------------|
| Γ_6 | 2 | 1 | $\sqrt{2}$ |
| Γ_7 | 2 | 1 | $-\sqrt{2}$ |
| Γ_8 | 4 | x' | y' |

This allows us to fill in many of the entries in the double group character table for group O (Table 14.3). For example, Γ_6 , Γ_7 and Γ_8 cannot have 5-dimensional representations, because then $\ell_j^2 = 25 > 24$. Among 1-, 2-, 3- and 4-dimensional irreducible representations, the only combination we can make to satisfy (14.24) is

$$2^2 + 2^2 + 4^2 = 24. \quad (14.25)$$

We already have identified a 2-dimensional irreducible representation of the double group, namely the “spinor” $D_{1/2}$ (see Table 14.2). We see immediately that $D_{1/2}$ obeys all the orthogonality relations, and the characters for $D_{1/2}$ can be added to the character table, using the notation $D_{1/2} = \Gamma_6$.

In Table 14.3 we have also filled in zeros for the characters for all the C_2 classes in the special double group representations Γ_6 , Γ_7 and Γ_8 . Using orthogonality and normalization conditions which follow from the wonderful orthogonality theorem on character, it is quite easy to complete this character table. To get the Γ_7 representation we have to consider the entries in Table 14.4 and orthogonality requires $4+8x+6\sqrt{2}y = 0$ which is satisfied for $x = \pm 1$, and $y = -\sqrt{2}$. Having filled in those entries it is easy to get the four-dimensional representation (see Table 14.5). Orthogonality now requires: $8+8x' \pm \sqrt{2}y' = 0$

Table 14.6. Double group character table for the group O

| O | E | \mathcal{R} | $3C_4^2 + 3\mathcal{R}C_4^2$ | $6C_4$ | $6\mathcal{R}C_4$ | $6C'_2 + 6\mathcal{R}C''_2$ | $8C_3$ | $8\mathcal{R}C_3$ |
|----------------|-----|---------------|------------------------------|-------------|-------------------|-----------------------------|--------|-------------------|
| Γ_1 | 1 | 1 | 1 | 1 | 1 | 1 | 1 | 1 |
| Γ_2 | 1 | 1 | 1 | -1 | -1 | -1 | 1 | 1 |
| Γ_{12} | 2 | 2 | 2 | 0 | 0 | 0 | -1 | -1 |
| $\Gamma_{15'}$ | 3 | 3 | -1 | 1 | 1 | -1 | 0 | 0 |
| $\Gamma_{25'}$ | 3 | 3 | -1 | -1 | -1 | 1 | 0 | 0 |
| Γ_6 | 2 | -2 | 0 | $\sqrt{2}$ | $-\sqrt{2}$ | 0 | 1 | -1 |
| Γ_7 | 2 | -2 | 0 | $-\sqrt{2}$ | $\sqrt{2}$ | 0 | 1 | -1 |
| Γ_8 | 4 | -4 | 0 | 0 | 0 | 0 | -1 | 1 |

Table 14.7. Direct products $\Gamma_i \otimes \Gamma_6^+$ for O_h symmetry

| | |
|---|---|
| $\Gamma_1^+ \otimes \Gamma_6^+ = \Gamma_6^+$ | $\Gamma_1^- \otimes \Gamma_6^+ = \Gamma_6^-$ |
| $\Gamma_2^+ \otimes \Gamma_6^+ = \Gamma_7^+$ | $\Gamma_2^- \otimes \Gamma_6^+ = \Gamma_7^-$ |
| $\Gamma_{12}^+ \otimes \Gamma_6^+ = \Gamma_8^+$ | $\Gamma_{12}^- \otimes \Gamma_6^+ = \Gamma_8^-$ |
| $\Gamma_{15}^+ \otimes \Gamma_6^+ = \Gamma_6^+ + \Gamma_8^+$ | $\Gamma_{15}^- \otimes \Gamma_6^+ = \Gamma_6^- + \Gamma_8^-$ |
| $\Gamma_{25}^+ \otimes \Gamma_6^+ = \Gamma_7^+ + \Gamma_8^+$ | $\Gamma_{25}^- \otimes \Gamma_6^+ = \Gamma_7^- + \Gamma_8^-$ |
| $\Gamma_6^+ \otimes \Gamma_6^+ = \Gamma_1^+ + \Gamma_{15}^+$ | $\Gamma_6^- \otimes \Gamma_6^+ = \Gamma_1^- + \Gamma_{15}^-$ |
| $\Gamma_7^+ \otimes \Gamma_6^+ = \Gamma_2^+ + \Gamma_{25}^+$ | $\Gamma_7^- \otimes \Gamma_6^+ = \Gamma_2^- + \Gamma_{25}^-$ |
| $\Gamma_8^+ \otimes \Gamma_6^+ = \Gamma_{12}^+ + \Gamma_{15}^+ + \Gamma_{25}^+$ | $\Gamma_8^- \otimes \Gamma_6^+ = \Gamma_{12}^- + \Gamma_{15}^- + \Gamma_{25}^-$ |

which is satisfied for $x' = -1$, $y' = 0$. So now we have the whole character table, as shown in Table 14.6.

In practice, we do not have to construct these character tables because the double group character tables have already been tabulated in the literature [47, 48, 54] or via the website cited in Ref. [54]. An example of a double group character table for O symmetry is given in Appendix D, Table D.1. Here you will see that a symmetry element RC_n is listed as \bar{R}_n following the notation in Koster's book. Other examples of double group character tables are found in Appendix D.

We will now apply the double group characters to a cubic crystal with O_h symmetry at the Γ point, $\mathbf{k} = 0$ and we make use of Table 14.6 or Table D.1 and $O_h = O \otimes i$ or Table D.1. The spin functions α and β transform as the partners of the irreducible representation $D_{1/2}$ which is written as Γ_6^+ for the double group O_h . Now we see that the appropriate double group representations (which must be used when the effects of the electron spin are included) are obtained by taking the direct product of the irreducible representation Γ_i with the spinor ($D_{1/2}$) as shown in Table 14.7. Since group $O_h = O \otimes i$, the number of classes in the double group O_h is $2 \times 8 = 16$ and the total number of irreducible representations is 16, and each is labeled according to whether

it is even or odd under the inversion operation, noting that $\Gamma'_{15} = \Gamma_{15}^+$ and $\Gamma'_{25} = \Gamma_{25}^+$, while $\Gamma_{15} = \Gamma_{15}^-$ and $\Gamma_{25} = \Gamma_{25}^-$.

When the spin–orbit interaction is introduced into the description of the electronic structure, then the energy bands are labeled by double group irreducible representations (e.g., Γ_6^\pm , Γ_7^\pm and Γ_8^\pm for the O_h group at $\mathbf{k} = 0$). Table 14.7 shows that the one-dimensional representations without the spin–orbit interaction Γ_1^\pm and Γ_2^\pm all become *doubly degenerate* after taking the direct product with the spinor $D_{1/2}$. This result is independent of the symmetry group. When the spin–orbit interaction is introduced, all formerly non-degenerate levels therefore become double degenerate as in Fig. 14.1(b). (This effect is called the *Kramers degeneracy*.)

In the case of the O_h group, the twofold levels Γ_{12}^\pm become fourfold degenerate when spin is included as is shown in Table 14.7. However, something different happens for the triply degenerate Γ_{15}^\pm and Γ_{25}^\pm states. These states would become sixfold degenerate with spin, but the spin–orbit interaction partly lifts this degeneracy so that these sixfold levels split into a twofold and a fourfold level, just as in the atomic case. Group theory does not tell us the ordering of these levels, nor the magnitude of the splitting, but it does give the symmetry of the levels. By including the spin–orbit interaction in dealing with the valence band of a semiconductor like germanium, the sixfold level can be partially diagonalized; the (6×6) $\mathbf{k} \cdot \mathbf{p}$ effective Hamiltonian breaks up into a (2×2) block and a (4×4) block.

Figure 14.1 shows the effect of the spin–orbit interaction on the energy bands of germanium. We note that the magnitudes of the spin–orbit splittings are \mathbf{k} dependent. Spin–orbit effects are largest at $\mathbf{k} = 0$, moderately large along the (111) direction (A) and at the L -point, but much smaller along the (100) direction (Δ) and at the X -point. Group theory does not provide information on these relative magnitudes. As was mentioned above, the spin–orbit interaction effects tend to be very *important* in the **III–V compound semiconductors**. Since in this case the two atoms in the unit cell correspond to different chemical species, the appropriate point group at $\mathbf{k} = 0$ is T_d and the bonding and antibonding bands both have symmetries Γ_1 and Γ_{15} for the s and p states, respectively. The general picture of the energy bands for the III–V compounds is qualitatively similar to that given in Fig. 14.1 except for a generally larger spin–orbit splitting and for a linear k term to be discussed with regard to time reversal symmetry (see Chap. 16).

Another important class of semiconductors where the spin–orbit interaction is important is the narrow gap lead salts (e.g., PbTe). Since Pb has a high atomic number, it is necessary to give a more exact theory for the spin–orbit interaction in this case, by including relativistic correction terms [21]. However, the group theoretical considerations given here apply equally well when relativistic corrections are included.

In writing down the double group irreducible representations, we see that a particular representation may be associated with various single group representations. For example, the direct products in Table 14.7 show that the

Γ_7^+ irreducible double group representation could be associated with either a Γ_1^+ or a Γ_{25}^+ irreducible single group representation. In dealing with basis functions in the double group representations, it is often useful to know which single group representation corresponds to a particular double group representation. The standard notation used for this association is for example $\Gamma_8^+(\Gamma_{12}^+)$, in which the appropriate single group representation is put in parenthesis, indicating that the particular Γ_8^+ basis functions of interest are those arising from the direct product $\Gamma_{12}^+ \otimes \Gamma_6^+$ rather than from one of the other possibilities listed in Table 14.7.

14.4 Crystal Field Splitting Including Spin–Orbit Coupling

In our treatment of crystal field splittings in solids in Chap. 5 we ignored the spin–orbit coupling, thus providing a first approximation for describing the crystal field levels for the impurity ions in a host lattice. To improve on this, we consider in this chapter the effect of the spin–orbit interaction which will allow us to treat crystal field splittings in host lattices with rare earth ions (where the spin–orbit interaction is in fact larger than the crystal field interaction), and also to obtain a better approximation to the crystal field splittings for $3d$ transition metal ions that were first discussed in Chap. 5.

The introduction of a transition-metal ion in an atomic d -state into an octahedral crystal field gives rise to crystal field splittings, as shown in Fig. 14.3 (see also Sect. 5.3).

For a single d -electron, $s = 1/2$ and in O_h symmetry the appropriate double group representation for the spinor is Γ_6^+ . Thus when the spin–orbit interaction is included in the crystal field problem, the d -levels are further split. Thus the twofold crystal field level in O_h cubic symmetry transforms as

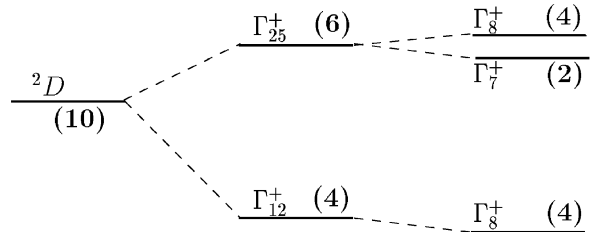
$$\Gamma_{12}^+ \otimes \Gamma_6^+ = \Gamma_8^+ \quad (14.26)$$

and the threefold crystal field level in O_h symmetry is split according to

$$\Gamma_{25}^+ \otimes \Gamma_6^+ = \Gamma_7^+ + \Gamma_8^+ . \quad (14.27)$$

In (14.26) and (14.27), Γ_{12}^+ and Γ_{25}^+ denote spatial wave-functions and Γ_6^+ denotes the spin wave-function. Here we see that the E_g (Γ_{12}^+) level does not split further by the spin–orbit interaction, but the T_{2g} (Γ_{25}^+) level splits into a twofold and a fourfold level.

For the 2D state of the free $3d$ transition-metal ion, we use to Fig. 14.3 to show the splitting induced by a large crystal field and a small spin–orbit interaction (where the number of states is given in parentheses and we use the notation $^{2s+1}X_J$ to denote the quantum numbers s and J while X denotes the orbital angular momentum). The analysis in Fig. 14.3 is valid only if the *crystal field interaction is large compared with the spin–orbit splitting*. This situation describes the iron-group transition metal ions.



Free ion
d-state
with spin

Crystal field
with spin but
no spin–orbit

Crystal field
with spin–orbit

| | |
|--|--|
| $\mathcal{H}_{\Gamma_{25}^+, \Gamma_{25}^+}$ | \mathcal{O} |
| \mathcal{O} | $\mathcal{H}_{\Gamma_{12}^+, \Gamma_{12}^+}$ |

| | | |
|--|--|--|
| $\mathcal{H}_{\Gamma_8^+, \Gamma_8^+}$ | \mathcal{O} | $\mathcal{H}_{\Gamma_8^+, \Gamma_8^+}$ |
| \mathcal{O} | $\mathcal{H}_{\Gamma_7^+, \Gamma_7^+}$ | \mathcal{O} |
| $\mathcal{H}_{\Gamma_8^+, \Gamma_8^+}$ | \mathcal{O} | $\mathcal{H}_{\Gamma_8^+, \Gamma_8^+}$ |

Fig. 14.3. Schematic diagram of the crystal field splitting of a 2D state with a tenfold degeneracy, followed by further splitting by the spin–orbit interaction. This model is appropriate for a $3d$ transition metal ion in a crystal with O_h symmetry for which the crystal field perturbation is large compared to the spin–orbit interaction. The degeneracy of each of the levels is indicated by the parentheses. Also shown in this figure are the labels for the crystal field levels associated with each of the Γ_8^+ levels in the absence of the spin–orbit interaction. Below the crystal field splitting diagram, the form of the crystal field Hamiltonian is indicated on the left in the absence of the spin–orbit interaction, and on the right when the spin–orbit interaction is included

When we move down the periodic table to the palladium group (4d) and the platinum group (5d), the spin–orbit interaction becomes large compared with the crystal field. In this case, we consider first the spin–orbit splitting of the free ion state as the major perturbation (see Fig. 14.4). We now have to consider the effect of the crystal field on levels described by half-integral j values. To compute the characters for the full rotation group, we use the formula

$$\chi_j(\alpha) = \frac{\sin(j + 1/2)\alpha}{\sin(\alpha/2)}. \quad (14.28)$$

We then find the characters for the $^2D_{5/2}$ and $^2D_{3/2}$ states to see how they split in the cubic field (see Table 14.8). Using Table 14.8 we see immediately

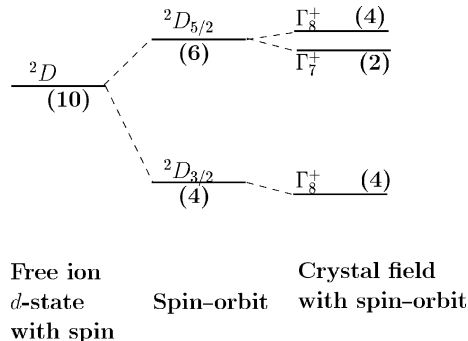


Fig. 14.4. Schematic diagram of the spin-orbit splitting of a 2D level with a tenfold degeneracy and of the subsequent crystal field splittings of these levels in a cubic field for an ion with a spin-orbit interaction that is large compared to the crystal field splittings (which might apply to a $4d$ or a $5d$ atomic level). The degeneracy of each level is shown in parentheses

that the irreducible representations for $^2D_{5/2}$ and $^2D_{3/2}$ become

$$^2D_{5/2} \rightarrow \Gamma_7 + \Gamma_8 \quad (14.29)$$

$$^2D_{3/2} \rightarrow \Gamma_8 \quad (14.30)$$

as indicated in Fig. 14.4. The symmetries in Figs. 14.3 and 14.4 for the levels in the presence of both the spin-orbit interaction and the cubic field of the crystalline solid are $\Gamma_7^+ + 2\Gamma_8^+$ in both cases with the + parity coming from the orbital angular momentum being a D -level (even parity state). In Fig. 14.4, the crystal field splittings are small compared with the spin-orbit splittings, in contrast to the case in Fig. 14.3.

Let us consider another example of crystal field levels that show some other important features. Consider the levels of the holmium ion Ho^{3+} in a cubic field (group O) for which the atomic configuration is $4f^{10}5s^25p^6$ so that by Hund's rule the ground state, after the spin-orbit interaction is included, becomes, $s = 2$, $l = 6$, $j = 8$ denoted by the spectroscopic notation 5I_8 (see page 404 of Ref. [45]). Since $j = 8$ is an integer, application of the formula

$$\chi_j(\alpha) = \left\{ \frac{\sin(j+1/2)\alpha}{\sin(\alpha/2)} \right\} \quad (14.31)$$

gives only ordinary irreducible representations, even though the electron spin is included. We thus get the characters for the ground state 5I_8 given in Table 14.9.

Decomposition of the $\Gamma(^5I_8)$ level into irreducible representations of O yields

$$\Gamma(^5I_8) \rightarrow \Gamma_1 + 2\Gamma_{12} + 2\Gamma_{15} + 2\Gamma_{25}, \quad (14.32)$$

Table 14.8. Decomposition into double group O_h representations for a $\ell = 2$ level

| | E | \mathcal{R} | $3C_4^2 + 3\mathcal{R}C_4^2$ | $6C_4$ | $6\mathcal{R}C_4$ | $6C_2 + 6\mathcal{R}C_2$ | $8C_3$ | $8\mathcal{R}C_3$ |
|-------------------|-----|---------------|------------------------------|-------------|-------------------|--------------------------|--------|-------------------|
| $\chi(^2D_{5/2})$ | 6 | -6 | 0 | $-\sqrt{2}$ | $\sqrt{2}$ | 0 | 0 | 0 |
| $\chi(^2D_{3/2})$ | 4 | -4 | 0 | 0 | 0 | 0 | -1 | 1 |

Table 14.9. Characters for the 5I_8 and ${}^4I_{15/2}$ states in O symmetry

| | E | $3C_4^2$ | $6C_4$ | $6C_2$ | $8C_3$ |
|------------------------|-----|----------|--------|--------|--------|
| $\Gamma({}^5I_8)$ | 17 | 1 | 1 | 1 | -1 |
| $\Gamma({}^4I_{15/2})$ | 16 | 0 | 0 | 0 | -1 |

where there are seven levels for 17 states. Finding the crystal field splittings for a 17-fold level would be a very difficult problem without group theory. As another example, let us consider the erbium ion Er^{3+} in a host crystal. This ion is the basis for applications of amplification capabilities in optical fibers. We consider the level splitting for the rare earth ion Er^{3+} in a $4f^{11}5s^2p^6$ which gives a ${}^4I_{15/2}$ ground state. The characters for the $j = 15/2$ state are given in Table 14.9 and the splitting of these states in a cubic O field is also included in this table. The $j = 15/2$ state in cubic O symmetry splits into

$$\Gamma({}^4I_{15/2}) \rightarrow \Gamma_6 + \Gamma_7 + 3\Gamma_8.$$

In dealing with the crystal field problem, we often encounter a situation where a perturbation is applied to lower the crystal symmetry. In such cases we follow the procedure which we have used many times before – the irreducible representation of the high symmetry group is treated as a reducible representation for the lower symmetry group and we look for the irreducible representations contained therein. The only difference in including the spin–orbit interaction is the use of double groups for all point groups – both for the high symmetry and the low symmetry groups. It is the case that the single group irreducible representations in a group of higher symmetry will always go into single group irreducible representations of the lower symmetry group. For example, the level Γ_8 in point group O goes into $\Gamma_4 + \Gamma_5 + \Gamma_6$ in point group D_3 , when the symmetry is lowered (see Table D.7 in Appendix D.)

In considering optical transitions in semiconductors which are described by either single or double group representations, the electromagnetic interaction Hamiltonian will in all cases transform as the vector within the single group representations. Suppose that we consider the application of an electromagnetic light wave on a Ge crystal where we are considering the coupling of light to the Γ_7^- conduction band at the center of the Brillouin zone. Then we can write

$$\Gamma_{15}^- \otimes \Gamma_7^- = \Gamma_7^+ + \Gamma_8^+, \quad (14.33)$$

and see that light couples the conduction band at $k = 0$ to the valence band and to its related split-off band. Thus, if single group states had been considered instead, such as the Γ_2^- conduction band in Ge without spin-orbit interaction, the coupling of the Γ_2^- band by light would be found by $(\Gamma_{15}^- \otimes \Gamma_2^- = \Gamma_{25}^+)$, which tells us that the Γ_7^- conduction band and the Γ_{25}^+ valence band are in this case also coupled by light. Then (14.33) shows that the corresponding double group conduction band state (Γ_7^-) is optically coupled to the corresponding double group valence band states ($\Gamma_7^+ + \Gamma_8^+$).

Whereas the wave function for a single electron transforms as $D_{1/2}$ (or Γ_6^+ for O_h symmetry), a two-electron wavefunction transforms as the direct product $D_{1/2} \otimes D_{1/2}$. For O_h symmetry, we have for this direct product

$$\Gamma_6^+ \otimes \Gamma_6^+ = \Gamma_1^+ + \Gamma_{15}^+, \quad (14.34)$$

where Γ_1^+ is the singlet $s = 0$ state and the Γ_{15}^+ corresponds to the triplet $s = 1$ level which has three values of m_s . More explicitly, using \uparrow and \downarrow to denote the two spin states and the numerals 1 and 2 to denote each of the two electrons, we can denote the $s = 0$ state by $1/\sqrt{2}(\uparrow_1\downarrow_2 - \downarrow_1\uparrow_2)$ and the three partners of $s = 1$ by $(\uparrow_1\uparrow_2)$, $1/\sqrt{2}(\uparrow_1\downarrow_2 + \downarrow_1\uparrow_2)$, and $(\downarrow_1\downarrow_2)$. We note that in both cases, the levels have integral values of spin angular momentum and thus the state transforms as a single group irreducible representation. Finally, we note that for a $D_{3/2}$ in full rotational symmetry generated by two p -electrons, the double group representation in cubic symmetry for two p electrons yields $D_{1/2}^+ \otimes \Gamma_{15}^- = \Gamma_6^- + \Gamma_8^-$. For the Γ_8^- level, the m_j values are $3/2, 1/2, -1/2$ and $-3/2$ with very different wave functions than arise for the case of two electrons in s states. The $\Gamma_{1/2}^-$ level is made up of p states with $m_j = 1/2$ and $-1/2$ values. These topics are further considered in the following sections.

14.5 Basis Functions for Double Group Representations

We will use the following notation for single electron spin states:

$$\begin{aligned} \uparrow &= \text{spin up} = \begin{pmatrix} 1 \\ 0 \end{pmatrix} \\ \downarrow &= \text{spin down} = \begin{pmatrix} 0 \\ 1 \end{pmatrix}. \end{aligned} \quad (14.35)$$

The states in (14.35) are the states for the spinor $D_{1/2}$ irreducible representation. For the cubic group O this spinor is denoted by the double group representation Γ_6 and for the O_h group by Γ_6^+ . Operation by the *Pauli spin matrices* σ_x, σ_y and σ_z

$$\begin{aligned}\sigma_x &= \begin{pmatrix} 0 & 1 \\ 1 & 0 \end{pmatrix} \\ \sigma_y &= \begin{pmatrix} 0 & -i \\ i & 0 \end{pmatrix} \\ \sigma_z &= \begin{pmatrix} 1 & 0 \\ 0 & -1 \end{pmatrix}\end{aligned}\tag{14.36}$$

on the pure spin up and spin down states yields

$$\begin{aligned}\sigma_x \uparrow &= \downarrow \\ -i\sigma_y \uparrow &= \downarrow \\ \sigma_z \uparrow &= \uparrow \\ \sigma_x \downarrow &= \uparrow \\ -i\sigma_y \downarrow &= -\uparrow \\ \sigma_z \downarrow &= -\downarrow.\end{aligned}\tag{14.37}$$

The Pauli spin matrices $\sigma_x, \sigma_y, \sigma_z$ together with the (2×2) unit matrix

$$\hat{1} = \begin{pmatrix} 1 & 0 \\ 0 & 1 \end{pmatrix}\tag{14.38}$$

span a 2×2 space, so that every 2×2 matrix can be expressed in terms of these four matrices, $\hat{1}, \sigma_x, -i\sigma_y, \sigma_z$. Also the raising σ_+ and lowering σ_- operators are defined by

$$\sigma_{\pm} = \sigma_x \pm i\sigma_y,\tag{14.39}$$

so that

$$\frac{1}{2}\sigma_- \uparrow = \downarrow \quad \text{and} \quad \frac{1}{2}\sigma_+ \downarrow = \uparrow.\tag{14.40}$$

One set of basis functions for Γ_6^+ is the pair \uparrow, \downarrow which form partners for Γ_6^+ relevant to spinors. This pair is also referred to as $[\phi(1/2, 1/2)$ and $\phi(1/2, -1/2)]$ denoting the s and m_s values for each partner. Any other pair can be found from multiplication of this pair by another basis function such as Γ_1^+ , since $\Gamma_6^+ = \Gamma_1^+ \otimes \Gamma_6^+$. We will see below how very different-looking basis functions can be used for Γ_6^+ depending on the single group representation with which Γ_6^+ is connected, such as a Γ_1^+ or a Γ_{15}^+ state. Thus, it is convenient to label the basis functions for any double group representation with the single group representation from which it comes. Thus the pair \uparrow, \downarrow would be associated with a $\Gamma_6^+(\Gamma_1^+)$ state, whereas $\Gamma_6^+(\Gamma_{15}^+)$ would have a different significance as discussed below.

To understand this notation better, consider the $\Gamma_8^+(\Gamma_{15}^+)$ state which comes from the direct product $\Gamma_{15}^+ \otimes \Gamma_6^+ = \Gamma_6^+ + \Gamma_8^+$. For the Γ_{15}^+ state

we may select the *basis functions* L_x, L_y, L_z (angular momentum components). Then the six functions $L_x\uparrow, L_x\downarrow, L_y\uparrow, L_y\downarrow, L_z\uparrow, L_z\downarrow$ make up basis functions for the combined Γ_6^+ and Γ_8^+ representations, assuming no spin-orbit interaction. However, when the spin-orbit interaction is included, we must now find the correct linear combinations of the above six functions so that two of these transform as Γ_6^+ and four transform as Γ_8^+ . The *correct linear combinations* are found by identifying those basis functions which arise in the electronic energy band problem with by making use of angular momentum states as discussed in Sect. 14.6. The principles of group theory tell us that if the group theory problem is solved for angular momentum functions, then the same group theoretical solution can be applied to the electronic energy band eigenfunctions with the same symmetry. This approach is utilized in the following two sections.

14.6 Some Explicit Basis Functions

In this section, we will generate the basis functions for the $j = 3/2, \ell = 1, s = 1/2$ states and for the $j = 1/2, \ell = 1, s = 1/2$ states. For the angular momentum functions in the $|\ell s m_\ell m_s\rangle$ representation, the six eigenfunctions correspond to the orbital states $\ell = 1, m_\ell = 1, 0, -1$ and the spin states $s = 1/2, m_s = 1/2, -1/2$. The transformations we are looking for will transform these states into $j = 3/2, m_j = 3/2, 1/2, -1/2, -3/2$ and $j = 1/2, m_j = 1/2, -1/2$. The matrices which carry out these transformations generate what are known as the Clebsch-Gordan coefficients. Tables of Clebsch-Gordan coefficients are found in quantum mechanics and group theory books for many of the useful combinations of spin and orbital angular momentum that occur in practical problems [20].

A basis set that is appropriate for $\ell = 1, s = 1/2$ is given below for a Γ_8^+ double group state derived from a Γ_{15}^+ single group state (see also Sect. 14.9)

| $ j, m_j\rangle$ State | Basis Function | |
|-------------------------------------|---|---------|
| $ \frac{3}{2}, \frac{3}{2}\rangle$ | $\xi_1 = \frac{1}{\sqrt{2}}(L_x + iL_y) \uparrow$ | |
| $ \frac{3}{2}, \frac{1}{2}\rangle$ | $\xi_2 = \frac{1}{\sqrt{6}}[(L_x + iL_y) \downarrow + 2L_z \uparrow]$ | (14.41) |
| $ \frac{3}{2}, -\frac{1}{2}\rangle$ | $\xi_3 = \frac{1}{\sqrt{6}}[(L_x - iL_y) \uparrow + 2L_z \downarrow]$ | |
| $ \frac{3}{2}, -\frac{3}{2}\rangle$ | $\xi_4 = \frac{1}{\sqrt{2}}(L_x - iL_y) \downarrow$ | |

These basis functions are obtained using the fundamental relations for raising operators

$$L_+ |\ell, m_\ell\rangle = \sqrt{(\ell - m_\ell)(\ell + m_\ell + 1)} |\ell, m_\ell + 1\rangle$$

$$J_+ |j, m_j\rangle = \sqrt{(j - m_j)(j + m_j + 1)} |j, m_j + 1\rangle. \quad (14.42)$$

We further note that the state $|j = 3/2, m_j = -3/2\rangle$ is identical with the state for $\ell = 1, s = 1/2$ and $|m_\ell = -1, m_s = -1/2\rangle$. Therefore, we start with the $j = 3/2, m_j = -3/2$ state and apply the raising operator to obtain the other states:

$$\begin{aligned}
 J_+ \left| j = \frac{3}{2}, m_j = -\frac{3}{2} \right\rangle &= \sqrt{\left(\frac{3}{2} + \frac{3}{2}\right) \left(\frac{3}{2} - \frac{3}{2} + 1\right)} \left| j = \frac{3}{2}, m_j = -\frac{1}{2} \right\rangle \\
 &= (L_+ + S_+) \left| m_\ell = -1, m_s = -\frac{1}{2} \right\rangle \\
 &= \sqrt{(1+1)(1-1+1)} \left| m_\ell = 0, m_s = -\frac{1}{2} \right\rangle \quad (14.43) \\
 &\quad + \sqrt{\left(\frac{1}{2} + \frac{1}{2}\right) \left(\frac{1}{2} - \frac{1}{2} + 1\right)} \left| m_\ell = -1, m_s = \frac{1}{2} \right\rangle.
 \end{aligned}$$

Collecting terms, we obtain

$$\left| j = \frac{3}{2}, m_j = -\frac{1}{2} \right\rangle = \frac{\sqrt{2}}{3} \left| m_\ell = 0, m_s = -\frac{1}{2} \right\rangle + \frac{1}{\sqrt{3}} \left| m_\ell = -1, m_s = \frac{1}{2} \right\rangle. \quad (14.44)$$

We make the identification:

$$\begin{aligned}
 m_\ell = +1 &\rightarrow \frac{1}{\sqrt{2}}(L_x + iL_y) \\
 m_\ell = 0 &\rightarrow L_z \\
 m_\ell = -1 &\rightarrow \frac{1}{\sqrt{2}}(L_x - iL_y) \\
 m_s = \frac{1}{2} &\rightarrow \uparrow \\
 m_s = -\frac{1}{2} &\rightarrow \downarrow,
 \end{aligned}$$

from which we obtain the basis functions

$$\begin{array}{lll}
 |j, m_j\rangle & \text{State} & \text{Basis Function} \\
 \left| \frac{3}{2}, -\frac{3}{2} \right\rangle & & \frac{1}{\sqrt{2}}(L_x - iL_y) \downarrow \\
 \left| \frac{3}{2}, -\frac{1}{2} \right\rangle & & \frac{1}{\sqrt{6}}[(L_x - iL_y) \uparrow + 2L_z \downarrow].
 \end{array} \quad (14.45)$$

Similarly, operation of J_+ on the state $|j = 3/2, m_j = 1/2\rangle$ results in a state $|j = 3/2, m_j = 1/2\rangle$ and operation of $L_+ + S_+$ on the corresponding functions of $|m_\ell = 0, m_s = -1/2\rangle$ and $|m_\ell = -1, m_s = 1/2\rangle$ results in states $|m_\ell = 0, m_s = 1/2\rangle$ and $|m_\ell = +1, m_s = -1/2\rangle$. In this way we obtain all the basis functions for $\Gamma_8^+(\Gamma_{15}^+)$ given in (14.41).

We will now proceed to obtain the basis functions for $\Gamma_6^+(\Gamma_{15}^+)$ which are

| $ j, m_j\rangle$ State | Basis Function |
|-------------------------------------|--|
| $ \frac{1}{2}, \frac{1}{2}\rangle$ | $\lambda_1 = \frac{1}{\sqrt{3}}[(L_x + iL_y) \downarrow -L_z \uparrow]$ |
| $ \frac{1}{2}, -\frac{1}{2}\rangle$ | $\lambda_2 = \frac{1}{\sqrt{3}}[-(L_x - iL_y) \uparrow +L_z \downarrow]$. |

The notation “ ξ_i ” was used in (14.41) to denote the four $\Gamma_8^+(\Gamma_{15}^+)$ basis functions for $j = 3/2$ and “ λ_i ” for the two $\Gamma_6^+(\Gamma_{15}^+)$ basis functions for $j = 1/2$. This notation “ ξ_i ” and “ λ_i ” is arbitrary and is not standard in the literature.

To obtain the $\Gamma_6^+(\Gamma_{15}^+)$ basis functions we note that the appropriate (m_ℓ, m_s) quantum numbers corresponding to $j = 1/2$ and $m_j = \pm 1/2$ are

$$\begin{aligned} m_\ell = 0, \quad m_s &= \pm \frac{1}{2}, \\ m_\ell = 1, \quad m_s &= -\frac{1}{2}, \\ m_\ell = -1, \quad m_s &= +\frac{1}{2}, \end{aligned}$$

so that the corresponding basis functions are completely specified by making them orthogonal to the $|j = 3/2, m_j = +1/2\rangle$ and $|j = 3/2, m_j = -1/2\rangle$ states. For example, the function orthogonal to

$$\sqrt{\frac{2}{3}} \left| m_\ell = 0, m_s = -\frac{1}{2} \right\rangle + \frac{1}{\sqrt{3}} \left| m_\ell = -1, m_s = +\frac{1}{2} \right\rangle \quad (14.47)$$

is the function

$$\frac{1}{\sqrt{3}} \left| m_\ell = 0, m_s = -\frac{1}{2} \right\rangle - \sqrt{\frac{2}{3}} \left| m_\ell = -1, m_s = +\frac{1}{2} \right\rangle, \quad (14.48)$$

which yields the basis functions for the $|j = 1/2, m_j = -1/2\rangle$ state:

$$\frac{1}{\sqrt{3}} |L_z \downarrow - (L_x - iL_y) \uparrow \rangle. \quad (14.49)$$

Similarly the basis function for the $|j = 1/2, m_j = +1/2\rangle$ state can be found by application of the raising operators J_+ and $(L_+ + S_+)$ to the $|j = 1/2, m_j = -1/2\rangle$ state, or alternatively by requiring orthogonality to the $|j = 3/2, m_j = +1/2\rangle$ state. Applying the raising operator to the state (14.48) yields

$$\begin{aligned} \frac{1}{\sqrt{3}} \left| m_\ell = 0, m_s = +\frac{1}{2} \right\rangle - \sqrt{\frac{2}{3}} \left| m_\ell = +1, m_s = -\frac{1}{2} \right\rangle \\ = \frac{1}{\sqrt{3}} [(L_x + iL_y) \downarrow -L_z \uparrow], \end{aligned} \quad (14.50)$$

which is seen to be orthogonal to

$$\frac{1}{\sqrt{6}}[(L_x + iL_y) \downarrow + 2L_z \uparrow]. \quad (14.51)$$

In finding the basis functions for $\Gamma_8^+(\Gamma_{15}^+)$ we have made use of the symmetry properties of the angular momentum operators. As far as the symmetry properties are concerned, it makes no difference whether \mathbf{L} is an angular momentum function or an electronic energy band wave function with Γ_{15}^+ symmetry. This concept allows us to write down wave functions with Γ_8^+ symmetry derived from other single group states, and examples of such results are given in Sect. 14.7, and others are taken from the literature [47] or elsewhere (see also Appendix D for tables of these coupling coefficients).

14.7 Basis Functions for Other Γ_8^+ States

Basis functions for the Γ_8^\pm state derived from $\Gamma_8^-(\Gamma_{15}^-)$, $\Gamma_8^+(\Gamma_{25}^+)$, $\Gamma_8^-(\Gamma_{25}^-)$, etc. can be found from $\Gamma_8^+(\Gamma_{15}^+)$ and $\Gamma_6^+(\Gamma_{15}^+)$, as explained below. To obtain the basis functions for $\Gamma_8^-(\Gamma_{15}^-)$, all we have to do is to replace

$$L_x, L_y, L_z \rightarrow x, y, z$$

in (14.41) of Sect. 14.6. This set of basis functions is also considered in Sect. 14.8 using tables available from the literature. Likewise to obtain $\Gamma_8^+(\Gamma_{25}^+)$, we have to replace

$$L_x, L_y, L_z \rightarrow \varepsilon_x, \varepsilon_y, \varepsilon_z,$$

where $\varepsilon_x = yz$, $\varepsilon_y = zx$, $\varepsilon_z = xy$. By using this prescription, the basis functions for Γ_8^\pm will be of the same form for all symmetry-related partners, whether the basis functions are derived from a Γ_{15}^\pm or a Γ_{25}^\pm single group representation. This correspondence is a highly desirable feature for working practical problems.

We note that the $\Gamma_8^+(\Gamma_{12}^+)$ representation can also be produced by considering the electron spin for a Γ_{12}^+ spinless level: $\Gamma_6^+ \otimes \Gamma_{12}^+ = \Gamma_8^+$. We can always make a set of four basis functions for this representation out of $f_1 \uparrow, f_1 \downarrow, f_2 \uparrow, f_2 \downarrow$ where $f_1 = x^2 + \omega y^2 + \omega^2 z^2$, $f_2 = f_1^*$ and $\omega = \exp(2\pi i/3)$. This makes up a perfectly good representation, but the actual functions that are partners look very different from those of $\Gamma_8^+(\Gamma_{15}^+)$ or $\Gamma_8^+(\Gamma_{25}^+)$. We can, however, make a unitary transformation of these four functions so that they look like the $\Gamma_8^+(\Gamma_{15}^+)$ set.

We can make use of these double group basis functions in many ways. For example, these basis functions are used to determine the nonvanishing

$\mathbf{k} \cdot \mathbf{p}$ matrix elements ($u_{n,0}^{\Gamma_i} | \mathcal{H}' | u_{n,0}^{\Gamma_j}$) (see Chap. 15 and (15.12)). These basis functions also determine which of the nonvanishing matrix elements are equal to each other for a given group of the wave vector.

One technique that can be used to determine the number of nonvanishing matrix elements in cases involving multidimensional representations is as follows. If the relevant matrix element is of the form ($\Gamma_i | \Gamma_{\text{interaction}} | \Gamma_j$) then the *number of independent matrix elements* is the number of times the identity representation (Γ_1^+) is contained in the triple direct product $\Gamma_i \otimes \Gamma_{\text{interaction}} \otimes \Gamma_j$. For example, the direct product of the matrix element ($\Gamma_1^+ | \Gamma_{15}^- | \Gamma_{15}^-$) is

$$\Gamma_1^+ \otimes \Gamma_{15}^- \otimes \Gamma_{15}^- = \Gamma_1^+ + \Gamma_{12}^+ + \Gamma_{15}^+ + \Gamma_{25}^+, \quad (14.52)$$

and since all nonvanishing matrix elements must be invariant under all symmetry operations of the group, only the Γ_1^+ term leads to a nonvanishing matrix element. This triple direct product then tells us that of the nine possible combinations of partners, there is only one independent nonvanishing matrix element, and therefore all nine possible combinations of partners must be related to this nonvanishing matrix element.

For the case of double groups, the matrix element ($\Gamma_6^+ | \Gamma_{15}^- | \Gamma_6^-$) has $2 \times 3 \times 2 = 12$ possible combinations. Now $\Gamma_6^+ \otimes \Gamma_{15}^- \otimes \Gamma_6^- = \Gamma_1^+ + \Gamma_{15}^+ + \Gamma_{12}^+ + \Gamma_{15}^+ + \Gamma_{25}^+$, so that once again there is only one independent matrix element. Finally, for the case ($\Gamma_6^+ | \Gamma_{15}^- | \Gamma_8^-$) there are 24 possible combinations. The direct product $\Gamma_6^+ \otimes \Gamma_{15}^- \otimes \Gamma_8^- = \Gamma_1^+ + \Gamma_2^+ + \Gamma_{12}^+ + 2\Gamma_{15}^+ + 2\Gamma_{25}^+$, and once again there is one independent matrix element. Furthermore, if Γ_6^- and Γ_8^- are both related through a Γ_{15}^- interaction term, then the *same independent matrix element* applies to both ($\Gamma_6^+ | \Gamma_{15}^- | \Gamma_6^-$) and ($\Gamma_6^+ | \Gamma_{15}^- | \Gamma_8^-$).

14.8 Comments on Double Group Character Tables

At this point, it is important to address the reader to Appendix D, which contains much information and many illustrative tables pertinent to double groups. This appendix provides an interface between this chapter and the literature [48, 54] and various sources of information about double groups.

In dealing with electronic energy bands for which the spin-orbit interaction is included, we use the $|j\ell sm_j\rangle$ representation, and this in general requires a transformation from the basis functions in the $|\ell sm_\ell m_s\rangle$ representation to the $|j\ell sm_j\rangle$ representation. Table D.4 in Appendix D gives us the following relations between the pertinent basis functions for the two representations for the double group O_h :

$$\begin{aligned}
\psi_{-1/2}^6 &= \left| \frac{1}{2}, -\frac{1}{2} \right\rangle = -(i/\sqrt{3})(u_x^4 - iu_y^4) \uparrow + (i/\sqrt{3})u_z^4 \downarrow \\
\psi_{1/2}^6 &= \left| \frac{1}{2}, \frac{1}{2} \right\rangle = -(i/\sqrt{3})(u_x^4 + iu_y^4) \downarrow - (i/\sqrt{3})u_z^4 \uparrow \\
\psi_{-3/2}^8 &= \left| \frac{3}{2}, -\frac{3}{2} \right\rangle = (i/\sqrt{2})(u_x^4 - iu_y^4) \downarrow \\
\psi_{-1/2}^8 &= \left| \frac{3}{2}, -\frac{1}{2} \right\rangle = (i/\sqrt{6})(u_x^4 - iu_y^4) \uparrow + (i\sqrt{2}/\sqrt{3})u_z^4 \downarrow \\
\psi_{1/2}^8 &= \left| \frac{3}{2}, \frac{1}{2} \right\rangle = -(i/\sqrt{6})(u_x^4 + iu_y^4) \downarrow + (i\sqrt{2}/\sqrt{3})u_z^4 \uparrow \\
\psi_{3/2}^8 &= \left| \frac{3}{2}, \frac{3}{2} \right\rangle = -(i/\sqrt{2})(u_x^4 + iu_y^4) \uparrow . \tag{14.53}
\end{aligned}$$

In Table D.4, Γ_{15}^- is denoted by Γ_4 , and (u_x^4, u_y^4, u_z^4) are the three partners of Γ_4 , while the spinor partners are denoted by $\uparrow = v_{1/2}^6$ and $\downarrow = v_{-1/2}^6$, thus constituting the $|\ell s m_\ell m_s\rangle$ representations. The linear combinations given in (14.53) and written above are basically the *Clebsch–Gordan coefficients* in quantum mechanics [20]. We make use of these equations in Sect. 14.9 when we discuss the introduction of spin and the spin–orbit interaction into the plane wave relations describing the energy eigenvalues and eigenfunctions of the empty lattice for an electron with spin.

Table D.1 gives the point group character tables for group O and group T_d including double groups, while Table D.7 gives the compatibility relations showing the decomposition of the irreducible representations of T_d and O into the irreducible representations of the appropriate lower symmetry groups. Note in Table D.7 that E refers to the electric field and H to the magnetic field. The table can be used for many applications, such as finding the resulting symmetries under crystal field splittings as for example $O_h \rightarrow D_3$ (see Sect. 14.4). The decomposition of the irreducible representations of the full rotation group into irreducible representations of groups O and T_d for the s, p, d, \dots functions, etc. is given in Tables D.8 and D.9. Note that all the irreducible representations of the full rotation group D_j^\pm are listed, with the \pm sign denoting the parity (even or odd under inversion) and the subscript giving the angular momentum quantum number (j), so that the dimensionality of the irreducible representation D_j^\pm is $(2j + 1)$.

14.9 Plane Wave Basis Functions for Double Group Representations

In Chap. 12 we discussed the nearly free electron approximation for the energy bands in crystalline solids, neglecting the electron spin. In this case, the

electron wave functions were expressed in terms of symmetrized linear combinations of plane waves transforming according to irreducible representations of the group of the wave vector. In the present section, we extend the presentation in Chap. 12 by giving an explicit example for O_h symmetry (space group #221 for the simple cubic lattice) focusing on the plane wave solutions at $k = 0$ for the corresponding situation where the spin of the electron is included and the wave functions are described in terms of the double group irreducible representations.

It is relatively simple to include the effect of the electron spin for the irreducible representations Γ_1^\pm and Γ_2^\pm because there are no splittings induced by the spin-orbit coupling. Thus the basis functions in this case are simple product functions given by $\Gamma_6^\pm = \Gamma_1^\pm \otimes \Gamma_6^+$ and $\Gamma_7^\pm = \Gamma_2^\pm \otimes \Gamma_6^+$ or more explicitly

$$\begin{aligned}\Psi_{\Gamma_6^\pm}(\mathbf{K}_{n_i}) &= \psi_{\Gamma_1^\pm}(\mathbf{K}_{n_i}) \begin{pmatrix} \alpha \\ \beta \end{pmatrix} \\ \Psi_{\Gamma_7^\pm}(\mathbf{K}_{n_i}) &= \psi_{\Gamma_2^\pm}(\mathbf{K}_{n_i}) \begin{pmatrix} \alpha \\ \beta \end{pmatrix},\end{aligned}\quad (14.54)$$

in which the \mathbf{K}_{n_i} denote reciprocal lattice vectors while $\psi_{\Gamma_1^\pm}(\mathbf{K}_{n_i})$ and $\psi_{\Gamma_2^\pm}(\mathbf{K}_{n_i})$ denote the symmetrized plane wave combinations considered in Chap. 12, but in that case ignoring the effect of the electron spin, while α and β here denote spin up and spin down functions, respectively, which form partners of the Γ_6^+ double group irreducible representation.

For the degenerate plane wave combinations, such as those with Γ_{12}^\pm , Γ_{15}^\pm and Γ_{25}^\pm symmetries, one method to find an appropriate set of basis functions when the electron spin is included is to use the tables presented in Appendix D. For example, basis functions for the four partners for $\Gamma_8^\pm = \Gamma_3^\pm \otimes \Gamma_6^+$ can be found in the Table D.5. Consider that the functions u_1^3, u_2^3 for Γ_3 in this table transform as

$$\begin{aligned}u_1^3 &\propto 3z^2 - r^2 \\ u_2^3 &\propto \sqrt{3}(x^2 - y^2)\end{aligned}\quad (14.55)$$

and the spinor functions are given by

$$\begin{aligned}v_{+1/2}^6 &\propto \alpha \\ v_{-1/2}^6 &\propto \beta.\end{aligned}\quad (14.56)$$

Then the application of Table D.5 gives

$$\Psi_{\Gamma_8^\pm}(\mathbf{K}_{n_i}) = \frac{1}{\sqrt{2}} \begin{pmatrix} \sqrt{3}(x^2 - y^2)\alpha \\ (3z^2 - r^2)\beta \\ -(3z^2 - r^2)\alpha \\ -\sqrt{3}(x^2 - y^2)\beta \end{pmatrix}. \quad (14.57)$$

A more symmetric set of basis functions for $\Gamma_8^\pm = \Gamma_{12}^\pm \otimes \Gamma_6^+$ is

$$\Psi_{\Gamma_8^\pm}(\mathbf{K}_{n_i}) = \frac{1}{\sqrt{2}} \begin{pmatrix} [\omega^2 \psi_{\Gamma_{12}^\pm}^*(\mathbf{K}_{n_i}) + \omega \psi_{\Gamma_{12}^\pm}(\mathbf{K}_{n_i})] \alpha \\ -i[\omega^2 \psi_{\Gamma_{12}^\pm}^*(\mathbf{K}_{n_i}) - \omega \psi_{\Gamma_{12}^\pm}(\mathbf{K}_{n_i})] \beta \\ i[\omega^2 \psi_{\Gamma_{12}^\pm}^*(\mathbf{K}_{n_i}) - \omega \psi_{\Gamma_{12}^\pm}(\mathbf{K}_{n_i})] \alpha \\ -[\omega^2 \psi_{\Gamma_{12}^\pm}^*(\mathbf{K}_{n_i}) + \omega \psi_{\Gamma_{12}^\pm}(\mathbf{K}_{n_i})] \beta \end{pmatrix}, \quad (14.58)$$

in which $\psi_{\Gamma_{12}^+}(\mathbf{K}_{n_i}) = x^2 + \omega y^2 + \omega^2 z^2$ and $\psi_{\Gamma_{12}^+}^*(\mathbf{K}_{n_i}) = x^2 + \omega^2 y^2 + \omega z^2$.

Since the three-dimensional levels Γ_{15}^\pm and Γ_{25}^\pm split under the spin–orbit interaction

$$\Gamma_{15}^\pm \otimes D_{1/2} = \Gamma_6^\pm + \Gamma_8^\pm$$

$$\Gamma_{25}^\pm \otimes D_{1/2} = \Gamma_7^\pm + \Gamma_8^\pm$$

the basis functions for these levels are somewhat more complicated, but the coupling coefficients can be found in Table D.4 for the case of $\Gamma_{15}^\pm \otimes D_{1/2}$ and in Table D.6 for the case of $\Gamma_{25}^\pm \otimes D_{1/2}$. In these tables, (u_x^4, u_y^4, u_z^4) and (u_x^5, u_y^5, u_z^5) are the three partners of Γ_{15}^\pm (Γ_4) and Γ_{25}^\pm (Γ_5), respectively, and from these tables we obtain for the twofold levels:

$$\begin{aligned} \Psi_{\Gamma_6^\pm}(\mathbf{K}_{n_i}) &= \frac{1}{\sqrt{3}} \begin{pmatrix} \left[-i \left(\psi_{\Gamma_{15}^\pm}^x(\mathbf{K}_{n_i}) - i \psi_{\Gamma_{15}^\pm}^y(\mathbf{K}_{n_i}) \right) \alpha + i \psi_{\Gamma_{15}^\pm}^z(\mathbf{K}_{n_i}) \beta \right] \\ \left[-i \left(\psi_{\Gamma_{15}^\pm}^x(\mathbf{K}_{n_i}) + i \psi_{\Gamma_{15}^\pm}^y(\mathbf{K}_{n_i}) \right) \beta - i \psi_{\Gamma_{15}^\pm}^z(\mathbf{K}_{n_i}) \alpha \right] \end{pmatrix} \\ \Psi_{\Gamma_7^\pm}(\mathbf{K}_{n_i}) &= \frac{1}{\sqrt{3}} \begin{pmatrix} \left[-i \left(\psi_{\Gamma_{25}^\pm}^x(\mathbf{K}_{n_i}) - i \psi_{\Gamma_{25}^\pm}^y(\mathbf{K}_{n_i}) \right) \alpha + i \psi_{\Gamma_{25}^\pm}^z(\mathbf{K}_{n_i}) \beta \right] \\ \left[-i \left(\psi_{\Gamma_{25}^\pm}^x(\mathbf{K}_{n_i}) + i \psi_{\Gamma_{25}^\pm}^y(\mathbf{K}_{n_i}) \right) \beta - i \psi_{\Gamma_{25}^\pm}^z(\mathbf{K}_{n_i}) \alpha \right] \end{pmatrix}. \end{aligned} \quad (14.59)$$

Problem 14.3 considers the corresponding fourfold levels obtained from taking the direct products of $\Gamma_{15}^\pm(\Gamma_4^\pm) \otimes \Gamma_6^+$ and $\Gamma_{25}^\pm(\Gamma_5^\pm) \otimes \Gamma_6^+$.

14.10 Group of the Wave Vector for Nonsymmorphic Double Groups

In the case of nonsymmorphic space groups, we found in Sect. 12.5 that bands are often required to stick together at certain high symmetry points on the Brillouin zone boundary where the structure factor vanishes. In Sect. 12.5 it was explicitly shown that for the diamond structure the nondegenerate Δ_1

and Δ_2 levels come into the X point with equal and opposite nonzero slopes, so that in the extended Brillouin zone, the $E(\mathbf{k})$ curves together with all their derivatives, pass through the X point continuously as they interchange their symmetry designations. It was shown in Sect. 12.5 that the physical basis for bands sticking together in this way is that the structure factor vanishes. In such cases it is as if there were no Brillouin zone boundary so that the energy eigenvalues continue through the symmetry point without interruption.

In this section, we consider the corresponding situation including the electron spin and the spin-orbit interaction. Here we explicitly illustrate the sticking together of energy bands in terms of another space group #194 for the hexagonal close packed structure. Another objective of this section is to gain further experience with using double group irreducible representations. Space group #194 was previously discussed in Problems 9.6 and 10.6 and in Sect. 11.4.3 in relation to the lattice modes in graphite. In the case of lattice modes, we only make use of the single group representations. Mention of space group #194 was also made in Sect. 12.5 in connection with bands sticking together at the zone boundary in cases where the structure factor vanishes for nonsymmorphic groups, but in Sect. 12.5 the electron spin and the spin-orbit interaction was neglected. We here consider the case where energy bands for the nonsymmorphic hexagonal close packed lattice stick together and the spin-orbit interaction is included [26] so that double groups must be considered.

Let us consider the wave vector to going from a high symmetry point (Γ) (see Fig. C.7) to a lower symmetry point (Δ) to the point A at the BZ boundary. The double group character tables for these three high symmetry points Γ , Δ and A are found in Tables D.10, D.11 and D.13, respectively. At the A point there are six classes for the group of the wave vector and six irreducible representations, three of which are ordinary irreducible representations Γ_1^A , Γ_2^A , Γ_3^A and three of which are double group representations (Γ_4^A , Γ_5^A , Γ_6^A).

The compatibility relations between the irreducible representations at A and at Δ :

$$\begin{array}{cccccc} (A) & 1 & 2 & 3 & 4+5 & 6 \\ & \downarrow & \downarrow & \downarrow & \downarrow & \downarrow \\ (\Delta) & (1+3) & (2+4) & (5+6) & 2(9) & (7+8) \end{array}$$

show that in the vicinity of the A point, we have band crossings for all the single group bands with A_1 , A_2 and A_3 symmetry. These band crossings, shown in Fig. 14.5, are based on these compatibility relations. The energy bands pass through the A point without interruption and merely change their symmetry designations, as for example $\Delta_1 \rightarrow A_1 \rightarrow \Delta_3$. Bands for the doubly degenerate double group irreducible representations Δ_7 and Δ_8 stick together as an A_6 band at the A point. At the A point ($k_z = \pi/c$) the phase factor $\exp[i(c/2)k_z]$, associated with the symmetry operations containing $\tau = (c/2)((0, 0, 1))$ such as $\{C_6|\tau\}$, becomes $e^{i\pi/2} = i$. Energy bands with double group representations A_4 and A_5 have complex characters and are complex conjugates of each

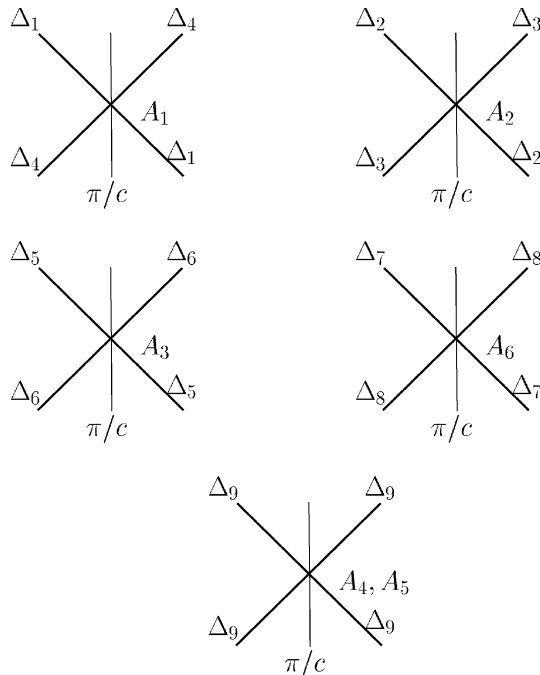


Fig. 14.5. Energy band dispersion relations for various irreducible representations for group #194 near the A point. The energy bands go through the A point without interruption because of the vanishing structure factor at the A point. Note that A_4 , A_5 , A_6 , Δ_7 , Δ_8 and Δ_9 are double group representations. The A_4 and A_5 levels stick together because of time reversal symmetry discussed in Chap. 16

other. In Chap. 16 we will see that such bands stick together because of time reversal symmetry. Thus two Δ_9 levels come into the A point to form $A_4 + A_5$ levels and leave the A point with the same Δ_9 symmetry (see Fig. 14.5).

Selected Problems

- 14.1.** (a) Following the procedure in Sect. 14.3, find the double group character table for the point group D_6 . First find the number of classes and the number of irreducible representations. Then identify the classes as listed in the character table, and the dimensionality of each irreducible representation. Finally find the entries in the character table.
- (b) Use the results in (a) to obtain the double group character table for the group of the wave vector at $k = 0$ for space group #194 which is a non-symmorphic group. Check your results against Table D.10.
- (c) To which double group states do the states Γ_7^+ , Γ_8^+ , and Γ_9^+ couple optically through electric dipole transitions?

14.2. Consider an Er^{3+} rare earth ion entering an insulating ionic crystal in a position with point group symmetry D_{4h} .

- (a) Find the double group irreducible representations of the crystal field (D_{4h} point group symmetry) corresponding to the ground state configuration for the free ion. Compare with the crystal field splitting that would occur for icosahedral point group symmetry I_h .
- (b) Use Hund's rules (see page 404 of Ref. [45]) to identify the lowest energy optical transitions that can be induced from the ground state level of the free Er^{3+} ion. Using group theory, find the lowest energy transitions expected for an Er^{3+} ion in a crystal with D_{4h} point group symmetry.
- (c) What changes in the spectra (b) are expected to occur if a stress is applied along the fourfold symmetry axis? in the direction along a twofold axis perpendicular to the fourfold axis?
- (d) Now suppose that a Dy^{3+} rare earth ion is introduced into the same lattice instead of the Er^{3+} ion. What are the symmetry types for levels to which optical transitions can be induced from a multiplet corresponding to the ground state level of the free Dy^{3+} ion. (Use Hund's rule to obtain the ground state energies.) Work the problem only for the D_{4h} point group symmetry. Comment on the expected differences in the optical spectrum for the Dy^{3+} and the Er^{3+} ions in part (c).

14.3. Using the linear combinations for plane waves given in Chap. 12 and the coupling coefficients in Appendix D (see Sect. 14.9), find the linear combination of the appropriate partners for $\Gamma_g^\pm(\mathbf{k}_{n_i})$ for the fourfold levels obtained from $\Gamma_5^+ \otimes \Gamma_6^+$ for a material crystallizing in the simple cubic structure.

Application of Double Groups to Energy Bands with Spin

In this chapter we apply the group theoretical background for the electron spin and the *spin-orbit* interaction (which is discussed in Chap. 14) to the treatment of electronic energy band models for solids (which is discussed in Chaps. 12 and 13 for the case when the electron spin is neglected). By including the spin-orbit interaction we can also discuss the effective *g*-factor, which together with the effective mass tensor, characterize the properties of a *semiconductor* in a magnetic field. We also review the *Slater-Koster* method for determination of the electronic energy band structure of crystalline solids by interpolation and extrapolation of energy eigenvalues and eigenfunctions that are accurately known at a few high symmetry points in the Brillouin zone either from *ab initio* calculations or from experiments.

15.1 Introduction

The one-electron Hamiltonian including spin-orbit interaction is written as

$$\mathcal{H} = \frac{p^2}{2m} + V(\mathbf{r}) + \frac{\hbar}{4m^2c^2}(\nabla V \times \mathbf{p}) \cdot \boldsymbol{\sigma}, \quad (15.1)$$

where $\boldsymbol{\sigma}$ is the dimensionless spin operator [$\mathbf{S} = (\hbar/2)\boldsymbol{\sigma}$]. The first two terms of (15.1) denote the kinetic energy and periodic potential of the one-electron Hamiltonian in a simple periodic potential $V(\mathbf{r})$ that reflects the crystal symmetry, and the third term denotes the spin-orbit interaction \mathcal{H}'_{SO}

$$\mathcal{H}'_{\text{SO}} = \frac{\hbar}{4m^2c^2}(\nabla V \times \mathbf{p}) \cdot \boldsymbol{\sigma}, \quad (15.2)$$

where $\mathcal{H} = \mathcal{H}_0 + \mathcal{H}'_{\text{SO}}$. The Hamiltonian (15.1) is appropriate when the spin-orbit splittings are significant compared with typical energy gaps. The presence of the spin operator $\boldsymbol{\sigma}$ in the spin-orbit term \mathcal{H}'_{SO} requires the use of *spin-dependent* wave functions with double group symmetry designations

for the energy bands. Since the magnitude of the spin-orbit interaction is comparable to energy band gaps for many important electronic materials, it is important in these cases to consider the spin-orbit interaction explicitly when carrying out energy band calculations.

Thus explicit band calculations of $E(\mathbf{k})$ with spin-orbit interaction have been carried out using all the standard techniques for energy band calculations. Quite independent of the particular calculational technique that is used, group theoretical techniques are introduced to classify the states and to bring the secular equation into block diagonal form. To illustrate these points we consider explicitly the use of group theory (i.e., double groups as discussed in Chap. 14) to treat the electronic energy bands for several situations, including the empty lattice, the nearly free electron approximation, for $\mathbf{k} \cdot \mathbf{p}$ perturbation theory and the Slater-Koster method. These examples are also designed to provide some experience with the handling of double groups.

15.2 $E(\mathbf{k})$ for the Empty Lattice Including Spin–Orbit Interaction

In this section the calculation of the empty lattice electronic energy dispersion relations is considered in the presence of spin-orbit interaction following the discussion in Chap. 12 for the case where the electron spin is neglected.

Referring to (15.2) we see that both $V(\mathbf{r})$ and $\nabla V(\mathbf{r})$ vanish for the empty lattice, and therefore it is only the change in irreducible representations from single group to double group representations that needs to be considered. Thus when considering the plane waves *labeled* by the reciprocal lattice vectors $\{\mathbf{K}_{n_i}\}$ in Table 12.2, we should now use double group irreducible representations, which are found by taking the direct product of each single group irreducible representation Γ_i with the spinor $D_{1/2}$. Here the spinor is demonstrated for the cubic O group where $D_{1/2}$ transforms as Γ_6 and the pertinent direct products are easily obtained from Table 14.7. As an example of the effect of spin on the empty lattice, consider the $E(\mathbf{k})$ diagram in Fig. 12.1 for the FCC empty lattice. The ground state label would now become Γ_6 , and for the next excited state we would have

$$\Gamma_6 \otimes \Gamma_1 + \Gamma_6 \otimes \Gamma_{2'} + \Gamma_6 \otimes \Gamma_{15} + \Gamma_6 \otimes \Gamma_{25'} = 2(\Gamma_6 + \Gamma_7 + \Gamma_8),$$

but the eigenstates now could be also labeled more completely by using also the single group irreducible representations to which they relate:

$$[\Gamma_6(\Gamma_1) + \Gamma_6(\Gamma_{15})] + [\Gamma_7(\Gamma_{2'}) + \Gamma_7(\Gamma_{25'})] + [\Gamma_8(\Gamma_{15}) + \Gamma_8(\Gamma_{25'})].$$

A similar procedure could then be applied to all the labels in Fig. 12.1 using the appropriate character tables for the various symmetry points in the Brillouin zone. The curves in Fig. 12.1 would not change because both $V(\mathbf{r}) = 0$ and

$\nabla V(\mathbf{r}) = 0$, and because the Kramers degeneracy applies. Introduction of spin into the nearly free electron approximation requires the use of double groups.

15.3 The $\mathbf{k} \cdot \mathbf{p}$ Perturbation with Spin–Orbit Interaction

Schrödinger's equation including the spin–orbit interaction can be written as

$$\left[\frac{p^2}{2m} + V(\mathbf{r}) + \frac{\hbar}{4m^2c^2} (\nabla V \times \mathbf{p}) \cdot \boldsymbol{\sigma} \right] \psi_{n\mathbf{k}}(\mathbf{r}) = E_n(\mathbf{k}) \psi_{n\mathbf{k}}(\mathbf{r}), \quad (15.3)$$

in which the Bloch functions $\psi_{n\mathbf{k}}(\mathbf{r})$ for \mathcal{H}'_{SO} include spinors $\psi_{n\mathbf{k}\uparrow}(\mathbf{r})$ and $\psi_{n\mathbf{k}\downarrow}(\mathbf{r})$ rather than the simple wave functions considered in Chap. 13. These spinor basis functions can be written in more expanded notation as

$$\begin{aligned} \psi_{n\mathbf{k}\uparrow}(\mathbf{r}) &= e^{i\mathbf{k}\cdot\mathbf{r}} u_{n\mathbf{k}\uparrow}(\mathbf{r}) \\ \psi_{n\mathbf{k}\downarrow}(\mathbf{r}) &= e^{i\mathbf{k}\cdot\mathbf{r}} u_{n\mathbf{k}\downarrow}(\mathbf{r}), \end{aligned} \quad (15.4)$$

where the arrow in the subscript of $\psi_{n\mathbf{k}\uparrow}(\mathbf{r})$ means that the state is generally spin up or the expectation value of σ_z in this state is positive, and the down arrow gives a negative expectation value for σ_z so that

$$\begin{aligned} \langle \psi_{n\mathbf{k}\uparrow} | \sigma_z | \psi_{n\mathbf{k}\uparrow} \rangle &> 0 \\ \langle \psi_{n\mathbf{k}\downarrow} | \sigma_z | \psi_{n\mathbf{k}\downarrow} \rangle &< 0. \end{aligned} \quad (15.5)$$

The Bloch states are only pure spin up or spin down states when the spin–orbit interaction is neglected ($\mathcal{H}'_{\text{SO}} \equiv 0$). The spin–orbit interaction mixes the spin-up and spin-down partners, and, as was discussed in Chap. 14 for the atomic case, the $|j, \ell, s, m_j\rangle$ representation becomes the appropriate irreducible representation for the spin–orbit coupled system rather than the $|\ell, s, m_\ell, m_s\rangle$ representation.

Let us focus our attention on one of the periodic spinor $u_{n\mathbf{k}}(\mathbf{r})$ functions (either of the components \uparrow or \downarrow in (15.4) which diagonalize the Schrödinger equation (15.3)). Using $\mathbf{k} \cdot \mathbf{p}$ perturbation theory, the corresponding differential equation for $u_{n\mathbf{k}}(\mathbf{r})$ is

$$\begin{aligned} &\left[\frac{p^2}{2m} + V(\mathbf{r}) + \frac{\hbar}{4m^2c^2} (\nabla V \times \mathbf{p}) \cdot \boldsymbol{\sigma} \right] u_{n\mathbf{k}}(\mathbf{r}) \\ &+ \frac{\hbar\mathbf{k}}{m} \cdot \left(\mathbf{p} + \frac{\hbar}{4mc^2} \boldsymbol{\sigma} \times \nabla V \right) u_{n\mathbf{k}}(\mathbf{r}) \\ &= \left[E_n(\mathbf{k}) - \frac{\hbar^2 k^2}{2m} \right] u_{n\mathbf{k}}(\mathbf{r}) \end{aligned} \quad (15.6)$$

in which we have made use of the vector identities:

$$(\mathbf{A} \times \mathbf{B}) \cdot \mathbf{C} = (\mathbf{B} \times \mathbf{C}) \cdot \mathbf{A} = (\mathbf{C} \times \mathbf{A}) \cdot \mathbf{B}, \quad (15.7)$$

or more explicitly

$$(\nabla V \times \mathbf{p}) \cdot \boldsymbol{\sigma} e^{i\mathbf{k} \cdot \mathbf{r}} u_{n\mathbf{k}}(\mathbf{r}) = (\boldsymbol{\sigma} \times \nabla V) \cdot \mathbf{p} e^{i\mathbf{k} \cdot \mathbf{r}} u_{n\mathbf{k}}(\mathbf{r}), \quad (15.8)$$

and

$$\mathbf{p} e^{i\mathbf{k} \cdot \mathbf{r}} u_{n\mathbf{k}}(\mathbf{r}) = e^{i\mathbf{k} \cdot \mathbf{r}} [\hbar \mathbf{k} u_{n\mathbf{k}}(\mathbf{r}) + \mathbf{p} u_{n\mathbf{k}}(\mathbf{r})]. \quad (15.9)$$

If we identify terms in (15.6) with an unperturbed Hamiltonian \mathcal{H}_0 and a perturbation Hamiltonian $\mathcal{H}'_{\mathbf{k} \cdot \mathbf{p}}$ we obtain

$$\mathcal{H}_0 = \frac{\mathbf{p}^2}{2m} + V(\mathbf{r}) + \frac{\hbar}{4m^2 c^2} (\nabla V \times \mathbf{p}) \cdot \boldsymbol{\sigma}, \quad (15.10)$$

and

$$\mathcal{H}'_{\mathbf{k} \cdot \mathbf{p}} = \frac{\hbar \mathbf{k}}{m} \cdot \left(\mathbf{p} + \frac{\hbar}{4mc^2} \boldsymbol{\sigma} \times \nabla V \right), \quad (15.11)$$

so that Rayleigh–Schrödinger perturbation theory for energy bands near $\mathbf{k} = 0$ yields the following expression for the nondegenerate state Γ_i [see (13.4) and (13.9)]

$$E_n^{\Gamma_i}(\mathbf{k}) = E_n^{\Gamma_i}(0) + (u_{n,0}^{\Gamma_i} | \mathcal{H}' | u_{n,0}^{\Gamma_i}) + \sum_{n' \neq n} \frac{(u_{n,0}^{\Gamma_i} | \mathcal{H}' | u_{n',0}^{\Gamma_j})(u_{n',0}^{\Gamma_j} | \mathcal{H}' | u_{n,0}^{\Gamma_i})}{E_n^{\Gamma_i}(0) - E_{n'}^{\Gamma_j}(0)}, \quad (15.12)$$

in which the unperturbed functions $u_{n,0}^{\Gamma_i}$ are evaluated at $\mathbf{k} = 0$ (the expansion point for the $\mathbf{k} \cdot \mathbf{p}$ perturbation) and Γ_j labels the irreducible representations for bands n' . The sum in (15.12) is over states Γ_j that couple to state Γ_i through the $\mathbf{k} \cdot \mathbf{p}$ perturbation Hamiltonian given by (15.11). We note that (15.12) has the same form as the corresponding expression without spin–orbit interaction (13.9) *except* that in (15.12):

- The unperturbed Hamiltonian yielding the energy eigenvalues at $\mathbf{k} = 0$ explicitly contains a spin–orbit term.
- The $\mathbf{k} \cdot \mathbf{p}$ perturbation Hamiltonian explicitly contains the spin operator and a spin–orbit term.
- The irreducible representations Γ_i and Γ_j are both double group representations.

In treating $\mathbf{k} \cdot \mathbf{p}$ perturbation theory without explicitly considering the electron spin (see Chap. 13), we have three possibilities: nondegenerate levels, degenerate (or nearly degenerate) levels that are treated in first-order degenerate perturbation theory, and degenerate levels that are treated in second-order degenerate perturbation theory. In all three of these cases, we use group theory

to determine which are the nonvanishing matrix elements of a vector operator taken between double group states, and which of the nonvanishing matrix elements are equal to each other. More explicitly, for the case of a crystal with O_h symmetry, all the Γ_i and Γ_j representations have either Γ_6^\pm , Γ_7^\pm and Γ_8^\pm symmetry at $k = 0$ since the spatial part of the wavefunctions transform according to one of the five ordinary irreducible representations and the direct product of an ordinary irreducible representation with the spinor D_6^+ yields one of the double group representations. By inspection, we find that for the O_h group all the irreducible representations Γ_i are at least twofold degenerate. But this degeneracy is maintained for all \mathbf{k} values and is lifted only by the application of an external (or internal) magnetic field. This twofold degeneracy, known as the *Kramers degeneracy*, is generally found in the absence of a magnetic field. We therefore look for this degeneracy when working practical problems, because it greatly reduces the *labor* in dealing with problems involving spin. Because of this Kramers degeneracy, we can effectively use *nondegenerate perturbation theory* to deal with twofold levels such as the Γ_6^\pm and Γ_7^\pm levels occurring in many applications.

Group theory can be used to greatly simplify the $\mathbf{k} \cdot \mathbf{p}$ expansion for one of the Γ_6^\pm or Γ_7^\pm levels. For example, take $\Gamma_i = \Gamma_6^+$ and note that the generalized momentum operator \mathbf{P} including the spin–orbit interaction explicitly

$$\mathbf{P} = \mathbf{p} + \frac{\hbar}{4mc^2} \boldsymbol{\sigma} \times \nabla V \quad (15.13)$$

transforms like the Γ_{15}^- irreducible representation. The *generalized* momentum operator \mathbf{P} transforms as Γ_{15}^- whether or not the spin–orbit interaction is included, since \mathbf{p} is a vector and so is $(\boldsymbol{\sigma} \times \nabla V)$, both being radial vectors. Since $\Gamma_6^+ \otimes \Gamma_{15}^- = \Gamma_6^- + \Gamma_8^-$ and since Γ_6^+ is orthogonal to Γ_6^- and Γ_8^- , we have no linear \mathbf{k} term in the $\mathbf{k} \cdot \mathbf{p}$ expansion of (15.12). In the quadratic term we can only have intermediate states with Γ_6^- and Γ_8^- symmetry. For example, if the spin–orbit interaction is neglected for a crystal with O_h symmetry, then a nondegenerate Γ_1^+ state is coupled by the $\mathbf{k} \cdot \mathbf{p}$ perturbation Hamiltonian only to a Γ_{15}^- intermediate state (see Sect. 13.3). When the spin–orbit interaction is included, the Γ_1^+ and Γ_{15}^- states become the following double group states (see Table 14.7):

$$\begin{aligned} \Gamma_1^+ &\rightarrow \Gamma_6^+ \\ \Gamma_{15}^- &\rightarrow \Gamma_6^- + \Gamma_8^- , \end{aligned} \quad (15.14)$$

so that, with the spin–orbit interaction, a Γ_6^+ band will couple to bands with Γ_6^- and Γ_8^- symmetries. We note that bands with Γ_8^- symmetry can arise from single-group bands with Γ_{12}^- , Γ_{15}^- and Γ_{25}^- symmetries. In this sense the spin–orbit interaction gives more possibilities for immediate states.

Again we can use group theory to show relations between the various nonvanishing matrix elements of \mathbf{P} , and as before, only a very small number

of matrix elements are independent. To study these matrix elements we use the basis functions for the double group irreducible representations discussed in Sects. 14.5–14.7.

15.4 $E(\mathbf{k})$ for a Nondegenerate Band Including Spin–Orbit Interaction

In this section we discuss the form of $E(\mathbf{k})$ for a nondegenerate band including spin–orbit interaction while in Sect. 15.5 the corresponding discussion is given for degenerate energy bands, which is followed by a discussion of the effective g -factor in Sect. 15.6, which is a topic that arises because of the presence of spin.

The form of $E(\mathbf{k})$ for a nondegenerate band is developed in Sect. 15.3 through nondegenerate $\mathbf{k} \cdot \mathbf{p}$ perturbation theory see (15.12) by considering the form of the $\mathbf{k} \cdot \mathbf{p}$ matrix elements implied by group theory. Since \mathbf{p} and \mathbf{P} both transform as Γ_{15}^- , the group theory is not changed and it is only in the numerical evaluation of the specific terms that we need distinguish between \mathbf{p} and \mathbf{P} . In this section, we illustrate the theory by an example, the nondegenerate Γ_6^+ band for a cubic crystal with O_h symmetry for the group of the wave vector at $k = 0$. From Sect. 14.5, we take as basis functions for the Γ_6^+ state:

$$\Gamma_6^+ : \quad \begin{cases} 1 \uparrow \\ 1 \downarrow \end{cases} \quad (15.15)$$

Within the framework of $\mathbf{k} \cdot \mathbf{p}$ perturbation theory, the Γ_6^+ state couples only to Γ_6^- and Γ_8^- since $\Gamma_6^+ \otimes \Gamma_{15}^- = \Gamma_6^- + \Gamma_8^-$. For the Γ_6^- and Γ_8^- states, we use the basis functions derived from (14.41) and (14.46), together with the extension $L_x, L_y, L_z \rightarrow x, y, z$ discussed in Sect. 14.7 so that for $\Gamma_6^- (\Gamma_{15}^-)$ we write

$$\begin{array}{lll} |j, m_j\rangle & \text{State} & \text{Basis Function} \\ | \frac{1}{2}, \frac{1}{2} \rangle & & \left(\frac{1}{\sqrt{3}} \right) [(x + iy) \downarrow -z \uparrow] \\ | \frac{1}{2}, -\frac{1}{2} \rangle & & \left(\frac{1}{\sqrt{3}} \right) [-(x - iy) \uparrow +z \downarrow], \end{array} \quad (15.16)$$

and for $\Gamma_8^- (\Gamma_{15}^-)$ we write

$$\begin{array}{lll} |j, m_j\rangle & \text{State} & \text{Basis Function} \\ | \frac{3}{2}, \frac{3}{2} \rangle & & \left(\frac{1}{\sqrt{2}} \right) (x + iy) \uparrow \\ | \frac{3}{2}, \frac{1}{2} \rangle & & \left(\frac{1}{\sqrt{6}} \right) [(x + iy) \downarrow +2z \uparrow] \\ | \frac{3}{2}, -\frac{1}{2} \rangle & & \left(\frac{1}{\sqrt{6}} \right) [(x - iy) \uparrow +2z \downarrow] \\ | \frac{3}{2}, -\frac{3}{2} \rangle & & \left(\frac{1}{\sqrt{2}} \right) (x - iy) \downarrow. \end{array} \quad (15.17)$$

We can read off the basis functions relating the $|j, m_j\rangle$ representation and the $|\ell s m_\ell m_s\rangle$ representation for the Γ_6^- ($j = 1/2$) and Γ_8^- ($j = 3/2$) states that are derived from the Γ_{15}^- level directly from (15.16) and (15.17). The x, y and z in (15.16) and (15.17) refer to the three partners of the Γ_{15}^- state. For this case there are no nonvanishing matrix elements in (15.12) in first-order perturbation theory. In second-order, the nonvanishing terms are

$$\begin{aligned}
& \left(1 \uparrow |P_x| \left(\frac{1}{\sqrt{2}} \right) (x + iy) \uparrow \right) = \left(\frac{1}{\sqrt{2}} \right) (1|P_x|x) \\
& \left(1 \uparrow |P_y| \left(\frac{1}{\sqrt{2}} \right) (x + iy) \uparrow \right) = \left(\frac{i}{\sqrt{2}} \right) (1|P_y|y) \\
& \left(1 \uparrow |P_z| \left(\frac{1}{\sqrt{6}} \right) \{(x + iy) \downarrow + 2z \uparrow\} \right) = \left(\frac{2}{\sqrt{6}} \right) (1|P_z|z) \\
& \left(1 \uparrow |P_x| \left(\frac{1}{\sqrt{6}} \right) \{(x - iy) \uparrow + 2z \downarrow\} \right) = \left(\frac{1}{\sqrt{6}} \right) (1|P_x|x) \\
& \left(1 \uparrow |P_y| \left(\frac{1}{\sqrt{6}} \right) \{(x - iy) \uparrow + 2z \downarrow\} \right) = - \left(\frac{i}{\sqrt{6}} \right) (1|P_y|y) \\
& \left(1 \uparrow |P_z| \left(\frac{1}{\sqrt{3}} \right) \{(x + iy) \downarrow - z \uparrow\} \right) = - \left(\frac{1}{\sqrt{3}} \right) (1|P_z|z) \\
& \left(1 \uparrow |P_x| \left(\frac{1}{\sqrt{3}} \right) \{(-x + iy) \uparrow + z \downarrow\} \right) = - \left(\frac{1}{\sqrt{3}} \right) (1|P_x|x) \\
& \left(1 \uparrow |P_y| \left(\frac{1}{\sqrt{3}} \right) \{(-x + iy) \uparrow + z \downarrow\} \right) = \left(\frac{i}{\sqrt{3}} \right) (1|P_y|y). \quad (15.18)
\end{aligned}$$

Summing up the second-order terms and *utilizing* the equality

$$(1|P_x|x) = (1|P_y|y) = (1|P_z|z), \quad (15.19)$$

we obtain

$$\begin{aligned}
E_{\Gamma_6^+}(\mathbf{k}) &= E_{\Gamma_6^+}(0) + \frac{\hbar^2 |(1|P_x|x)|^2}{m^2 E_g} \left\{ \frac{1}{3} k_x^2 + \frac{1}{3} k_y^2 + \frac{1}{3} k_z^2 \right\} \\
&\quad + \frac{\hbar^2 |(1|P_x|x)|^2}{m^2 (E_g + \Delta)} \left\{ \frac{1}{2} k_x^2 + \frac{1}{2} k_y^2 + \frac{2}{3} k_z^2 + \frac{1}{6} k_x^2 + \frac{1}{6} k_y^2 \right\} \\
&= E_{\Gamma_6^+}(0) + \frac{\hbar^2 k^2}{m^2} |(1|P_x|x)|^2 \left\{ \frac{1}{3E_g} + \frac{2}{3(E_g + \Delta)} \right\}, \quad (15.20)
\end{aligned}$$

where E_g and $E_g + \Delta$ are defined in Fig. 15.1. One can note that the energy bands in (15.12) have subscripts n and n' to denote their band index identification. The $E_{\Gamma_6^+}(\mathbf{k})$ in (15.20) denotes the s -band lying low in the

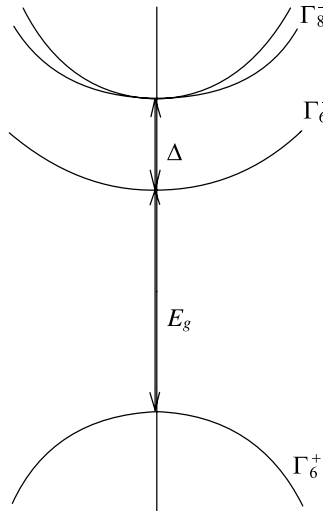


Fig. 15.1. Energy versus k at the Γ point showing the effect of the spin-orbit interaction in splitting the p -level. The relevant bands are labeled by the double group representations for a cubic group near $k = 0$ with O_h symmetry

valence band which through $\mathbf{k} \cdot \mathbf{p}$ perturbation theory is shown to couple to the conduction band levels with Γ_6^- and Γ_8^- symmetries arising from the conduction p bands (see Fig. 15.1).

15.5 $E(\mathbf{k})$ for Degenerate Bands Including Spin–Orbit Interaction

In dealing with $\mathbf{k} \cdot \mathbf{p}$ perturbation theory for degenerate states we again use basis functions such as are given by (14.41) and (14.46) to classify the degenerate states. For example, instead of the (3×3) secular equation for p -bands (Γ_{15}^- symmetry) without spin–orbit coupling that was discussed in Sect. 13.5, inclusion of the spin–orbit interaction leads to solution of a (6×6) secular equation. This (6×6) equation assumes block diagonal form containing a (4×4) block with Γ_8^- symmetry and a (2×2) block with Γ_6^- symmetry, because the spin functions transform as $D_{1/2}$ or Γ_6^+ and because

$$\Gamma_6^+ \otimes \Gamma_{15}^- = \Gamma_6^- + \Gamma_8^- , \quad (15.21)$$

where Γ_6^- corresponds to a $j = 1/2$ state and Γ_8^- to a $j = 3/2$ state (see Fig. 15.1). Thus the Γ_{15}^- conduction band for the case of no spin becomes Γ_6^- and Γ_8^- when spin–orbit interaction is included (see Fig. 15.1).

An important application of degenerate $\mathbf{k} \cdot \mathbf{p}$ perturbation theory including the effects of spin–orbit interaction is to the valence band of the group IV

and III–V compound semiconductors. A description of $E(\mathbf{k})$ for the valence band is needed to construct the constant energy surfaces for holes in these semiconductors. The $\mathbf{k} \cdot \mathbf{p}$ perturbation theory method is useful for analysis of cyclotron resonance measurements on holes in group IV and III–V semiconductors, which were studied in the 1950s and 1960s for 3D crystals and 40–50 years later these measurements are being used to study low-dimensional nanostructured systems.

One way to solve for the energy levels of the valence band of a group IV semiconductor about the valence band maximum $\mathbf{k} = 0$ (Γ_{25}^+ single group level) is to start with the (6×6) matrix labeled by the double group basis functions. The secular equation is constructed by considering

$$\mathcal{H} = \mathcal{H}_0 + \mathcal{H}'_{\mathbf{k} \cdot \mathbf{p}}, \quad (15.22)$$

in which the matrix elements for $\mathcal{H}'_{\mathbf{k} \cdot \mathbf{p}}$ vanish in first-order. Therefore in degenerate second-order perturbation theory we must replace each matrix element $\langle i|\mathcal{H}'|j\rangle$ by

$$\langle i|\mathcal{H}'|j\rangle + \sum_{\alpha} \frac{\langle i|\mathcal{H}'|\alpha\rangle\langle\alpha|\mathcal{H}'|j\rangle}{E_i - E_{\alpha}}, \quad (15.23)$$

in which \mathcal{H}' denotes the $\mathbf{k} \cdot \mathbf{p}$ perturbation Hamiltonian (see Sect. 13.5), and i, j, α all denote double group irreducible representations. In this case we obtain the appropriate basis functions for the Γ_7^+ and Γ_8^+ states from the combination that we previously derived using the raising operator $J_+ = L_+ + S_+$ see (14.41) and (14.46) and making the transcription $L_x, L_y, L_z \rightarrow \varepsilon_x, \varepsilon_y, \varepsilon_z$ discussed in Sect. 14.7. Thus for the $\Gamma_7^+(\Gamma_{25}^+)$ states, the basis functions are

$$\begin{array}{ll} |j, m_j\rangle & \text{State} \quad \text{Basis Function} \\ \left| \frac{1}{2}, \frac{1}{2} \right\rangle & \mu_1 = \frac{1}{\sqrt{3}} [(\varepsilon_x + i\varepsilon_y) \downarrow -\varepsilon_z \uparrow] \\ \left| \frac{1}{2}, \frac{1}{2} \right\rangle & \mu_2 = \frac{1}{\sqrt{3}} [-(\varepsilon_x - i\varepsilon_y) \uparrow +\varepsilon_z \downarrow], \end{array} \quad (15.24)$$

and for the $\Gamma_8^+(\Gamma_{25}^+)$ states, the basis functions are

$$\begin{array}{ll} |j, m_j\rangle & \text{State} \quad \text{Basis Function} \\ \left| \frac{3}{2}, \frac{3}{2} \right\rangle & \nu_1 = \frac{1}{\sqrt{2}} (\varepsilon_x + i\varepsilon_y) \uparrow \\ \left| \frac{3}{2}, \frac{1}{2} \right\rangle & \nu_2 = \frac{1}{\sqrt{6}} [(\varepsilon_x + i\varepsilon_y) \downarrow + 2\varepsilon_z \uparrow] \\ \left| \frac{3}{2}, -\frac{1}{2} \right\rangle & \nu_3 = \frac{1}{\sqrt{6}} [(\varepsilon_x - i\varepsilon_y) \uparrow + 2\varepsilon_z \downarrow] \\ \left| \frac{3}{2}, -\frac{3}{2} \right\rangle & \nu_4 = \frac{1}{\sqrt{2}} (\varepsilon_x - i\varepsilon_y) \downarrow, \end{array} \quad (15.25)$$

in which the states Γ_7^+ and Γ_8^+ are labeled by $|j, m_j\rangle$ and the components of the function ε_i relate to x, y, z partners according to

$$\begin{aligned}\varepsilon_x &= yz \\ \varepsilon_y &= zx \\ \varepsilon_z &= xy.\end{aligned}\tag{15.26}$$

In solving for $E(\mathbf{k})$ for the valence band of a semiconductor, such as germanium, we use the unperturbed and perturbed Hamiltonians given by (15.10) and (15.11), respectively. The states used to solve the eigenvalue problem are labeled by the wave functions that diagonalize the “unperturbed” Hamiltonian \mathcal{H}_0 of (15.10). Since $\mathcal{H}'_{\mathbf{k}, \mathbf{p}}$ transforms as Γ_{15}^- and since $\Gamma_{15}^- \otimes \Gamma_7^+ = \Gamma_7^- + \Gamma_8^-$, we conclude that $\mathcal{H}'_{\mathbf{k}, \mathbf{p}}$ does not couple band Γ_7^+ to band Γ_8^- . This same result follows more easily just from parity arguments (i.e., the evenness and oddness of states for systems exhibiting inversion symmetry).

A solution to the resulting (6×6) secular equation involves explicit computation of matrix elements as was done for the spinless case in Sect. 13.5. For brevity, we will not include a detailed evaluation of all the matrix elements, but we will instead just *summarize* the results. For the $\Gamma_7^+(\Gamma_{25}^+)$ level, the dispersion relation (see Fig. 14.1) $E(\mathbf{k})$ assumes the form

$$E(\Gamma_7^+) = k^2 \left(\frac{\hbar^2}{2m} + 4C_1 + \frac{4}{3}C_2 + C_3 \right),\tag{15.27}$$

where

$$\begin{aligned}C_1 &= \frac{\hbar^2}{m^2} \left\{ \sum_{\Gamma_8^-(\Gamma_{12})} \frac{|\langle \Gamma_7^+ | P_x | \Gamma_8^- \rangle|^2}{E_0 - E_\ell} + \sum_{\Gamma_8^-(\Gamma_{25}^-)} \frac{|\langle \Gamma_7^+ | P_x | \Gamma_8^- \rangle|^2}{E_0 - E_\ell} \right\} \\ C_2 &= \frac{\hbar^2}{m^2} \sum_{\Gamma_8^-(\Gamma_{15}^-)} \frac{|\langle \Gamma_7^+ | P_x | \Gamma_8^- \rangle|^2}{E_0 - E_\ell} \\ C_3 &= \frac{\hbar^2}{m^2} \sum_{\Gamma_7^-(\Gamma_2^-)} \frac{|\langle \Gamma_7^+ | P_z | \Gamma_7^- \rangle|^2}{E_0 - E_\ell},\end{aligned}\tag{15.28}$$

in which

$$\mathbf{P} = \mathbf{p} + \frac{\hbar}{4m^2c^2}(\boldsymbol{\sigma} \times \boldsymbol{\nabla}V),\tag{15.29}$$

and E_ℓ is an intermediate state with the indicated symmetries. Since bands with Γ_{12}^- and Γ_{25}^- symmetries do not lie close to the valence band Γ_{25}^+ in a typical cubic semiconductor, we would expect C_1 to be much smaller than C_2 or C_3 .

The solution for the $\Gamma_8^+(\Gamma_{25}^+)$ level in the valence band is a good deal more complicated than that for the Γ_7^+ level, and yields the result

$$E[\Gamma_8^+(\Gamma_{25}^+)] = A k^2 \pm \sqrt{B^2 k^4 + C^2(k_x^2 k_y^2 + k_y^2 k_z^2 + k_z^2 k_x^2)},\tag{15.30}$$

where

$$\begin{aligned} A &= \frac{\hbar^2}{2m} + \frac{2}{3}E_1 + 2E_2 + E_3 + 5E_4 + \frac{1}{2}E_5 \\ B^2 &= \frac{4}{9}E_1^2 + 4E_2^2 + 16E_4^2 + \frac{1}{4}E_5^2 - \frac{8}{3}E_1E_2 + \frac{16}{3}E_1E_4 \\ &\quad - \frac{2}{3}E_1E_5 - 16E_2E_4 + 2E_2E_5 - 4E_4E_5 \\ C^2 &= -\frac{9}{16}E_5^2 + 16E_1E_2 - 32E_1E_4 + E_1E_5 - 9E_2E_5 + 18E_4E_5, \end{aligned} \quad (15.31)$$

and where

$$\begin{aligned} E_1 &= \frac{\hbar^2}{m^2} \sum_{\Gamma_6^-(\Gamma_{15}^-)} \frac{|\langle \Gamma_8^+ | P_x | \Gamma_6^- \rangle|^2}{E_0 - E_\ell} \\ E_2 &= \frac{\hbar^2}{m^2} \sum_{\Gamma_7^-(\Gamma_2^-)} \frac{|\langle \Gamma_8^+ | P_x | \Gamma_7^- \rangle|^2}{E_0 - E_\ell} \\ E_3 &= \frac{\hbar^2}{m^2} \sum_{\Gamma_8^-(\Gamma_{15}^-)} \frac{|\langle \Gamma_8^+ (\Gamma_{25}^+) | P_z | \Gamma_8^- (\Gamma_{15}^-) \rangle|^2}{E_0 - E_\ell} \\ E_4 &= \frac{\hbar^2}{m^2} \sum_{\Gamma_8^-(\Gamma_{25}^-)} \frac{|\langle \Gamma_8^+ (\Gamma_{25}^+) | P_z | \Gamma_8^- (\Gamma_{25}^-) \rangle|^2}{E_0 - E_\ell} \\ E_5 &= \frac{\hbar^2}{m^2} \sum_{\Gamma_8^-(\Gamma_{12}^-)} \frac{|\langle \Gamma_8^+ (\Gamma_{25}^+) | P_z | \Gamma_8^- (\Gamma_{12}^-) \rangle|^2}{E_0 - E_\ell}. \end{aligned} \quad (15.32)$$

In (15.32), E_4 and E_5 are expected to be small using arguments similar to those given in (15.28) for the $E[\Gamma_7^+(\Gamma_{25}^+)]$ band dispersion. Because of the $E_0 - E_\ell$ denominator that enters second-order degenerate perturbation theory, the most important contributions to $\mathbf{k} \cdot \mathbf{p}$ perturbation theory come from bands lying close in energy to the E_0 level, which in this case refers to the Γ -point valence band energy extrema. For germanium the levels lying relatively close to the Fermi level have Γ_{25}^+ , Γ_1^+ , Γ_2^- and Γ_{15}^- symmetries (see Fig. 14.1) so that only the double group states derived from these states will contribute significantly to the sums in (15.32). The far-lying levels only contribute small correction terms. See Problem 15.2 for more details on the solutions to $E[\Gamma_8^+(\Gamma_{25}^+)]$ and $E[\Gamma_7^+(\Gamma_{25}^+)]$. To construct $E(\mathbf{k})$ throughout the Brillouin zone as in Fig. 14.1, we use compatibility relations to move away from $\mathbf{k} = 0$, and then we use different compatibility relations to get to the BZ boundary.

Although the spin–orbit perturbation term contained in \mathcal{H}_0 in (15.10) does not depend on \mathbf{k} , the resulting energy bands show a \mathbf{k} -dependent spin–orbit splitting. For example, in Fig. 14.1 we note that the spin–orbit splitting of the Γ_8^+ (Γ_{25}^+) level is $\Delta = 0.29$ eV at the Γ point in

Ge while along the Λ axis, the splitting is only about $2/3$ this value and remains constant over most of the Λ axis. For the corresponding levels along the Δ or (100) direction, the spin-orbit splitting is very much smaller (see Fig. 14.1). When the spin-orbit interaction is weak, it is convenient to deal with this interaction in perturbation theory. We note that the spin-orbit interaction can be written in a diagonal form using the $|j, m_j\rangle$ representation. Therefore instead of writing the wavefunctions for the unperturbed problem in the $|\ell, s, m_\ell, m_s\rangle$ representation, as we did here, it is convenient to use the $|j, m_j\rangle$ representation for the whole perturbation theory problem. A classic work on spin-orbit interaction in solids [33] has been applied to $\mathbf{k} \cdot \mathbf{p}$ perturbation theory [31].

15.6 Effective g -Factor

One of the important applications of double groups in *solid-state physics* is to the treatment of the effective g -factor which directly relates to the electron spin. In calculating the effective g -factor (g_{eff}), we employ $\mathbf{k} \cdot \mathbf{p}$ perturbation theory with spin, and show that in a magnetic field B , new terms arise in the one-electron Hamiltonian. Some of these new terms have the symmetry of an axial vector (e.g., the magnetic moment μ_{eff}), giving rise to an interaction $\mu_{\text{eff}} \cdot \mathbf{B}$. We review first the origin of the effective g -factor in solid state physics and show the important role of group theory in the evaluation of the pertinent matrix elements. In this problem we consider three perturbations:

- (a) Spin-orbit interaction,
- (b) $\mathbf{k} \cdot \mathbf{p}$ perturbation,
- (c) Perturbation by a magnetic field.

We will see that the effective one-electron Hamiltonian for an electron in a solid in an applied magnetic field can be written as

$$\mathcal{H}_{\text{eff}} = \frac{1}{2m_{\alpha\beta}^*} \left(\mathbf{p} - \frac{e}{c} \mathbf{A} \right)^2 - g_{\text{eff}} \mu_B m_s B, \quad (15.33)$$

which implies that in effective mass theory, the periodic potential is replaced by both an effective mass tensor and an effective g -factor. Just as the effective mass of an electron can differ greatly from the free electron value, so can the effective g -factor differ greatly from the free electron value of 2. To see how this comes about, let us consider energy bands about a band extrema in a crystal with O_h symmetry. The discussion given here follows closely that given for $\mathbf{k} \cdot \mathbf{p}$ perturbation theory in Chap. 13, and as expanded in this chapter by including the spin-orbit interaction.

Every entry in the secular equation for the $\mathbf{k} \cdot \mathbf{p}$ Hamiltonian is of the following form since there are no entries in *first-order* that couple the degenerate states:

$$\frac{\hbar^2 k^2}{2m} \delta_{n,n'} + \sum_{n''} \frac{\langle n | \mathcal{H}' | n'' \rangle \langle n'' | \mathcal{H}' | n' \rangle}{E_n - E_{n''}}, \quad (15.34)$$

where $\sum_{n''}$ denotes the sum over states outside the nearly degenerate set (NDS, see Sect. 13.5) and where we are assuming that every member in the NDS is of approximately the same energy, like the situation for degenerate p -bands or of strongly coupled s and p bands. The $\mathbf{k} \cdot \mathbf{p}$ perturbation Hamiltonian is either $\mathcal{H}' = (\hbar/m)\mathbf{k} \cdot \mathbf{p}$ for the spinless problem or it is $\mathcal{H}' = (\hbar/m)\mathbf{k} \cdot \mathbf{P}$ for the problem with spin, where $\mathbf{P} = \mathbf{p} + (\hbar/4mc^2)\boldsymbol{\sigma} \times \nabla V$. With this identification of \mathcal{H}' we can rewrite the entries to the secular equation (15.34) as

$$\sum_{\alpha\beta} D_{nn'\alpha\beta} k_\alpha k_\beta = \sum_{\alpha\beta} k_\alpha k_\beta \left\{ \frac{\hbar^2}{2m} \delta_{nn'} \delta_{\alpha\beta} + \frac{\hbar^2}{m^2} \sum_{n''} \frac{\langle n | P_\alpha | n'' \rangle \langle n'' | P_\beta | n' \rangle}{E_n^{(0)} - E_{n''}^{(0)}} \right\}, \quad (15.35)$$

where $\sum_{\alpha\beta}$ denotes a sum on components of the \mathbf{k} vectors, and $\sum_{n''}$ denotes a sum over members outside the NDS, and where $D_{nn'\alpha\beta}$ denotes the term in curly brackets, and depends on the band indices n, n' . The eigenvalues are found by solving the secular equation

$$\sum_{n'} \left[\sum_{\alpha\beta} D_{nn'\alpha\beta} k_\alpha k_\beta - E \delta_{nn'} \right] f_{n'} = 0. \quad (15.36)$$

Equation (15.36) is the eigenvalue problem in zero magnetic field. The same form for the secular equation also applies when $B \neq 0$. This equation symbolically represents the problem with spin if the $f_{n'}$ functions are taken to transform as irreducible representations of the crystal double group and the \mathbf{P} vectors are chosen so that they include the spin-orbit interaction $\mathbf{P} = \mathbf{p} + (\hbar/4mc^2)(\boldsymbol{\sigma} \times \nabla V)$.

In an external magnetic field we replace the operator $\mathbf{p} \rightarrow \mathbf{p} - (e/c)\mathbf{A}$ (where \mathbf{A} is the vector potential, and the magnetic field \mathbf{B} is related to \mathbf{A} by $\mathbf{B} = \nabla \times \mathbf{A}$), in the Hamiltonian and from this it follows generally that in (15.36) we must make the transcription

$$\hbar \mathbf{k} \rightarrow \frac{\hbar}{i} \nabla - \frac{e}{c} \mathbf{A}, \quad (15.37)$$

when a magnetic field is applied. The relation (15.37) is called the Kohn–Luttinger transcription and is widely used in the solution of magnetic field problems in semiconductor physics. As a result of (15.37), \mathbf{k} in a magnetic field becomes a noncommuting operator, rather than just a simple commuting

operator in zero magnetic field. Let us, for example, select a gauge for the vector potential

$$A_x = -By \quad (15.38)$$

$$A_y = 0 \quad (15.39)$$

$$A_z = 0, \quad (15.40)$$

so that $\mathbf{B} = B\hat{z}$, and from (15.37), $\hbar k_z$ becomes

$$\hbar k_x = \frac{\hbar}{i} \frac{\partial}{\partial x} + \frac{e}{c} By, \quad (15.41)$$

$$\hbar k_y = \frac{\hbar}{i} \frac{\partial}{\partial y}, \quad (15.42)$$

so that k_x and k_y no longer commute and we obtain the commutation relation

$$[k_x, k_y] = \frac{ieB}{\hbar c}. \quad (15.43)$$

The commutation relation (15.43) tells us that the amount by which the operators k_x and k_y fail to commute is proportional to B . We note that all other pairs of wave vector components, such as $[k_x, k_z]$, etc. still commute. Since the order of operators is important in a magnetic field, we will need to rewrite the secular equation (15.36) when $B \neq 0$ in terms of a symmetric and an antisymmetric part:

$$D_{nn'\alpha\beta} k_\alpha k_\beta = \frac{1}{2} D_{nn'\alpha\beta}^S \underbrace{\{k_\alpha, k_\beta\}}_{\text{anticommutator}} + \frac{1}{2} D_{nn'\alpha\beta}^A \underbrace{[k_\alpha, k_\beta]}_{\text{commutator}}, \quad (15.44)$$

where the symmetric part is

$$D_{nn'\alpha\beta}^S = \frac{1}{2} [D_{nn'\alpha\beta} + D_{nn'\beta\alpha}], \quad (15.45)$$

and the antisymmetric part is

$$D_{nn'\alpha\beta}^A = \frac{1}{2} [D_{nn'\alpha\beta} - D_{nn'\beta\alpha}], \quad (15.46)$$

in which the commutator is $[k_\alpha, k_\beta] = k_\alpha k_\beta - k_\beta k_\alpha$ and the anticommutator is $\{k_\alpha, k_\beta\} = k_\alpha k_\beta + k_\beta k_\alpha$. Thus the symmetric part $D_{nn'\alpha\beta}^S$ can be written explicitly as

$$D_{nn'\alpha\beta}^S = \frac{\hbar^2}{2m} \delta_{nn'} \delta_{\alpha\beta} + \frac{\hbar^2}{2m^2} \sum_{n''} \frac{\langle n | P_\alpha | n'' \rangle \langle n'' | P_\beta | n' \rangle + \langle n | P_\beta | n'' \rangle \langle n'' | P_\alpha | n' \rangle}{E_n(0) - E_{n''}(0)} \quad (15.47)$$

and gives the effective mass tensor through the relation

$$\frac{1}{m_{\alpha\beta}^*} = \frac{\partial^2 E_n}{\hbar^2 \partial k_\alpha \partial k_\beta}. \quad (15.48)$$

Since the electron spin is now included, the states in (15.47) are labeled by irreducible representations of the double groups and \mathbf{P} is a function of σ , as seen in (15.11).

The antisymmetric part $D_{nn'\alpha\beta}^A$ is from the above definition:

$$D_{nn'\alpha\beta}^A = \frac{\hbar^2}{2m^2} \sum_{n''} \frac{\langle n|P_\alpha|n''\rangle\langle n''|P_\beta|n' \rangle - \langle n|P_\beta|n''\rangle\langle n''|P_\alpha|n' \rangle}{E_n(0) - E_{n''}(0)}. \quad (15.49)$$

In the case of a spinless electron in a cubic crystal, $D_{nn'\alpha\beta}^A$ would vanish identically because there is only one independent momentum matrix element in cubic O_h symmetry in the absence of a magnetic field. If now we also include the electron spin and the double group representations, these arguments do not apply and we will find that $D_{nn'\alpha\beta}^A$ does not generally vanish and in fact contributes strongly to the effective g -factor. By way of comparison, the zero magnetic field eigenvalue problem is

$$\sum_{n'} \left[\sum_{\alpha\beta} D_{nn'\alpha\beta} k_\alpha k_\beta - E \delta_{nn'} \right] f_{n'} = 0, \quad (15.50)$$

and the magnetic field eigenvalue problem then becomes

$$\sum_{n'} \left\{ \sum_{\alpha\beta} \frac{1}{2} [D_{nn'\alpha\beta}^S \{k_\alpha, k_\beta\} + D_{nn'\alpha\beta}^A [k_\alpha, k_\beta]] - \mu_B \sigma \cdot \mathbf{B} - E \delta_{nn'} \right\} f_{n'} = 0, \quad (15.51)$$

where μ_B is the Bohr magneton

$$\mu_B = -\frac{|e|\hbar}{2mc},$$

and $\sigma = 2\mathbf{S}/\hbar$. The term $D_{nn'\alpha\beta}^S$ gives rise to a replacement of the periodic potential by an effective mass tensor. In computing $m_{\alpha\beta}^*$ we ordinarily neglect the difference between \mathbf{p} and \mathbf{P} .

In the presence of a magnetic field, the wavevectors \mathbf{k} are operators which act on the effective mass wave functions $f_{n'}$. From (15.43) we see that the components of the wave vector operator do not commute, so that

$$[k_\alpha, k_\beta] = \frac{ieB_\gamma}{\hbar c}, \quad (15.52)$$

and the commutator in (15.52) vanishes in zero magnetic field, as it should. Here the α, β, γ directions form a right-handed coordinate system. The term

$D_{nn'\alpha\beta}^A$ vanishes if there is no spin. The commutator $[k_\alpha, k_\beta]$ transforms as an axial vector. Because of the form of $D_{nn'\alpha\beta}^A$ given in (15.49), we see that $D_{nn'\alpha\beta}^A$ also transforms as an axial vector. Therefore the term $D_{nn'\alpha\beta}^A$ has the same symmetry properties as $-\mu_B \boldsymbol{\sigma}$ and gives rise to an effective magnetic moment different from the free electron value of the Bohr magneton μ_B . If we now write

$$[k_x, k_y] = \frac{ieB_z}{\hbar c} = iB_z \left(\frac{e\hbar}{2mc} \right) \left(\frac{2m}{\hbar^2} \right) = i\mu_B B_z \frac{2m}{\hbar^2}, \quad (15.53)$$

then

$$D_{N's}^A [k_x, k_y] = \frac{iB_z}{m} \mu_B \sum_{n''} \frac{\langle n | P_x | n'' \rangle \langle n'' | P_y | n' \rangle - \langle n | P_y | n'' \rangle \langle n'' | P_x | n' \rangle}{E_n(0) - E_{n''}(0)}, \quad (15.54)$$

so that the effective magnetic moment of an electron in a crystal is

$$\mu_{\alpha\beta}^* = |\mu_B| \left[\delta_{\alpha\beta} + \frac{i}{m} \sum_{n''} \frac{\langle n | P_\alpha | n'' \rangle \langle n'' | P_\beta | n \rangle - \langle n | P_\beta | n'' \rangle \langle n'' | P_\alpha | n \rangle}{E_n(0) - E_{n''}(0)} \right], \quad (15.55)$$

where the effective g -factor is related to $\mu_{\alpha\beta}^*$ by

$$g_{\text{eff } \alpha\beta} = 2\mu_{\alpha\beta}^*/\mu_B. \quad (15.56)$$

We recall that the energy levels of a free electron in a magnetic field are

$$E_{m_s} = g\mu_B m_s B, \quad (15.57)$$

so that for spin $1/2$, the spin splitting of the levels is $2\mu_B B$. In a crystalline solid, the spin splitting becomes $2\mu^* B$.

For comparison we include the corresponding formula for the effective mass tensor component

$$\frac{1}{m_{\alpha\beta}^*} = \frac{\delta_{\alpha\beta}}{m} + \frac{1}{m^2} \sum_{n''} \frac{\langle n | P_\alpha | n'' \rangle \langle n'' | P_\beta | n \rangle + \langle n | P_\beta | n'' \rangle \langle n'' | P_\alpha | n \rangle}{E_n(0) - E_{n''}(0)}, \quad (15.58)$$

in which

$$\mathbf{P} = \mathbf{p} + \frac{\hbar}{4mc^2} \boldsymbol{\sigma} \times \nabla V. \quad (15.59)$$

Thus an electron in a magnetic field and in a periodic potential acts as if the periodic potential can be replaced by letting $m \rightarrow m_{\alpha\beta}^*$ and $\mu_B \rightarrow \mu_{\alpha\beta}^*$. Thus, symbolically we would write an effective Hamiltonian as

$$H_{\text{eff}} = \frac{1}{2m^*} \left(\mathbf{p} - \frac{e}{c} \mathbf{A} \right)^2 - \mu^* \boldsymbol{\sigma} \cdot \mathbf{B}, \quad (15.60)$$

where

$$\mu^* = \mu_B g_{\text{eff}}/2. \quad (15.61)$$

In deriving the formula for the effective g -factor above, we did not pay much attention to whether \mathbf{P} was merely the momentum operator \mathbf{p} or the more complete quantity including the spin-orbit interaction

$$\mathbf{p} + \frac{\hbar}{4mc^2}(\boldsymbol{\sigma} \times \boldsymbol{\nabla}V).$$

It turns out that it is not very important whether we distinguish between matrix elements of \mathbf{p} and of \mathbf{P} since the matrix element of

$$\frac{\hbar}{4mc^2}(\boldsymbol{\sigma} \times \boldsymbol{\nabla}V)$$

is generally quite small. However, what is important, and even crucial, is that we consider the states n, n', n'' in the above expressions as states characterized by the irreducible representations of the crystal double groups.

Let us illustrate how we would proceed to calculate an effective g -factor for a typical semiconductor. Let us consider the effective g -factor for germanium at the Γ point ($\mathbf{k} = 0$). In Fig. 15.2 we let E_g denote the energy gap between the conduction band and the uppermost valence band, and we let Δ denote the spin-orbit splitting of the valence band. In germanium $E_g \sim 0.8$ eV and $\Delta \sim 0.3$ eV. We will assume in this simple example that these are the only bands to be included in carrying out the sum on n'' . Since the band extrema occur at $k = 0$, the effect of the translations $\boldsymbol{\tau} = (a/4)(1, 1, 1)$ are not important for Ge in this limit and can be neglected.

To evaluate μ^* and m^* in (15.55) and (15.58) we use the basis functions discussed in Sects. 14.6 and 14.7 to find the nonvanishing matrix elements of $\hbar\mathbf{k} \cdot \mathbf{p}/m$. We write the basis functions for $\Gamma_8^+(\Gamma_{25}^+)$ and $\Gamma_7^+(\Gamma_{25}^+)$ in a symbolic form from (15.24) and (15.25) so that we can make use of all the group theory ideas that were discussed in Sect. 13.5 in connection with the corresponding problem without spin. This approximation is valid if $\Delta \ll E_g$ and each double group level can be clearly identified with the single group level from which it originates. Otherwise the Γ_8^+ levels mix appreciably with one another and all matrix elements must be evaluated in the double group representation directly, so that the numerical estimates obtained here would have to be revised.

Now let us evaluate the matrix elements that go into (15.55) for μ^* . One set of matrix elements have the form:

$$\left\langle \gamma^- \uparrow | p_x | \frac{3}{2}, \frac{3}{2} \right\rangle = \left\langle \gamma^- \uparrow | p_x | \frac{1}{\sqrt{2}}(\varepsilon_x + i\varepsilon_y) \uparrow \right\rangle. \quad (15.62)$$

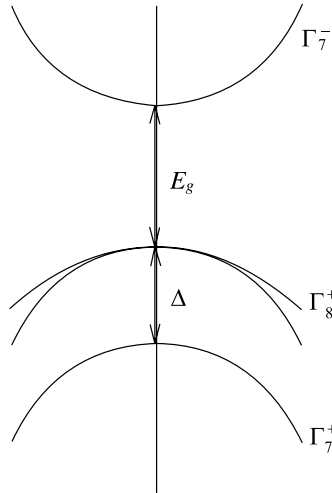


Fig. 15.2. Level ordering at the Γ point in Ge for the energy bands near the Fermi level

For the Γ_7^- state we take the basis functions to be $(\gamma^- \uparrow, \gamma^- \downarrow)$ where γ^- is a basis function for the Γ_2^- representation. For the basis functions for Γ_8^+ (Γ_{25}^+) we use

| $ j, m_j\rangle$ | State | Basis Function |
|-------------------------------------|-------|---|
| $ \frac{3}{2}, \frac{3}{2}\rangle$ | | $\nu_1 = \frac{1}{\sqrt{2}}(\varepsilon_x + i\varepsilon_y) \uparrow$ |
| $ \frac{3}{2}, \frac{1}{2}\rangle$ | | $\nu_2 = \frac{1}{\sqrt{6}}[(\varepsilon_x + i\varepsilon_y) \downarrow + 2\varepsilon_z \uparrow]$ |
| $ \frac{3}{2}, -\frac{1}{2}\rangle$ | | $\nu_3 = \frac{1}{\sqrt{6}}[(\varepsilon_x - i\varepsilon_y) \uparrow + 2\varepsilon_z \downarrow]$ |
| $ \frac{3}{2}, -\frac{3}{2}\rangle$ | | $\nu_4 = \frac{1}{\sqrt{2}}(\varepsilon_x - i\varepsilon_y) \downarrow .$ |

From Sect. 13.5 we have $(\Gamma_2^\pm | \mathcal{H}' | \Gamma_{25,\alpha}^\mp) = A_2 \hbar k_\alpha / m$, where $A_2 = (\Gamma_2^\pm | p_x | \Gamma_{25,x}^\mp)$ is the only independent matrix element connecting these symmetry types, where we note that the basis function for Γ_2^- symmetry is xyz . Using the basis functions for Γ_8^+ (Γ_{25}^+) given by (15.63) we obtain

$$\langle \gamma^- \uparrow | p_x | \frac{3}{2}, \frac{3}{2} \rangle = \frac{1}{\sqrt{2}} A_2$$

$$\langle \gamma^- \uparrow | p_x | \frac{3}{2}, \frac{1}{2} \rangle = 0$$

$$\langle \gamma^- \uparrow | p_x | \frac{3}{2}, -\frac{1}{2} \rangle = \frac{1}{\sqrt{6}} A_2$$

$$\langle \gamma^- \uparrow | p_x | \frac{3}{2}, -\frac{3}{2} \rangle = 0,$$

where we consider the *ortho-normality* of both the spin and orbital states. For the p_y matrix, the same procedure gives

$$\begin{aligned}\langle \gamma^- \uparrow | p_y | \frac{3}{2}, \frac{3}{2} \rangle &= \frac{i}{\sqrt{2}} A_2 \\ \langle \gamma^- \uparrow | p_y | \frac{3}{2}, \frac{1}{2} \rangle &= 0 \\ \langle \gamma^- \uparrow | p_y | \frac{3}{2}, -\frac{1}{2} \rangle &= -\frac{i}{\sqrt{6}} A_2 \\ \langle \gamma^- \uparrow | p_y | \frac{3}{2}, -\frac{3}{2} \rangle &= 0.\end{aligned}$$

To find the contribution to μ^*/μ_B , we sum (15.55) over the four Γ_8^+ levels to obtain

$$\begin{aligned}\sum_i \frac{[\langle \gamma^- \uparrow | p_x | \nu_i \rangle \langle \nu_i | p_y | \gamma^- \uparrow \rangle - \langle \gamma^- \uparrow | p_y | \nu_i \rangle \langle \nu_i | p_x | \gamma^- \uparrow \rangle]}{E_g} \\ = \frac{1}{E_g} \left[\left\{ \frac{A_2}{\sqrt{2}} \right\} \left\{ -\frac{iA_2^*}{\sqrt{2}} \right\} + \left\{ \frac{A_2}{\sqrt{6}} \right\} \left\{ \frac{iA_2^*}{\sqrt{6}} \right\} \right. \\ \left. - \left\{ \frac{iA_2}{\sqrt{2}} \right\} \left\{ \frac{A_2^*}{\sqrt{2}} \right\} - \left\{ -\frac{iA_2}{\sqrt{6}} \right\} \left\{ \frac{A_2^*}{\sqrt{6}} \right\} \right] \\ = \frac{|A_2|^2}{E_g} \left[-\frac{2i}{3} \right].\end{aligned}\quad (15.64)$$

We thus obtain for the contribution from the $\Gamma_8^+(\Gamma_{25}^+)$ levels to (μ^*/μ_B) a value of

$$\frac{i}{m} \left(-\frac{2i}{3} \right) \frac{|A_2|^2}{E_g} = \frac{2|A_2|^2}{3mE_g}.\quad (15.65)$$

Let us now find the contribution to μ^*/μ_B from the spin-orbit split-off bands. Here we use the basis functions for $\Gamma_7^+(\Gamma_{25}^+)$

$$\begin{array}{lll}|j, m_j\rangle & \text{State} & \text{Basis Function} \\ |\frac{1}{2}, \frac{1}{2}\rangle & & \mu_1 = \frac{1}{\sqrt{3}} [(\varepsilon_x + i\varepsilon_y) \downarrow - \varepsilon_z \uparrow] \\ |\frac{1}{2}, -\frac{1}{2}\rangle & & \mu_2 = \frac{1}{\sqrt{3}} [-(\varepsilon_x - i\varepsilon_y) \uparrow + \varepsilon_z \downarrow],\end{array}\quad (15.66)$$

so that the matrix elements for p_x and p_y become

$$\begin{aligned}\langle \gamma^- \uparrow | p_x | \frac{1}{2}, \frac{1}{2} \rangle &= 0 \\ \langle \gamma^- \uparrow | p_x | \frac{1}{2}, -\frac{1}{2} \rangle &= -\frac{1}{\sqrt{3}} A_2\end{aligned}$$

$$\begin{aligned}\langle \gamma^- \uparrow | p_y | \frac{1}{2}, \frac{1}{2} \rangle &= 0 \\ \langle \gamma^- \uparrow | p_y | \frac{1}{2}, -\frac{1}{2} \rangle &= \frac{i}{\sqrt{3}} A_2.\end{aligned}$$

We thus obtain the contribution of

$$\frac{i}{m(E_g + \Delta)} \left[\frac{2i}{3} |A_2|^2 \right] = -\frac{2}{3} \frac{|A_2|^2}{m(E_g + \Delta)} \quad (15.67)$$

to μ^*/μ_B in (15.55) from the $\Gamma_7^+(\Gamma_{25}^+)$ levels. Adding up the two contributions from (15.65) and (15.67) we finally obtain

$$\left(\frac{\mu^*}{\mu_B} \right)_{\text{orbital}} = -\frac{2|A_2|^2}{3m} \left[\frac{1}{E_g + \Delta} - \frac{1}{E_g} \right] + 1, \quad (15.68)$$

where +1 in (15.68) is the free electron contribution.

We can now evaluate $|A_2|^2$ in terms of the conduction band effective mass using the symmetric contribution $D_{nn'\alpha\beta}^S$ and for this term we can use the relation

$$\frac{m}{m^*} = 1 + \frac{2}{m} \sum_n \frac{|\langle \gamma^- \uparrow | p_x | n \rangle|^2}{E_{T_{2'}}(0) - E_n(0)}. \quad (15.69)$$

Evaluating the matrix elements in (15.69), we thus obtain

$$\frac{m}{m^*} = 1 + \frac{2}{m} \left[\frac{|A_2|^2}{2E_g} + \frac{|A_2|^2}{6E_g} + \frac{|A_2|^2}{3(E_g + \Delta)} \right] \approx \frac{2}{3m} |A_2|^2 \left[\frac{2}{E_g} + \frac{1}{E_g + \Delta} \right], \quad (15.70)$$

where the free electron term of unity is usually small compared to other terms in the sum in (15.70) and can be neglected in many cases. Neglecting this term, we now substitute for $|A_2|^2$ in terms of m^* to obtain

$$g_{\text{eff}} = \frac{2\mu^*}{\mu_B} = 2 - \frac{2m}{m^*} \left(\frac{\Delta}{3E_g + 2\Delta} \right). \quad (15.71)$$

In the limit, $\Delta \rightarrow 0$, then $g \rightarrow 2$ in agreement with the results for the free electron g -factor. In the limit $\Delta \gg E_g$

$$g_{\text{eff}} \rightarrow 2 - \frac{m}{m^*}, \quad (15.72)$$

which implies $g_{\text{eff}} \rightarrow -m/m^*$ for carriers with very light masses.

For germanium, for which $m^*/m \sim 0.12$, $\Delta \sim 0.3$ eV, and $E_g \sim 0.8$ eV, the effective g -factor mostly cancels the free electron contribution:

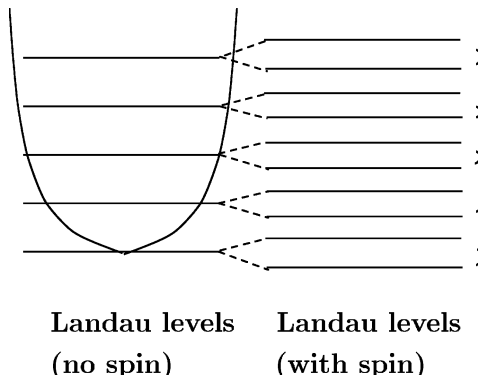


Fig. 15.3. Landau levels in InSb showing the spin splitting resulting from the large negative effective g -factor

$$g_{\text{eff}} = 2 \left[1 - \left(\frac{1}{0.12} \right) \frac{0.3}{3(0.8) + 2(0.3)} \right] = 2 \left[1 - \frac{1}{1.2} \right] \simeq \frac{1}{3}. \quad (15.73)$$

For InSb the spin-orbit splitting is large compared with the direct band gap $m^*/m \sim 0.013$, $\Delta \sim 0.9$ eV, and $E_g \sim 0.2$ eV

$$g_{\text{eff}} \sim 2 \left[1 - \left(\frac{1}{0.013} \right) \frac{0.9}{3(0.2) + 2(0.9)} \right] \sim 2(1 - 28) \simeq -54 \quad (15.74)$$

leading to the picture for InSb shown in Fig. 15.3. In InSb, the spin splitting is almost as large as the Landau level separation. However, the g_{eff} has the opposite sign as compared with the free electron spin g -value, where we note that because of the negative sign of the charge on the electron and on the Bohr magneton, the free electron spin state of lowest energy is aligned antiparallel to the applied field. Sometimes it is convenient to define the spin effective mass by the relation

$$\frac{\mu^*}{\mu_B} = \frac{m}{m_s^*}, \quad (15.75)$$

where m_s^* denotes spin effective mass, so that $g_{\text{eff}} = 2m/m_s^*$ [19, 52, 62, 74, 77].

In general, the spin and orbital effective masses will not be the same. If they are (see Fig. 15.4), the Landau level spacing is equal to the spacing between spin levels. The physical reason why these masses are not expected to be equal is that the orbital mass is determined by a momentum matrix element (which transforms as a radial vector). Since the spin mass depends on the coupling between electronic energy bands through an operator which transforms as an axial vector, different energy bands with different symmetries are coupled for the two cases.

In treating cyclotron resonance transitions, the transitions are spin conserving and the g -factors usually cancel out. They are, however, important for

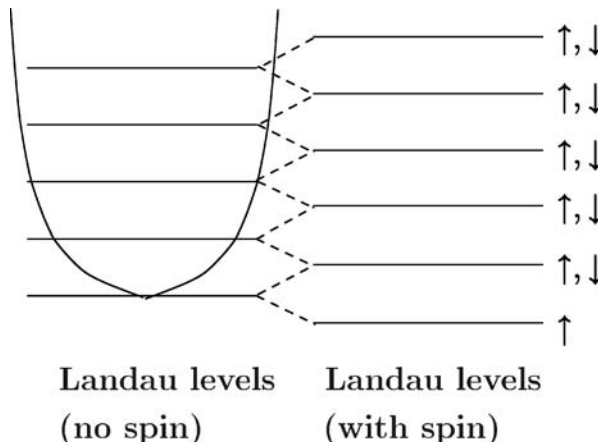


Fig. 15.4. Strict two-band model where the Landau level separation is equal to the spin splitting, as occurs for the case of a free electron gas. This limit applies quite well to the L -point Landau levels for the conduction band in bismuth

interband Landau level transitions even though the transitions are spin conserving, since the g -factors in the valence and conduction bands can be different. Thus spin up and spin down transitions can occur at different energies. The effective g -factors are directly observed in spin resonance experiments which occur between the same Landau level but involve a spin flip.

Of interest also is the case where the spin effective mass and the orbital effective mass are equal to one another. In a strict two-band model this must be the case. For bismuth, the strongly coupled two-band model is approximately valid and $m_s^* \simeq m^*$ (see Fig. 15.4). Landau level separations equal to the spin splitting also occur for the free electron magnetic energy levels. However, for band electrons, the Landau level separations are proportional to the inverse cyclotron effective mass rather than the inverse free electron mass.

For high mobility (low effective mass) materials with a small spin-orbit interaction, the Landau level separation is large compared with the spin splitting (see Fig. 15.3). On the other hand, some high mobility narrow gap semiconductors with a large spin-orbit interaction can have spin splittings larger than the Landau level separations; such a situation gives rise to interesting phenomena at high magnetic fields.

Summarizing, the effective mass Hamiltonian was considered in the presence of a magnetic field, taking into account the spin on the electron. In this case, we form the following symmetrized combinations of wave vectors:

$$\begin{aligned}
 \Gamma_1^+ &\rightarrow k_x^2 + k_y^2 + k_z^2 \\
 \Gamma_{12}^+ &\rightarrow k_x^2 + \omega k_y^2 + \omega^2 k_z^2, k_x^2 + \omega^2 k_y^2 + \omega k_z^2, \\
 \Gamma_{25}^+ &\rightarrow (\{k_y, k_z\}, \{k_z, k_x\}, \{k_x, k_y\}) \\
 \Gamma_{15}^+ &\rightarrow ([k_y, k_z], [k_z, k_x], [k_x, k_y])
 \end{aligned} \tag{15.76}$$

in which the wave vector is taken as an operator. These symmetrized forms of the wave vector are used in connection with the effective g -factor for an electron in a periodic solid to which a magnetic field is applied [19, 52, 62, 74, 77].

We will return to the g -factor in semiconductors in Chap. 16 where we discuss time reversal symmetry. Since a magnetic field breaks time reversal symmetry, the form of $E(\mathbf{k})$ is sensitive to spin and time reversal symmetry. These considerations are very important to the field of spintronics.

15.7 Fourier Expansion of Energy Bands: Slater–Koster Method

The Slater–Koster technique uses group theory to provide the most general form for the energy bands throughout the Brillouin zone which is consistent with the crystal symmetry. The method is used when experiments or theory provide information relevant to $E(\mathbf{k})$ at different points in the Brillouin zone. The method provides the best fit to the form of $E(\mathbf{k})$ consistent with the experimental or theoretical constraints. Like the $\mathbf{k} \cdot \mathbf{p}$ method, it is an approach whereby the energy bands can be determined from experimental data without recourse to a definite energy band model or to a specific crystal potential. In contrast to $\mathbf{k} \cdot \mathbf{p}$ perturbation theory which makes use of the group of the wave-vector for an expansion of $E(\mathbf{k})$ about a specific point in the Brillouin zone such as $k = 0$, the Slater–Koster method considers the entire Brillouin zone and makes use of the full space group symmetry to form $E(\mathbf{k})$ on an equal basis. The original work done by Slater and Koster provided an interpolation formula for calculating energy bands at high symmetry points in the Brillouin zone [66], and the method was later applied to silicon and germanium [29]. We will illustrate the method here for a simple cubic lattice [27].

Because of the periodicity of the lattice, the energy bands $E_n(\mathbf{k})$ are periodic in the extended Brillouin zone

$$E_n(\mathbf{k} + \mathbf{K}_{n_i}) = E_n(\mathbf{k}), \quad (15.77)$$

where \mathbf{K}_{n_i} is a reciprocal lattice vector so that $\mathbf{K}_{n_i} \cdot \mathbf{R}_m = 2\pi p$, with p an integer. The energy bands $E_n(\mathbf{k})$ are furthermore continuous across a zone boundary and they approach this boundary with zero slope (giving the electrons zero velocity at a zone boundary). We make use of this periodicity as follows. Suppose that we have a function $V(\mathbf{r})$ which is periodic in the three-dimensional lattice. This function reflects the full symmetry of the crystal and symmetry operations of the space group. The function $V(\mathbf{r})$ can be Fourier expanded in the reciprocal lattice

$$V(\mathbf{r}) = \sum_{\mathbf{K}_{n_i}} v(\mathbf{K}_{n_i}) e^{i\mathbf{K}_{n_i} \cdot \mathbf{r}} \quad (15.78)$$

in which the summation is over all reciprocal lattice vectors. In the extended zone scheme, the energy $E_n(\mathbf{k})$ is periodic in a three-dimensional space defined

by the reciprocal lattice vectors. Therefore it is possible to Fourier expand $E_n(\mathbf{k})$ in a space “reciprocal” to the reciprocal lattice, i.e., in the direct lattice, to obtain:

$$E_n(\mathbf{k}) = \sum_{\mathbf{d}} \varepsilon_n(\mathbf{d}) e^{i\mathbf{k} \cdot \mathbf{d}}, \quad (15.79)$$

where $\mathbf{d} = \mathbf{R}_m$ are Bravais lattice vectors and $\varepsilon_n(\mathbf{d})$ can be interpreted as an overlap integral in the tight binding approximation. What is important here is that the tight binding wave functions reflect the symmetry operations of the space group. Crystal symmetry restricts the number of independent expansion coefficients $\varepsilon_n(\mathbf{d})$ following the principles that govern the determination of the number of independent nonvanishing matrix elements (see Sect. 6.6). Provided that the Fourier series of (15.79) is rapidly convergent, it is possible to describe $E_n(\mathbf{k})$ in terms of a small number of expansion parameters $\varepsilon_n(\mathbf{d})$. The number of $\varepsilon_n(\mathbf{d})$ is determined by group theory and their values, in principle, can be determined by experiment.

For example, let us consider a nondegenerate, isolated s -band in a simple cubic crystal. Such a band has Γ_1^+ symmetry and is invariant under the point group operations of the cubic group. The Fourier expansion would then take the form of the tight binding functions and relate to linear combinations of plane waves (see Sect. 12.2):

$$\begin{aligned} E_n(\mathbf{k}) = & \varepsilon_n(0) + \varepsilon_n(1) [\cos ak_x + \cos ak_y + \cos ak_z] \\ & + \varepsilon_n(2) [\cos a(k_y + k_z) + \cos a(k_y - k_z) + \cos a(k_z + k_x)] \\ & + \cos a(k_z - k_x) + \cos a(k_x + k_y) + \cos a(k_x - k_y)] \\ & + \varepsilon_n(3) [\cos a(k_x + k_y + k_z) + \cos a(k_x - k_y - k_z) \\ & + \cos a(-k_x + k_y - k_z) + \cos a(-k_x - k_y + k_z)] + \dots \quad (15.80) \end{aligned}$$

where $d = 0$ is the zeroth *neighbor* at $a(0, 0, 0)$
 $d = 1$ is the nearest neighbor at $a(1, 0, 0)$
 $d = 2$ is the next nearest neighbor at $a(1, 1, 0)$
 $d = 3$ is the next–next nearest neighbor at $a(1, 1, 1)$, etc.

In the tight binding approximation, the expansion coefficients appear as overlap integrals and transfer integrals of various kinds. Thus, the tight binding form is written to satisfy the symmetry of the space group and is of the Slater–Koster form. Now suppose that *ab initio* calculations provide the energy levels and wave functions with high accuracy at a few points in the Brillouin zone. The Slater–Koster method allows all these solutions to be brought together to give $E(\mathbf{k})$ throughout the Brillouin zone, consistent with space group symmetry. For example in Ge, we could have experimental data relevant to the Γ point from measurements of the hole

constant energy surfaces at the Γ point, and electron constant energy surfaces about the L points in the Brillouin zone [29] and optical transitions at both the Γ point and the L point. The Slater-Koster method provides a framework that allows use of each of these experiments to aid in the determination of the electronic energy band structure throughout the Brillouin zone [27].

Now for energy bands of practical interest, we will not have isolated non-degenerate bands, but rather coupled bands of some sort. We can express the eigenvalue problem for n coupled bands in terms of an $(n \times n)$ secular equation of the form

$$|\langle i|\mathcal{H}|j \rangle - E_n(\mathbf{k})\delta_{ij}| = 0. \quad (15.81)$$

In (15.81) the indices i and j denote Bloch wave functions which diagonalize the Hamiltonian

$$\mathcal{H} = \frac{p^2}{2m} + V(\mathbf{r}), \quad (15.82)$$

and are labeled by the wave vector \mathbf{k} . The matrix elements $\langle i|\mathcal{H}|j \rangle$ thus constitute a \mathbf{k} -dependent matrix. But at each \mathbf{k} point, these matrix elements are invariant under the symmetry operations of the group of the wave vector at \mathbf{k} . The Hamiltonian at $\mathbf{k} = 0$ has Γ_1^+ symmetry just like its eigenvalues $E_n(\mathbf{k})$. This matrix is also periodic in the reciprocal lattice in the extended zone scheme and therefore can be Fourier expanded.

The expansion is carried out in terms of a complete set of basis matrices which are taken as angular momentum matrices in the spirit of Sect. 14.6. For example, a (2×2) Hamiltonian including the electron spin (i.e., the double group representations Γ_6^\pm or Γ_7^\pm in Chap. 14) would be expanded in terms of four basis matrices $1, S_x, S_y$ and S_z , representing the angular momentum matrices for spin 1/2. A (3×3) Hamiltonian, such as would be used to describe the valence bands of many common semiconductors, is expanded in terms of the nine linearly independent basis matrices which span this space, namely, $\hat{1}, S_x, S_y, S_z, S_x^2, S_y^2, \{S_z, S_y\}, \{S_z, S_x\}$ and $\{S_x, S_y\}$, in which $\hat{1}$ is a (3×3) unit matrix, S_x, S_y, S_z are angular momentum matrices for spin 1, and $\{S_i, S_j\}$ denotes the anticommutator for matrices S_i and S_j . Under the point group operations of the group of the wave vector, the angular momentum matrices S_i transform as an axial vector – i.e., at $\mathbf{k} = 0$, S_i transforms as Γ_{15}^+ , while the matrix Hamiltonian still is required to be invariant. Therefore, it is necessary to take products of symmetrized combinations of the n basis matrices with appropriate symmetrized combinations of the Fourier expansion functions so that an invariant matrix Hamiltonian results.

The $(n \times n)$ matrix Hamiltonian which is denoted by $D_{\Gamma_1}(\mathbf{k})$ can be Fourier expanded in terms of these basis function matrices in the form

$$D_{\Gamma_1}(\mathbf{k}) = \sum_{\mathbf{d}} \alpha_{d, \Gamma_j} \mathcal{C}_{\Gamma_j}(\mathbf{d}) \cdot \mathcal{S}_{\Gamma_j}, \quad (15.83)$$

which is a generalization of (15.79). In (15.83), \mathcal{S}_{Γ_j} denotes a collection of basis matrices which transforms as Γ_j , and these symmetrized products of angular momentum matrices are given in Table 15.1 for the simple cubic lattice (space group #221). The distance d denotes the order of the expansion in (15.83) and corresponds to the distance of neighbors in the Fourier expansion in the tight binding sense, so that orders 0, 1, 2, ..., etc. correspond to $d = 0$ or $d = 1$ (nearest neighbor terms) or $d = 2$ (next nearest neighbor terms), etc. The angular momentum matrices in Table 15.1 are given by

$$S_x = \begin{pmatrix} 0 & 0 & 0 \\ 0 & 0 & i \\ 0 & -i & 0 \end{pmatrix}, \quad S_y = \begin{pmatrix} 0 & 0 & -i \\ 0 & 0 & 0 \\ i & 0 & 0 \end{pmatrix}, \quad S_z = \begin{pmatrix} 0 & i & 0 \\ -i & 0 & 0 \\ 0 & 0 & 0 \end{pmatrix}. \quad (15.84)$$

Products of the dimensionless angular momentum matrices S_i are listed representations of cubic group in Table 15.1, using an abbreviated notation. For example, $\mathcal{S}_{\Gamma_{15}^+}^{(x)}(1)$ denotes the x component of a three component vector S_x, S_y, S_z and all three components would appear in (15.83). Similarly, $\mathcal{S}_{\Gamma_{12}^+}^{(i)}(2)$ is a two component vector with partners

$$S_x^2 + \omega S_y^2 + \omega^2 S_z^2$$

and

$$S_x^2 + \omega^2 S_y^2 + \omega S_z^2,$$

and only one of the partners is listed in Table 15.1, where several other three component matrices are found, such as $\mathcal{S}_{\Gamma_{25}^+}^{(\alpha)}(2)$ for which the x component is the anticommutator $\{S_y, S_z\}$ and the y and z components of $\mathcal{S}_{\Gamma_{25}^+}^{(\alpha)}(2)$ are found by cyclic permutation of the indices x, y, z . It is worth

Table 15.1. Symmetrized products of angular momenta for the cubic group

| order | representation | notation | symmetrized products |
|-------|-----------------|--|---|
| 0 | Γ_1^+ | $\mathcal{S}_{\Gamma_1^+}(0)$ | 1 |
| 1 | Γ_{15}^+ | $\mathcal{S}_{\Gamma_{15}^+}^x(1)$ | S_x |
| 2 | Γ_{12}^+ | $\mathcal{S}_{\Gamma_{12}^+}^{(1)}(2)$ | $S_x^2 + \omega S_y^2 + \omega^2 S_z^2$ |
| | Γ_{25}^+ | $\mathcal{S}_{\Gamma_{25}^+}^{(x)}(2)$ | $\{S_y, S_z\}$ |
| 3 | Γ_2^+ | $\mathcal{S}_{\Gamma_2^+}(3)$ | $S_x S_y S_z + S_x S_z S_y$ |
| | Γ_{15}^+ | $\mathcal{S}_{\Gamma_{15}^+}^{(x)}(3)$ | S_x^3 |
| | Γ_{25}^+ | $\mathcal{S}_{\Gamma_{25}^+}^{(x)}(3)$ | $\{S_x, (S_y^2 - S_z^2)\}$ |

mentioning that all of the \mathcal{S} matrices in (15.83) are 3×3 matrices which are found explicitly by carrying out the indicated matrix operations. For example:

$$\{S_y, S_z\} = S_y S_z + S_z S_y = \begin{pmatrix} 0 & 0 & 0 \\ 0 & 0 & 0 \\ 0 & -1 & 0 \end{pmatrix} + \begin{pmatrix} 0 & 0 & 0 \\ 0 & 0 & -1 \\ 0 & 0 & 0 \end{pmatrix} = \begin{pmatrix} 0 & 0 & 0 \\ 0 & 0 & -1 \\ 0 & -1 & 0 \end{pmatrix}. \quad (15.85)$$

Also useful for carrying out matrix operations are the definitions:

$$S_x = \frac{\hbar}{i} \left(y \frac{\partial}{\partial z} - z \frac{\partial}{\partial y} \right) \quad (15.86)$$

so that

$$S_x \begin{pmatrix} x \\ y \\ z \end{pmatrix} = \frac{\hbar}{i} \begin{pmatrix} 0 \\ -z \\ y \end{pmatrix}. \quad (15.87)$$

Another point worth mentioning about Table 15.1 concerns the terms that do *not* appear. For example, in second-order we could have terms like $S_x^2 + S_y^2 + S_z^2$ but this matrix is just the unit matrix which has already been listed in the table. Similarly, the commutators $[S_y, S_z]$ which enter in second-order are matrices that have already appeared in first-order as iS_x .

We give below the nine basis matrices that span the (3×3) matrices for spin 1, where we note that $(\Gamma_{15}^+ \otimes \Gamma_{15}^+) = \Gamma_1^+ + \Gamma_{12}^+ + \Gamma_{15}^+ + \Gamma_{25}^+$:

$$\mathcal{S}_{\Gamma_1^+} = \begin{pmatrix} 1 & 0 & 0 \\ 0 & 1 & 0 \\ 0 & 0 & 1 \end{pmatrix}, \quad (15.88)$$

$$\mathcal{S}_{\Gamma_{12}^+}^{(1)} = \begin{pmatrix} -1 & 0 & 0 \\ 0 & 1 + \omega^2 & 0 \\ 0 & 0 & 1 + \omega \end{pmatrix} = \begin{pmatrix} -1 & 0 & 0 \\ 0 & -\omega & 0 \\ 0 & 0 & -\omega^2 \end{pmatrix}, \quad (15.89)$$

$$\mathcal{S}_{\Gamma_{12}^+}^{(2)} = \begin{pmatrix} -1 & 0 & 0 \\ 0 & 1 + \omega & 0 \\ 0 & 0 & 1 + \omega^2 \end{pmatrix}, \quad (15.90)$$

$$\mathcal{S}_{\Gamma_{15}^+}^{(x)} = \begin{pmatrix} 0 & 0 & 0 \\ 0 & 0 & i \\ 0 & -i & 0 \end{pmatrix}, \quad (15.91)$$

$$\mathcal{S}_{\Gamma_{15}^+}^{(y)} = \begin{pmatrix} 0 & 0 & -i \\ 0 & 0 & 0 \\ i & 0 & 0 \end{pmatrix}, \quad (15.92)$$

$$\mathcal{S}_{\Gamma_{15}^+}^{(z)} = \begin{pmatrix} 0 & i & 0 \\ -i & 0 & 0 \\ 0 & 0 & 0 \end{pmatrix}, \quad (15.93)$$

$$\mathcal{S}_{\Gamma_{25}^+}^{(x)} = \begin{pmatrix} 0 & 0 & 0 \\ 0 & 0 & 1 \\ 0 & 1 & 0 \end{pmatrix}, \quad (15.94)$$

$$\mathcal{S}_{\Gamma_{25}^+}^{(y)} = \begin{pmatrix} 0 & 0 & 1 \\ 0 & 0 & 0 \\ 1 & 0 & 0 \end{pmatrix}, \quad (15.95)$$

$$\mathcal{S}_{\Gamma_{25}^+}^{(z)} = \begin{pmatrix} 0 & 1 & 0 \\ 1 & 0 & 0 \\ 0 & 0 & 0 \end{pmatrix}, \quad (15.96)$$

Any arbitrary (3×3) matrix can be written as a linear combination of these nine matrices.

Table 15.1 however was constructed to be more general than just to describe interacting p -bands in a 3×3 matrix formulation. The table can equally well be used to form the appropriate 16 basis matrices which are needed to deal with interacting s and p bands, such as would arise in semiconductor physics. Such interacting s and p bands give rise to a 4×4 matrix Hamiltonian and therefore 16 basis matrices are needed to span the space for the secular equation in this case. The symmetries involved for order 0, 1, 2, 3, ... correspond to the symmetries of the angular momentum matrices in cubic symmetry.

Now let us return to the Fourier expansion of (15.83). For each neighbor distance $|\mathbf{d}|$ there are several lattice vectors that enter, just as in the plane wave problem of Chap. 12 where we considered sets of \mathbf{K}_{n_i} vectors of equal magnitude. The terms in (15.83) can be labeled by their symmetry types so that the sum on \mathbf{d} breaks up into a sum on the magnitude $|\mathbf{d}|$ and on the symmetry type Γ_j occurring at distance \mathbf{d} . The linear combinations of the exponential functions $\exp(i\mathbf{k} \cdot \mathbf{d})$ which transform as the pertinent irreducible representations of the cubic group are given in Table 15.2 out through third nearest neighbor distances. Once again, if a representation is one-dimensional, the basis function itself is given. For the two-dimensional representations, only one of the functions is listed, the partner being the complex conjugate of the listed function. For the three-dimensional representations, only the x -component is listed; the partners are easily found by cyclic permutations of the indices.

The combinations of plane waves and basis functions that enter the Fourier expansion of (15.83) are the scalar products of these symmetrized Fourier functions $\mathcal{C}_{\Gamma_j}(\mathbf{d})$ and the basis functions $\mathcal{S}_{\Gamma_j}(\mathbf{d})$. This means that for the two-dimensional representations, we write

$$\mathcal{C}_{\Gamma_{12}^+}^{(1)} \left(\mathcal{S}_{\Gamma_{12}^+}^{(1)} \right)^* + \mathcal{C}_{\Gamma_{12}^+}^{(2)} \left(\mathcal{S}_{\Gamma_{12}^+}^{(2)} \right)^*, \quad (15.97)$$

Table 15.2. Symmetrized Fourier functions for a simple cubic lattice

| d | repr. | notation | symmetrized Fourier functions |
|--------------|-----------------|--|---|
| $a(0, 0, 0)$ | Γ_1^+ | $\mathcal{C}_{\Gamma_1^+}(000)$ | 1 |
| $a(1, 0, 0)$ | Γ_1^+ | $\mathcal{C}_{\Gamma_1^+}(100)$ | $\cos ak_x + \cos ak_y + \cos ak_z$ |
| | Γ_{12}^+ | $\mathcal{C}_{\Gamma_{12}^+}^{(1)}(100)$ | $\cos ak_x + \omega \cos ak_y + \omega^2 \cos ak_z$ |
| | Γ_{15}^- | $\mathcal{C}_{\Gamma_{15}^-}^{(x)}(100)$ | $\sin ak_x$ |
| $a(1, 1, 0)$ | Γ_1^+ | $\mathcal{C}_{\Gamma_1^+}(110)$ | $\cos a(k_y + k_z) + \cos a(k_y - k_z) + \cos a(k_z + k_x) + \cos a(k_z - k_x) + \cos a(k_x + k_y) + \cos a(k_x - k_y)$ |
| | Γ_{12}^+ | $\mathcal{C}_{\Gamma_{12}^+}^{(1)}(110)$ | $[\cos a(k_y + k_z) + \cos a(k_y - k_z)] + \omega [\cos a(k_z + k_x) + \cos a(k_z - k_x)] + \omega^2 [\cos a(k_x + k_y) + \cos a(k_x - k_y)]$ |
| | Γ_{15}^- | $\mathcal{C}_{\Gamma_{15}^-}^{(x)}(110)$ | $\sin a(k_x + k_y) + \sin a(k_x - k_y) + \sin a(k_x + k_z) + \sin a(k_x - k_z)$ |
| | Γ_{25}^- | $\mathcal{C}_{\Gamma_{25}^-}^{(x)}(110)$ | $\sin a(k_x + k_y) + \sin a(k_x - k_y) - \sin a(k_x + k_z) - \sin a(k_x - k_z)$ |
| | Γ_{25}^+ | $\mathcal{C}_{\Gamma_{25}^+}^{(x)}(110)$ | $\cos a(k_y + k_z) - \cos a(k_y - k_z)$ |
| $a(1, 1, 1)$ | Γ_1^+ | $\mathcal{C}_{\Gamma_1^+}(111)$ | $\cos a(k_x + k_y + k_z) + \cos a(k_x - k_y - k_z) + \cos a(-k_x + k_y - k_z) + \cos a(-k_x - k_y + k_z)$ |
| | Γ_2^- | $\mathcal{C}_{\Gamma_2^-}(111)$ | $\sin a(k_x + k_y + k_z) + \sin a(k_x - k_y - k_z) + \sin a(-k_x + k_y - k_z) + \sin a(-k_x - k_y + k_z)$ |
| | Γ_{15}^- | $\mathcal{C}_{\Gamma_{15}^-}^{(x)}(111)$ | $\sin a(k_x + k_y + k_z) + \sin a(k_x - k_y - k_z) - \sin a(-k_x + k_y - k_z) - \sin a(-k_x - k_y + k_z)$ |
| | Γ_{25}^+ | $\mathcal{C}_{\Gamma_{25}^+}^{(x)}(111)$ | $\cos a(k_x + k_y + k_z) + \cos a(k_x - k_y - k_z) - \cos a(-k_x + k_y - k_z) - \cos a(-k_x - k_y + k_z)$ |

$\omega = \exp(2\pi i/3)$ and a is the lattice constant

where the second term is the complex conjugate of the first so that the sum is real. For the three-dimensional representations we write for the scalar product

$$\mathcal{C}^x \mathcal{S}^x + \mathcal{C}^y \mathcal{S}^y + \mathcal{C}^z \mathcal{S}^z. \quad (15.98)$$

Finally, the Fourier expansion parameters α_{d, Γ_j} are just numbers that give the magnitude of all the terms which enter the Fourier expansion. By taking the C_{Γ_i} and S_{Γ_i} to transform according to the same irreducible representation, the direct product will contain Γ_1 which is invariant under the symmetry operations of the group. These coefficients are often evaluated from experimental data.

Now suppose that we are going to do a Fourier expansion for p -bands. If the spin-orbit interaction is neglected, the p -bands have Γ_{15}^- symmetry. We

ask what symmetry types can we have in the coupling between p -bands – clearly only the symmetries that enter into the direct product

$$\Gamma_{15}^- \otimes \Gamma_{15}^- = \Gamma_1^+ + \Gamma_{12}^+ + \Gamma_{15}^+ + \Gamma_{25}^+. \quad (15.99)$$

We will now indicate the terms which contribute at each neighbor distance to (15.83).

15.7.1 Contributions at $d = 0$

From Table 15.2 we can have only Γ_1^+ symmetry at $d = 0$ for which the basis matrix is

$$\begin{pmatrix} 1 & 0 & 0 \\ 0 & 1 & 0 \\ 0 & 0 & 1 \end{pmatrix}, \quad (15.100)$$

and the symmetrical Fourier function is the number 1, so that the net contribution to (15.83) is

$$\alpha_{0,\Gamma_1^+} \begin{pmatrix} 1 & 0 & 0 \\ 0 & 1 & 0 \\ 0 & 0 & 1 \end{pmatrix}. \quad (15.101)$$

15.7.2 Contributions at $d = 1$

For Γ_1^+ symmetry the contribution is in analogy to (15.101)

$$\alpha_{1,\Gamma_1^+} \mathcal{C}_{\Gamma_1^+}(100) \begin{pmatrix} 1 & 0 & 0 \\ 0 & 1 & 0 \\ 0 & 0 & 1 \end{pmatrix}, \quad (15.102)$$

while for Γ_{12}^+ symmetry, the contribution is

$$\alpha_{1,\Gamma_{12}^+} \mathcal{C}_{\Gamma_{12}^+}^{(1)} \begin{pmatrix} \omega + \omega^2 & 0 & 0 \\ 0 & 1 + \omega^2 & 0 \\ 0 & 0 & 1 + \omega \end{pmatrix} + \alpha_{1,\Gamma_{12}^+} \mathcal{C}_{\Gamma_{12}^+}^{(2)} \begin{pmatrix} \omega + \omega^2 & 0 & 0 \\ 0 & 1 + \omega & 0 \\ 0 & 0 & 1 + \omega^2 \end{pmatrix}, \quad (15.103)$$

where we have used the relation $S_{\Gamma_{12}^+}^{(1)} = S_x^2 + \omega S_y^2 + \omega^2 S_z^2$ to obtain the appropriate matrices. We also use the relations $1 + \omega + \omega^2 = 0$ for the cube roots of unity to simplify (15.103). We note that both terms in (15.103) have the same expansion parameter α_{1,Γ_{12}^+} .

These are all the contributions for $d = 1$. The symmetry type Γ_{15}^- does not enter into this sum since there are no basis matrices with symmetries Γ_{15}^- for $\mathbf{d} = 1$ (see Table 15.1). This symmetry would however enter into treating the interaction between s and p bands. Group theory thus tells us that we get no off-diagonal terms until we go to second-neighbor distances. This should not be surprising to us since this is exactly what happens in the $\mathbf{k} \cdot \mathbf{p}$ treatment of p bands. In fact, *the Fourier expansion technique contains in it a $\mathbf{k} \cdot \mathbf{p}$ expansion for every point in the Brillouin zone*.

15.7.3 Contributions at $d = 2$

At the second-neighbor distance Table 15.2 yields contributions from Γ_1^+ , Γ_{12}^+ and Γ_{25}^+ symmetries. These contributions at $d = 2$ are:

$$\Gamma_1^+ \text{ symmetry } \alpha_{2,\Gamma_1^+} \mathcal{C}_{\Gamma_1^+}(110) \begin{pmatrix} 1 & 0 & 0 \\ 0 & 1 & 0 \\ 0 & 0 & 1 \end{pmatrix}, \quad (15.104)$$

$$\Gamma_{12}^+ \text{ symmetry } \alpha_{2,\Gamma_{12}^+} \left[\mathcal{C}_{\Gamma_{12}^+}^{(1)}(110) \begin{pmatrix} -1 & 0 & 0 \\ 0 & -\omega & 0 \\ 0 & 0 & -\omega^2 \end{pmatrix} + c.c. \right] \quad (15.105)$$

$$\Gamma_{25}^+ \text{ symmetry } \alpha_{2,\Gamma_{25}^+} \begin{pmatrix} 0 & \mathcal{C}_{\Gamma_{25}^+}^{(z)}(110) & \mathcal{C}_{\Gamma_{25}^+}^{(y)}(110) \\ \mathcal{C}_{\Gamma_{25}^+}^{(z)}(110) & 0 & \mathcal{C}_{\Gamma_{25}^+}^{(x)}(110) \\ \mathcal{C}_{\Gamma_{25}^+}^{(y)}(110) & \mathcal{C}_{\Gamma_{25}^+}^{(x)}(110) & 0 \end{pmatrix} \quad (15.106)$$

Terms with Γ_{15}^- and Γ_{25}^- symmetries in Table 15.2 do not enter because there are no basis matrices with these symmetries.

15.7.4 Summing Contributions through $d = 2$

Symmetries Γ_1^+ and Γ_{25}^+ contribute and these are written down as above. To get the matrix Hamiltonian we add up contributions from (15.101)–(15.106). There are six parameters α_{d,Γ_j} that enter into the Fourier expansion through second-neighbor terms ($d = 0, 1, 2$). The Γ_1^+ representation at $d = 0$ contributes to the (1,1) position in the secular equation a term in α_{0,Γ_1^+} and at $d = 1$ contributes a term $\alpha_{1,\Gamma_1^+}(\cos ak_x + \cos ak_y + \cos ak_z)$ in which the two coefficients α_{0,Γ_1^+} and α_{1,Γ_1^+} will have different numerical values. The other entries into the (3×3) matrix are found similarly. The resulting (3×3) matrix Hamiltonian is then diagonalized and the eigenvalues are the $E_n(\mathbf{k})$ we are looking for. This $E_n(\mathbf{k})$ properly expresses the crystal symmetry at all points in the Brillouin zone.

It is instructive to write out this matrix Hamiltonian in detail along the (100), (110) and (111) directions and to verify that all connectivity relations and symmetry requirements are automatically satisfied. It is directly shown that near $\mathbf{k} = 0$, the Hamiltonian of (15.83) is of the $\mathbf{k} \cdot \mathbf{p}$ form previously derived. As stated above, the Fourier expansion approach contains the $\mathbf{k} \cdot \mathbf{p}$ form for all expansion points \mathbf{k}_0 in the Brillouin zone.

15.7.5 Other Degenerate Levels

The Fourier expansion can also be applied to the twofold Γ_{12}^+ levels in cubic symmetry arising from d -bands, or to Γ_{12}^\pm levels more generally. Of particular

interest is application of the Slater–Koster method [66] to coupled s and p bands as has been done for silicon and germanium, both of which crystallize in the diamond structure. In the case of coupled s and p bands, the 3×3 expansion in Sect. 15.7 and the s -band expansion are coupled with the Fourier terms from Table 15.2 having symmetries $\Gamma_i \otimes \Gamma_{15}^-$. We give an outline in this section for setting up the secular equation to solve the Fourier expansion for these two interesting cases.

The four 2×2 matrices that are used as basis matrices for Fourier expanding the Γ_{12}^\pm levels are implied by $\Gamma_{12}^\pm \otimes \Gamma_{12}^\pm = \Gamma_1^+ + \Gamma_2^+ + \Gamma_{12}^+$:

$$\text{for } \Gamma_1^+ \text{ symmetry } \mathcal{S}_{\Gamma_1^+} = \begin{pmatrix} 1 & 0 \\ 0 & 1 \end{pmatrix}, \quad (15.107)$$

$$\text{for } \Gamma_2^+ \text{ symmetry } \mathcal{S}_{\Gamma_2^+} = \begin{pmatrix} 1 & 0 \\ 0 & -1 \end{pmatrix}, \quad (15.108)$$

$$\text{for } \Gamma_{12}^+ \text{ symmetry } \mathcal{S}_{\Gamma_{12,1}^+} = \begin{pmatrix} 0 & 1 \\ 0 & 0 \end{pmatrix}, \quad (15.109)$$

where the partner of $\mathcal{S}_{\Gamma_{12,1}^+}$ is the Hermitian transpose

$$\mathcal{S}_{\Gamma_{12,2}^+} = \mathcal{S}_{\Gamma_{12,1}^+}^* = \mathcal{S}_{\Gamma_{12,1}^+}^\dagger = \begin{pmatrix} 0 & 0 \\ 1 & 0 \end{pmatrix}. \quad (15.110)$$

Using these matrices we see that

$$\mathcal{S}_{\Gamma_{12,1}^+} \mathcal{S}_{\Gamma_{12,1}^+}^\dagger + \mathcal{S}_{\Gamma_{12,2}^+} \mathcal{S}_{\Gamma_{12,2}^+}^\dagger = \begin{pmatrix} 1 & 0 \\ 0 & 1 \end{pmatrix} = \mathcal{S}_{\Gamma_1^+}, \quad (15.111)$$

and

$$\mathcal{S}_{\Gamma_{12,1}^+} \mathcal{S}_{\Gamma_{12,1}^+}^\dagger - \mathcal{S}_{\Gamma_{12,2}^+} \mathcal{S}_{\Gamma_{12,2}^+}^\dagger = \begin{pmatrix} 1 & 0 \\ 0 & -1 \end{pmatrix} = \mathcal{S}_{\Gamma_2^+}. \quad (15.112)$$

The dispersion relation of $E(\mathbf{k})$ for a band with Γ_{12}^+ symmetry at $\mathbf{k} = 0$ can then be Fourier expanded throughout the Brillouin zone in terms of the basis functions in (15.107)–(15.110) as

$$\begin{aligned} E_{\Gamma_{12}^\pm}(\mathbf{k}) = & \sum_{\mathbf{d}} \alpha_{d, \Gamma_1^+} \mathcal{C}_{\Gamma_1^+}(\mathbf{d}) \begin{pmatrix} 1 & 0 \\ 0 & 1 \end{pmatrix} + \sum_{\mathbf{d}} \alpha_{d, \Gamma_2^+} \mathcal{C}_{\Gamma_2^+}(\mathbf{d}) \begin{pmatrix} 1 & 0 \\ 0 & -1 \end{pmatrix} \\ & + \sum_{\mathbf{d}} \alpha_{d, \Gamma_{12}^+} \mathcal{C}_{\Gamma_{12}^+}^{(1)}(\mathbf{d}) \begin{pmatrix} 0 & 1 \\ 0 & 0 \end{pmatrix} + \sum_{\mathbf{d}} \alpha_{d, \Gamma_{12}^+} \mathcal{C}_{\Gamma_{12}^+}^{(2)}(\mathbf{d}) \begin{pmatrix} 0 & 0 \\ 1 & 0 \end{pmatrix}, \end{aligned} \quad (15.113)$$

where $\mathcal{C}_{\Gamma_{12}^\pm}^{(2)}(\mathbf{d}) = \mathcal{C}_{\Gamma_{12}^\pm}^{(1)*}(\mathbf{d})$ and the $\mathcal{C}_{\Gamma_i^\pm}(\mathbf{d})$ functions are found in Table 15.2.

For the case of interacting s (Γ_1^+) and p (Γ_{15}^-) bands, the interaction terms have $\Gamma_1^+ \otimes \Gamma_{15}^- = \Gamma_{15}^-$ symmetry so the 4×4 expansion matrices must be supplemented by the matrices

$$\mathcal{S}_{\Gamma_{15}^-}^x = \begin{pmatrix} 0 & 1 & 0 & 0 \\ 1 & 0 & 0 & 0 \\ 0 & 0 & 0 & 0 \\ 0 & 0 & 0 & 0 \end{pmatrix}, \quad (15.114)$$

and the two partners

$$\mathcal{S}_{\Gamma_{15}^-}^y = \begin{pmatrix} 0 & 0 & 1 & 0 \\ 0 & 0 & 0 & 0 \\ 1 & 0 & 0 & 0 \\ 0 & 0 & 0 & 0 \end{pmatrix}, \quad \mathcal{S}_{\Gamma_{15}^-}^z = \begin{pmatrix} 0 & 0 & 0 & 1 \\ 0 & 0 & 0 & 0 \\ 0 & 0 & 0 & 0 \\ 1 & 0 & 0 & 0 \end{pmatrix}. \quad (15.115)$$

The detailed treatment of the Fourier expansion for the eight coupled s and p bonding and antibonding bands in the nonsymmorphic diamond structure has been presented [29] and was used to describe the Si and Ge bands throughout the Brillouin zone. The nonsymmorphic diamond structure requires certain restrictions on the energy bands, as discussed in Sect. 12.5 and in Appendix C. The same basic treatment without the s bands was used to treat the lattice dynamics for the diamond structure [30].

Selected Problems

15.1. Consider the empty lattice $E(\mathbf{k})$ diagram in Fig. 12.1 for an FCC structure, but now also including the electron spin.

- (a) Find the symmetry designations and energy for the lowest nonzero double group energy level which arises from the single group L_1 and $L_{2'}$ levels.
- (b) Then find the symmetry designations and energy for the next lowest energy level which is derived from the X_1 and $X_{4'}$ levels.
- (c) What are the corresponding basis functions for these levels?
- (d) What is the difference between these lowest energy levels for the case of the diamond structure in comparison to the symmorphic FCC space group? The character tables for the group of the wave vector for the diamond structure can be found in Appendix C.

15.2. (a) Give more details to show how group theory leads to the form of $E(\Gamma_7^+)$ given by (15.27).

- (b) Similarly, give more details to show how the form of $E(\mathbf{k})$ for the four-fold degenerate valence band of Ge is obtained.

- (c) The derivation given in Sect. 15.5 was for a symmorphic cubic group. However, Ge is described by the space group #227 which is nonsymmorphic. What is the effect of the screw axis in the diamond structure on the forms of $E(\Gamma_7^+)$ and $E(\Gamma_8^+)$ discussed in (a) and (b)? When would the sticking together of bands discussed in Sect. 12.5 become important? You may find the character tables for the diamond structure in Appendix C useful for this problem.

15.3. Find the form of $E(\mathbf{k})$ including the spin-orbit interaction for a non-degenerate valence band level in a column IV semiconductor (2 atoms/unit cell) with a simple symmorphic hexagonal structure (space group #191) at the Γ point and at the K point in the Brillouin zone using $\mathbf{k} \cdot \mathbf{p}$ perturbation theory. Assume that at $k = 0$, the energy bands have D_{6h} symmetry and that the nondegenerate band in this problem is derived from the fully symmetric single group irreducible representation Γ_1 .

15.4. Apply the formalism in Sect. 15.6 to find the effective g -factor for a carrier pocket at the Γ point for a nondegenerate valence band for a crystal with hexagonal symmetry (space group #191) as in Problem 15.3.

- 15.5.** (a) Using the procedure in Sect. 15.7, write down the matrices for S_x , S_y and S_z for angular momentum 3/2. Products of these matrices and the (4×4) unit matrix form the 16 matrix basis functions which span the vector space for the (4×4) Slater-Koster secular equation for coupled s and p bands for a simple cubic lattice. Find these 16 matrices and indicate the combination of S_x , S_y and S_z used and indicate the symmetry type of each.
- (b) Returning to the Slater-Koster (3×3) secular determinant for a simple cubic lattice, write the explicit expression for this matrix along a (100) direction. Show that by doing a Taylor's expansion of the Slater-Koster Hamiltonian about the X point, the proper $\mathbf{k} \cdot \mathbf{p}$ Hamiltonian is obtained at the X point.

- 15.6.** (a) Using the Slater-Koster technique [66], find the form for $E(\mathbf{k})$ for the lowest two levels for a face centered cubic lattice at the X point, the L point and the K point (see Table C.6).
- (b) Using your results in (a), expand $E(\mathbf{k})$ about the L -point in a Taylor expansion and compare your results with those obtained using $\mathbf{k} \cdot \mathbf{p}$ perturbation theory.

Part VI

Other Symmetries

Time Reversal Symmetry

In this chapter we consider the properties of the time reversal operator (Sects. 16.1 and 16.2) and the topic of time reversal symmetry. We then consider the effect of time reversal symmetry on the form of the electronic dispersion relations and this topic is discussed here for the case of no spin (Sect. 16.3) and when the spin-orbit interaction is included (Sect. 16.4). As a second illustration of time reversal symmetry, we consider magnetic space groups in Sect. 16.5, where the time reversal operator itself can become a symmetry element of the group.

In high energy physics, arguments regarding time inversion were essential in providing guidance for the development of a theory for the fundamental particles. The CPT invariance in particle physics deals with charge conjugation (C) which is the reversal of the sign of the electrical charge, parity (P) which is spatial inversion, and time inversion (T).

16.1 The Time Reversal Operator

Knowledge of the state of a system at any instant of time t and the deterministic laws of physics are sufficient to determine the state of the system both into the future and into the past. If the wave function $\psi(\mathbf{r}, t)$ specifies the time evolution of state $\psi(\mathbf{r}, 0)$, then $\psi(\mathbf{r}, -t)$ is called the *time-reversed conjugate* of $\psi(\mathbf{r}, t)$. The time-reversed conjugate state is achieved by running the system backwards in time or reversing all the velocities (or momenta) of the system.

The time evolution of a state is governed by Schrödinger's equation (one of the deterministic laws of physics)

$$i\hbar \frac{\partial \psi}{\partial t} = \mathcal{H}\psi, \quad (16.1)$$

which is satisfied by a time-dependent wave function of the form

$$\psi(\mathbf{r}, t) = e^{\frac{-i\mathcal{H}t}{\hbar}} \psi(\mathbf{r}, 0), \quad (16.2)$$

where $\exp[-i\mathcal{H}t/\hbar]$ is the time evolution factor. The effect of time reversal $t \rightarrow -t$ (which we denote by the operator \hat{T}) on the wave function is that of complex conjugation $\psi \rightarrow \psi^*$ so that

$$\hat{T}\psi(\mathbf{r}, t) = \psi(\mathbf{r}, -t) = \psi^*(\mathbf{r}, t). \quad (16.3)$$

In Sect. 16.2, we discuss some of the important properties of \hat{T} .

16.2 Properties of the Time Reversal Operator

The important properties of the time reversal operator \hat{T} include:

- (a) *Commutation*: $[\hat{T}, \mathcal{H}] = 0$

Because of *energy conservation*, the time reversal operator \hat{T} commutes with the Hamiltonian $\hat{T}\mathcal{H} = \mathcal{H}\hat{T}$. Since \hat{T} commutes with the Hamiltonian, eigenstates of the time reversal operator are also eigenstates of the Hamiltonian.

- (b) *Antilinear*: $\hat{T}i = -i$

From Schrödinger's equation (16.1), it is seen that the reversal of time corresponds to a change of $i \rightarrow -i$, which implies that $\hat{T}i = -i$. We call an operator *antilinear* if its operation on a complex number yields the complex conjugate of the number $\hat{T}a = a^*$ rather than the number itself.

- (c) *Complex conjugation of wave functions*:

Since \hat{T} is an antilinear operator, we have $\hat{T}\psi = \psi^*$. Since $\hat{T}\psi = \psi^*$, the action of \hat{T} on a scalar product is

$$\hat{T}(\psi, \phi) = \int \phi^*(\mathbf{r})\psi(\mathbf{r})d^3r = (\psi, \phi)^*. \quad (16.4)$$

- (d) In the case of no spin, we have $\hat{T} = \hat{K}$ where \hat{K} is the complex conjugation operator. With spin, we show below that $\hat{T} = \hat{K}\sigma_y$ where σ_y is the Pauli spin operator,

$$\sigma_y = \begin{pmatrix} 0 & -i \\ i & 0 \end{pmatrix}.$$

We will see below that both \hat{T} and \hat{K} are antiunitary operators. From Schrödinger's equation (no spin), the effect of \hat{T} on \mathbf{p} is to reverse \mathbf{p} (time goes backward) and \hat{T} leaves $V(\mathbf{r})$ invariant, so that indeed \mathcal{H} is invariant under \hat{T} . When spin is included, however, the Hamiltonian \mathcal{H} must still be invariant under \hat{T} . We note that $\hat{T}\mathbf{p} = -\mathbf{p}$ and $\hat{T}\mathbf{L} = -\mathbf{L}$ (orbital angular momentum). We likewise require that $\hat{T}\mathbf{S} = -\mathbf{S}$ where \mathbf{S} = spin angular momentum. If these requirements are imposed, we show below that the \mathcal{H} is still invariant under \hat{T} , that is \mathcal{H} commutes with \hat{T} when the spin-orbit interaction is included:

$$\mathcal{H} = \frac{p^2}{2m} + V(\mathbf{r}) + \frac{\hbar}{4m^2c^2} \boldsymbol{\sigma} \cdot (\boldsymbol{\nabla}V \times \mathbf{p}) . \quad (16.5)$$

To show that \hat{T} commutes with \mathcal{H} when the spin-orbit interaction is included, we first note that $\hat{K}[\sigma_x, \sigma_y, \sigma_z] = [\sigma_x, -\sigma_y, \sigma_z]$ when the spin components are written in terms of the Pauli matrices

$$\begin{aligned} \sigma_x &= \begin{pmatrix} 0 & 1 \\ 1 & 0 \end{pmatrix}, \\ \sigma_y &= \begin{pmatrix} 0 & -i \\ i & 0 \end{pmatrix}, \\ \sigma_z &= \begin{pmatrix} 1 & 0 \\ 0 & -1 \end{pmatrix}, \end{aligned} \quad (16.6)$$

since only the Pauli matrix σ_y contains i . Thus \hat{K} by itself is not sufficient to describe the time reversal operation on the Hamiltonian \mathcal{H} (16.5) when the spin-orbit interaction is included. We will however see below that the product $\hat{K}\sigma_y$ can describe the time reversal of \mathcal{H} .

Let us now consider the effect of $\hat{K}\sigma_y$ on the spin matrices $\hat{K}\sigma_y[\sigma_x, \sigma_y, \sigma_z]$. We note that

$$\begin{aligned} \sigma_y\sigma_x &= -\sigma_x\sigma_y \quad \text{so that} \quad \hat{K}\sigma_y\sigma_x = -\hat{K}\sigma_x\sigma_y = -\sigma_x\hat{K}\sigma_y \\ \sigma_y\sigma_z &= -\sigma_z\sigma_y \quad \text{so that} \quad \hat{K}\sigma_y\sigma_z = -\hat{K}\sigma_z\sigma_y = -\sigma_z\hat{K}\sigma_y . \end{aligned}$$

Also we have $\hat{K}\sigma_y\sigma_y = -\sigma_y\hat{K}\sigma_y$ since, from above $\hat{K}\sigma_y = -\sigma_y\hat{K}$. Thus we obtain

$$\hat{K}\sigma_y\boldsymbol{\sigma} = -\boldsymbol{\sigma}\hat{K}\sigma_y ,$$

so that the operator $\hat{K}\sigma_y$ transforms $\boldsymbol{\sigma}$ (or \mathbf{S}) into $-\boldsymbol{\sigma}$ (or $-\mathbf{S}$). Clearly σ_y does not act on any of the other terms in the Hamiltonian.

Since $\hat{K}\hat{K} = \hat{K}^2 = \hat{1}$, where $\hat{1}$ is the unit matrix, we can write the important relation $\hat{T} = \hat{K}\sigma_y$ which implies $\hat{K}\hat{T} = \sigma_y = \text{unitary operator}$ since $\sigma_y^\dagger\sigma_y^{-1} = \hat{1}$. But also $\sigma_y^2 = \sigma_y\sigma_y = \hat{1}$ so we have $\sigma_y^\dagger = \sigma_y$ and $\sigma_y^{\dagger 2} = \hat{1}$, where the symbol \dagger is used to denote the adjoint of an operator.

- (e) In the case of no spin $\hat{T}^2 = \hat{1}$, since $\hat{K}^2 = \hat{1}$ and $\hat{T} = \hat{K}$. With spin we will now show that $\hat{T}^2 = -\hat{1}$. Since $\hat{T} = \hat{K}\sigma_y$ when the effect of the electron spin is included, then

$$\hat{T}^2 = (\hat{K}\sigma_y)(\hat{K}\sigma_y) = -(\sigma_y\hat{K})(\hat{K}\sigma_y) = -\sigma_y\hat{K}^2\sigma_y = -\sigma_y\sigma_y = -\hat{1} .$$

More generally if we write $\hat{K}\hat{T} = \hat{U} = \text{unitary operator}$ (not necessarily σ_y), we can then show that $\hat{T}^2 = \pm\hat{1}$. Since two consecutive operations by \hat{T} on a state ψ must produce the same physical state ψ , we have $\hat{T}^2 = C\hat{1}$

where C is a phase factor $e^{i\phi}$ of unit magnitude. Since $\hat{K}^2 = \hat{1}$, we can write

$$\hat{K}^2 \hat{T} = \hat{T} = \hat{K}\hat{U} = \hat{U}^* \hat{K}, \quad (16.7)$$

$$\hat{T}^2 = \hat{K}\hat{U}\hat{K}\hat{U} = \hat{U}^* \hat{K}^2 \hat{U} = \hat{U}^* \hat{U} = C\hat{1}. \quad (16.8)$$

We show below that $C = \pm\hat{1}$. Making use of the unitary property $\hat{U}^\dagger \hat{U} = \hat{U}\hat{U}^\dagger = \hat{1}$, we obtain by writing $\hat{U}^* = \hat{U}^* \hat{U}\hat{U}^\dagger = C\hat{U}^\dagger$,

$$\hat{U}^* = C\hat{U}^\dagger = C\tilde{\hat{U}}, \quad (16.9)$$

where $\tilde{\hat{U}}$ denotes the transpose of \hat{U} . Taking the transpose of both sides of (16.9) yields

$$\tilde{\hat{U}}^* = \hat{U}^\dagger = C\hat{U}^* = C(C\tilde{\hat{U}}^*) = C^2\hat{U}^\dagger \quad \text{or} \quad C^2 = 1 \quad \text{and} \quad C = \pm 1. \quad (16.10)$$

We thus obtain either $\hat{T}^2 = +\hat{1}$ or $\hat{T}^2 = -\hat{1}$.

- (f) Operators $H, \mathbf{r}, V(\mathbf{r})$ are even under time reversal \hat{T} ; operators $\mathbf{p}, \mathbf{L}, \boldsymbol{\sigma}$ are odd under \hat{T} . Operators are either even or odd under time reversal. We can think of spin angular momentum classically as due to a current loop in a plane \perp to the z -axis. Time reversal causes the current to flow in the opposite direction.

- (g) \hat{T} and \hat{K} are antiunitary operators, as shown below.

In this subsection we show that \hat{T} and \hat{K} are antiunitary operators which means $\hat{T}\hat{T}^\dagger = -\hat{1}$ and $\hat{K}\hat{K}^\dagger = -\hat{1}$. We show below that \hat{T} and \hat{K} are antiunitary whether or not the spin is considered explicitly. The properties of the inverse of \hat{T} and \hat{K} are readily found. Since $\hat{K}^2 = \hat{1}$, then $\hat{K}\hat{K} = \hat{1}$ and $\hat{K}^{-1} = \hat{K}$. If for the case where the spin is treated explicitly $\hat{T}^2 = -\hat{1}$, then $\hat{T}\hat{T} = -\hat{1}$ and $\hat{T}^{-1} = -\hat{T}$; $\hat{T} = \hat{K}\sigma_y$ for the case of spin. For the spinless case, $\hat{T}^2 = \hat{1}$ and $\hat{T}^{-1} = \hat{T}$. Since complex conjugation changes $i \rightarrow -i$, we can write $\hat{K}^\dagger = -\hat{K}$ so that \hat{K} is antiunitary.

We now use this result to show that both \hat{T} and \hat{K} are *antiunitary*. This is the most important property of \hat{T} from the point of view of group theory. Since $\hat{K} = \hat{T}$ in the absence of spin, and since \hat{K} is antiunitary, it follows that \hat{T} is antiunitary in this case. However, when spin is included, $\hat{T} = \hat{K}\sigma_y$ and

$$\begin{aligned} \sigma_y &= \hat{K}\hat{T} \\ \sigma_y^\dagger &= \hat{T}^\dagger \hat{K}^\dagger. \end{aligned} \quad (16.11)$$

Since σ_y is a unitary operator, thus $\hat{T}^\dagger \hat{K}^\dagger \hat{K}\hat{T} = \hat{1}$ but since $\hat{K}^\dagger \hat{K} = -\hat{1}$ it follows that $\hat{T}^\dagger \hat{T} = -\hat{1}$, showing that \hat{T} is also *antiunitary*.

Furthermore \hat{K} and \hat{T} behave differently from all the operators that we have thus far encountered in group theory, such as the point group operations (rotations, improper rotations, mirror planes, inversion and \mathcal{R} = rotation of

2π must be considered for spin dependent Hamiltonians). Thus in considering symmetry operations in group theory, we treat all the unitary operators separately by use of character tables and all the associated apparatus, and then we treat *time reversal symmetry* as an *additional symmetry constraint*. We will see in Sect. 16.5 how time reversal symmetry enters directly as a symmetry element for magnetic point groups.

We discuss first in Sects. 16.3 and 16.4 the general effect of \hat{T} on the form of $E(\mathbf{k})$ for the case of electronic bands neglecting spin (Sect. 16.3) and including spin (Sect. 16.4). In these sections we also consider the question of degeneracies imposed on energy levels by time reversal symmetry (the Herring Rules) [39].

16.3 The Effect of \hat{T} on $E(\mathbf{k})$, Neglecting Spin

If for the moment we neglect spin, then the time reversal operation acting on a solution of Schrödinger's equation yields

$$\hat{T}\psi(\mathbf{r}) = \psi^*(\mathbf{r}). \quad (16.12)$$

Since the Hamiltonian commutes with \hat{T} , then both $\psi(\mathbf{r})$ and $\psi^*(\mathbf{r})$ satisfy Schrödinger's equation for the same energy eigenvalue, so that a twofold degeneracy occurs. We will now show that time reversal symmetry leads to two symmetry properties for the energy eigenvalues for Bloch states: the evenness of the energy eigenvalues $E(\mathbf{k}) = E(-\mathbf{k})$, and the zero slope of $E_n(\mathbf{k})$ at the Brillouin zone boundaries.

The effect of the translation operation on a Bloch state is

$$\psi_k(\mathbf{r} + \mathbf{R}_n) = e^{i\mathbf{k}\cdot\mathbf{R}_n} \psi_k(\mathbf{r}), \quad (16.13)$$

and the effect of time reversal is

$$\hat{T}\psi_k(\mathbf{r}) = \psi_k^*(\mathbf{r}). \quad (16.14)$$

We can write the following relation for the complex conjugate of Bloch's theorem

$$\psi_k^*(\mathbf{r} + \mathbf{R}_n) = e^{-i\mathbf{k}\cdot\mathbf{R}_n} \psi_k^*(\mathbf{r}), \quad (16.15)$$

and we can also rewrite (16.15) in terms of $\mathbf{k} \rightarrow -\mathbf{k}$ as

$$\psi_{-k}^*(\mathbf{r} + \mathbf{R}_n) = e^{i\mathbf{k}\cdot\mathbf{R}_n} \psi_{-k}^*(\mathbf{r}), \quad (16.16)$$

which upon comparing (16.13), (16.15) and (16.16) implies that for nondegenerate levels the time reversal operator transforms $\mathbf{k} \rightarrow -\mathbf{k}$

$$\hat{T}\psi_k(\mathbf{r}) = \psi_{-k}(\mathbf{r}) = \psi_k^*(\mathbf{r}). \quad (16.17)$$

If the level is doubly degenerate and $\psi_k(\mathbf{r})$ and $\phi_k(\mathbf{r})$ are the corresponding eigenstates, then if $\hat{T}\psi_k(\mathbf{r}) = \phi_k(\mathbf{r}) = \psi_{-k}(\mathbf{r})$, and no additional degeneracy

is required by time reversal symmetry. Time reversal symmetry thus implies that for a spinless system

$$E_n(\mathbf{k}) = E_n(-\mathbf{k}), \quad (16.18)$$

and the energy is an even function of wave vector \mathbf{k} whether or not there is spatial inversion symmetry.

Using this result (16.18) and the $E(\mathbf{k}) = E(\mathbf{k} + \mathbf{K})$ periodicity in \mathbf{k} space, where \mathbf{K} is a reciprocal lattice vector, we obtain

$$E\left(\frac{\mathbf{K}}{2} - \delta\mathbf{k}\right) = E\left(-\frac{\mathbf{K}}{2} + \delta\mathbf{k}\right) = E\left(\frac{\mathbf{K}}{2} + \delta\mathbf{k}\right), \quad (16.19)$$

where $\delta\mathbf{k}$ is an infinitesimal distance to the Brillouin zone boundary. Thus referring to Fig. 16.1, $E(\mathbf{k})$ comes into the zone boundary with *zero slope* for both the lower and upper branches of the solutions in Fig. 16.1. For the case where the energy band shows a degeneracy at the zone boundary, the upper and lower bands will have *equal and opposite slopes*.

We have been using the symmetry properties in (16.18) and (16.19) throughout our solid state physics courses. In the most familiar cases, $E(\mathbf{k})$ depends on k^2 . Figure 16.1 illustrates the symmetry properties of (16.18) and (16.19) for a simple parabolic band at $\mathbf{k} = 0$ and at the Brillouin zone boundary.

Let us now consider the consequences of these ideas from a group theoretical point of view, and enumerate Herring's rules which summarize the effect of time reversal \hat{T} on the irreducible representations of a group. If $\psi(\mathbf{r})$ belongs to the irreducible representation D , then $\hat{T}\psi(\mathbf{r}) = \psi^*(\mathbf{r})$ will transform according to D^* which consists of the complex conjugate of all the matrices in D . We can distinguish three different possibilities in the case of *no spin*:

- (a) All of the matrices in the representation D are real matrices or can be made into real matrices by a unitary transformation. In this case, the time reversal operator leaves the representation D invariant and no additional degeneracies in $E(\mathbf{k})$ result.
- (b) If the representations D and D^* cannot be brought into equivalence by a unitary transformation, there is a doubling of the degeneracy of such levels due to time reversal symmetry. Then the representations D and D^* are said to form a *time reversal symmetry pair* and these levels will stick together.
- (c) If the representations D and D^* can be made equivalent under a suitable unitary transformation, but the matrices in this representation cannot be made real, then the time reversal symmetry also requires a doubling of the degeneracy of D and the bands will stick together.

To illustrate these possibilities, consider the point group C_4 (see Table 16.1). Here irreducible representations A and B are of type (a) above and each of

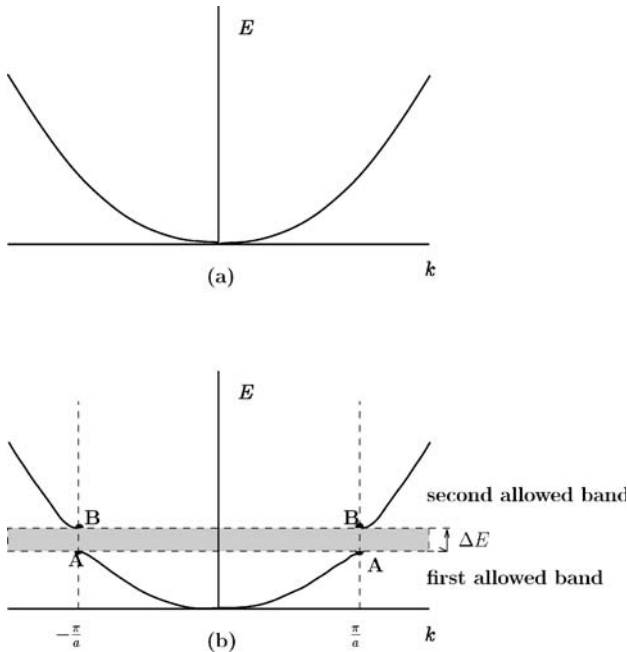


Fig. 16.1. Simple $E(\mathbf{k})$ diagram for a spinless electron illustrating both $E(\mathbf{k}) = E(-\mathbf{k})$ and the zero slope of $E(\mathbf{k})$ at the Brillouin zone boundary

Table 16.1. Character table for point group C_4

| C_4 (4) | | E | C_2 | C_4 | C_4^3 | time reversal |
|------------------|----------------------------|-----|-------|-------|---------|---------------|
| $x^2 + y^2, z^2$ | R_z, z | A | 1 | 1 | 1 | (a) |
| $x^2 - y^2, xy$ | | B | 1 | 1 | -1 | (a) |
| (xz, yz) | (x, y) $\{R_x, R_y\}$ | E | 1 | -1 | i | (b) |
| | | | 1 | -1 | $-i$ | (b) |

these representations correspond to nondegenerate energy levels. However, the two representations labeled E are complex conjugates of each other and are of type (b) since there is no unitary transformation that can bring them into equivalence. Thus because of the time reversal symmetry requirement, representation E corresponds to a doubly degenerate level. This illustrates the case where time reversal symmetry gives rise to an additional level degeneracy.

The time reversal partners are treated as different representations when applying the following rules on character:

- The number of irreducible representations is equal to the number of classes.
- $\sum_i \ell_i^2 = h$.

Using the character table for the group of the wave vector, we can distinguish which of the three cases apply for a given irreducible representation using the Herring test [39], which is now discussed. Let Q_0 be an element in the space group which transforms \mathbf{k} into $-\mathbf{k}$. Then Q_0^2 is an element in the group of the wave vector \mathbf{k} , since all elements in the group of the wave vector leave \mathbf{k} invariant and therefore each of these group elements are elements with the properties of Q_0^2 . If the inversion operator i is contained in the group of the wave vector \mathbf{k} , then all the elements Q_0 are in the group of the wave vector \mathbf{k} . If i is not an element of the group of the wave vector \mathbf{k} , then the elements Q_0 may or may not be an element in the group of the wave vector. Let h_{Q_0} equal the number of elements Q_0 . The Herring space group test is then

$$\begin{aligned}\sum_R \chi(Q_0^2) &= h_{Q_0} \quad \text{case (a)} \\ &= 0 \quad \text{case (b)} \\ &= -h_{Q_0} \quad \text{case (c)},\end{aligned}$$

where χ is the character for a representation of the group of the wave vector \mathbf{k} and the sum is over all the elements of the group. These tests can be used to decide whether or not time reversal symmetry introduces any additional degeneracies to this representation. Information on the Herring test is normally presented in each of the 32 point groups in the character tables in Koster's book [47, 48].

To apply the Herring test to the point group C_4 , and consider the group of the wave vector for $\mathbf{k} = 0$. Then all four symmetry operations take $\mathbf{k} \rightarrow -\mathbf{k}$ since $\mathbf{k} = 0$. Furthermore, $E^2 = E$, $C_2^2 = E$, $C_4^2 = C_2$ and $(C_4^3)^2 = C_2$ so that for representations A and B

$$\sum_R \chi(Q_0^2) = 1 + 1 + 1 + 1 = 4 \quad (16.20)$$

from which we conclude that A and B correspond to case (a), in agreement with Koster's tables. On the other hand, for each representation under E ,

$$\sum_R \chi(Q_0^2) = 1 + 1 + (-1) + (-1) = 0 \quad (16.21)$$

from which we conclude that representations E correspond to case (b). Therefore the two irreducible representations under E correspond to the same energy and the corresponding $E(\mathbf{k})$ will stick together. The two representations under E are called *time reversal conjugate representations*.

16.4 The Effect of \hat{T} on $E(\mathbf{k})$, Including the Spin–Orbit Interaction

When the *spin–orbit interaction is included*, then the Bloch functions transform as irreducible representations of the double group. The degeneracy of the energy levels is different from the spinless situation, and in particular every level is at least doubly degenerate.

When the spin–orbit interaction is included, $\hat{T} = \hat{K}\sigma_y$ and not only do we have $\mathbf{k} \rightarrow -\mathbf{k}$, but we also have $\boldsymbol{\sigma} \rightarrow -\boldsymbol{\sigma}$ under time reversal symmetry. This is written schematically as

$$\hat{T}\psi_{n,k\uparrow}(\mathbf{r}) = \psi_{n,-k\downarrow}(\mathbf{r}), \quad (16.22)$$

so that the time reversal conjugate states are

$$E_{n\uparrow}(\mathbf{k}) = E_{n\downarrow}(-\mathbf{k}) \quad (16.23)$$

and

$$E_{n\downarrow}(\mathbf{k}) = E_{n\uparrow}(-\mathbf{k}). \quad (16.24)$$

If inversion symmetry exists as well,

$$E_n(\mathbf{k}) = E_n(-\mathbf{k}), \quad (16.25)$$

then

$$E_{n\uparrow}(\mathbf{k}) = E_{n\uparrow}(-\mathbf{k}) \quad \text{and} \quad E_{n\downarrow}(\mathbf{k}) = E_{n\downarrow}(-\mathbf{k}) \quad (16.26)$$

making $E_{n\uparrow}(\mathbf{k})$ and $E_{n\downarrow}(\mathbf{k})$ degenerate. In more detail, since $\hat{T} = \hat{K}\sigma_y$ and since

$$\begin{aligned} \sigma_y \uparrow &= \begin{pmatrix} 0 & -i \\ i & 0 \end{pmatrix} \begin{pmatrix} 1 \\ 0 \end{pmatrix} = i \begin{pmatrix} 0 \\ 1 \end{pmatrix} = i \downarrow \\ \sigma_y \downarrow &= \begin{pmatrix} 0 & -i \\ i & 0 \end{pmatrix} \begin{pmatrix} 0 \\ 1 \end{pmatrix} = -i \begin{pmatrix} 1 \\ 0 \end{pmatrix} = -i \uparrow, \end{aligned}$$

we obtain

$$\begin{aligned} \hat{T}\psi_{n,k\uparrow}(\mathbf{r}) &= \hat{T}e^{i\mathbf{k}\cdot\mathbf{r}} \left[u_{n,k\uparrow} \begin{pmatrix} 1 \\ 0 \end{pmatrix} \right] = e^{-i\mathbf{k}\cdot\mathbf{r}} \left[iu_{n,k\uparrow}^* \begin{pmatrix} 0 \\ 1 \end{pmatrix} \right] \\ &= e^{-i\mathbf{k}\cdot\mathbf{r}} u_{n,-k\downarrow} \begin{pmatrix} 0 \\ 1 \end{pmatrix}, \end{aligned} \quad (16.27)$$

which is a Bloch state for wave vector $-\mathbf{k}$ and spin \downarrow . Likewise

$$\begin{aligned} \hat{T}\psi_{n,k\downarrow}(\mathbf{r}) &= \hat{T}e^{i\mathbf{k}\cdot\mathbf{r}} \left[u_{n,k\downarrow} \begin{pmatrix} 0 \\ 1 \end{pmatrix} \right] = e^{-i\mathbf{k}\cdot\mathbf{r}} \left[-iu_{n,k\downarrow}^* \begin{pmatrix} 1 \\ 0 \end{pmatrix} \right] \\ &= e^{-i\mathbf{k}\cdot\mathbf{r}} u_{n,-k\uparrow} \begin{pmatrix} 1 \\ 0 \end{pmatrix} \end{aligned} \quad (16.28)$$

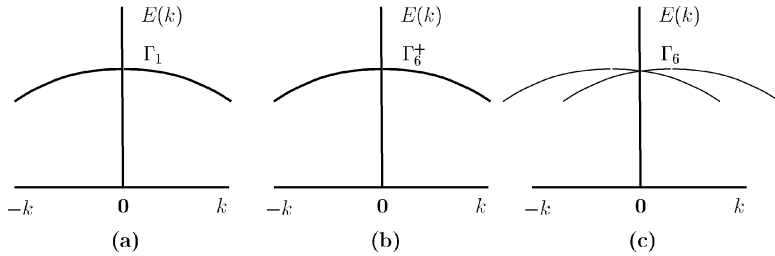


Fig. 16.2. Schematic example of Kramers degeneracy in a crystal in the case of: (a) no spin-orbit interaction where each level is doubly degenerate (\uparrow, \downarrow), (b) both spin-orbit interaction and inversion symmetry are present and the levels are doubly degenerate, (c) spin-orbit interaction and no spatial inversion symmetry where the relations (16.23) and (16.24) apply

which is a Bloch state for wave vector $-\mathbf{k}$ and spin \uparrow in which we have written

$$iu_{n,k\uparrow}^* = u_{n,-k\downarrow}$$

and

$$-iu_{n,k\downarrow}^* = u_{n,-k\uparrow}.$$

For a general point in the Brillouin zone, and in the absence of spin-orbit coupling, but including the spin on the electron, the energy levels have a *necessary twofold spin degeneracy* and also exhibit the property $E(\mathbf{k}) = E(-\mathbf{k})$, whether or not there is inversion symmetry. This is illustrated in Fig. 16.2(a). When the spin-orbit interaction is turned on and there is inversion symmetry, then we get the situation illustrated in Fig. 16.2(b), where the twofold degeneracy remains.

However, if there is no inversion symmetry, then the only relationships that remain are those of (16.23) and (16.24) shown in Fig. 16.2(c), and the Kramers degeneracy results in $E_\uparrow(\mathbf{k}) = E_\downarrow(-\mathbf{k})$ and $E_\downarrow(\mathbf{k}) = E_\uparrow(-\mathbf{k})$.

The role of inversion symmetry is also important for the $E(\mathbf{k})$ relations for degenerate bands. This is illustrated in Fig. 16.3 for degenerate bands near $\mathbf{k} = 0$. We take as examples: (a) diamond for which the spin-orbit interaction can be neglected and all levels are doubly degenerate at a general point in the Brillouin zone, (c) InSb or GaAs which have T_d symmetry (lacking inversion) so that relations (16.23) and (16.24) apply and the twofold Kramers degeneracy is lifted by the Dresselhaus-spin-orbit term [25], (b) Ge or Si which have O_h symmetry (including inversion) and the twofold Kramers degeneracy is retained at a general point in the Brillouin zone.

We give in Table 16.2 the general Herring rules (see Sect. 16.3) which apply whether or not the spin-orbit interaction is included. When the spin-orbit interaction is included, there are also three cases which can be distinguished. When the time reversal operator \hat{T} acts on a spin dependent wavefunction ψ

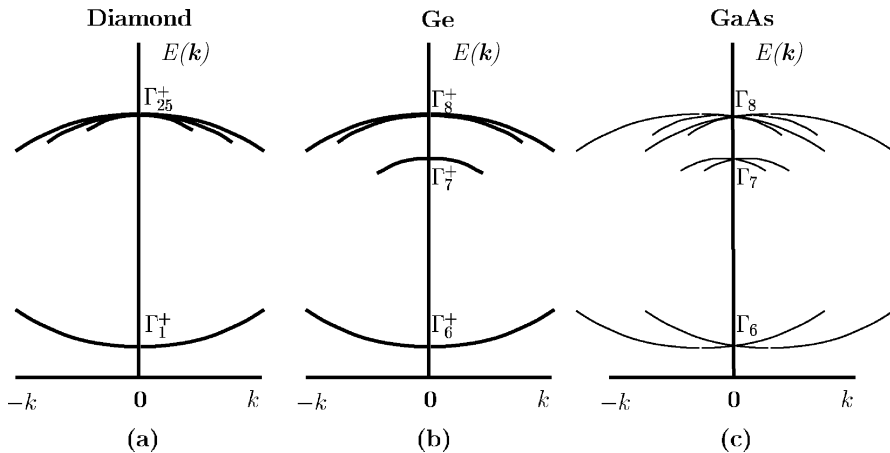


Fig. 16.3. Schematic examples of energy bands $E(\mathbf{k})$ near $\mathbf{k} = 0$: (a) in diamond without spin-orbit interaction, each band having a twofold spin degeneracy. (b) in Ge where the spin-orbit interaction split bands, with each band remaining at least doubly degenerate. (c) in GaAs where the Γ_8 bands are split by the spin-orbit interaction and the degeneracy occurs only at $\mathbf{k} = 0$. At a general \mathbf{k} point the levels do not stick together. The magnitudes of the splittings are not to scale

Table 16.2. Summary of Herring rules regarding degeneracies and time reversal

| case | relation between D and D^* | Frobenius–Schur test | spinless electron | half-integral spin electron |
|------|---|---------------------------|---------------------|-----------------------------|
| (a) | D and D^* are equivalent to the same real irreducible representation | $\sum_R \chi(Q_0^2) = h$ | no extra degeneracy | doubled degeneracy |
| (b) | D and D^* are inequivalent | $\sum_R \chi(Q_0^2) = 0$ | doubled degeneracy | doubled degeneracy |
| (c) | D and D^* are equivalent to each other but not to a real representation | $\sum_R \chi(Q_0^2) = -h$ | double degeneracy | no extra degeneracy |

which transforms according to an irreducible representation D , then we have three possibilities:

- If the representation D is real, or can be transformed by a unitary transformation into a set of real matrices, then the action of \hat{T} on these matrices will yield the same set of matrices. To achieve the required additional degeneracy, we must have D occur twice.
- If representations D and D^* cannot be brought into equivalence by a unitary transformation, then the corresponding levels must stick together in pairs to satisfy the time reversal degeneracy requirement.

Table 16.3. Character table for the double group C_4 ^a

| C_4 | E | \bar{E} | C_4 | \bar{C}_4 | C_2 | \bar{C}_2 | C_4^{-1} | \bar{C}_4^{-1} | time inv. | basis for group C_4 |
|------------|-----|-----------|-------------|-------------|-------|-------------|-------------|------------------|--------------|------------------------------------|
| Γ_1 | 1 | 1 | 1 | 1 | 1 | 1 | 1 | 1 | a | z or S_z |
| Γ_2 | 1 | 1 | -1 | -1 | 1 | 1 | -1 | -1 | a | xy |
| Γ_3 | 1 | 1 | i | i | -1 | -1 | $-i$ | $-i$ | b | $-i(x + iy)$ or $-(S_x + iS_y)$ |
| Γ_4 | 1 | 1 | $-i$ | $-i$ | -1 | -1 | i | i | b | $i(x - iy)$ or $(S_x - iS_y)$ |
| Γ_5 | 1 | -1 | ω | $-\omega$ | i | $-i$ | $-\omega^3$ | ω^3 | b | $\phi(1/2, 1/2)$ |
| Γ_6 | 1 | -1 | $-\omega^3$ | ω^3 | $-i$ | i | ω | $-\omega$ | b | $\phi(1/2, -1/2)$ |
| Γ_7 | 1 | -1 | $-\omega$ | ω | i | $-i$ | ω^3 | $-\omega^3$ | b | $\phi(3/2, -3/2)$ |
| Γ_8 | 1 | -1 | ω^3 | $-\omega^3$ | $-i$ | i | $-\omega$ | ω | b | $\phi(3/2, 3/2)$ |

^a In the table $i = e^{i\pi/2}$ and $\omega = e^{i\pi/4}$, and \bar{E} , \bar{C}_4 , \bar{C}_2 and \bar{C}_4^{-1} denote $\mathcal{R}E$, $\mathcal{R}C_4$, $\mathcal{R}C_2$ and $\mathcal{R}C_4^{-1}$ where \mathcal{R} is rotation by 2π (see Chap. 14)

- (c) If representations D and D^* can be brought into equivalence but neither can be made all real, then no additional degeneracy need be introduced and both make up the time reversal degenerate pair.

These results are summarized in Table 16.2 for both the case of no spin and when spin-orbit interaction is included. We now illustrate these rules with two cases:

- (i) The double group representations of point group C_4 (symmorphic);
- (ii) The double group representation at the L point in Ge (or Si) where the levels are degenerate by time reversal symmetry (nonsymmorphic).

For the first illustration, we give in Table 16.3 the character table for the double group C_4 discussed in the literature [47, 48]. We note that the double group tables contain an entry for time inversion, which summarizes the results discussed in Sect. 16.1 for the spinless bands. Inspection of this character table shows that the double group representations involve the 4th roots of unity (as shown below) and obey the relation $\chi(A_i) = -\chi(\bar{A}_i)$ for each of the pairs of symmetry operations A_i and \bar{A}_i where $\bar{A}_i = \mathcal{R}A_i$. Note that the character table originally given in Koster has some misprints with regard to $\chi(C_4^{-1}) = -\chi(\bar{C}_4^{-1})$, which are corrected in Table 16.3. Table 16.4 clearly shows that the characters for the Γ_5 and Γ_6 irreducible representations are time reversal degenerate pairs, and likewise for the Γ_7 and Γ_8 irreducible representations.

For the double group representations, we consider the character $\chi(Q_0\bar{Q}_0)$ in applying the Herring rules which is also known in the literature as the Frobenius-Schur test. Application of the Frobenius-Schur test for Γ_5 gives

Table 16.4. Characters for Γ_5 , Γ_6 , Γ_7 and Γ_8 irreducible representations in terms of $\omega = e^{i\pi/4}$

| | E | \bar{E} | C_4 | \bar{C}_4 | C_2 | \bar{C}_2 | C_4^{-1} | \bar{C}_4^{-1} |
|--------------|------------|------------|------------|-------------|------------|-------------|------------|------------------|
| Γ_5 : | ω^0 | ω^4 | ω | ω^5 | ω^2 | ω^6 | ω^7 | ω^3 |
| Γ_6 : | ω^0 | ω^4 | ω^7 | ω^3 | ω^6 | ω^2 | ω | ω^5 |
| Γ_7 : | ω^0 | ω^4 | ω^5 | ω | ω^2 | ω^6 | ω^3 | ω^7 |
| Γ_8 : | ω^0 | ω^4 | ω^3 | ω^7 | ω^6 | ω^2 | ω^5 | ω |

$$\begin{aligned} \sum \chi(Q_0 \bar{Q}_0) &= (1)(-1) + (1)(-1) - \omega^2 - \omega^2 + 1 + 1 - \omega^6 - \omega^6 \\ &= -1 - 1 - i - i + 1 + 1 + i + i = 0, \end{aligned} \quad (16.29)$$

and shows that Γ_5 is type “b” under time reversal symmetry. By doing a similar Frobenius–Schur test for the other double group irreducible representations of double group C_4 we find that the representations Γ_6 , Γ_7 and Γ_8 are also of the *b* type with respect to time reversal symmetry and this information is also given in Table 16.3.

For the second illustration involving the L -point levels in Ge, see the $E(\mathbf{k})$ diagram in Fig. 14.1(b) for the case where the spin–orbit interaction is included. The character table appropriate to the L -point (group D_{3d}) is given in Table 16.5. The character table for the group of the wave vector for the L point for the diamond structure is given in Table C.18 in the absence of spin. Since the translation $\tau_d = (a/4)(1, 1, 1)$ does not enter into any of the symmetry operations, the classes can be simply represented as in Table 16.5.

The designations for the L -point representations have been added on the left column of Koster’s table which is given in general in Table 16.5 for a double group for D_{3d} symmetry. This example shows the importance of checking the notation used in the literature for dispersion relations (Fig. 14.1(b)) and the notation used in general tables for double groups (Table 16.5) to verify that they are internally consistent.

For a A point (group D_3), the operations E , $2C_3$ and $3C'_2$ take $\mathbf{k} \rightarrow -\mathbf{k}$ so each symmetry operation corresponds to an operator of the Q_0 type. For the L -point (group D_{3d}) also, all operations are of the Q_0 type, so that for the representations L_1 , L_2 and L_3 , we have $\Sigma \chi(Q_0 \bar{Q}_0) = 12$, yielding representations of type *a*, in agreement with the character table for D_{3d} (Table 16.5). For the double group representation L_6^+ we obtain

$$L_6^+ = \Sigma \chi(Q_0 \bar{Q}_0) = -4 - 2 + 0 - 4 - 2 + 0 = -12 \quad \text{type (c)}, \quad (16.30)$$

where again we write $Q_0 \bar{Q}_0$ or $Q_0 \mathcal{R} Q_0$ for Q_0^2 . For the double group representation L_4^+ , the Frobenius–Schur test yields

$$L_4^+ : \Sigma \chi(Q_0 \bar{Q}_0) = -1 - 2 + 3 - 1 - 2 + 3 = 0 \quad \text{type (b)}. \quad (16.31)$$

Table 16.5. Character table and basis functions for the double group D_{3d} [48]

| D_{3d} | E | \bar{E} | $2C_3$ | $2\bar{C}_2$ | $3C'_2$ | $3\bar{C}'_2$ | I | \bar{I} | $2S_6$ | $2\bar{S}_6$ | $3\sigma_d$ | $3\bar{\sigma}_d$ | time inv. | bases | |
|----------|--------------|-----------|--------|--------------|---------|---------------|------|-----------|--------|--------------|-------------|-------------------|-----------|-------|---|
| L_1^+ | Γ_1^+ | 1 | 1 | 1 | 1 | 1 | 1 | 1 | 1 | 1 | 1 | 1 | 1 | a | R |
| L_2^+ | Γ_2^+ | 1 | 1 | 1 | 1 | -1 | -1 | 1 | 1 | 1 | 1 | -1 | -1 | a | S_x |
| L_3^+ | Γ_3^+ | 2 | 2 | -1 | -1 | 0 | 0 | 2 | 2 | -1 | -1 | 0 | 0 | a | $(S_x - iS_y),$ $-(S_x + iS_y)$ |
| L_1^- | Γ_1^- | 1 | 1 | 1 | 1 | 1 | -1 | -1 | -1 | -1 | -1 | -1 | -1 | a | zS_z |
| L_2^- | Γ_2^- | 1 | 1 | 1 | 1 | -1 | -1 | -1 | -1 | -1 | -1 | 1 | 1 | a | z |
| L_3^- | Γ_3^- | 2 | 2 | -1 | -1 | 0 | 0 | -2 | -2 | 1 | 1 | 0 | 0 | a | $(x - iy),$ $-(x + iy)$ |
| L_6^+ | Γ_4^+ | 2 | -2 | 1 | -1 | 0 | 0 | 2 | -2 | 1 | -1 | 0 | 0 | c | $\phi(1/2, -1/2)$ |
| L_4^+ | Γ_5^+ | 1 | -1 | -1 | 1 | i | $-i$ | 1 | -1 | -1 | 1 | i | $-i$ | b | $\phi(3/2, -3/2)$ $-i\phi(3/2, 3/2)$ |
| L_5^+ | Γ_6^+ | 1 | -1 | -1 | 1 | $-i$ | i | 1 | -1 | -1 | 1 | $-i$ | i | b | $-(\phi(3/2, 3/2))$ $-i\phi(3/2, -3/2))$ |
| L_6^- | Γ_4^- | 2 | -2 | 1 | -1 | 0 | 0 | -2 | 2 | -1 | 1 | 0 | 0 | c | $\Gamma_4^+ \times \Gamma_1^-$ |
| L_4^- | Γ_5^- | 1 | -1 | -1 | 1 | i | $-i$ | -1 | 1 | 1 | -1 | $-i$ | i | b | $\Gamma_5^+ \times \Gamma_1^-$ |
| L_5^- | Γ_6^- | 1 | -1 | -1 | 1 | $-i$ | i | -1 | 1 | 1 | -1 | i | $-i$ | b | $\Gamma_6^+ \times \Gamma_1^-$ |

Likewise L_5^+ is of type b . Since L_4^+ and L_5^+ are complex conjugate representations, L_4^+ and L_5^+ form time reversal degenerate pairs. Similarly, L_4^- and L_5^- are type b representations and form time reversal degenerate pairs (see Figs. 14.1(b) and 16.2(b)). For both L_4^+ and L_5^+ (and likewise for L_4^- and L_5^-) which are type (b) under time reversal symmetry, the dispersion shown in Fig. 16.2(b) applies. To obtain the regime shown in Fig. 16.2(c), the crystal should have no spatial inversion symmetry, which is pertinent to the zinc blende structure. Finally in Table 16.5 we see basis function entries of the form $\phi(1/2, -1/2)$ which denote spherical harmonics for which the two entries $1/2$ and $-1/2$, respectively, denote $j = 1/2$ and $m_j = -1/2$.

With this discussion of time reversal symmetry, we have explained all the entries to the character tables, and have explained why because of time reversal symmetry certain bands stick together on the $E(\mathbf{k})$ diagrams, such as in Fig. 14.1(b).

16.5 Magnetic Groups

If atoms at each lattice site can be represented as a charge distribution $\rho(\mathbf{r})$ with no particular spin symmetry (paramagnetic or diamagnetic), the ordi-

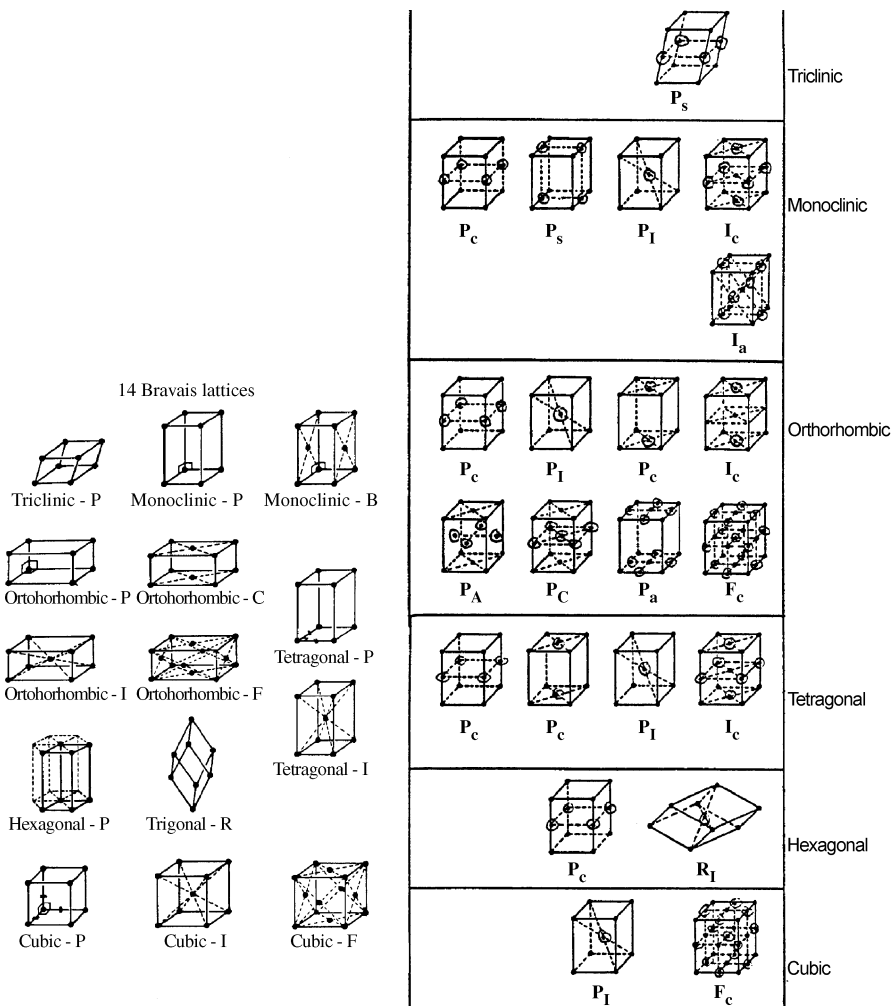


Fig. 16.4. (a) The 14 ordinary Bravais lattices on the *left* and (b) the 22 additional magnetic Bravais lattices on the *right*. The *open circles* represent the time reversed sites

nary space groups are used. If, however, we have ordered arrangements of spins, then the time reversal operator (which reverses the spin direction) can be combined with other group elements to form elements of a new type of symmetry group. Groups in which the time reversal operator forms group elements are called *magnetic space groups* and the corresponding point groups are called *magnetic point groups*. In this section we present some of the essential properties of magnetic space groups and give some examples of interest to solid state physics [54, 70].

16.5.1 Introduction

When magnetically ordered phases are taken into account, the magnetic unit cell is often larger than the chemical unit cell, as for example in an antiferromagnetic system. Additional symmetry elements are introduced (see Sect. 16.5.2), and as a result many more point groups and space groups are possible (see Sect. 16.5.3).

There are, in fact, **122** ($58 + 2 \times 32$) magnetic point groups (rather than 32), and **1,651** ($1,191 + 2 \times 230$) magnetic space groups (rather than 230), and 36 ($22 + 14$) magnetic Bravais lattices rather than 14. The magnetic Bravais lattices which are important for describing antiferromagnetic structures are shown in Fig. 16.4(b), and for comparison the 14 ordinary Bravais lattices are also shown in Fig. 16.4(a), and are further explained below. We will confine our brief discussion to magnetic single groups (not double groups) and we shall only discuss magnetic point groups, and showing their connection to time reversal symmetry.

16.5.2 Types of Elements

Magnetic groups have symmetry elements corresponding to unitary operators (denoted by A_i) and antielements $M_k = \hat{T}A_k$ corresponding to antiunitary operators, where \hat{T} is the antiunitary time reversal operator (see Sect. 16.2). We show in Fig. 16.5(a) a one-dimensional lattice in which \hat{T} when combined with a translation is a symmetry operation. However, by displacing the nonmagnetic white atoms relative to the magnetic shaded atoms in Fig. 16.5(b) relative to their positions in Fig. 16.5(a), we see that \hat{T} is no longer a symmetry operation. The lowering of the symmetry of the chain of atoms introduced by the spin on the magnetic ion breaks the time reversal symmetry in Fig. 16.5(b) as the spin-up magnetic species attracts the nonmagnetic ion relative to the interaction with the spin-down magnetic ion. This structural

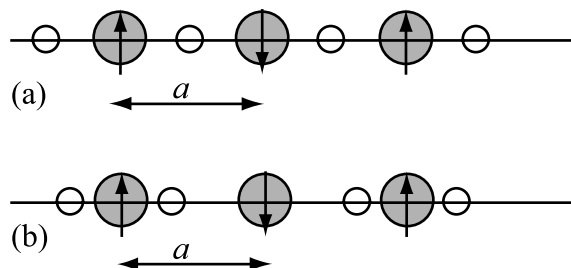


Fig. 16.5. Diagram showing a one-dimensional lattice where the white atoms are nonmagnetic and the shaded atoms are magnetic with the indicated direction of spin angular momentum: (a) the operation \hat{T} is combined with translation as a space group symmetry operation, (b) \hat{T} is not a symmetry operation of the group, even if combined with translations

lattice distortion represents another manifestation of the Jahn–Teller effect (see Sect. 7.7).

The product of two unitary elements A_i or of two antiunitary elements M_k yields a unitary element, while the product of a unitary element A_i with an antiunitary element M_k yields an antiunitary element:

$$\begin{aligned} A_i A_{i'} &= A_{i''} \\ A_i M_k &= M_{k'} \\ M_k A_i &= M_{k''} \\ M_k M_{k'''} &= A_{i'''} . \end{aligned} \quad (16.32)$$

To satisfy these relations, group properties and the rearrangement theorem, there must be *equal numbers* of elements of the type A_i and of the type M_k in a magnetic point group.

16.5.3 Types of Magnetic Point Groups

In classifying the magnetic point groups we must consider three types of point groups:

- (a) 32 ordinary point groups G' where \hat{T} is not an element.
- (b) 32 ordinary point groups $G' \otimes \hat{T}$. In these magnetic point groups, all elements A_i of G' are contained together with all elements $\hat{T}A_i$.
- (c) 58 point groups G in which half of the elements are $\{A_i\}$ and half are $\{M_k\}$ where $M_k = \hat{T}A_k$ and the $\{A_i, A_k\}$ form an ordinary point group G' . Also $\{A_i\}$ is a subgroup of G' . It is important to emphasize that the M_k elements are made from A_k elements that are different from the A_i elements.

Summing the number of types (a), (b), and (c) we obtain $(32 + 32 + 58) = 122$ magnetic point groups. Case (a) can apply to nonmagnetic materials and some ferromagnetic materials. Case (b) can apply to some antiferromagnetic materials. Case (c) can apply to magnetic materials with a variety of spin orderings.

We list in Table 16.6 the 58 magnetic point groups of type (c) and denoted by G ; also included in the table are the 32 ordinary point groups of type (a) which are denoted by G' [70]. The 32 point groups of type (b), obtained from those in type (a) as $G' \otimes \hat{T}$, are not listed. The magnetic groups of type (c) are related to elements of a group G' and a subgroup H_r and are denoted by $G'(H_r)$. The appropriate group G' contains the symmetry elements $\{A_i, A_k\}$ while the subgroup H_r of G' only has elements $\{A_i\}$.

16.5.4 Properties of the 58 Magnetic Point Groups $\{A_i, M_k\}$

We list below some of the properties of the magnetic point groups [type (c)] that contain both unitary and antiunitary symmetry elements, A_i and $M_k =$

Table 16.6. The magnetic point groups of type (a) and type (c)

| crystal system | group G' | number of elements | invariant unitary subgroup H | Shubnikov notation | international notation | magnetic order |
|----------------|---|----------------------------------|---|---|---|---|
| triclinic | C_1 $S_2(C_i)$ | 1 2 | C_1 S_2 C_1 | $\bar{1}$ $\bar{2}$ $\bar{2}$ | $\bar{1}$ $\bar{1}$ $\bar{1}$ | F F AF |
| monoclinic | C_{1h} C_2 C_{2h} | 2 2 4 | C_{1h} C_1 C_2 C_1 C_{2h} C_i C_2 C_{1h} | m \bar{m} $\bar{2}$ $\bar{2}$ $\bar{2}:m$ $\bar{2}:m$ $\bar{2}:\underline{m}$ $\bar{2}:m$ | m \bar{m} $\bar{2}$ $\bar{2}$ $\bar{2}/m$ $\bar{2}/m$ $\bar{2}/\underline{m}$ $\bar{2}/m$ | F F F F F F AF AF |
| rhombic | C_{2v} D_2 D_{2h} | 4 4 8 | C_{2v} C_{1h} C_2 D_2 C_2 D_{2h} C_{2h} C_{2v} D_2 | $2\cdot m$ $\bar{2}\cdot m$ $\bar{2}\cdot m$ $2\cdot\bar{2}$ $2\cdot\bar{2}$ $m\cdot\bar{2}:m$ $\underline{m}\cdot\bar{2}:m$ $m\cdot\bar{2}:m$ $\underline{m}\cdot\bar{2}:m$ | $2mm$ $\bar{2}mm$ $\bar{2}mm$ $\bar{2}22$ $\bar{2}22$ mmm \underline{mmm} mmm \underline{mmm} | AF F F AF F AF F AF AF |
| tetragonal | C_4 S_4 C_{4h} D_{2d} C_{4v} D_4 D_{4h} | 4 4 8 8 8 8 16 | C_4 C_2 S_4 C_2 C_{4h} C_{2h} C_4 S_4 D_{2d} C_{2v} D_2 S_4 C_{4v} C_{2v} C_4 D_4 D_2 C_4 D_{4h} D_{2h} C_{4h} D_{2d} C_{4v} D_4 | 4 $\bar{4}$ $\bar{4}$ $\bar{4}$ $4:m$ $\bar{4}:m$ $\bar{4}:m$ $\bar{4}\cdot m$ $\bar{4}\cdot m$ $\bar{4}\cdot m$ $\bar{4}\cdot m$ $4:m$ $\bar{4}:m$ $\bar{4}:m$ $4:2$ $\bar{4}:2$ $\bar{4}\cdot\bar{2}$ $m\cdot 4:m$ $\bar{m}\cdot 4:m$ $\bar{m}\cdot 4:m$ $m\cdot 4:m$ $\bar{m}\cdot 4:m$ | 4 $\bar{4}$ $\bar{4}$ $\bar{4}$ $4/m$ $\bar{4}/m$ $\bar{4}/m$ $\bar{4}2m$ $\bar{4}2m$ $\bar{4}2m$ $\bar{4}2m$ $4/m$ $\bar{4}/m$ $\bar{4}/m$ $42(422)$ $\bar{4}2$ $\bar{4}2$ $4/mmm$ $\bar{4}/mmmm$ $\bar{4}/mmmm$ $4/mmm$ $\bar{4}/mmmm$ | F AF F AF AF F AF AF AF AF F AF F F AF AF AF F AF AF AF AF |

(Group G' is a point group and the underscores on the Shubnikov notation denote elements of G' to which \hat{T} has been adjoined. F and AF denote ferromagnetic and antiferromagnetic ordering, respectively)

Table 16.6. (continued)

| crystal system | group G' | number of elements | invariant unitary subgroup H | Shubnikov notation | international notation | magnetic order |
|----------------|------------|--------------------|--------------------------------|---------------------|------------------------|----------------|
| rhombohedral | C_3 | 3 | C_3 | 3 | 3 | F |
| | S_6 | 6 | S_6 | $\bar{6}$ | $\bar{3}$ | F |
| | C_{3r} | 6 | C_3 | $\bar{6}$ | $\bar{3}$ | AF |
| | | | C_{3v} | $\bar{3} \cdot m$ | $\bar{3}m$ | AF |
| | D_3 | 6 | C_3 | $\bar{3} \cdot m$ | $\bar{3}m$ | F |
| | | | D_3 | 3:2 | $\bar{3}2$ | AF |
| | D_{3d} | 12 | C_3 | 3:2 | $\bar{3}2$ | F |
| | | | D_{3d} | $\bar{6} \cdot m$ | $\bar{3}m$ | AF |
| | | | S_6 | $\bar{6} \cdot m$ | $\bar{3}m$ | F |
| | | | C_{3v} | $\bar{6} \cdot m$ | $\bar{3}m$ | AF |
| | | | D_3 | $\bar{6} \cdot m$ | $\bar{3}m$ | AF |
| hexagonal | C_{3h} | 6 | C_{3h} | $3 \cdot m$ | $\bar{6}$ | F |
| | | | C_3 | $3 \cdot m$ | $\bar{6}$ | AF |
| | C_6 | 6 | C_6 | 6 | 6 | F |
| | | | C_3 | 6 | 6 | AF |
| | C_{6h} | 12 | C_{6h} | $6 \cdot m$ | $\bar{6}m$ | F |
| | | | S_6 | $6 \cdot m$ | $\bar{6}m$ | AF |
| | | | C_{3h} | $6 \cdot m$ | $\bar{6}m$ | AF |
| | | | C_6 | $6 \cdot m$ | $\bar{6}m$ | AF |
| | D_{3h} | 12 | D_{3h} | $m \cdot 3 \cdot m$ | $\bar{6}m2$ | AF |
| | | | C_{3v} | $m \cdot 3 \cdot m$ | $\bar{6}m2$ | AF |
| | | | D_3 | $m \cdot 3 \cdot m$ | $\bar{6}m2$ | AF |
| | | | C_{3h} | $m \cdot 3 \cdot m$ | $\bar{6}m2$ | F |
| | | | C_{6h} | $6 \cdot m$ | $6mm$ | AF |
| | | | C_{3v} | $6 \cdot m$ | $6mm$ | AF |
| | D_6 | 12 | C_6 | $6 \cdot m$ | $6mm$ | F |
| | | | D_6 | 6:2 | $62(622)$ | AF |
| | | | D_3 | 6:2 | 62 | AF |
| | D_{6h} | 24 | C_6 | 6:2 | 62 | F |
| | | | D_{6h} | $m \cdot 6 \cdot m$ | $6/mmm$ | AF |
| | | | D_{3d} | $m \cdot 6 \cdot m$ | $6/mmm$ | AF |
| | | | C_{3h} | $m \cdot 6 \cdot m$ | $6/mmm$ | F |
| | | | D_{3h} | $m \cdot 6 \cdot m$ | $6/mmm$ | AF |
| | | | C_{6v} | $m \cdot 6 \cdot m$ | $6/mmm$ | AF |
| | | | D_6 | $m \cdot 6 \cdot m$ | $6/mmm$ | AF |
| cubic | T | 12 | T | $3/2$ | 23 | AF |
| | T_h | 24 | T_h | $\bar{6}/2$ | $m3$ | AF |
| | | | T | $\bar{6}/2$ | $m3$ | AF |
| | T_d | 24 | T_d | $3/4$ | $\bar{4}3m$ | AF |
| | | | T | $3/4$ | $\bar{4}3m$ | AF |
| | O | 24 | O | $3/4$ | $\bar{4}3(432)$ | AF |
| | | | T | $3/4$ | $\bar{4}3$ | AF |
| | O_h | 48 | O_h | $\bar{6}/4$ | $m3m$ | AF |
| | | | T_h | $\bar{6}/4$ | $m3m$ | AF |
| | | | T_d | $\bar{6}/4$ | $m3m$ | AF |
| | | | O | $\bar{6}/4$ | $m3m$ | AF |

$\hat{T}A_k$, respectively. We denote a typical magnetic point group of this category by $G = \{A_i, M_k\}$.

- (a) \hat{T} is not an element in the magnetic point group G (since the identity element is one of the elements of $\{A_i\}$ but not of $\{A_k\}$).
- (b) A_i and A_k are distinct, so that no element in the set $\{A_i\}$ is also in $\{A_k\}$ where $\{M_k\} = \{\hat{T}A_k\}$. If there were one A_j in common, then we could have $\hat{T}A_j$ in $\{M_k\}$ and A_j^{-1} in $\{A_i\}$, which on multiplication $\hat{T}A_j A_j^{-1}$ implies that \hat{T} is in G , in contradiction with property (a).
- (c) $G' \equiv \{A_i, A_k\}$ is one of the 32 ordinary point groups.
- (d) The set $H_r = \{A_i\}$ forms an invariant unitary subgroup of G . This subgroup is selfconjugate because conjugation of an element in A_i with any element in $\{M_k\}$ written as $M_k A_i M_k^{-1}$ yields an element in $\{A_i\}$ as a result of (16.32), and likewise the conjugation $A_i M_k A_i^{-1}$ yields an element in $\{M_k\}$.
- (e) The number of unitary operators A_i = the number of antiunitary operators M_k , to satisfy the multiplication rules in (16.32) and the group properties of G .
- (f) $\{A_i\}$ is the only coset of H_r in G and $\{A_k\}$ is the only coset of H_r in G' .
- (g) Since H_r and G' are groups, and properties (e) and (f) apply, then G is a group of the form

$$G = H_r + \hat{T}(G' - H_r). \quad (16.33)$$

- (h) From property (g), we see that the procedure for finding magnetic point groups is to start with one of the 32 point groups G' and find all invariant subgroups H_r of *index 2* where half of the elements in G' are in H_r and half are not. Denoting each such subgroup by H_r we can form a magnetic group G_r such that

$$G_r = H_r + \hat{T}(G' - H_r). \quad (16.34)$$

We denote each magnetic group G_r thus formed by $G'(H_r)$ in which the relevant G' and H_r for each G_r are listed. This notation is used in Table 16.6 and the various $G'(H_r)$ can be found in this table.

To illustrate the elements of magnetic point groups, we consider the four entries under C_{2h} in Table 16.6. We then list below the symmetry elements of each of the $C_{2h}(H_r)$ magnetic point groups.

$$\begin{aligned} C_{2h}(C_{2h}) : & E, C_2, i, iC_2, \quad (iC_2 = \sigma_h) \\ C_{2h}(C_2) : & E, C_2, \hat{T}i, \hat{T}iC_2 \\ C_{2h}(C_i) : & E, i, \hat{T}C_2, \hat{T}iC_2 \\ C_{2h}(C_{1h}) : & E, iC_2, \hat{T}i, \hat{T}C_2, \end{aligned} \quad (16.35)$$

in which the magnetic point group $C_{2h}(C_{2h})$ is of type (a), and the other three are of type (c). Not listed is the magnetic space group $C_{2h} \otimes \hat{T}$ of type (b) which contains the eight symmetry elements $\{A_i\} = \{E, C_2, i, iC_2\}$ and

$\{\hat{T} \otimes A_i\} = \{\hat{T}, \hat{T}C_2, \hat{T}i, \hat{T}iC_2\}$ (see Table A.6 in Appendix A for the character table for C_{2h}). We note that the time reversal operator of \hat{T} reverses the sign of a spin, while the *inversion operator* i leaves a spin invariant (since the angular momentum \mathbf{L} is even under inversion, while \mathbf{r} and \mathbf{p} are each odd).

16.5.5 Examples of Magnetic Structures

We give below three examples of magnetic structures in each case illustrating a different aspect of magnetic structures. First we illustrate an orthorhombic ferromagnetic structure for which the magnetic unit cell and the chemical unit cell are the same (see Fig. 16.6).

The symmetry of this magnetic structure is denoted by D_{2h} (C_{2h}) which denotes a point group D_{2h} from which the subgroup (C_{2h}) forms the set of symmetry elements $\{A_i\}$ and the remaining symmetry elements of G' are $\{A_k\}$ where the elements M_k in G are of the form $M_k = \hat{T}A_k$. We note from Table 16.6 that D_{2h} (C_{2h}) corresponds to a ferromagnetic structure such as the one shown in Fig. 16.6. In the paramagnetic state, the proper symmetry group for this structure is D_{2h} .

The symmetry operations for $D_{2h} = D_2 \otimes i$ are $E, C_{2x}, C_{2y}, C_{2z}, i, iC_{2x}, iC_{2y}, iC_{2z}$ [see Appendix A for character tables for D_{2h} (Table A.7) and C_{2h} (Table A.6)]. It is immediately seen that the subgroup of D_{2h} which leaves the spin invariant consists of the elements $\{A_i\} = E, C_{2z}, i, iC_{2z}$, since both orbital and spin angular momentum are invariant under inversion. These four elements form the group $C_{2h} = C_2 \otimes i$, noting again that the spin angular momentum S is even under inversion. The remaining elements of D_{2h} reverse the spins, so that the time reversal operator \hat{T} is needed to keep all the spins

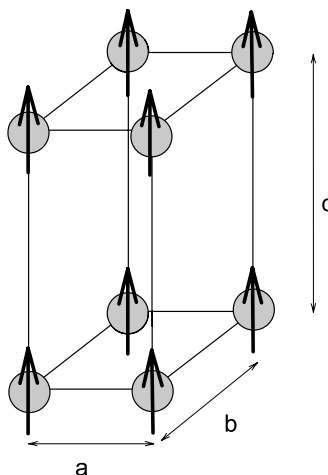


Fig. 16.6. Magnetic spin arrangement in $D_{2h}(C_{2h})$ symmetry for an orthorhombic ferromagnetic system

ferro-magnetically aligned. We therefore obtain $\{M_k\} = \hat{T}C_{2x}, \hat{T}C_{2y}, \hat{T}iC_{2x}$ and $\hat{T}iC_{2y}$ for the remaining symmetry elements of D_{2h} (C_{2h}). The appropriate Bravais lattice in this case is the orthorhombic-P Bravais lattice for the nonmagnetic groups (see Fig. 16.4(a)). The magnetic space group D_{2h} (C_{2h}) is further developed in Problem 16.5.

Next we consider for our second example antiferromagnets with the Rutile structure as shown in Fig. 16.7. The open circles are the F ions while the black circles with spins denote the magnetic cations. The point group for this structure in the paramagnetic state is $D_{4h} = D_4 \otimes i$. In the antiferromagnetic state, each unit cell has one spin up and one spin down cation. The chemical and magnetic unit cells contain the atoms shown in Fig. 16.7. The space group symmetry operations for D_{4h} pertinent to the rutile structure are the 16 operations listed below:

$$\begin{array}{ll}
 1. \{E|0\} & 9. \{i|0\} \\
 2. \{C_2|0\} & 10. \{\sigma_h|0\} = \{C_2|0\}\{i|0\} \\
 3. \{C_{2\xi}|0\} & 11. \{\sigma_{d\xi}|0\} = \{C_{2\xi}|0\}\{i|0\} \\
 4. \{C_{2\nu}|0\} & 12. \{\sigma_{d\nu}|0\} = \{C_{2\nu}|0\}\{i|0\} \\
 5. \{C_4|\tau_0\} & 13. \{S_4^{-1}|\tau_0\} = \{C_4|\tau_0\}\{i|0\} \\
 6. \{C_4^{-1}|\tau_0\} & 14. \{S_4|\tau_0\} = \{C_4^{-1}|\tau_0\}\{i|0\} \\
 7. \{C_{2x}|\tau_0\} & 15. \{\sigma_{vx}|\tau_0\} = \{C_{2x}|\tau_0\}\{i|0\} \\
 8. \{C_{2y}|\tau_0\} & 16. \{\sigma_{vy}|\tau_0\} = \{C_{2y}|\tau_0\}\{i|0\}, \\
 \end{array} \tag{16.36}$$

where the axes $\xi = (110)$ and $\nu = (1\bar{1}0)$ denote twofold axes and the translation $\tau_0 = 1/2(\mathbf{a}_1 + \mathbf{a}_2 + \mathbf{a}_3)$ is from the origin at the lower left hand corner of the figure to the body center of the unit cell (see Fig. 16.7). The point group

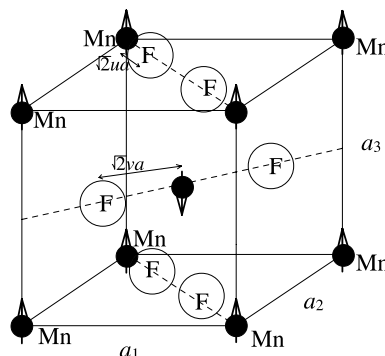


Fig. 16.7. Common antiferromagnets MnF_2 , FeF_2 and CoF_2 crystallize in the rutile structure with $|a_1| = |a_2| = a$; $|a_3| = c$; $c \neq a$. The diagram emphasizes the magnetic unit cell for the rutile structure that has the magnetic point group D_{4h} (D_{2d}) which describes the antiferromagnetic spin alignment of these magnetic materials

D_{4h} corresponding to these space group operations is found by setting $\tau_0 = 0$. The character table for D_4 is given in Table A.18 where $D_{4h} = D_4 \otimes i$. The operations listed in (16.36) correspond to the space group for the chemical unit cell for the rutile structure.

The unitary subgroup that forms the symmetry group for antiferromagnetic MF_2 ($\text{M} = \text{magnetic cation}$) consists of the four elements of the symmetry group D_2 $\{E|0\}$, $\{C_2|0\}$, $\{C_{2x}|\tau_0\}$, $\{C_{2y}|\tau_0\}$ and four additional elements formed by combining these with inversion. These eight elements constitute $\{A_i\}$ which corresponds to the group $D_{2h} = D_2 \otimes i$ (see Table A.7). From Fig. 16.7 we see that the operations C_{2x} and C_{2y} invert the spins. The appropriate Bravais lattice for MnF_2 is the tetragonal Bravais lattice P_I for the magnetic groups (see Fig. 16.4). If we ignore the fluorine anions, the chemical unit cell would be half as large containing only one magnetic cation. The magnetic unit cell would then be twice as large as the chemical unit cell. Nevertheless the magnetic point group for the antiferromagnetic chemical structure remains D_{4h} (D_{2h}). Further elaboration on this space group is given in Problem 16.7.

As a third example we consider the magnetic states of EuSe because the nearest and next-nearest exchange constants are of approximately equal magnitude and of opposite sign, and for this reason EuSe exhibits several different and interesting magnetic phases, depending on the magnetic field and temperature variables. In Figs. 16.8(a)–(c) we see, respectively, the spin arrangement for the antiferromagnetic (AF-II) two spin ($\uparrow\downarrow$) phase, the ferri-

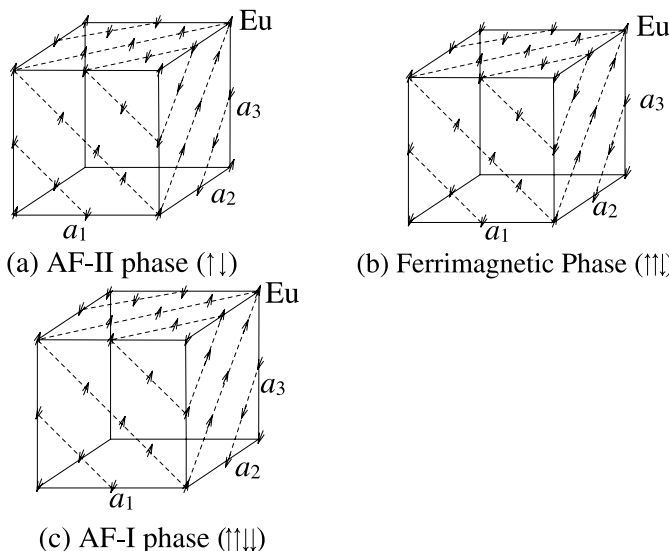


Fig. 16.8. Magnetic structure of EuSe in (a) the AF-II phase ($\uparrow\downarrow$), (b) the ferrimagnetic phase ($\uparrow\downarrow\downarrow$), and (c) the antiferromagnetic AF-I phase ($\uparrow\uparrow\downarrow\downarrow$) in which the magnetic Eu spins are shown

magnetic three spin ($\uparrow\uparrow\downarrow$) phase, and the antiferromagnetic (AF-I) four spin ($\uparrow\uparrow\downarrow\downarrow$) phase.

A ferromagnetic phase is also found upon application of a high applied magnetic field. In all four magnetically ordered phases, the spins in a given $(1\bar{1}\bar{1})$ plane are parallel to each other and are oriented along the $[011]$ direction. The resulting magnetic space group has very low symmetry. For the AF-II phase, the symmetry elements are $\{E|0\}$, $\{i|0\}$, $\hat{T}\{E|\tau_0\}$, $\hat{T}\{i|\tau_0\}$ in which the vector τ_0 takes the spins from one sublattice to the other

$$\tau_0 = \frac{1}{4}(a_x, 0, a_z). \quad (16.37)$$

Thus the magnetic point group is $S_2 \otimes \hat{T}$.

If, however, the spins were oriented instead along $[1\bar{1}1]$ and $[\bar{1}1\bar{1}]$ directions in alternate (111) planes, then the magnetic symmetry of the group increases and is $C_3 \otimes \hat{T}$. Thus the spin direction is important in determining the magnetic point group and the magnetic space group. We note that the number of sublattices (1, 2, 3, or 4) is also important in determining the symmetry operations in the magnetic space groups. For some cases it is useful to ignore the spin directions and just to consider each atom on a given sublattice as a colored atom. Such groups are called *color groups* [43]. Color groups have more symmetry than the magnetic groups.

16.5.6 Effect of Symmetry on the Spin Hamiltonian for the 32 Ordinary Point Groups

The n lowest energy states for electrons in a paramagnetic center where an external magnetic field H has been applied can be described by an Effective Spin Hamiltonian $\mathcal{H}_{\text{spin}}$ generally given by [59]:

$$\mathcal{H}_{\text{spin}} = \mathcal{H}_Z + \mathcal{H}_F + \mathcal{H}_{hf} + \mathcal{H}_{shf} + \mathcal{H}_{ZN} + \mathcal{H}_Q, \quad (16.38)$$

where the contributions from the electronic Zeeman effect \mathcal{H}_Z , the fine interaction \mathcal{H}_F , the hyper-fine interaction \mathcal{H}_{hf} , the super-hyper-fine interactions \mathcal{H}_{shf} , the nuclear Zeeman effect \mathcal{H}_{ZN} and the nuclear quadrupole interaction \mathcal{H}_Q are taken into account. Each of these contributions are represented by tensors, and the symmetries of the system can be used to evaluate the nonzero and the independent terms in $\mathcal{H}_{\text{spin}}$. The group theory procedure for dealing with general tensors is discussed in Chap. 18.

It is however interesting to comment here on the influence of symmetries in the spin Hamiltonian. If we limit ourselves to spin operators S transforming like angular momentum (invariant under spatial inversion and odd under time reversal symmetry), it is clear that different Hamiltonians related to each other by the spatial inversion are identical. Therefore, two groups obtained from each other by the direct multiplication with the inversion operator will indeed give the same $\mathcal{H}_{\text{spin}}$. They will be *magnetically equivalent*.

Table 16.7. Categories of magnetic equivalence for the 32 ordinary point groups

| categories | 1 | 2 | 3 | 4 | 5 | 6 | 7 | 8 | 9 | 10 | 11 |
|------------|-------|----------|----------|-------|----------|----------|----------|----------|----------|-------|----------|
| | C_1 | C_2 | D_2 | C_3 | D_3 | C_4 | D_4 | C_6 | D_6 | T | O |
| | S_2 | C_{1h} | C_{2v} | S_6 | C_{3v} | S_4 | C_{4v} | C_{6h} | C_{6v} | T_h | T_d |
| | | C_{2h} | D_{2h} | | D_{3d} | C_{4h} | D_{2d} | C_{3h} | D_{3h} | | O_h |
| | | | | | | | | D_{4h} | | | D_{6h} |

Considering the 32 ordinary point groups, Table 16.7 gives the 11 categories of *magnetically equivalent* groups. It is enough to find $\mathcal{H}_{\text{spin}}$ for the lowest symmetry point groups for each of the 11 categories, and the spin Hamiltonian for the higher symmetry groups will be identical.

Selected Problems

16.1. Consider the space group D_{6h}^4 (#194) which we discussed in connection with the lattice modes for graphite (see Problem 11.1). We will now concern ourselves with the electronic structure of graphite. Since the Fermi surfaces are located close to the HK axes in the Brillouin zone, it is important to work with the group of the wave vector at points H , K and A (see Fig. 16.9).

- (a) Using Appendix D and other literature references [47, 54] give the character table including double groups for the group of the wave vector at point K . Classify each of the irreducible representations according to whether they behave as a, b or c under time reversal symmetry.
- (a) Find the compatibility relations as we move away from K toward H .

16.2. Now consider a 2D graphene sheet, which by definition is one atomic layer of 3D graphite.

- (a) What are the symmetry operations for this structure and what is the appropriate 2D space group?

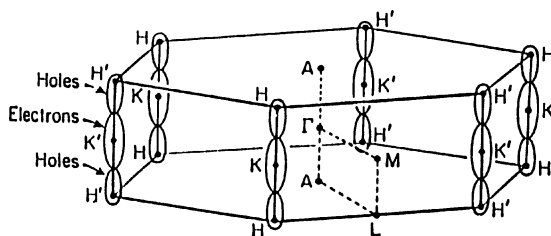


Fig. 16.9. Brillouin zone and Fermi surfaces for electrons and holes of semimetallic graphite

- (b) Give the character table for the group of the wave vector at the Γ point (center of the Brillouin zone), and include the time reversal classification for the cases where the spin-orbit interaction is neglected and where it is included.
- (c) Repeat part (b) for the group of the wave vector at the K point where the valence and conduction band are degenerate right at the K point (corner of the Brillouin zone) and have a linear k dependence as we move away from the K point. What is the relation between the K and K' points in the 2D Brillouin zone under time reversal symmetry? Consider the symmetry relation between $E_{\uparrow(k)}$ and $E_{\downarrow(k)}$ in the vicinity of the K and K' points for the linear k bands and for those coming into points K and K' with zero slope.

16.3. Consider the zinc blende space group (#227) which lacks inversion symmetry. For an energy band with two fold degeneracy, time reversal symmetry gives the relation $E(\mathbf{k}, \uparrow) = E(-\mathbf{k}, \downarrow)$ (see Sect. 16.4)

- (a) What is the form of $E(\mathbf{k})$ as we move away from $\mathbf{k} = 0$?
- (b) What is the form of the constant energy surface for the case where the carrier concentration is 10^{17} carriers/cm³? Does time reversal symmetry have an effect on the constant energy surface at the Fermi level? What happens in the presence of a magnetic field for which $\mu^*B > E_F$ and $\mu^*B < E_F$?

16.4. Consider the symmetry operations of the arrangement of the chains of magnetic and nonmagnetic atoms in Fig. 16.5.

- (a) What are the symmetry operations of the chain shown in Fig. 16.5(a)? What type of magnetic group would be applicable to the group of the wave vector for $k = 0$, using the classifications in Sect. 16.5.3.
- (b) Repeat (a) for the case of the chain shown in Fig. 16.5(b). Fig. 16.5 for $E(k, \uparrow)$ under spatial and time inversion symmetry?

16.5. (a) For the ferromagnetic structure in Fig. 16.6, what is the difference between the chemical and magnetic unit cell [51]? What are the differences in the symmetry operations when the system is in the ferromagnetic state as compared to the paramagnetic states?

(b) What difference do you expect for $E(k)$ for the two cases in (a)? What is the effect of the time reversal operator on $E(k)$? Do you expect a change in $E(k)$ when a phase transition from a paramagnetic to a ferromagnetic state occurs?

(c) Suppose now that the spins were all aligned by a high magnetic field along the \mathbf{a} axis. What would be the new magnetic group? On physical arguments, would you expect this to be a stable configuration when you turn off the magnetic field? Why? What information does group theory provide regarding this question?

16.6. Suppose that we have a magnetic compound MX (where M is the magnetic species) that crystallizes in the zinc-blende structure. Suppose that

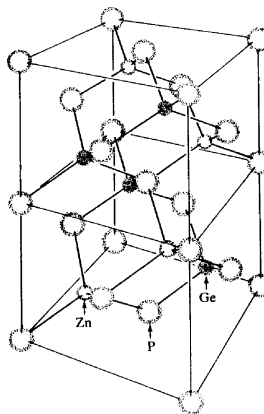


Fig. 16.10. In the chalcopyrite structure for ZnGeP_2 , the lattice is compressed slightly along the vertical direction and the phosphorus atoms are slightly displaced from the positions they would have in the zinc blende structure

at the Neél temperature the magnetic species undergo a magnetic phase transition to an antiferromagnetic two sublattice phase such that by treating the $\text{M}\uparrow$ and $\text{M}\downarrow$ as different species, the magnetic crystal is described by the chalcopyrite structure (Fig. 16.10).

- Reconfigure the prototype chalcopyrite structure, shown in Fig. 16.10 for ZnGeP_2 , to correspond to the antiferromagnetic MX compound with the two spin states. What is the space group for this structure?
- Find the change in the Raman spectra associated with this magnetic phase transition from the zinc-blende to the chalcopyrite structures shown in Fig. 16.10.

16.7. Consider the structure shown for MnF_2 in Fig. 16.7.

- What are the classes formed by the elements in (16.36)? What is the effect of time reversal symmetry on each of these classes?
- What is the appropriate space group for MnF_2 in the paramagnetic state? What changes occur at the magnetic phase transition to an antiferromagnetic state?
- The Raman effect probes certain lattice modes in this structure. Find the Raman active modes in the paramagnetic phase?
- What changes would you expect to see in the Raman spectra when the MnF_2 undergoes a magnetic phase transition to the magnetic D_{4h} (D_{2d})?

16.8. The ferrites (XFe_2O_4 , X^{2+} = metallic ion) are important magnetic materials belonging to the cubic $Fd3m$ (O_h^7) space group. To calculate the spin Hamiltonian $\mathcal{H}_{\text{spin}}$ for this material, it is enough to obtain $\mathcal{H}_{\text{spin}}$ for one of the ordinary point groups of class 11 in Table 16.7. Show that the spin Hamiltonian can be written in the following form [3, 15, 34, 41]:

$$\mathcal{H}_{\text{spin}} = g\mu\mathbf{H}\cdot\mathbf{S} - g_N\mu_N\mathbf{H}\cdot\mathbf{I} + A\mathbf{I}\cdot\mathbf{S} + B_{40}(O_{40} + 5O_{44}) + B_{60}(O_{60} + 21O_{64}), \quad (16.39)$$

where

$$O_{40} = 35S_z^4 + 25S_z^3 - 30S(S+1)S_z^2 + 3S^2(S+1)^2 - 6S(S+1),$$

$$O_{44} = (1/2)(S_+^4 + S_-^4),$$

$$O_{60} = 231S_z^6 - 315S(S+1)S_z^4 + 735S_z^4 + 105S^2(S+1)^2S_z^2 - 525S(S+1)S_z^2 \\ + 294S_z^2 - 5S^3(S+1)^3 + 40S^2(S+1)^2 - 60S(S+1),$$

$$O_{64} = (1/2)(S_+^4 + S_-^4)(11S_z^2 - S(S+1) - 38).$$

Permutation Groups and Many-Electron States

In this chapter we discuss the properties of permutation groups, which are known as “Symmetric Groups” in the mathematics literature. Although permutation groups are quite generally applicable to many-body systems, they are used in this chapter to classify the symmetry in many-electron states. This discussion applies to the symmetries of both the spin and orbital states. In Chap. 18 we apply the results of this chapter for the permutation groups to show a very different use of permutation groups, which is to classify the symmetry properties for tensors occurring in solid state physics in a powerful way.

The main application of the permutation group in this chapter is to describe atoms with full rotational symmetry. We give explicit results for two, three, four, and five electron systems. Whereas two electron systems can be handled without group theory, the power of group theory is evident for three, four, five, and even larger electron systems. With a five-electron system, we can treat all multielectron states arising from s , p , and d electrons, since five electrons fill half of a d level, and a more than half-filled level such as for eight d electrons can be treated as two d level holes, using concepts equivalent to the presence of hole states in solid state physics. To deal with all multielectron states that could be made with f electrons we would need to also consider the permutation groups for six and seven objects. In the solid state, multielectron states occur predominantly in the context of crystal fields, as for example the substitution of a transition metal ion (having d electrons) on a crystal site which experiences the symmetry of the crystal environment. The crystal field lowers the full rotational symmetry of the free ion giving rise to crystal field splittings. In this case the effect of the crystal field must be considered once the symmetry of the electronic configuration of the free ion has been determined using the permutation groups discussed in this chapter.

17.1 Introduction

In the physics of a many-electron atom or molecule we are interested in solutions to a Hamiltonian of the form

$$\mathcal{H}(\mathbf{r}_1, \dots, \mathbf{r}_n) = \sum_{i=1}^n \left(\frac{p_i^2}{2m} + V(\mathbf{r}_i) \right) + \frac{1}{2} \sum_{i \neq j} \frac{e^2}{r_{ij}}, \quad (17.1)$$

where $V(\mathbf{r}_i)$ is a one-electron potential and the Coulomb electron–electron interaction term is explicitly included. The one-electron potential determines the rotational and translational symmetry of the Hamiltonian.

In addition to symmetry operations in space, the Hamiltonian in (17.1) is invariant under interchanges of electrons, i.e., permutation operations P of the type

$$P = \begin{pmatrix} 1 & 2 & \dots & n \\ a_1 & a_2 & \dots & a_n \end{pmatrix}, \quad (17.2)$$

where the operation P replaces 1 by a_1 , 2 by a_2 , etc. and n by a_n . We have already seen that these permutation operations form a group (see Sect. 1.2), i.e., there exists the inverse operation

$$P^{-1} = \begin{pmatrix} a_1 & a_2 & \dots & a_n \\ 1 & 2 & \dots & n \end{pmatrix}, \quad (17.3)$$

and the identity element is given by

$$E = \begin{pmatrix} 1 & 2 & \dots & n \\ 1 & 2 & \dots & n \end{pmatrix}, \quad (17.4)$$

which leaves the n electrons unchanged. Multiplication involves sequential permutation operations of the type given by (17.2). The number of symmetry operations in a permutation group of n objects is $n!$, which gives the order of the permutation group to be $n!$. Thus the group $P(3)$ in Sect. 1.2 has $h = 3! = 3 \cdot 2 \cdot 1 = 6$ elements.

The wave function solutions of the many-electron Hamiltonian (17.1) are denoted by $\Psi_{\Gamma_i}(\mathbf{r}_1, \dots, \mathbf{r}_n)$. Since all electrons are indistinguishable, the permutation P commutes with the Hamiltonian, and we, therefore, can classify the wave functions of the group of the Schrödinger equation according to an irreducible representation Γ_i of the permutation or the symmetric group. Some permutations give rise to symmetric states, others to antisymmetric states, and the remainder are neither. In some cases, all possible states are either symmetric or antisymmetric, and there are no states that are neither fully symmetric nor fully antisymmetric.

For the permutation group of n objects amongst the various possible irreducible representations, there are two special one-dimensional irreducible representations: one that is *symmetric* and one that is *antisymmetric* under the interchange of two particles. The basis function for the *symmetric* representation Γ_1^s of an orbital state is just the product wave function

$$\Psi_{\Gamma_1^s}(\mathbf{r}_1, \mathbf{r}_2, \dots, \mathbf{r}_n) = \frac{1}{\sqrt{n!}} \sum_{\text{permutations}} \psi_1(\mathbf{r}_1) \psi_2(\mathbf{r}_2) \dots \psi_n(\mathbf{r}_n). \quad (17.5)$$

The total wave function for a many-electron system is the product of the orbital and spin wave functions. The basis function for the antisymmetric representation Γ_1^a is conveniently written in terms of the Slater determinant [6]:

$$\Psi_{\Gamma_1^a}(\mathbf{x}_1, \mathbf{x}_2, \dots, \mathbf{x}_n) = \frac{1}{\sqrt{n!}} \begin{vmatrix} \psi_1(\mathbf{r}_1, \sigma_1) & \psi_1(\mathbf{r}_2, \sigma_2) & \dots & \psi_1(\mathbf{r}_n, \sigma_n) \\ \psi_2(\mathbf{r}_1, \sigma_1) & \psi_2(\mathbf{r}_2, \sigma_2) & \dots & \psi_2(\mathbf{r}_n, \sigma_n) \\ \vdots & \vdots & \ddots & \vdots \\ \psi_n(\mathbf{r}_1, \sigma_1) & \psi_n(\mathbf{r}_2, \sigma_2) & \dots & \psi_n(\mathbf{r}_n, \sigma_n) \end{vmatrix}, \quad (17.6)$$

where \mathbf{x}_i denotes a generalized coordinate, consisting of \mathbf{r}_i , the spatial coordinate and σ_i , the spin coordinate. When written in this form, the many-body wave function automatically satisfies the Pauli principle since the repetition of either a row or a column results in a zero determinant, thereby guaranteeing that every electron is in a different state.

The higher dimensional irreducible representations of the permutation group are also important in determining many-electron states which satisfy the Pauli principle. For example, in the $\mathbf{L} \cdot \mathbf{S}$ coupling scheme for angular momentum, one must take combinations of n spins to get the total S . These must be combined with the orbital angular momentum combinations to get the total L . Both the spin states and the orbital states will transform as some irreducible representation of the permutation group. When combined to make a total J , only those combinations which transform as the antisymmetric representation Γ_1^a are allowed by the Pauli principle. We will illustrate these concepts with several examples in this chapter, including the three-electron p^3 state and the four-electron p^4 state.

In this chapter we will use the permutation groups to yield information about the symmetry and the degeneracy of the states for a many-electron system. We emphasize that in contrast to the case of rotational invariance, the ground state of (17.1) does not transform as the totally symmetric representation of the permutation group Γ_1^s . But rather for electrons (or half integral spin (Fermion) particles), the ground state and all allowed excited states transform as the antisymmetric one-dimensional irreducible representation Γ_1^a since any physical perturbation \mathcal{H}' will not distinguish between like particles. The perturbation \mathcal{H}' itself transforms as the totally symmetric

irreducible representation of the permutation group. Only integral spin particles (Bosons) have ground states that transform as the totally symmetric irreducible representation Γ_1^s .

Mathematicians also study another aspect of permutations called braids [36], where both the permutation and the ordered sequence of the permutation is part of the definition of the group element. The group theory and application of braids to solid state physics is not considered in this chapter.

In this chapter we first discuss the classes of the permutation groups (Sect. 17.2), their irreducible representations (Sect. 17.2), and their basis functions (Sect. 17.3). Applications of the permutation groups are then made (Sect. 17.4) to classify two-electron, three-electron, four-electron and five-electron states.

17.2 Classes and Irreducible Representations of Permutation Groups

Of particular interest to the symmetry properties of permutation groups are cyclic permutations.

Definition 26. A cyclic permutation is here defined in terms of an example:

If a permutation group has n objects, one of the group elements of a cyclic permutation of n objects is

$$\begin{pmatrix} 1 & 2 & 3 & \dots & (n-1) & n \\ 2 & 3 & 4 & \dots & n & 1 \end{pmatrix} \equiv (23\dots n1),$$

where the permutation $(123\dots n)$ denotes the identity element. It is clear that the n cyclic permutations of n identical objects are all related to one another by an equivalence transformation

$$(123\dots n) = (234\dots n1) = (34\dots n12) = \text{etc.} \quad (17.7)$$

Since all of these group elements are identical, and all these cyclic permutations have $1 \rightarrow 2$, $2 \rightarrow 3$, $3 \rightarrow 4$, all are the same permutation of n identical objects, all are related by an equivalence transformation, i.e., all of these cyclic permutations represent the same physics.

Theorem. Any permutation can be decomposed into cycles.

Proof. The decomposition of a given permutation is demonstrated by the following example.

$$P_i = \begin{pmatrix} 1 & 2 & 3 & 4 & 5 & 6 & 7 \\ 4 & 3 & 2 & 5 & 7 & 6 & 1 \end{pmatrix} \equiv (1\ 4\ 5\ 7)(2\ 3)(6) \quad (17.8)$$

can be decomposed into three cycles as indicated in (17.8). The decomposition of a permutation into cycles is unique, since different arrangements of cycles correspond to different permutations. \square

Definition 27. *Length of a cycle.*

Let us assume that a permutation of n objects is decomposed into cycles as follows: there are λ_1 cycles of one element, i.e., of length 1, λ_2 cycles of length 2, \dots , λ_q cycles of length q :

$$n = \lambda_1 + 2\lambda_2 + \dots + q\lambda_q. \quad (17.9)$$

It is easily seen that there are

$$\frac{n!}{1^{\lambda_1} \lambda_1! 2^{\lambda_2} \lambda_2! \dots q^{\lambda_q} \lambda_q!} \quad (17.10)$$

permutations that have the same cycle structure. An example of the length of the cycle for permutation group $P(4)$ will be given after the next theorem.

Theorem. *Permutations with the same cycle structure belong to the same class.*

Proof. Consider two permutations P and P' with the same cycle structure given by

$$\begin{aligned} P &= (a_1 a_2 \dots a_{\lambda_1})(b_1 b_2 \dots b_{\lambda_2}) \dots (d_1 d_2 \dots d_{\lambda_r}) \\ P' &= (a'_1 a'_2 \dots a'_{\lambda_1})(b'_1 b'_2 \dots b'_{\lambda_2}) \dots (d'_1 d'_2 \dots d'_{\lambda_r}). \end{aligned} \quad (17.11)$$

Here P takes $a_1 \rightarrow a_2$, etc. $b_1 \rightarrow b_2$, etc., $d_1 \rightarrow d_2$, etc. while P' does the corresponding permutation for the primed quantities. Now we introduce the permutation operation T which takes the primed quantities into the unprimed quantities (e.g., $a'_i \rightarrow a_i$)

$$T = \begin{pmatrix} a'_1 & \dots & a'_{\lambda_1} & b'_1 & \dots & b'_{\lambda_2} & \dots & d'_1 & \dots & d'_{\lambda_r} \\ a_1 & \dots & a_{\lambda_1} & b_1 & \dots & b_{\lambda_2} & \dots & d_1 & \dots & d_{\lambda_r} \end{pmatrix} \quad (17.12)$$

and T^{-1} takes $a_i \rightarrow a'_i$. Thus $T^{-1}PT$ does the following sequence: $a'_i \rightarrow a_i$, $a_i \rightarrow a_{i+1} \rightarrow a'_{i+1}$ and finally $a_{i+1} \rightarrow a'_{i+1}$. But this is equivalent to $a'_i \rightarrow a'_{i+1}$ which is precisely the permutation P' . Therefore,

$$T^{-1}PT = P'.$$

P' is related to P by conjugation, thus completing the proof of the theorem. The number of elements in each class is found from (17.10). \square

From the above theorem it follows that the number k of different classes (and hence the number of irreducible representations) of the permutation group of n objects is the number of different cycle structures that can be formed. Thus, the number of classes is just the number of ways in which the number n can be written as the sum of positive integers. For example, $n = 4$ objects can be constituted into five different cycle structures as enumerated below:

$$\begin{aligned}
 n = 4 & \quad 4 = 4 & (1, 2, 3, 4) \\
 & \quad 4 = 3 + 1 & (1, 2, 3)(4) \\
 & \quad 4 = 2 + 1 + 1 & (1, 2)(3)(4) \\
 & \quad 4 = 2 + 2 & (1, 2)(3, 4) \\
 & \quad 4 = 1 + 1 + 1 + 1 & (1)(2)(3)(4)
 \end{aligned} \tag{17.13}$$

giving rise to five classes and the number of members in each class can be found from (17.10).

As an example of this theorem consider the cycle structure $(abc)(d)$ of the permutation group $P(4)$, which is isomorphic to the point group T_d for the symmetry operations of a regular tetrahedron. The cycle structure $(abc)(d)$ in $P(4)$ corresponds to the rotation about a threefold axis, which also forms a class. The number of symmetry operations k in this class according to (17.10) is

$$\frac{4!}{(1^1)(1!)(3^1)(1!)} = 8,$$

which is in agreement with the number of elements in $8C_3$ in the group T_d . Another example is finding the number of symmetry operations in the class $(ab)(cd)$ of the point group $P(4)$, corresponding to the twofold axes around x, y, z , would be $4!/[2^2(2!)] = 3$ from (17.10), as expected for k from the isomorphism of $(ab)(cd)$ of $P(4)$ and $3C_2$ in T_d .

In the same way, $n = 5$ objects can be constituted in seven different cycle structures giving rise to 7 classes. Correspondingly $q = 6$ gives rise to 11 classes, $q = 7$ gives rise to 15 classes, $q = 8$ gives rise to 22 classes, etc. as further discussed in Problem 17.1(a).

Since the number of classes is equal to the number of irreducible representations, we can construct Table 17.1 where $P(n)$ labels the permutation group of n objects. Since the permutation groups are finite groups, we can appeal to our experience regarding finite groups and use the Theorem (3.40)

$$h = \sum_i \ell_i^2, \tag{17.14}$$

where ℓ_i is the dimensionality of the representation i , and h is the order of the group. For a permutation group of n objects, the order of the group is $h = n!$. From Table 17.1 we note that $P(3)$ is isomorphic with group C_{3v} or alternatively with group D_3 . Similarly $P(4)$ is isomorphic with the tetrahedral group T_d . Although the groups $P(5)$ and I_h both have 120 symmetry

Table 17.1. The number of classes and a listing of the dimensionalities of the irreducible representations

| group | classes | number of group elements $\sum_i \ell_i^2$ |
|--------|---------|--|
| $P(1)$ | 1 | $1! = 1^2 = 1$ |
| $P(2)$ | 2 | $2! = 1^2 + 1^2 = 2$ |
| $P(3)$ | 3 | $3! = 1^2 + 1^2 + 2^2 = 6$ |
| $P(4)$ | 5 | $4! = 1^2 + 1^2 + 2^2 + 3^2 + 3^2 = 24$ |
| $P(5)$ | 7 | $5! = 1^2 + 1^2 + 4^2 + 4^2 + 5^2 + 5^2 + 6^2 = 120$ |
| $P(6)$ | 11 | $6! = 1^2 + 1^2 + 5^2 + 5^2 + 5^2 + 5^2 + 9^2 + 9^2 + 10^2 + 10^2 + 16^2 = 720$ |
| $P(7)$ | 15 | $7! = 1^2 + 1^2 + 6^2 + 6^2 + 14^2 + 14^2 + 14^2 + 14^2 + 15^2 + 15^2$ $+ 21^2 + 21^2 + 35^2 + 35^2 + 20^2 = 5040$ |
| $P(8)$ | 22 | $8! = 1^2 + 1^2 + 7^2 + 7^2 + 14^2 + 14^2 + 20^2 + 20^2 + 21^2 + 21^2$ $+ 28^2 + 28^2 + 35^2 + 35^2 + 56^2 + 56^2 + 64^2 + 64^2 + 70^2 + 70^2$ $+ 42^2 + 90^2 = 40320$ |
| : | | |

operations, $P(5)$ is *not* isomorphic to the icosahedral group I_h since the two groups have different numbers of classes. The number of classes of $P(5)$ is seven while the number of classes of I_h is 10. The dimensions ℓ_i of the seven classes in the group $P(5)$ are listed in Table 17.1, and include two irreducible representations with $\ell_i = 1$, two with $\ell_i = 4$, two with $\ell_i = 5$ icosahedral group I_h , and one with $\ell_i = 6$. The 10 irreducible representations of I_h have the following dimensionalities: $2[1+3+3+4+5]$ (the 2 refers to two irreducible representations for each dimensionality arising from the inversion symmetry). Making use of the isomorphism of $P(3)$ and $P(4)$ mentioned above, matrix representations for the symmetry operations of these groups are easily written down.

17.3 Basis Functions of Permutation Groups

The basis functions considered here are for the particular application of permutation groups to many-particle systems. For example, the one-electron Hamiltonian

$$\mathcal{H}_0(\mathbf{r}_1) = \frac{p_1^2}{2m} + V(\mathbf{r}_1) \quad (17.15)$$

has one-electron solutions $\psi_0(\mathbf{r}_1)$, $\psi_1(\mathbf{r}_1)$, etc. Thus the solutions of the many-electron problem can be expanded in terms of products of the one-electron wave functions for the Hamiltonian in (17.15). Below, we write down the ground state many-electron wave function formed by putting all electrons in the ground state, and the lowest excited states are formed by putting one electron in an excited state.

Since electrons are Fermions, we present the discussion more generally in terms of particles. We will first consider the ground state of lowest energy which is a fully symmetric state with Γ_1^s symmetry. Every n -particle (electron) system also has one fully antisymmetric state with Γ_1^a symmetry. Because of the Pauli principle, we know that every allowed Fermion state must have Γ_1^a symmetry and thus we always look for the product of orbital and spin states that transform as Γ_1^a .

Ground State: (Boson gas)

The many-particle ground state wave function Ψ_0 is found by putting all the particles into the one-particle ground state:

$$\Psi_0 = \psi_0(\mathbf{r}_1)\psi_0(\mathbf{r}_2)\dots\psi_0(\mathbf{r}_n) \rightarrow \Gamma_1^s \quad (17.16)$$

and from a group theoretical point of view, this orbital state transforms at the totally symmetric representation Γ_1^s .

Single Excitation: (e.g., “phonons” or “magnons”)

To form the first excited state, consider the functions g_i found by placing the i th particle in the first excited state $\psi_1(\mathbf{r}_i)$:

$$\begin{aligned} \psi_1(\mathbf{r}_1)\psi_0(\mathbf{r}_2)\dots\psi_0(\mathbf{r}_n) &= g_1, \\ \psi_0(\mathbf{r}_1)\psi_1(\mathbf{r}_2)\dots\psi_0(\mathbf{r}_n) &= g_2, \\ &\vdots \\ \psi_0(\mathbf{r}_1)\psi_0(\mathbf{r}_2)\dots\psi_1(\mathbf{r}_n) &= g_n. \end{aligned} \quad (17.17)$$

The basis functions given by (17.17) transform as an n -dimensional reducible representation. Decomposition of this reducible representation yields

$$I_n(\text{reducible}) = \Gamma_1^s + \Gamma_{n-1},$$

where Γ_1^s refers to the totally symmetric representation, with basis functions is given by

$$\Psi'_{\Gamma_1^s} = \frac{1}{\sqrt{n}} \sum_{i=1}^n g_i \rightarrow \Gamma_1^s \quad (17.18)$$

and Γ_{n-1} is the $(n-1)$ dimensional irreducible representation, the basis functions depending on the ensemble of phase factors forming all possible n^{th} roots of unity

$$\Psi'_{\Gamma_{n-1}} = \left\{ \begin{array}{l} \frac{1}{\sqrt{n}} \sum_{i=1}^n \omega^{(i-1)} g_i \\ \frac{1}{\sqrt{n}} \sum_{i=1}^n \omega^{2(i-1)} g_i \\ \vdots \\ \frac{1}{\sqrt{n}} \sum_{i=1}^n \omega^{n(i-1)} g_i \end{array} \right\} \rightarrow \Gamma_{n-1} \quad (17.19)$$

where ω are phase factors given by $\omega = e^{2\pi i/n}$. For the special case $n = 2$, where $\omega = -1$, we obtain

$$\Psi'_{\Gamma_1=\Gamma_1^a} = \frac{1}{\sqrt{2}} [\psi_1(r_1)\psi_0(r_2) - \psi_0(r_1)\psi_1(r_2)].$$

For the case $n = 3$, where $\omega = e^{2\pi i/3}$, we obtain

$$\begin{aligned} \Psi'_{\Gamma_2} = \frac{1}{\sqrt{3}} & \{ \psi_1(r_1)\psi_0(r_2)\psi_0(r_3) + \omega\psi_0(r_1)\psi_1(r_2)\psi_0(r_3) \\ & + \omega^2\psi_0(r_1)\psi_0(r_2)\psi_1(r_3) \} \end{aligned}$$

and its partner

$$\begin{aligned} \Psi''_{\Gamma_2} = \frac{1}{\sqrt{3}} & (\psi_1(r_1)\psi_0(r_2)\psi_0(r_3) + \omega^2\psi_0(r_1)\psi_1(r_2)\psi_0(r_3) \\ & + \omega\psi_0(r_1)\psi_0(r_2)\psi_1(r_3)) \end{aligned}$$

for the two-dimensional irreducible representation.

The $(n-1)$ cyclic permutations $(1)(23\dots n)$, $(1)(n23\dots (n-1))$, \dots all commute with each other. Hence the eigenfunctions can be chosen so that these matrices are brought into diagonal form. This means that the $(n-1)$ diagonal terms become eigenvalues, given by

$$e^{\frac{2\pi i}{n}(\frac{n-2}{2})}, \dots, e^{\frac{-2\pi i}{n}(\frac{n-2}{2})}.$$

This Γ_{n-1} irreducible representation is present in every permutation group $P(n)$.

Irreducible Representation Γ_1^a . Also present in every permutation group is a one-dimensional irreducible representation Γ_1^a which is totally antisymmetric and Γ_1^a can be found from the regular representation which contains every irreducible representation (see Sect. 3.7) of the group in accordance with its dimensionality.

Regular Representation. Since all n electrons are in distinct states, they have different eigenfunctions. The Slater determinant (Sect. 17.1) formed from these eigenfunctions is distinct, and does not vanish. Furthermore the Slater determinant forms the basis function for the antisymmetric representation Γ_1^a . For the case where all n one-electron functions are distinct, the $n!$ functions form a regular representation of the permutation group, and the character for the identity element for the regular representation is the order of the group and according to (3.42) we have

$$\chi^{\text{regular}} = \sum_j^n \ell_j \chi^{\Gamma_j} = h = n!, \quad (17.20)$$

where ℓ_j is the dimension of the irreducible representation Γ_j and each representation occurs a number of times which is equal to the dimension of the representation, and h is the order of the group $= n!$.

17.4 Pauli Principle in Atomic Spectra

We will in the following subsections of this section apply the results in Sect. 17.3 to specify the symmetry of many-body wave-functions formed by two electrons, three electrons, etc. For each case, we will point out the states corresponding to the representations Γ_1^s , Γ_1^a , and Γ_{n-1} discussed in Sect. 17.3.

17.4.1 Two-Electron States

For the case of two electrons, the use of group theory is not especially needed for selecting the proper linear combinations of wave functions. The same results can be found just from consideration of even and odd states, since there are only two classes and two irreducible representations for $P(2)$. We discuss this case here largely for review and pedagogic reasons. The Slater determinant for the two-electron problem can be written as

$$\Psi(\mathbf{x}_1, \mathbf{x}_2) = \frac{1}{\sqrt{2}} \begin{vmatrix} \psi_1(\mathbf{r}_1, \sigma_1) & \psi_1(\mathbf{r}_2, \sigma_2) \\ \psi_2(\mathbf{r}_1, \sigma_1) & \psi_2(\mathbf{r}_2, \sigma_2) \end{vmatrix}, \quad (17.21)$$

where $\Psi(\mathbf{x}_1, \mathbf{x}_2)$ denotes the many-electron wave function for the case of two electrons. The wave-functions $\psi_i(\mathbf{r}_j, \sigma_j)$, $j = 1, 2$ denote the one-electron wave functions with each electron having spatial \mathbf{r}_j and spin σ_j coordinates. The subscript i ($i = 1, 2$) refers to two distinct electron states that obey the Pauli Principle. We use the vector \mathbf{x}_i to denote both the orbital and spin variables (\mathbf{r}_i, σ_i) . The two electron state defined by the Slater determinant in (17.21) has Γ_1^a symmetry.

The lowest energy state for the two-electron problem is achieved by putting both electrons in $1s$ orbital states, taking the *symmetric* (s) linear combination of spatial orbitals and taking the spins antiparallel. This choice provides two different states for the two electrons by the Pauli Principle, and minimizes the energy. Multiplying out the Slater determinant in this case yields

$$\Psi(1, 2) = \frac{1}{\sqrt{2}} \psi_s^{1s}(1) \psi_s^{1s}(2) [\alpha_1 \beta_2 - \alpha_2 \beta_1], \quad (17.22)$$

where the spin up state is denoted by α or \uparrow and the spin down state by β , or \downarrow , and $\Psi(1, 2)$ denotes the two-electron ground state. The function $[\alpha_1 \beta_2 - \alpha_2 \beta_1]$ denotes the antisymmetric spin function where the subscripts refer to the individual electrons.

Let us now consider the transformation properties of these two electrons more generally, including their excited states. The possible spin states for two electrons are $S = 0, 1$ where capital S denotes the total spin for the many electron system. The phase factor for the two-electron problem is $\omega = e^{2\pi i/2} = -1$ so that the linear combinations simply involve ± 1 . For the two-electron problem we can form a symmetric and an antisymmetric combination of α and β as given in Table 17.2.

Table 17.2. Transformation properties of two-electron states under permutations

| configuration | state | irreducible representations | allowed states |
|---|---------|-----------------------------|----------------|
| $(\alpha_1\beta_2 - \beta_1\alpha_2)/\sqrt{2}$ | $S = 0$ | Γ_1^a | |
| $(\alpha_1\alpha_2 + \alpha_2\alpha_1)/\sqrt{2}, \dots$ | $S = 1$ | Γ_1^s | |
| s^2 | $L = 0$ | Γ_1^s | 1S |
| $1s2s$ | $L = 0$ | $\Gamma_1^s + \Gamma_1^a$ | $^1S, ^3S$ |
| sp | $L = 1$ | $\Gamma_1^s + \Gamma_1^a$ | $^1P, ^3P$ |
| p^2 | $L = 0$ | Γ_1^s | 1S |
| p^2 | $L = 1$ | Γ_1^a | 3P |
| p^2 | $L = 2$ | Γ_1^s | 1D |
| pd | $L = 1$ | $\Gamma_1^s + \Gamma_1^a$ | $^1P + ^3P$ |
| pd | $L = 2$ | $\Gamma_1^s + \Gamma_1^a$ | $^1D + ^3D$ |
| pd | $L = 3$ | $\Gamma_1^s + \Gamma_1^a$ | $^1F + ^3F$ |
| d^2 | $L = 0$ | Γ_1^s | 1S |
| d^2 | $L = 1$ | Γ_1^a | 3P |
| d^2 | $L = 2$ | Γ_1^s | 1D |
| d^2 | $L = 3$ | Γ_1^a | 3F |
| d^2 | $L = 4$ | Γ_1^s | 1G |
| f^2 | $L = 0$ | Γ_1^s | 1S |
| f^2 | $L = 1$ | Γ_1^a | 3P |
| f^2 | $L = 2$ | Γ_1^s | 1D |
| f^2 | $L = 3$ | Γ_1^a | 3F |
| f^2 | $L = 4$ | Γ_1^s | 1G |
| f^2 | $L = 5$ | Γ_1^a | 3H |
| f^2 | $L = 6$ | Γ_1^s | 1I |

The symmetries of the irreducible representations of the permutation group $P(2)$ label the various spin and orbital angular momentum states. To obtain states allowed by the Pauli Principle, the direct product of the symmetries between the orbital and spin states must contain Γ_1^a

For the antisymmetric combination ($S = 0$) as in (17.22), we can have only $M_S = 0$ and the corresponding linear combination of spin states is given in Table 17.2. For the symmetric spin combination ($S = 1$), we can have three linear combinations. Only the $M_S = 1$ combination $(\alpha_1\alpha_2 + \alpha_2\alpha_1)/\sqrt{2}$ is listed explicitly in Table 17.2. The $M_S = 0$ combination $(\alpha_1\beta_2 + \beta_1\alpha_2)/\sqrt{2}$ and the $M_S = -1$ combination $(\beta_1\beta_2 + \beta_2\beta_1)/\sqrt{2}$ do not appear in the table.

We also make entries in Table 17.2 for the symmetries of the orbital angular momentum states. If the two electrons are in the same symmetric orbital s

state ($L = 0$), then the spin functions must transform as an antisymmetric linear combination Γ_1^a in Table 17.2 and corresponding to the spectroscopic notation 1S as in (17.22). However, if the two s electrons have different principal quantum numbers, then we can make both a symmetric and an antisymmetric combination of orbital states, as is illustrated here for the two electrons occupying $1s$ and $2s$ states, where the symmetric and antisymmetric combinations are

$$(\psi_{1s}(\mathbf{r}_1)\psi_{2s}(\mathbf{r}_2) + \psi_{1s}(\mathbf{r}_2)\psi_{2s}(\mathbf{r}_1))/\sqrt{2},$$

which transforms as Γ_1^s and

$$(\psi_{1s}(\mathbf{r}_1)\psi_{2s}(\mathbf{r}_2) - \psi_{1s}(\mathbf{r}_2)\psi_{2s}(\mathbf{r}_1))/\sqrt{2},$$

which transforms as Γ_1^a . Because of the Pauli principle, the orbital Γ_1^s combination goes with the Γ_1^a spin state leading to an 1S level, while the Γ_1^a orbital state goes with the Γ_1^s spin state leading to an 3S level (see Table 17.2). The state with Γ_{n-1} symmetry will be a one-dimensional representation also, but we already have two one-dimensional representations and there can be no more than two irreducible representations for $P(2)$ because we have only two classes.

We now consider the next category of entries in Table 17.2. If one electron is in an s state and the second is in a p state (configuration labeled sp), the total L value must be $L = 1$. We however have two choices for the orbital states: a symmetric Γ_1^s state or an antisymmetric Γ_1^a state. The symmetric combination of orbital wave functions (Γ_1^s) must then correspond to the $S = 0$ antisymmetric spin state (Γ_1^a), resulting in the 1P level, whereas the antisymmetric orbital combination (transforming as Γ_1^a) goes with the symmetric triplet Γ_1^s spin state and yields the 3P level (see Table 17.2).

Placing two electrons in p states with the same principal quantum number (configuration p^2 in Table 17.2) allows for a total angular momentum of $L = 0$ (which must have Γ_1^s symmetry), of $L = 1$ (with Γ_1^a symmetry) and of $L = 2$ (again with Γ_1^s symmetry). Each p electron can be in one of the three orbital states (p^+, p^0, p^-), corresponding to $m_l = 1, 0, -1$, respectively, for each one-electron state. Combining the p^+p^+ product yields an $M_L = 2$ state which belongs exclusively to the $L = 2$ multiplet, whereas combining the p^+p^0 states symmetrically yields the $M_L = 1$ state of the $L = 2$ multiplet. We use the notation p^+p^0 to denote $\psi_{p^+}(\mathbf{r}_1)\psi_{p^0}(\mathbf{r}_2)$. However, combining p^+p^0 antisymmetrically yields the $M_L = 1$ state of the $L = 1$ multiplet. The formation of the two-electron states for the various L and M_L values occurring for the p^2 configuration is given below. Since the orbital functions for the $L = 1$ state transform as Γ_1^a the spin functions transform as Γ_1^s and the $L = 1$ multiplet is a triplet spin state 3P . The $L = 0$ and $L = 2$ states both transform as Γ_1^s and thus the allowed spin states must be the singlet spin state $S = 0$ (see Table 17.2).

The wave functions for the p^2 configuration sketched above can be found in many standard quantum mechanics text books and are:

$L = 2$ symmetry (Γ_1^s) going with Γ_1^a for the spins to yield a 1D state.

$$\begin{aligned}\Psi(L = 2, M_L = 2) &= (p^+p^+) \\ \Psi(L = 2, M_L = 1) &= (p^0p^+ + p^+p^0)/\sqrt{2} \\ \Psi(L = 2, M_L = 0) &= [(p^0p^0) + (p^+p^- + p^-p^+)/\sqrt{2}]/\sqrt{2} \\ \Psi(L = 2, M_L = -1) &= (p^0p^- + p^-p^0)/\sqrt{2} \\ \Psi(L = 2, M_L = -2) &= (p^-p^-).\end{aligned}\quad (17.23)$$

$L = 1$ symmetry (Γ_1^a) going with a symmetric spin state (Γ_1^s) to yield a 3P state.

$$\begin{aligned}\Psi(L = 1, M_L = 1) &= (p^0p^+ - p^+p^0)/\sqrt{2} \\ \Psi(L = 1, M_L = 0) &= (p^+p^- - p^-p^+)/\sqrt{2} \\ \Psi(L = 1, M_L = -1) &= (p^0p^- - p^-p^0)/\sqrt{2}.\end{aligned}\quad (17.24)$$

$L = 0$ symmetry (Γ_1^s) going with an antisymmetric spin state (Γ_1^a) to yield a 1S state.

$$\Psi(L = 0, M_L = 0) = [(p^0p^0) - (p^+p^- + p^-p^+)/\sqrt{2}]/\sqrt{2}. \quad (17.25)$$

Following this explanation for the p^2 configuration, the reader can now fill in the corresponding explanations for the states formed from two-electron states derived from the pd , d^2 or f^2 configurations listed in Table 17.2.

17.4.2 Three-Electron States

For the case of three electrons, the use of group theory becomes more important. In this case we have the permutation group of three objects $P(3)$ which has six elements, three classes and three irreducible representations (see Table 17.3). In the extended character table above, we label the class

Table 17.3. Extended character table for permutation group $P(3)$

| | $\chi(E)$ | $\chi(A, B, C)$ | $\chi(D, F)$ | |
|---|-----------|-----------------|--------------|---|
| $P(3)$ | (1^3) | $3(2, 1)$ | $2(3)$ | |
| Γ_1^s | 1 | 1 | 1 | |
| Γ_1^a | 1 | -1 | 1 | |
| Γ_2 | 2 | 0 | -1 | |
| $\Gamma_{\text{perm.}}(\psi_1\psi_1\psi_1)$ | 1 | 1 | 1 | $\Rightarrow \Gamma_1^s$ |
| $\Gamma_{\text{perm.}}(\psi_1\psi_1\psi_2)$ | 3 | 1 | 0 | $\Rightarrow \Gamma_1^s + \Gamma_2$ |
| $\Gamma_{\text{perm.}}(\psi_1\psi_2\psi_3)$ | 6 | 0 | 0 | $\Rightarrow \Gamma_1^s + \Gamma_1^a + 2\Gamma_2$ |

(1^3) to denote the cyclic structure $(1)(2)(3)$ and class $(2, 1)$ to denote the cyclic structures $(1\ 2)(3)$, $(2)(1\ 3)$, $(1)(2\ 3)$, and class (3) to denote the cyclic structure $(1\ 2\ 3)$. The correspondence between the six symmetry elements E, A, B, C, D, F and these three classes is immediate and is given in the table explicitly. Also given below the character table are all the possible symmetries of the permutations for three-electron wave functions. Because of these additional listings, we call this an extended character table. The first permutation representation Γ_{perm} for the three-electron state would correspond to having all the same one-electron states $(\psi_1\psi_1\psi_1)$. This function is invariant under any of the six permutations of the group, so that all characters are one and the function $(\psi_1\psi_1\psi_1)$ transforms as Γ_1^s . In the second possible case, one of the electrons is in a different state $(\psi_1\psi_1\psi_2)$, and since there are three possible combinations that can be formed with the ψ_2 one-electron wave function, we have three distinct functions that can be obtained from permutation of the electrons. Hence $(\psi_1\psi_1\psi_2)$ transforms as a three-dimensional reducible representation of the permutation group $P(3)$ with three partners for this state. The identity operation leaves the three partners invariant so we get a character three. Each of the permutation operations $[3(2, 1)]$ leaves one of the partners invariant, so we get a character of one, while the cyclic permutations change all partners yielding a character of zero. The reduction of this reducible representation to its irreducible components yields $\Gamma_1^s + \Gamma_2$ as indicated on the table. Finally, we consider the case when all three electrons are in different states $(\psi_1\psi_2\psi_3)$. This choice gives rise to six partners, and it is only the identity operation which leaves the partners $(\psi_1\psi_2\psi_3)$ invariant. This reducible representation [like the regular representation can be expressed in terms of its irreducible constituents using the relation $h = \sum_i (\ell_i^2)$] contains $\Gamma_1^s + \Gamma_1^a + 2\Gamma_2$ as is expected for the regular representation. The equivalence principle is thus used to form reducible representations such as those for $P(3)$ given in Table 17.3. This table is also given in Appendix F as Table F.1.

Let us now look at the spin states that can be made from three electrons. Referring to Sect. 17.3 we can make a symmetric state

$$(\alpha_1\alpha_2\alpha_3)$$

with symmetry Γ_1^s that corresponds to the $S = 3/2$ and $M_S = 3/2$ spin state. To obtain the linear combination of spin states for the three other M_S values ($M_S = 1/2, -1/2, -3/2$), we must apply lowering operators to the $M_S = 3/2$ state $(\alpha_1\alpha_2\alpha_3)$. With regard to the $S = 1/2$ state, (17.17) tells us that this state is a two-dimensional representation with partners:

$$\Psi'_{\Gamma_2} = \begin{cases} (g_1 + \omega g_2 + \omega^2 g_3) \\ (g_1 + \omega^2 g_2 + \omega g_3), \end{cases} \quad (17.26)$$

where $\omega = \exp(2\pi i/3)$ and where the functions g_i are assembled by sequentially selecting the spin down state β at each of the sites 1, 2 or 3. This explains the first two entries in Table 17.4. The state Ψ'_{Γ_2} corresponds to the

Table 17.4. Transformation properties of three-electron states under permutations^(a)

| configuration | state | irreducible representation | allowed state |
|--------------------------------|-----------|--|----------------------|
| $(\uparrow\uparrow\downarrow)$ | $S = 1/2$ | Γ_2 | |
| $(\uparrow\uparrow\uparrow)$ | $S = 3/2$ | Γ_1^s | |
| s^3 | $L = 0$ | Γ_1^s | — |
| $1s^2 2s$ | $L = 0$ | $\Gamma_1^s + \Gamma_2$ | 2S |
| $s^2 p$ | $L = 1$ | $\Gamma_1^s + \Gamma_2$ | 2P |
| sp^2 | $L = 0$ | $\Gamma_1^s + \Gamma_2$ | 2S |
| sp^2 | $L = 1$ | $\Gamma_1^a + \Gamma_2$ | $^2P, ^4P$ |
| sp^2 | $L = 2$ | $\Gamma_1^s + \Gamma_2$ | 2D |
| $(2p)^2 (3p)$ | $L = 0$ | $\Gamma_1^a + \Gamma_2$ | $^2S, ^4S$ |
| $(2p)^2 (3p)$ | $L = 1$ | $2\Gamma_1^s + \Gamma_1^a + 3\Gamma_2$ | $^2P, ^2P, ^2P, ^4P$ |
| $(2p)^2 (3p)$ | $L = 2$ | $\Gamma_1^s + \Gamma_1^a + 2\Gamma_2$ | $^2D, ^2D, ^4D$ |
| $(2p)^2 (3p)$ | $L = 3$ | $\Gamma_1^s + \Gamma_2$ | 2F |
| p^3 | $L = 0$ | Γ_1^a | 4S |
| p^3 | $L = 1$ | $\Gamma_1^s + \Gamma_2$ | 2P |
| p^3 | $L = 2$ | Γ_2 | 2D |
| p^3 | $L = 3$ | Γ_1^s | — |
| d^3 | $L = 0$ | Γ_1^s | — |
| d^3 | $L = 1$ | $\Gamma_1^a + \Gamma_2$ | $^2P, ^4P$ |
| d^3 | $L = 2$ | $\Gamma_1^s + 2\Gamma_2$ | $^2D, ^2D$ |
| d^3 | $L = 3$ | $\Gamma_1^s + \Gamma_1^a + \Gamma_2$ | $^2F, ^4F$ |
| d^3 | $L = 4$ | $\Gamma_1^s + \Gamma_2$ | 2G |
| d^3 | $L = 5$ | Γ_2 | 2H |
| d^3 | $L = 6$ | Γ_1^s | — |
| f^3 | $L = 0$ | Γ_1^a | 4S |
| f^3 | $L = 1$ | $\Gamma_1^s + \Gamma_2$ | 2P |
| f^3 | $L = 2$ | $\Gamma_1^a + 2\Gamma_2$ | $^2D, ^2D, ^4D$ |
| f^3 | $L = 3$ | $2\Gamma_1^s + \Gamma_1^a + 2\Gamma_2$ | $^2F, ^2F, ^4F$ |
| f^3 | $L = 4$ | $\Gamma_1^s + \Gamma_1^a + 2\Gamma_2$ | $^2G, ^2G, ^4G$ |
| f^3 | $L = 5$ | $\Gamma_1^s + 2\Gamma_2$ | $^2H, ^2H$ |
| f^3 | $L = 6$ | $\Gamma_1^s + \Gamma_1^a + \Gamma_2$ | $^2I, ^4I$ |
| f^3 | $L = 7$ | $\Gamma_1^s + \Gamma_2$ | 2J |
| f^3 | $L = 8$ | Γ_2 | 2K |
| f^3 | $L = 9$ | Γ_1^s | — |

(a) The symmetries of the irreducible representations of the permutation group $P(3)$ label the various spin and orbital angular momentum states. To obtain the states allowed by the Pauli Principle, the direct product of the symmetries between the orbital and spin states must contain Γ_1^a

state with Γ_{n-1} symmetry in Table 17.4. Using the g_1 , g_2 , and g_3 functions we can write the state with Γ_1^s symmetry as

$$\Psi'_{\Gamma_1^s} = \frac{1}{\sqrt{3}}(g_1 + g_2 + g_3) \quad (17.27)$$

and the state with Γ_1^a symmetry as the Slater determinant

$$\Psi'_{\Gamma_1^a} = \frac{1}{\sqrt{3}} \begin{vmatrix} g_1(x_1) & g_1(x_2) & g_1(x_3) \\ g_2(x_1) & g_2(x_2) & g_2(x_3) \\ g_3(x_1) & g_3(x_2) & g_3(x_3) \end{vmatrix}. \quad (17.28)$$

Now let us examine the spatial states. Putting all three electrons in the same s state would yield a state with $L = 0$, $M_L = 0$ and having Γ_1^s symmetry. Taking the direct product between Γ_1^s for the orbital $L = 0$ state and either of the spin states $\Gamma_1^s \otimes (\Gamma_1^s + \Gamma_2)$ does not yield a state with Γ_1^a symmetry, and therefore the s^3 configuration is not allowed because of the Pauli principle. This is a group theoretical statement of the fact that a particular s level can only accommodate one spin up and one spin down electron. If now one of the electrons is promoted to a $2s$ state, then we can make an Γ_1^s state and a Γ_2 state in accordance with Sect. 17.3 and with the character table for $P(3)$ in Table 17.3, taking $g_1 = \psi_{2s}(\mathbf{r}_1)\psi_{1s}(\mathbf{r}_2)\psi_{1s}(\mathbf{r}_3)$, etc. and forming states such as given in (17.18) and (17.19). The direct product

$$\Gamma_2 \otimes \Gamma_2 = \Gamma_1^s + \Gamma_1^a + \Gamma_2$$

then ensures that a state with Γ_1^a symmetry can be assembled to satisfy the Pauli principle. Since the spin state with Γ_2 symmetry corresponds to a Pauli-allowed component $S = 1/2$, the allowed $1s^22s$ state will be a doublet 2S state as shown in Table 17.4. Similar arguments apply to the formation of s^2p states with $L = 1$.

For the sp^2 configuration the orbital angular momentum can be $L = 0$, $L = 1$ and $L = 2$. This corresponds to $(2 \times 6 \times 6 = 72)$ possible states in the multiplet. We show below using the Pauli principle and group theory arguments that the number of allowed states is 30. The spatial states for the sp^2 configuration with $L = 2$ are formed from products of the type sp^+p^+ for the $M_L = 2$ state (see (17.23)–(17.25)). Once again from the character table (Table 17.3) for $P(3)$, the symmetries which are contained in the three-electron wave function sp^+p^+ (denoting $\psi_s(\mathbf{r}_1)\psi_{p^+}(\mathbf{r}_2)\psi_{p^+}(\mathbf{r}_3)$) are Γ_1^s and Γ_2 just as was obtained for the $1s^22s$ configuration. The only possible allowed state for $L = 2$ has $S = 1/2$ which results in the 2D state listed in the table. The $M_L = 1$ states are linear combinations of the sp^+p^0 functions which have the symmetries $\Gamma_1^s + \Gamma_1^a + 2\Gamma_2$, since this case corresponds to $(\psi_1\psi_2\psi_3)$ in the character table. Of these symmetry types, the $\Gamma_1^s + \Gamma_2$ states are associated with the $M_L = 1$ state of the $L = 2$ multiplet, since the irreducible representation is specified by the quantum number L and the M_L only specify the partners

of that irreducible representation. After this subtraction has been performed the symmetry types $\Gamma_1^a + \Gamma_2$ for the $L = 1$, $M_L = 1$ level are obtained.

Referring to Table 17.4, the symmetry for the $L = 0$ state of the sp^2 configuration could arise from a sp^0p^0 state which is of the $(\psi_1\psi_1\psi_2)$ form and therefore transforms according to $\Gamma_1^s + \Gamma_2$ symmetry (see the character table (Table 17.3) for $P(3)$). These orbital states go with the spin states Γ_1^a .

For the $L = 1$ state, the orbital Γ_1^a irreducible representation goes with the Γ_1^s spin 3/2 state to give rise to a quartet 4P state while the Γ_2 orbital state can only go with the Γ_2 spin state to give a Γ_1^a state when taking the direct product of the symmetries of the orbital and spin states ($\Gamma_2 \otimes \Gamma_2$). The case of the p^3 configuration is an instructive example where we can see how group theory can be used to simplify the analysis of the symmetries of multi-electron states. As the number of electrons increases, the use of group theory becomes essential to keep track of the symmetries that are possible by the addition of angular momentum and the symmetries that are allowed by the Pauli principle. For the p^3 configuration, we can have a total of $6 \times 6 \times 6 = 216$ states. We will show below that if all electrons have the same principal quantum number, only 20 of these states are allowed by the Pauli principle and we will here classify their symmetry types.

For the p^3 configuration we can have $L = 3, 2, 1$ and 0 total orbital angular momentum states. In the discussion that follows we will assume that all electrons have the same principal quantum number (e.g., $2p^3$). For the $L = 3$ state to be allowed, we must be able to put all three electrons into a $(p^+p^+p^+)$ state to make the $M_L = 3$ state. From the extended character table (Table 17.3) for $P(3)$, we see that $L = 3$ must transform as Γ_1^s . Since the direct product of the orbital and spin states $\Gamma_1^s \otimes (\Gamma_1^s + \Gamma_2)$ does not contain Γ_1^a this state is not allowed. The $L = 2$ multiplet is constructed from an $M_L = 2$ state having $p^+p^+p^0$ combinations which from the character table (Table 17.3) for $P(3)$ transform as $\Gamma_1^s + \Gamma_2$. Since $M_L = 2$ also contributes to the $L = 3$ state with symmetry Γ_1^s , we must subtract Γ_1^s from $\Gamma_1^s + \Gamma_2$ to get the symmetry Γ_2 for the $L = 2$ state. If we take a direct product of the orbital and spin states for this case, we obtain

$$\Gamma_2 \otimes (\Gamma_1^s + \Gamma_2) = \Gamma_1^s + \Gamma_1^a + 2\Gamma_2,$$

but it is only the direct product $\Gamma_2 \otimes \Gamma_2$ which contributes a state with Γ_1^a symmetry that is allowed by the Pauli principle. Thus only the 2D state is symmetry-allowed as indicated in Table 17.4. To get the symmetry of the $L = 1$ state, consider the combinations $p^+p^0p^0$ and $p^+p^+p^-$ which contribute to the $M_L = 1$ state. In this case the $M_L = 1$ state contains irreducible representations $2(\Gamma_1^s + \Gamma_2)$. Since $M_L = 1$ also appears for $L = 2$ and $L = 3$, we need to subtract $(\Gamma_1^s + \Gamma_2)$ to obtain $(\Gamma_1^s + \Gamma_2)$ for the symmetries of the orbital $L = 1$ state (see Table 17.4). For the $M_L = 0$ levels we have the combinations $p^0p^0p^0$ and $p^+p^-p^0$, the first transforming as Γ_1^s and the second as $\Gamma_1^s + \Gamma_1^a + 2\Gamma_2$ to give a total of $2\Gamma_1^s + \Gamma_1^a + 2\Gamma_2$. However $M_L = 0$ is also present in the $L = 3, 2$ and 1 multiplets, so we must subtract the irreducible

representations $(\Gamma_1^s) + (\Gamma_2) + (\Gamma_1^s + \Gamma_2)$ to obtain Γ_1^a for the $L = 0$ state. For an orbital angular momentum with symmetry Γ_1^a , it is only the $S = 3/2$ Γ_1^s spin state that is allowed by the Pauli principle (see Table 17.4).

The same procedure can be used to obtain all the other entries in Table 17.4, as well as the many three-electron states not listed. As the angular momentum increases (e.g., for the case of d^3 or f^3 configurations), group theoretical concepts become increasingly important.

17.4.3 Four-Electron States

In consideration of the four-electron problem we must consider the permutation group $P(4)$. The character table for the group $P(4)$ is given in Table 17.5 and also in Table F.2. The irreducible representations are denoted by subscripts referring to their dimensionality. Also shown in Table 17.5 are the transformation properties for the various products of functions. These transformation properties are obtained in the same way as for the case of the group $P(3)$ discussed in Sect. 17.4.2. The various four-electron states of a free ion or atom that are consistent with the Pauli principle are formed with the help of this extended character table.

We first consider the possible spin states for the four-electron configuration. The transformation of the spin states under the operations of the permutation group are shown in Table 17.6. The four spins can be arranged to give a total spin of $S = 2$, $S = 1$ and $S = 0$. The representation for the fully symmetric ($\alpha_1\alpha_2\alpha_3\alpha_4$) state, which appears in Table 17.5 as $\Gamma_{\text{perm.}}(\psi_1\psi_1\psi_1\psi_1)$, has $S = 2$ and clearly transforms as Γ_1^s . The $S = 1$ state is formed from a combination ($\alpha_1\alpha_2\alpha_3\beta_4$) with $M_S = 1$ and the product wave-function is of the form $(\psi_1\psi_1\psi_1\psi_2)$, which from the extended character table in Table 17.5 transforms as $\Gamma_1^s + \Gamma_3$. But $M_S = 1$ also contributes to the $S = 2$ state which transforms as Γ_1^s . Thus by subtraction, $S = 1$ transforms as Γ_3 . Likewise, the $S = 0$

Table 17.5. Extended character table for group $P(4)$

| $P(4)$ | (1^4) | $8(3, 1)$ | $3(2^2)$ | $6(2, 1^2)$ | $6(4)$ |
|---|---------|-----------|----------|-------------|--|
| Γ_1^s | 1 | 1 | 1 | 1 | 1 |
| Γ_1^a | 1 | 1 | 1 | -1 | -1 |
| Γ_2 | 2 | -1 | 2 | 0 | 0 |
| Γ_3 | 3 | 0 | -1 | 1 | -1 |
| $\Gamma_{3'}$ | 3 | 0 | -1 | -1 | 1 |
| $\Gamma_{\text{perm.}}(\psi_1\psi_1\psi_1\psi_1)$ | 1 | 1 | 1 | 1 | $1 \Rightarrow \Gamma_1^s$ |
| $\Gamma_{\text{perm.}}(\psi_1\psi_1\psi_1\psi_2)$ | 4 | 1 | 0 | 2 | $0 \Rightarrow \Gamma_1^s + \Gamma_3$ |
| $\Gamma_{\text{perm.}}(\psi_1\psi_1\psi_2\psi_2)$ | 6 | 0 | 2 | 2 | $0 \Rightarrow \Gamma_1^s + \Gamma_2 + \Gamma_3$ |
| $\Gamma_{\text{perm.}}(\psi_1\psi_1\psi_2\psi_3)$ | 12 | 0 | 0 | 2 | $0 \Rightarrow \Gamma_1^s + \Gamma_2 + 2\Gamma_3 + \Gamma_{3'}$ |
| $\Gamma_{\text{perm.}}(\psi_1\psi_2\psi_3\psi_4)$ | 24 | 0 | 0 | 0 | $0 \Rightarrow \Gamma_1^s + \Gamma_1^a + 2\Gamma_2 + 3\Gamma_3 + 3\Gamma_{3'}$ |

Table 17.6. Transformation properties of four-electron states under permutations^(a)

| configu- ration | state | irreducible representation | allowed state |
|--|----------|---|-------------------------------------|
| $(\uparrow\uparrow\downarrow\downarrow)$ | $S = 0$ | Γ_2 | — |
| $(\uparrow\uparrow\uparrow\downarrow)$ | $S = 1$ | Γ_3 | — |
| $(\uparrow\uparrow\uparrow\uparrow)$ | $S = 2$ | Γ_1^s | — |
| s^4 | $L = 0$ | Γ_1^s | — |
| $1s^3 2s$ | $L = 0$ | $\Gamma_1^s + \Gamma_3$ | — |
| $1s^2 2s^2$ | $L = 0$ | $\Gamma_1^s + \Gamma_2 + \Gamma_3$ | 1S |
| sp^3 | $L = 0$ | $\Gamma_1^a + \Gamma_3'$ | $^3S, ^5S$ |
| sp^3 | $L = 1$ | $\Gamma_1^s + \Gamma_2 + 2\Gamma_3 + \Gamma_3'$ | $^1P, ^3P$ |
| sp^3 | $L = 2$ | $\Gamma_2 + \Gamma_3 + \Gamma_3'$ | $^1D, ^3D$ |
| sp^3 | $L = 3$ | $\Gamma_1^s + \Gamma_3$ | — |
| $(2p)^3 (3p)$ | $L = 0$ | $\Gamma_1^s + \Gamma_2 + 2\Gamma_3 + \Gamma_3'$ | $^1S, ^3S$ |
| $(2p)^3 (3p)$ | $L = 1$ | $\Gamma_1^s + \Gamma_1^a + 2\Gamma_2 + 3\Gamma_3 + 3\Gamma_3'$ | $^1P, ^1P, ^3P, ^3P, ^3P, ^5P$ |
| $(2p)^3 (3p)$ | $L = 2$ | $2\Gamma_1^s + 2\Gamma_2 + 4\Gamma_3 + 2\Gamma_3'$ | $^1D, ^1D, ^3D, ^3D$ |
| $(2p)^3 (3p)$ | $L = 3$ | $\Gamma_1^s + \Gamma_2 + 2\Gamma_3 + \Gamma_3'$ | $^1F, ^3F$ |
| $(2p)^3 (3p)$ | $L = 4$ | $\Gamma_1^s + \Gamma_3$ | — |
| p^4 | $L = 0$ | $\Gamma_1^s + \Gamma_2$ | 1S |
| p^4 | $L = 1$ | $\Gamma_3 + \Gamma_3'$ | 3P |
| p^4 | $L = 2$ | $\Gamma_1^s + \Gamma_2 + \Gamma_3$ | 1D |
| p^4 | $L = 3$ | Γ_3 | — |
| p^4 | $L = 4$ | Γ_1^s | — |
| d^4 | $L = 0$ | $\Gamma_1^s + 2\Gamma_2$ | $^1S, ^1S$ |
| d^4 | $L = 1$ | $2\Gamma_3 + 2\Gamma_3'$ | $^3P, ^3P$ |
| d^4 | $L = 2$ | $2\Gamma_1^s + \Gamma_1^a + 2\Gamma_2 + 2\Gamma_3 + \Gamma_3'$ | $^1D, ^1D, ^3D, ^5D$ |
| d^4 | $L = 3$ | $\Gamma_2 + 3\Gamma_3 + 2\Gamma_3'$ | $^1F, ^3F, ^3F$ |
| d^4 | $L = 4$ | $2\Gamma_1^s + 2\Gamma_2 + 2\Gamma_3 + \Gamma_3'$ | $^1G, ^1G, ^3G$ |
| d^4 | $L = 5$ | $\Gamma_1^s + 2\Gamma_3 + \Gamma_3'$ | 3H |
| d^4 | $L = 6$ | $\Gamma_1^s + \Gamma_2 + \Gamma_3$ | 1I |
| d^4 | $L = 7$ | Γ_3 | — |
| d^4 | $L = 8$ | Γ_1^s | — |
| f^4 | $L = 0$ | $2\Gamma_1^s + \Gamma_1^a + 3\Gamma_3$ | 5S |
| f^4 | $L = 1$ | $2\Gamma_2 + 3\Gamma_3 + 3\Gamma_3'$ | $^1P, ^1P, ^3P, ^3P, ^3P$ |
| f^4 | $L = 2$ | $2\Gamma_1^s + \Gamma_1^a + 4\Gamma_2 + 3\Gamma_3 + 2\Gamma_3'$ | $^1D, ^1D, ^1D, ^1D, ^3D, ^3D, ^5D$ |
| f^4 | $L = 3$ | $\Gamma_1^s + \Gamma_1^a + \Gamma_2 + 5\Gamma_3 + 4\Gamma_3'$ | $^1F, ^3F, ^3F, ^3F, ^3F, ^5F$ |
| f^4 | $L = 4$ | $3\Gamma_1^s + \Gamma_1^a + 4\Gamma_2 + 4\Gamma_3 + 3\Gamma_3'$ | $^1G, ^1G, ^1G, ^3G, ^3G, ^3G, ^5G$ |
| f^4 | $L = 5$ | $\Gamma_1^s + 2\Gamma_2 + 5\Gamma_3 + 4\Gamma_3'$ | $^1H, ^1H, ^3H, ^3H, ^3H$ |
| f^4 | $L = 6$ | $3\Gamma_1^s + \Gamma_1^a + 3\Gamma_2 + 4\Gamma_3 + 2\Gamma_3'$ | $^1I, ^1I, ^1I, ^3I, ^3I, ^5I$ |
| f^4 | $L = 7$ | $\Gamma_1^s + \Gamma_2 + 4\Gamma_3 + 2\Gamma_3'$ | $^1J, ^3J, ^3J$ |
| f^4 | $L = 8$ | $2\Gamma_1^s + 2\Gamma_2 + 2\Gamma_3 + \Gamma_3'$ | $^1K, ^1K, ^3K$ |
| f^4 | $L = 9$ | $\Gamma_1^s + 2\Gamma_3 + \Gamma_3'$ | 3L |
| f^4 | $L = 10$ | $\Gamma_1^s + \Gamma_2 + \Gamma_3$ | 1M |
| f^4 | $L = 11$ | Γ_3 | — |
| f^4 | $L = 12$ | Γ_1^s | — |

(a) The symmetries of the irreducible representations of the permutation group $P(4)$ label the various spin and orbital angular momentum states. To obtain the states allowed by the Pauli Principle the direct product of the symmetries between the orbital and spin states must contain Γ_1^a

state is formed from a configuration $(\alpha_1\alpha_2\beta_3\beta_4)$ with $M_S = 0$ which from the extended character Table 17.5 is of the form $(\psi_1\psi_1\psi_2\psi_2)$ and transforms as $\Gamma_1^s + \Gamma_2 + \Gamma_3$. Upon subtraction of the symmetry types for the $S = 1$ and $S = 2$ states $(\Gamma_3 + \Gamma_1^s)$, we obtain the symmetry Γ_2 for the $S = 0$ state, as shown in Table 17.6. This completes the discussion for the spin entries to Table 17.6.

The allowed states resulting from the s^4 , $1s^32s$ and $1s^22s^2$ orbital states follow from the discussion in Sect. 17.4.2. Some similarity is also found for the sp^3 states in Table 17.6. We now illustrate the four-electron problem with the p^4 electron configuration, assuming the same principal quantum number for all four electrons as for example in a $(2p^4)$ state. Here we can have $L = 4, 3, 2, 1$ and 0 (see Table 17.6). Starting with the $L = 4$ multiplet, the $M_L = 4$ state $p^+p^+p^+p^+$ would have Γ_1^s symmetry. This state is forbidden by the Pauli principle since the direct product of the orbital and spin states $\Gamma_1^s \otimes (\Gamma_1^s + \Gamma_2 + \Gamma_3)$ does not contain Γ_1^a symmetry. To find the symmetry for the $L = 3$ multiplet, we consider the $M_L = 3$ states which arise from a $p^+p^+p^+p^0$ configuration and from Table 17.5 (giving the character table for $P(4)$), we see that $(\psi_1\psi_1\psi_1\psi_2)$ contains the irreducible representations $\Gamma_1^s + \Gamma_3$. Thus subtracting Γ_1^s for the $L = 4$ state gives the symmetry Γ_3 for the $L = 3$ multiplet. The direct product of the orbital and spin states

$$\Gamma_3 \otimes (\Gamma_1^s + \Gamma_2 + \Gamma_3) = \Gamma_1^s + \Gamma_2 + 3\Gamma_3 + 2\Gamma_3'$$

again does not contain Γ_1^a and therefore is not allowed by the Pauli principle. However the $L = 2$ state is allowed and gives rise to a 1D level since $M_L = 2$ arises from $p^+p^+p^0p^0$ or $p^+p^+p^+p^-$ which, respectively, correspond to the symmetries

$$(\Gamma_1^s + \Gamma_2 + \Gamma_3) + (\Gamma_1^s + \Gamma_3) .$$

Thus subtracting the contributions of $M_L = 2$ to the $L = 3$ and $L = 4$ states gives $(\Gamma_1^a + \Gamma_2 + \Gamma_3)$. Now taking the direct product between the orbital and spin states

$$(\Gamma_1^s + \Gamma_2 + \Gamma_3) \otimes (\Gamma_1^s + \Gamma_2 + \Gamma_3) = 3\Gamma_1^s + \Gamma_1^a + 4\Gamma_2 + 5\Gamma_3 + 3\Gamma_3'$$

does contain the Γ_1^a symmetry arising from the direct product of $\Gamma_2 \otimes \Gamma_2$ and corresponding to the $S = 0$ spin state which is a singlet state. Likewise the symmetries of the 3P and 1S states for $L = 1$ and $L = 0$, respectively, can be found, and the results are given in Table 17.6. Since a p^4 electron configuration is equivalent to a p^2 hole configuration the allowed states for p^4 should be the same as for p^2 . This can be verified by comparing the allowed states for p^2 in Table 17.2 with those (1S , 3P , 1D) for p^4 in Table 17.6.

It is left to the reader to verify the other entries in Table 17.6 and to explore the symmetries of other four-electron combinations not listed. In finding these entries it should be noted that

$$\Gamma_2 \otimes \Gamma_2 = \Gamma_1^s + \Gamma_1^a + \Gamma_2$$

and

$$\Gamma_3 \otimes \Gamma_{3'} = \Gamma_1^a + \Gamma_2 + \Gamma_3 + \Gamma_{3'}$$

so that the spatial functions with Γ_1^a , Γ_2 and $\Gamma_{3'}$ all can give rise to states allowed by the Pauli principle.

17.4.4 Five-Electron States

The character table for the permutation group of five electrons is shown in Table F.3 of Appendix F. Note that there are no 2D or 3D irreducible representations, but rather there are four, five and six-dimensional irreducible representations, yielding $h = \sum l_i^2 = 120 = 5!$, as required. Also listed in Table F.3 of Appendix F are the characters for all possible distinct products of five functions considered within the equivalence representation. The irreducible representations of $P(5)$ contained in the decomposition of the reducible equivalence representation $\Gamma_{\text{perm.}}$ are listed below the character table for $P(5)$ (Table F.3 of Appendix F). With the help of these tables, the entries in Table 17.7 can be obtained for the spin and orbital symmetries for a number of the five-electron states that are listed in this table. The possible spin states are $S = 1/2$ which occurs ten times, the $S = 3/2$ which occurs five times and the $S = 5/2$ which occurs once. In making the antisymmetric combinations it should be noted that

$$\Gamma_4 \otimes \Gamma_{4'} = \Gamma_1^a + \Gamma_{4'} + \Gamma_{5'} + \Gamma_6 \quad \text{and}$$

$$\Gamma_5 \otimes \Gamma_{5'} = \Gamma_1^a + \Gamma_4 + \Gamma_{4'} + \Gamma_5 + \Gamma_{5'} + \Gamma_6,$$

so that the spatial functions with Γ_1^a , $\Gamma_{4'}$ and $\Gamma_{5'}$ may all give rise to states that are allowed by the Pauli Principle. Five-electron states occur in a half-filled d level. Such half-filled d levels are important in describing the magnetic ions in magnetic semiconductors formed by the substitution of Mn^{2+} for Cd in CdTe or CdSe .

17.4.5 General Comments on Many-Electron States

The Pauli-allowed states for n electrons in a more than half filled p shell and for $6 - n$ holes are the same. For example, referring to Table 17.7, the only Pauli-allowed state for p^5 is an $L = 1$, 2P state. But this state corresponds to a single hole in a p -shell, which has the same allowed angular momentum states as a single p electron ($S = 1/2$) in a p -shell. We can denote both of these states by p^1 corresponding to the level designation 2P . Using the same arguments, we find that p^2 and p^4 have the same allowed states. Similarly, the states for the d^6 electron configuration are identical to those for the d^4 hole configuration which are worked out in the

Table 17.7. Transformation properties of five-electron states under permutations^(a)

| configuration | state | irreducible representation | allowed state |
|--|-----------|--|----------------------|
| $(\uparrow\uparrow\uparrow\downarrow\downarrow)$ | $S = 1/2$ | Γ_5 | |
| $(\uparrow\uparrow\uparrow\downarrow\downarrow)$ | $S = 3/2$ | Γ_4 | |
| $(\uparrow\uparrow\uparrow\uparrow\downarrow)$ | $S = 5/2$ | Γ_1^s | |
| s^5 | $L = 0$ | Γ_1^s | — |
| $1s^4 2s$ | $L = 0$ | $\Gamma_1^s + \Gamma_4$ | — |
| $1s^2 2s^2 3s$ | $L = 0$ | $\Gamma_1^s + 2\Gamma_4 + 2\Gamma_5 + \Gamma_{5'} + \Gamma_6$ | 2S |
| p^5 | $L = 0$ | Γ_6 | — |
| p^5 | $L = 1$ | $\Gamma_1^s + \Gamma_4 + \Gamma_5 + \Gamma_{5'}$ | 2P |
| p^5 | $L = 2$ | $\Gamma_4 + \Gamma_5 + \Gamma_6$ | — |
| p^5 | $L = 3$ | $\Gamma_1^s + \Gamma_4 + \Gamma_5$ | — |
| p^5 | $L = 4$ | Γ_4 | — |
| p^5 | $L = 5$ | Γ_1^s | — |
| d^5 | $L = 0$ | $\Gamma_1^a + \Gamma_4 + \Gamma_{5'} + \Gamma_6$ | $^2S, ^6S$ |
| d^5 | $L = 1$ | $\Gamma_1^s + 2\Gamma_4 + \Gamma_{4'} + 3\Gamma_5 + \Gamma_{5'} + 2\Gamma_6$ | $^2P, ^4P$ |
| d^5 | $L = 2$ | $2\Gamma_1^s + 3\Gamma_4 + \Gamma_{4'} + 4\Gamma_5 + 3\Gamma_{5'} + 2\Gamma_6$ | $^2D, ^2D, ^2D, ^4D$ |
| d^5 | $L = 3$ | $\Gamma_1^s + 4\Gamma_4 + \Gamma_{4'} + 3\Gamma_5 + 2\Gamma_{5'} + 4\Gamma_6$ | $^2F, ^2F, ^4F$ |
| d^5 | $L = 4$ | $2\Gamma_1^s + 4\Gamma_4 + \Gamma_{4'} + 4\Gamma_5 + 2\Gamma_{5'} + 2\Gamma_6$ | $^2G, ^2G, ^4G$ |
| d^5 | $L = 5$ | $\Gamma_1^s + 3\Gamma_4 + 3\Gamma_5 + \Gamma_{5'} + 3\Gamma_6$ | 2H |
| d^5 | $L = 6$ | $2\Gamma_1^s + 3\Gamma_4 + 2\Gamma_5 + \Gamma_{5'} + \Gamma_6$ | 2I |
| d^5 | $L = 7$ | $\Gamma_1^s + 2\Gamma_4 + \Gamma_5 + \Gamma_6$ | — |
| d^5 | $L = 8$ | $\Gamma_1^s + \Gamma_4 + \Gamma_5$ | — |
| d^5 | $L = 9$ | Γ_4 | — |
| d^5 | $L = 10$ | Γ_1^s | — |

^(a) The symmetries of the irreducible representations of the permutation group $P(5)$ label the various spin and orbital angular momentum states. To obtain the states allowed by the Pauli Principle the direct product of the symmetries between the orbital and spin states must contain Γ_1^a

Table 17.6, etc. In this sense, the tables that are provided in this chapter are sufficient to handle all atomic s , p and d levels. To treat the f levels completely we would need to construct tables for the permutation groups $P(6)$ and $P(7)$, and the character tables for $P(6)$ and $P(7)$ are found in Appendix F.

In solids and molecules where point group symmetry rather than full rotational symmetry applies, the application of permutation groups to the many-electron states is identical. Thus the $3d$ levels of a transition metal ion in a crystal field of cubic symmetry are split into a E_g and a T_{2g} level (see Sect. 5.3) and the allowed d^2 levels would be either a 1E_g or a $^1T_{2g}$,

${}^3T_{2g}$ level. In general, crystal field splittings are applied to the many-electron states whose symmetries are given in Tables 17.2, 17.4, 17.6 and 17.7. The d states in icosahedral symmetry do not experience any crystal field splitting and all the arguments of this chapter apply directly. Character tables for the groups $P(3)$, $P(4)$, $P(5)$, $P(6)$ and $P(7)$ are found in Appendix F.

Selected Problems

17.1. Use the following character table for the permutation group $P(5)$ given in Table F.3.

- (a) Using (17.10) find the number of symmetry elements in each of the classes for the permutation group $P(5)$, and check the entries to Table F.3.
- (b) What are the characters for the equivalence transformation for a state where three of the five electrons are in one state (e.g., a d -state) and two electrons are in another state (e.g., a p -state)? Explain how you obtained your result. What irreducible representations are contained in this equivalence transformation (see Table F.3)?
- (c) Multiply element

$$P_i = \begin{pmatrix} 1 & 2 & 3 & 4 & 5 \\ 3 & 2 & 1 & 4 & 5 \end{pmatrix}$$

by element

$$P_j = \begin{pmatrix} 1 & 2 & 3 & 4 & 5 \\ 4 & 2 & 5 & 1 & 3 \end{pmatrix}$$

to form $P_i P_j$ and $P_j P_i$. Are your results consistent with the character table?

- (c) Referring to Table 17.7, what are the irreducible representations for the spin configuration $(\uparrow\uparrow\downarrow\downarrow\downarrow)$? How did you obtain this result?
- (e) What are the Pauli allowed states (as would be given in Table 17.7) with the largest L value for the p^3d^2 configuration? Note that this calculation would make a new entry to Table 17.7.

17.2. (a) Consider the addition of Mn^{2+} as a substitutional magnetic impurity for CdTe. Since Mn^{2+} has five $3d$ electrons, use the permutation group $P(5)$ to find the Pauli-allowed states for the Mn^{2+} ion in CdTe (Table F.3 in Appendix F). Of these Pauli-allowed d^5 states, which is the ground state based on Hund's rule?

(b) Using the electric dipole selection rule for optical transitions, find the allowed transitions from the ground state in (a) to Pauli-allowed states in the $3d^34p^2$ configuration (see Problem 17.1(e)).

17.3. Use the character table for the permutation group $P(6)$ (Table F.4 in Appendix F).

- (a) Starting with $q = 6$ objects, show that there are 11 classes of the form given in the character table for $P(6)$ (see Sect. 17.2). Show that all $6!$ symmetry elements are contained in these classes.
- (b) Show that there are 45 symmetry elements in the class $(2^2, 1^2)$ and 40 symmetry elements in class $(3, 1^3)$.
- (c) Show that the irreducible representations Γ_5''' and Γ_9 as given in the character table are orthogonal. (This is a check that the entries in the character table in Table F.4 are correct.) Which of the four five-dimensional irreducible representations correspond to the basis functions $\Psi'_{\Gamma_{n-1}}$ in (17.19)?
- (d) What are the irreducible representations in $P(6)$ that represent the spin angular momentum states $S = 3, 2, 1, 0$? To solve this problem, you will have to find the equivalence transformations corresponding to selected permutations of spin configurations that are needed to construct the various spin angular momentum states (see Tables F.3 and F.4 for the permutation group $P(5)$ to provide guidance for solving this problem for $P(6)$).
- (e) According to Hund's rule, what are the S , L and J values for placing six electrons in a d^6 electronic configuration. To which irreducible representations of $P(6)$ do the spin and spatial parts of this Hund's rule ground state correspond?

17.4. In this chapter, we considered multielectron occupation of atomic states. Consider both the case of no spin-orbit interaction and of including the spin-orbit interaction for the following cases.

- (a) What is the effect of time inversion on two $1s$ electrons in an atomic state?
What is the effect of time inversion symmetry on two $2p$ electrons?
- (b) What is the effect of time inversion symmetry on three $2p$ electrons?

Symmetry Properties of Tensors

In theories and experiments involving physical systems with high symmetry, one frequently encounters the question of how many independent terms are required by symmetry to specify a tensor of a given rank for each symmetry group. These questions have simple group theoretical answers [75]. This chapter deals with the symmetry properties of tensors, with particular attention given to those tensors of rank 2 and higher that arise in the physics of condensed matter concerning nonlinear optics and elasticity theory. In this analysis we consider the symmetry implied by the permutation group which gives the number of independent components in the case of no point group symmetry. We then consider the additional symmetry that is introduced by the presence of symmetry elements such as rotations, reflections and inversions. We explicitly discuss full rotational symmetry and several point group symmetries.

18.1 Introduction

We start by listing a few commonly occurring examples of tensors of rank 2, 3, and 4 that occur in condensed matter physics. Second rank symmetric tensors occur in the constitutive equations of Electromagnetic Theory, as for example in the linear equations relating the current density to the electric field intensity

$$\mathbf{J}^{(1)} = \overset{\leftrightarrow}{\sigma^e}^{(2)} \cdot \mathbf{E}, \quad (18.1)$$

where the electrical conductivity $\overset{\leftrightarrow}{\sigma^e}^{(2)}$ is a symmetric ($\sigma_{ij}^e = \sigma_{ji}^e$) second rank tensor. We use the superscript (2) to distinguish the second rank linear conductivity tensor from the nonlinear higher order tensor terms that depend on higher powers of the electric field \mathbf{E} discussed below. A similar situation holds for the relation between the polarization and the electric field

$$\mathbf{P}^{(2)} = \overset{\leftrightarrow}{\alpha}^{(2)} \cdot \mathbf{E}, \quad (18.2)$$

where the polarizability $\overset{\leftrightarrow}{\alpha}^{(2)}$ is a symmetric second rank tensor, and where $\overset{\leftrightarrow}{\alpha}^{(2)} \equiv \overset{\leftrightarrow}{\chi}_E^{(2)}$ is often called the electrical susceptibility. A similar situation also holds for the relation between the magnetization and the magnetic field

$$\mathbf{M}^{(2)} = \overset{\leftrightarrow}{\chi}_H^{(2)} \cdot \mathbf{H}, \quad (18.3)$$

where the magnetic susceptibility $\overset{\leftrightarrow}{\chi}_H^{(2)}$ is also a symmetric second rank tensor. These relations all involve second rank symmetric tensors: $\overset{\leftrightarrow}{\sigma}^{(2)}$, $\overset{\leftrightarrow}{\alpha}^{(2)}$ and $\overset{\leftrightarrow}{\chi}_H^{(2)}$. Each second (3×3) rank tensor T_{ij} has nine components but because it is a symmetric tensor $T_{ij} = T_{ji}$ only six coefficients (rather than nine) are required to represent these symmetric second rank tensors. Thus, a symmetric second rank tensor, such as the polarizability tensor or the Raman tensor, has only six independent components. In this chapter we are concerned with the symmetry properties of these and other tensors under permutations and point group symmetry operations.

As an example of higher rank tensors, consider nonlinear optical phenomena, where the polarization in (18.2) is further expanded to higher order terms in \mathbf{E} as

$$\mathbf{P} = \overset{\leftrightarrow}{\alpha}^{(2)} \cdot \mathbf{E} + \overset{\leftrightarrow}{\alpha}^{(3)} \cdot \mathbf{EE} + \overset{\leftrightarrow}{\alpha}^{(4)} \cdot \mathbf{EEE} + \dots, \quad (18.4)$$

where we can consider the polarizability tensor $\overset{\leftrightarrow}{\alpha}$ to be field dependent

$$\overset{\leftrightarrow}{\alpha} = \overset{\leftrightarrow}{\alpha}^{(2)} + \overset{\leftrightarrow}{\alpha}^{(3)} \cdot \mathbf{E} + \overset{\leftrightarrow}{\alpha}^{(4)} \cdot \mathbf{EE} + \dots, \quad (18.5)$$

because an increase in the magnitude of \mathbf{E} will make the nonlinear terms in (18.4) and (18.5) more important. More will be said about the symmetry of the various $\overset{\leftrightarrow}{\alpha}^{(i)}$ tensors under permutations and point group operations in Sect. 18.3. Similar expansions can be made for (18.1) and (18.3).

As another example, consider the *piezoelectric* tensor which is a third rank tensor relating the polarization per unit volume \mathbf{P} to the strain tensor, $\overset{\leftrightarrow}{e}$, where \mathbf{P} is given by

$$\mathbf{P} = \overset{\leftrightarrow}{d}^{(3)} \cdot \overset{\leftrightarrow}{e}, \quad (18.6)$$

which can be rewritten to show the rank of each tensor explicitly

$$P_k = \sum_{i,j} d_{kij} \frac{u_i}{x_j}, \quad (18.7)$$

in which the vector u_i denotes the change in the length while x_j refers to the actual length. We note that there are 27 components in the tensor $\overset{\leftrightarrow}{d}^{(3)}$ without

considering any symmetry of the system under permutation operations. A frequently used fourth rank tensor is the elastic constant tensor $\overset{\leftrightarrow}{C}^{(4)}$ defined by

$$\overset{\leftrightarrow}{\sigma}^m = \overset{\leftrightarrow}{C}^{(4)} \cdot \overset{\leftrightarrow}{e}, \quad (18.8)$$

where the second rank symmetric stress tensor $\overset{\leftrightarrow}{\sigma}^m$ and strain tensor $\overset{\leftrightarrow}{e}$ (i.e., the gradient of the displacement) are related through the fourth rank elastic constant tensor $\overset{\leftrightarrow}{C}^{(4)}$ (or C_{ijkl}), which neglecting permutation symmetry would have 81 components. More will be said about the elastic constant tensor below (see Sect. 18.6) where we will use $\overset{\leftrightarrow}{\sigma}^m$ to denote the mechanical stress tensor, but it should be noted that σ_{ij}^e is used to denote the linear electrical conductivity tensors (18.1). The superscripts m and e are used to distinguish σ_{ij}^m for the stress tensor from σ_{ij}^e for the electrical conductivity tensor.

These tensors and many more are discussed in a book by Nye [57]. The discussion of tensors which we give in this chapter is group theoretical, whereas Nye's book gives tables of the tensors which summarize many of the results which we can deduce from our group theoretical analysis.

In this chapter we use group theory to find the smallest number of independent coefficients for commonly occurring tensors in condensed matter physics, including permutation symmetry and point group symmetry. Let us now consider the total number of tensor components. As stated above $\overset{\leftrightarrow}{\alpha}^{(2)}$ has $3^2 = 9$ coefficients (six for the symmetric components, $\alpha_{ij} = \alpha_{ji}$). There are $3^3 = 27$ coefficients (10 symmetric) in $\overset{\leftrightarrow}{\alpha}^{(3)}$, $3^4 = 81$ coefficients (only 15 symmetric) in $\overset{\leftrightarrow}{\alpha}^{(4)}$, and $3^5 = 243$ coefficients (21 symmetric) in $\overset{\leftrightarrow}{\alpha}^{(5)}$, etc. We ask how many tensor components are independent? Which components are related to one another? How many independent experiments must be carried out to completely characterize these tensors? These are important questions that occur in many areas of condensed matter physics and materials science. We address these questions in this chapter.

In Sect. 18.2, we discuss the reduction in the number of independent coefficients arising from symmetries associated with the permutation of tensor indices while in Sect. 18.3 we discuss the corresponding reduction in the number of independent components of tensors obtained from point group symmetry (rotations, reflections and inversion). The number of independent coefficients for the case of complete isotropy (full rotational symmetry) is considered in Sect. 18.4, while lower point group symmetries are treated in Sect. 18.5. The independent coefficients of the elastic modulus tensor C_{ijkl} are discussed in Sect. 18.6. Since the number of independent symmetry elements can be found by considering the crystal symmetry group as a subgroup of the full rotation group without making contact to translational symmetry, point group symmetry is considered in finding the form of tensors in condensed matter systems.

18.2 Independent Components of Tensors Under Permutation Group Symmetry

In this section we consider the effect of permutation symmetry on reducing the number of independent components of tensors. For example, second rank symmetric tensors occur frequently in condensed matter physics. In this case, the symmetry $\alpha_{ij} = \alpha_{ji}$ implied by the term symmetric tensor restricts the off-diagonal matrix elements to follow this additional permutation relation $ij = ji$, thereby reducing the number of allowed off-diagonal elements from six to three, since the symmetric combinations $(\alpha_{ij} + \alpha_{ji})/2$ are allowed and the combinations $(\alpha_{ij} - \alpha_{ji})/2$ vanish by symmetry. Furthermore, the three elements $(\alpha_{ij} - \alpha_{ji})/2$ constitute the three components of an antisymmetric second rank tensor, also called an axial vector; the angular momentum (listed in character tables as R_i) is an example of an antisymmetric second-rank tensor which has three components L_x, L_y, L_z .

Group theory is not needed to deal with the symmetry of a second-rank tensor because of its simplicity. As the rank of the tensor increases, group theory becomes increasingly helpful in the classification of symmetric tensors. Just for illustrative purposes, we now consider the case of the second-rank tensor from the point of view of permutation group symmetry. For this purpose we have listed in Table 18.1 the permutation groups which are needed to handle the tensors mentioned in Sect. 18.1. Referring to Table 18.1 (which is constructed from tables in Chap. 17), we see that a second rank symmetric tensor like the electrical conductivity tensor $\overset{\leftrightarrow}{\sigma}^e$ is represented in Table 18.1 by pp , which we can consider as the generic prototype of a second rank symmetric tensor. From the discussion of Chap. 17, we found that p^2 could have angular momentum states $L = 0, 1, 2$ with the indicated permutation group symmetries labeled “irreducible representations” in Table 18.1, and yielding a total number of states equal to the sum of $(2L + 1)$ to yield $1 + 3 + 5 = 9$. From the table, it is seen that the symmetric states (Γ_1^s) arise from the $L = 0$ and $L = 2$ entries, corresponding to $1+5=6$ states. Thus we obtain six independent coefficients for a symmetric second rank tensor based on permutation symmetry alone. The number of independent coefficients for the second rank antisymmetric tensor (transforming Γ_1^a) is correspondingly equal to 3, and the antisymmetric contribution arises from the $L = 1$ state.

A third-rank symmetric tensor (such as $\overset{\leftrightarrow}{\alpha}^{(3)}$) is more interesting from a group theoretical standpoint. Here we need to consider permutations in Table 18.1 of the type p^3 , so that p^3 can be considered as the appropriate basis function of the permutation group $P(3)$ for the permutation symmetry of $\overset{\leftrightarrow}{\alpha}^{(3)}$. Referring to (18.4), we note that the $\mathbf{E}\mathbf{E}$ fields are clearly symmetric under interchange of $\mathbf{E} \leftrightarrow \mathbf{E}$; but since (18.5) defines the general nonlinear polarizability tensor $\overset{\leftrightarrow}{\alpha}$, then all terms in the expansion of $\overset{\leftrightarrow}{\alpha}$ must be symmetric under interchange of $\alpha_{ij} \rightarrow \alpha_{ji}$. From Table 18.1, we see that p^3 consists of $L = 0, 1, 2, 3$ angular momentum states. The entries for the p^3 configuration

Table 18.1. Transformation properties of various tensors under permutations^(a)

| tensor | configuration | state | irreducible representations | group |
|----------------|---------------|---------|---|--------|
| | SS | $L = 0$ | Γ_1^s | $P(2)$ |
| | SD | $L = 2$ | $\Gamma_1^s + \Gamma_1^a$ | $P(2)$ |
| | DD | $L = 0$ | Γ_1^s | $P(2)$ |
| $C_{(ij)(kl)}$ | DD | $L = 1$ | Γ_1^a | $P(2)$ |
| | DD | $L = 2$ | Γ_1^s | $P(2)$ |
| | DD | $L = 3$ | Γ_1^a | $P(2)$ |
| | DD | $L = 4$ | Γ_1^s | $P(2)$ |
| $d_{i(jk)}$ | pS | $L = 1$ | $\Gamma_1^s + \Gamma_1^a$ | $P(2)$ |
| | pD | $L = 1$ | $\Gamma_1^s + \Gamma_1^a$ | $P(2)$ |
| | pD | $L = 2$ | $\Gamma_1^s + \Gamma_1^a$ | $P(2)$ |
| | pD | $L = 3$ | $\Gamma_1^s + \Gamma_1^a$ | $P(2)$ |
| $\alpha^{(2)}$ | p^2 | $L = 0$ | Γ_1^s | $P(2)$ |
| | p^2 | $L = 1$ | Γ_1^a | $P(2)$ |
| | p^2 | $L = 2$ | Γ_1^s | $P(2)$ |
| $\alpha^{(3)}$ | p^3 | $L = 0$ | Γ_1^a | $P(3)$ |
| | p^3 | $L = 1$ | $\Gamma_1^s + \Gamma_2$ | $P(3)$ |
| | p^3 | $L = 2$ | Γ_2 | $P(3)$ |
| | p^3 | $L = 3$ | Γ_1^s | $P(3)$ |
| $\alpha^{(4)}$ | p^4 | $L = 0$ | $\Gamma_1^s + \Gamma_2$ | $P(4)$ |
| | p^4 | $L = 1$ | $\Gamma_3 + \Gamma_{3'}$ | $P(4)$ |
| | p^4 | $L = 2$ | $\Gamma_1^s + \Gamma_2 + \Gamma_3$ | $P(4)$ |
| | p^4 | $L = 3$ | Γ_3 | $P(4)$ |
| | p^4 | $L = 4$ | Γ_1^s | $P(4)$ |
| $\alpha^{(5)}$ | p^5 | $L = 0$ | Γ_6 | $P(5)$ |
| | p^5 | $L = 1$ | $\Gamma_1^s + \Gamma_4 + \Gamma_5 + \Gamma_{5'}$ | $P(5)$ |
| | p^5 | $L = 2$ | $\Gamma_4 + \Gamma_5 + \Gamma_6$ | $P(5)$ |
| | p^5 | $L = 3$ | $\Gamma_1^s + \Gamma_4 + \Gamma_5$ | $P(5)$ |
| | p^5 | $L = 4$ | Γ_4 | $P(5)$ |
| | p^5 | $L = 5$ | Γ_1^s | $P(5)$ |
| $\alpha^{(6)}$ | p^6 | $L = 0$ | $\Gamma_1^s + \Gamma_{5'''} + \Gamma_9$ | $P(6)$ |
| | p^6 | $L = 1$ | $\Gamma_5 + \Gamma_{5''} + \Gamma_{10} + \Gamma_{16}$ | $P(6)$ |
| | p^6 | $L = 2$ | $\Gamma_1^s + \Gamma_5 + 2\Gamma_9 + \Gamma_{16}$ | $P(6)$ |
| | p^6 | $L = 3$ | $\Gamma_5 + \Gamma_{5''} + \Gamma_9 + \Gamma_{10}$ | $P(6)$ |
| | p^6 | $L = 4$ | $\Gamma_1^s + \Gamma_5 + \Gamma_9$ | $P(6)$ |
| | p^6 | $L = 5$ | Γ_5 | $P(6)$ |
| | p^6 | $L = 6$ | Γ_1^s | $P(6)$ |

^(a) The irreducible representations associated with the designated permutation group, configuration and state are listed

Table 18.2. Number of independent components for various tensors for the listed group symmetries

| group | repr. ^a | angular momentum values ^b | number of independent coefficients | | | | | |
|----------------|--------------------|--------------------------------------|------------------------------------|-------------|----------------|----------------|----------------|----------------|
| | | | $C_{(ij)(kl)}$ | $d_{k(ij)}$ | $\alpha^{(2)}$ | $\alpha^{(3)}$ | $\alpha^{(4)}$ | $\alpha^{(5)}$ |
| R_∞^c | $\Gamma_{\ell=0}$ | $\ell = 0$ | 2 | 0 | 1 | 0 | 1 | 0 |
| I_h | A_{1g} | $\ell = 0, 6, 10, \dots$ | 2 | 0 | 1 | 0 | 1 | 0 |
| O_h | A_{1g} | $\ell = 0, 4, 6, 8, 10, \dots$ | 3 | 0 | 1 | 0 | 2 | 0 |
| T_d | A_1 | $\ell = 0, 3, 4, 6, 7, 8, 9, \dots$ | 3 | 1 | 1 | 1 | 2 | 1 |
| $D_{\infty h}$ | A_{1g} | $\ell = 0, 2, 4, 6, \dots$ | 5 | 1 | 2 | 0 | 3 | 0 |
| $C_{\infty v}$ | A_1 | $\ell = 0, 1, 2, 3, 4, 5, \dots$ | 5 | 4 | 2 | 2 | 3 | 3 |
| D_{6h} | A_{1g} | $\ell = 0, 2, 4, 6, \dots$ | 5 | 1 | 2 | 0 | 3 | 0 |
| C_1 | A_1 | $\ell = 0, 1, 2, 3, 4, 5, \dots^d$ | 21 | 18 | 6 | 10 | 15 | 21 |

^a The notation for the totally symmetric irreducible representation for each group is given

^b The angular momentum states that contain the A_1 (or A_{1g}) irreducible representation for the various symmetry groups (see Table 18.1)

^c The full rotational symmetry group is denoted by R_∞

^d For this lowest point group symmetry, the A_1 representation occurs $2\ell + 1$ times. For the other groups in this table, there is only one occurrence of A_1 for each listed ℓ value. However, for higher ℓ values, multiple occurrences of A_1 may arise (e.g., in O_h symmetry, the $\ell = 12$ state has two A_{1g} modes)

in Table 18.1 come from Table 17.4 which contains a variety of configurations of the permutation group $P(3)$ that can be constructed from three electrons (or more generally from three interchangeable vectors). The total number of states in the p^3 configuration is found by multiplying the degeneracy ($2L + 1$) of each angular momentum state along with the corresponding number of irreducible representations occurring for each of the $L = 0, 1, 2, 3$ multiplets and then summing all of these products to get

$$(1)(1) + 3(1 + 2) + 5(2) + 7(1) = 27$$

which includes all 3^3 combinations. Of this total, the number of symmetric combinations that go with Γ_1^s is only $3(1) + 7(1) = 10$. Similarly Table 18.1 shows that there is only one antisymmetric combination (for $L = 0$). Of interest is the large number of combinations that are neither symmetric nor antisymmetric: $3(2) + 5(2) = 16$ for $\overset{\leftrightarrow}{\alpha}^{(3)}$ for the $P(3)$ permutation group. Thus, Table 18.1 shows that on the basis of permutation symmetry, there are only ten independent coefficients for $\overset{\leftrightarrow}{\alpha}^{(3)}$, assuming no additional point group symmetry. This result is summarized in Table 18.2.

As the next example, consider $\overset{\leftrightarrow}{\alpha}^{(4)}$ which is a fourth rank tensor that couples \mathbf{P} and \mathbf{EEE} symmetrically. The generic tensor for this case is p^4 in Table 18.1 (taken from Table 17.6 for $P(4)$ for four electrons) with $3^4 = 81$

coefficients neglecting permutational and point group symmetries, which is also obtained from the entries in Table 18.1 for p^4 as follows:

$$(1)(1+2) + (3)(3+3) + 5(1+2+3) + 7(3) + 9(1) = 81.$$

Of these, $1+5+9=15$ are symmetric (transforms as Γ_1^s) and this entry is included in Table 18.2. There are no antisymmetric combinations (i.e., there is no Γ_1^a for p^4 in $P(4)$).

Another commonly occurring tensor in solid state physics is the elastic modulus tensor $C_{ijkl} = C_{(ij)(kl)}$ which relates two symmetric tensors $\overset{\leftrightarrow}{\sigma^m}$ and $\overset{\leftrightarrow}{e}$, each having six independent components, and thus leading to $6 \times 6 = 36$ components for the product. But $C_{(ij)(kl)}$ is further symmetric under interchange of $ij \leftrightarrow kl$, reducing the 30 off-diagonal components of the 6×6 matrix into 15 symmetric and 15 antisymmetric combinations, in addition to the six diagonal symmetric components. This gives a total of 21 independent symmetric coefficients, as is explained in standard condensed matter physics texts. From a group theoretical standpoint, the (ij) and (kl) are each treated as p^2 units which form total angular momentum states of $L = 0$ (labeled S in Table 18.1) and $L = 2$ (labeled D). Under the permutation group $P(2)$, we can make one SS combination ($L = 0$), one symmetric and one antisymmetric SD combination ($L = 2$), and finally DD combinations can be made with $L = 0, 1, 2, 3, 4$. Adding up the total number of combinations that can be made from $C_{(ij)(kl)}$ we get

$$(1)(1) + 5(1+1) + 1(1) + 3(1) + 5(1) + 7(1) + 9(1) = 36,$$

in agreement with the simple argument given above. Of these, 21 are symmetric (i.e., go with Γ_1^s) while 15 are antisymmetric (i.e., go with Γ_1^a), and the number 21 appears in Table 18.2. If we had instead used p^4 in Table 18.1 as the basis function for the permutation of the elastic tensor C_{ijkl} , we would have neglected the symmetric interchange of the stress and strain tensors $(ij) \leftrightarrow (kl)$.

The final tensor that we will consider is the piezoelectric tensor $d_{i(jk)}$ formed as the symmetric direct product of a vector and a symmetric second rank tensor ($3 \times 6 = 18$ components). The symmetries are calculated following the pS and pD combinations, using the concepts discussed for the transformation properties of the $\overset{\leftrightarrow}{\alpha}^{(2)}$ and $C_{(ij)(kl)}$ tensors. This discussion yields 18 independent coefficients for $d_{i(jk)}$ under permutation symmetry.

In summary, each second rank symmetric tensor is composed of irreducible representations $L = 0$ and $L = 2$ of the full rotation group, the third rank symmetric tensor from $L = 1$ and $L = 3$, the fourth rank symmetric tensor from $L = 0, L = 2$ and $L = 4$, the elastic tensor from $L = 0, 2L = 2$ and $L = 4$, and the piezoelectric tensor from $2L = 1, L = 2$ and $L = 3$. We use these results to now incorporate the various rotational symmetries to further reduce the number of independent coefficients for each symmetry group.

18.3 Independent Components of Tensors: Point Symmetry Groups

In this section we discuss a very general group theoretical result for tensor components arising from point group symmetry operations such as rotations, reflections and inversions. These symmetry operations further reduce the number of independent coefficients that need to be introduced for the various tensors in crystals having various point group symmetries.

Let us consider a relation between a tensor of arbitrary rank $J_{ij\dots}$ and another tensor $F_{i'j'\dots}$ also of arbitrary rank and arbitrary form where the two tensors in general will be of different ranks.

$$J_{ij\dots} = \sum_{i'j'\dots} \{t_{ij\dots, i'j'\dots}\} F_{i'j'\dots} \quad (18.9)$$

What we have in mind in (18.9) are relations such as are given in (18.1) to (18.8), where $J_{ij\dots}$ appears as either a simple vector or as a second rank symmetrical tensor. Likewise $F_{i'j'\dots}$ denotes either a simple vector, the product of two vectors, the product of three vectors, or a symmetric second rank tensor etc.

Theorem. *The number of independent non-zero tensor components $t_{ij\dots, i'j'\dots}$ allowed by point group symmetry in (18.9) is determined by finding the irreducible representations contained in both $\{\Gamma_{J_{ij\dots}}\} = \sum \alpha_i \Gamma_i$ and $\{\Gamma_{F_{i'j'\dots}}\} = \sum \beta_j \Gamma_j$.*

Proof. Only coefficients $t_{ij\dots, i'j'\dots}$ coupling $\{\mathbf{J}\}_{\Gamma_i}$ and $\{\mathbf{F}\}_{\Gamma_j}$ that correspond to the same partner of the same irreducible representation contained in both Γ_i and Γ_j can be nonzero, since $\overset{\leftrightarrow}{t}$ must be invariant under the symmetry operations of the group. Thus the number of independent matrix elements in the tensor $t_{ij\dots, i'j'\dots}$ is the number of times the scalar representation Γ_1^+ occurs in the decomposition of the direct product

$$\{\Gamma_{\mathbf{J}}\} \otimes \{\Gamma_{\mathbf{F}}\} = \sum_i \alpha_i \Gamma_i \otimes \sum_j \beta_j \Gamma_j = \sum_k \gamma_k \Gamma_k, \quad (18.10)$$

thus completing the proof. \square

The only nonvanishing couplings between $\{\mathbf{J}\}_{\Gamma_i}$ and $\{\mathbf{F}\}_{\Gamma_j}$ are between partners transforming according to the same irreducible representation because only these lead to matrix elements that are invariant under the symmetry operations of the group. We therefore transform (18.9) to make use of the symmetrized form

$$\{\mathbf{J}\}_{\Gamma_i} = t_{\Gamma_1^+} \{\mathbf{F}\}_{\Gamma_i}, \quad (18.11)$$

where the $\{\mathbf{J}\}_{\Gamma_i}$ and $\{\mathbf{F}\}_{\Gamma_i}$ correspond to the same partners of the same irreducible representation and $t_{\Gamma_1^+}$ transforms as a scalar which has Γ_1^+ symmetry.

In most cases of interest, permutation symmetry requirements on the products $\{\mathbf{F}\}_{\Gamma_i}$ further limit the number of independent matrix elements of a tensor matrix, as discussed below (Sect. 18.4).

Application of this theorem is given for the maximum amount of rotational symmetry (the full rotation group) in Sect. 18.4 and for specific point group symmetries in Sect. 18.5 and Sect. 18.6.

18.4 Independent Components of Tensors Under Full Rotational Symmetry

The highest point group symmetry is the full isotropy provided by the full rotation group R_∞ . In Sect. 18.3 we showed that the number of independent coefficients in a tensor $t_{ij\dots i'j'\dots}$ in (18.9) coupling two tensors is the number of times the direct product in (18.10) contains Γ_1^s . For full rotational symmetry we use in the fully symmetric irreducible representation $L = 0$. Thus we must look for the occurrence of $L = 0$ in Table 18.1.

Referring to Table 18.1, we find $\Gamma_{L=0}$ and that for the second rank tensor, we have Γ_1 contained once, giving only a single independent coefficient $\{\Gamma_j\} \otimes \{\Gamma_t\}$. Consequently, group theory tells us that the one independent coefficient is $\alpha_{11} = \alpha_{22} = \alpha_{33}$ while the off-diagonal terms vanish $\alpha_{12} = \alpha_{23} = \alpha_{31} = 0$ for a symmetric second rank tensor in a medium with full rotational symmetry. This result for the number of independent components is given in Table 18.2.

Likewise Table 18.1 shows that there are no independent coefficients for $\overset{\leftrightarrow}{\alpha}^{(3)}$ in full rotational symmetry. Group theory thus tells us that this tensor vanishes by symmetry for the case of full rotational symmetry. This analysis further tells us that we cannot have any non-vanishing tensors of odd rank given by (18.4).

With regard to the fourth rank tensor, $\overset{\leftrightarrow}{\alpha}^{(4)}$, Table 18.1 shows that we can have only one independent coefficient for full rotational symmetry. In contrast, the $C_{(ij)(kl)}$ fourth rank tensor contains two independent coefficients in full rotational symmetry and the components of $d_{i(jk)}$ all vanish by symmetry.

This completes the discussion for the form of the various tensors in Table 18.2 under full rotational symmetry. Also listed in the table are the number of independent coefficients for several point group symmetries, including I_h , O_h , T_d , $D_{\infty h}$, $C_{\infty v}$, D_{6h} , and C_1 . These results can be derived by considering these groups as subgroups of the full rotational group, and going from higher to lower symmetry. Some illustrative examples of the various point group symmetries are given in the following sections.

18.5 Tensors in Nonlinear Optics

In this section we consider polarizability tensors arising in nonlinear optics, including symmetric second rank, third rank and fourth rank tensors, such

as those appearing in (18.5). We now consider these tensors for groups with symmetries lower than the full rotational group thereby filling in entries in Table 18.2.

18.5.1 Cubic Symmetry: O_h

The character table for group O_h is shown in Table 10.2 using solid state physics notation together with basis functions for each irreducible representation. We first consider the transformation properties of the linear response tensor $\overset{\leftrightarrow}{\alpha}^{(2)}$ and the nonlinear polarizability tensors $\overset{\leftrightarrow}{\alpha}^{(3)}$ and $\overset{\leftrightarrow}{\alpha}^{(4)}$ (see (18.5)). Consider for example the second rank tensor $\overset{\leftrightarrow}{\alpha}^{(2)}$ defined by

$$\mathbf{P} = \overset{\leftrightarrow}{\alpha}^{(2)} \cdot \mathbf{E} \quad (18.12)$$

in linear response theory. Both \mathbf{P} and \mathbf{E} transform as Γ_{15}^- (or Γ_{15} in Table 10.2), which gives for the direct product:

$$\Gamma_{\mathbf{P}} \otimes \Gamma_{\mathbf{E}} = \Gamma_{15}^- \otimes \Gamma_{15}^- = \Gamma_1^+ + \Gamma_{12}^+ + \Gamma_{15}^+ + \Gamma_{25}^+, \quad (18.13)$$

in which we use a notation which explicitly displays the irreducible representations that are even (+) or odd (−) under inversion, as can immediately be identified from the basis functions given in Table 10.2. But since the symmetry elements in Γ_{15}^+ are represented by a 3×3 matrix for the angular momentum R_{ij} , this 3×3 matrix is antisymmetric under interchange of $i \leftrightarrow j$ so that $R_{ij} = -R_{ji}$ and we have

$$\Gamma_{\overset{\leftrightarrow}{\alpha}}^{(s)} = \Gamma_1^+ + \Gamma_{12}^+ + \Gamma_{25}^+, \quad \Gamma_{\overset{\leftrightarrow}{\alpha}}^{(a)} = \Gamma_{15}^+ \quad (18.14)$$

showing the symmetries of the six partners for the second rank symmetric tensor, and the three partners for the second rank antisymmetric tensor. These results can also be obtained starting from the full rotation group, considering the decomposition of the $L = 0$ and $L = 2$ states for the symmetric partners and the $L = 1$ states for the antisymmetric partners.

Since Γ_1^+ is contained only once in the direct product $\Gamma_{15}^- \otimes \Gamma_{15}^-$ in cubic O_h symmetry (18.13), there is only one independent tensor component for $\overset{\leftrightarrow}{\alpha}^{(2)}$ and we can write $\overset{\leftrightarrow}{\alpha}^{(2)} = \alpha^0 \overset{\leftrightarrow}{1}$, where $\overset{\leftrightarrow}{1}$ is the unit tensor and α^0 is a constant. As a consequence of this general result, the electrical conductivity in cubic symmetry (O_h or T_d) is independent of the direction of the fields relative to the crystal axes and only one experiment is required to measure the polarizability or the conductivity of an unoriented cubic crystal.

In non-linear optics the lowest order non-linear term is $\overset{\leftrightarrow}{\alpha}^{(2)} \cdot \mathbf{E}\mathbf{E}$ in (18.4) where $\overset{\leftrightarrow}{\alpha}^{(2)}$ is a third rank tensor. Since $(\mathbf{E}\mathbf{E})$ is symmetric under interchange, then $(\mathbf{E}\mathbf{E})$ transforms as

$$\Gamma_{\mathbf{EE}}^{(s)} = \Gamma_1^+ + \Gamma_{12}^+ + \Gamma_{25}^+, \quad (18.15)$$

where we have thrown out the Γ_{15}^+ term because it is antisymmetric under interchange of $E_i E_j \rightarrow E_j E_i$. Thus, we obtain the irreducible representations contained in the direct product:

$$\begin{aligned} \Gamma_{\mathbf{P}} \otimes \Gamma_{\mathbf{EE}}^{(s)} &= \Gamma_{15}^- \otimes \{\Gamma_1^+ + \Gamma_{12}^+ + \Gamma_{25}^+\} \\ &= (\Gamma_2^- + 2\Gamma_{15}^- + \Gamma_{25}^-)^{(s)} \\ &\quad + (\Gamma_{12}^- + \Gamma_{15}^- + \Gamma_{25}^-) \end{aligned} \quad (18.16)$$

yielding 18 partners, ten of which are symmetric, in agreement with the general result in Table 18.1. Of particular significance is the fact that none of the ten symmetric irreducible representations have Γ_1^+ symmetry. Thus there are no nonvanishing tensor components for a third rank tensor (such as $\overset{\leftrightarrow}{\alpha}^{(3)}$) in O_h symmetry, a result which could also be obtained by going from full rotational symmetry to O_h symmetry. The ten symmetric partners are found from Table 18.1 and includes angular momentum states $L = 1$ (corresponding to Γ_{15}^-) and $L = 3$ (corresponding to $\Gamma_2^- + \Gamma_{15}^- + \Gamma_{25}^-$) and the decomposition of these angular momentum states in full rotational symmetry yields the irreducible representations of group O_h as shown in Table 5.6 in Chap. 5.

We will now use the symmetric partners of the third rank tensor to discuss the fourth rank tensors. The next order term in (18.4) for the nonlinear response to a strong optical beam (e.g., multiple photon generation) is the fourth rank tensor $\overset{\leftrightarrow}{\alpha}^{(4)}$ defined by

$$\mathbf{P}^{(3)} = \overset{\leftrightarrow}{\alpha}^{(4)} \cdot \mathbf{EEE}. \quad (18.17)$$

If we consider the product \mathbf{EEE} to arise from the symmetric combination for a third rank tensor (see (18.16)), then

$$\Gamma_{\mathbf{EEE}}^{(s)} = \Gamma_2^- + 2\Gamma_{15}^- + \Gamma_{25}^- \quad (18.18)$$

in cubic O_h symmetry, and

$$\begin{aligned} \Gamma_{\mathbf{P}} \otimes \Gamma_{\mathbf{EEE}}^{(s)} &= \Gamma_{15}^- \otimes \{\Gamma_2^- + 2\Gamma_{15}^- + \Gamma_{25}^-\} \\ &= 2\Gamma_1^+ + \Gamma_2^+ + 3\Gamma_{12}^+ + 3\Gamma_{15}^+ + 4\Gamma_{25}^+. \end{aligned} \quad (18.19)$$

Referring to Table 18.1 we see that the symmetric partners for p^4 correspond to $L = 0$ (giving Γ_1^+), $L = 2$ (giving $\Gamma_{12}^+ + \Gamma_{25}^+$) and $L = 4$ (giving $\Gamma_1^+ + \Gamma_{12}^+ + \Gamma_{15}^+ + \Gamma_{25}^+$) yielding the 15 symmetric partners

$$(2\Gamma_1^+ + 2\Gamma_{12}^+ + \Gamma_{15}^+ + 2\Gamma_{25}^+)^{(s)},$$

showing which irreducible representations of (18.19) correspond to symmetric tensors. Since Γ_1^+ is contained twice among the 15 symmetric partners in cubic O_h symmetry, the symmetric fourth rank tensor $\overset{\leftrightarrow}{\alpha}^{(4)}$ has two independent coefficients that would need to be determined by experiments.

18.5.2 Tetrahedral Symmetry: T_d

The group T_d has half the number of symmetry operations of the group O_h , has slightly different classes from group O , and lacks inversion symmetry. Since $\Gamma_2^-(O_h) \rightarrow \Gamma_1(T_d)$, the corresponding relations to (18.16) shows that there exists one nonvanishing tensor component in T_d symmetry for a third rank tensor $\overset{\leftrightarrow}{\alpha}^{(3)}$. This means that zinc-blende structures such as (GaAs and InSb) can have nonvanishing nonlinear optical terms in $\overset{\leftrightarrow}{\alpha}^{(3)}$ because in T_d symmetry, the symmetric partners of the direct product transform as

$$(\Gamma_P \otimes \Gamma_{EE}^{(s)})^{(s)} = \Gamma_1 + 2\Gamma_{25} + \Gamma_{15} \quad (18.20)$$

and the Γ_1 representation is contained once (see Table 18.2).

18.5.3 Hexagonal Symmetry: D_{6h}

The character table for D_{6h} (hexagonal symmetry) is shown in Table A.21. In this subsection we will use the notation found in this character table. Vector forces in hexagonal symmetry decompose into two irreducible representations

$$\Gamma_{\text{vector}} = A_{2u} + E_{1u} . \quad (18.21)$$

Thus the second rank conductivity tensor requires consideration of

$$\begin{aligned} \Gamma_P \otimes \Gamma_E &= (A_{2u} + E_{1u}) \otimes (A_{2u} + E_{1u}) \\ &= 2A_{1g} + A_{2g} + 2E_{1g} + E_{2g} \\ &= (2A_{1g} + E_{1g} + E_{2g})^{(s)} + (A_{2g} + E_{1g})^{(a)} . \end{aligned} \quad (18.22)$$

Equation (18.22) indicates that there are two independent components for a symmetric second rank tensor such as the conductivity tensor. Hence, one must measure both in-plane and out-of-plane conductivity components to determine the conductivity tensor, which is as expected because of the equivalence of transport in the in-plane directions and along the c -axis. The symmetric tensor components (six partners) of (18.22) are

$$\Gamma_{EE}^{(s)} = 2A_{1g} + E_{1g} + E_{2g} \quad (18.23)$$

and the antisymmetric components (three partners) are $(A_{2g} + E_{1g})$. Hence for the symmetric third rank tensor we can write

$$\begin{aligned} \Gamma_P \otimes \Gamma_{EE}^{(s)} &= (A_{2u} + E_{1u}) \otimes (2A_{1g} + E_{1g} + E_{2g}) \\ &= (A_{1u} + A_{2u} + B_{1u} + B_{2u} + 2E_{1u} + E_{2u})^{(s)} \\ &\quad + (2A_{2u} + 4E_{1u} + E_{2u})^{(a)} \end{aligned} \quad (18.24)$$

and there are thus no nonvanishing third rank tensor components in hexagonal D_{6h} symmetry because of parity considerations. For the fourth rank tensor we have

$$\begin{aligned}\Gamma_P \otimes \Gamma_{\mathbf{EE}\mathbf{E}}^{(s)} &= (A_{2u} + E_{1u}) \otimes (A_{1u} + A_{2u} + B_{1u} + B_{2u} + 2E_{1u} + 2E_{2u}) \\ &= (3A_{1g} + B_{1g} + B_{2g} + 2E_{1g} + 3E_{2g})^{(s)} \\ &\quad + (3A_{2g} + 2B_{1g} + 2B_{2g} + 4E_{1g} + 3E_{2g})^{(a)}\end{aligned}\quad (18.25)$$

and there are three independent tensor components. This result could also be obtained by going from full rotational symmetry ($L = 0$, $L = 2$, and $L = 4$), yielding the identical result

$$[A_{1g} + (A_{1g} + E_{1g} + E_{2g}) + (A_{1g} + B_{1g} + B_{2g} + E_{1g} + 2E_{2g})]^{(s)}.$$

The results for D_{6h} and $D_{\infty h}$ (see Table 18.2) show great similarity in behavior between all the tensors that are enumerated in this table, and these similarities stem from the angular momentum states to which they relate (see Table 5.6).

In lowering the symmetry from D_{6h} to D_{3h} which has no inversion symmetry, we get $\Gamma_i^{\pm}(D_{6h}) \rightarrow \Gamma_i(D_{3h})$ for the various irreducible representations. The only difference between the tensor properties in D_{6h} and D_{3d} symmetries involves odd rank tensors. Referring to (18.24) we can see that for D_{3h} there is a nonvanishing third rank tensor component and once again piezoelectric phenomena are symmetry allowed.

18.6 Elastic Modulus Tensor

The elastic modulus tensor represents a special case of a fourth rank tensor (see (18.8)). The elastic energy is written as

$$W = \frac{1}{2} \mathcal{C}_{ijkl} e_{ij} e_{kl}, \quad (18.26)$$

where W transforms as a scalar, the e_{ij} strain tensors transform as second rank symmetric tensors, and the \mathcal{C}_{ijkl} matrices transform as a fourth rank tensor formed by the direct product of two symmetric second rank tensors. The symmetry of \mathcal{C}_{ijkl} with regard to permutations was considered in Sect. 18.2. With regard to point group symmetry, we have the result following (18.10) that the maximum number of independent components of the \mathcal{C}_{ijkl} tensor is the number of times the totally symmetric representation A_{1g} is contained in the direct product of the symmetric part of $\Gamma_{e_{ij}} \otimes \Gamma_{e_{kl}}$. In this section we provide a review of the conventions used to describe the \mathcal{C}_{ijkl} tensor and then give results for a few crystal symmetries.

To make a connection between the elastic constants as discussed from the group theory perspective and in conventional solid state physics books, we introduce a contracted notation for the stress tensor and the strain tensor [57]:

$$\begin{aligned}
\sigma_1^m &= \sigma_{11}^m & \varepsilon_1 &= e_{11} \\
\sigma_2^m &= \sigma_{22}^m & \varepsilon_2 &= e_{22} \\
\sigma_3^m &= \sigma_{33}^m & \varepsilon_3 &= e_{33} \\
\sigma_4^m &= (\sigma_{12}^m + \sigma_{23}^m)/2 & \varepsilon_4 &= (e_{23} + e_{32}) \\
\sigma_5^m &= (\sigma_{13}^m + \sigma_{31}^m)/2 & \varepsilon_5 &= (e_{13} + e_{31}) \\
\sigma_6^m &= (\sigma_{12}^m + \sigma_{21}^m)/2 & \varepsilon_6 &= (e_{12} + e_{21}).
\end{aligned} \tag{18.27}$$

Since both the stress and strain tensors are symmetric, then \mathcal{C}_{ijkl} can have no more than 36 components. We further note from (18.26) that the \mathcal{C}_{ijkl} are symmetric under the interchange of $ij \leftrightarrow kl$, thereby reducing the number of independent components to 21 for a crystal with no symmetry operations beyond translational symmetry of the lattice. Crystals with non-trivial symmetry operations such as rotations, reflections and inversions will have fewer than 21 independent coefficients. Using the notation of (18.27) for the stress and strain tensors, the stress-strain relations can be written as

$$\begin{bmatrix} \sigma_1^m \\ \sigma_2^m \\ \sigma_3^m \\ \sigma_4^m \\ \sigma_5^m \\ \sigma_6^m \end{bmatrix} = \begin{bmatrix} C_{11} & C_{12} & C_{13} & C_{14} & C_{15} & C_{16} \\ C_{21} & C_{22} & C_{23} & C_{24} & C_{25} & C_{26} \\ C_{31} & C_{32} & C_{33} & C_{34} & C_{35} & C_{36} \\ C_{41} & C_{42} & C_{43} & C_{44} & C_{45} & C_{46} \\ C_{51} & C_{52} & C_{53} & C_{54} & C_{55} & C_{56} \\ C_{61} & C_{62} & C_{63} & C_{64} & C_{65} & C_{66} \end{bmatrix} \begin{bmatrix} \varepsilon_1 \\ \varepsilon_2 \\ \varepsilon_3 \\ \varepsilon_4 \\ \varepsilon_5 \\ \varepsilon_6 \end{bmatrix}, \tag{18.28}$$

where the contracted C_{ij} matrix is symmetric, with the 21 independent coefficients containing 15 off-diagonal components and six diagonal components. In the most compact form, we write

$$\sigma_i^m = C_{ij}\varepsilon_j, \quad i, j = 1, \dots, 6, \tag{18.29}$$

where the C_{ij} components are normally used in the description of the mechanical properties of solids. The introduction of additional symmetry operations reduces the number of independent components from the maximum of 21 for a monoclinic crystal group C_1 with no symmetry to a much smaller number (e.g., two for the full rotational group R_∞). We consider here the case of full rotational symmetry, icosahedral symmetry, cubic symmetry, full axial symmetry, and hexagonal symmetry.

Fiber reinforced composites represent an interesting application of these symmetry forms. If the fibers are oriented in three-dimensional space in the six directions prescribed by icosahedral symmetry, then isotropy of the elastic modulus tensor will be obtained. In the corresponding two dimensional situation, if the fibers are oriented at 60° intervals, then isotropy is obtained in the plane. It is standard practice in the field of fiber composites to use fiber composite sheets stacked at 60° angular intervals to obtain “quasiplanar isotropy”.

18.6.1 Full Rotational Symmetry: 3D Isotropy

The highest overall symmetry for an elastic medium is the full rotation group which corresponds to “jellium”. For the case of full rotational symmetry, the rules for the addition of angular momentum tell us that a general second rank tensor transforms according to the representations that can be written as a sum of symmetric and an antisymmetric part

$$\Gamma = \Gamma^{(s)} + \Gamma^{(a)}, \quad (18.30)$$

where the symmetric components for full rotational symmetry transform as the irreducible representations

$$\Gamma^{(s)} = \Gamma_{\ell=0} + \Gamma_{\ell=2} \quad (18.31)$$

and the antisymmetric components transform as

$$\Gamma^{(a)} = \Gamma_{\ell=1}, \quad (18.32)$$

in which the irreducible representations of the full rotation group are denoted by their total angular momentum values ℓ , which are symmetric (antisymmetric) if ℓ is even (odd). Since the stress tensor $\nabla \cdot \mathbf{F} \equiv \overset{\leftrightarrow}{\sigma^m}$ and the strain tensor $\overset{\leftrightarrow}{e}$ are *symmetric* second rank tensors, both σ_α^m and e_{ij} transform according to $(\Gamma_{\ell=0} + \Gamma_{\ell=2})$ in full rotational symmetry, where σ_α^m denotes a force in the x direction applied to a plane whose normal is in the α direction.

The fourth rank symmetric \mathcal{C}_{ijkl} tensor of (18.26) transforms according to the symmetric part of the direct product of two second rank symmetric tensors $\overset{\leftrightarrow}{\Gamma_e^{(s)}} \otimes \overset{\leftrightarrow}{\Gamma_e^{(s)}}$ yielding

$$\begin{aligned} (\Gamma_{\ell=0} + \Gamma_{\ell=2}) \otimes (\Gamma_{\ell=0} + \Gamma_{\ell=2}) &= (2\Gamma_{\ell=0} + 2\Gamma_{\ell=2} + \Gamma_{\ell=4})^{(s)} \\ &\quad + (\Gamma_{\ell=1} + \Gamma_{\ell=2} + \Gamma_{\ell=3})^{(a)}, \end{aligned} \quad (18.33)$$

in which the direct product has been broken up into the 21 partners that transform as symmetric irreducible representations (s) and the 15 partners for the antisymmetric irreducible representations (a). In the case of no crystal symmetry e_{ij} is specified by six constants and the \mathcal{C}_{ijkl} tensor by 21 constants because \mathcal{C}_{ijkl} is symmetrical under the interchange of $ij \leftrightarrow kl$. Since all the symmetry groups of interest are subgroups of the full rotation group, the procedure of going from higher to lower symmetry can be used to determine the irreducible representations for less symmetric groups that correspond to the stress and strain tensors and to the elastic tensor \mathcal{C}_{ijkl} .

As stated in Sect. 18.3 and in Sect. 18.4, the number of times the totally symmetric representation (e.g., $\Gamma_{\ell=0}$ for the full rotational group) is contained in the irreducible representations of a general matrix of arbitrary rank determines the minimum number of independent nonvanishing constants needed

to specify that matrix. In the case of full rotational symmetry, (18.33) shows that the totally symmetric representation ($\Gamma_{\ell=0}$) is contained only twice in the direct product of the irreducible representations for two second rank symmetric tensors, indicating that only two independent nonvanishing constants are needed to describe the 21 constants of the C_{ijkl} tensor in full rotational symmetry, a result that is well known in elasticity theory for isotropic media and is discussed above (see Sect. 18.4).

We denote the two independent non-vanishing constants needed to specify the C_{ijkl} tensor by C_0 for $\Gamma_{\ell=0}$ and by C_2 for $\Gamma_{\ell=2}$ symmetry. We then use these two constants to relate symmetrized stresses and strains labeled by the irreducible representations $\Gamma_{\ell=0}$ and $\Gamma_{\ell=2}$ in the full rotation group. The symmetrized stress-strain equations are first written in full rotational symmetry, using basis functions for the partners of the pertinent irreducible representations (one for $\ell = 0$ and five for the $\ell = 2$ partners):

$$\begin{aligned}
 (X_x + Y_y + Z_z) &= C_0(e_{xx} + e_{yy} + e_{zz}) & \text{for } \ell = 0, m = 0 \\
 (X_x - Y_y + iY_x + iX_y) &= C_2(e_{xx} - e_{yy} + ie_{xy} + ie_{yx}) & \text{for } \ell = 2, m = 2 \\
 (Z_x + X_z + iY_z + iZ_y) &= C_2(e_{zx} + e_{xz} + ie_{yz} + ie_{zy}) & \text{for } \ell = 2, m = 1 \\
 (Z_z - \frac{1}{2}(X_x + Y_y)) &= C_2(e_{zz} - \frac{1}{2}(e_{xx} + e_{yy})) & \text{for } \ell = 2, m = 0 \\
 (Z_x + X_z - iY_z - iZ_y) &= C_2(e_{zx} + e_{xz} - ie_{yz} - ie_{zy}) & \text{for } \ell = 2, m = -1 \\
 (X_x - Y_y - iY_x - iX_y) &= C_2(e_{xx} - e_{yy} - ie_{xy} - ie_{yx}) & \text{for } \ell = 2, m = -2
 \end{aligned} \tag{18.34}$$

in which X , Y and Z are the Cartesian components of the stress tensor $\overset{\leftrightarrow}{\sigma}^m$ and the subscripts denote the shear directions. Since the basis functions in full rotational symmetry are specified by angular momentum states, the quantum numbers ℓ and m are used to denote the irreducible representations and their partners.

From the first, second, fourth and sixth relations in (18.34) we solve for X_x in terms of the strains, yielding

$$X_x = \left(\frac{C_0}{3} + \frac{2C_2}{3} \right) e_{xx} + \left(\frac{C_0}{3} - \frac{C_2}{3} \right) (e_{yy} + e_{zz}) . \tag{18.35}$$

Likewise five additional relations are then written down for the other five stress components in (18.34).

$$Y_y = \left(\frac{C_0}{3} + \frac{2C_2}{3} \right) e_{yy} + \left(\frac{C_0}{3} - \frac{C_2}{3} \right) (e_{zz} + e_{xx}) , \tag{18.36}$$

$$Z_z = \left(\frac{C_0}{3} + \frac{2C_2}{3} \right) e_{zz} + \left(\frac{C_0}{3} - \frac{C_2}{3} \right) (e_{xx} + e_{yy}) , \tag{18.37}$$

$$Z_y + Y_z = C_2 (e_{zy} + e_{yz}) , \tag{18.38}$$

$$Y_x + X_y = C_2 (e_{yx} + e_{xy}) , \tag{18.39}$$

$$Z_x + X_z = C_2 (e_{zx} + e_{xz}) . \quad (18.40)$$

In the notation that is commonly used in elasticity theory, we write the stress-strain relations as

$$\sigma_i^m = \sum_{j=1,6} C_{ij} \varepsilon_j , \quad (18.41)$$

where the six components of the symmetric stress and strain tensors are written in accordance with (18.27) as

$$\begin{aligned} \sigma_1^m &= X_x & \varepsilon_1 &= e_{xx} \\ \sigma_2^m &= Y_y & \varepsilon_2 &= e_{yy} \\ \sigma_3^m &= Z_z & \varepsilon_3 &= e_{zz} \\ \sigma_4^m &= \frac{1}{2}(Y_z + Z_y) & \text{and} & \varepsilon_4 = (e_{yz} + e_{zy}) \\ \sigma_5^m &= \frac{1}{2}(Z_x + X_z) & \varepsilon_5 &= (e_{zx} + e_{xz}) \\ \sigma_6^m &= \frac{1}{2}(X_y + Y_x) & \varepsilon_6 &= (e_{xy} + e_{yx}) \end{aligned} \quad (18.42)$$

and C_{ij} is the 6×6 elastic modulus matrix. In this notation the 21 partners that transform as $(2\Gamma_{\ell=0} + 2\Gamma_{\ell=2} + \Gamma_{\ell=4})$ in (18.33) correspond to the symmetric coefficients of C_{ij} . From the six relations for the six stress components (given explicitly by (18.35) through (18.40)), the relations between the C_0 and C_2 and the C_{ij} coefficients follow:

$$\begin{aligned} C_{11} &= \frac{1}{3}(C_0 + 2C_2) = C_{22} = C_{33} \\ C_{12} &= \frac{1}{3}(C_0 - C_2) = C_{13} = C_{23} \\ C_{44} &= \frac{1}{2}C_2 = C_{55} = C_{66} \\ C_{ij} &= C_{ji} \end{aligned} \quad (18.43)$$

from which we construct the C_{ij} matrix for a 3D isotropic medium. Note that the elastic modulus tensor for full rotational symmetry only two independent constants C_{11} and C_{12}

$$C_{ij} = \begin{bmatrix} C_{11} & C_{12} & C_{12} & 0 & 0 & 0 \\ C_{11} & C_{12} & 0 & 0 & 0 & 0 \\ C_{11} & 0 & 0 & 0 & 0 & 0 \\ & & \frac{1}{2}(C_{11} - C_{12}) & 0 & 0 & 0 \\ & & & \frac{1}{2}(C_{11} - C_{12}) & 0 & 0 \\ & & & & \frac{1}{2}(C_{11} - C_{12}) & \end{bmatrix} . \quad (18.44)$$

18.6.2 Icosahedral Symmetry

Any subgroup of the full rotation group for which the fivefold $\Gamma_{\ell=2}$ level degeneracy is not lifted will leave the form of the C_{ij} matrix invariant. The icosahedral group with inversion symmetry I_h , which is a subgroup of the full rotation group, and the icosahedral group without inversion I , which is a subgroup of both the full rotation group and the group I_h , are two examples of groups which preserve the fivefold degenerate level of the full rotation group and hence retain the form of the C_{ij} matrix given by (18.44). This result follows from at least two related arguments. The first argument relates to the compatibility relations between the full rotation group and the I_h group for which the basis functions follow the compatibility relations

$$\Gamma_{\ell=0} \longrightarrow (A_g)_{I_h} \quad \text{and} \quad \Gamma_{\ell=2} \longrightarrow (H_g)_{I_h} . \quad (18.45)$$

Thus, for the icosahedral group, we have for a symmetric second rank tensor:

$$\Gamma_{\overset{\leftrightarrow}{e}}^{(s)} = (A_g)_{I_h} + (H_g)_{I_h} . \quad (18.46)$$

From (18.46) we see that with respect to second rank tensors no lifting of degeneracy occurs in going from full rotational symmetry to I_h symmetry from which it follows that the number of nonvanishing independent constants in the C_{ij} matrix remains at 2 for I_h (and I) symmetry.

The same conclusion follows from the fact that the basis functions for $\Gamma_{\ell=0}$ and $\Gamma_{\ell=2}$ for the full rotation group can also be used as basis functions for the A_g and H_g irreducible representations of I_h . Therefore the same stress-strain relations are obtained in I_h symmetry as are given in (18.34) for full rotational symmetry. It therefore follows that the form of the C_{ij} matrix will also be the same for either group I_h or full rotational symmetry, thereby completing the proof.

Clearly, the direct product $\Gamma_{\overset{\leftrightarrow}{e}}^{(s)} \otimes \Gamma_{\overset{\leftrightarrow}{e}}^{(s)}$ given by (18.33) is not invariant as the symmetry is reduced from full rotational symmetry to I_h symmetry since the ninefold representation $\Gamma_{\ell=4}$ in (18.33) splits into the irreducible representations $(G_g + H_g)$ in going to the lower symmetry group I_h . But this is not of importance to the linear stress-strain equations which are invariant to this particular lowering of symmetry. However, when nonlinear effects are taken into account, and perturbations from (18.26) are needed to specify the nonlinear stress-strain relations, different mechanical behavior would be expected to occur in I_h symmetry in comparison to the full rotation group.

18.6.3 Cubic Symmetry

It should be noted that all symmetry groups forming Bravais lattices in condensed matter physics have too few symmetry operations to preserve the fivefold degeneracy of the $\ell = 2$ level of the full rotation group. For example, the Bravais lattice with the highest symmetry is the cubic group O_h .

The $\ell = 2$ irreducible representation in full rotational symmetry corresponds to a reducible representation of group O_h which splits into a threefold and a twofold level (the T_{2g} and E_g levels), so that in this case we will see below, three elastic constants are needed to specify the 6×6 matrix for C_{ij} in cubic O_h symmetry.

Since e_{ij} (where $i, j = x, y, z$) is a symmetric second rank tensor, the irreducible representations for e_{ij} in cubic symmetry are found as

$$\Gamma_{\overset{\leftrightarrow}{e}}^{(s)} = \Gamma_1^+ + \Gamma_{12}^+ + \Gamma_{25}^+. \quad (18.47)$$

From the direct product we obtain

$$\begin{aligned} \Gamma_{\overset{\leftrightarrow}{e}}^{(s)} \otimes \Gamma_{\overset{\leftrightarrow}{e}}^{(s)} &= (\Gamma_1^+ + \Gamma_{12}^+ + \Gamma_{25}^+) \otimes (\Gamma_1^+ + \Gamma_{12}^+ + \Gamma_{25}^+) \\ &= 3\Gamma_1^+ + \Gamma_2^+ + 4\Gamma_{12}^+ + 3\Gamma_{15}^+ + 5\Gamma_{25}^+, \end{aligned} \quad (18.48)$$

which has 21 symmetric partners ($3\Gamma_1^+ + 3\Gamma_{12}^+ + \Gamma_{15}^+ + 3\Gamma_{25}^+$) and 15 antisymmetric partners ($\Gamma_2^+ + \Gamma_{12}^+ + 2\Gamma_{15}^+ + 2\Gamma_{25}^+$) and three independent C_{ij} coefficients. These results could also be obtained by going from higher (full rotational R_∞) symmetry to lower (O_h) symmetry using the cubic field splittings of the angular momenta shown in Table 5.6.

Forming basis functions for the irreducible representations of the stress and strain tensors in cubic O_h symmetry, we can then write the symmetrized elastic constant equations as

$$\begin{aligned} (X_x + Y_y + Z_z) &= C_{\Gamma_1^+}(e_{xx} + e_{yy} + e_{zz}) & \text{for } \Gamma_1^+ \\ (X_x + \omega Y_y + \omega^2 Z_z) &= C_{\Gamma_{12}^+}(e_{xx} + \omega e_{yy} + \omega^2 e_{zz}) & \text{for } \Gamma_{12}^+ \\ (X_x + \omega^2 Y_y + \omega Z_z) &= C_{\Gamma_{12}^{+*}}(e_{xx} + \omega^2 e_{yy} + \omega e_{zz}) & \text{for } \Gamma_{12}^{+*} \\ (Y_z + Z_y) &= C_{\Gamma_{25}^+}(e_{yz}) & \text{for } \Gamma_{25x}^+ \\ (Z_x + X_z) &= C_{\Gamma_{25}^+}(e_{xz}) & \text{for } \Gamma_{25y}^+ \\ (X_y + Y_x) &= C_{\Gamma_{25}^+}(e_{xy}) & \text{for } \Gamma_{25z}^+. \end{aligned} \quad (18.49)$$

As in Sect. 18.6.1, we now solve for X_x , Y_y and Z_z in terms of e_{xx} , e_{yy} and e_{zz} to connect the three symmetry-based elastic constants $C_{\Gamma_1^+}^+$, $C_{\Gamma_{12}^+}^+$ and $C_{\Gamma_{25}^+}^+$ and the C_{11} , C_{12} and C_{44} in Nye's book (and other solid state physics books)

$$\begin{aligned} C_{11} &= (C_{\Gamma_1^+}^+ + 2C_{\Gamma_{12}^+}^+)/3 \\ C_{12} &= (C_{\Gamma_1^+}^+ - C_{\Gamma_{12}^+}^+)/3 \\ C_{44} &= C_{\Gamma_{25}^+}^+/2, \end{aligned} \quad (18.50)$$

yielding an elastic tensor for cubic symmetry O_h in the form

$$C_{ij} = \begin{bmatrix} C_{11} & C_{12} & C_{12} & 0 & 0 & 0 \\ & C_{11} & C_{12} & 0 & 0 & 0 \\ & & C_{11} & 0 & 0 & 0 \\ & & & C_{44} & 0 & 0 \\ & & & & C_{44} & 0 \\ & & & & & C_{44} \end{bmatrix}. \quad (18.51)$$

18.6.4 Other Symmetry Groups

We briefly sketch results for C_{ijkl} for several groups of lower symmetry.

One simple method for finding the irreducible representations for lower symmetry groups is to make use of the compatibility relations between the full rotation group and the lower symmetry groups. For example, for group $D_{\infty h}$ (see character Table A.34) we have

$$\begin{aligned} \Gamma_{\ell=0} &\longrightarrow A_{1g} \\ \Gamma_{\ell=1} &\longrightarrow A_{2u} + E_{1u} \\ \Gamma_{\ell=2} &\longrightarrow A_{1g} + E_{1g} + E_{2g} \\ \Gamma_{\ell=3} &\longrightarrow A_{2u} + E_{1u} + E_{2u} + E_{3u} \\ \Gamma_{\ell=4} &\longrightarrow A_{1g} + E_{1g} + E_{2g} + E_{3g} + E_{4g}. \end{aligned} \quad (18.52)$$

Since the symmetric second rank tensor e_{ij} transforms according to the sum $\Gamma_{\ell=0} + \Gamma_{\ell=2}$, then we look for the irreducible representations contained therein. For $D_{\infty h}$ symmetry we would then obtain

$$\Gamma_{\overrightarrow{e}}^{(s)} = A_{1g} + (A_{1g} + E_{1g} + E_{2g}) = 2A_{1g} + E_{1g} + E_{2g}, \quad (18.53)$$

and a similar procedure would be used for other low symmetry groups.

From the symmetric terms in (18.33) and (18.52), we find that the C_{ijkl} tensor transforms according to $2\Gamma_{\ell=0} + 2\Gamma_{\ell=2} + \Gamma_{\ell=4}$ which for $D_{\infty h}$ symmetry becomes

$$\begin{aligned} \Gamma_{C_{ijkl}} &= (2A_{1g}) + (2A_{1g} + 2E_{1g} + 2E_{2g}) + (A_{1g} + E_{1g} + E_{2g} + E_{3g} + E_{4g}) \\ &= 5A_{1g} + 3E_{1g} + 3E_{2g} + E_{3g} + E_{4g}. \end{aligned} \quad (18.54)$$

The same result as in (18.54) can be obtained by taking the direct product of $(A_{1g} + E_{1g} + E_{2g}) \otimes (A_{1g} + E_{1g} + E_{2g})$ which comes from $\Gamma_{\ell=2} \otimes \Gamma_{\ell=2}$ and retaining only the symmetric terms. From (18.54), we see that there are only five independent elastic constants remain for $D_{\infty h}$ symmetry.

To find the form of the elasticity matrix C_{ij} we go through the process of finding the (6×6) stress-strain relations for $\ell = 0, m = 0$ and

$\ell = 2, m = 2, 1, 0, -1, -2$ and then relate symmetry coefficients to obtain the C_{ij} coefficients and the relation between these to obtain the C_{ij} matrix for full axial $D_{\infty h}$ symmetry:

$$C_{ij} = \begin{bmatrix} C_{11} & C_{12} & C_{13} & 0 & 0 & 0 \\ & C_{11} & C_{13} & 0 & 0 & 0 \\ & & C_{33} & 0 & 0 & 0 \\ & & & C_{44} & 0 & 0 \\ & & & & C_{44} & 0 \\ & & & & & \frac{1}{2}(C_{11} - C_{12}) \end{bmatrix}. \quad (18.55)$$

The symmetric combination of irreducible representations for the group D_{6h} is

$$\Gamma_{\vec{e}}^{(s)} = 2A_{1g} + E_{1g} + E_{2g}, \quad (18.56)$$

which is isomorphic to $D_{\infty h}$. Using (18.33) and the irreducible representations contained in the angular momentum states $\ell = 0$, $\ell = 2$, and $\ell = 4$ in D_{6h} symmetry, we get

$$\begin{aligned} \Gamma_{\ell=0} &\rightarrow A_{1g} \\ \Gamma_{\ell=1} &\rightarrow A_{2u} + E_{1u} \\ \Gamma_{\ell=2} &\rightarrow A_{1g} + E_{1g} + E_{2g} \\ \Gamma_{\ell=3} &\rightarrow A_{2u} + B_{1u} + B_{2u} + E_{1u} + E_{2u} \\ \Gamma_{\ell=4} &\rightarrow A_{1g} + B_{1g} + B_{2g} + E_{1g} + 2E_{2g}, \end{aligned} \quad (18.57)$$

which gives

$$\Gamma_{C_{(ij)(kl)}} = 5A_{1g} + B_{1g} + B_{2g} + 3E_{1g} + 4E_{2g} \quad (18.58)$$

yielding five independent C_{ij} coefficients.

A similar analysis to that for the group $D_{\infty h}$, yields for D_{6h} the same form of C_{ij} as for $D_{\infty h}$ given by (18.55). As we go to lower symmetry more independent coefficients are needed.

For D_{2h} group symmetry which is the case of symmetry with respect to three mutually orthogonal planes (called *orthotropy* in the engineering mechanics literature), there remain nine independent components of C_{ij} . The C_{ij} tensor in this case assumes the form

$$C_{ij} = \begin{bmatrix} C_{11} & C_{12} & C_{13} & 0 & 0 & 0 \\ & C_{22} & C_{23} & 0 & 0 & 0 \\ & & C_{33} & 0 & 0 & 0 \\ & & & C_{44} & 0 & 0 \\ & & & & C_{55} & 0 \\ & & & & & C_{66} \end{bmatrix}. \quad (18.59)$$

The lowest nontrivial symmetry group for consideration of the elastic tensor is group C_{2h} with a single symmetry plane. In this case C_{ij} has 13 independent components and assumes the form

$$C_{ij} = \begin{bmatrix} C_{11} & C_{12} & C_{13} & 0 & 0 & C_{16} \\ C_{22} & C_{23} & 0 & 0 & C_{26} & \\ C_{33} & 0 & 0 & C_{36} & & \\ C_{44} & C_{45} & 0 & & & \\ C_{55} & 0 & & & & \\ C_{66} & & & & & \end{bmatrix}. \quad (18.60)$$

Selected Problems

18.1. Consider the third rank tensor $d_{i(jk)}$ in (18.6) and (18.7).

- (a) Show from Table 18.1 that there are exactly 18 independent coefficients after taking permutational symmetry into account.
- (b) Find the number of independent coefficients for full rotational symmetry.
- (c) Find the number of independent coefficients for O_h and T_d symmetries.
- (d) Finally find the number of independent coefficients for D_{4h} symmetry.

18.2. Suppose that stress is applied to FCC aluminum Al in the (100) direction, and suppose that the effect of the resulting strain is to lower the symmetry of aluminum from cubic O_h symmetry to tetragonal D_{4h} symmetry. The situation outlined here arises in the fabrication of superlattices using the molecular beam epitaxy technique.

- (a) How many independent elastic constants are there in the stressed aluminum Al?
- (b) What is the new symmetrized form of the stress-strain relations (see (18.34))?
- (c) What is the form of the C_{ijkl} tensor for D_{4h} symmetry (see (18.44))?

18.3. (a) Assume that the material in Problem 18.2 is a nonlinear elastic material and the stress-strain relation is of the form

$$\sigma_{ij}^m = C_{ijkl}^{(2)} \varepsilon_{kl} + C_{ijklmn}^{(3)} \varepsilon_{kl} \varepsilon_{mn} + \dots$$

Consider the symmetry of the nonlinear tensor coefficient $C_{ijklmn}^{(3)}$ explicitly. How many independent constants are there in $C_{ijklmn}^{(3)}$ assuming that the point group symmetry is C_1 (i.e., no rotational symmetry elements other than the identity operation), but taking into account permutation symmetry?

- (b) How many independent constants are there when taking into account both permutation and crystal (O_h) symmetry? (Note: To do this problem, you may have to make a new entry to Table 18.1.)

18.4. Suppose that we prepare a quantum well using as the constituents GaAs and $\text{GaAs}_{1-x}\text{P}_x$. In bulk form GaAs and similar III–V compounds have T_d symmetry. The lattice mismatch introduces lattice strain and lowers the symmetry. Denote by \hat{z} the direction normal to the layer. Find the number of independent coefficients in the polarizability tensor, including $\overset{\leftrightarrow}{\alpha}^{(2)}$, $\overset{\leftrightarrow}{\alpha}^{(3)}$, and $\overset{\leftrightarrow}{\alpha}^{(4)}$, for

- (i) $\hat{z} \parallel (100)$
- (ii) $\hat{z} \parallel (111)$
- (iii) $\hat{z} \parallel (110)$

Using these results, how can infrared and Raman spectroscopy be used to distinguish between the crystalline orientation of the quantum well?

A

Point Group Character Tables

Appendix A contains Point Group Character (Tables A.1–A.34) to be used throughout the chapters of this book. Pedagogic material to assist the reader in the use of these character tables can be found in Chap. 3. The Schoenflies symmetry (Sect. 3.9) and Hermann–Mauguin notations (Sect. 3.10) for the point groups are also discussed in Chap. 3.

Some of the more novel listings in this appendix are the groups with five-fold symmetry C_5 , C_{5h} , C_{5v} , D_5 , D_{5d} , D_{5h} , I , I_h . The cubic point group O_h in Table A.31 lists basis functions for all the irreducible representations of O_h and uses the standard solid state physics notation for the irreducible representations.

Table A.1. Character table for group C_1 (triclinic)

| C_1 (1) | E |
|-----------|-----|
| A | 1 |

Table A.2. Character table for group $C_i = S_2$ (triclinic)

| S_2 ($\bar{1}$) | | E | i |
|---------------------|-----------------|-------|-----|
| x^2, y^2, z^2 | R_x, R_y, R_z | A_g | 1 |
| xy, xz, yz | x, y, z | A_u | 1 |
| | | | -1 |

Table A.3. Character table for group $C_{1h} = S_1$ (monoclinic)

| $C_{1h}(m)$ | | E | σ_h |
|---------------------|---------------|-------|------------|
| x^2, y^2, z^2, xy | R_z, x, y | A' | 1 |
| xz, yz | R_x, R_y, z | A'' | 1 |
| | | | -1 |

Table A.4. Character table for group C_2 (monoclinic)

| C_2 (2) | | | E | C_2 |
|---------------------|--------------------------|-----|-----|-------|
| x^2, y^2, z^2, xy | R_z, z | A | 1 | 1 |
| | (x, y) (R_x, R_y) | B | 1 | -1 |

Table A.5. Character table for group C_{2v} (orthorhombic)

| C_{2v} (2mm) | | | E | C_2 | σ_v | σ'_v |
|-----------------|----------|-------|-----|-------|------------|-------------|
| x^2, y^2, z^2 | z | A_1 | 1 | 1 | 1 | 1 |
| xy | R_z | A_2 | 1 | 1 | -1 | -1 |
| xz | R_y, x | B_1 | 1 | -1 | 1 | -1 |
| yz | R_x, y | B_2 | 1 | -1 | -1 | 1 |

Table A.6. Character table for group C_{2h} (monoclinic)

| C_{2h} (2/m) | | | E | C_2 | σ_h | i |
|---------------------|------------|-------|-----|-------|------------|-----|
| x^2, y^2, z^2, xy | R_z | A_g | 1 | 1 | 1 | 1 |
| | z | A_u | 1 | 1 | -1 | -1 |
| | R_x, R_y | B_g | 1 | -1 | -1 | 1 |
| | x, y | B_u | 1 | -1 | 1 | -1 |

Table A.7. Character table for group $D_2 = V$ (orthorhombic)

| D_2 (222) | | | E | C_2^z | C_2^y | C_2^x |
|-----------------|----------|-------|-----|---------|---------|---------|
| x^2, y^2, z^2 | | A_1 | 1 | 1 | 1 | 1 |
| xy | R_z, z | B_1 | 1 | 1 | -1 | -1 |
| xz | R_y, y | B_2 | 1 | -1 | 1 | -1 |
| yz | R_x, x | B_3 | 1 | -1 | -1 | 1 |

Table A.8. Character table for group $D_{2d} = V_d$ (tetragonal)

| D_{2d} (42m) | | | E | C_2 | $2S_4$ | $2C'_2$ | $2\sigma_d$ |
|------------------|--------------------------|-------|-----|-------|--------|---------|-------------|
| $x^2 + y^2, z^2$ | R_z | A_1 | 1 | 1 | 1 | 1 | 1 |
| | | A_2 | 1 | 1 | 1 | -1 | -1 |
| $x^2 - y^2$ | z | B_1 | 1 | 1 | -1 | 1 | -1 |
| | | B_2 | 1 | 1 | -1 | -1 | 1 |
| (xz, yz) | (x, y) (R_x, R_y) | E | 2 | -2 | 0 | 0 | 0 |

 $D_{2h} = D_2 \otimes i$ (mmm) (orthorhombic)

Table A.9. Character table for group C_3 (rhombohedral)

| $C_3(3)$ | | | E | C_3 | C_3^2 |
|---------------------------------|--------------------------|-----|------------------------------------|--|--|
| $x^2 + y^2, z^2$ | R_z, z | A | 1 | 1 | 1 |
| (xz, yz) $(x^2 - y^2, xy)$ | (x, y) (R_x, R_y) | E | $\begin{cases} 1 \\ 1 \end{cases}$ | $\begin{cases} \omega \\ \omega^2 \end{cases}$ | $\begin{cases} \omega^2 \\ \omega \end{cases}$ |

$$\omega = e^{2\pi i/3}$$

Table A.10. Character table for group C_{3v} (rhombohedral)

| $C_{3v} (3m)$ | | | E | $2C_3$ | $3\sigma_v$ |
|---------------------------------|--------------------------|-------|-----|--------|-------------|
| $x^2 + y^2, z^2$ | z | A_1 | 1 | 1 | 1 |
| | R_z | A_2 | 1 | 1 | -1 |
| $(x^2 - y^2, xy)$ (xz, yz) | (x, y) (R_x, R_y) | E | 2 | -1 | 0 |

Table A.11. Character table for group $C_{3h} = S_3$ (hexagonal)

| $C_{3h} = C_3 \otimes \sigma_h (\bar{6})$ | | | E | C_3 | C_3^2 | σ_h | S_3 | $(\sigma_h C_3^2)$ |
|---|--------------|-------|------------------------------------|--|--|------------|------------|--------------------|
| $x^2 + y^2, z^2$ | R_z | A' | 1 | 1 | 1 | 1 | 1 | 1 |
| | z | A'' | 1 | 1 | 1 | -1 | -1 | -1 |
| $(x^2 - y^2, xy)$ | (x, y) | E' | $\begin{cases} 1 \\ 1 \end{cases}$ | $\begin{cases} \omega \\ \omega^2 \end{cases}$ | $\begin{cases} \omega^2 \\ \omega \end{cases}$ | 1 | ω | ω^2 |
| (xz, yz) | (R_x, R_y) | E'' | $\begin{cases} 1 \\ 1 \end{cases}$ | $\begin{cases} \omega \\ \omega^2 \end{cases}$ | $\begin{cases} \omega \\ \omega \end{cases}$ | -1 | ω^2 | ω |

$$\omega = e^{2\pi i/3}$$

Table A.12. Character table for group D_3 (rhombohedral)

| $D_3 (32)$ | | | E | $2C_3$ | $3C_2'$ |
|---------------------------------|--------------------------|-------|-----|--------|---------|
| $x^2 + y^2, z^2$ | | A_1 | 1 | 1 | 1 |
| | R_z, z | A_2 | 1 | 1 | -1 |
| (xz, yz) $(x^2 - y^2, xy)$ | (x, y) (R_x, R_y) | E | 2 | -1 | 0 |

Table A.13. Character table for group D_{3d} (rhombohedral)

| $D_{3d} = D_3 \otimes i (\bar{3}m)$ | | | E | $2C_3$ | $3C_2'$ | i | $2iC_3$ | $3iC_2'$ |
|-------------------------------------|--------------|----------|-----|--------|---------|-----|---------|----------|
| $x^2 + y^2, z^2$ | | A_{1g} | 1 | 1 | 1 | 1 | 1 | 1 |
| | R_z | A_{2g} | 1 | 1 | -1 | 1 | 1 | -1 |
| $(xz, yz), (x^2 - y^2, xy)$ | (R_x, R_y) | E_g | 2 | -1 | 0 | 2 | -1 | 0 |
| | z | A_{1u} | 1 | 1 | 1 | -1 | -1 | -1 |
| | | A_{2u} | 1 | 1 | -1 | -1 | -1 | 1 |
| | (x, y) | E_u | 2 | -1 | 0 | -2 | 1 | 0 |

Table A.14. Character table for group D_{3h} (hexagonal)

| $D_{3h} = D_3 \otimes \sigma_h$ ($\bar{6}m2$) | | | E | σ_h | $2C_3$ | $2S_3$ | $3C'_2$ | $3\sigma_v$ |
|---|-------|---------|-----|------------|--------|--------|---------|-------------|
| $x^2 + y^2, z^2$ | R_z | A'_1 | 1 | 1 | 1 | 1 | 1 | 1 |
| | | A'_2 | 1 | 1 | 1 | 1 | -1 | -1 |
| | | A''_1 | 1 | -1 | 1 | -1 | 1 | -1 |
| | z | A''_2 | 1 | -1 | 1 | -1 | -1 | 1 |
| $(x^2 - y^2, xy)$ | | E' | 2 | 2 | -1 | -1 | 0 | 0 |
| (xz, yz) | | E'' | 2 | -2 | -1 | 1 | 0 | 0 |

Table A.15. Character table for group C_4 (tetragonal)

| C_4 (4) | | | E | C_2 | C_4 | C_4^3 |
|------------------|----------|-----|--|--|--|--|
| $x^2 + y^2, z^2$ | R_z, z | A | 1 | 1 | 1 | 1 |
| | | B | 1 | 1 | -1 | -1 |
| | | E | $\begin{cases} 1 & -1 \\ 1 & -1 \end{cases}$ | $\begin{cases} i & -i \\ -i & i \end{cases}$ | $\begin{cases} i & -i \\ -i & i \end{cases}$ | $\begin{cases} i & -i \\ -i & i \end{cases}$ |
| | | E | $\begin{cases} 1 & -1 \\ 1 & -1 \end{cases}$ | $\begin{cases} i & -i \\ -i & i \end{cases}$ | $\begin{cases} i & -i \\ -i & i \end{cases}$ | $\begin{cases} i & -i \\ -i & i \end{cases}$ |

Table A.16. Character table for group C_{4v} (tetragonal)

| C_{4v} (4mm) | | | E | C_2 | $2C_4$ | $2\sigma_v$ | $2\sigma_d$ |
|-------------------|--------------------------|-------|--|--|--|--|--|
| $x^2 + y^2, z^2$ | R_z | A_1 | 1 | 1 | 1 | 1 | 1 |
| | | A_2 | 1 | 1 | 1 | -1 | -1 |
| | | B_1 | 1 | 1 | -1 | 1 | -1 |
| | | B_2 | 1 | 1 | -1 | -1 | 1 |
| (xz, yz) | (x, y) (R_x, R_y) | E | 2 | -2 | 0 | 0 | 0 |
| $(x^2 - y^2, xy)$ | | E | $\begin{cases} 1 & -1 \\ 1 & -1 \end{cases}$ | $\begin{cases} i & -i \\ -i & i \end{cases}$ | $\begin{cases} i & -i \\ -i & i \end{cases}$ | $\begin{cases} i & -i \\ -i & i \end{cases}$ | $\begin{cases} i & -i \\ -i & i \end{cases}$ |

 $C_{4h} = C_4 \otimes i$ (4/m) (tetragonal)**Table A.17.** Character table for group S_4 (tetragonal)

| S_4 ($\bar{4}$) | | | E | C_2 | S_4 | S_4^3 |
|---------------------|-------|-----|--|--|--|--|
| $x^2 + y^2, z^2$ | R_z | A | 1 | 1 | 1 | 1 |
| | | B | 1 | 1 | -1 | -1 |
| | | E | $\begin{cases} 1 & -1 \\ 1 & -1 \end{cases}$ | $\begin{cases} i & -i \\ -i & i \end{cases}$ | $\begin{cases} i & -i \\ -i & i \end{cases}$ | $\begin{cases} i & -i \\ -i & i \end{cases}$ |
| | | E | $\begin{cases} 1 & -1 \\ 1 & -1 \end{cases}$ | $\begin{cases} i & -i \\ -i & i \end{cases}$ | $\begin{cases} i & -i \\ -i & i \end{cases}$ | $\begin{cases} i & -i \\ -i & i \end{cases}$ |

Table A.18. Character table for group D_4 (tetragonal)

| D_4 (422) | | | E | $C_2 = C_4^2$ | $2C_4$ | $2C'_2$ | $2C''_2$ |
|-------------------|--------------------------|-------|--|--|--|--|--|
| $x^2 + y^2, z^2$ | R_z, z | A_1 | 1 | 1 | 1 | 1 | 1 |
| | | A_2 | 1 | 1 | 1 | -1 | -1 |
| | | B_1 | 1 | 1 | -1 | 1 | -1 |
| | | B_2 | 1 | 1 | -1 | -1 | 1 |
| (xz, yz) | (x, y) (R_x, R_y) | E | 2 | -2 | 0 | 0 | 0 |
| $(x^2 - y^2, xy)$ | | E | $\begin{cases} 1 & -1 \\ 1 & -1 \end{cases}$ | $\begin{cases} i & -i \\ -i & i \end{cases}$ | $\begin{cases} i & -i \\ -i & i \end{cases}$ | $\begin{cases} i & -i \\ -i & i \end{cases}$ | $\begin{cases} i & -i \\ -i & i \end{cases}$ |

 $D_{4h} = D_4 \otimes i$ (4/mmm) (tetragonal)

Table A.19. Character table for group C_6 (hexagonal)

| C_6 (6) | | | E | C_6 | C_3 | C_2 | C_3^2 | C_6^5 |
|------------------|--|-------|--|--|--|--|--|---------|
| $x^2 + y^2, z^2$ | R_z, z | A | 1 | 1 | 1 | 1 | 1 | 1 |
| | | B | 1 | -1 | 1 | -1 | 1 | -1 |
| (xz, yz) | $\begin{matrix} (x, y) \\ (R_x, R_y) \end{matrix}$ | E' | $\begin{cases} 1 & \omega \\ 1 & \omega^5 \end{cases}$ | $\begin{matrix} \omega^2 \\ \omega^4 \end{matrix}$ | $\begin{matrix} \omega^3 \\ \omega^3 \end{matrix}$ | $\begin{matrix} \omega^4 \\ \omega^2 \end{matrix}$ | $\begin{matrix} \omega^5 \\ \omega \end{matrix}$ | |
| | | E'' | $\begin{cases} 1 & \omega^2 \\ 1 & \omega^4 \end{cases}$ | $\begin{matrix} \omega^4 \\ \omega^2 \end{matrix}$ | 1 | $\begin{matrix} \omega^2 \\ \omega^4 \end{matrix}$ | $\begin{matrix} \omega^4 \\ \omega^2 \end{matrix}$ | |

$$\omega = e^{2\pi i/6}$$

Table A.20. Character table for group C_{6v} (hexagonal)

| C_{6v} (6mm) | | | E | C_2 | $2C_3$ | $2C_6$ | $3\sigma_d$ | $3\sigma_v$ |
|------------------|--|-------|-----|-------|--------|--------|-------------|-------------|
| $x^2 + y^2, z^2$ | R_z | A_1 | 1 | 1 | 1 | 1 | 1 | 1 |
| | | A_2 | 1 | 1 | 1 | 1 | -1 | -1 |
| | | B_1 | 1 | -1 | 1 | -1 | -1 | 1 |
| | | B_2 | 1 | -1 | 1 | -1 | 1 | -1 |
| (xz, yz) | $\begin{matrix} (x, y) \\ (R_x, R_y) \end{matrix}$ | E_1 | 2 | -2 | -1 | 1 | 0 | 0 |
| | | E_2 | 2 | 2 | -1 | -1 | 0 | 0 |

$$C_{6h} = C_6 \otimes i \text{ (6/m) (hexagonal); } S_6 = C_3 \otimes i \text{ (\overline{3}) (rhombohedral)}$$

Table A.21. Character table for group D_6 (hexagonal)

| D_6 (622) | | | E | C_2 | $2C_3$ | $2C_6$ | $3C_2'$ | $3C_2''$ |
|------------------|--|-------|-----|-------|--------|--------|---------|----------|
| $x^2 + y^2, z^2$ | R_z, z | A_1 | 1 | 1 | 1 | 1 | 1 | 1 |
| | | A_2 | 1 | 1 | 1 | 1 | -1 | -1 |
| | | B_1 | 1 | -1 | 1 | -1 | 1 | -1 |
| | | B_2 | 1 | -1 | 1 | -1 | -1 | 1 |
| (xz, yz) | $\begin{matrix} (x, y) \\ (R_x, R_y) \end{matrix}$ | E_1 | 2 | -2 | -1 | 1 | 0 | 0 |
| | | E_2 | 2 | 2 | -1 | -1 | 0 | 0 |

$$D_{6h} = D_6 \otimes i \text{ (6/mmm) (hexagonal)}$$

Table A.22. Character table for group C_5 (icosahedral)

| C_5 (5) | | | E | C_5 | C_5^2 | C_5^3 | C_5^4 |
|------------------|--|-------|--|--|--|--|--|
| $x^2 + y^2, z^2$ | R_z, z | A | 1 | 1 | 1 | 1 | 1 |
| | | E' | $\begin{cases} 1 & \omega \\ 1 & \omega^4 \end{cases}$ | $\begin{matrix} \omega^2 \\ \omega^3 \end{matrix}$ | $\begin{matrix} \omega^3 \\ \omega^2 \end{matrix}$ | $\begin{matrix} \omega^4 \\ \omega \end{matrix}$ | $\begin{matrix} \omega^4 \\ \omega \end{matrix}$ |
| (xz, yz) | $\begin{matrix} (x, y) \\ (R_x, R_y) \end{matrix}$ | E'' | $\begin{cases} 1 & \omega^2 \\ 1 & \omega^3 \end{cases}$ | $\begin{matrix} \omega^4 \\ \omega \end{matrix}$ | $\begin{matrix} \omega \\ \omega^4 \end{matrix}$ | $\begin{matrix} \omega \\ \omega^4 \end{matrix}$ | $\begin{matrix} \omega^3 \\ \omega^2 \end{matrix}$ |
| | | | | | | | |

$$\omega = e^{2\pi i/5}. \text{ Note group } C_{5h} = C_5 \otimes \sigma_h = S_{10}(\overline{10})$$

Table A.23. Character table for group C_{5v} (icosahedral)

| C_{5v} ($5m$) | | | E | $2C_5$ | $2C_5^2$ | $5\sigma_v$ |
|-------------------------------------|--|-------|-----|------------------|------------------|-------------|
| $x^2 + y^2, z^2, z^3, z(x^2 + y^2)$ | z | A_1 | 1 | 1 | 1 | 1 |
| | R_z | A_2 | 1 | 1 | 1 | -1 |
| | (x, y) $\{(R_x, R_y)\}$ | E_1 | 2 | $2 \cos \alpha$ | $2 \cos 2\alpha$ | 0 |
| | $(x^2 - y^2, xy), z(x^2 - y^2, xy),$ $[x(x^2 - 3y^2), y(3x^2 - y^2)]$ | E_2 | 2 | $2 \cos 2\alpha$ | $2 \cos 4\alpha$ | 0 |

$\alpha = 2\pi/5 = 72^\circ$. Note that $\tau = (1 + \sqrt{5})/2$ so that $\tau = -2 \cos 2\alpha = -2 \cos 4\pi/5$ and $\tau - 1 = 2 \cos \alpha = 2 \cos 2\pi/5$

Table A.24. Character table for group D_5 (icosahedral)

| D_5 (52) | | | E | $2C_5$ | $2C_5^2$ | $5C'_2$ |
|------------------|--|-------|-----|------------------|------------------|---------|
| $x^2 + y^2, z^2$ | R_z, z (x, y) $\{(R_x, R_y)\}$ | A_1 | 1 | 1 | 1 | 1 |
| | | A_2 | 1 | 1 | 1 | -1 |
| | | E_1 | 2 | $2 \cos \alpha$ | $2 \cos 2\alpha$ | 0 |
| | | E_2 | 2 | $2 \cos 2\alpha$ | $2 \cos 4\alpha$ | 0 |

Table A.25. Character table for D_{5d} (icosahedral)

| D_{5d} | E | $2C_5$ | $2C_5^2$ | $5C'_2$ | i | $2S_{10}^{-1}$ | $2S_{10}$ | $5\sigma_d$ | $(h = 20)$ |
|----------|-----|------------|------------|---------|-----|----------------|------------|-------------|----------------------------|
| A_{1g} | +1 | +1 | +1 | +1 | +1 | +1 | +1 | +1 | $(x^2 + y^2), z^2$ |
| A_{2g} | +1 | +1 | +1 | -1 | +1 | +1 | +1 | -1 | R_z |
| E_{1g} | +2 | $\tau - 1$ | $-\tau$ | 0 | +2 | $\tau - 1$ | $-\tau$ | 0 | $z(x + iy, x - iy)$ |
| E_{2g} | +2 | $-\tau$ | $\tau - 1$ | 0 | +2 | $-\tau$ | $\tau - 1$ | 0 | $[(x + iy)^2, (x - iy)^2]$ |
| A_{1u} | +1 | +1 | +1 | +1 | -1 | -1 | -1 | -1 | |
| A_{2u} | +1 | +1 | +1 | -1 | -1 | -1 | -1 | +1 | z |
| E_{1u} | +2 | $\tau - 1$ | $-\tau$ | 0 | -2 | $1 - \tau$ | $+\tau$ | 0 | $(x + iy, x - iy)$ |
| E_{2u} | +2 | $-\tau$ | $\tau - 1$ | 0 | -2 | $+\tau$ | $1 - \tau$ | 0 | |

Note: $D_{5d} = D_5 \otimes i$, $iC_5 = S_{10}^{-1}$ and $iC_5^2 = S_{10}$. Also $iC'_2 = \sigma_d$

Table A.26. Character table for D_{5h} (icosahedral)

| D_{5h} ($\bar{10}2m$) | E | $2C_5$ | $2C_5^2$ | $5C'_2$ | σ_h | $2S_5$ | $2S_5^3$ | $5\sigma_v$ | $(h = 20)$ |
|---------------------------|-----|------------|------------|---------|------------|------------|------------|-------------|---|
| A'_1 | +1 | +1 | +1 | +1 | +1 | +1 | +1 | +1 | $x^2 + y^2, z^2$ |
| A'_2 | +1 | +1 | +1 | -1 | +1 | +1 | +1 | -1 | R_z |
| E'_1 | +2 | $\tau - 1$ | $-\tau$ | 0 | +2 | $\tau - 1$ | $-\tau$ | 0 | $(x, y), (xz^2, yz^2),$ $[x(x^2 + y^2), y(x^2 + y^2)]$ |
| E'_2 | +2 | $-\tau$ | $\tau - 1$ | 0 | +2 | $-\tau$ | $\tau - 1$ | 0 | $(x^2 - y^2, xy),$ $[y(3x^2 - y^2), x(x^2 - 3y^2)]$ |
| A''_1 | +1 | +1 | +1 | +1 | -1 | -1 | -1 | -1 | |
| A''_2 | +1 | +1 | +1 | -1 | -1 | -1 | -1 | +1 | $z, z^3, z(x^2 + y^2)$ |
| E''_1 | +2 | $\tau - 1$ | $-\tau$ | 0 | -2 | $1 - \tau$ | $+\tau$ | 0 | $(R_x, R_y), (xz, yz)$ |
| E''_2 | +2 | $-\tau$ | $\tau - 1$ | 0 | -2 | $+\tau$ | $1 - \tau$ | 0 | $[xyz, z(x^2 - y^2)]$ |

$D_{5h} = D_5 \otimes \sigma_h$

Table A.27. Character table for the icosahedral group I (icosahedral)

| I (532) | E | $12C_5$ | $12C_5^2$ | $20C_3$ | $15C_2$ | $(h = 60)$ |
|-----------|-----|-----------|-----------|---------|---------|---|
| A | +1 | +1 | +1 | +1 | +1 | $x^2 + y^2 + z^2$ |
| F_1 | +3 | + τ | 1- τ | 0 | -1 | $(x, y, z); (R_x, R_y, R_z)$ |
| F_2 | +3 | 1- τ | + τ | 0 | -1 | |
| G | +4 | -1 | -1 | +1 | 0 | |
| H | +5 | 0 | 0 | -1 | +1 | $\begin{cases} 2z^2 - x^2 - y^2 \\ x^2 - y^2 \\ xy \\ xz \\ yz \end{cases}$ |

Table A.28. Character table for I_h (icosahedral)

| I_h | E | $12C_5$ | $12C_5^2$ | $20C_3$ | $15C_2$ | i | $12S_{10}^3$ | $12S_{10}$ | $20S_6$ | 15σ | $(h = 120)$ |
|----------|-----|-----------|-----------|---------|---------|-----|--------------|------------|---------|------------|---|
| A_g | +1 | +1 | +1 | +1 | +1 | +1 | +1 | +1 | +1 | +1 | $x^2 + y^2 + z^2$ |
| F_{1g} | +3 | + τ | 1- τ | 0 | -1 | +3 | τ | 1- τ | 0 | -1 | R_x, R_y, R_z |
| F_{2g} | +3 | 1- τ | + τ | 0 | -1 | +3 | 1- τ | τ | 0 | -1 | |
| G_g | +4 | -1 | -1 | +1 | 0 | +4 | -1 | -1 | +1 | 0 | |
| H_g | +5 | 0 | 0 | -1 | +1 | +5 | 0 | 0 | -1 | +1 | $\begin{cases} 2z^2 - x^2 - y^2 \\ x^2 - y^2 \\ xy \\ xz \\ yz \end{cases}$ |
| A_u | +1 | +1 | +1 | +1 | +1 | -1 | -1 | -1 | -1 | -1 | |
| F_{1u} | +3 | + τ | 1- τ | 0 | -1 | -3 | - τ | $\tau - 1$ | 0 | +1 | (x, y, z) |
| F_{2u} | +3 | 1- τ | + τ | 0 | -1 | -3 | $\tau - 1$ | - τ | 0 | +1 | |
| G_u | +4 | -1 | -1 | +1 | 0 | -4 | +1 | +1 | -1 | 0 | |
| H_u | +5 | 0 | 0 | -1 | +1 | -5 | 0 | 0 | +1 | -1 | |

$\tau = (1 + \sqrt{5})/2$. Note: C_5 and C_5^{-1} are in different classes, labeled $12C_5$ and $12C_5^2$ in the character table. Then $iC_5 = S_{10}^{-1}$ and $iC_5^{-1} = S_{10}$ are in the classes labeled $12S_{10}^3$ and $12S_{10}$, respectively. Also $iC_2 = \sigma_v$ and $I_h = I \otimes i$

Table A.29. Character table for group T (cubic)

| T (23) | | E | $3C_2$ | $4C_3$ | $4C'_3$ |
|---------------------------|-----|---|--------|----------|------------|
| $x^2 + y^2 + z^2$ | A | 1 | 1 | 1 | 1 |
| $(x^2 - y^2, 3z^2 - r^2)$ | E | $\begin{cases} 1 \\ 1 \\ 1 \end{cases}$ | 1 | ω | ω^2 |
| (R_x, R_y, R_z) | T | 3 | -1 | 0 | 0 |
| (x, y, z) | | | | | |
| (yz, zx, xy) | | | | | |

$\omega = e^{2\pi i/3}$; $T_h = T \otimes i$, (m3) (cubic)

Table A.30. Character table for group O (cubic)

| O (432) | | E | $8C_3$ | $3C_2 = 3C_4^2$ | $6C'_2$ | $6C_4$ |
|---------------------------|-------|-----|--------|-----------------|---------|--------|
| $(x^2 + y^2 + z^2)$ | A_1 | 1 | 1 | | 1 | 1 |
| | A_2 | 1 | 1 | | 1 | -1 |
| $(x^2 - y^2, 3z^2 - r^2)$ | E | 2 | -1 | | 2 | 0 |
| | T_1 | 3 | 0 | | -1 | -1 |
| (x, y, z) | | | | | | 1 |
| | T_2 | 3 | 0 | | -1 | -1 |

$O_h = O \otimes i$, ($m3m$) (cubic)

Table A.31. Character table for the cubic group O_h (cubic)†

| repr. basis functions | E | $3C_4^2$ | $6C_4$ | $6C'_2$ | $8C_3$ | i | $3iC_4^2$ | $6iC_4$ | $6iC'_2$ | $8iC_3$ |
|---|-----|----------|--------|---------|--------|-----|-----------|---------|----------|---------|
| A_1^+ 1 | | 1 | 1 | 1 | 1 | 1 | 1 | 1 | 1 | 1 |
| A_2^+ $\begin{cases} x^4(y^2 - z^2) + \\ y^4(z^2 - x^2) + \\ z^4(x^2 - y^2) \end{cases}$ | | 1 | 1 | -1 | -1 | 1 | 1 | -1 | -1 | 1 |
| E^+ $\begin{cases} x^2 - y^2 \\ 2z^2 - x^2 - y^2 \end{cases}$ | | 2 | 2 | 0 | 0 | -1 | 2 | 2 | 0 | 0 |
| T_1^- x, y, z | | 3 | -1 | 1 | -1 | 0 | -3 | 1 | -1 | 1 |
| T_2^- $z(x^2 - y^2) \dots$ | | 3 | -1 | -1 | 1 | 0 | -3 | 1 | 1 | -1 |
| A_1^- $\begin{cases} xyz[x^4(y^2 - z^2) + \\ y^4(z^2 - x^2) + \\ z^4(x^2 - y^2)] \end{cases}$ | | 1 | 1 | 1 | 1 | 1 | -1 | -1 | -1 | -1 |
| A_2^- xyz | | 1 | 1 | -1 | -1 | 1 | -1 | -1 | 1 | 1 |
| E^- $xyz(x^2 - y^2) \dots$ | | 2 | 2 | 0 | 0 | -1 | -2 | -2 | 0 | 0 |
| T_1^+ $xy(x^2 - y^2) \dots$ | | 3 | -1 | 1 | -1 | 0 | 3 | -1 | 1 | -1 |
| T_2^+ xy, yz, zx | | 3 | -1 | -1 | 1 | 0 | 3 | -1 | -1 | 1 |

† The basis functions for T_2^- are $z(x^2 - y^2)$, $x(y^2 - z^2)$, $y(z^2 - x^2)$, for E^- are $xyz(x^2 - y^2)$, $xyz(3z^2 - s^2)$ and for T_1^+ are $xy(x^2 - y^2)$, $yz(y^2 - z^2)$, $zx(z^2 - x^2)$

Table A.32. Character table for group T_d (cubic)^a

| T_d ($\bar{4}3m$) | | E | $8C_3$ | $3C_2$ | $6\sigma_d$ | $6S_4$ |
|---------------------------|-------|-----|--------|--------|-------------|--------|
| $x^2 + y^2 + z^2$ | A_1 | 1 | 1 | 1 | 1 | 1 |
| | A_2 | 1 | 1 | 1 | -1 | -1 |
| $(x^2 - y^2, 3z^2 - r^2)$ | E | 2 | -1 | 2 | 0 | 0 |
| | T_1 | 3 | 0 | -1 | -1 | 1 |
| (R_x, R_y, R_z) | | | | | | |
| | T_2 | 3 | 0 | -1 | 1 | -1 |

^a Note that (yz, zx, xy) transforms as representation T_1

Table A.33. Character table for group $C_{\infty v}$

| $C_{\infty v}(\infty m)$ | | | E | $2C_\phi$ | σ_v |
|--------------------------|---|-----------------|----------|----------------|------------|
| $(x^2 + y^2, z^2)$ | z | $A_1(\Sigma^+)$ | 1 | 1 | 1 |
| | R_z | $A_2(\Sigma^-)$ | 1 | 1 | -1 |
| (xz, yz) | $\begin{matrix} (x, y) \\ (R_x, R_y) \end{matrix} \Big\}$ | $E_1(\Pi)$ | 2 | $2 \cos \phi$ | 0 |
| $(x^2 - y^2, xy)$ | | $E_2(\Delta)$ | 2 | $2 \cos 2\phi$ | 0 |
| | | \vdots | \vdots | \vdots | \vdots |

Table A.34. Character table for group $D_{\infty h}$

B

Two-Dimensional Space Groups

We include in this appendix a summary of the crystallographic symmetries for all 17 of the 2D space groups, taken from the “International Tables for X-ray Crystallography” [58].

Table B.1. The two-dimensional oblique space group $p1$ or #1 ($p1$)

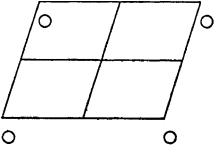
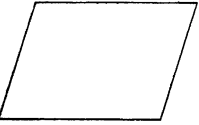
| $p1$ | No. 1 | $p1$ | 1 Oblique |
|---|---|---|-----------|
|  |  | | |
| | Origin on 1 | | |
| Number of positions Wyckoff notation, and point symmetry | Co-ordinates of equivalent positions | Conditions limiting possible reflections | |
| $1 \ a \ 1 \ x, y$ | | General: No conditions | |

Table B.2. The two-dimensional oblique space group $p2$ or #2 ($p2111$)

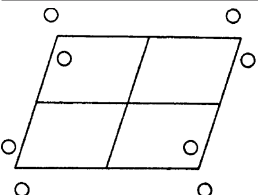
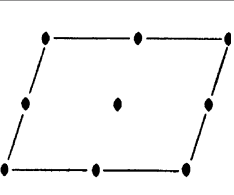
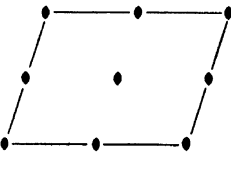
| $p2$ | No. 2 | $p2111$ | 2 Oblique |
|---|---|---|------------------------|
|  |  |  | |
| Origin at 2 | | | |
| 2 e 1 $x, y; \bar{x}, \bar{y}$ | | | General: No conditions |
| 1 d 2 $\frac{1}{2}, \frac{1}{2}$ | | | Special: No conditions |
| 1 c 2 $\frac{1}{2}, 0$ | | | |
| 1 b 2 $0, \frac{1}{2}$ | | | |
| 1 a 2 $0, 0$ | | | |

Table B.3. The two-dimensional rectangular space group pm or #3 ($p1m1$)

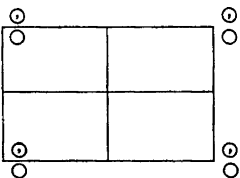
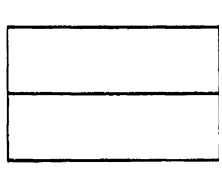
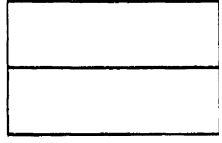
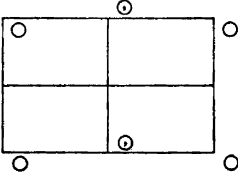
| pm | No. 3 | $p1m1$ | m Rectangular |
|---|---|---|---------------------------|
|  |  |  | |
| Origin on m | | | |
| Number of positions | Co-ordinates of | | Conditions limiting |
| Wyckoff notation, | equivalent positions | | possible reflections |
| and point symmetry | | | |
| 2 c 1 $x, y; \bar{x}, \bar{y}$ | | | General: No conditions |
| 1 b m $\frac{1}{2}, y$ | | | Special: No conditions |
| 1 a m $0, y$ | | | |

Table B.4. The two-dimensional space group pg or #4 ($p1g1$)

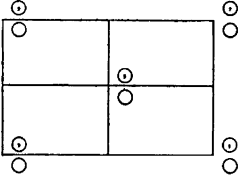
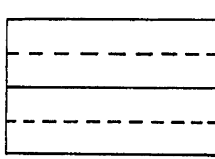
| pg | No. 4 | $p1g1$ | m Rectangular |
|---|-------|---|-----------------|
|  | |  | |

Origin on g

$2 \quad a \quad 1 \quad x, y; \bar{x}, \frac{1}{2} + y$

General:
 hk : No conditions
 $0k$: $k = 2n$

Table B.5. The two-dimensional rectangular space group cm or #5 ($c1m1$)

| cm | No. 5 | $c1m1$ | m Rectangular |
|---|-------|---|-----------------|
|  | |  | |

Origin on m

Number of positions
Wyckoff notation,
and point symmetry

$4 \quad b \quad 1 \quad x, y; \bar{x}, y$

Co-ordinates of
equivalent positions
 $(0, 0; \frac{1}{2}, \frac{1}{2}) +$

Conditions limiting
possible reflections

General:
 hk : $h + k = 2n$
Special:
as above only

Table B.6. The two-dimensional rectangular space group pmm or #6 ($p2mm$)

| pmm | No. 6 | $p2m\bar{m}$ | $m\bar{m}$ Rectangular |
|--|-------|--------------------------------------|--|
| | | | |
| Origin at $2mm$ | | | |
| Number of positions | | Co-ordinates of equivalent positions | Conditions limiting possible reflections |
| Wyckoff notation, and point symmetry | | | |
| 4 i 1 $x, y; \bar{x}, y; \bar{x}, \bar{y}; x, \bar{y}$ | | | General: no conditions |
| 2 h m $\frac{1}{2}, y; \frac{1}{2}, \bar{y}$ | | | Special: No condition |
| 2 g m $0, y; 0, \bar{y}$ | | | |
| 2 f m $x, \frac{1}{2}; \bar{x}, \frac{1}{2}$ | | | |
| 2 e m $x, 0; \bar{x}, 0$ | | | |
| 1 d mm $\frac{1}{2}, \frac{1}{2}$ | | | |
| 1 c mm $\frac{1}{2}, 0$ | | | |
| 1 b mm $0, \frac{1}{2}$ | | | |
| 1 a mm $0, 0$ | | | |

Table B.7. The two-dimensional rectangular space group pmg or #7 ($p2mg$)

| pmg | No. 7 | $p2m\bar{g}$ | $m\bar{m}$ Rectangular |
|--|-------|--------------------------------------|---|
| | | | |
| Origin at 2 | | | |
| Number of positions | | Co-ordinates of equivalent positions | Conditions limiting possible reflections |
| Wyckoff notation, and point symmetry | | | |
| 4 d 1 $x, y; \bar{x}, \bar{y}; \frac{1}{2} + x, \bar{y}; \frac{1}{2} - x, y$ | | | General: hk : No conditions $h0$: $h = 2n$ |
| 2 c m $\frac{1}{4}, y; \frac{3}{4}, \bar{y}$ | | | Special: as above, plus no extra conditions |
| 2 b 2 $0, \frac{1}{2}; \frac{1}{2}, \frac{1}{2}$ | | | |
| 2 a 2 $0, 0; \frac{1}{2}, 0$ | | | $\} hk: h = 2n$ |

Table B.8. The two-dimensional rectangular space group pgg or #8 ($p2gg$)

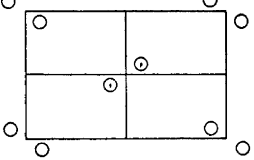
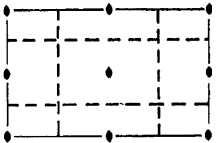
| pgg | No. 8 | $p2gg$ | mm Rectangular |
|--|-------------|---|--|
|  | |  | |
| | Origin at 2 | | |
| Number of positions | | Co-ordinates of equivalent positions | Conditions limiting possible reflections |
| Wyckoff notation, and point symmetry | | | |
| 4 c 1 $x, y; \bar{x}, \bar{y}; \frac{1}{2} + x, \frac{1}{2} - y; \frac{1}{2} - x, \frac{1}{2} + y$ | | | General: hk : no conditions |
| 2 b 2 $\frac{1}{2}, 0; 0, \frac{1}{2}$ | | | $h0: h = 2n$ |
| 2 a 2 $0, 0; \frac{1}{2}, \frac{1}{2}$ | | | $0l: k = 2n$ |
| | | | Special: as above, plus |
| | | | $\} hk: h + k = 2n$ |

Table B.9. The two-dimensional rectangular space group cmm or #9 ($c2mm$)

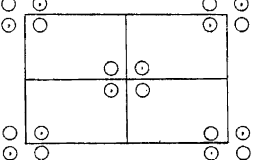
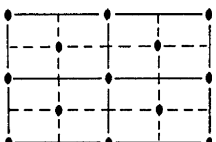
| cmm | No. 9 | $c2mm$ | mm Rectangular |
|--|-----------------|--|--|
|  | |  | |
| | Origin at $2mm$ | | |
| Number of positions | | Co-ordinates of equivalent positions | Conditions limiting possible reflections |
| Wyckoff notation, and point symmetry | | $(0, 0; \frac{1}{2}, \frac{1}{2}) +$ | |
| 8 f 1 $x, y; \bar{x}, \bar{y}; \bar{x}, \bar{y}; x, \bar{y}$ | | | General: $hk: h + k = 2n$ |
| 4 e m $0, y; 0, \bar{y}$ | | | Special: as above, plus |
| 4 d m $x, 0; \bar{x}, 0$ | | | $\} $ no extra conditions |
| 4 c 2 $\frac{1}{4}, \frac{1}{4}; \frac{1}{4}, \frac{3}{4}$ | | | $hk: h = 2n; (k = 2n)$ |
| 2 b mm $0, \frac{1}{2}$ | | | $\} $ no extra conditions |
| 2 a mm $0, 0$ | | | |

Table B.10. The two-dimensional square space group $p4$ or #10 ($p4$)

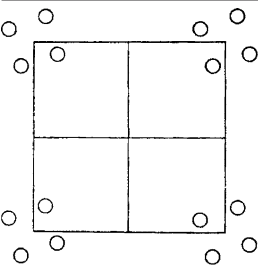
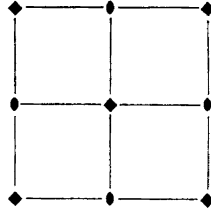
| $p4$ | No. 10 | $p4$ | 4 Square |
|---|---|--------------------------------------|--|
|  |  | | |
| Origin at 4 | | | |
| Number of positions | | Co-ordinates of equivalent positions | Conditions limiting possible reflections |
| Wyckoff notation, and point symmetry | | | |
| 4 d 1 $x, y; \bar{x}, \bar{y}; y, \bar{x}; \bar{y}, x$ | | | General: No conditions |
| 2 c 2 $\frac{1}{2}, 0; 0, \frac{1}{2}$ | | | Special: $hk: h + k = 2n$ |
| 1 b 4 $\frac{1}{2}, \frac{1}{2}$ | | | $\}$ No conditions |
| 1 a 4 0, 0 | | | |

Table B.11. The two-dimensional square space group $p4m$ or #11 ($p4mm$)

| $p4m$ | No. 11 | $p4m m$ | $4mm$ Square |
|--|---|---|--------------|
| | | | |
| Origin at $4mm$ | | | |
| Number of positions Wyckoff notation, and point symmetry | Co-ordinates of equivalent positions | Conditions limiting possible reflections | |
| 8 g 1 $x, y; \bar{x}, \bar{y}; y, \bar{x}; \bar{y}, x; \bar{x}, y; x, \bar{y}; \bar{y}, \bar{x}, y, x$ | | General: No conditions Special: $\left. \begin{array}{l} \text{no conditions} \\ h \bar{k}: h + k = 2n \end{array} \right\}$ | |
| 4 f m $x, x; \bar{x}, \bar{x}; \bar{x}, x; x, \bar{x}$ | | | |
| 4 e m $x, \frac{1}{2}; \bar{x}, \frac{1}{2}; \frac{1}{2}, x; \frac{1}{2}, \bar{x}$ | | | |
| 4 d m $x, 0; \bar{x}, 0; 0, x; 0, \bar{x}$ | | | |
| 2 c mm $\frac{1}{2}, 0; 0, \frac{1}{2}$ | | | |
| 1 b $4mm$ $\frac{1}{2}, \frac{1}{2}$ | | | |
| 1 a $4mm$ $0, 0$ | | | |

Table B.12. The two-dimensional square space group $p4g$ or #12 ($p4gm$)

| $p4g$ | No. 12 | $p4gm$ | $4mm$ Square |
|--|--|--|---|
| | | | |
| | Origin at 4 | | |
| Number of positions Wyckoff notation, and point symmetry | Co-ordinates of equivalent positions | | Conditions limiting possible reflections |
| 8 d 1 $x, y; y, \bar{x}; \frac{1}{2} - x, \frac{1}{2} + y; \frac{1}{2} - y, \frac{1}{2} - x$ $\bar{x}, \bar{y}; \bar{y}, x; \frac{1}{2} + x, \frac{1}{2} - y; \frac{1}{2} + y, \frac{1}{2} + x$ | General: $x, \frac{1}{2} + x; \bar{x}, \frac{1}{2} - x; \frac{1}{2} + x, \bar{x}; \frac{1}{2} - x, x$ | | hk : No conditions $h0$: $h = 2n$ ($0k$: $k = 2n$) hh : No conditions |
| 4 c m $x, \frac{1}{2} + x; \bar{x}, \frac{1}{2} - x; \frac{1}{2} + x, \bar{x}; \frac{1}{2} - x, x$ | | Special: as above, plus no extra conditions | |
| 2 b $4mm$ $\frac{1}{2}, 0; 0, \frac{1}{2}$ | | | $\} \quad hk: h + k = 2n$ |
| 2 a 4 $0, 0; \frac{1}{2}, \frac{1}{2}$ | | | |

Table B.13. The two-dimensional hexagonal space group $p3$ or #13 ($p3$)

| $p3$ | No. 13 | $p3$ | 3 Hexagonal |
|--|---|--|---|
| | | | |
| | Origin at 3 | | |
| Number of positions Wyckoff notation, and point symmetry | Co-ordinates of equivalent positions | | Conditions limiting possible reflections |
| 3 d 1 $\bar{y}, x - y; y - x, \bar{x}$ | | General: No conditions Special: no conditions | |
| 1 c 3 $\frac{1}{3}, \frac{1}{3}$ | | | |
| 1 b 3 $\frac{1}{3}, \frac{1}{3}$ | | | |
| 1 a 3 $0, 0$ | | | |

Table B.14. The two-dimensional hexagonal space group $p3m1$ or #14 ($p3m1$)

| $p3m1$ | No. 14 | $p3m1$ | 3m Hexagonal |
|--|---|---|--------------|
| | | | |
| Origin at $3m$ | | | |
| Number of positions Wyckoff notation, and point symmetry | Co-ordinates of equivalent positions | Conditions limiting possible reflections | |
| 6 e m $x, y; \bar{y}, x - y; y - x, \bar{x}$ $\bar{y}, \bar{x}; x, x - y; y - x, y$ | | General: No conditions | |
| 3 d m $x, \bar{x}; x, 2x; 2\bar{x}, x$ | | Special: No conditions | |
| 1 c $3m$ $\frac{2}{3}, \frac{1}{3}$ | | | |
| 1 b $3m$ $\frac{1}{3}, \frac{2}{3}$ | | | |
| 1 a $3m$ $0, 0$ | | | |

Table B.15. The two-dimensional hexagonal space group $p31m$ or #15 ($p31m$)

| $p31m$ | No. 15 | $p31m$ | 3m Hexagonal |
|--|---|---|--------------|
| | | | |
| Origin at $31m$ | | | |
| Number of positions Wyckoff notation, and point symmetry | Co-ordinates of equivalent positions | Conditions limiting possible reflections | |
| 6 d 1 $x, y; \bar{y}, x - y; y - x, \bar{x}$ $y, x; \bar{x}, y - x; x - y, \bar{y}$ | | General: No conditions | |
| 3 c m $x, 0; 0, x; \bar{x}, \bar{x}$ | | Special: no conditions | |
| 2 b 3 $\frac{1}{3}, \frac{2}{3}; \frac{2}{3}, \frac{1}{3}$ | | | |
| 1 a $3m$ $0, 0$ | | | |

Table B.16. The two-dimensional hexagonal space group $p6$ or #16 ($p6$)

| $p6$ | No. 16 | $p6$ | Hexagonal 6 |
|--|---|---------------------------|---|
| | | | |
| | Origin at 6 | | |
| Number of positions Wyckoff notation, and point symmetry | Co-ordinates of equivalent positions | | Conditions limiting possible reflections |
| 6 d 1 $x, y; \bar{y}, x - y; y - x, \bar{x}$ $\bar{x}, \bar{y}; y, y - x; x - y, x$ | | General: No conditions | |
| 3 c 2 $\frac{1}{2}, 0; 0, \frac{1}{2}; \frac{1}{2}, \frac{1}{2}$ | | Special: No conditions | |
| 2 b 3 $\frac{1}{3}, \frac{2}{3}; \frac{2}{3}, \frac{1}{3}$ | | | |
| 1 a 6 0, 0 | | | |

Table B.17. The two-dimensional hexagonal space group $p6m$ or #17 ($p6mm$)

| $p6m$ | No. 17 | $p6mm$ | 6mm Hexagonal |
|---|---|---------------------------|---|
| | | | |
| | Origin at 6mm | | |
| Number of positions Wyckoff notation, and point symmetry | Co-ordinates of equivalent positions | | Conditions limiting possible reflections |
| 12 f 1 $x, y; \bar{y}, x - y; y - x, \bar{x}; y, x; \bar{x}, y - x; x - y, \bar{y}$ $\bar{x}, \bar{y}; y, y - x; x - y, x; \bar{y}, \bar{x}; x, x - y; y - x, y$ | | General: No conditions | |
| 6 e m $x, \bar{x}; x, 2x; 2\bar{x}, \bar{x}; \bar{x}, x; \bar{x}, 2\bar{x}; 2x, x$ | | Special: No conditions | |
| 6 d m $x, 0; 0, x; \bar{x}, \bar{x}; \bar{x}, 0; 0, \bar{x}; x, x$ | | | |
| 3 c mm $\frac{1}{2}, 0; 0, \frac{1}{2}; \frac{1}{2}, \frac{1}{2}$ | | | |
| 2 b $3m$ $\frac{1}{3}, \frac{2}{3}; \frac{2}{3}, \frac{1}{3}$ | | | |
| 1 a $6mm$ 0, 0 | | | |

C

Tables for 3D Space Groups

In this appendix, selected tables and figures for 3D space groups in real space and in reciprocal space are presented. The real space tables¹ and figures given in the first part of the appendix (Sect. C.1) pertain mainly to crystallographic information and are used for illustrative purposes in various chapters of this book. The tables which pertain to reciprocal space appear in the second part of the appendix (Sect. C.2) and are mainly for tables for the group of the wave vector for various high symmetry points in the Brillouin zone for various cubic space groups and other space groups selected for illustrative purposes.

C.1 Real Space

A list of the 230 space groups and their Hermann–Mauguin symmetry designations (Sect. 3.10) is given in Table C.1, taken from the web [54]. Most of the current literature presently follows the notation of reference [58]. The reader will find Table C.1 to differ in two ways from entries in the International Tables for X-ray Crystallography [58]. Firstly, a minus sign ($-n$) is used in [54] rather than \bar{n} in [58] to denote improper rotations (see Sect. 3.9) for many of the groups, including #81-82, #111-122, #147-148, #162-167, #174, #187-190, #215-220. Secondly, a minus sign ($-n$) is used in [54], rather than n itself [58] to denote other groups, including #200-206 and #221-230. Some of the special space groups referred to in the book text are the rhombohedral space group #166, the hexagonal space group #194, the simple cubic space group #221, the face-centered cubic space group #225, the space group #227 for the diamond structure, and the body-centered cubic space group #229.

Space groups have in addition to translational symmetry, point group symmetries which single out special high symmetry points. Tables C.2, C.3, and

¹The notation for these tables is discussed in Chap. 9.

Table C.1. Listing of the Hermann–Mauguin symmetry space group symbol designations for the 230 space groups. The table is taken from the web [54] (see text)

| 1 | <i>P1</i> | 2 | <i>P</i> – 1 | 3 | <i>P2</i> | 4 | <i>P2</i> ₁ | 5 | <i>C2</i> |
|-----|---|-----|---|-----|---|-----|--|-----|--|
| 6 | <i>Pm</i> | 7 | <i>Pc</i> | 8 | <i>Cm</i> | 9 | <i>Cc</i> | 10 | <i>P2</i> / <i>m</i> |
| 11 | <i>P2</i> ₁ / <i>m</i> | 12 | <i>C2</i> / <i>m</i> | 13 | <i>P2</i> / <i>c</i> | 14 | <i>P2</i> ₁ / <i>c</i> | 15 | <i>C2</i> / <i>c</i> |
| 16 | <i>P222</i> | 17 | <i>P222</i> ₁ | 18 | <i>P2</i> ₁ <i>2</i> ₁ <i>2</i> | 19 | <i>P2</i> ₁ <i>2</i> ₁ <i>2</i> ₁ | 20 | <i>C222</i> ₁ |
| 21 | <i>C222</i> | 22 | <i>F222</i> | 23 | <i>I222</i> | 24 | <i>I2</i> ₁ <i>2</i> ₁ <i>2</i> ₁ | 25 | <i>Pmm</i> 2 |
| 26 | <i>Pmc</i> ₂ ₁ | 27 | <i>Pcc</i> 2 | 28 | <i>Pma</i> 2 | 29 | <i>Pca</i> ₂ ₁ | 30 | <i>Pnc</i> 2 |
| 31 | <i>Pmn</i> ₂ ₁ | 32 | <i>Pba</i> 2 | 33 | <i>Pna</i> ₂ ₁ | 34 | <i>Pmn</i> 2 | 35 | <i>Cmm</i> 2 |
| 36 | <i>Cmc</i> ₂ ₁ | 37 | <i>Ccc</i> 2 | 38 | <i>Amm</i> 2 | 39 | <i>Abm</i> 2 | 40 | <i>Ama</i> 2 |
| 41 | <i>AbA</i> 2 | 42 | <i>Fmm</i> 2 | 43 | <i>Fdd</i> 2 | 44 | <i>Imm</i> 2 | 45 | <i>Iba</i> 2 |
| 46 | <i>Ima</i> 2 | 47 | <i>Pmmm</i> | 48 | <i>Pnnn</i> | 49 | <i>Pccm</i> | 50 | <i>Pban</i> |
| 51 | <i>Pmma</i> | 52 | <i>Pnna</i> | 53 | <i>Pnna</i> | 54 | <i>Pcca</i> | 55 | <i>Pbam</i> |
| 56 | <i>Pccn</i> | 57 | <i>Pbcm</i> | 58 | <i>Pnnm</i> | 59 | <i>Pmmn</i> | 60 | <i>Pbcn</i> |
| 61 | <i>Pbca</i> | 62 | <i>Pnma</i> | 63 | <i>Cmcm</i> | 64 | <i>Cmca</i> | 65 | <i>Cmmm</i> |
| 66 | <i>Cccm</i> | 67 | <i>Cmma</i> | 68 | <i>Ccca</i> | 69 | <i>Fmmm</i> | 70 | <i>Fddd</i> |
| 71 | <i>Immm</i> | 72 | <i>Ibam</i> | 73 | <i>Ibca</i> | 74 | <i>Imma</i> | 75 | <i>P4</i> |
| 76 | <i>P4</i> ₁ | 77 | <i>P4</i> ₂ | 78 | <i>P4</i> ₃ | 79 | <i>I4</i> | 80 | <i>I4</i> ₁ |
| 81 | <i>P</i> – 4 | 82 | <i>I</i> – 4 | 83 | <i>P4</i> / <i>m</i> | 84 | <i>P4</i> _{2/<i>m</i>} | 85 | <i>P4</i> / <i>n</i> |
| 86 | <i>P4</i> ₂ / <i>n</i> | 87 | <i>I4</i> / <i>m</i> | 88 | <i>I4</i> ₁ / <i>a</i> | 89 | <i>P422</i> | 90 | <i>P42</i> ₁ <i>2</i> |
| 91 | <i>P4</i> ₁ <i>2</i> ₂ | 92 | <i>P4</i> ₁ <i>2</i> ₁ <i>2</i> | 93 | <i>P4</i> ₂ <i>2</i> ₂ | 94 | <i>P4</i> ₂ <i>1</i> ₂ <i>2</i> | 95 | <i>P4</i> ₃ <i>2</i> ₂ |
| 96 | <i>P4</i> ₃ <i>2</i> ₁ <i>2</i> | 97 | <i>I422</i> | 98 | <i>I4</i> ₁ <i>22</i> | 99 | <i>P4mm</i> | 100 | <i>P4bm</i> |
| 101 | <i>P4</i> ₂ <i>cm</i> | 102 | <i>P4</i> ₂ <i>nm</i> | 103 | <i>P4cc</i> | 104 | <i>P4nc</i> | 105 | <i>P4</i> ₂ <i>mc</i> |
| 106 | <i>P4</i> ₂ <i>bc</i> | 107 | <i>I4mm</i> | 108 | <i>I4cm</i> | 109 | <i>I4</i> ₁ <i>md</i> | 110 | <i>I4</i> ₁ <i>cd</i> |
| 111 | <i>P</i> – 4 <i>2m</i> | 112 | <i>P</i> – 4 <i>2c</i> | 113 | <i>P</i> – 4 <i>21m</i> | 114 | <i>P</i> – 4 <i>21c</i> | 115 | <i>P</i> – 4 <i>m</i> ₂ |
| 116 | <i>P</i> – 4 <i>c</i> ₂ | 117 | <i>P</i> – 4 <i>b</i> ₂ | 118 | <i>P</i> – 4 <i>n</i> ₂ | 119 | <i>I</i> – 4 <i>m</i> ₂ | 120 | <i>I</i> – 4 <i>c</i> ₂ |
| 121 | <i>I</i> – 4 <i>2m</i> | 122 | <i>I</i> – 4 <i>2d</i> | 123 | <i>P4</i> / <i>mmm</i> | 124 | <i>P4</i> / <i>mcc</i> | 125 | <i>P4</i> / <i>nbm</i> |
| 126 | <i>P4</i> / <i>nnc</i> | 127 | <i>P4</i> / <i>mbm</i> | 128 | <i>P4</i> / <i>mnc</i> | 129 | <i>P4</i> / <i>nmm</i> | 130 | <i>P4</i> / <i>ncc</i> |
| 131 | <i>P4</i> ₂ / <i>mmc</i> | 132 | <i>P4</i> ₂ / <i>mcm</i> | 133 | <i>P4</i> ₂ / <i>nbc</i> | 134 | <i>P4</i> ₂ / <i>nmm</i> | 135 | <i>P4</i> ₂ / <i>mbc</i> |
| 136 | <i>P4</i> ₂ / <i>mmm</i> | 137 | <i>P4</i> ₂ / <i>nmc</i> | 138 | <i>P4</i> ₂ / <i>ncm</i> | 139 | <i>I4</i> / <i>mmm</i> | 140 | <i>I4</i> / <i>mcm</i> |
| 141 | <i>I4</i> ₁ / <i>amd</i> | 142 | <i>PI</i> ₁ / <i>acd</i> | 143 | <i>P3</i> | 144 | <i>P3</i> ₁ | 145 | <i>P3</i> ₂ |
| 146 | <i>R</i> ₃ | 147 | <i>P</i> – 3 | 148 | <i>R</i> – 3 | 149 | <i>P3</i> ₁₂ | 150 | <i>P3</i> ₂₁ |
| 151 | <i>P3</i> ₁ <i>12</i> | 152 | <i>P3</i> ₁ <i>21</i> | 153 | <i>P3</i> ₂ ₁₂ | 154 | <i>P3</i> ₂ ₂₁ | 155 | <i>R3</i> ₂ |
| 156 | <i>P3m</i> 1 | 157 | <i>P31m</i> | 158 | <i>P3c</i> 1 | 159 | <i>P31c</i> | 160 | <i>R3m</i> |
| 161 | <i>R3c</i> | 162 | <i>P</i> – 3 <i>1m</i> | 163 | <i>P</i> – 3 <i>1c</i> | 164 | <i>P</i> – 3 <i>m</i> 1 | 165 | <i>P</i> – 3 <i>c</i> 1 |
| 166 | <i>R</i> – 3 <i>m</i> | 167 | <i>R</i> – 3 <i>c</i> | 168 | <i>P6</i> | 169 | <i>P6</i> ₁ | 170 | <i>P6</i> ₅ |
| 171 | <i>P6</i> ₂ | 172 | <i>P6</i> ₄ | 173 | <i>P6</i> ₃ | 174 | <i>P</i> – 6 | 175 | <i>P6</i> / <i>m</i> |
| 176 | <i>P6</i> ₂ / <i>m</i> | 177 | <i>P622</i> | 178 | <i>P6</i> ₁ <i>22</i> | 179 | <i>P6</i> ₅ <i>22</i> | 180 | <i>P6</i> ₂ <i>22</i> |
| 181 | <i>P6</i> ₄ <i>22</i> | 182 | <i>P6</i> ₃ <i>22</i> | 183 | <i>P6mm</i> | 184 | <i>P6cc</i> | 185 | <i>P6</i> ₃ <i>cm</i> |
| 186 | <i>P6</i> ₃ <i>mc</i> | 187 | <i>P</i> – 6 <i>m</i> 2 | 188 | <i>P</i> – 6 <i>c</i> 2 | 189 | <i>P</i> – 6 <i>2m</i> | 190 | <i>P</i> – 6 <i>2c</i> |
| 191 | <i>P6</i> / <i>mmm</i> | 192 | <i>P6</i> / <i>mcc</i> | 193 | <i>P6</i> ₃ / <i>mcm</i> | 194 | <i>P6</i> ₃ / <i>mmc</i> | 195 | <i>P2</i> 3 |
| 196 | <i>F2</i> 3 | 197 | <i>I2</i> 3 | 198 | <i>P2</i> ₁ 3 | 199 | <i>I2</i> ₁ 3 | 200 | <i>Pm</i> – 3 |
| 201 | <i>Pn</i> – 3 | 202 | <i>Fm</i> – 3 | 203 | <i>Fd</i> – 3 | 204 | <i>Im</i> – 3 | 205 | <i>Pa</i> – 3 |
| 206 | <i>Ia</i> – 3 | 207 | <i>P432</i> | 208 | <i>P4</i> ₂ <i>32</i> | 209 | <i>F432</i> | 210 | <i>F4</i> ₁ <i>32</i> |
| 211 | <i>I4</i> ₃ 2 | 212 | <i>P4</i> ₃ 2 | 213 | <i>P4</i> ₁ <i>32</i> | 214 | <i>I4</i> ₁ <i>32</i> | 215 | <i>P</i> – 4 <i>3m</i> |
| 216 | <i>F</i> – 4 <i>3m</i> | 217 | <i>I</i> – 4 <i>3m</i> | 218 | <i>P</i> – 4 <i>3n</i> | 219 | <i>F</i> – 4 <i>3c</i> | 220 | <i>I</i> – 4 <i>3d</i> |
| 221 | <i>Pm</i> – 3 <i>m</i> | 222 | <i>Pn</i> – 3 <i>n</i> | 223 | <i>Pm</i> – 3 <i>n</i> | 224 | <i>Pn</i> – 3 <i>m</i> | 225 | <i>Fm</i> – 3 <i>m</i> |
| 226 | <i>Fm</i> – 3 <i>c</i> | 227 | <i>Fd</i> – 3 <i>m</i> | 228 | <i>Fd</i> – 3 <i>c</i> | 229 | <i>Im</i> – 3 <i>m</i> | 230 | <i>Ia</i> – 3 <i>d</i> |

Table C.2. Symmetry positions for space group #221 denoted by O_h^1 and ($Pm3m$) using the Schoenflies and Hermann–Mauguin notations, respectively (see Fig. 9.7) [58]

| $Pm3m$ | | | No. 221 | $P4/m\bar{3}2/m$ | $m\bar{3}m$ Cubic |
|---|--|--|---------|--|-------------------|
| Origin at centre ($m\bar{3}m$) | | | | | |
| Number of positions, Wyckoff notation, and point symmetry | Co-ordinates of equivalent positions | | | Conditions limiting possible reflections | |
| 48 n 1 | $x, y, z; z, x, y; y, z, x; x, \bar{z}, y; y, \bar{x}, z; z, y, \bar{x};$ $x, \bar{y}, \bar{z}; z, \bar{x}, \bar{y}; y, \bar{z}, \bar{x}; x, \bar{z}, \bar{y}; y, \bar{x}, \bar{z}; z, \bar{y}, \bar{x};$ $\bar{x}, y, \bar{z}; \bar{z}, x, \bar{y}; \bar{y}, z, \bar{x}; \bar{x}, \bar{z}, \bar{y}; \bar{y}, \bar{x}, \bar{z}; \bar{z}, y, \bar{x};$ $\bar{x}, \bar{y}, z; \bar{z}, \bar{x}, y; \bar{y}, \bar{z}, x; \bar{x}, \bar{z}, y; \bar{y}, \bar{x}, z; \bar{z}, \bar{y}, x;$ $\bar{x}, \bar{y}, \bar{z}; \bar{z}, \bar{x}, \bar{y}; \bar{y}, \bar{z}, \bar{x}; \bar{x}, \bar{z}, \bar{y}; \bar{y}, \bar{x}, \bar{z}; \bar{z}, \bar{y}, \bar{x};$ $\bar{x}, y, \bar{z}; \bar{z}, x, \bar{y}; \bar{y}, z, \bar{x}; \bar{x}, \bar{z}, y; \bar{y}, \bar{x}, z; \bar{z}, y, \bar{x};$ $x, \bar{y}, z; z, \bar{x}, y; y, \bar{z}, x; x, \bar{z}, y; y, \bar{x}, z; z, \bar{y}, x;$ $x, y, \bar{z}; z, x, \bar{y}; y, z, \bar{x}; x, z, \bar{y}; y, x, \bar{z}; z, y, \bar{x};$ | | | General: $h\bar{k}l; \bar{h}k\bar{l}; \bar{h}\bar{k}l; \bar{h}\bar{k}\bar{l}; \bar{h}k\bar{l}; h\bar{k}\bar{l}$ } No conditions $0kl; \bar{0}k\bar{l}; \bar{0}\bar{k}l; \bar{0}\bar{k}\bar{l}; \bar{0}k\bar{l}; 0\bar{k}\bar{l}$ } No conditions | |
| 24 m m | $x, x, z; z, x, x; x, z, x; \bar{x}, \bar{x}, \bar{z}; \bar{x}, \bar{x}, \bar{x}; \bar{x}, \bar{x}, \bar{x};$ $x, \bar{x}, \bar{z}; z, \bar{x}, \bar{x}; x, \bar{x}, \bar{x}; \bar{x}, x, z; \bar{x}, x, x; \bar{x}, z, x;$ $\bar{x}, x, \bar{z}; \bar{z}, x, \bar{x}; \bar{x}, z, \bar{x}; x, \bar{x}, z; x, \bar{x}, x; x, z, \bar{x};$ $\bar{x}, \bar{x}, z; \bar{z}, \bar{x}, x; \bar{x}, \bar{x}, x; x, \bar{x}, \bar{z}; z, x, \bar{x}; x, z, \bar{x};$ | | | Special: No conditions | |
| 24 l m | $\frac{1}{2}, y, z; z, \frac{1}{2}, y; y, z, \frac{1}{2}; \frac{1}{2}, z, y; y, \frac{1}{2}, z; z, y, \frac{1}{2};$ $\frac{1}{2}, \bar{y}, \bar{z}; \bar{z}, \frac{1}{2}, \bar{y}; \bar{y}, \bar{z}, \frac{1}{2}; \frac{1}{2}, \bar{z}, \bar{y}; \bar{y}, \frac{1}{2}, \bar{z}; \bar{z}, \bar{y}, \frac{1}{2};$ $\frac{1}{2}, y, \bar{z}; \bar{z}, \frac{1}{2}, y; y, \bar{z}, \frac{1}{2}; \frac{1}{2}, z, y; y, \frac{1}{2}, z; \bar{z}, y, \frac{1}{2};$ $\frac{1}{2}, \bar{y}, z; z, \frac{1}{2}, \bar{y}; \bar{y}, z, \frac{1}{2}; \frac{1}{2}, z, \bar{y}; \bar{y}, \frac{1}{2}, z; z, \bar{y}, \frac{1}{2};$ | | | | |
| 24 k m | $0, y, z; z, 0, y; y, z, 0; 0, z, y; y, 0, z; z, y, 0;$ $0, \bar{y}, \bar{z}; \bar{z}, 0, \bar{y}; \bar{y}, \bar{z}, 0; 0, \bar{z}, \bar{y}; \bar{y}, 0, \bar{z}; \bar{z}, \bar{y}, 0;$ $0, y, \bar{z}; z, 0, y; y, \bar{z}, 0; 0, \bar{z}, y; y, 0, \bar{z}; \bar{z}, y, 0;$ $0, \bar{y}, z; z, 0, \bar{y}; \bar{y}, z, 0; 0, z, \bar{y}; \bar{y}, 0, z; z, \bar{y}, 0.$ | | | | |
| 12 j mm | $\frac{1}{2}, x, x; x, \frac{1}{2}, x; x, x, \frac{1}{2}; \frac{1}{2}, x, \bar{x}; \bar{x}, \frac{1}{2}, x; x, \bar{x}, \frac{1}{2};$ $\frac{1}{2}, \bar{x}, \bar{x}; \bar{x}, \frac{1}{2}, \bar{x}; \bar{x}, \bar{x}, \frac{1}{2}; \frac{1}{2}, \bar{x}, x; x, \frac{1}{2}, \bar{x}; \bar{x}, x, \frac{1}{2};$ | | | | |
| 12 i mm | $0, x, x; x, 0, x; x, x, 0; 0, x, \bar{x}; \bar{x}, 0, x; x, x, 0;$ $0, \bar{x}, \bar{x}; \bar{x}, 0, \bar{x}; \bar{x}, \bar{x}, 0; 0, \bar{x}, x; x, 0, \bar{x}; \bar{x}, x, 0.$ | | | | |
| 12 h mm | $x, \frac{1}{2}, 0; 0, x, \frac{1}{2}; \frac{1}{2}, 0, x; x, 0, \frac{1}{2}; \frac{1}{2}, x, 0; 0, \frac{1}{2}, x;$ $\bar{x}, \frac{1}{2}, 0; 0, \bar{x}, \frac{1}{2}; \frac{1}{2}, 0, \bar{x}; \bar{x}, 0, \frac{1}{2}; \frac{1}{2}, \bar{x}, 0; 0, \frac{1}{2}, \bar{x}.$ | | | | |
| 8 g $3m$ | $x, x, x; x, \bar{x}, \bar{x}; \bar{x}, x, \bar{x}; \bar{x}, \bar{x}, x;$ $\bar{x}, \bar{x}, \bar{x}; \bar{x}, x, x; x, \bar{x}, x; x, x, \bar{x}.$ | | | | |
| 6 f $4mm$ | $x, \frac{1}{2}, \frac{1}{2}; \frac{1}{2}, x, \frac{1}{2}; \frac{1}{2}, \frac{1}{2}, x; \bar{x}, \frac{1}{2}, \frac{1}{2}; \frac{1}{2}, \bar{x}, \frac{1}{2}; \frac{1}{2}, \frac{1}{2}, \bar{x}.$ | | | | |
| 6 e $4mm$ | $x, 0, 0; 0, x, 0; 0, 0, x; \bar{x}, 0, 0; 0, \bar{x}, 0; 0, 0, \bar{x}.$ | | | | |
| 3 d $4/mmm$ | $\frac{1}{2}, 0, 0; 0, \frac{1}{2}, 0; 0, 0, \frac{1}{2}.$ | | | | |
| 3 c $4/mmm$ | $0, \frac{1}{2}, \frac{1}{2}; \frac{1}{2}, 0, \frac{1}{2}; \frac{1}{2}, \frac{1}{2}, 0.$ | | | | |
| 1 b $m3m$ | $\frac{1}{2}, \frac{1}{2}, \frac{1}{2}.$ | | | | |
| 1 a $m3m$ | $0, 0, 0.$ | | | | |

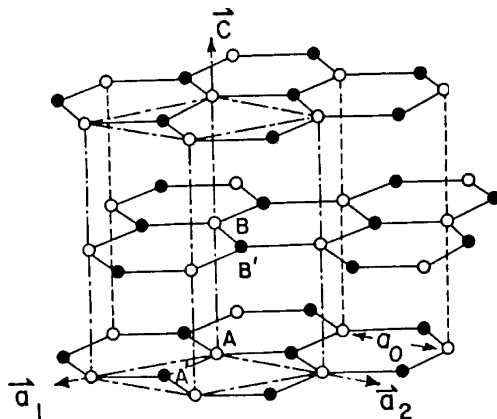


Fig. C.1. Crystal structure of hexagonal graphite, space group #194

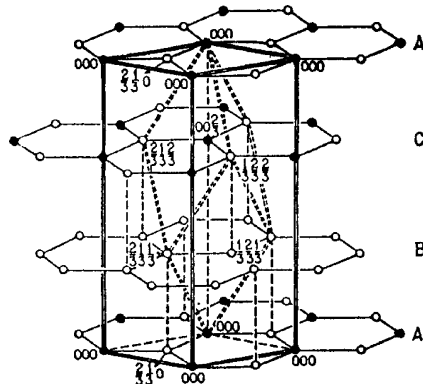


Fig. C.2. Crystal structure of rhombohedral graphite showing *ABC* stacking of the individual sheets, space group #166 $\bar{R}3m$. Also shown with *dashed lines* is the rhombohedral unit cell

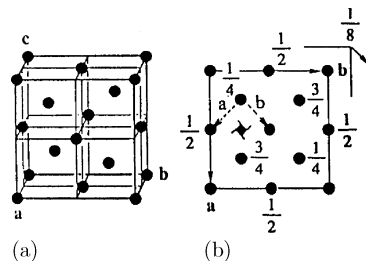


Fig. C.3. (a) Diamond structure $Fd\bar{3}m$ ($O\bar{h}$, #227) showing a unit cell with two distinct atom site locations. For the zinc blende structure (see Fig. 10.6) the atoms on the two sites are distinct and belong to group $F\bar{4}3m$ #216. (b) The screw axis in the diamond structure shown looking at the projection of the various atoms with their z -axis distances given

C.4 taken from the International Crystallographic Tables [58] list these site symmetries for high symmetry points for a few illustrative 3D space groups in analogy to the Tables in Appendix B which pertain to two-dimensional space groups. For example in Table C.2 for the simple cubic lattice (#221), the general point n has no additional symmetry (C_1), while points a and b have full O_h point group symmetry. The points c through m have more symmetry than the general point n , but less symmetry than points a and b . For each symmetry point a through n , the Wyckoff positions are listed and the corresponding point symmetry for each high symmetry point is given.

To better visualize 3D crystal structures, it is important to show ball and stick models when working with specific crystals. Figure C.1 shows such a model for the crystal structure of 3D hexagonal graphite (space group #194), while Fig. C.2 shows the crystal structure of 3D rhombohedral graphite (space group #166). Both hexagonal and rhombohedral graphite are composed of the same individual 2D graphene layers, but hexagonal graphite has an *ABAB* stacking sequence of these layer planes, while rhombohedral graphite has an *ABCABC* stacking of these layers. Because of the differences in their stacking sequences, the structure with the *ABAB* stacking sequence is described by a nonsymmorphic space group #194, while the structure with the *ABCABC* stacking sequence is described by a symmorphic space group #166. Figure C.3(a) shows the crystal structure for diamond together with a diagram showing the diamond screw axis (Fig. C.3(b)) that explains the non-symmorphic nature of the diamond structure.

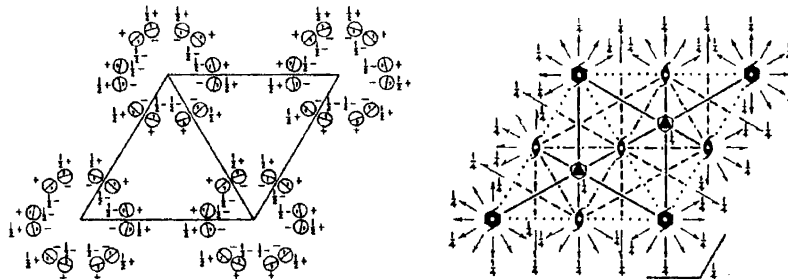
Table C.3 gives a listing similar to Table C.2, but now for the hexagonal non-symmorphic space group $P6_3/mmc$ (D_{6h}^4) which is the appropriate space group for 3D graphite, while Table C.4 gives a similar listing for the rhombohedral symmorphic space group #166 which describes rhombohedral graphite. Group #166 is unusual because it can be specified either within a rhombohedral description or a hexagonal description, as seen in Table C.4. The information provided in the International Crystallographic Tables [58], as exemplified by Table C.4 for group #166, can also be found on the web. Table C.5 taken from the web-site [58] gives the same information on the Wyckoff positions and point symmetries as is contained in Table C.4. The notation in Table C.5 which is taken from the web [54] differs from the notation used in the International Tables for X-ray Crystallography [58] insofar as $-x$, $-y$, $-z$ in [54] are used to denote \bar{x} , \bar{y} , \bar{z} in [58], and some of the entries are given in a different but equivalent order.

C.2 Reciprocal Space

In this section character tables are presented for the group of the wave vector for a variety of high symmetry points in the Brillouin zone for various space

Table C.3. International Crystallography Table for point group symmetries for the hexagonal space group #194 ($P6_3/mmc$) or D_{6h}^4 (see Fig. C.1)

$P6_3/mmc$ No. 194 $P6_3/m\ 2/m\ 2/c$ $6/m\ m\ m$ Hexagonal
 D_{6h}^4



Origin at centre ($\bar{3}m1$)

| Number of positions, Wyckoff notation, and point symmetry | | | Co-ordinates of equivalent positions | Conditions limiting possible reflections |
|---|----------|-----------|--|--|
| 24 | <i>l</i> | 1 | $x, y, z; \bar{y}, x-y, z; y-x, \bar{x}, z; \bar{y}, \bar{x}, z; x, x-y, z; y-x, y, z;$ $\bar{x}, \bar{y}, \bar{z}; y, y-x, \bar{z}; x-y, x, \bar{z}; y, x, \bar{z}; \bar{x}, y-x, \bar{z}; x-y, \bar{y}, \bar{z};$ $\bar{x}, y, \frac{1}{2}+z; y, y-x, \frac{1}{2}+z; x-y, x, \frac{1}{2}+z;$ $x, y, \frac{1}{2}-z; \bar{y}, x-y, \frac{1}{2}-z; y-x, \bar{x}, \frac{1}{2}-z;$ $y, x, \frac{1}{2}+z; \bar{x}, y-x, \frac{1}{2}+z; x-y, \bar{y}, \frac{1}{2}+z;$ $\bar{y}, x, \frac{1}{2}-z; x, x-y, \frac{1}{2}-z; y-x, y, \frac{1}{2}-z.$ | General: $hkil$: No conditions $h\bar{l}2\bar{h}l$: $l=2n$ $h\bar{h}0l$: No conditions |
| 12 | <i>k</i> | <i>m</i> | $x, 2x, z; 2\bar{x}, \bar{x}, z; x, \bar{x}, z; \bar{x}, 2\bar{x}, \bar{z}; 2x, x, \bar{z}; \bar{x}, x, \bar{z};$ $\bar{x}, 2x, \frac{1}{2}+z; 2x, x, \frac{1}{2}+z; x, x, \frac{1}{2}+z;$ $x, 2x, \frac{1}{2}-z; 2\bar{x}, \bar{x}, \frac{1}{2}-z; x, \bar{x}, \frac{1}{2}-z.$ | Special: as above, plus no extra conditions |
| 12 | <i>j</i> | <i>m</i> | $x, y, \frac{1}{2}; \bar{y}, x-y, \frac{1}{2}; y-x, \bar{x}, \frac{1}{2}; \bar{y}, x, \frac{1}{2}; x, x-y, \frac{1}{2}; y-x, y, \frac{1}{2};$ $\bar{x}, \bar{y}, \frac{1}{2}; y, y-x, \frac{1}{2}; x-y, x, \frac{1}{2}; y, x, \frac{1}{2}; \bar{x}, y-x, \frac{1}{2}; x-y, \bar{y}, \frac{1}{2}.$ | |
| 12 | <i>i</i> | 2 | $x, 0, 0; 0, x, 0; \bar{x}, \bar{x}, 0; x, 0, \frac{1}{2}; 0, x, \frac{1}{2}; \bar{x}, \bar{x}, \frac{1}{2};$ $\bar{x}, 0, 0; 0, \bar{x}, 0; x, x, 0; \bar{x}, 0, \frac{1}{2}; 0, \bar{x}, \frac{1}{2}; x, x, \frac{1}{2}.$ | $hkil$: $l=2n$ |
| 6 | <i>h</i> | <i>mm</i> | $x, 2x, \frac{1}{2}; 2\bar{x}, \bar{x}, \frac{1}{2}; x, \bar{x}, \frac{1}{2}; \bar{x}, 2\bar{x}, \frac{1}{2}; 2x, x, \frac{1}{2}; \bar{x}, x, \frac{1}{2}.$ | no extra conditions |
| 6 | <i>g</i> | $2/m$ | $\frac{1}{2}, 0, 0; 0, \frac{1}{2}, 0; \frac{1}{2}, 1, 0; \frac{1}{2}, 0, \frac{1}{2}; 0, \frac{1}{2}, 1; \frac{1}{2}, \frac{1}{2}, \frac{1}{2}.$ | $hkil$: $l=2n$ |
| 4 | <i>f</i> | $3m$ | $\frac{1}{2}, \frac{1}{2}, z; \frac{1}{2}, \frac{1}{2}, \bar{z}; \frac{1}{2}, \frac{1}{2}, \frac{1}{2}+z; \frac{1}{2}, \frac{1}{2}, \frac{1}{2}-z.$ | $hkil$: If $h-k=3n$, then $l=2n$ |
| 4 | <i>e</i> | $3m$ | $0, 0, z; 0, 0, \bar{z}; 0, 0, \frac{1}{2}+z; 0, 0, \frac{1}{2}-z.$ | $hkil$: $l=2n$ |
| 2 | <i>d</i> | $3m2$ | $\frac{1}{2}, \frac{1}{2}, \frac{1}{2}; \frac{1}{2}, \frac{1}{2}, \frac{1}{2}.$ | $hkil$: If $h-k=3n$, then $l=2n$ |
| 2 | <i>c</i> | $3m2$ | $\frac{1}{2}, \frac{1}{2}, \frac{1}{2}; \frac{1}{2}, \frac{1}{2}, \frac{1}{2}.$ | |
| 2 | <i>b</i> | $3m2$ | $0, 0, \frac{1}{2}; 0, 0, \frac{1}{2}.$ | $hkil$: $l=2n$ |
| 2 | <i>a</i> | $3m$ | $0, 0, 0; 0, 0, \frac{1}{2}.$ | |

Table C.4. Stereographs for space group #166 $R\text{-}3m$, along with the Wyckoff positions and point symmetries for each high symmetry point a through l , listed for both the rhombohedral and hexagonal systems

Origin at centre (3m)

Number of positions,
Wyckoff notation,
and point symmetry

Co-ordinates of equivalent positions

(1) RHOMBOHEDRAL AXES:

Conditions limiting
possible reflections

General:
No conditions

Special:
No conditions

12 i 1 $x,y,z; z,x,y; y,z,x; y,x,z; z,y,x; x,z,y; \bar{x},\bar{y},\bar{z}; \bar{z},\bar{x},\bar{y}; \bar{y},\bar{z},\bar{x}; \bar{z},\bar{y},\bar{x}; \bar{x},\bar{z},\bar{y}$.

6 h m $x,x,z; x,z,x; z,x,x; \bar{x},\bar{x},\bar{z}; \bar{x},\bar{z},\bar{x}; \bar{z},\bar{x},\bar{x}$.

6 g 2 $x,\bar{x},\frac{1}{2}; \bar{x},\frac{1}{2},x; \frac{1}{2},x,\bar{x}; \bar{x},x,\frac{1}{2}; x,\frac{1}{2},\bar{x}; \frac{1}{2},\bar{x},x$.

6 f 2 $x,\bar{x},0; \bar{x},0,x; 0,x,\bar{x}; \bar{x},x,0; x,0,\bar{x}; 0,\bar{x},x$.

3 e $2/m$ $0,\frac{1}{2},\frac{1}{2}; \frac{1}{2},0,\frac{1}{2}; \frac{1}{2},\frac{1}{2},0$.

3 d $2/m$ $\frac{1}{2},0,0; 0,\frac{1}{2},0; 0,0,\frac{1}{2}$.

2 c $3m$ $x,x,x; \bar{x},\bar{x},\bar{x}$.

1 b $\bar{3}m$ $\frac{1}{2},\frac{1}{2},\frac{1}{2}$.

1 a $\bar{3}m$ $0,0,0$.

(2) HEXAGONAL AXES:
(0,0,0; $\frac{1}{2},\frac{1}{2},\frac{1}{2}$; $\frac{1}{2},\frac{1}{2},\frac{1}{2}$)+

36 i 1 $x,y,z; \bar{y},x,-y,z; y,-x,\bar{z},z; \bar{x},\bar{y},\bar{z}; y,y,-x,z; x-y,\bar{x},\bar{z}; \bar{y},\bar{x},z; x,x-y,z; y-x,y,z; y,x,\bar{z}; \bar{x},y-x,\bar{z}; x-y,\bar{y},\bar{z}$.

General:
 $h\bar{k}\bar{l}h$; $-h+k+l=3n$
 $h\bar{h}2\bar{h}h$; $(l=3n)$
 $h\bar{h}0\bar{h}$; $(h+l=3n)$

18 h m $x,\bar{x},z; x,2\bar{x},z; 2\bar{x},\bar{x},z; \bar{x},x,\bar{z}; \bar{x},2\bar{x},\bar{z}; 2x,x,\bar{z}$.

Special: as above only

18 g 2 $x,0,\frac{1}{2}; 0,x,\frac{1}{2}; \bar{x},\bar{x},\frac{1}{2}; \bar{x},0,\frac{1}{2}; 0,\bar{x},\frac{1}{2}; x,x,\frac{1}{2}$.

18 f 2 $x,0,0; 0,x,0; \bar{x},\bar{x},0; \bar{x},0,0; 0,\bar{x},0; x,x,0$.

9 e $2/m$ $\frac{1}{2},0,0; 0,\frac{1}{2},0; \frac{1}{2},\frac{1}{2},0$.

9 d $2/m$ $\frac{1}{2},0,\frac{1}{2}; 0,\frac{1}{2},\frac{1}{2}; \frac{1}{2},\frac{1}{2},\frac{1}{2}$.

6 c $3m$ $0,0,z; 0,0,\bar{z}$.

3 b $\bar{3}m$ $0,0,\frac{1}{2}$.

3 a $\bar{3}m$ $0,0,0$.

Table C.5. Wyckoff positions for space group #166 $R\bar{3}m$ (taken from the website given in [54])

| Multi- plicity | Wyckoff letter | Site sym- metry | Coordinates |
|-------------------|-------------------|-----------------------|---|
| 36 | <i>i</i> | 1 | $(0, 0, 0) + (2/3, 1/3, 1/3) + (1/3, 2/3, 2/3) +$ $(x, y, z) (-y, x - y, z) (-x + y, -x, z) (y, x, -z)$ $(x - y, -y, -z) (-x, -x + y, -z) (-x, -y, -z)$ $(y, -x + y, -z) (x - y, x, -z) (-y, -x, z)$ $(-x + y, y, z) (x, x - y, z)$ |
| 18 | <i>h</i> | <i>m</i> | $(x, -x, z) (x, 2x, z) (-2x, -x, z) (-x, x, -z)$ $(2x, x, -z) (-x, -2x, -z)$ |
| 18 | <i>g</i> | 2 | $(x, 0, 1/2) (0, x, 1/2) (-x, -x, 1/2) (-x, 0, 1/2)$ $(0, -x, 1/2) (x, x, 1/2)$ |
| 18 | <i>f</i> | 2 | $(x, 0, 0) (0, x, 0) (-x, -x, 0) (-x, 0, 0)$ $(0, -x, 0) (x, x, 0)$ |
| 9 | <i>e</i> | $2/m$ | $(1/2, 0, 0) (0, 1/2, 0) (1/2, 1/2, 0)$ |
| 9 | <i>d</i> | $2/m$ | $(1/2, 0, 1/2) (0, 1/2, 1/2) (1/2, 1/2, 1/2)$ |
| 6 | <i>c</i> | $3m$ | $(0, 0, z) (0, 0, -z)$ |
| 3 | <i>b</i> | $-3m$ | $(0, 0, 1/2)$ |
| 3 | <i>a</i> | $-3m$ | $(0, 0, 0)$ |

groups. Diagrams for the high symmetry points are also presented for a few representative examples. The high symmetry points of the Brillouin zone for the simple cubic lattice are shown in Fig. C.4, and correspondingly, the high symmetry points for the FCC and BCC space groups #225 and #229 are shown in Fig. C.5(a), C.5(b), respectively. Table C.6 gives a summary of space groups listed in this appendix, together with the high symmetry points for the various groups that are considered in this appendix, giving the road-map for three isomorphous cubic groups (#221 for the simple cubic lattice, #225 for the FCC lattice, and #229 for the BCC lattice). For each high symmetry point and space group that is listed, its symmetry and the table number where the character table appears is given.

When the tables for the group of the wave vector are given (as for example in Tables C.7, C.8 and C.10), the caption cites a specific high symmetry point for a particular space group. Below the table are listed other high symmetry points for the same or other space groups for which the character table applies. Following Table C.8 which applies to point group C_{4v} , the multiplication table for the elements of group C_{4v} is given in Table C.9. Some high symmetry points which pertain to the same group of the wave vector may have classes containing different twofold axes. For this reason, when basis functions are given with the character table, they apply only to the high symmetry point

given in the caption to the table. Sometimes a high symmetry point is within the Brillouin zone such as point Λ in Table C.10, while point F for the BCC structure is on the Brillouin zone boundary. Many of these issues are illustrated in Table C.11 which gives the character table for point group C_{2v} (see Table A.5), but the symmetry operations for the twofold axes can refer to different twofold axes, as for example for points Σ and Z . A similar situation applies for Table C.15 for the X and M points for space group #221 regarding their twofold axes. With regard to Table C.12 for the W point for the FCC lattice, we see that the group of the wave vector has C_{4v} symmetry, but in contrast to the symmetry operations for the Δ point in Table C.8 which is an interior point in the Brillouin zone with C_{4v} symmetry, only four of the symmetry operations E , C_4^2 , iC_4^2 , and iC_2 take W into itself while four other symmetry operations $2C_4$, iC_4^2 , and iC_2 require a reciprocal lattice vector to take W into itself (Table C.12).

Also included in Table C.6 is a road-map for the character tables provided for the group of the wave vector for the nonsymmorphic diamond structure (#227). For this structure, the symmetry operations of classes that pertain to the O_h point group but are not in the T_d point group, include a translation $\tau_d = (a/4)(1, 1, 1)$ and the entries for the character tables for these classes includes a phase factor $\exp(i\mathbf{k} \cdot \boldsymbol{\tau}_d)$ (see Table C.17 for the Γ point and Table C.18 for the L point). The special points X , W , and Z on the square face for the diamond structure (#227) do not correspond to Bragg reflections and along this face, and the energy levels stick together (see Sect. 12.5) at these high symmetry points (see Tables C.19 and C.20). Additional character tables for the group of the wave vector at high symmetry points Λ , Σ , Δ , and X for the diamond structure are found in Sect. 10.8 (Tables 10.9–10.12).

Next we consider the group of the wave vector for crystals with hexagonal/rhombohedral symmetry as occurs for graphite with $ABCABC$ stacking (symmorphic space group #166) which has high symmetry points shown in Fig. C.6(a) and (b). Since the space group #166 is symmorphic, the group of the wave vector at high symmetry points is simply found. Explicit examples are given in Tables C.21–C.23 for three points of high symmetry for space group #166. From Figure C.6 it can be seen that the group of the wave vector for the Γ point $k = 0$ has the highest symmetry of D_{3d} , which is shared by point Z at the center of the hexagonal face in Fig. C.6(b) (see Table C.21). The point Δ has a twofold axis with C_2 symmetry (Table C.23) and leads to the point X with C_{3v} point group symmetry at the center of the rectangular face (see Table C.22). The compatibility of the Δ point with the Γ and X points can be verified.

Finally, we present in Tables C.24–C.29 the character tables for the group of the wave vector for selected high symmetry points for the nonsymmorphic hexagonal structure given by space group #194, which is descriptive of 3D graphite with $ABAB$ layer stacking. The high symmetry points in the Brillouin zone for the hexagonal structure are shown in Fig. C.7. Specific character tables are given for the high symmetry points Γ ($k = 0$) in Table C.24, a Δ

Table C.6. Group of the wave vector at various symmetry points in the Brillouin zone for some specific space groups

| lattice | point | \mathbf{k} | symmetry | Table |
|-------------------|-----------|-------------------------------------|----------|-------|
| #221 ^a | Γ | (0,0,0) | O_h | C.7 |
| | R | $[(2\pi/a)(1, 1, 1)]$ | O_h | C.7 |
| | X | $[(2\pi/a)(1, 0, 0)]$ | D_{4h} | C.15 |
| | M | $[(2\pi/a)(1, 1, 0)]$ | D_{4h} | C.15 |
| | Λ | $[(2\pi/a)(x, x, x)]$ | C_{3v} | C.10 |
| | Σ | $[(2\pi/a)(x, x, 0)]$ | C_{2v} | C.11 |
| | Δ | $[(2\pi/a)(x, 0, 0)]$ | C_{4v} | C.8 |
| | S | $[(2\pi/a)(1, z, z)]$ | C_{2v} | C.11 |
| | T | $[(2\pi/a)(1, 1, z)]$ | C_{4v} | C.8 |
| | Z | $[(2\pi/a)(1, y, 0)]$ | C_{2v} | C.11 |
| #225 ^b | Γ | (0,0,0) | O_h | C.7 |
| | X | $[(2\pi/a)(1, 0, 0)]$ | D_{4h} | C.15 |
| | W | $[(\pi/a)(2, 1, 0)]$ | C_{4v} | C.12 |
| | L | $[(\pi/a)(1, 1, 1)]$ | D_{3d} | C.16 |
| | Λ | $[(\pi/a)(x, x, x)]$ | C_{3v} | C.10 |
| | Σ | $[(2\pi/a)(x, x, 0)]$ | C_{2v} | C.11 |
| | Δ | $[(2\pi/a)(x, 0, 0)]$ | C_{4v} | C.8 |
| | K | $[(2\pi/a)(0, 3/4, 3/4)]$ | C_{2v} | C.11 |
| | U | $[(2\pi/a)(1, 1/4, 1/4)]$ | C_{2v} | C.11 |
| | Z | $[(2\pi/a)(1, y, 0)]$ | C_{2v} | C.11 |
| #227 ^c | Γ | (0,0,0) | O_h | C.17 |
| | X | $[(2\pi/a)(1, 0, 0)]$ | D_2 | 10.12 |
| | W | $[(\pi/a)(2, 1, 0)]$ | C_{4v} | C.19 |
| | L | $[(\pi/a)(1, 1, 1)]$ | D_{3d} | C.18 |
| | Λ | $[(2\pi/a)(x, x, x)]$ | C_{3v} | 10.11 |
| | Σ | $[(2\pi/a)(x, x, 0)]$ | C_{2v} | 10.10 |
| | Δ | $[(2\pi/a)(x, 0, 0)]$ | C_{4v} | 10.9 |
| | $Z(V)$ | $[(2\pi/a)(1, y, 0)]$ | C_{2v} | C.20 |
| | Q | $[(4\pi/a)(1/4, 1/2 - y, y)]$ | C_{2v} | A.5 |
| | | | | |
| #229 ^d | Γ | (0,0,0) | O_h | C.7 |
| | Λ | $[(\pi/a)(x, x, x)]$ | C_{3v} | C.10 |
| | Σ | $[(\pi/a)(x, x, 0)]$ | C_{2v} | C.11 |
| | Δ | $[(2\pi/a)(x, 0, 0)]$ | C_{4v} | C.8 |
| | H | $[(2\pi/a)(1, 0, 0)]$ | D_{4h} | C.15 |
| | P | $[(\pi/a)(1, 1, 1)]$ | T_d | C.13 |
| | F | $[(\pi/a)(1 + 2x, 1 - 2x, 1 - 2x)]$ | C_{3v} | C.10 |
| | G | $[(\pi/a)(1 + 2x, 1 - 2x, 0)]$ | C_{2v} | C.11 |

^aSee Fig. C.4; ^bSee Fig. C.5(a); ^cSee Figs. C.3 and C.5(a); ^dSee Fig. C.5(b)

Table C.6 (continued)

| lattice | point | \mathbf{k} | symmetry | Table |
|-------------------|----------|------------------------------|----------|-------|
| | D | $[(\pi/a)(1, 1, z)]$ | C_{2v} | C.11 |
| | N | $[(\pi/a)(1, 1, 0)]$ | D_{2h} | C.14 |
| #166 ^e | Γ | (0,0,0) | D_{3d} | C.21 |
| | A | $[(2\pi/c)(0, 0, z)]$ | D_3 | C.22 |
| | Δ | $[(2\pi/a)(x, 0, 0)]$ | C_2 | C.23 |
| | Z | $[(2\pi/c)(0, 0, 1)]$ | D_{3d} | C.21 |
| | X | $[(2\pi/a)(1, 0, 0)]$ | D_3 | C.22 |
| #194 ^f | Γ | (0,0,0) | D_{6h} | C.24 |
| | A | $[(2\pi/c)(0, 0, 1)]$ | D_{3h} | C.26 |
| | K | $[(2\pi/a)(1/3, 1/3, 0)]$ | D_{3h} | C.27 |
| | H | $[(2\pi)(1/3a, 1/3a, 1/c)]$ | D_{3h} | C.28 |
| | Δ | $[(2\pi/c)(0, 0, z)]$ | C_{6v} | C.25 |
| | P | $[(2\pi)(1/3a, 1/3a, z/c)]$ | C_{3v} | C.29 |
| | M | $[(\pi/a)(1, -1, 0)]$ | D_{2h} | C.30 |
| | T | $[(\pi/a)(1 - x, 1 + x, 0)]$ | C_{2v} | C.31 |
| | Σ | $[(\pi/a)(x, -x, 0)]$ | C_{2v} | C.32 |
| | U | $[(2\pi)(1/3a, -1/3a, x/c)]$ | C_{1h} | C.33 |

^eSee Fig. C.6; ^fSee Fig. C.7

point in Table C.25, an A point in Table C.26 together with some compatibility relations, a K point in Table C.27, an H point in Table C.28 and a P point in Table C.29.

In the character Table C.24 for the Γ point ($k = 0$), the six classes which are in D_{6h} but not in D_{3d} have a translation vector $\tau = (c/2)(0, 0, 1)$ in their symmetry operations $\{R|\tau\}$. Phase factors are seen in Table C.25 for the Δ point which is at an interior $k \neq 0$ point in the Brillouin zone. The phase factors $T_\Delta = \exp(i\mathbf{k}_\Delta \cdot \tau)$ appear in the character table for the classes containing a translation vector τ . Points A and H are special high symmetry points where energy levels stick together because the points in reciprocal space associated with this plane do not correspond to a true Bragg reflection, i.e., the calculated structure factor for these points is zero. Character Tables for other high symmetry points for group #194 are also given in Table C.30 for point M , Table C.31 for point T , Table C.32 for point Σ , Table C.33 for point U while Table C.34 gives pertinent compatibility relations for group #194. Appendix D gives further character tables for double groups based on group #194 where the spin on the electron is considered in formulating the symmetry for the electronic energy band structure (Tables D.10–D.14).

Table C.7. Character table (for group O_h) for the group of the wave-vector at a Γ point for various cubic space groups

| representation | basis functions | E | $3C_4^2$ | $6C_4$ | $6C_2$ | $8C_3$ | i | $3iC_4^2$ | $6iC_4$ | $6iC_2$ | $8iC_3$ |
|----------------|---|-----|----------|--------|--------|--------|-----|-----------|---------|---------|---------|
| Γ_1 | 1 | | 1 | 1 | 1 | 1 | 1 | 1 | 1 | 1 | 1 |
| Γ_2 | $\begin{cases} x^4(y^2 - z^2) + \\ y^4(z^2 - x^2) + \\ z^4(x^2 - y^2) \end{cases}$ | | 1 | 1 | -1 | -1 | 1 | 1 | 1 | -1 | -1 |
| Γ_{12} | $\begin{cases} x^2 - y^2 \\ 2z^2 - x^2 - y^2 \end{cases}$ | | 2 | 2 | 0 | 0 | -1 | 2 | 2 | 0 | 0 |
| Γ_{15} | x, y, z | | 3 | -1 | 1 | -1 | 0 | -3 | 1 | -1 | 1 |
| Γ_{25} | $z(x^2 - y^2)$, etc. | | 3 | -1 | -1 | 1 | 0 | -3 | 1 | 1 | -1 |
| Γ'_1 | $\begin{cases} xyz[x^4(y^2 - z^2) + \\ y^4(z^2 - x^2) + \\ z^4(x^2 - y^2)] \end{cases}$ | | 1 | 1 | 1 | 1 | 1 | -1 | -1 | -1 | -1 |
| Γ'_2 | xyz | | 1 | 1 | -1 | -1 | 1 | -1 | -1 | 1 | -1 |
| Γ'_{12} | $xyz(x^2 - y^2)$, etc. | | 2 | 2 | 0 | 0 | -1 | -2 | -2 | 0 | 0 |
| Γ'_{15} | $xy(x^2 - y^2)$, etc. | | 3 | -1 | 1 | -1 | 0 | 3 | -1 | 1 | -1 |
| Γ'_{25} | xy, yz, zx | | 3 | -1 | -1 | 1 | 0 | 3 | -1 | -1 | 1 |

$\Gamma = (0, 0, 0)$ [SC (#221), FCC (#225), BCC (#229)]. $R = (2\pi/a)(1, 1, 1)$ [SC (#221)]. The partners for Γ_{25} are $z(x^2 - y^2)$, $x(y^2 - z^2)$, $y(z^2 - x^2)$, for Γ'_{12} are $xyz(x^2 - y^2)$, $xyz(2z^2 - x^2 - y^2)$, for Γ'_{25} are $xy(x^2 - y^2)$, $yz(y^2 - z^2)$, $zx(z^2 - x^2)$

Table C.8. Character table (for group C_{4v}) for the group of the wave-vector at a Δ point for various cubic space groups

| representation | basis functions | E | C_4^2 | $2C_4$ | $2iC_4^2$ | $2iC_2'$ |
|----------------|--------------------------|-----|---------|--------|-----------|----------|
| Δ_1 | $1; x; 2x^2 - y^2 - z^2$ | 1 | 1 | 1 | 1 | 1 |
| Δ_2 | $y^2 - z^2$ | 1 | 1 | -1 | 1 | -1 |
| Δ'_2 | yz | 1 | 1 | -1 | -1 | 1 |
| Δ'_1 | $yz(y^2 - z^2)$ | 1 | 1 | 1 | -1 | -1 |
| Δ_5 | $y, z; xy, xz$ | 2 | -2 | 0 | 0 | 0 |

$\Delta = (2\pi/a)(x, 0, 0)$ (SC, FCC, BCC). $T = (2\pi/a)(1, 1, z)$ (SC)

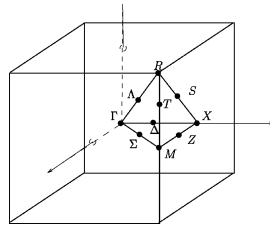


Fig. C.4. Brillouin zone for a simple cubic lattice (#221) showing the high symmetry points and axes

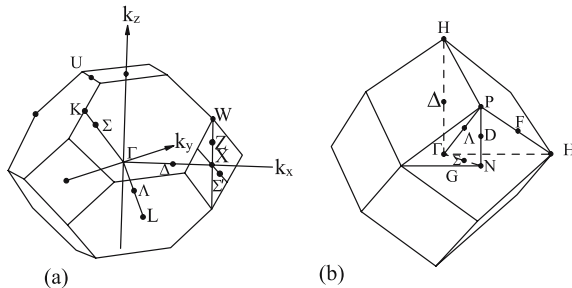


Fig. C.5. Brillouin zones for the (a) face-centered (#225) and (b) body-centered (#229) cubic lattices. Points and lines of high symmetry are indicated

Table C.9. Multiplication table for group C_{4v}

| class | operation | | | designation | E | α | β | γ | δ | ε | ζ | η |
|-----------|-----------|------|------|---------------|---------------|---------------|---------------|---------------|---------------|---------------|---------------|---------------|
| E | x | y | z | E | E | α | β | γ | δ | ε | ζ | η |
| C_4^2 | x | $-y$ | $-z$ | α | α | E | γ | β | ε | δ | η | ζ |
| $2C_4$ | x | $-z$ | y | β | β | γ | α | E | ζ | η | ε | δ |
| | x | z | $-y$ | γ | γ | β | E | α | η | ζ | δ | ε |
| $2iC_4^2$ | x | $-y$ | z | δ | δ | ε | η | ζ | E | α | γ | β |
| | x | y | $-z$ | ε | ε | δ | ζ | η | α | E | β | γ |
| $2iC_2$ | x | $-z$ | $-y$ | ζ | ζ | η | δ | ε | β | γ | E | α |
| | x | z | y | η | η | ζ | ε | δ | γ | β | α | E |

The rule for using the multiplication table is $\alpha\beta = (x, -y, -z)(x, -z, y) = [x, -(-z), -(y)] = (x, z, -y) = \gamma$, $\beta\delta = (x, -z, y)(x, -y, z) = (x, z, y) = \eta$, where the right operator (β) designates the row and the left operator (α) designates the column.

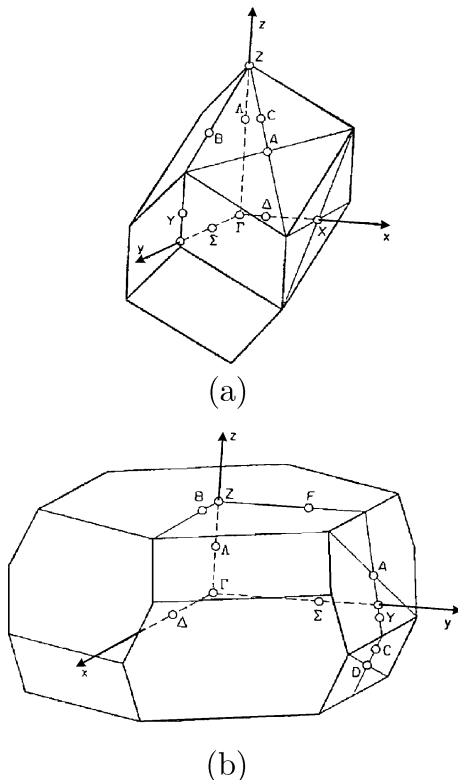


Fig. C.6. Brillouin zones for a rhombohedral lattice shown in (a) for rhombohedral axes and in (b) for hexagonal axes as presented in Table C.4 where the site symmetries corresponding to (a) and (b) are both presented for one of the rhombohedral groups

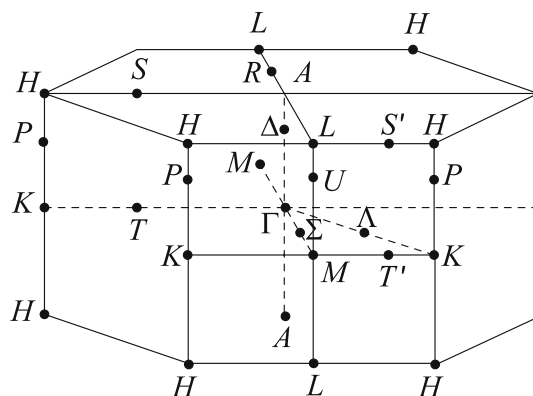


Fig. C.7. Brillouin zone for a hexagonal Bravais lattice showing high symmetry points for hexagonal structures

Table C.10. Character table for group C_{3v} for point A for various cubic space groups

| representation | basis | E | $2C_3$ | $3iC_2$ |
|----------------|--|-----|--------|---------|
| A_1 | $1; x + y + z$ | 1 | 1 | 1 |
| A_2 | $x(y^2 - z^2) + y(z^2 - x^2) + z(x^2 - y^2)$ | 1 | 1 | -1 |
| A_3 | $2x - y - z, y - z$ | 2 | -1 | 0 |

$\Lambda = (2\pi/a)(x, x, x)$ (SC, FCC, BCC). $F = (\pi/a)(1 + 2x, 1 - 2x, 1 - 2x)$ (BCC)

Table C.11. Character table for the group C_{2v} of the wave vector Σ for various cubic space groups

| represen- tation | Z | E | C_4^2 | iC_4^2 | $iC_{4\perp}^2$ |
|---------------------|--------------|-----|---------|----------|-----------------|
| | Σ | E | C_2 | iC_4^2 | iC_2 |
| | G, K, U, S | E | C_2 | iC_4^2 | iC_2 |
| | D | E | C_4^2 | iC_2 | $iC_{2\perp}$ |
| Σ_1 | | 1 | 1 | 1 | 1 |
| Σ_2 | | 1 | 1 | -1 | -1 |
| Σ_3 | | 1 | -1 | -1 | 1 |
| Σ_4 | | 1 | -1 | 1 | -1 |

$\Sigma = (2\pi/a)(x, x, 0)$ (SC, FCC, BCC) $G = (\pi/a)(1 + 2x, 1 - 2x, 0)$ (BCC) $K = (2\pi/a)(0, \frac{3}{4}, \frac{3}{4})$ (FCC) $U = (2\pi/a)(1, \frac{1}{4}, \frac{1}{4})$ (FCC) $D = (\pi/a)(1, 1, z)$ (BCC) $Z = (2\pi/a)(1, y, 0)$ (SC, FCC) $S = (2\pi/a)(1, z, z)$ (SC)

Table C.12. Character table for group C_{4v} of the wave vector for W for a symmorphic FCC lattice (#225)

| representation | E | C_4^2 | $2C_4$ | $2iC_4^2$ | $2iC_{2'}$ |
|----------------|-----|---------|--------|-----------|------------|
| W_1 | 1 | 1 | 1 | 1 | 1 |
| W_2 | 1 | 1 | -1 | 1 | -1 |
| W_3 | 1 | 1 | -1 | -1 | 1 |
| W_4 | 1 | 1 | 1 | -1 | -1 |
| W_5 | 2 | -2 | 0 | 0 | 0 |

$W = (\pi/a)(2, 1, 0)$ (FCC)

Table C.13. Character table for group T_d for the group of the wave vector for the P point in the BCC lattice

| representation | E | $3C_4^2$ | $8C_3$ | $6iC_4$ | $6iC_2$ |
|----------------|-----|----------|--------|---------|---------|
| P_1 | 1 | 1 | 1 | 1 | 1 |
| P_2 | 1 | 1 | 1 | -1 | -1 |
| P_3 | 2 | 2 | -1 | 0 | 0 |
| P_4 | 3 | -1 | 0 | -1 | 1 |
| P_5 | 3 | -1 | 0 | 1 | -1 |

$P = (\pi/a)(1, 1, 1)$ (BCC)

Table C.14. Character table for group $D_{2h} = D_2 \otimes i$ for the group of the wave vector for point N (BCC)

| representation | E | C_4^2 | $C_{2\parallel}$ | $C_{2\perp}$ | i | iC_4^2 | $iC_{2\parallel}$ | $iC_{2\perp}$ |
|----------------|-----|---------|------------------|--------------|-----|----------|-------------------|---------------|
| N_1 | 1 | 1 | 1 | 1 | 1 | 1 | 1 | 1 |
| N_2 | 1 | -1 | 1 | -1 | 1 | -1 | 1 | -1 |
| N_3 | 1 | -1 | -1 | 1 | 1 | -1 | -1 | 1 |
| N_4 | 1 | 1 | -1 | -1 | 1 | 1 | -1 | -1 |
| N'_1 | 1 | 1 | 1 | 1 | -1 | -1 | -1 | -1 |
| N'_2 | 1 | -1 | 1 | -1 | -1 | 1 | -1 | 1 |
| N'_3 | 1 | 1 | -1 | -1 | -1 | -1 | 1 | 1 |
| N'_4 | 1 | -1 | -1 | 1 | -1 | 1 | 1 | -1 |

 $N = (\pi/a)(1, 1, 0)$ (BCC)
Table C.15. Character table for D_{4h} for the group of the wave vector for point X for various cubic space groups

| representation | basis | E | $2C_{4\perp}^2$ | $C_{4\parallel}^2$ | $2C_{4\parallel}^2$ | $2C_2$ | i | $2iC_{4\perp}^2$ | $iC_{4\parallel}^2$ | $2iC_{4\parallel}$ | $2iC_2$ |
|----------------|-----------------------|-----|-----------------|--------------------|---------------------|--------|-----|------------------|---------------------|--------------------|---------|
| X_1 | $1; 2x^2 - y^2 - z^2$ | 1 | 1 | 1 | 1 | 1 | 1 | 1 | 1 | 1 | 1 |
| X_2 | $y^2 - z^2$ | 1 | 1 | 1 | -1 | -1 | 1 | 1 | 1 | -1 | -1 |
| X_3 | yz | 1 | -1 | 1 | -1 | 1 | 1 | -1 | 1 | -1 | 1 |
| X_4 | $yz(y^2 - z^2)$ | 1 | -1 | 1 | 1 | -1 | 1 | -1 | 1 | 1 | -1 |
| X_5 | xy, xz | 2 | 0 | -2 | 0 | 0 | 2 | 0 | -2 | 0 | 0 |
| X'_1 | $xyz(y^2 - z^2)$ | 1 | 1 | 1 | 1 | 1 | -1 | -1 | -1 | -1 | -1 |
| X'_2 | xyz | 1 | 1 | 1 | -1 | -1 | -1 | -1 | 1 | 1 | 1 |
| X'_3 | $x(y^2 - z^2)$ | 1 | -1 | 1 | -1 | 1 | -1 | 1 | -1 | 1 | -1 |
| X'_4 | x | 1 | -1 | 1 | 1 | -1 | -1 | 1 | -1 | -1 | 1 |
| X'_5 | y, z | 2 | 0 | -2 | 0 | 0 | -2 | 0 | 2 | 0 | 0 |

 $X = (2\pi/a)(1, 0, 0)$ (SC, FCC). $M = (2\pi/a)(1, 1, 0)$ (SC). $H = (2\pi/a)(1, 0, 0)$ (BCC)
Table C.16. Character table for D_{3d} for the group of the wave vector for point L (FCC)

| representation | basis | E | $2C_3$ | $3C_2$ | i | $2iC_3$ | $3iC_2$ |
|----------------|---|-----|--------|--------|-----|---------|---------|
| L_1 | $1; xy + yz + xz$ | 1 | 1 | 1 | 1 | 1 | 1 |
| L_2 | $yz(y^2 - z^2) + xy(x^2 - y^2) + xz(z^2 - x^2)$ | 1 | 1 | -1 | 1 | 1 | -1 |
| L_3 | $2x^2 - y^2 - z^2, y^2 - z^2$ | 2 | -1 | 0 | 2 | -1 | 0 |
| L'_1 | $x(y^2 - z^2) + y(z^2 - x^2) + z(x^2 - y^2)$ | 1 | 1 | 1 | -1 | -1 | -1 |
| L'_2 | $x + y + z$ | 1 | 1 | -1 | -1 | -1 | 1 |
| L'_3 | $y - z, 2x - y - z$ | 2 | -1 | 0 | -2 | 1 | 0 |

 $L = (\pi/a)(1, 1, 1)$ (FCC)

Table C.17. Character table for group O_h appropriately modified to describe the group of the wave vector for $k = 0$ (the Γ -point) for the diamond structure (#227)

| representation | $\{E 0\}$ | $3\{C_4^2 0\}$ | $6\{C_4 0\}$ | $6\{C_2 0\}$ | $8\{C_3 0\}$ | $8\{C_2' 0\}$ | $3\{iC_4^2 \tau_d\}$ | $\{i \tau_d\}$ | $3\{iC_4 0\}$ | $6\{iC_2 0\}$ | $6\{iC_3 0\}$ | $8\{iC_2' 0\}$ | $8\{iC_3 \tau_d\}$ |
|----------------|-----------|----------------|--------------|--------------|--------------|---------------|----------------------|----------------|---------------|---------------|---------------|----------------|--------------------|
| Γ_1 | 1 | 1 | 1 | 1 | 1 | 1 | 1 | 1 | 1 | 1 | 1 | 1 | 1 |
| Γ_2 | 1 | 1 | -1 | -1 | 1 | 1 | 1 | 1 | -1 | -1 | -1 | 1 | 1 |
| Γ_{12} | 2 | 2 | 0 | 0 | -1 | 2 | 2 | 0 | 0 | 0 | -1 | -1 | -1 |
| Γ_{15} | 3 | -1 | 1 | -1 | 0 | -3 | 1 | -1 | 1 | 1 | 0 | 0 | 0 |
| Γ_{25} | 3 | -1 | -1 | 1 | 0 | -3 | 1 | 1 | 1 | -1 | 0 | 0 | 0 |
| Γ'_1 | 1 | 1 | 1 | 1 | 1 | -1 | -1 | -1 | -1 | -1 | -1 | -1 | -1 |
| Γ'_2 | 1 | 1 | -1 | -1 | 1 | -1 | -1 | -1 | 1 | 1 | 1 | -1 | -1 |
| Γ'_2 | 2 | 2 | 0 | 0 | -1 | -2 | -2 | 0 | 0 | 0 | 0 | 1 | 1 |
| Γ'_{12} | 3 | -1 | 1 | -1 | 0 | 3 | -1 | 1 | -1 | -1 | 0 | 0 | 0 |
| Γ'_{15} | 3 | -1 | -1 | 1 | 0 | 3 | -1 | -1 | 1 | -1 | 1 | 0 | 0 |
| Γ'_{25} | | | | | | | | | -1 | -1 | 1 | 0 | 0 |

$\tau_d = (a/4)(1, 1, 1)$. The classes involving τ_d translations are classes in the O_h point group that are not in the T_d point group

Table C.18. Character table for group D_{3d} of the wave vector for point L for the diamond structure (#227)

| representation | basis | $\{E 0\}$ | $2\{C_3 0\}$ | $3\{C_2 0\}$ | $\{i 0\}$ | $2\{C_{2'} 0\}$ | $3\{iC_3 0\}$ | $3\{iC_{2'} 0\}$ |
|----------------|---|-----------|--------------|--------------|-----------|-----------------|---------------|------------------|
| L_1 | $1; xy + yz + xz$ | 1 | 1 | 1 | 1 | 1 | 1 | 1 |
| L_2 | $yz(y^2 - z^2) + xy(x^2 - y^2) + xz(z^2 - x^2)$ | 1 | 1 | -1 | 1 | 1 | 1 | -1 |
| L_3 | $2x^2 - y^2 - z^2, y^2 - z^2$ | 2 | -1 | 0 | 2 | -1 | 0 | 0 |
| L'_1 | $x(y^2 - z^2) + y(z^2 - x^2) + z(x^2 - y^2)$ | 1 | 1 | 1 | -1 | -1 | -1 | -1 |
| L'_2 | $x + y + z$ | 1 | 1 | -1 | -1 | -1 | 1 | 1 |
| L'_3 | $y - z, 2x - y - z$ | 2 | -1 | 0 | -2 | 1 | 0 | 0 |

For the L point $(\pi/a)(1, 1, 1)$, the group of the wave vector has no symmetry operations involving the translation vector $\tau_d = (a/4)(1, 1, 1)$

Table C.19. Character table for group C_{4v} for the group of the wave vector for the W point for the diamond structure (#227)

| representation ^a | $\{E 0\}$ | $\{C_4^2 0\}$ | $2\{C_4 \tau_d\}$ | $2\{iC_4^2 \tau_d\}$ | $2\{iC_{2'} 0\}$ |
|-----------------------------|-----------|---------------|-------------------|----------------------|------------------|
| W_1 | 2 | 2 | 0 | 0 | 0 |
| W_2 | 2 | -2 | 0 | 0 | 0 |

^a Note $\tau_d = (a/4)(1, 1, 1)$ $W = (\pi/a)(2, 1, 0)$. Note the W point is not a point with Bragg reflections, so energy levels stick together at this point.

Table C.20. Character table for group C_{2v} of the group of the wave vector for the Z (or V) point for the diamond structure (#227)

| representation ^a | $\{E 0\}$ | $\{C_4^2 0\}$ | $\{iC_4^2 \tau_d\}$ | $\{iC_{4\perp}^2 \tau_d\}$ |
|-----------------------------|-----------|---------------|---------------------|----------------------------|
| Z_1 | 2 | 2 | 0 | 0 |
| Z_2 | 2 | -2 | 0 | 0 |

$Z = (2\pi/a)(1, y, 0)$ and $\tau_d = (a/4)(1, 1, 1)$. Note that the Z (or V) point is not a point with Bragg reflections, so energy bands stick together at this point

Table C.21. Character table with point group symmetry D_{3d} ($\bar{3}m$), for the group of the wave vector at the Γ point ($\mathbf{k} = 0$) for the space group #166 $R\bar{3}m$

| D_{3d} ($\bar{3}m$) | representation | E | $2C_3$ | $3C_{2'}$ | i | $2iC_3$ | $3iC_{2'}$ |
|-------------------------|----------------|-----|--------|-----------|-----|---------|------------|
| Γ_1^+ | | 1 | 1 | 1 | 1 | 1 | 1 |
| Γ_2^+ | | 1 | 1 | -1 | 1 | 1 | -1 |
| Γ_3^+ | | 2 | -1 | 0 | 2 | -1 | 0 |
| Γ_1^- | | 1 | 1 | 1 | -1 | -1 | -1 |
| Γ_2^- | | 1 | 1 | -1 | -1 | -1 | 1 |
| Γ_3^- | | 2 | -1 | 0 | -2 | 1 | 0 |

$\Gamma = (0, 0, 0)$. $Z = (2\pi/c)(0, 0, 1)$

Table C.22. Character table with point group symmetry $C_{3v}(3m)$ for group of the wave vector for a point A for the space group #166 $R\bar{3}m$

| $C_{3v}(3m)$ | E | $2C_3$ | $3\sigma_v$ |
|--------------|-----|--------|-------------|
| A_1 | 1 | 1 | 1 |
| A_2 | 1 | 1 | -1 |
| A_3 | 2 | -1 | 0 |

$A = (2\pi/c)(0, 0, z)$. $X = (2\pi/a)(1, 0, 0)$

Table C.23. Character table with point group symmetry $C_2(2)$ for the group of the wave vector for a point Δ for the space group #166 $R\bar{3}m$

| $C_2(2)$ | E | $C_{2'}$ |
|------------|-----|----------|
| Δ_1 | 1 | 1 |
| Δ_2 | 1 | -1 |

$\Delta = (2\pi/a)(x, 0, 0)$

Table C.24. Character table with point group symmetry D_{6h} appropriately modified to describe the group of the wave vector for a point Γ ($k = 0$) for the space group #194 D_{6h}^4 ($P6_3/mmc$)^{a,b}

| | $\{C_3^+\ 0\}$ | $\{C_3^-\ \tau\}$ | $\{C_2^+\ 0\}$ | $\{C_2^-\ \tau\}$ | $\{C_2'^A\ 0\}$ | $\{C_2''^A\ \tau\}$ | $\{C_2'^B\ 0\}$ | $\{C_2''^B\ \tau\}$ | $\{S_6^+\ 0\}$ | $\{S_6^-\ \tau\}$ | $\{S_6^+\ \tau\}$ | $\{S_6^-\ 0\}$ | $\{S_h\ \tau\}$ | $\{S^+\ \tau\}$ | $\{S^-\ 0\}$ | $\{\sigma_d^A\ 0\}$ | $\{\sigma_d^B\ 0\}$ | $\{\sigma_d^C\ 0\}$ | $\{\sigma_v^A\ \tau\}$ | $\{\sigma_v^B\ 0\}$ | $\{\sigma_v^C\ \tau\}$ |
|---------|----------------|-------------------|----------------|-------------------|-----------------|---------------------|-----------------|---------------------|----------------|-------------------|-------------------|----------------|-----------------|-----------------|--------------|---------------------|---------------------|---------------------|------------------------|---------------------|------------------------|
| I_1^+ | 1 | 1 | 1 | 1 | 1 | 1 | 1 | 1 | 1 | 1 | 1 | 1 | 1 | 1 | 1 | 1 | 1 | 1 | 1 | 1 | 1 |
| I_1^+ | 1 | 1 | 1 | 1 | -1 | -1 | 1 | 1 | 1 | 1 | 1 | 1 | -1 | -1 | -1 | -1 | -1 | -1 | -1 | -1 | -1 |
| I_2^+ | 1 | -1 | 1 | -1 | 1 | -1 | 1 | -1 | 1 | -1 | 1 | -1 | 1 | -1 | 1 | -1 | -1 | -1 | -1 | -1 | -1 |
| I_3^+ | 1 | -1 | 1 | -1 | -1 | -1 | 1 | 1 | -1 | 1 | -1 | 1 | -1 | 1 | -1 | -1 | -1 | -1 | -1 | -1 | -1 |
| I_4^+ | 1 | -1 | 1 | -1 | -1 | -1 | 1 | 1 | 1 | -1 | 1 | -1 | 1 | -1 | 1 | -1 | -1 | -1 | -1 | -1 | -1 |
| I_4^+ | 2 | -2 | -1 | 1 | 0 | 0 | 2 | 2 | -2 | -1 | -1 | 1 | 0 | 0 | 0 | 0 | 0 | 0 | 0 | 0 | 0 |
| I_5^+ | 2 | 2 | -1 | -1 | 0 | 0 | 0 | 2 | 2 | -1 | -1 | -1 | 0 | 0 | 0 | 0 | 0 | 0 | 0 | 0 | 0 |
| I_6^+ | 2 | 2 | 1 | 1 | 1 | 1 | -1 | -1 | -1 | -1 | -1 | -1 | -1 | -1 | -1 | -1 | -1 | -1 | -1 | -1 | -1 |
| I_1^- | 1 | 1 | 1 | 1 | 1 | 1 | 1 | 1 | 1 | 1 | 1 | 1 | 1 | 1 | 1 | 1 | 1 | 1 | 1 | 1 | 1 |
| I_2^- | 1 | 1 | 1 | 1 | -1 | -1 | -1 | -1 | -1 | -1 | -1 | -1 | -1 | -1 | -1 | -1 | -1 | -1 | -1 | -1 | -1 |
| I_3^- | 1 | -1 | 1 | -1 | 1 | -1 | 1 | -1 | 1 | -1 | 1 | -1 | 1 | -1 | 1 | -1 | -1 | -1 | -1 | -1 | -1 |
| I_4^- | 1 | -1 | 1 | -1 | -1 | -1 | 1 | 1 | 1 | -1 | 1 | -1 | 1 | -1 | 1 | -1 | -1 | -1 | -1 | -1 | -1 |
| I_5^- | 2 | -2 | -1 | 1 | 0 | 0 | -2 | 2 | 1 | -1 | 1 | -1 | 1 | -1 | 1 | -1 | -1 | -1 | -1 | -1 | -1 |
| I_6^- | 2 | 2 | -1 | -1 | 0 | 0 | -2 | -2 | 1 | -1 | 1 | -1 | 1 | -1 | 1 | -1 | 0 | 0 | 0 | 0 | 0 |

^a Since $D_{6h} = D_6 \otimes i$, the group D_{6h} has 12 classes and 12 irreducible representations

^b Note that the symmetry operations for the nonsymmorphic group of the wave vector at $k = 0$ have translations $\tau = (c/2)(0, 0, 1)$ if they are elements of group D_{6h} but are not in group D_{3d}

Table C.25. Character table with point group symmetry C_{6v} for the group of the wave vector for a point Δ for the space group #194

| C_{6v} | $\{E 0\}$ | $\{C_2 \tau\}$ | $2\{C_3 0\}$ | $2\{C_6 \tau\}$ | $3\{\sigma_d 0\}$ | $3\{\sigma_v \tau\}$ |
|------------|-----------|---------------------|--------------|---------------------|-------------------|----------------------|
| Δ_1 | 1 | $1 \cdot T_\Delta$ | 1 | $1 \cdot T_\Delta$ | 1 | $1 \cdot T_\Delta$ |
| Δ_2 | 1 | $1 \cdot T_\Delta$ | 1 | $1 \cdot T_\Delta$ | -1 | $-1 \cdot T_\Delta$ |
| Δ_3 | 1 | $-1 \cdot T_\Delta$ | 1 | $-1 \cdot T_\Delta$ | 1 | $-1 \cdot T_\Delta$ |
| Δ_4 | 1 | $-1 \cdot T_\Delta$ | 1 | $-1 \cdot T_\Delta$ | -1 | $1 \cdot T_\Delta$ |
| Δ_5 | 2 | $-2 \cdot T_\Delta$ | -1 | $1 \cdot T_\Delta$ | 0 | 0 |
| Δ_6 | 2 | $2 \cdot T_\Delta$ | -1 | $-1 \cdot T_\Delta$ | 0 | 0 |

The symmetry operations with translations for point $\Delta = (2\pi/c)(0, 0, z)$, where $0 \leq z \leq 1$ are consistent with those in Table C.24 for $k = 0$. The translation here is $\tau = (c/2)(0, 0, 1)$ and the phase factor is $T_\Delta = \exp(i\mathbf{k} \cdot \tau)$ so that at the dimensionless z end points we have $T_\Delta = 1$ at $z = 0$ and $T_\Delta = -1$ at $z = 1$. See Table C.34 for compatibility relations.

Table C.26. Character table with point group symmetry C_{3v} for the group of the wave vector for point A for the space group #194

| C_{3v} | $\{E 0\}$ | $\{2C_3 0\}$ | $3\{\sigma_d 0\}$ | compatibility relations |
|----------|-----------|--------------|-------------------|---------------------------------------|
| A_1 | 2 | 2 | 2 | $A_1 \rightarrow \Delta_1 + \Delta_3$ |
| A_2 | 2 | 2 | -2 | $A_2 \rightarrow \Delta_2 + \Delta_4$ |
| A_3 | 4 | -2 | 0 | $A_3 \rightarrow \Delta_5 + \Delta_6$ |

Point $A = (2\pi/c)(0, 0, 1)$. At the A point in the Brillouin zone, the structure factor vanishes so that Bragg reflections do not occur. Therefore the compatibility relations given on the right side of Table C.26 show that at the A point the Δ point bands stick together.

Table C.27. Character table with point group symmetry D_{3h} for the group of the wave vector for a point K for the space group #194

| | $\{C_2'^A 0\}$ | $\{\sigma_v^A \tau\}$ | | |
|---------|--|--|----|----------------------------------|
| | $\{C_3^+ 0\}$ $\{C_2'^B 0\}$ | $\{S_3^- \tau\}$ $\{\sigma_v^B \tau\}$ | | |
| | $\{E 0\}$ $\{C_3^- 0\}$ $\{C_2'^C 0\}$ | $\{\sigma_h \tau\}$ $\{S_3^+ \tau\}$ $\{\sigma_v^C \tau\}$ | | |
| K_1^+ | 1 | 1 | 1 | $x^2 + y^2, z^2$ |
| K_2^+ | 1 | 1 | -1 | R_z |
| K_3^+ | 2 | -1 | 0 | $(x^2 - y^2, xy)$ (R_x, R_y) |
| K_1^- | 1 | 1 | 1 | $(x^2 - y^2, xy)$ (R_x, R_y) |
| K_2^- | 1 | 1 | -1 | z |
| K_3^- | 2 | -1 | 0 | $0(x, y)$ |

compatibility relations

$K_1^+ \rightarrow P_1$; $K_2^+ \rightarrow P_2$; $K_3^+ \rightarrow P_3$; $K_1^- \rightarrow P_2$; $K_2^- \rightarrow P_1$; $K_3^- \rightarrow P_3$

$K = (2\pi/a)(1/3, 1/3, 0)$

Table C.28. Character table with point group symmetry D_{3h} for the group of the wave vector for point H for the space group #194

| $D_{3h}(\bar{6}m2)$ | $\{E 0\}$ | $2\{C_3 0\}$ | $3\{C_{2'} 0\}$ | $\{\sigma_h \tau\}$ | $2\{S_3 \tau\}^a$ | $3\{\sigma_v \tau\}$ | compatibility relations |
|---------------------|-----------|--------------|-----------------|---------------------|-------------------|----------------------|-------------------------------|
| H_1 | 2 | -1 | 0 | 0 | $-\sqrt{3}i$ | $\sqrt{3}i$ | 0 $H_1 \rightarrow P_3$ |
| H_2 | 2 | -1 | 0 | 0 | $\sqrt{3}i$ | $-\sqrt{3}i$ | 0 $H_2 \rightarrow P_3$ |
| H_3 | 2 | 2 | 0 | 0 | 0 | 0 | 0 $H_3 \rightarrow P_1 + P_2$ |
| H_4 | 1 | -1 | i | i | i | $-i$ | 1 $H_4 \rightarrow P_1$ |
| H_5 | 1 | -1 | i | $-i$ | $-i$ | i | -1 $H_5 \rightarrow P_1$ |
| H_6 | 1 | -1 | $-i$ | $-i$ | $-i$ | i | 1 $H_6 \rightarrow P_2$ |

$$H = 2\pi(1/3a, 1/3a, 1/c)$$

^a Note that the two columns under class $2\{S_3|\tau\}$ refer to two symmetry operations in this class which have characters that are complex conjugates of one another.

Table C.29. Character table with point group symmetry C_{3v} for the group of the wave vector for point P for the space group #194

| C_{3v} | $\{E 0\}$ | $2\{C_3 0\}$ | $3\{\sigma_v \tau\}$ |
|----------|-----------|--------------|----------------------|
| P_1 | 1 | 1 | $1 \cdot T_p$ |
| P_2 | 1 | 1 | $-1 \cdot T_p$ |
| P_3 | 2 | -1 | 0 |

$$P = 2\pi(1/3a, 1/3a, z/c). T_p = \exp i\mathbf{k}_p \cdot \boldsymbol{\tau} \text{ where } 0 < z < 1 \text{ and } \boldsymbol{\tau} = (c/2)(0, 0, 1)$$

Table C.30. Character table with point group symmetry D_{2h} for the group of the wave vector of the M point of space group #194

| | $\{E 0\}$ | $\{C_2 \tau\}$ | $\left\{C_2'^A 0\right\}$ | $\left\{C_2''^A \tau\right\}$ | $\{i 0\}$ | $\{\sigma_h \tau\}$ | $\{\sigma_d^A 0\}$ | $\{\sigma_v^A \tau\}$ | |
|---------|-----------|----------------|---------------------------|-------------------------------|-----------|---------------------|--------------------|-----------------------|-----------------|
| M_1^+ | 1 | 1 | 1 | 1 | 1 | 1 | 1 | 1 | x^2, y^2, z^2 |
| M_2^+ | 1 | 1 | -1 | -1 | 1 | 1 | -1 | -1 | xy |
| M_3^+ | 1 | -1 | 1 | -1 | 1 | -1 | 1 | -1 | xz |
| M_4^+ | 1 | -1 | -1 | 1 | 1 | -1 | -1 | 1 | yz |
| M_1^- | 1 | 1 | 1 | 1 | -1 | -1 | -1 | -1 | |
| M_2^- | 1 | 1 | -1 | -1 | -1 | -1 | 1 | 1 | z |
| M_3^- | 1 | -1 | 1 | -1 | -1 | 1 | -1 | 1 | y |
| M_4^- | 1 | -1 | -1 | 1 | -1 | 1 | 1 | -1 | x |

compatibility relations

$$M_1^+ \rightarrow \Sigma_1; M_2^+ \rightarrow \Sigma_3; M_3^+ \rightarrow \Sigma_4; M_4^+ \rightarrow \Sigma_2;$$

$$M_1^- \rightarrow \Sigma_2; M_2^- \rightarrow \Sigma_4; M_3^- \rightarrow \Sigma_3; M_4^- \rightarrow \Sigma_1$$

$$M = (\pi/a)(1, -1, 0)$$

Table C.31. Character table for the group of the wave vector for point T for space group #194

| | $\{E 0\}$ | $\{C_2'^A 0\}$ | $\{\sigma_h \tau\}$ | $\{\sigma_v^A \tau\}$ | | |
|-------|-----------|----------------|---------------------|-----------------------|-----|-----------------|
| T_1 | 1 | 1 | 1 | 1 | y | x^2, y^2, z^2 |
| T_2 | 1 | 1 | -1 | -1 | | xz |
| T_3 | 1 | -1 | 1 | -1 | x | xy |
| T_4 | 1 | -1 | -1 | 1 | z | yz |

$$T = (\pi/a)(1-x, 1+x, 0)$$

Table C.32. Character table for Σ point for space group #194 (C_s^3 , Cm , #8)

| | $\{E 0\}$ | $\{C_2''^A \tau\}$ | $\{\sigma_h \tau\}$ | $\{\sigma_d^A 0\}$ | | |
|------------|-----------|--------------------|---------------------|--------------------|-----|-----------------|
| Σ_1 | 1 | 1 | 1 | 1 | x | x^2, y^2, z^2 |
| Σ_2 | 1 | 1 | -1 | -1 | | zy |
| Σ_3 | 1 | -1 | 1 | -1 | y | xy |
| Σ_4 | 1 | -1 | -1 | 1 | z | zx |

$$\Sigma = (\pi/a)(x, -x, 0)$$

Table C.33. Character table with point group C_{1h} for the group of the wave vector for point U for space group #194

| | $\{E 0\}$ | $\{\sigma_h \tau\}$ | | |
|-------|-----------|---------------------|--------|---------------------|
| U_1 | 1 | 1 | x, y | x^2, y^2, z^2, xy |
| U_2 | 1 | -1 | z | zy, zx |

$$U = 2\pi(1/3a, -1/3a, p/c)$$

Table C.34. Compatibility relations for Γ , Δ , Σ , and T

| Γ | Δ | Σ | T |
|--------------|------------|-----------------------|-------------|
| Γ_1^+ | Δ_1 | Σ_1 | T_1 |
| Γ_2^+ | Δ_2 | Σ_3 | T_3 |
| Γ_3^+ | Δ_3 | Σ_4 | T_2 |
| Γ_4^+ | Δ_4 | Σ_2 | T_4 |
| Γ_5^+ | Δ_5 | $\Sigma_2 + \Sigma_4$ | $T_2 + T_4$ |
| Γ_6^+ | Δ_6 | $\Sigma_1 + \Sigma_3$ | $T_1 + T_3$ |
| Γ_1^- | Δ_2 | Σ_2 | T_2 |
| Γ_2^- | Δ_1 | Σ_4 | T_4 |
| Γ_3^- | Δ_4 | Σ_3 | T_1 |
| Γ_4^- | Δ_3 | Σ_1 | T_3 |
| Γ_5^- | Δ_5 | $\Sigma_1 + \Sigma_3$ | $T_1 + T_3$ |
| Γ_6^- | Δ_6 | $\Sigma_2 + \Sigma_4$ | $T_2 + T_4$ |

D

Tables for Double Groups

In this appendix we provide tables useful for handling problems associated with double groups. Many of these tables can be found in two references, one by Koster et al. [48] and another by Miller and Love [54]. The first reference book “Properties of the Thirty-Two Point Groups,” by G.F. Koster, J.O. Dimmock, R.G. Wheeler, and H. Statz gives many tables for each of the 32 point groups, while the second gives many character tables for the group of the wave vector for each of the high symmetry points for each of the 230 space groups and many other kinds of related space groups.

The tables in the first reference for the 32 point groups include:

1. A character table including the double group representations (see, for example Table D.1 for groups O and T_d).
2. A table giving the decomposition of the direct product of any two irreducible representations (an example of such a table is given in Table D.2).
3. Tables of coupling coefficients for the product of any two basis functions. Two examples of tables of coupling coefficients are given in Tables D.3 and D.4.¹
4. Compatibility tables between point groups (e.g., Table D.7).
5. Compatibility tables with the Full Rotation Group (e.g., Table D.8).

We now illustrate some examples of these tables. Table D.1 shows the double group character table for the group O , which is tabulated together with T_d and includes classes, irreducible representations and basis functions for the double group. For example, the basis functions for $\Gamma_4(\Gamma_{15})$ are S_x, S_y, S_z which refer to the three Cartesian components of the angular momentum (integral values of angular momentum)¹ [47]. The basis functions for the Γ_6 and Γ_8 irreducible representations are written in the basic form $\phi(j, m_j)$ for the angular momentum and all the m_j partners are listed. Koster et al. use the notation \overline{E} for \mathcal{R} (rotation by 2π) and the notation \overline{C}_3 for class \mathcal{RC}_3 . The meaning of the time

¹Table 83 of [47] is continued over 10 pages of the book pages 90–99. We have reproduced some of the sections of this complete compilation.

Table D.1. Character table and basis functions for double groups O and T_d

| O | E | \bar{E} | $8C_3$ | $8\bar{C}_3$ | $\frac{3C_2}{3\bar{C}_2}$ | $6C_4$ | $6\bar{C}_4$ | $\frac{6C'_2}{6\bar{C}'_2}$ | | | |
|-------------------------|-----|-----------|--------|--------------|---------------------------|-------------|--------------|-------------------------------------|-------------------|--|-----------------------------|
| T_d | E | \bar{E} | $8C_3$ | $8\bar{C}_3$ | $\frac{3C_2}{3\bar{C}_2}$ | $6S_4$ | $6\bar{S}_4$ | $\frac{6\sigma_d}{6\bar{\sigma}_d}$ | time inversion | bases for O | bases for T_d |
| Γ_1 | 1 | 1 | 1 | 1 | 1 | 1 | 1 | 1 | a | R | R or xyz |
| Γ_2 | 1 | 1 | 1 | 1 | 1 | -1 | -1 | -1 | a | xyz | $S_x S_y S_z$ |
| $\Gamma_3(\Gamma_{12})$ | 2 | 2 | -1 | -1 | 2 | 0 | 0 | 0 | a | $(2z^2 - x^2 - y^2), (2z^2 - x^2 - y^2),$ $\sqrt{3}(x^2 - y^2)$ | $\sqrt{3}(x^2 - y^2)$ |
| $\Gamma_4(\Gamma_{15})$ | 3 | 3 | 0 | 0 | -1 | 1 | 1 | -1 | a | S_x, S_y, S_z | S_x, S_y, S_z |
| $\Gamma_5(\Gamma_{25})$ | 3 | 3 | 0 | 0 | -1 | -1 | -1 | 1 | a | yz, xz, xy | x, y, z |
| Γ_6 | 2 | -2 | 1 | -1 | 0 | $\sqrt{2}$ | $-\sqrt{2}$ | 0 | c | $\phi(1/2, -1/2), \phi(1/2, -1/2),$ $\phi(1/2, 1/2)$ | $\phi(1/2, 1/2)$ |
| Γ_7 | 2 | -2 | 1 | -1 | 0 | $-\sqrt{2}$ | $\sqrt{2}$ | 0 | c | $\Gamma_6 \otimes \Gamma_2$ | $\Gamma_6 \otimes \Gamma_2$ |
| Γ_8 | 4 | -4 | -1 | 1 | 0 | 0 | 0 | 0 | c | $\phi(3/2, -3/2), \phi(3/2, -3/2),$ $\phi(3/2, -1/2), \phi(3/2, -1/2),$ $\phi(3/2, 1/2), \phi(3/2, 1/2),$ $\phi(3/2, 3/2) \phi(3/2, 3/2)$ | $\phi(3/2, 3/2)$ |

inversion (Time Inversion) entries a, b and c are explained in Chap. 16 where *time inversion symmetry* is discussed.

Table D.2 for groups O and T_d gives the decomposition of the direct product of any irreducible representation Γ_i labeling a column with another irreducible representation Γ_j labeling a row. The irreducible representations contained in the decomposition of the direct product are $\Gamma_i \otimes \Gamma_j$ entered in the matrix position of their intersection.

The extensive tables of coupling coefficients are perhaps the most useful tables in Koster et al. [48]. These tables give the basis functions for the irreducible representations obtained by taking the direct product of two irreducible representations. We illustrate in Table D.3 the basis functions obtained by taking the direct product of each of the two partners of the Γ_{12} representation (denoted by Koster et al. as u_1^3 and u_2^3) with each of the three partners of the Γ_{15} representation (denoted by v_x^4, v_y^4, v_z^4) to yield three partners with Γ_{15} symmetry (denoted by $\psi_x^4, \psi_y^4, \psi_z^4$) and 3 partners with Γ_{25} symmetry (denoted by $\psi_{yz}^5, \psi_{zx}^5, \psi_{xy}^5$). This is Table 83 on p. 91 of Koster et al. [48]. From Table D.3 we see that the appropriate linear combinations for the ψ^4 and ψ^5 functions are (see Sect. 14.8)

Table D.2. Table of direct products of irreducible representations for the groups O and T_d

| Γ_1 | Γ_2 | Γ_3 | Γ_4 | Γ_5 | Γ_6 | Γ_7 | Γ_8 | |
|----------------------------------|------------|---|---|-----------------------|-----------------------|-----------------------------------|--------------------------|------------|
| Γ_1 | Γ_2 | Γ_3 | Γ_4 | Γ_5 | Γ_6 | Γ_7 | Γ_8 | Γ_1 |
| Γ_1 | Γ_3 | Γ_5 | Γ_4 | Γ_7 | Γ_6 | Γ_8 | Γ_2 | |
| $\Gamma_1 + \Gamma_2 + \Gamma_3$ | | $\Gamma_4 + \Gamma_5$ | $\Gamma_4 + \Gamma_5$ | $\Gamma_4 + \Gamma_5$ | Γ_8 | $\Gamma_6 + \Gamma_7 + \Gamma_8$ | Γ_3 | |
| | | $\Gamma_1 + \Gamma_3 + \Gamma_4 + \Gamma_5$ | $\Gamma_2 + \Gamma_3 + \Gamma_4 + \Gamma_5$ | $\Gamma_6 + \Gamma_8$ | $\Gamma_7 + \Gamma_8$ | $\Gamma_6 + \Gamma_7 + 2\Gamma_8$ | Γ_4 | |
| | | | $\Gamma_1 + \Gamma_3 + \Gamma_4 + \Gamma_5$ | $\Gamma_7 + \Gamma_8$ | $\Gamma_6 + \Gamma_8$ | $\Gamma_6 + \Gamma_7 + 2\Gamma_8$ | Γ_5 | |
| | | | | $\Gamma_1 + \Gamma_4$ | $\Gamma_2 + \Gamma_5$ | $\Gamma_3 + \Gamma_4 + \Gamma_5$ | Γ_6 | |
| | | | | | $\Gamma_1 + \Gamma_4$ | $\Gamma_3 + \Gamma_4 + \Gamma_5$ | Γ_7 | |
| | | | | | | $\Gamma_1 + \Gamma_2 + \Gamma_3$ | Γ_8 | |
| | | | | | | | $+2\Gamma_4 + 2\Gamma_5$ | |

Table D.3. Coupling coefficients for selected basis functions for single group O

| | $u_1^3 v_x^4$ | $u_1^3 v_y^4$ | $u_1^3 v_z^4$ | $u_2^3 v_x^4$ | $u_2^3 v_y^4$ | $u_2^3 v_z^4$ |
|---------------|---------------|---------------|---------------|---------------|---------------|---------------|
| ψ_x^4 | $-1/2$ | 0 | 0 | $\sqrt{3}/2$ | 0 | 0 |
| ψ_y^4 | 0 | $-1/2$ | 0 | 0 | $-\sqrt{3}/2$ | 0 |
| ψ_z^4 | 0 | 0 | 1 | 0 | 0 | 0 |
| ψ_{yz}^5 | $-\sqrt{3}/2$ | 0 | 0 | $-1/2$ | 0 | 0 |
| ψ_{xz}^5 | 0 | $\sqrt{3}/2$ | 0 | 0 | $-1/2$ | 0 |
| ψ_{xy}^5 | 0 | 0 | 0 | 0 | 0 | 1 |

Table D.4. Coupling coefficient tables for the indicated basis functions for double group O_h

| | $u_x^4 v_{-1/2}^6$ | $u_x^4 v_{1/2}^6$ | $u_y^4 v_{-1/2}^6$ | $u_y^4 v_{1/2}^6$ | $u_z^4 v_{-1/2}^6$ | $u_z^4 v_{1/2}^6$ |
|-----------------|--------------------|-------------------|--------------------|-------------------|----------------------|----------------------|
| $\psi_{-1/2}^6$ | 0 | $-i/\sqrt{3}$ | 0 | $-1/\sqrt{3}$ | $i/\sqrt{3}$ | 0 |
| $\psi_{1/2}^6$ | $-i/\sqrt{3}$ | 0 | $1/\sqrt{3}$ | 0 | 0 | $-i/\sqrt{3}$ |
| $\psi_{-3/2}^8$ | $i/\sqrt{2}$ | 0 | $1/\sqrt{2}$ | 0 | 0 | 0 |
| $\psi_{-1/2}^8$ | 0 | $i/\sqrt{6}$ | 0 | $1/\sqrt{6}$ | $i\sqrt{2}/\sqrt{3}$ | 0 |
| $\psi_{1/2}^8$ | $-i/\sqrt{6}$ | 0 | $1/\sqrt{6}$ | 0 | 0 | $i\sqrt{2}/\sqrt{3}$ |
| $\psi_{3/2}^8$ | 0 | $-i/\sqrt{2}$ | 0 | $1/\sqrt{2}$ | 0 | 0 |

Table D.5. Coupling coefficient table for coupling the basis functions of $\Gamma_3 \otimes \Gamma_6^+$ to Γ_8 where $\Gamma_3 \otimes \Gamma_6^+ = \Gamma_8$ in the double group for O_h

| | $u_1^3 v_{-1/2}^6$ | $u_1^3 v_{+1/2}^6$ | $u_2^3 v_{-1/2}^6$ | $u_2^3 v_{+1/2}^6$ |
|-----------------|--------------------|--------------------|--------------------|--------------------|
| $\psi_{-3/2}^8$ | 0 | 0 | 0 | 1 |
| $\psi_{-1/2}^8$ | 1 | 0 | 0 | 0 |
| $\psi_{+1/2}^8$ | 0 | -1 | 0 | 0 |
| $\psi_{+3/2}^8$ | 0 | 0 | -1 | 0 |

$$\begin{aligned}
\psi_x^4 &= -(1/2)u_1^3 v_x^4 + (\sqrt{3}/2)u_2^3 v_x^4 \\
\psi_y^4 &= -(1/2)u_1^3 v_y^4 - (\sqrt{3}/2)u_2^3 v_y^4 \\
\psi_z^4 &= u_1^3 v_z^4 \\
\psi_{yz}^5 &= -(\sqrt{3}/2)u_1^3 v_x^4 - (1/2)u_2^3 v_x^4 \\
\psi_{xz}^5 &= (\sqrt{3}/2)u_1^3 v_y^4 - (1/2)u_2^3 v_y^4 \\
\psi_{xy}^5 &= u_2^3 v_z^4.
\end{aligned}$$

Note that the basis functions for the ψ^4 and ψ^5 functions depend on the choice of basis functions for u and v . Journal articles often use the notation

$$\Gamma_{15} \otimes \Gamma_{12} = \Gamma_{15} + \Gamma_{25}, \quad (\text{D.1})$$

Table D.6. Coupling coefficient table for coupling the basis functions of $\Gamma_5 \otimes \Gamma_6^+$ to the basis functions Γ_7 and Γ_8 in the double group for O_h

| | $u_x^5 v_{-1/2}^6$ | $u_x^5 v_{+1/2}^6$ | $u_y^5 v_{-1/2}^6$ | $u_y^5 v_{+1/2}^6$ | $u_z^5 v_{-1/2}^6$ | $u_z^5 v_{+1/2}^6$ |
|-----------------|--------------------|--------------------|--------------------|--------------------|----------------------|----------------------|
| $\psi_{-1/2}^7$ | 0 | $-i/\sqrt{3}$ | 0 | $-1/\sqrt{3}$ | $i/\sqrt{3}$ | 0 |
| $\psi_{+1/2}^7$ | $-i/\sqrt{3}$ | 0 | $1/\sqrt{3}$ | 0 | 0 | $-i/\sqrt{3}$ |
| $\psi_{-3/2}^8$ | $-i/\sqrt{6}$ | 0 | $1/\sqrt{6}$ | 0 | 0 | $i\sqrt{2}/\sqrt{3}$ |
| $\psi_{-1/2}^8$ | 0 | $i/\sqrt{2}$ | 0 | $-1/\sqrt{2}$ | 0 | 0 |
| $\psi_{+1/2}^8$ | $-i/\sqrt{2}$ | 0 | $-1/\sqrt{2}$ | 0 | 0 | 0 |
| $\psi_{+3/2}^8$ | 0 | $i/\sqrt{6}$ | 0 | $1/\sqrt{6}$ | $i\sqrt{2}/\sqrt{3}$ | 0 |

where $\Gamma_4 \leftrightarrow \Gamma_{15}$ and $\Gamma_3 \leftrightarrow \Gamma_{12}$. Thus taking the direct product between irreducible representations Γ_3 and Γ_4 in O or T_d symmetries yields:

$$\Gamma_4 \otimes \Gamma_3 = \Gamma_4 + \Gamma_5, \quad (\text{D.2})$$

where $\Gamma_5 \leftrightarrow \Gamma_{25}$.

We next illustrate the use of a typical coupling coefficient table relevant to the introduction of spin into the electronic energy level problem. In this case we need to take a direct product of Γ_6^+ with a single group representation, where Γ_6^+ is the representation for the spinor ($D_{1/2}$). For example, for a p -level $\Gamma_{15}^- \otimes \Gamma_6^+ = \Gamma_6^- + \Gamma_8^-$ and the appropriate coupling coefficient table is Table D.4 (in Koster et al. Table 83, p. 92).

Table D.4 gives us the following relations between basis functions:

$$\begin{aligned}
 \psi_{-1/2}^6 &= \left| \frac{1}{2}, -\frac{1}{2} \right\rangle = -(i/\sqrt{3})(u_x^4 - iu_y^4) \uparrow + (i/\sqrt{3})u_z^4 \downarrow \\
 \psi_{1/2}^6 &= \left| \frac{1}{2}, \frac{1}{2} \right\rangle = -(i/\sqrt{3})(u_x^4 + iu_y^4) \downarrow - (i/\sqrt{3})u_z^4 \uparrow \\
 \psi_{-3/2}^8 &= \left| \frac{3}{2}, -\frac{3}{2} \right\rangle = (i/\sqrt{2})(u_x^4 - iu_y^4) \downarrow \\
 \psi_{-1/2}^8 &= \left| \frac{3}{2}, -\frac{1}{2} \right\rangle = (i/\sqrt{6})(u_x^4 - iu_y^4) \uparrow + (i\sqrt{2}/\sqrt{3})u_z^4 \downarrow \\
 \psi_{1/2}^8 &= \left| \frac{3}{2}, \frac{1}{2} \right\rangle = -(i/\sqrt{6})(u_x^4 + iu_y^4) \downarrow + (i\sqrt{2}/\sqrt{3})u_z^4 \uparrow \\
 \psi_{3/2}^8 &= \left| \frac{3}{2}, \frac{3}{2} \right\rangle = -(i/\sqrt{2})(u_x^4 + iu_y^4) \uparrow,
 \end{aligned} \quad (\text{D.3})$$

and $v_{-1/2}^6 = \downarrow$. The relations in (D.3) give the transformation of basis functions in the $|\ell sm_\ell m_s\rangle$ representation to the $|j \ell sm_j\rangle$ representation, appropriate to

Table D.7. Compatibility table for the decomposition of the irreducible representations of the double groups O and T_d into the irreducible representations of their subgroups

| T_d | O | T_1 | T_2 | T_3 | T_4 |
|---------------------|---------------------|---------------------|-------------|-------------|-------------------------|
| T | T | T_1 | T_1 | $T_2 + T_3$ | T_4 |
| D_{2d} | D_4 | T_1 | T_3 | $T_1 + T_3$ | $T_2 + T_5$ |
| $C_{3v}; E(w)$ | D_3 | T_1 | T_2 | T_3 | $T_2 + T_3$ |
| $S_4 : H(z)$ | $C_4 : H(z) : E(z)$ | T_1 | T_1 | $T_2 + T_3$ | $T_1 + T_2 + T_3$ |
| $C_{2v} : E(z)$ | | T_1 | T_3 | $T_1 + T_3$ | $T_2 + T_3 + T_4$ |
| $C_s : E(v) : H(v)$ | $C_2 : E(v) : H(v)$ | T_1 | T_2 | $T_1 + T_2$ | $T_1 + 2T_2$ |
| T_d | O | T_5 | T_6 | T_7 | T_8 |
| T | T | T_4 | T_5 | T_5 | $T_6 + T_7$ |
| D_{2d} | D_4 | $T_4 + T_5$ | T_6 | T_7 | $T_6 + T_7$ |
| $C_{3v}; E(w)$ | D_3 | $T_1 + T_3$ | T_4 | T_4 | $T_4 + T_5 + T_6$ |
| $S_4 : H(z)$ | $C_4 : H(z) : E(z)$ | $T_1 + T_2 + T_3$ | $T_4 + T_5$ | $T_4 + T_5$ | $T_5 + T_6 + T_7 + T_8$ |
| $C_{2v} : E(z)$ | | $T_1 + T_2 + T_4$ | T_5 | T_5 | $2T_5$ |
| $C_s : E(v) : H(v)$ | $2T_1 + T_2$ | $C_2 : E(v) : H(v)$ | $T_3 + T_4$ | $T_3 + T_4$ | $2T_3 + 2T_4$ |

Table D.8. Full rotation group compatibility table for the group O

| | | |
|---|----------------|---|
| S | D_0^+ | Γ_1 |
| P | D_1^- | Γ_4 |
| D | D_2^+ | $\Gamma_3 + \Gamma_5$ |
| F | D_3^- | $\Gamma_2 + \Gamma_4 + \Gamma_5$ |
| G | D_4^+ | $\Gamma_1 + \Gamma_3 + \Gamma_4 + \Gamma_5$ |
| H | D_5^- | $\Gamma_3 + 2\Gamma_4 + \Gamma_5$ |
| I | D_6^+ | $\Gamma_1 + \Gamma_2 + \Gamma_3 + \Gamma_4 + 2\Gamma_5$ |
| | $D_{1/2}^\pm$ | Γ_6 |
| | $D_{3/2}^\pm$ | Γ_8 |
| | $D_{5/2}^\pm$ | $\Gamma_7 + \Gamma_8$ |
| | $D_{7/2}^\pm$ | $\Gamma_6 + \Gamma_7 + \Gamma_8$ |
| | $D_{9/2}^\pm$ | $\Gamma_6 + 2\Gamma_8$ |
| | $D_{11/2}^\pm$ | $\Gamma_6 + \Gamma_7 + 2\Gamma_8$ |
| | $D_{13/2}^\pm$ | $\Gamma_6 + 2\Gamma_7 + 2\Gamma_8$ |
| | $D_{15/2}^\pm$ | $\Gamma_6 + \Gamma_7 + 3\Gamma_8$ |

energy bands for which the spin-orbit interaction is included. These linear combinations are basically the *Clebsch–Gordan coefficients* in quantum mechanics [18]. We make use of (D.3) when we introduce spin and spin-orbit interaction into the plane wave relations of the energy eigenvalues and eigenfunctions of the empty lattice.

Tables similar to Table D.4, but allowing us to find the basis functions for the direct products $\Gamma_{12}^\pm \otimes \Gamma_6^+$ and $\Gamma_{25}^\pm \otimes \Gamma_6^+$, are given in Tables D.5 and D.6, respectively, where Γ_{12}^\pm and Γ_{25}^\pm are denoted by Γ_3^\pm and Γ_5^\pm , respectively, in the Koster tables [47].

Table D.7 gives the point groups that are subgroups of groups T_d and O , and gives the decomposition of the irreducible representations of T_d and O into the irreducible representations of the lower symmetry group. Note in Table D.7 that E refers to the electric field and H to the magnetic field. The table can be used for many applications such as finding the resulting symmetries under crystal field splittings as for example $O_h \rightarrow D_3$.

The notation for each of the irreducible representations is consistent with that given in the character tables of Koster's book [47,48]. The decompositions of the irreducible representations of the full rotation group into irreducible representations of groups O and T_d are given, respectively, in Tables D.8 and D.9. Note that all the irreducible representations of the full rotation group are listed, with the \pm sign denoting the parity (even or odd under inversion) and the subscript giving the angular momentum quantum number (j), so that the dimensionality of the irreducible representation D_j^\pm is $(2j + 1)$. In

Table D.9. Full rotation group compatibility table for the group T_d

| | | | |
|--------------|---|--------------|---|
| D_0^+ | Γ_1 | D_0^- | Γ_2 |
| D_1^+ | Γ_4 | D_1^- | Γ_5 |
| D_2^+ | $\Gamma_3 + \Gamma_5$ | D_2^- | $\Gamma_3 + \Gamma_4$ |
| D_3^+ | $\Gamma_2 + \Gamma_4 + \Gamma_5$ | D_3^- | $\Gamma_1 + \Gamma_4 + \Gamma_5$ |
| D_4^+ | $\Gamma_1 + \Gamma_3 + \Gamma_4 + \Gamma_5$ | D_4^- | $\Gamma_2 + \Gamma_3 + \Gamma_4 + \Gamma_5$ |
| D_5^+ | $\Gamma_3 + 2\Gamma_4 + \Gamma_5$ | D_5^- | $\Gamma_3 + \Gamma_4 + 2\Gamma_5$ |
| D_6^+ | $\Gamma_1 + \Gamma_2 + \Gamma_3 + \Gamma_4 + 2\Gamma_5$ | D_6^- | $\Gamma_1 + \Gamma_2 + \Gamma_3 + 2\Gamma_4 + \Gamma_5$ |
| $D_{1/2}^+$ | Γ_6 | $D_{1/2}^-$ | Γ_7 |
| $D_{3/2}^+$ | Γ_8 | $D_{3/2}^-$ | Γ_8 |
| $D_{5/2}^+$ | $\Gamma_7 + \Gamma_8$ | $D_{5/2}^-$ | $\Gamma_6 + \Gamma_8$ |
| $D_{7/2}^+$ | $\Gamma_6 + \Gamma_7 + \Gamma_8$ | $D_{7/2}^-$ | $\Gamma_6 + \Gamma_7 + \Gamma_8$ |
| $D_{9/2}^+$ | $\Gamma_6 + 2\Gamma_8$ | $D_{9/2}^-$ | $\Gamma_7 + 2\Gamma_8$ |
| $D_{11/2}^+$ | $\Gamma_6 + \Gamma_7 + 2\Gamma_8$ | $D_{11/2}^-$ | $\Gamma_6 + \Gamma_7 + 2\Gamma_8$ |
| $D_{13/2}^+$ | $\Gamma_6 + 2\Gamma_7 + 2\Gamma_8$ | $D_{13/2}^-$ | $2\Gamma_6 + \Gamma_7 + 2\Gamma_8$ |

summary, we note that the double group character table shown in Table D.1 is applicable to a symmorphic space group, like the O_h point group ($O_h = O \otimes i$) which applies to the group of the wave vector at $k = 0$ for cubic space groups #221, #225, and #229. A double group character table like Table D.1 is also useful for specifying the group of the wave vector for high symmetry points of a nonsymmorphic space group where the double group has to be modified to take into account symmetry operations involving translations. For illustrative purposes we consider the nonsymmorphic space group #194 that applies to 3D graphite ($P6_3/mmc$) or D_{6h}^4 with $ABAB$ layer stacking (see Fig. C.1).

The simplest case to consider is the group of the wave vector for $k = 0$ (the Γ point) where the phase factor is unity. Then the character table for this nonsymmorphic space group looks quite similar to that for a symmorphic space group, the only difference being the labeling of the classes, some of which include translations. This is illustrated in Table D.10 where eight of the classes require translations. Those classes with translations $\tau = (c/2)(0, 0, 1)$ correspond to symmetry operations occurring in group D_{6h} but not in D_{3d} , and are indicated in Table D.10 by a τ symbol underneath the class listing (see also Table C.24 for the corresponding ordinary irreducible representations for which spin is not considered).

As we move away from the Γ point in the k_z direction, the symmetry is lowered from D_{6h} to C_{6v} and the appropriate group of the wave vector is that for a Δ point, as shown in Table D.11. The corresponding point group is C_{6v} which has nine classes, as listed in the character table, showing a compatibility between the classes in C_{6v} and D_{6h} regarding which classes contain

Table D.10. Character table for the double group D_{6h} [48] appropriately modified to pertain to the group of the wave vector at the Γ point ($k = 0$) for space group #194 D_{6h}^4 ($P6_3/mmc$)^a

| D_{6h} | E | C_2 | | $2C_3$ | | $2\bar{C}_3$ | | $2C_6$ | | $2\bar{C}_6$ | | $3C'_2$ | | $3\bar{C}'_2$ | | I | \bar{I} | σ_h | $2S_6$ | $2\bar{S}_6$ | $2S_3$ | $2\bar{S}_3$ | $3\sigma_d$ | $3\sigma_v$ | time |
|--------------|-----|--------|--------|--------|--------|--------------|-------------|--------|--------|--------------|--------|---------|--------|---------------|-------------|-------------|-----------|------------|--------|--------------|--------|--------------|-------------|-------------|------|
| | | τ | τ | τ | τ | τ | τ | τ | τ | τ | τ | τ | τ | τ | τ | | | | | | | | | | |
| Γ_1^+ | 1 | 1 | 1 | 1 | 1 | 1 | 1 | 1 | 1 | 1 | 1 | 1 | 1 | 1 | 1 | 1 | 1 | 1 | 1 | 1 | 1 | 1 | 1 | a | |
| Γ_2^+ | 1 | 1 | 1 | 1 | 1 | 1 | 1 | -1 | -1 | 1 | 1 | 1 | 1 | 1 | 1 | 1 | 1 | 1 | 1 | -1 | -1 | -1 | -1 | a | |
| Γ_3^+ | 1 | 1 | -1 | 1 | 1 | -1 | -1 | 1 | -1 | 1 | 1 | -1 | 1 | 1 | 1 | -1 | -1 | -1 | -1 | 1 | -1 | a | | | |
| Γ_4^+ | 1 | 1 | -1 | 1 | 1 | -1 | -1 | -1 | 1 | 1 | 1 | -1 | 1 | 1 | -1 | -1 | -1 | -1 | -1 | 1 | 1 | -1 | a | | |
| Γ_5^+ | 2 | 2 | -2 | -1 | -1 | 1 | 1 | 0 | 0 | 2 | 2 | -2 | -1 | -1 | 1 | 1 | 0 | 0 | 0 | 0 | 0 | 0 | a | | |
| Γ_6^+ | 2 | 2 | 2 | -1 | -1 | -1 | -1 | 0 | 0 | 2 | 2 | 2 | -1 | -1 | -1 | -1 | -1 | 0 | 0 | 0 | 0 | 0 | a | | |
| Γ_1^- | 1 | 1 | 1 | 1 | 1 | 1 | 1 | 1 | 1 | 1 | 1 | -1 | -1 | -1 | -1 | -1 | -1 | -1 | -1 | -1 | -1 | -1 | a | | |
| Γ_2^- | 1 | 1 | 1 | 1 | 1 | 1 | 1 | -1 | -1 | -1 | -1 | -1 | -1 | -1 | -1 | -1 | -1 | 1 | 1 | 1 | 1 | 1 | a | | |
| Γ_3^- | 1 | 1 | -1 | 1 | 1 | -1 | -1 | 1 | -1 | -1 | -1 | 1 | -1 | -1 | 1 | 1 | -1 | 1 | 1 | -1 | 1 | 1 | a | | |
| Γ_4^- | 1 | 1 | -1 | 1 | 1 | -1 | -1 | -1 | 1 | -1 | -1 | 1 | -1 | -1 | 1 | 1 | 1 | 1 | 1 | 1 | -1 | -1 | a | | |
| Γ_5^- | 2 | 2 | -2 | -1 | -1 | 1 | 1 | 0 | 0 | -2 | -2 | 2 | 1 | 1 | -1 | -1 | 0 | 0 | 0 | 0 | 0 | 0 | a | | |
| Γ_6^- | 2 | 2 | 2 | -1 | -1 | -1 | -1 | 0 | 0 | -2 | -2 | -2 | 1 | 1 | 1 | 1 | 0 | 0 | 0 | 0 | 0 | 0 | a | | |
| Γ_7^+ | 2 | -2 | 0 | 1 | -1 | $\sqrt{3}$ | $-\sqrt{3}$ | 0 | 0 | 2 | -2 | 0 | 1 | -1 | $\sqrt{3}$ | $-\sqrt{3}$ | 0 | 0 | 0 | c | | | | | |
| Γ_8^+ | 2 | -2 | 0 | 1 | -1 | $-\sqrt{3}$ | $\sqrt{3}$ | 0 | 0 | 2 | -2 | 0 | 1 | -1 | $-\sqrt{3}$ | $\sqrt{3}$ | 0 | 0 | 0 | c | | | | | |
| Γ_9^+ | 2 | -2 | 0 | -2 | 2 | 0 | 0 | 0 | 0 | 2 | -2 | 0 | -2 | 2 | 0 | 0 | 0 | 0 | 0 | c | | | | | |
| Γ_7^- | 2 | -2 | 0 | 1 | -1 | $\sqrt{3}$ | $-\sqrt{3}$ | 0 | 0 | -2 | 2 | 0 | -1 | 1 | $-\sqrt{3}$ | $\sqrt{3}$ | 0 | 0 | 0 | c | | | | | |
| Γ_8^- | 2 | -2 | 0 | 1 | -1 | $-\sqrt{3}$ | $\sqrt{3}$ | 0 | 0 | -2 | 2 | 0 | -1 | 1 | $\sqrt{3}$ | $-\sqrt{3}$ | 0 | 0 | 0 | c | | | | | |
| Γ_9^- | 2 | -2 | 0 | -2 | 2 | 0 | 0 | 0 | 0 | -2 | 2 | 0 | 2 | -2 | 0 | 0 | 0 | 0 | 0 | c | | | | | |

^a For the group of the wave vector for $k = 0$ for the space group #194, the eight classes in the double group D_{6h} that are not in group D_{3d} [namely (C_2 , \bar{C}_2), $2C_6$, $2\bar{C}_6$, ($3C'_2$, $3\bar{C}'_2$), (σ_h , $\bar{\sigma}_h$), $2S_3$, $2\bar{S}_3$, and ($3\sigma_v$, $3\bar{\sigma}_v$)] have, in addition to the point group operations $\{R|0\}$ or $\{\bar{R}|0\}$, additional operations $\{R|\tau\}$ or $\{\bar{R}|\tau\}$ involving the translation $\tau = (0, 0, c/2)$. A phase factor $T = \exp(i\mathbf{k} \cdot \tau)$, which is equal to unity at $k = 0$, accompanies the characters for the classes corresponding to $\{R|\tau\}$ or $\{\bar{R}|\tau\}$. In listing the classes, the symbol τ is placed below the class symbol, such as $2C_6$, to distinguish the classes that involve translations $\{R|\tau\}$. For the special classes containing both the $\{R|0\}$ and $\{\bar{R}|0\}$ symmetry operations, the symbols are stacked above one another, as in $3\sigma_d$ and $3\bar{\sigma}_d$.

translations τ and which do not. All characters corresponding to symmetry operations containing τ must be multiplied by a phase factor $T_\Delta = \exp[i\pi\Delta]$ which is indicated in Table D.11 by T_Δ , where Δ is a dimensionless variable $0 \leq \Delta \leq 1$.

From Tables D.10 and D.11 we can write down compatibility relations between the Γ point and the Δ point representations (see Table D.12), and we note that in the limit $k \rightarrow 0$ all the phase factors $T_\Delta = \exp[i\pi\Delta]$ in Table D.11 go to unity as Δ goes to zero.

Table D.11. Character table and basis functions for the double group C_{6v} [48] as modified to pertain to the group of the wave vector along the Δ direction for space group #194^{a,b}

| C_{6v} (6mm) | E | \bar{E} | $\frac{C_2}{\bar{C}_2}$ | $2C_3$ | $2\bar{C}_3$ | $2C_6$ | $2\bar{C}_6$ | $\frac{3\sigma_v}{3\bar{\sigma}_d}$ | $\frac{3\sigma_v}{3\bar{\sigma}_v}$ | time inversion |
|-------------------|-----|-----------------------------|-------------------------|-------------------|--------------|--------|---------------------|-------------------------------------|-------------------------------------|----------------|
| | | | τ | | | τ | | τ | τ | |
| $x^2 + y^2, z^2$ | z | | | Δ_1 | 1 | 1 | $1 \cdot T_\Delta$ | 1 | $1 \cdot T_\Delta$ | a |
| R_z | | R_z | | Δ_2 | 1 | 1 | $1 \cdot T_\Delta$ | 1 | $1 \cdot T_\Delta$ | a |
| $x^3 - 3xy^2$ | | | | Δ_3 | 1 | 1 | $-1 \cdot T_\Delta$ | 1 | $-1 \cdot T_\Delta$ | a |
| $x^3 - 3yx^2$ | | | | Δ_4 | 1 | 1 | $-1 \cdot T_\Delta$ | 1 | $-1 \cdot T_\Delta$ | a |
| (x, y) | | | | | | | $-1 \cdot T_\Delta$ | $-1 \cdot T_\Delta$ | $-1 \cdot T_\Delta$ | a |
| (x, y, z) | | (R_x, R_y) | | Δ_5 | 2 | 2 | $-2 \cdot T_\Delta$ | -1 | $1 \cdot T_\Delta$ | a |
| $(x^2 - y^2, xy)$ | | $\Delta_3 \otimes \Delta_5$ | | Δ_6 | 2 | 2 | $2 \cdot T_\Delta$ | -1 | $-1 \cdot T_\Delta$ | a |
| | | | | | | | | $-1 \cdot T_\Delta$ | 0 | a |
| | | | | $\phi(1/2, 1/2)$ | | | | | 0 | a |
| | | | | $\phi(1/2, -1/2)$ | | | | | 0 | a |
| | | | | Δ_7 | 2 | -2 | 0 | 1 | $-\sqrt{3} \cdot T_\Delta$ | c |
| | | | | Δ_8 | 2 | -2 | 0 | 1 | $-\sqrt{3} \cdot T_\Delta$ | c |
| | | | | Δ_9 | 2 | -2 | 0 | -2 | 0 | c |
| | | | | | | | | 0 | 0 | c |

^a The notation for the symmetry elements and classes is the same as in Table D.10

^b For the group of the wave vector for a k point along the Δ axis for group #194, the four classes in group C_{6v} that are not in group C_{3v} [namely (C_2, \bar{C}_2) , $2C_6$, $2\bar{C}_6$, and $(3\sigma_v, 3\bar{\sigma}_v)$] have, in addition to the point group operation R (or \bar{R}), a translation $\tau = (0, 0, c/2)$ to form the operation $\{R|\tau\}$, and the irreducible representations have a phase factor $T_\Delta = \exp(i\pi\Delta)$ for these classes. The remaining classes have symmetry operations of the form $\{R|0\}$ and have no phase factors.

Table D.12. Compatibility relations between the irreducible representations of the group of the wave vector at Γ ($k = 0$) and Δ [$k = (2\pi/a)(0, 0, \Delta)$] for space group #194

| Γ point representation | Δ point representation | Γ point representation | Δ point representation |
|-------------------------------|-------------------------------|-------------------------------|-------------------------------|
| Γ_1^+ | $\rightarrow \Delta_1$ | Γ_1^- | $\rightarrow \Delta_2$ |
| Γ_2^+ | $\rightarrow \Delta_2$ | Γ_2^- | $\rightarrow \Delta_1$ |
| Γ_3^+ | $\rightarrow \Delta_3$ | Γ_3^- | $\rightarrow \Delta_3$ |
| Γ_4^+ | $\rightarrow \Delta_4$ | Γ_4^- | $\rightarrow \Delta_4$ |
| Γ_5^+ | $\rightarrow \Delta_5$ | Γ_5^- | $\rightarrow \Delta_5$ |
| Γ_6^+ | $\rightarrow \Delta_6$ | Γ_6^- | $\rightarrow \Delta_6$ |
| Γ_7^+ | $\rightarrow \Delta_7$ | Γ_7^- | $\rightarrow \Delta_7$ |
| Γ_8^+ | $\rightarrow \Delta_8$ | Γ_8^- | $\rightarrow \Delta_8$ |
| Γ_9^+ | $\rightarrow \Delta_9$ | Γ_9^- | $\rightarrow \Delta_9$ |

Table D.13. Character table for the group of the wave vector at the point A for space group #194 from Koster [48]

| | E | \bar{E} | $2C_3$ | $2\bar{C}_3$ | $\frac{3C'_2}{3C'_2}$ | $\frac{3\sigma_d}{3\bar{\sigma}_d}$ | time inversion |
|-------|-----|-----------|--------|--------------|-----------------------|-------------------------------------|----------------|
| A_1 | 2 | 2 | 2 | 2 | 0 | 2 | a |
| A_2 | 2 | 2 | 2 | 2 | 0 | -2 | a |
| A_3 | 4 | 4 | -2 | -2 | 0 | 0 | a |
| A_4 | 2 | -2 | -2 | 2 | $2i$ | 0 | c |
| A_5 | 2 | -2 | -2 | 2 | $-2i$ | 0 | c |
| A_6 | 4 | -4 | 2 | -2 | 0 | 0 | c |

All classes have symmetry operations of the form $\{R|0\}$ or $\{\bar{R}|0\}$ and do not involve τ translations.

Table D.14. Compatibility relations between the irreducible representations of the group of the wave vector at A [$k = (2\pi/c)(001)$] and Δ [$k = (2\pi/c)(00\Delta)$] for space group #194

| A point representation | Δ point representation |
|--------------------------|-----------------------------------|
| A_1 | $\rightarrow \Delta_1 + \Delta_3$ |
| A_2 | $\rightarrow \Delta_2 + \Delta_4$ |
| A_3 | $\rightarrow \Delta_5 + \Delta_6$ |
| $A_4 + A_5$ | $\rightarrow 2\Delta_9$ |
| A_6 | $\rightarrow \Delta_7 + \Delta_8$ |

At the A point (D_{6h} symmetry) we have six irreducible representations, three of which are ordinary irreducible representations Γ_1^A , Γ_2^A , Γ_3^A and three of which are double group representations (Γ_4^A , Γ_5^A , Γ_6^A). There are only six classes with nonvanishing characters (see Table D.13) for the A point. We

note that all the characters in the group of the wave vector are multiples of 2, consistent with bands sticking together. For example, the compatibility relations given in Table D.14 show Δ point bands sticking together in pairs at the A point. In the plane defined by $\Delta = 1$, containing the A point and the H point among others (see Fig. C.7), the structure factor vanishes and Bragg reflections do not occur.

E

Group Theory Aspects of Carbon Nanotubes

In this appendix we provide information needed for solving problems related to carbon nanotubes (see Sect. 9.4). Carbon nanotubes in general exhibit compound rotation-translation operations and therefore belong to nonsymmorphic space groups. From the symmetry point of view, there are two types of carbon nanotubes, namely chiral and achiral tubes. We here discuss the structure of carbon nanotubes and provide the character tables for the group of the wavevectors at $k = 0$ and $k \neq 0$, for both chiral and achiral tubes [8].

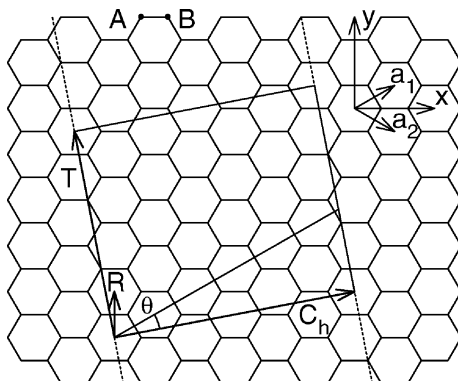


Fig. E.1. An unrolled carbon nanotube projected on a graphene layer (a single layer of crystalline graphite). When the nanotube is rolled up, the chiral vector \mathbf{C}_h turns into the circumference of the cylinder, and the translation vector \mathbf{T} is aligned along the cylinder axis. \mathbf{R} is the symmetry vector (Sect. E.4) and θ is the chiral angle. The unit vectors $(\mathbf{a}_1, \mathbf{a}_2)$ of the graphene layer are indicated in the figure along with the inequivalent A and B sites within the unit cell of the graphene layer [64]

E.1 Nanotube Geometry and the (n, m) Indices

A single wall carbon nanotube (SWNT) is constructed starting from a graphene layer (see Fig. E.1) by rolling it up into a seamless cylinder. The nanotube structure is uniquely determined by the chiral vector \mathbf{C}_h which spans the circumference of the cylinder when the graphene layer is rolled up into a tube. The chiral vector can be written in the form

$$\mathbf{C}_h = n\mathbf{a}_1 + m\mathbf{a}_2, \quad (\text{E.1})$$

where the vectors \mathbf{a}_1 and \mathbf{a}_2 bounding the unit cell of the graphene layer contain two distinct carbon atom sites A and B , as shown in Fig. E.1, while n and m are arbitrary integer numbers. In the shortened (n, m) form, the chiral vector is written as a pair of integers. The (n, m) notation is widely used to characterize the geometry of each distinct (n, m) nanotube [63, 64].

The nanotube can also be characterized by its diameter d_t and chiral angle θ , which determine the length $C_h = |\mathbf{C}_h| = \pi d_t$ of the chiral vector and its orientation on the graphene layer (see Fig. E.1). Both d_t and θ are expressed in terms of the indices n and m by the relations $d_t = a\sqrt{n^2 + nm + m^2}/\pi$ and $\tan \theta = \sqrt{3}m/(2n+m)$, as one can derive from Fig. E.1, where $a = \sqrt{3}a_{\text{C-C}} = 0.246$ nm is the lattice constant for the graphene layer and $a_{\text{C-C}} = 0.142$ nm is the nearest neighbor C-C distance. As an example, the chiral vector \mathbf{C}_h shown in Fig. E.1 is given by $\mathbf{C}_h = 4\mathbf{a}_1 + 2\mathbf{a}_2$, and thus the corresponding nanotube can be identified by the integer pair $(4, 2)$. Due to the sixfold symmetry of the graphene layer, all nonequivalent nanotubes can be characterized by the (n, m) pairs of integers where $0 \leq m \leq n$. It is also possible to define nanotubes with opposite handedness, for which $0 \leq n \leq m$ [65]. The nanotubes are classified as chiral ($0 < m < n$) and achiral ($m = 0$ or $m = n$), which in turn are known as zigzag ($m = 0$) and armchair ($m = n$) nanotubes (see Figs. 9.11 and E.1).

E.2 Lattice Vectors in Real Space

To specify the symmetry properties of carbon nanotubes as 1D systems, it is necessary to define the lattice vector or translation vector \mathbf{T} along the nanotube axis and normal to the chiral vector \mathbf{C}_h defined in Fig. E.1. The vectors \mathbf{T} and \mathbf{C}_h define the unit cell of the 1D nanotube. The translation vector \mathbf{T} , of a general chiral nanotube as a function of n and m , can be written as

$$\mathbf{T} = (t_1\mathbf{a}_1 + t_2\mathbf{a}_2) = [(2m+n)\mathbf{a}_1 - (2n+m)\mathbf{a}_2]/d_R, \quad (\text{E.2})$$

with a length $T = \sqrt{3}C_h/d_R$, where d is the greatest common divisor of (n, m) , and d_R is the greatest common divisor of $2n+m$ and $2m+n$. Then d and d_R are related by

$$d_R = \begin{cases} d & \text{if } n-m \text{ is not a multiple of } 3d \\ 3d & \text{if } n-m \text{ is a multiple of } 3d. \end{cases} \quad (\text{E.3})$$

For the (4, 2) nanotube shown in Fig. E.1, we have $d_R = d = 2$ and $(t_1, t_2) = (4, -5)$. For armchair and zigzag achiral tubes, $T = a$ and $T = \sqrt{3}a$, respectively. The unit cell of an unrolled nanotube on a graphene layer is a rectangle bounded by the vectors \mathbf{C}_h and \mathbf{T} (see the rectangle shown in Fig. E.1 for the (4, 2) nanotube). The area of the nanotube unit cell can be easily calculated as a vector product of these two vectors, $|\mathbf{C}_h \times \mathbf{T}| = \sqrt{3}a^2(n^2 + nm + m^2)/d_R$. Dividing this product by the area of the unit cell of a graphene layer $|\mathbf{a}_1 \times \mathbf{a}_2| = \sqrt{3}a^2/2$, one can get the number of hexagons in the unit cell of a nanotube,

$$N = \frac{2(n^2 + nm + m^2)}{d_R}. \quad (\text{E.4})$$

For the (4, 2) nanotube we have $N = 28$, so that the unit cell of the (4, 2) nanotube (see the rectangle shown in Fig. E.1) contains 28 hexagons, or $2 \times 28 = 56$ carbon atoms. For armchair (n, n) and zigzag $(n, 0)$ nanotubes, $N = 2n$.

E.3 Lattice Vectors in Reciprocal Space

The unit cell of a graphene layer is defined by the vectors \mathbf{a}_1 and \mathbf{a}_2 . The graphene reciprocal lattice unit vectors \mathbf{b}_1 and \mathbf{b}_2 can be constructed from \mathbf{a}_1 and \mathbf{a}_2 using the standard definition $\mathbf{a}_i \cdot \mathbf{b}_j = 2\pi\delta_{ij}$, where δ_{ij} is the Kronecker delta symbol. In Fig. E.2, we show a diagram for the real space unit cell of a graphene sheet (Fig. E.2(a)) and its corresponding reciprocal lattice unit cell

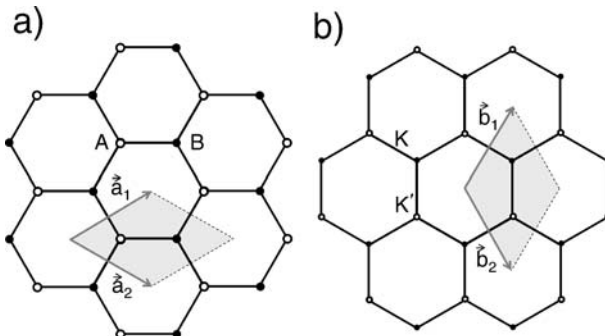


Fig. E.2. (a) Real space structure of a graphene layer. The gray rhombus represents the graphene unit cell with the lattice vectors denoted by \mathbf{a}_1 and \mathbf{a}_2 delimiting it. Note that this area encloses a total of two atoms, one A atom and one B atom. (b) Reciprocal space unit cell of the graphene layer denoted by the unit vectors \mathbf{b}_1 and \mathbf{b}_2 . Note also that the reciprocal space structure has two inequivalent points K and K' [8]

is shown in Fig. E.2(b). Note the rotation by the angle 30° of the hexagons in real space (Fig. E.2(a)) with respect to those in reciprocal space (Fig. E.2(b)).

In a similar fashion, the reciprocal space of a nanotube can be constructed, if we consider the nanotube as a 1D system with an internal structure that is composed of the $2N$ atoms in its unit cell and with a translational symmetry given by the translation vector \mathbf{T} . The reciprocal space of the nanotube can be constructed by finding a pair of reciprocal lattice vectors \mathbf{K}_1 and \mathbf{K}_2 which satisfy: $\mathbf{C}_h \cdot \mathbf{K}_1 = \mathbf{T} \cdot \mathbf{K}_2 = 2\pi$ and $\mathbf{C}_h \cdot \mathbf{K}_2 = \mathbf{T} \cdot \mathbf{K}_1 = 0$. Due to the spatial confinement of the nanotube in the radial direction, the vector \mathbf{C}_h does not play the role of a translation vector but rather of a generator of pure rotations, and the relation $\mathbf{C}_h \cdot \mathbf{K}_1 = 2\pi$ can only be satisfied for integer multiples of $2\pi/d_t$, where d_t is the diameter of the nanotube.

E.4 Compound Operations and Tube Helicity

All multiples of the translation vector \mathbf{T} will be translational symmetry operations of the nanotube [73]. However, to be more general, it is necessary to consider that any lattice vector

$$\mathbf{t}_{p,q} = p\mathbf{a}_1 + q\mathbf{a}_2, \quad (\text{E.5})$$

with p and q integers, of the unfolded graphene layer will also be a symmetry operation of the tube. In fact, the symmetry operation that arises from $\mathbf{t}_{p,q}$ will appear as a screw translation of the nanotube. Screw translations are combinations of a rotation (R_ϕ) by an angle ϕ and a small translation of \mathbf{r} in the axial direction of the nanotube, and can be written as $\{R_\phi|\tau\}$, using the notation common for space group operations [8, 64].

Any lattice vector $\mathbf{t}_{p,q}$ can also be written in terms of components of the nanotube lattice vectors, \mathbf{T} and \mathbf{C}_h , as

$$\mathbf{t}_{p,q} = \mathbf{t}_{u,v} = (u/N)\mathbf{C}_h + (v/N)\mathbf{T}, \quad (\text{E.6})$$

where u and v are negative or positive integers given by

$$u = \frac{(2n+m)p + (2m+n)q}{d_R} \quad (\text{E.7})$$

and

$$v = mp - nq. \quad (\text{E.8})$$

The screw translation of the nanotube which is associated with the graphene lattice vector $\mathbf{t}_{u,v}$ can then be written as

$$\mathbf{t}_{u,v} = \{C_N^u | vT/N\}, \quad (\text{E.9})$$

where C_N^u is a rotation of $u(2\pi/N)$ around the nanotube axis, and $\{E|vT/N\}$ is a translation of vT/N along the nanotube axis, with T being the magnitude

of the primitive translation vector \mathbf{T} , and E being the identity operation. It is clear that if a screw vector $\{C_N^u|vT/N\}$ is a symmetry operation of the nanotube, then the vectors $\{C_N^u|vT/N\}^s$, for any integer value of s , are also symmetry operations of the nanotube. The number of hexagons in the unit-cell N assumes the role of the “order” of the screw axis, since the symmetry operation $\{C_N^u|vT/N\}^N = \{E|vT\}$, where E is the identity operator, and vT is a primitive translation of the nanotube.

The nanotube structure can be obtained from a small number of atoms by using any choice of two noncolinear screw vectors $\{C_N^{u_1}|v_1T/N\}$ and $\{C_N^{u_2}|v_2T/N\}$. The two vectors will be colinear if there exists a pair of integers s and l different from 1, for which $lu_1 = su_2 + \lambda N$, and $lv_1 = sv_2 + \gamma T$, where, λ and γ are two arbitrary integers. The area of the nanotube cylindrical surface delimited by these two noncolinear vectors can be regarded as a reduced unit cell. Note that the number of atoms in this reduced unit cell is given by the ratio between the area delimited by these vectors ($|\mathbf{t}_{u_1, v_1} \times \mathbf{t}_{u_2, v_2} \mathbf{|}$) and the area of the unit cell of a graphene sheet ($|\mathbf{a}_1 \times \mathbf{a}_2|$) multiplied by 2, which is the number of carbon atoms in the graphene unit cell. Thus the number of atoms in the reduced unit cell defined by t_{u_1, v_1} and t_{u_2, v_2} is given by

$$2 \frac{|\mathbf{t}_{u_1, v_1} \times \mathbf{t}_{u_2, v_2}|}{|\mathbf{a}_1 \times \mathbf{a}_2|} = 2 \frac{|v_2 u_1 - u_2 v_1|}{N}. \quad (\text{E.10})$$

It is important to point out that, in this case, the nanotube ceases to be described as a quasi-1D system, but as a system with two quasitranslational dimensions, which are generated by the two screw vectors.

There are many combinations of screw vectors which can be used to construct the structure of the nanotube. These combinations can be divided into four categories: helical–helical, linear–helical, helical–angular, and linear–angular, as described below. Either one of these constructions can be used to obtain the nanotube structure. The helical–helical construction is characterized by choosing two general screw vectors, for the construction of the nanotube structure (see Fig. E.3(a)). Although this scheme permits the definition of a 2-atom unit cell, the unit cell does not exhibit the full symmetries of the nanotube, and thus is inadequate for representing the nanotube. The linear–helical scheme is characterized by using the translation vector \mathbf{T} and a general screw vector as unit vectors (see Fig. E.3(b)). This scheme maintains the translational symmetry of the nanotube, but not the point group operations, and it also permits the definition of a two-atom unit cell. In the helical–angular construction, a general screw vector is used along with a vector in the circumferential direction of the nanotube (see Fig. E.3(c)). This construction also permits the definition of a 2-atom unit cell. However, the 2-atom unit cell does not exhibit many of the symmetries of the nanotube. Instead it is convenient to define a $2d$ -atom unit cell, where the integer d is given by $d = \text{gcd}(n, m)$, and this unit cell will exhibit all the point group symmetry operations of the nanotube, but not the translational symmetry. The linear–angular construction uses as unit vectors the translational vector

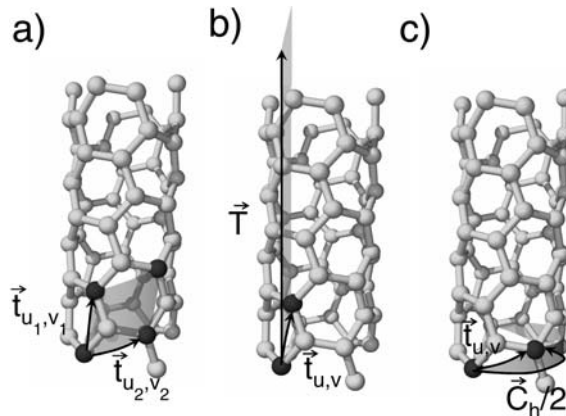


Fig. E.3. The 2-atom reduced unit cell for the: (a) helical–helical, (b) linear–helical, and (c) helical–angular construction for a (4, 2) nanotube. In (b) the deformed rhombus, which delimits the reduced unit cell that connects points both inside and outside the nanotube unit cell, had to be truncated to stay within the figure [8]

T and a vector in the circumferential direction, and thus parallel to C_h . The linear–angular construction does not permit the definition of a 2-atom unit cell. However, by choosing the vector in the circumferential direction to be C_h , the total unit cell of the nanotube, which exhibits all the translational and point symmetries of the nanotube, is restored.

E.5 Character Tables for Carbon Nanotubes

In this section we present the character tables for dealing with carbon nanotubes. Tables E.1 and E.2 give the character tables for the group of the wavevectors for chiral carbon nanotubes, at $k = 0, \pi/T$ and $0 < k < \pi/T$, respectively. Tables E.3 and E.4 give the character tables for the group of the wavevectors for achiral carbon nanotubes, at $k = 0, \pi/T$ and $0 < k < \pi/T$, respectively. Some of the point symmetry operations in these tables are shown in Fig. E.4.

Table E.1. Character table for the group of the wavevectors $k = 0$ and $k = \pi/T$ for chiral tubes

| D_N | $\{E 0\}$ | $2\{C_N^u vT/N\}$ | $2\{C_N^u vT/N\}^2$ | $\dots 2\{C_N^u vT/N\}^{(N/2)-1}$ | $2\{C_N^u vT/N\}^{N/2}$ | $(N/2)\{C_2' 0\}$ | $(N/2)\{C_2'' 0\}$ |
|---------------|-----------|------------------------|------------------------|-----------------------------------|-------------------------|-------------------|--------------------|
| A_1 | 1 | 1 | 1 | ... | 1 | 1 | 1 |
| A_2 | 1 | 1 | 1 | ... | 1 | -1 | -1 |
| B_1 | 1 | -1 | 1 | ... | $(-1)^{(N/2-1)}$ | $(-1)^{N/2}$ | -1 |
| B_2 | 1 | -1 | 1 | ... | $(-1)^{(N/2-1)}$ | $(-1)^{N/2}$ | 1 |
| E_1 | 2 | $2 \cos 2\pi/N$ | $2 \cos 4\pi/N$ | $\dots 2 \cos 2(N/2-1)\pi/N$ | -2 | 0 | 0 |
| E_2 | 2 | $2 \cos 4\pi/N$ | $2 \cos 8\pi/N$ | $\dots 2 \cos 4(N/2-1)\pi/N$ | 2 | 0 | 0 |
| : | : | : | : | : | : | : | : |
| $E_{(N/2-1)}$ | 2 | $2 \cos 2(N/2-1)\pi/N$ | $2 \cos 4(N/2-1)\pi/N$ | $\dots 2 \cos 2(N/2-1)^2\pi/N$ | $2 \cos (N/2-1)\pi$ | 0 | 0 |

This group is isomorphic to the point group D_N

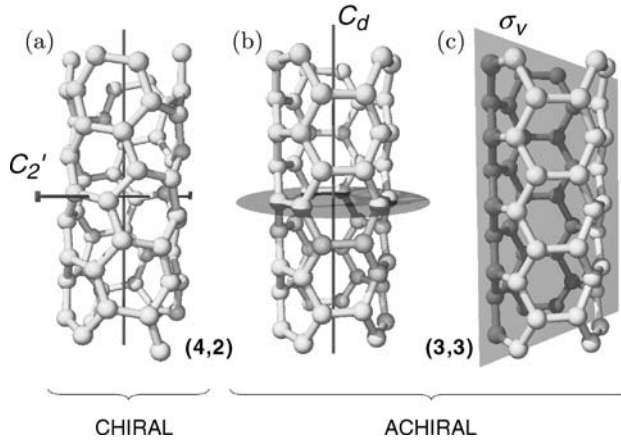


Fig. E.4. (a) Unit cell of the chiral (4,2) nanotube, showing the C_d rotation around the nanotube axis, with $d = 2$, and one of the C'_2 rotations perpendicular to the nanotube axis. A different class of two-fold rotations (C''_2), which is present for both chiral and achiral nanotubes, is not shown here. (b) A section of an achiral armchair (3,3) nanotube is shown emphasizing the horizontal mirror plane σ_h and the symmetry operation C_d , with $d = 3$. (c) The same (3,3) armchair nanotube is shown but now emphasizing of the vertical mirror planes σ_v [8]

Table E.2. Character table for the group of the wavevector $0 < k < \pi/T$ for chiral nanotubes

| C_N | $\{E 0\}$ | $\{C_N^u vT/N\}^1$ | $\{C_N^u vT/N\}^2$ | \dots | $\{C_N^u vT/N\}^\ell$ | \dots | $\{C_N^u vT/N\}^{N-1}$ |
|--------------------------|------------------------------------|---|---|----------|---|----------|---|
| A | 1 | 1 | 1 | \dots | 1 | \dots | 1 |
| B | 1 | -1 | 1 | \dots | $(-1)^\ell$ | \dots | -1 |
| $E_{\pm 1}$ | $\begin{cases} 1 \\ 1 \end{cases}$ | $\begin{cases} \epsilon \\ \epsilon^* \end{cases}$ | $\begin{cases} \epsilon^2 \\ \epsilon^{*2} \end{cases}$ | \dots | $\begin{cases} \epsilon^\ell \\ \epsilon^{*\ell} \end{cases}$ | \dots | $\begin{cases} \epsilon^{N-1} \\ \epsilon^{*(N-1)} \end{cases}$ |
| $E_{\pm 2}$ | $\begin{cases} 1 \\ 1 \end{cases}$ | $\begin{cases} \epsilon^2 \\ \epsilon^{*2} \end{cases}$ | $\begin{cases} \epsilon^4 \\ \epsilon^{*4} \end{cases}$ | \dots | $\begin{cases} \epsilon^{2\ell} \\ \epsilon^{*2\ell} \end{cases}$ | \dots | $\begin{cases} \epsilon^{2(N-1)} \\ \epsilon^{*2(N-1)} \end{cases}$ |
| \vdots | \vdots | \vdots | \vdots | \vdots | \vdots | \vdots | \vdots |
| $E_{\pm(\frac{N}{2}-1)}$ | $\begin{cases} 1 \\ 1 \end{cases}$ | $\begin{cases} \epsilon^{\frac{N}{2}-1} \\ \epsilon^{*\frac{N}{2}-1} \end{cases}$ | $\begin{cases} \epsilon^{2(\frac{N}{2}-1)} \\ \epsilon^{*2(\frac{N}{2}-1)} \end{cases}$ | \dots | $\begin{cases} \epsilon^{\ell(\frac{N}{2}-1)} \\ \epsilon^{*\ell(\frac{N}{2}-1)} \end{cases}$ | \dots | $\begin{cases} \epsilon^{(N-1)(\frac{N}{2}-1)} \\ \epsilon^{*(N-1)(\frac{N}{2}-1)} \end{cases}$ |

This group is isomorphic to the point group C_N . The \pm signs label the different representations with characters which are complex conjugates of each other. These irreducible representations are degenerate due to time reversal symmetry. The complex number ϵ is $e^{2\pi i/N}$.

Table E.3. Character table for the group of the wavevectors $k = 0$ and $k = \pi/T$ for achiral carbon tubes. This group is isomorphic to the point group D_{2nh}

| D_{2nh} | $\{E 0\}$ | \cdots | $2\{C_{2n}^u vT/2n\}^s$ | \cdots | $\{C_{2n}^u vT/2n\}^s$ | \cdots | $\{C_2'' 0\}$ | $n\{C_2'' 0\}$ | $\{I 0\}$ | \cdots | $2\{IC_{2n}^u vT/2n\}^s$ | \cdots | $\{\sigma_h 0\}$ | $n\{\sigma_v' 0\}$ | $n\{\sigma_v'' T/2\}$ | |
|-------------|-----------|----------|-------------------------|----------|------------------------|----------|---------------|----------------|-----------|----------|--------------------------|----------|------------------|--------------------|-----------------------|----------|
| A_{1g} | 1 | \cdots | 1 | \cdots | 1 | \cdots | 1 | \cdots | 1 | \cdots | 1 | \cdots | 1 | \cdots | 1 | 1 |
| A_{2g} | 1 | \cdots | 1 | \cdots | 1 | \cdots | -1 | \cdots | 1 | \cdots | 1 | \cdots | 1 | \cdots | -1 | -1 |
| B_{1g} | 1 | \cdots | $(-1)^s$ | \cdots | $(-1)^n$ | \cdots | -1 | \cdots | $(-1)^s$ | \cdots | $(-1)^s$ | \cdots | $(-1)^n$ | \cdots | -1 | 1 |
| B_{2g} | 1 | \cdots | $(-1)^s$ | \cdots | $(-1)^n$ | \cdots | -1 | \cdots | $(-1)^s$ | \cdots | $(-1)^n$ | \cdots | $(-1)^n$ | \cdots | -1 | -1 |
| \vdots | \vdots | \vdots | \vdots | \vdots | \vdots | \vdots | \vdots | \vdots | \vdots | \vdots | \vdots | \vdots | \vdots | \vdots | \vdots | \vdots |
| $E_{\mu g}$ | 2 | \cdots | $2\cos(\mu s\pi/n)$ | \cdots | $2(-1)^\mu$ | \cdots | 0 | 0 | 2 | \cdots | $2\cos(\mu s\pi/n)$ | \cdots | $2(-1)^\mu$ | \cdots | 0 | 0 |
| \vdots | \vdots | \vdots | \vdots | \vdots | \vdots | \vdots | \vdots | \vdots | \vdots | \vdots | \vdots | \vdots | \vdots | \vdots | \vdots | \vdots |
| A_{1u} | 1 | \cdots | 1 | \cdots | 1 | \cdots | 1 | \cdots | -1 | \cdots | -1 | \cdots | -1 | \cdots | -1 | -1 |
| A_{2u} | 1 | \cdots | 1 | \cdots | 1 | \cdots | -1 | \cdots | -1 | \cdots | -1 | \cdots | -1 | \cdots | 1 | 1 |
| B_{1u} | 1 | \cdots | $(-1)^s$ | \cdots | $(-1)^n$ | \cdots | -1 | \cdots | $(-1)^s$ | \cdots | $(-1)^n$ | \cdots | $(-1)^n$ | \cdots | -1 | -1 |
| B_{2u} | 1 | \cdots | $(-1)^s$ | \cdots | $(-1)^n$ | \cdots | 1 | \cdots | -1 | \cdots | $(-1)^s$ | \cdots | $(-1)^n$ | \cdots | -1 | 1 |
| \vdots | \vdots | \vdots | \vdots | \vdots | \vdots | \vdots | \vdots | \vdots | \vdots | \vdots | \vdots | \vdots | \vdots | \vdots | \vdots | \vdots |
| $E_{\mu u}$ | 2 | \cdots | $2\cos(\mu s\pi/n)$ | \cdots | $2(-1)^\mu$ | \cdots | 0 | 0 | -2 | \cdots | $-2\cos(\mu s\pi/n)$ | \cdots | $-2(-1)^\mu$ | \cdots | 0 | 0 |
| \vdots | \vdots | \vdots | \vdots | \vdots | \vdots | \vdots | \vdots | \vdots | \vdots | \vdots | \vdots | \vdots | \vdots | \vdots | \vdots | \vdots |

The values of s and μ span the integer values between 1 and $n - 1$.

Table E.4. Character table for the group of the wavevectors $0 < k\pi/T$ for achiral carbon nanotubes

| $C_{2n}v$ | $\{E 0\}$ | $2\{C_{2n}^u vT/2n\}^1$ | $\{C_{2n}^u vT/2n\}^2$ | \dots | $2\{C_{2n}^u vT/2n\}^{n-1}$ | $\{C_{2n}^u vT/2n\}^n$ | $n\{\sigma'_v \tau'\}$ | $n\{\sigma''_v \tau''\}$ |
|-------------|-----------|-------------------------|------------------------|----------|-----------------------------|------------------------|------------------------|--------------------------|
| A' | 1 | 1 | 1 | \dots | 1 | 1 | 1 | 1 |
| A'' | 1 | 1 | 1 | \dots | 1 | 1 | -1 | -1 |
| B' | 1 | -1 | 1 | \dots | $(-1)^{n-1}$ | $(-1)^n$ | 1 | -1 |
| B'' | 1 | -1 | 1 | \dots | $(-1)^{n-1}$ | $(-1)^n$ | -1 | 1 |
| E_1 | 2 | $2\cos\pi/n$ | $2\cos2\pi/n$ | \dots | $2\cos2(n-1)\pi/n$ | -2 | 0 | 0 |
| E_2 | 2 | $2\cos2\pi/n$ | $2\cos4\pi/n$ | \dots | $2\cos4(n-1)\pi/n$ | 2 | 0 | 0 |
| \vdots | \vdots | \vdots | \vdots | \vdots | \vdots | \vdots | \vdots | \vdots |
| $E_{(n-1)}$ | 2 | $2\cos(n-1)\pi/n$ | $2\cos2(n-1)\pi/n$ | \dots | $2\cos(n-1)^2\pi/n$ | $2\cos(n-1)\pi$ | 0 | 0 |

This group is isomorphic to the point group C_{2m1} . For zigzag nanotubes with n odd, $\tau' = \tau'' = T/2$, while for armchair nanotubes and zigzag nanotubes with n even, $\tau' = 0$ and $\tau'' = T/2$.

F

Permutation Group Character Tables

In this appendix we provide tables to be used with permutation groups. Tables F.1 and F.2 are the extended character tables for the permutation groups of 3 and 4 objects $P(3)$ and $P(4)$, respectively, and are discussed in Sects. 17.4.2 and 17.4.3, respectively. The discussion in these sections can also be used to understand the extended character tables for the permutation groups $P(5)$, $P(6)$, and $P(7)$ which have many more symmetry elements, namely $5! = 120$, $6! = 720$, and $7! = 5,040$, respectively (see Tables F.3 and F.4). These character tables are sufficient to describe the permutation groups arising for the filling of s, p, d , and f electron states, as discussed in Chap. 17. In Table F.5 for the group $P(7)$ only a few entries are made. The corresponding entries can also be made for permutation groups $P(n)$ of higher order.

When one considers a wave function of n identical particles (e.g., permutation groups in Chap. 17) then the interchange of identical particles is a symmetry operation that must be included. The number of irreducible representations is equal to the number of classes. Table F.6 contains the number of classes and the dimensionalities of the irreducible representations where $P(n)$ labels the permutation group of n objects.

Table F.1. Extended character table for permutation group $P(3)$

| | $\chi(E)$ | $\chi(A, B, C)$ | $\chi(D, F)$ | |
|---|-----------|-----------------|--------------|---|
| $P(3)$ | (1^3) | $3(2, 1)$ | $2(3)$ | |
| Γ_1^s | 1 | 1 | 1 | |
| Γ_1^a | 1 | -1 | 1 | |
| Γ_2 | 2 | 0 | -1 | |
| $\chi_{\text{perm.}}(\psi_1\psi_1\psi_1)$ | 1 | 1 | 1 | $\Rightarrow \Gamma_1^s$ |
| $\chi_{\text{perm.}}(\psi_1\psi_1\psi_2)$ | 3 | 1 | 0 | $\Rightarrow \Gamma_1^s + \Gamma_2$ |
| $\chi_{\text{perm.}}(\psi_1\psi_2\psi_3)$ | 6 | 0 | 0 | $\Rightarrow \Gamma_1^s + \Gamma_1^a + 2\Gamma_2$ |

Table F.2. Extended character table for the permutation group $P(4)$

| $P(4)$ | (1 ⁴) | 8(3,1) | 3(2 ²) | 6(2,1 ²) | 6(4) | |
|---|-------------------|--------|--------------------|----------------------|------|--|
| Γ_1^s | 1 | 1 | 1 | 1 | 1 | |
| Γ_1^a | 1 | 1 | 1 | -1 | -1 | |
| Γ_2 | 2 | -1 | 2 | 0 | 0 | |
| Γ_3 | 3 | 0 | -1 | 1 | -1 | |
| $\Gamma_{3'}$ | 3 | 0 | -1 | -1 | 1 | |
| $\chi_{\text{perm.}}(\psi_1\psi_1\psi_1\psi_1)$ | 1 | 1 | 1 | 1 | 1 | $\Rightarrow \Gamma_1^s$ |
| $\chi_{\text{perm.}}(\psi_1\psi_1\psi_1\psi_2)$ | 4 | 1 | 0 | 2 | 0 | $\Rightarrow \Gamma_1^s + \Gamma_3$ |
| $\chi_{\text{perm.}}(\psi_1\psi_1\psi_2\psi_2)$ | 6 | 0 | 2 | 2 | 0 | $\Rightarrow \Gamma_1^s + \Gamma_2 + \Gamma_3$ |
| $\chi_{\text{perm.}}(\psi_1\psi_1\psi_2\psi_3)$ | 12 | 0 | 0 | 2 | 0 | $\Rightarrow \Gamma_1^s + \Gamma_2 + 2\Gamma_3 + \Gamma_{3'}$ |
| $\chi_{\text{perm.}}(\psi_1\psi_2\psi_3\psi_4)$ | 24 | 0 | 0 | 0 | 0 | $\Rightarrow \Gamma_1^s + \Gamma_1^a + 2\Gamma_2 + 3\Gamma_3 + 3\Gamma_{3'}$ |

Here the Γ_{n-1} irreducible representation is Γ_3 (see Sect. 17.3)

Table F.3. Extended character table for permutation group $P(5)$

| $P(5)$ or S_5 | (1 ⁵) | 10(2, 1 ³) | 15(2 ² , 1) | 20(3, 1 ²) | 20(3, 2) | 30(4, 1) | 24(5) |
|---|---|------------------------|------------------------|------------------------|----------|----------|-------|
| Γ_1^s | 1 | 1 | 1 | 1 | 1 | 1 | 1 |
| Γ_1^a | 1 | -1 | 1 | 1 | -1 | -1 | 1 |
| Γ_4 | 4 | 2 | 0 | 1 | -1 | 0 | -1 |
| $\Gamma_{4'}$ | 4 | -2 | 0 | 1 | 1 | 0 | -1 |
| Γ_5 | 5 | 1 | 1 | -1 | 1 | -1 | 0 |
| $\Gamma_{5'}$ | 5 | -1 | 1 | -1 | -1 | 1 | 0 |
| Γ_6 | 6 | 0 | -2 | 0 | 0 | 0 | 1 |
| $\chi_{\text{perm.}}(\psi_1\psi_1\psi_1\psi_1\psi_1)$ | 1 | 1 | 1 | 1 | 1 | 1 | 1 |
| $\chi_{\text{perm.}}(\psi_1\psi_1\psi_1\psi_1\psi_2)$ | 5 | 3 | 1 | 2 | 0 | 1 | 0 |
| $\chi_{\text{perm.}}(\psi_1\psi_1\psi_1\psi_2\psi_2)$ | 10 | 4 | 2 | 1 | 1 | 0 | 0 |
| $\chi_{\text{perm.}}(\psi_1\psi_1\psi_1\psi_2\psi_3)$ | 20 | 6 | 0 | 2 | 0 | 0 | 0 |
| $\chi_{\text{perm.}}(\psi_1\psi_1\psi_2\psi_2\psi_3)$ | 30 | 6 | 2 | 0 | 0 | 0 | 0 |
| $\chi_{\text{perm.}}(\psi_1\psi_1\psi_2\psi_3\psi_4)$ | 60 | 6 | 0 | 0 | 0 | 0 | 0 |
| $\chi_{\text{perm.}}(\psi_1\psi_2\psi_3\psi_4\psi_5)$ | 120 | 0 | 0 | 0 | 0 | 0 | 0 |
| S_5 | irreducible representations | | | | | | |
| $\chi_{\text{perm.}}(\psi_1\psi_1\psi_1\psi_1\psi_1)$ | $\Rightarrow \Gamma_1^s$ | | | | | | |
| $\chi_{\text{perm.}}(\psi_1\psi_1\psi_1\psi_1\psi_2)$ | $\Rightarrow \Gamma_1^s + \Gamma_4$ | | | | | | |
| $\chi_{\text{perm.}}(\psi_1\psi_1\psi_1\psi_2\psi_2)$ | $\Rightarrow \Gamma_1^s + \Gamma_4 + \Gamma_5$ | | | | | | |
| $\chi_{\text{perm.}}(\psi_1\psi_1\psi_1\psi_2\psi_3)$ | $\Rightarrow \Gamma_1^s + 2\Gamma_4 + \Gamma_5 + \Gamma_6$ | | | | | | |
| $\chi_{\text{perm.}}(\psi_1\psi_1\psi_2\psi_2\psi_3)$ | $\Rightarrow \Gamma_1^s + 2\Gamma_4 + 2\Gamma_5 + \Gamma_{5'} + \Gamma_6$ | | | | | | |
| $\chi_{\text{perm.}}(\psi_1\psi_1\psi_2\psi_3\psi_4)$ | $\Rightarrow \Gamma_1^s + 3\Gamma_4 + \Gamma_{4'} + 3\Gamma_5 + 2\Gamma_{5'} + 3\Gamma_6$ | | | | | | |
| $\chi_{\text{perm.}}(\psi_1\psi_2\psi_3\psi_4\psi_5)$ | $\Rightarrow \Gamma_1^s + \Gamma_1^a + 4\Gamma_4 + 4\Gamma_{4'} + 5\Gamma_5 + 5\Gamma_{5'} + 6\Gamma_6$ | | | | | | |

Here the Γ_{n-1} irreducible representation of $P(5)$ is Γ_4 "

Table F.4. Extended character table for permutation group $P(6)$

| $P(6)$ | 1 | 15 | 45 | 15 | 40 | 120 | 40 | 90 | 90 | 144 | 120 |
|--|---|------------|--------------|---------|------------|-------------|---------|------------|----------|----------|-------|
| | (1^6) | $(2, 1^4)$ | $(2^2, 1^2)$ | (2^3) | $(3, 1^3)$ | $(3, 2, 1)$ | (3^2) | $(4, 1^2)$ | $(4, 2)$ | $(5, 1)$ | (6) |
| Γ_1^s | 1 | 1 | 1 | 1 | 1 | 1 | 1 | 1 | 1 | 1 | 1 |
| Γ_1^a | 1 | -1 | 1 | -1 | 1 | -1 | 1 | -1 | 1 | 1 | -1 |
| Γ_5 | 5 | 3 | 1 | -1 | 2 | 0 | -1 | 1 | -1 | 0 | -1 |
| $\Gamma_{5'}$ | 5 | -3 | 1 | 1 | 2 | 0 | -1 | -1 | -1 | 0 | 1 |
| $\Gamma_{5''}$ | 5 | 1 | 1 | -3 | -1 | 1 | 2 | -1 | -1 | 0 | 0 |
| $\Gamma_{5'''}$ | 5 | -1 | 1 | 3 | -1 | -1 | 2 | 1 | -1 | 0 | 0 |
| Γ_9 | 9 | 3 | 1 | 3 | 0 | 0 | 0 | -1 | 1 | -1 | 0 |
| $\Gamma_{9'}$ | 9 | -3 | 1 | -3 | 0 | 0 | 0 | 1 | 1 | -1 | 0 |
| Γ_{10} | 10 | 2 | -2 | -2 | 1 | -1 | 1 | 0 | 0 | 0 | 1 |
| $\Gamma_{10'}$ | 10 | -2 | -2 | 2 | 1 | 1 | 1 | 0 | 0 | 0 | -1 |
| Γ_{16} | 16 | 0 | 0 | 0 | -2 | 0 | -2 | 0 | 0 | 1 | 0 |
| $\chi_{\text{perm.}}(\psi_1 \psi_1 \psi_1 \psi_1 \psi_1 \psi_1)$ | 1 | 1 | 1 | 1 | 1 | 1 | 1 | 1 | 1 | 1 | 1 |
| $\chi_{\text{perm.}}(\psi_1 \psi_1 \psi_1 \psi_1 \psi_1 \psi_2)$ | 6 | 4 | 2 | 0 | 3 | 1 | 0 | 1 | 0 | 1 | 0 |
| \vdots | ... | | | | | | | | | | |
| $\chi_{\text{perm.}}(\psi_1 \psi_2 \psi_3 \psi_4 \psi_5 \psi_6)$ | 720 | 0 | 0 | 0 | 0 | 0 | 0 | 0 | 0 | 0 | 0 |
| S_6 | irreducible representations | | | | | | | | | | |
| $\Gamma_{\text{perm.}}(\psi_1 \psi_1 \psi_1 \psi_1 \psi_1 \psi_1)$ | $\Rightarrow \Gamma_1^s$ | | | | | | | | | | |
| $\Gamma_{\text{perm.}}(\psi_1 \psi_1 \psi_1 \psi_1 \psi_1 \psi_2)$ | $\Rightarrow \Gamma_1^s + \Gamma_5$ | | | | | | | | | | |
| \vdots | \vdots | | | | | | | | | | |
| $\Gamma_{\text{perm.}}(\psi_1 \psi_2 \psi_3 \psi_4 \psi_5 \psi_6)$ | $\Rightarrow \Gamma_1^s + \Gamma_1^a + 5\Gamma_5 + 5\Gamma_{5'} + 5\Gamma_{5''} + 5\Gamma_{5'''} + 9\Gamma_9 + 9\Gamma_{9'} + 10\Gamma_{10} + 10\Gamma_{10'} + 16\Gamma_{16}$ | | | | | | | | | | |

Here the Γ_{n-1} irreducible representation of $P(6)$ is Γ_{5e}

Table F.5. Character table (schematic) for group $P(7)$

| $P(7)$ or S_7 | $(1^7) \dots$ |
|---|---|
| Γ_1^s | 1 \dots |
| Γ_1^a | 1 \dots |
| Γ_6 | 6 \dots |
| $\Gamma_{6'}$ | 6 \dots |
| Γ_{14} | 14 \dots |
| $\Gamma_{14'}$ | 14 \dots |
| $\Gamma_{14''}$ | 14 \dots |
| $\Gamma_{14'''}$ | 14 \dots |
| Γ_{15} | 15 \dots |
| $\Gamma_{15'}$ | 15 \dots |
| Γ_{21} | 21 \dots |
| $\Gamma_{21'}$ | 21 \dots |
| Γ_{35} | 35 \dots |
| $\Gamma_{35'}$ | 35 \dots |
| Γ_{20} | 20 \dots |
| $\chi_{\text{perm.}}(\psi_1 \psi_1 \psi_1 \psi_1 \psi_1 \psi_1 \psi_1)$ | 1 \dots |
| $\chi_{\text{perm.}}(\psi_1 \psi_1 \psi_1 \psi_1 \psi_1 \psi_1 \psi_2)$ | 7 \dots |
| \vdots | $\vdots \vdots$ |
| $\chi_{\text{perm.}}(\psi_1 \psi_2 \psi_3 \psi_4 \psi_5 \psi_6 \psi_7)$ | 5,040 \dots |
| S_7 | irreducible representations |
| $\Gamma_{\text{perm.}}(\psi_1 \psi_1 \psi_1 \psi_1 \psi_1 \psi_1 \psi_1)$ | $\Rightarrow \Gamma_1^s$ |
| $\Gamma_{\text{perm.}}(\psi_1 \psi_1 \psi_1 \psi_1 \psi_1 \psi_2)$ | $\Rightarrow \Gamma_1^s + \Gamma_6$ |
| \vdots | \vdots |
| $\Gamma_{\text{perm.}}(\psi_1 \psi_2 \psi_3 \psi_4 \psi_5 \psi_6 \psi_7)$ | $\Rightarrow \Gamma_1^s + \Gamma_1^a + 6\Gamma_6 + 6\Gamma_{6'} + 14\Gamma_{14} + 14\Gamma_{14'} + 14\Gamma_{14''} + 14\Gamma_{14'''} + 15\Gamma_{15} + 15\Gamma_{15'} + 21\Gamma_{21} + 21\Gamma_{21'} + 35\Gamma_{35} + 35\Gamma_{35'} + 20\Gamma_{20}$ |

Table F.6. Number of classes and the dimensionalities of the Γ_i in $P(n)$

| group classes | number of group elements | $\sum_i \ell_i^2$ |
|---------------|--------------------------|---|
| $P(1)$ | 1 | $1! = 1^2 = 1$ |
| $P(2)$ | 2 | $2! = 1^2 + 1^2 = 2$ |
| $P(3)$ | 3 | $3! = 1^2 + 1^2 + 2^2 = 6$ |
| $P(4)$ | 5 | $4! = 1^2 + 1^2 + 2^2 + 3^2 + 3^2 = 24$ |
| $P(5)$ | 7 | $5! = 1^2 + 1^2 + 4^2 + 4^2 + 5^2 + 5^2 + 6^2 = 120$ |
| $P(6)$ | 11 | $6! = 1^2 + 1^2 + 5^2 + 5^2 + 5^2 + 9^2 + 10^2 + 16^2 = 720$ |
| $P(7)$ | 15 | $7! = 1^2 + 1^2 + 6^2 + 6^2 + 14^2 + 14^2 + 15^2 + 15^2 + 21^2 + 21^2 +$ $+35^2 + 35^2 + 20^2 = 5,040$ |
| $P(8)$ | 22 | $8! = 1^2 + 1^2 + 7^2 + 7^2 + 14^2 + 14^2 + 20^2 + 20^2 + 21^2 + 21^2 +$ $+35^2 + 35^2 + 56^2 + 56^2 + 64^2 + 64^2 + 70^2 + 70^2 + 42^2 + 90^2 = 40,320$ |
| $P(9)$ | 31 | $9! = 1^2 + 1^2 + 8^2 + 8^2 + \dots = 362,880$ |
| $P(10)$ | 37 | $10! = 1^2 + 1^2 + 9^2 + 9^2 + \dots = 3,628,800$ |
| $P(11)$ | 52 | $11! = 1^2 + 1^2 + 10^2 + 10^2 + \dots = 39,916,800$ |
| $P(12)$ | 67 | $12! = 1^2 + 1^2 + 11^2 + 11^2 + \dots = 479,001,600$ |
| \vdots | \vdots | \vdots |
| $P(n)$ | | $n! = 1^2 + 1^2 + (n-1)^2 + (n-1)^2 + \dots = n!$ |

References

1. L.P. Bouckaert, R. Smoluchowski, and E. Wigner, *Theory of Brillouin zones and symmetry properties of wave functions in crystals*. Phys. Rev. **50**, 58 (1936)
2. E. Wigner, *Gruppentheorie und ihre Anwendung auf die Quantenmechanik der Atomspektren*. (Vieweg, Braunschweig 1931)
3. A. Abragam and B. Bleaney, *Electron Paramagnetic Resonance of Transition Ions*. (Clarendon Press, Oxford 1970)
4. R.L. Aggarwal and A.K. Ramdas, *Optical determination of the symmetry of the ground states of group-V donors in silicon*. Phys. Rev. **140**, A1246 (1965)
5. G.B. Arfken and H.J. Weber, *Mathematical Methods for Physicists*. 5th Edn. (Academic Press, New York 2000)
6. N.W. Ashcroft and N.D. Mermin, *Solid State Physics*. (Holt, Rinehart and Winston, New York 1976)
7. C.S. Barrett, *Structure of Metals: Crystallographic Methods, Principles and Data*. (McGraw-Hill, New York 1952) p. 14
8. E.B. Barros, A. Jorio, Ge.G. Samsonidze, R.B. Capaz, A.G. Souza Filho, J. Mendes Filho, G. Dresselhaus, and M.S. Dresselhaus, *Review on the symmetry-related properties of carbon nanotubes*. Phys. Reports **431**, 261–302 (2006)
9. J.-L. Basdevant and J. Dalibard, *The Quantum Mechanics Solver: How to Apply Quantum Theory to Modern Physics*. (Springer, Berlin Heidelberg New York Tokyo 2000)
10. F. Bassani and G. Pastori Parravicini, *Electronic States and Optical Transitions in Solids*. (Pergamon Press, Oxford 1975)
11. H.A. Bethe, *Term-splitting in crystals*. Ann. Phys. **3**, 133–208 (1959)
12. B.N. Brockhouse, *Inelastic Scattering of Neutrons in Solids and Liquids*. (IAEA, Vienna 1961) p. 113
13. B.N. Brockhouse, L.M. Corliss, and J.M. Hastings, *Multiple scattering of slow neutrons by flat specimens and magnetic scattering by zinc ferrite*. Phys. Rev. **98**, 1721–1727 (1955)
14. B. Brockhouse and P. Iyengar, Phys. Rev. **111**, 747 (1958)
15. H.A. Buckmaster, Can. J. Phys. **40**, 11670 (1962)
16. G. Burns and A.M. Glaser, *Space Groups for Solid State Physicists*. (Academic Press, New York 1978)
17. M. Cardona and F.H. Pollack, *Energy band structure of Ge and Si: the $k \cdot p$ method*. Phys. Rev. **142**, 530 (1966)

18. Clebsch and Gordon, *Tables of Clebsch–Gordon Coefficients*.
<http://pdg.lbl.gov/2005/reviews/sclerpp.pdf>
19. M.H. Cohen and E.I. Blount, *The g-factor and de Haas–van Alphen effect of electrons in bismuth*. Phil. Mag. **5**, 115–126 (1960)
20. E.U. Condon and G.Shortley, *Theory of Atomic Spectra*. (Cambridge University Press, Cambridge 1951) pp. 56–78
21. J.B. Conklin, Jr., L.E. Johnson, and G.W. Pratt, Jr., *Energy bands in PbTe*. Phys. Rev. **137**, A1282 (1965)
22. M. Damnjanović and M. Vujićić, *Magnetic line groups*. Phys. Rev. B **25**, 6987 (1982)
23. M. Damnjanović, I. Milosević, M. Vujićić, and R. Sredanović, *Full symmetry, optical activity and potentials of single- and multi-wall nanotubes*. Phys. Rev. B **60**, 2728 (1999)
24. M. Damnjanović, I. Milosević, M. Vujićić, and R. Sredanović, *Symmetry and lattices of single wall nanotubes*. J. Phys. A: Math. Gen. **32**, 4097–4104 (1999)
25. G. Dresselhaus, *Spin–orbit interaction in zinc-blende structures*. Phys. Rev. **100**, 580–586 (1955)
26. G. Dresselhaus and M.S. Dresselhaus, *Spin–orbit interaction in graphite*. Phys. Rev. **140**, A401–A412 (1965)
27. G. Dresselhaus and M.S. Dresselhaus, *Magneto-optical effects in solids*. (XXXIV Corso) (Academic Press, New York 1966) pp. 198–256
28. G. Dresselhaus and M.S. Dresselhaus, *An effective hamiltonian for the optical properties of silicon and germanium*. Int. J. Quant. Chem. **IS**, 595 (1967)
29. G. Dresselhaus and M.S. Dresselhaus, *Fourier expansion for the electronic energy bands in silicon and germanium*. Phys. Rev. **160**, 649–679 (1967)
30. G. Dresselhaus and M.S. Dresselhaus, *Interpolation methods for phonon spectra in crystals*. Int. J. Quant. Chem. **IIS**, 333–345 (1968)
31. G. Dresselhaus, A.F. Kip, and C. Kittel, *Cyclotron resonance of electrons and holes in silicon and germanium crystals*. Phys. Rev. **98**, 368–384 (1955)
32. M.S. Dresselhaus, G. Dresselhaus and P. C. Eklund, *Science of Fullerenes and Carbon Nanotubes*. (Academic Press, New York, San Diego, 1996)
33. R.J. Elliott, *Theory of the effect of spin–orbit coupling on magnetic resonance in some semiconductors*. Phys. Rev. **96**, 266–279 (1954)
34. R.J. Elliott and K.W.H. Stevens, Proc. Roy. Soc. A **215**, 437 (1952)
35. G. Feher, *Electron spin resonance experiments on donors in silicon*. i. electronic structure of donors by the electron nuclear double resonance technique (ENDOR). Phys. Rev. **114**, 1219–1244 (1959)
36. E. Guadagnini, M. Martellini, and M. Mintchev, *Braids and quantum group symmetry in Chern–Simons theory*. Nuclear Phys. B **336**, 581–609 (1990)
37. V. Heine, *Group Theory in Quantum Mechanics*. (Pergamon Press, Oxford 1960)
38. F. Herman and S. Skillman, *Atomic Structure Calculations*. (Prentice-Hall, Englewood Cliffs 1963)
39. C. Herring, *Effect of time reversal symmetry on energy levels of crystals*. Phys. Rev. **52**, 361 (1937)
40. G.F. Herzberg, *Infrared and Raman Spectra of Polyatomic Molecules, Molecular Spectra and Molecular Structure II*. (Van Nostrand Reinhold, New York 1949)
41. M.T. Hutchings, Sol. State Phys. **16**, 227 (1964)
42. H.A. Jahn and E.R. Teller, *Stability of polyatomic molecules in degenerate electronic states*. Part I – orbital degeneracy. Proc. Roy. Soc. A **161**, 220–235 (1937)

43. C.K. Johnson, *Crystallographic Topology 2: Overview and Work in Progress*. (International Press, Cambridge 1999)
44. H. Kamimura, *Theoretical aspects of band structures and electronic properties of pseudo-one-dimensional solids*. (Kluwer, Hingham 1985)
45. C. Kittel, *Introduction to Solid State Physics*. (Wiley, New York 1996)
46. W. Kohn and J.M.G. Luttinger, *Hyperfine splitting of donor states in silicon*. Phys. Rev. **97**, 883 (1955)
47. G.F. Koster, *Space groups and their representations*. (Solid State Physics, vol. 5) (Academic Press, New York 1957) p. 173
48. G.F. Koster, J.O. Dimmock, R.G. Wheeler, and H. Statz, *Properties of the Thirty-Two Point Groups*. (MIT Press, Cambridge 1964)
49. O.V. Kovalev, *Irreducible Representations of the Space Groups*. (Gordon and Breach, New York 1965) [Academy of Sciences USSR Press, Kiev 1961]
50. M. Lax, *Symmetry Principles in Solid State and Molecular Physics*. (Wiley, New York 1974)
51. D.B. Litvin, *Magnetic space-group types*. Act. Crystall. A **57(6)**, 729–730 (2001)
52. J.M. Luttinger, *Quantum theory of cyclotron resonance in semiconductors: general theory*. Phys. Rev. **102**, 1030 (1956)
53. G.Ya. Lyubarskii, *Application of Group Theory in Physics*. (Pergamon, New York 1960)
54. S.C. Miller and W.H. Love, *Tables of Irreducible Representations of Space Groups and Co-Representations of Magnetic Space Groups*. (Pruett Press, Denver 1967) Much of this material is also available on the web: <http://www.cryst.ehu.es/> (Bilbao Crystallographic Server, University of the Basque Country, Bilbao, Basque Country, Spain)
55. C.E. Moore, *Atomic Energy Levels (National Bureau of Standards, Circular #467)*. (NBS Press, Washington, 1949 [Vol. 1], 1952 [Vol. 2], 1958 [Vol. 3]). See <http://physicsnist.gov/PhysRefData/DFTdata/> as well as <http://physicsnist.gov/PhysRefData/ASD/>
56. A. Nussbaum, *Applied Group Theory for Chemists, Physicists and Engineers*. (Prentice-Hall, Englewood Cliffs 1971)
57. J.F. Nye, *Physical Properties of Crystals: Their Representation by Tensors and Matrices*. (Oxford University Press, Oxford 1985)
58. International Union of Crystallography, *International Tables for X-Ray Crystallography*. (Kynoch Press, Birmingham 1952) See <http://www.crystallography.net/> as well as <http://www.cryst.ehu.es/>
59. G.E. Pake and T.L. Estle, *The Physical Principles of Electron Paramagnetic Resonance*. (W.A. Benjamin, Cambridge 1973)
60. Yu.E. Perlin and M. Wagner, *Modern Problems in Condensed Matter Sciences*. Vol. 7: The dynamical Jahn–Teller Effect in Localized Systems. (North-Holland Physics Publishing, Amsterdam 1984)
61. B.M. Powell and P. Martel, *Crystal dynamics of tellurium*. Proc. 10th Int. Conf on Physics of Semiconductors 1970, pp. 851–855
62. L.M. Roth, *g factor and donor spin-lattice relaxation for electrons in germanium and silicon*. Phys. Rev. **118**, 1534–1540 (1960)
63. R. Saito, G. Dresselhaus, and M.S. Dresselhaus, *Physical Properties of Carbon Nanotubes*. (Imperial College Press, London 1998)
64. E.B. Barros, R.B. Capaz, A. Jorio, Ge.G. Samsonidze, A.G. Souza-Filho, S. Ismail-Beigi, C.D. Spataru, S.G. Louie, G. Dresselhaus, and M.S. Dresselhaus,

- Selection rules for one and two-photon absorption for excitons in carbon nanotubes.* Phys. Rev. **B73**, 242406 (R) (2006)
65. Ge.G. Samsonidze, A. Grüneis, R. Saito, A. Jorio, A.G. Souza Filho, G. Dresselhaus, and M.S. Dresselhaus, *Interband optical transitions in left- and right-handed single-wall carbon nanotubes.* Phys. Rev. B **69**, 205402–(1–11) (2004)
66. J. Slater and G. Koster, *Simplified LCAO method for the periodic potential problem.* Phys. Rev. **94**, 1498–1524 (1959)
67. V.J. Tekippe, H.R. Chandrasekhar, P. Fisher, and A.K. Ramdas, *Determination of the deformation-potential constant of the conduction band of silicon from the piezospectroscopy of donors.* Phys. Rev. B **6**, 2348–2356 (1972)
68. The International Tables for X-Ray Crystallographers, Vol. A, published by the International Union of Crystallography (1987) (also check web site)
69. The Optical Properties of Solids, Proceedings of the International School of Physics, Enrico Fermi Course XXXIV (Academic Press, 1966) p. 198–256
70. M. Tinkham, *Group Theory and Quantum Mechanics.* (McGraw-Hill, New York 1964)
71. M. Vujović, I.B. Bozović, and F. Herbut, *Construction of the symmetry groups of polymer molecules.* J. Phys. A: Math. Gen. **10**, 1271 (1977)
72. S.A. Werner, R. Colella, A.W. Overhauser, and C.F. Eagen, *Observation of the phase shift of a neutron due to precession in a magnetic field.* Phys. Rev. Lett. **35**, 1053 (1975)
73. C.T. White, D.H. Roberston, and J.W. Mintmire, *Helical and rotational symmetries of nanoscale graphite tubules.* Phys. Rev. B **47**, 5485 (1993)
74. P.A. Wolff, *Matrix elements and selection rules for the two-band model of bismuth.* J. Phys. Chem. Solids **25**, 1057–1068 (1964)
75. W.A. Wooster, *Tensors and Group Theory for Physical Properties of Crystals.* (Clarendon Press, Oxford 1973)
76. R.W.G. Wyckoff, *Crystal Structures.* 2nd Edn. (Krieger, New York 1981) Also available on the web: <http://www.cryst.ehu.es/> and <http://www.crystallography.net/>
77. Y. Yafet, *Space groups and their representations.* (Solid State Physics, vol. 14) (Academic Press, New York 1963) pp. 1–98

Index

- A*₃*B*₃ molecule 54
Abelian group 3, 9, 44, 211–213
commuting operator 211
cyclic group 212
irreducible matrix representations 211
Abelian subgroup 7
achiral nanotubes 541, 542
characters for group *D*_{2nh} 541
characters for group *D*_{2nv} 542
 α -quartz 262, 268–273, 275
combined normal modes for Si and O atoms 270–272
comparsion to tellurium 268, 269
crystal structure 268, 269
effect of stress on symmetry of crystal 273
lattice modes 268–274
mixing of normal modes by stress 272
nonsymmorphic 268
normal modes 269–272, 275
normal modes for oxygen atoms 270–272
normal modes for Si and for O 275
normal modes for Si atoms 270
orientational effect 273
polarizability tensor 273, 274
Raman spectra 274
site symmetries 269
space group 262
stress effects in normal modes 272–275
angular momentum 433
orbital states 433
spin states 433
state degeneracy 433
state symmetry 433
transformation of Hamiltonian 433
angular momentum states 127, 128
characters in *T*_d symmetry 127, 128
irreducible representation 128
antiunitary matrix 21
antiunitary operator 406
associative law 3, 4
axial point group 204
improper rotations 204
inversion 204
rotations 204
axial stress effects on phonons 272, 273
example of α -quartz 273
orientational effect 272, 273
polarizability tensor 273
stress effect 273
symmetry lowering 272
symmetry of strain tensor 272, 273
axial vectors 161
*B*₁₂*H*₁₂ molecule 144
basis functions 57–59, 72–75, 150, 355–358
arbitrary function 63
basis function table 59, 60
basis vectors 57–59, 61–75
Clebsch–Gordan coefficients 355–358

- definition 57–59, 61–75
 derivation of Γ_6^+ (Γ_{15}^+) 356, 357
 derivation of Γ_8^+ (Γ_{15}^+) 355, 356
 examples in cubic symmetry 73
 $\mathbf{k} \cdot \mathbf{p}$ matrix elements 359
 generalization of basis functions 358, 359
 generating irreducible representations 58–63
 irreducible representations 57–75
 irreducible representations of double group 355
 matrix elements of a symmetry operator 58–63
 matrix representation 57, 61, 62
 orthogonality of basis functions 357
 partners 57, 64
 projection operators 64
 raising and lowering operator 355, 357
 splitting of $j = 3/2$ level in cubic symmetry 356
 square symmetry 73
 symmetry operations 57–75
 tables for coupling coefficients 358
 trace 63
 transformation from $|\ell s m_\ell m_s\rangle >$ representation to $|jm\rangle$ 355–357, 359
 wave functions 57, 58, 62–65, 67–75
 basis functions for double group 353–362
 matrix representation 353
 matrix representation for spin components 354
 notation for double groups based on single group 354
 Pauli spin matrices 353, 354
 spin raising and lowering operators 354
 unit matrix 354
 basis functions of permutation groups 437–439
 first excited state 438
 for many electron system 437
 ground state 438
 $(n-1)$ dimensional 439
 $P(2)$ basis functions 439
 $P(3)$ basis functions 439
 Pauli principle 438
 phase factors 438
 transforms as Γ_1^a antisymmetric state 438
 transforms at totally symmetric state 438
 BaTiO_3 247–250, 256–258
 basis functions 258
 equivalence transformation 256, 258
 irreducible representations 258
 normal mode patterns 258
 normal mode patterns at X point 256–258
 Bloch function 215, 217, 220
 basis functions 217
 effect of point group operations 215
 effect of symmetry operation 217
 effect of translation 215, 217
 eigenfunction 215
 irreducible representation for group of the wave vector 215
 orthonormality relation 217
 periodic part 215, 217
 plane wave factor 217
 transformation properties 215
 Bloch theorem 212, 213, 216
 Bloch function 213, 214
 eigenfunction 212
 eigenvalue of translation 213
 periodic boundary conditions 213
 phase factor 213
 quantum number of translations 213
 reciprocal lattice vector 213
 translation group 212
 translational symmetry 213
 wave vector 213
 body centered cubic lattice 222–227
 basis functions 224
 Brillouin zone 222
 character table $k = 0$ 224
 character table for Δ point 224
 character tables at high symmetry points 224, 225, 232
 compatibility relations 227
 group #229 222
 group of the wave vector along the Λ axis 226

- group of the wave vector at high symmetry points 226, 227
- bonding 114, 115
- antibonding states 115
 - atomic orbital 115
 - bonding states 115
 - charge overlap 114, 115
 - chemical bond 114, 115
 - concept of equivalence 115
 - diatomic molecule 115
 - directed valence bond 114, 115
 - exchange interaction 114, 115
- braids 434
- Bravais lattice 45, 188–190, 192, 196, 199, 207, 209, 210, 241
- 14 space lattices 192
 - 2D lattices 199, 210, 211
 - 3D space groups 192
 - acoustic modes 241
 - allowed wave vector states 241
 - Bloch theorem 209
 - body centered 191
 - body centered cubic lattice 209
 - centered 210
 - crystallographic lattices 190
 - cubic 191, 196, 209
 - definition 188
 - degrees of freedom 241
 - dispersion relation 209
 - examples 192
 - face centered 191
 - face centered cubic lattice 209
 - fivefold axis 207, 208
 - fourfold axis 207
 - hexagonal 191, 210
 - holohedral group 190
 - invariance under translation 188
 - lattice constants 211
 - lattice vectors 210, 220
 - monoclinic 191
 - oblique 210
 - orthorhombic 191
 - periodic boundary conditions 211
 - periodic potential 209
 - primitive 210
 - primitive translation vectors 189, 190, 210
 - reciprocal lattice vector 210
 - reciprocal space 209
- rectangular 210
- restriction on symmetries 114, 207, 208
- restrictions on possible rotations 191
- simple cubic lattice 209
- space groups 190, 192
- square 210
 - subgroup 190
 - tetragonal 191
 - threefold axis 207
 - translational symmetry 207, 209
 - triclinic 191
- Brillouin zone 213, 218, 219, 235, 245, 280
- body-centered cubic lattice (#229) 511
 - compatibility relations 219
 - essential degeneracy 218
 - extended 213, 280
 - extended Brillouin zone 213, 280
 - face-centered cubic lattice (#225) 511
 - first Brillouin zone 213
 - general point 219
 - graphite lattice 512
 - hexagonal lattice 512
 - high symmetry points 218, 219, 235
 - reciprocal lattice vector 213, 218
 - reduced Brillouin zone 280
 - rhombohedral lattice 512
 - simple cubic lattice (#221) 511
- bromine 276
- crystal structure 276
 - infrared activity 275, 276
 - lattice modes 276
 - Raman activity 275, 276
 - space group 276
 - Wyckoff positions 276
- C_2H_2 molecule 143, 164
- equivalence transformation 164
 - infrared activity 164
 - normal modes 164, 166, 177
 - optical polarization 164
 - Raman activity 164
- C_2H_4 molecule 143, 178
- normal mode displacement 178
 - normal modes symmetries 178

- carbon nanotubes 205, 208, 237, 276, 533
 achiral 205, 208, 237
 armchair 205
 character tables 538
 chiral 205, 208, 237, 539, 540
 compatibility relations 237
 1D Brillouin zone 237
 2D Brillouin zone 208
 factor group 237
 graphene 205
 helicity 536
 infrared active modes 276
 isogonal point groups 237
 lattice vector 237
 line groups 208, 237
 metallic 208, 237
 mode symmetries 276
 notation 208, 534
 phonon modes 276
 physical properties 205
 point groups operations 205
 polarization effects 276
 quantum numbers 208
 Raman active modes 276
 selection rules for Raman scattering 276
 semiconducting 208, 237
 space group 208
 structure 205, 534
 translation vector 205
 tubular 205
 unit cell 533, 537
 zigzag 205, 237
- CH_4 molecule 125–129, 168–170, 178
 basis functions 169
 combination modes 169, 170
 equivalence transformation 168
 irreducible representation of angular momentum 178
 linear combination of 4 hydrogen orbitals 168
 normal modes 169
 overtones 169, 170
 polarization effects in rotational interaction spectra 178
 rotational levels 178
 rotational–vibrational interaction symmetries 178
- character 29
 definition 29
 invariance under unitary transformation 29
 character of a representation 29, 33
 importance of 33
 character tables 30, 31, 40, 43, 86, 89, 104, 110
 carbon nanotubes 538
 cubic group 86
 cyclic groups 44
 definition 30
 direct product of groups 110
 example 110
 example of $P(3)$ 30
 group C_{4h} 104, 110
 group $D_3(32)$ 63
 group D_{3h} 137
 group T_d 126
 higher to lower symmetry 86
 irreducible representation 110
 matrix representation 40–43
 point groups 44
 setting them up 40–43
 symmetry operations 86
 tetragonal group 89
- characters of direct product 103
 direct product for two groups 103
 direct product for two irreducible representations 103
 direct product representation 103
 chiral carbon nanotubes 539, 540
 characters for group D_N 539, 540
- class 9, 30, 31, 435–437
 character of class elements 30
 definition 9
 example of D_3 31
 example of $P(3)$ 31
 classes of permutations 435–437
 class structure 436
 example of $P(4)$ 436
 example of $P(5)$ 436
 irreducible representations 436
 isomorphic 436
 number of classes 435–437
 number of elements 435
 number of elements in a class 436, 437
- $P(3)$ isomorphic to C_{3v} 436

- CO molecule 120–122, 128, 162
 equivalence transformation 162
 molecular vibration 162
 normal modes 162
 symmetry operations 162
- CO₂ molecule 54, 164, 165, 177
 atomic displacements 177
 equivalence transformation 164
 infrared active modes 164, 177
 normal modes 164, 165
 Raman active modes 164, 177
 rotational modes 177
 symmetries for electronic states 177
 symmetries for normal modes 177
 symmetry group 177
 use of blocks of atoms 165
- combination modes 156, 157, 159, 161
 CH₄ molecule 156, 157, 169
 direct product 156
 effect of inversion symmetry 159
 infrared active 156, 157, 159
 irreducible representation 156
 Raman active 156, 157, 159, 161
- compatibility between tetragonal (T_d) and cubic (O) representations 526
- compatibility relations 219, 227–229
 along A axis for cubic groups 228
 around a circuit 229
 basis functions 227, 229
 Brillouin zone 227
 connectivity 227
 degeneracy 227
 high to lower symmetry 229
 labeling energy bands 229
 level anticrossings 230
 level crossings 230
 lower to higher symmetry 230
- compatibility relations for space group #194 520, 531
 $\Gamma, \Delta, \Sigma, T$ 520, 531
- complex conjugation 16
- conjugation 9
- coset 7–10
 definition 7
 example 8
 left coset 7, 10
 multiplication 10
 right coset 7, 10
- coupling coefficient table for double group basis functions 525
 coupling coefficients for selected basis functions for single group O 524
 crystal double groups 341–365
 additional irreducible representations of full rotation group 344
 additional symmetry classes 344
 additional symmetry elements 344
 bands sticking together 363, 364
 basis functions 353, 359, 360
 Bloch function with spin 344
 character for rotation by an angle α and $\alpha + 2\pi$ for half integral j 341
 character for rotation for $j = 1/2$ for rotation group 345
 character table for O double group 346, 347
 character table for the point group D_6 364
 character tables 341, 359, 360
 character tables from the literature 347
 characters for symmetry operations 343
 Clebsch–Gordan coefficients 360
 compatibility relations 360, 363
 dimensionality of each representation 345, 348, 364
 direct product of double group 347
 direct product of irreducible representation with spinor $D_{1/2}$ 344, 347
 even-dimensional irreducible representations of full rotation group 341, 343, 348
 example of double group for O cubic symmetry point group 344
 experimental verification of 4π periodicity for Fermions 342
 half integral angular momentum 341
 history 342
 identity element 342
 irreducible representation for spinor $D_{1/2}$ 346
 irreducible representation notation $\Gamma_8^+(\Gamma_{12}^+)$ 348, 349
 irreducible representations 344

- Kramers degeneracy 348
 matrix elements 359
 matrix representation 353
 new symmetry element for rotation
 by 2π 342
 nonsymmorphic groups 362, 363
 notation for double group 341, 343
 number of classes 343, 345
 number of elements 342, 343
 number of irreducible representations
 345
 odd-dimensional irreducible representations of full rotation group
 341, 343
 orthogonality requirements of
 irreducible representations 346
 plane wave basis functions for double group representations 360–362
 rotation by 4π 341
 space group 363, 364
 special role of C_2 operation 343
 splitting of six-fold levels in cubic symmetry 348
 states for spinor 353
 symmetry operation $\mathcal{R}A_k$ 343
 symmorphic groups 361, 362
 time reversal symmetry 364
 vanishing structure factor 362, 364
 wonderful orthogonality theorem on
 character 346
 crystal field level splitting 79, 80, 85,
 88, 90, 92–94, 349
 angular momentum state 88, 92
 axial field 90
 basis functions 90
 bonding orbitals 94
 character tables 85, 350–352
 crystal field > spin-orbit interaction
 349
 crystal potential 79, 81, 85
 cubic field 85, 88, 90–92, 94
 direct product 85, 349, 353
 hexagonal field 95
 higher to lower symmetry 85, 88, 90,
 91
 icosahedral field 95
 impurity levels 79, 80, 94
 inversion symmetry 88
 irreducible representations 92
 Laplace equation 93
 level degeneracy 85
 notation for quantum number of
 designations (s, l, j) 351
 notation to label states 349
 octahedral crystal field 88, 90, 91
 optical transitions between crystal field levels 352, 353
 orthorhombic field 93
 perturbation theory 79
 quantum numbers for a transition
 metal ion 349
 rare earth ions 349
 reducible representation 88
 spherical harmonics 88, 91–95
 spin-orbit interaction 80
 splitting of sixfold level in a cubic field 349
 splitting of spin-orbit levels in a crystal field 352
 substitutional impurity 94
 symmetry operation 85
 tetragonal field 88, 90
 two-electron states 353
 weak field 90
 crystal field theory 79–92, 452
 Coulomb interaction 80
 crystal field 452
 Dy³⁺ ion in D_{4h} crystal field 365
 effect of application of stress along
 two fold axis 365
 Er³⁺ ion in D_{4h} crystal field 365
 Er³⁺ ion in I_h crystal field 365
 hyperfine interaction 80
 spin-orbit interaction 80, 349–351
 strong field case 80, 81
 transition metal ions 452
 weak field case 81
 crystal structure determination
 examples 206
 experimental techniques 206
 references 206
 symmetry 206
 cubic point groups 87, 88
 character table 86
 characters 87
 classes 87
 cubic field 88
 decomposition theorem 87

- irreducible representation 86, 88
- reducible representation 86–88
- site symmetries 196
- cubic space group #221 501
 - Hermann–Mauguin notation 501
 - Schoenflies notation 501
 - Wyckoff positions 501
- cubic space groups 194, 196, 222
 - basis functions 223
 - BCC #229 195, 196
 - Bravais lattice 196
 - character table 223
 - diamond structure #227 195
 - equivalence transformation 194
 - example of space group #221 195
 - example of space group #223 195
 - example of space group #225 195
 - example of space group #227 195
 - FCC #225 195, 196
 - irreducible representation 223
 - simple cubic #221 222, 501
 - site symmetries 196
 - zinc blende structure #203 195, 196
- cyclic group 211
 - commuting elements 211
- cyclic permutation 434
 - decomposition into cycles 434
 - definition 434
 - equivalence transformation 434
- 1D line groups
 - line groups 183
 - translations 183
- 2D Bravais lattice 235
 - translation vectors in real space 235
 - translation vectors in reciprocal space 235
- 2D hexagonal space groups 203
 - group $p31m$ 203
 - group $p3m1$ 203
 - group $p6$ 203
 - group $p6mm$ 203
 - symmorphic 207
- 2D oblique space groups 200, 201
 - general point 201
 - group $P1$ 200
 - group $p2$ 201
 - group $p211$ 200
- International Crystallography Tables
 - 201
 - motif 200
 - notation 200
 - oblique lattices 200
 - site symmetry 201
 - special points 201
 - twofold axis 200
 - Wyckoff letter 201
 - Wyckoff position 201
- 2D rectangular space groups 201, 202
 - $c1m1$ 202
 - centered lattice 201, 202
 - full rectangular point symmetry 201
 - general point 201
 - glide planes 202
 - group $2mm$ 201
 - group $c1m1$ 202
 - group $c2mm$ 202
 - group $p1g1$ 202
 - group $p1m1$ 201, 202
 - group $p2gg$ 202
 - group $p2mg$ 202, 294, 295
 - group $p2mm$ 202
 - lower symmetry motif 201
 - Miller indices 202
 - mirror planes 202
 - nonsymmorphic 202
 - notation 201
 - primitive lattice 201, 202
 - site symmetry 202
 - symmorphic 201, 202
 - Wyckoff position 202
- 2D space groups 183, 198–203, 207, 489–498
 - 2D square space groups 207
 - Brillouin zone 294, 295
 - 2D oblique space groups 200, 201
 - 2D rectangular space groups 201
 - full point group symmetry 202
 - group $p4gm$ 203, 207
 - line groups 183
 - nonsymmorphic 183
 - symmetry operations 183, 294, 295
- 2D square space groups 203, 207
 - centered 207
 - combining translation vectors with glide planes 203
 - full point group symmetry 203

- glide planes 203
- group $p3$ 203
- group $p4mm$ 202, 203
- nonsymmorphic 203, 207
- notation 203, 207
- symmorphic 203
- 3D space groups 183–198, 205–208
- D_{2d} point group 193
 - combined with tetragonal Bravais lattice 193
 - rotation axes 193
 - symmetry operations 193
- d^6 configuration for $P(6)$ 454
- decomposition theorem 34, 35, 39
- crystal field splitting 35
 - example 35
 - proof 34
 - uniqueness 34
- degeneracy 218
 - accidental degeneracy 218
 - essential degeneracy 218
 - non-essential degeneracy 218
- degenerate second order $\mathbf{k} \cdot \mathbf{p}$ perturbation theory 316–324
 - Brillouin–Wigner degenerate perturbation theory 318
 - coupling of Γ_{15}^- to states outside NDS 318
 - coupling of Γ_{15}^- to states within NDS 318
 - coupling strength of the Γ_{15}^- level to other levels 324
 - cyclotron resonance experiments 323, 324
 - determination of number of equivalent matrix elements 319
 - energy bands throughout the Brillouin zone 324
 - evaluation of non-vanishing elements 319
 - for a cubic Γ_{25}^+ level 317
 - intermediate states coupling to Γ_{15}^- 319
 - matrix element coupling to states outside NDS 319
 - matrix element coupling to states within NDS 319
 - matrix elements of $\mathbf{k} \cdot \mathbf{p}$ Hamiltonian coupling to Γ_{15}^- 319, 320
- nearly degenerate set of states (NDS) 317, 318
- off-diagonal contribution 322
- secular equations 317, 319
- states outside the NDS 317
- symmetries coupling to Γ_{15}^- band 319
- Taylor expansion along high symmetry directions 323
- Taylor expansion of secular equation 322
- vanishing terms 316, 317
- diamond structure 207, 231, 232, 234, 236, 250–252, 296–303, 508, 515, 516
 - 8 atoms per cubic unit cell 232
 - basis functions at the X point 300, 301
 - Bragg reflection at X point 299
 - character tables for high symmetry points 232, 233
 - characters for the equivalence transformation 231
 - classes for the diamond structure 231
 - compatibility relations 233, 234, 251
 - connection to zinc blende structure #216 231
 - effect of symmetry operations on basis functions at X point 303
 - electronic band structure 232, 299
 - empty lattice calculations along ΓL and ΓX 298
 - energy bands for Ge 299
 - energy bands sticking together 298, 300, 302
 - energy dispersion about the X point 299, 302
 - equivalence transformation 231, 250
 - equivalence transformation for symmetry operations and classes 236
 - essential degeneracies 298
 - extra degeneracy at X point 234
 - form of symmetry operators 232
 - group of the wave vector at high symmetry points 232–234, 236, 296, 303

- group of the wave vector on the square face 234
 Hermann–Mauguin notation 502
 high symmetry points on the square face 234, 235
 irreducible representation of group of the wave vector at high symmetry points 232, 251
 LA branch 251
 lattice modes 250
 LO branch 251
 multiplication of symmetry elements 232
 nonsymmorphic 250, 296
 phase factor 232–234
 phonon dispersion relations 232, 251, 252
 phonon modes 251, 252
 primitive unit cell 232
 product of symmetry operations at high symmetry points 236
 Raman activity 250, 252
 Raman tensor 252
 screw axis 250
 space group #227 502, 508, 515, 516
 structure factor vanishes at X point 299
 symmetry interchange at X point 301
 TA branch 251
 TO branch 251
 translation vectors 232, 296
 two atoms per unit cell 232
 two sublattices 232
 vanishing structure factor on square face of Brillouin zone 300
 Wyckoff positions 502
 diatomic molecules 117–124, 142
 antibonding 119–123, 143
 bonding 119–123, 142
 character table 119
 directed valence bonding 120, 123
 electron energy level 123
 equivalence transformation 119, 123
 evenness 118
 group $C_{\infty v}$ 118
 group $D_{\infty h}$ 118, 119
 group of Schrödinger's equation 119
 heteronuclear 117, 120–123
 HOMO 122
 homonuclear 117–121
 homopolar 117
 inversion symmetry 118
 irreducible representation 119
 linear combination of atomic orbitals 119, 121
 LUMO 122
 matrix Hamiltonian 124
 mirror plane 118
 molecular energy levels 122, 124
 oddness 118
 Pauli principle 120
 secular equation 123
 selection rules 120
 singlet states 120, 122
 triplet states 120, 122
 unitary transformation 120
 diffraction pattern 45
 direct product 98, 100, 101, 104, 109, 158–161, 170, 172, 175, 189, 204
 definition 189
 electron–photon scattering 160
 for groups 98, 100, 101, 109
 for representations 98, 101, 102
 infrared selection rules 158, 159
 selection rules for CH_4 molecule 169
 selection rules for Raman tensor 160
 semi-direct product 189, 204
 two vectors 172
 vibrational and rotational angular momentum irreducible representation 175
 weak direct product 204
 direct product of groups 100, 101, 109
 definition 100, 101
 examples 100, 101, 109
 notation 101
 direct product of irreducible representations 101, 102
 definition 101
 direct product group 101, 102
 irreducible representations 102
 matrix multiplication 102
 notation 101
 proof 101, 102
 direct product of matrices 109
 direct product representations 104

- character table 104
 decomposition theorem 104
 example 104
 irreducible representation 104
 notation 104
 directed valence bonding 113,
 117–120, 128, 129
 antibonding 117
 bond strengths 113, 129
 bonding 117, 128
 diatomic molecule 117–119, 121
 directed valence representation 118
 equivalence transformation 118
 example 128
 linear combination of atomic orbitals
 117, 118
 molecular orbitals 118
 sp^3 bonds 128
 dispersion relations 209
 Brillouin zone 209
 degeneracy 209
 group of the wave vector 209
 high symmetry points 209
 symmetry of wave function 209
 symmetry operator 209
 double groups *see* crystal double
 groups
 effect of time reversal operator on
 energy dispersion relations 407,
 408
 action of time reversal operator 407
 action on Bloch wave function 407
 bands sticking together 408
 degeneracies imposed by 407
 equal and opposite slopes for $E(\mathbf{k})$ at
 zone boundary 408
 Herring's rules 408
 time reversal symmetry pair 408
 zero slope of $E(\mathbf{k})$ at zone boundary
 408
 effective g -factor 378–383, 385–387,
 389, 400
 anticommutator of wave vector
 components 380
 antisymmetric part of secular
 equation 380, 381
 basis functions for $\Gamma_7^+ (\Gamma_{25}^+)$ 385
 basis functions for $\Gamma_7^- (\Gamma_2^-)$ 383
 basis functions for $\Gamma_8^+ (\Gamma_{25}^+)$ 383
 Bohr magneton 381
 commutation relation 380
 commutator of wave vector compo-
 nents 380, 381
 conduction band effective mass 386
 connection of spin and orbital
 effective mass tensors 388
 contribution from $\Gamma_7^+ (\Gamma_{25}^+)$ levels
 385
 contribution from $\Gamma_8^+ (\Gamma_{25}^+)$ levels
 385
 contribution to effective magnetic
 moment 385
 cyclotron resonance transitions 387
 effective g -factor for germanium at
 $k = 0$ 383, 385
 effective g -factor formula 386
 effective g -factor sum 385
 effective magnetic moment 382, 385
 effective mass approximation in
 a magnetic field 378
 effective mass tensor 380, 382
 effective mass wave functions 381
 eigenvalues 379
 energy levels of a free electron in
 a magnetic field 382
 evaluate effective magnetic moment
 383
 evaluate effective mass 383
 for germanium conduction electrons
 in Γ_7^- levels 386
 for InSb conduction electrons 386
 generalized momentum vector 382
 Hamiltonian for electron in a mag-
 netic field 378
 identification of double group with
 single group of origin 383
 interband Landau level transitions
 388
 \mathbf{k} as noncommuting operator 379,
 380
 Kohn–Luttinger transcription 379
 Landau level separation 387
 Landau level separation and spin
 splitting 388
 Landau level separation larger than
 spin splitting 388
 matrix elements for p_x, p_y 385

- matrix elements for evaluating
 effective magnetic moment 383
 nearly degenerate set of levels 379
 noncommuting wave vector compo-
 nents 381
 nondegenerate valence band for
 hexagonal symmetry (group
 #191) 400
 secular equation for $\mathbf{k} \cdot \mathbf{p}$ Hamiltonian
 379
 spin effective mass 387
 spin resonance experiments 388
 spin splitting 387
 symmetrized plane waves for various
 irreducible representations 389
 symmetrized secular equation 380
 transformation properties of antisym-
 metric part of secular equation
 381
 transformation properties of commu-
 tator of wave vector components
 381
 two-band model 388
 Zeeman effect 382
 elastic modulus tensor 467
 direct product of stress and strain
 tensors 467
 form of elastic modulus tensor 467
 notation as 6×6 matrix 468
 elastic modulus tensor under full
 rotational symmetry 469, 471
 antisymmetric irreducible representa-
 tions 469
 effect of full rotational symmetry
 469
 effect of permutation symmetry 469
 evaluation of elastic constants 6×6
 471
 nonvanishing constants 470
 symmetric irreducible representations
 469
 symmetrized stress-strain relations
 470
 elastic modulus tensor under lower
 symmetry groups 472–476
 evaluation from direct product of
 stress and strain tensors 472
 going from full rotational symmetry
 to icosahedral symmetry 472
 electromagnetic interaction 97, 98,
 157, 158, 327
 connection to $\mathbf{k} \cdot \mathbf{p}$ perturbation
 theory 327
 electromagnetic interaction Hamilto-
 nian 97, 98, 157, 158, 327
 matrix element of momentum 327
 relation of electromagnetic interaction
 to effective mass tensor 327
 selection rules 158
 transformation properties 157, 158
 vector potential 98
 electron–photon scattering 160
 electronic energy levels 279, 291
 BCC lattice 293, 294
 Brillouin zone for simple cubic
 structure 279, 288
 compatibility relations between X
 point and Δ point 289
 diamond structure 299
 dispersion of $E(k)$ near X point 299
 electronic dispersion relations 279
 empty lattice along Γ – R for simple
 cubic structure 293, 294
 empty lattice along Γ – X for simple
 cubic structure 293, 294
 empty lattice at Δ point cubic lattice
 286, 288
 empty lattice at X point for simple
 cubic group 288–294
 empty lattice at high symmetry
 points 286
 empty lattice for BCC structure at
 high symmetry points 293
 empty lattice for diamond structure
 at high symmetry points 297
 equivalence transformation 290, 291
 FCC lattice 294
 for simple cubic 302
 group of the wave vector 302
 lifting degeneracies 294
 linear combinations of plane waves
 forming basis functions 302
 nearly free electron model 279
 nonsymmorphic structures 294–301
 symmetrized plane waves 286, 288,
 290–292
 symmetrized plane waves at X point
 289

- symmorphic structures 293, 294
 weak periodic potential with BCC symmetry 294
 electronic states 113–115
 basis functions 114
 block diagonal form 114
 eigenfunctions 114, 279
 eigenvalues 114, 279
 energy eigenvalues 113
 equivalence concept 114
 free atomic orbitals 114
 many electron states 114, 115
 one-electron potential 113
 Pauli principle 114, 115
 secular equation 114
 valence electrons 114
 wavefunctions 115
 electronic–rotational level interactions
 (λ -doubling) 175, 176
 electronic–vibrational level interactions
 (vibronic levels) 175, 176
 empty lattice 279–281, 303
 2D hexagonal lattice #17 $p6mm$ at $k = 0$ 302
 diamond structure at $k = 0$ 303
 diamond structure at X point 303
 for 2D hexagonal lattice #17 $p6mm$ at Γ point 303
 for BCC structure at $k = 0$ 303
 for FCC structure at L point 302
 for FCC structure at X point 302
 for simple cubic structure 302
 lifting degeneracy by periodic potential 303
 linear combinations of plane waves
 forming basis functions 302
 symmetry operations on diamond structure wave functions at X point 303
 empty lattice at $k = 0$ 282–284, 286
 basis functions for irreducible representations 285
 BCC structure #229 286
 Brillouin zone for simple cubic lattice 288
 character table for symmetry operations of group of the wave vector 290
 compatibility relations 288, 289
 cubic symmetry operations 282, 284
 degeneracy symmetry 283
 diagonalizing matrix Hamiltonian 286
 diamond structure #227 at high symmetry points 297
 eigenfunctions at X point 289–292
 energy eigenvalues 282, 283, 286, 293
 equivalence transformation 282, 284, 289, 292
 group of the wave vector 282, 288, 290
 Hamiltonian in block diagonal form 282, 284, 286
 irreducible representations 282, 284, 291
 level symmetry 282, 284
 lifting level degeneracies 286, 289, 303
 linear combination of plane wave states 282–286, 288–293, 302
 notation 290
 reciprocal lattice vector 282, 283, 286
 simple cubic lattice #221 286, 287, 302
 standard references 288
 structure factor 297
 weak periodic potential 286
 empty lattice with spin–orbit interaction 368, 399
 direct product of spinor 368
 double group at high symmetry points 399
 double group irreducible representations 368
 double group representation related to single group origin 368
 Kramers degeneracy 368, 369
 energy bands with spin–orbit interaction 367, 368, 376–383, 385–387, 389–399
 bands sticking together 399
 basis functions 375
 connection between the Slater–Koster method and $\mathbf{k} \cdot \mathbf{p}$ perturbation theory 389, 396, 397
 double groups 367

- effect of screw axes 399
 effective *g*-factor 378–383, 385–387, 389
 Hamiltonian 367
 secular equation for valence band of group IV semiconductor 375–377
 secular equation into block diagonal form 368
 wave functions 367
 equilateral triangle 4, 6, 67
 matrix representation 5
 symmetry operations 4
 equivalence concept 113, 115
 atomic sites 115
 equivalence representation 115
 linear combination of atomic orbitals 114
 equivalence representation 36, 115, 116
 characters 116
 equivalent sites 116
 linear combination of atomic orbitals 116
 matrix representation 115, 116
 equivalence transformation 17, 117, 221
 characters 117, 150, 221
 decomposition into irreducible representations 221
 equivalent atoms (sites) 221
 for H_2O molecule 154
 irreducible representations 221
 phase factor for translations 221
 reducible representation 221
- F*43*m* (diamond structure, group #227) 230
 effect of symmetry operation on A and B atoms 230
 effect of symmetry operation on basis function of diamond structure 230
 factor group 231
 phase factor 231
 primitive unit cell 231
 screw axis 231
 two interpenetrating FCC sublattices 231
- face centered cubic lattice (FCC, group #225)
 basis functions 224
 character tables 223–227
 compatibility relations 227
 factor group 7, 11, 13, 110, 189, 190, 231
 cosets 188, 189
 definition 11
 example 11, 13
 form of symmetry operations 231
 group properties 189
 irreducible representations 190
 isomorphic to point group 189, 231
 multiplication of cosets 189
 multiplication table 13
 multiplier algebra 190
 multiplier groups 190
 multiplier representation 190
 self-conjugate subgroup 11
 five-electron states 451–454
 allowed states 452
 antisymmetric irreducible representation 451
 character table for $P(5)$ 451, 453
 classes of $P(5)$ 451, 453
 d^5 configuration for $P(5)$ 453, 454
 direct product 452
 equivalence transformation 453
 irreducible representations 451, 452
 multiplication of elements 453, 454
 p^3d^2 configuration 453, 454
 Pauli allowed states 453, 454
 symmetries 452
 table of transformation properties 452
- fivefold symmetry body centered cubic (BCC) structure 45, 46, 50, 53, 191, 207, 208
- Fm*3*m* (O_h^5) group 223
 Brillouin zone 223
 high symmetry axes and points 223
- four-electron states 448–451
 $1s^32s$ configuration 449
 allowed states 450, 451
 character table for $P(4)$ 449
 classes 448
 equivalence between p^4 electron and p^2 hole states 450, 451

- irreducible representations 448–450
- $P(4)$ permutation group 448
- p^4 configuration 449, 451
- s^4 configuration 449
- spin configurations 448
- table of transformation properties 449
- free electron energy bands 279–281
 - Bloch function 279–281
 - empty lattice 279–281
 - FCC structure 280, 281
 - first Brillouin zone 280
 - full rotation group 280
 - glide planes 280
 - group of the wave vector 280
 - high symmetry points 280, 281
 - irreducible representations 280
 - level degeneracies 280, 281
 - lifting level degeneracy 281
 - periodic potential 280, 281
 - phase factor 281
 - plane waves 279, 280
 - reduced Brillouin zone 280
 - screw axes 280
 - simple cubic crystal 280
 - wave vector 280
 - full rotation group 80–90, 95, 172
 - addition of angular momentum 172, 173
 - addition theorem for spherical harmonics 82
 - angular momentum 81, 82, 84, 172
 - axis of quantization 82
 - azimuthal angle 82
 - basis functions 80–84
 - characters for inversion 83
 - characters for rotation 80–84, 95
 - compatibility to group O 527
 - compatibility to group T_d 528
 - compound operation 84
 - continuous group 81
 - dimensionality of representations 84
 - direct product 84, 172
 - eigenfunctions 80–84
 - higher to lower symmetry 80, 84
 - inversion operation 84
 - irreducible representation 80–86
 - Legendre polynomials 81
 - level degeneracy 84, 85
 - matrix representation 82, 83
 - odd-dimensional representations 82
 - polar angle 82
 - polar coordinate system 82
 - reducible representation 84
 - rotation operator 82
 - selection rules 172
 - spherical harmonics 80–84, 95
 - Wigner coefficient 172
 - Wigner–Eckart theorem 172
 - glide planes 186, 187, 198
 - axial glide 187
 - definition 187
 - diagonal glide 187
 - diamond glide 187, 198
 - examples 186
 - n -glide 187
 - graphene 258–262, 427
 - eigenvector 262
 - equivalence transformation 260, 261
 - group of the wave vector 259, 260
 - hexagonal Bravais lattice 259
 - high symmetry points 259
 - lattice distortion 262
 - lattice modes at K point 261, 262
 - lattice vector 259
 - mode degeneracy 261
 - normal mode displacements 261, 262
 - phase factor 262
 - projection algebra 262
 - real space vector 260
 - reciprocal lattice vector 259–261
 - symmetry group #191 (D_{6h}^1)
 - $P6/mmm$ 258
 - symmetry operations 260
 - time reversal symmetry effects 427, 428
 - graphite 237, 303, 427
 - electron band structure 237
 - equivalence transformation for 4 atoms per unit cell 236
 - structure factor at various high symmetry points 303
 - symmetry operations of the group of the wave vector 237
 - time reversal symmetry 427
 - graphite space group #166 505

- Hermann–Mauguin notation 505
 Schoenflies notation 505
 Wyckoff positions 505
 group 3, 10, 11, 15
 abstract group 15
 commuting 3
 definition 3
 element 3
 group of Schrödinger's equation 11, 12, 71, 149, 160
 simple group 10
 substitution group 15
 group C_{2v} 154, 155
 application to H_2O molecule 154
 character table 154, 155
 group $C_{\infty v}$ 162
 application to CO molecule 162
 heterogenous linear molecule 162
 homogenous linear molecule 162
 molecular vibrations 162
 symmetry operations 162
 group $D_{\infty h}$ 162–165
 application to CO_2 molecule 164, 165
 eigenvalue transformation 163
 for linear homogeneous molecule 164, 165
 for O_2 molecule 163
 infrared active 163
 molecular vibrations 163
 Raman active 163
 symmetry operations 163
 to C_2H_2 molecule 164, 165
 group element 3, 4
 commuting 3
 group of Schrödinger's equation 12, 71, 149, 160
 definition 12
 eigenfunctions 12
 Hamiltonian 12
 higher to lower symmetry 71
 irreducible representations 71
 matrix representation 12
 group of the wave vector 209, 214–237
 2D hexagonal lattice 215, 235
 2D square lattice 214, 215
 at general point 215
 at high symmetry point 215, 222–237
 basis functions 217–219, 223
 BCC lattice 210, 225
 Bloch functions 219
 character tables 223–226, 234, 235, 237
 classes 231
 compatibility relations 225, 235
 cubic groups at $k = 0$ 223
 definition 215
 degeneracy 215
 diamond structure 210, 230–235
 equivalence transformation 231
 factor group 218, 219
 FCC lattice 210, 225
 higher to lower symmetry 225
 irreducible representation of group of the wave vector at high symmetry points 215, 219, 232, 235
 large representations 219, 220
 lower to higher symmetry 225
 matrix representation 219
 multiplication tables 224
 multiplier algebra 219, 220
 nonsymmorphic structures 218, 220, 232–234
 phase factor 234
 phonon dispersion relations 232
 point group 209, 219, 220
 reciprocal lattice vector 214
 references 235
 simple cubic lattice 209, 222–230
 small representation 219, 220
 special high symmetry points 235
 star of a wave vector 214, 218
 subgroup 219
 symmetry elements 215
 translations 209, 214, 215, 219
- H_2^- ion 120, 142, 143
 Hamiltonian for vibrations 148
 eigenfunctions 148
 eigenvalues 148
 kinetic energy 148
 matrix elements 148
 potential energy 148
 helium molecule He_2 142
 Hermann–Mauguin symmetry notation 47, 479, 500

- complete 230 space groups listing of
3D groups 500
- Hermitian matrix 16, 21
- Herring's rules 408
- band sticking together 410
 - example with group C_4 409, 410
 - time reversal 409, 410
- hexagonal space group #194 502, 504
- Hermann–Mauguin notation 502,
504
- Schoenflies notation 502, 504
- Wyckoff positions 502, 504
- higher to lower symmetry 17, 55, 74,
110
- icosahedron and dodecahedron 74
 - polarization effects 110
 - selection rules 110
- homomorphic 15, 16
- hydrogen molecular ion 120, 142, 143
- hydrogen molecule 119, 120
- hydrogenic impurity problem 328
- crystal potential of periodic lattice
329, 330
 - donor states 329
 - effective Bohr radius 329
 - effective mass Hamiltonian 328
 - effective mass theorem 328, 329
 - hydrogenic impurity levels 329
 - lost symmetry information 328, 329
 - screened Coulomb potential 329
 - substitutional impurity 329
 - valley–orbit interaction 329
- icosahedral molecule 144, 178
- equivalence transformation 178
 - infrared activity 178
 - normal modes 178
 - polarization selection rules 178
 - Raman activity 178
 - rotational–vibrational interaction
symmetries 178
 - symmetries of rotational levels 178
- icosahedron symmetry 142, 144
- identity element 3
- independent components of tensors
- application of irreducible representation $L = 0$ to all tensors 463
- cubic O_h symmetry 464, 465
- direct evaluation from theorem
464–467
- for nonlinear optic tensors 464–467
- full rotational symmetry 463
- going from full rotational to D_{6h}
symmetry 467
- going from higher to lower symmetry
- from full rotational group 464
 - hexagonal D_{6h} symmetry 466, 467
 - nonvanishing third rank tensor 467
 - tetrahedral T_d symmetry 466
- index of a subgroup 11
- infrared activity 157–160
- combination modes 158, 159
 - complementary to Raman activity
160
 - direct product 158, 159
 - H_2O molecule 158
 - oscillating dipole moment 157, 158
 - perturbation Hamiltonian 157
 - selection rules 158–160
- inverse element 3
- irreducible representation for space
groups 224
- basis functions 224
 - character table 224
 - even function 224
 - notation 223
 - odd function 224
- irreducible representations 17, 18, 22,
28, 31–33, 35
- definition 17
 - dimensionality 31
 - examples 28
 - number of representations 35
 - orthogonality 31
 - primitive characters 31–33
 - uniqueness 33
 - vector space 35
- irreducible representations for permuta-
tion groups 438
- antisymmetric Γ_1^s 438
 - (n–1) dimensional representation
 Γ_{n-1} 438
 - phase factors 438
 - symmetric Γ_1^a 438
- isomorphic 15, 16
- Jahn–Teller effect 141, 142

- definition 141
 dynamic 141
 example 142
 geometric distortion 141
 linear effect 142
 Renner–Teller effect 142
 static 141
 symmetry-lowering 141
 time reversal symmetry 142
- $\mathbf{k} \cdot \mathbf{p}$** perturbation theory 305–312,
 316–327, 335, 336, 369–378, 399,
 400
 antibonding bands 306
 bonding bands 306
 connection to valley–orbit interaction
 in semiconductors 327–335
 coupling to intermediate states in sec-
 ond order degenerate perturbation
 theory 335, 336
 degenerate second order **$\mathbf{k} \cdot \mathbf{p}$**
 perturbation theory 324
 effect of small periodic potential to
 split degeneracy of BCC empty
 lattice energy band at H point
 336
 effective mass formula 310
 equivalence transformation 306
 extrapolation method 305, 324
 for hybridized s -bands and p -bands
 306
 independent matrix elements 309
 interpolation method 305, 324
 interpretation of optical experiments
 326, 327
 longitudinal effective mass component
 311
 momentum matrix element 309–311
 nondegenerate **$\mathbf{k} \cdot \mathbf{p}$** perturbation
 theory 308–311, 324, 326, 335,
 336
 oscillator strength 311
 symmetry based energy band model
 305
 transformation properties of
 perturbation Hamiltonian 308
 transverse effective mass component
 311
 two-band model 311–314
- $\mathbf{k} \cdot \mathbf{p}$** perturbation with spin–orbit
 interaction 369–378, 399, 400
 basis functions 372
 Bloch functions with spin 369
 coupling to intermediate states 371,
 374
 for valence band of group IV
 semiconductor 374, 399
 form of $E(\mathbf{k})$ for Γ_6^+ level 373
 generalized momentum operator
 371
 independent matrix elements
 370–372
 irreducible representations 370
 $\mathbf{k} \cdot \mathbf{p}$ expansion for nondegenerate Γ_6^+
 level in the simple cubic structure
 371–374
 $\mathbf{k} \cdot \mathbf{p}$ perturbation Hamiltonian with
 spin and spin–orbit perturbation
 370
 nondegenerate perturbation theory
 $E_n^{I_i}(\mathbf{k})$ 370, 399, 400
 Schrödinger’s equation for periodic
 part of Bloch function 369
 transformation from $|\ell s m_\ell m_s\rangle$
 representation to $|j \ell s m_j\rangle$ 369
- lattice modes 241–277
 at high symmetry points 244, 253
 at zone center 245–253
 block diagonal form 241
 compared to molecular vibrations
 241, 244, 245
 compatibility relations 244
 degeneracies 244
 degrees of freedom 245
 dependence on wavevector 244
 effect of symmetry operation on
 normal modes 245
 effect of translations 245
 eigenvector 244
 equivalence transformation 244,
 245, 253
 group of the wave vector 244, 245,
 253
 infrared activity 241, 244
 irreducible representations 244
 NaCl structure 253
 nonsymmorphic space group 245

- normal modes 241, 244
 number of phonon branches 245
 phase factor 245, 253
 phonon-assisted optical transitions
 244
 polarization effects 244
 Raman activity 241, 244
 secular determinant 241
 selection rules 244
 symmetry classification 244
 symmorphic space group 245
 transformation of the vector 244
 zinc blende structure 253
- line group 204, 205, 208, 237
 axial point group 204
 carbon nanotubes 204, 205, 208, 237
 commutation 204
 direct product 204
 families 204, 205
 identity operation 204
 irreducible representations 237
 symmetry elements 204
 translational symmetry 204
 weak direct product 204, 205
- linear combinations of atomic orbitals
 (LCAO) 67–70, 74
 arbitrary functions 69
 basis functions 69
 example $P(3)$ 67–70, 74
 irreducible representations 67, 68
 matrix representation 68, 70
 projection operator 68
 unitary representation 70
- linear molecules 161–166, 173
 application to C_2H_2 164–166
 application to CO 161–163
 application to CO_2 164
 application to H_2 161
 application to HCl molecule 171
 application to O_2 163
 breathing mode 162, 163
 dipole moment 173
 equivalence transformation 164
 infrared activity 162–164
 molecular vibrations 161–166
 permanent dipole moments 171
 Raman activity 162–165
 rigid rotator spectra 171
 rotational selection rules 171, 173
- magnetic point groups 416–426, 428, 429
 antiferromagnetic ordering 420, 421, 424–426
 antiunitary operators 418
 chalcopyrite structure 429
 chemical unit cell 424
 classification of magnetic point
 groups 420, 421
 color groups 426
 cosets 422
 examples of magnetic structures
 423–426, 428, 429
 ferromagnetic ordering 420, 421, 423, 428
 group D_{4h} (D_{2h}) 425
 invariant unitary subgroup 422
 inversion operator 423, 428
 Jahn–Teller effect 419
 magnetic Bravais lattices 418–421, 424, 425
 magnetic field effect 428
 magnetic phases of EuSe 425
 magnetic subgroup 422, 423, 425
 magnetic symmetry elements 418
 MnF_2 424
 multiplication rules for symmetry
 elements 418, 422
 notation 420–423
 orthorhombic structure D_{2h} (C_{2h})
 423
 Rutile structure 424, 425
 spin flipping operations 425
 structural lattice distortion 419
 symmetry elements 419, 422, 425, 426
 tetragonal group D_{4h} (D_{2d}) 425
 time reversal operator 416, 418, 419, 423, 428, 429
 translation vector 426
 type of magnetic point groups 418
 unitary operators 418
 zinc blende structure 429
- matrix elements 359
 for double groups 359
 number of independent matrix
 elements 359
- matrix representation 15–18, 186
 definition 15

- degeneracy 18
- dimensionality 17
- examples for $P(3)$ 18
- inverse 186
- matrix algebra 16
- multiplication 186
- notation 185, 187
- orthogonal matrices 17
- orthonormal matrices 17
- symmetric elements 18
- trace 17
- translations 185
- uniqueness 17
- unitary matrices 17
- mirror planes 48
- molecular bonding 121
 - antibonding 121
 - bonding 121
 - diatomic molecule 121
- molecular electronic states 149
- molecular energy levels 113
 - Born–Oppenheimer approximation 113
 - electronic motion 113
 - rotational motion 113
 - vibrational motion 113
- molecular Hamiltonian 149
 - block diagonal form 149
 - eigenvalues 149
 - harmonic oscillator 149
- molecular vibrations 154–156, 158–166, 168, 169
 - antisymmetric stretch mode 154, 156, 164
 - bending modes 164–166
 - blocks of atoms within a molecule 165
 - breathing mode 154–156, 162, 166, 167
- C_2H_2 molecule 164, 166
- CH_4 molecule 157, 168–170
- characters for irreducible representations 151
- characters for pure rotations 150, 151
- characters for the vector 150
- characters for translation 151
- CO molecule 162
- CO_2 molecule 164
- combination modes 156–159, 161, 170
- coupling between rotational and vibrational states 171, 173, 174
- coupling of modes with the same symmetries 169
- degrees of freedom 150
- dynamical matrix 147
- eigenvalues 149, 150
- examples 151
- H_2O molecule 154–156, 158
- Hamiltonian 147–149
- infrared active 151, 157–159, 164, 169
- linear molecule 161–166
- NH_3 molecule 165, 167, 168
- normal modes 147–151, 157, 164–167
- O_2 molecule 163
- overtones 156–158
- phase related normal modes 168
- polarization 158
- potential function 147, 148
- Raman active 151, 157, 159–161, 164, 169
- reducible representation 150
- restoring forces 147
- rotations 155, 161
- secular equation 148, 149
- selection rules 147, 151, 160, 161, 171
- symmetric stretch mode 154, 156, 164, 166
 - motion of center of mass 156
 - translations 155
- multiaatomic molecule 124–141
 - angular momentum states 127, 133, 143, 144
 - antibonding 125, 132, 145
 - bonding 125, 132, 145
 - configuration mixing 134
 - directed valence bonding 124, 125, 133, 134, 144
 - electron energy levels 123
 - electronic orbitals 126, 127
 - equivalence transformation 124, 126, 130, 133, 134, 143
 - hexagonal symmetry 129, 130

- irreducible representations 126, 127, 129, 135
- linear combination of atomic orbitals 124, 126, 127, 129, 130, 132, 133, 144
- matrix representation 126, 131
- octahedral bonding 133
- secular equation 131, 144
- tetrahedral bonding 125
- multiplication tables 4, 5, 7, 37, 43, 511
- multiplier group 221
 - effect of symmetry operations 221
 - irreducible representation 221
 - multiplication rules 220, 221
 - multiplier algebra 221
 - phase factor 221
- multivalley semiconductor impurity problem 330, 331
 - central cell corrections 331
 - $D_{\infty h}$ symmetry 330, 331
 - ellipsoidal constant energy surfaces for donor impurities 330
 - Ge with 4 valleys 330
 - Si with 6 valleys 330
 - splitting of impurity levels due to crystal field 330, 331
- N_2O molecule 177
 - atomic displacements 177
 - infrared active modes 177
 - Raman active modes 177
 - rotational modes 177
 - symmetry group 177
- NaCl structure 246, 247, 254, 255
 - at high symmetry points 254
 - compatibility relations 247, 254
 - equivalence transformation 246, 254
 - infrared activity 247
 - lattice modes 246, 254
 - optical branches 247, 255
 - phase factor 255
 - phonon modes 246, 254, 255
- nanotube *see* carbon nanotubes
- Nb_3Sn 207, 275
 - infrared activity 275
 - normal modes 275
 - polarization effect 275
 - Raman activity 275
 - structure 207
- Wyckoff positions 207
- NH_3 molecule 124, 125, 165–168
 - breathing modes 166, 167
 - building blocks 166
 - 3D crystal structure 165
 - equivalence transformation 166
 - linear combination of hydrogen orbitals 167, 168
 - normal modes 168
 - polarization selection rules 168
 - Raman active 168
 - tetrahedral bonding 125
- nondegenerate $\mathbf{k} \cdot \mathbf{p}$ perturbation
 - theory at a Δ point *see* $\mathbf{k} \cdot \mathbf{p}$ perturbation theory, 324–326
 - carrier pockets for electrons and holes 324, 326
- compatibility relations 325, 326
- $E(k)$ for cubic semiconductors at high symmetry points 324
- extrapolation method 324
- group III–V semiconductors (GaAs, InSb) 325
- group IV semiconductors (Si, Ge) 325
- interpolation method 324
- longitudinal matrix elements 325, 326
- transformation of p and $\mathbf{k} \cdot \mathbf{p}$ 325, 326
- vanishing of first order term 326
- nonsymmorphic groups 190, 220
 - multiplier algebra 220, 221
 - multiplier groups 220
 - phase factor 220
 - relevant representations 220
 - small representation 221
- nonsymmorphic space groups 190, 196–198, 220, 221, 230, 294–298
 - definition 189
 - diamond structure #227 196, 198, 230–235, 294–296
 - energy bands sticking together 294–296, 298
 - essential degeneracies 298
 - factor group 190, 220
 - glide plane 198
 - glide plane translation 189
 - group $p2mg$ 294–296

- group of the wave vector 294, 296
 hexagonal close packed structure
 group #194 294–296
 point group operations 189, 230
 screw axis 189, 197, 198
 tetragonal space groups 197, 198
 translation 220, 230
 normal modes 147–154, 159–161,
 163–168, 177
 antisymmetric stretch mode 154
 basis function 149, 150, 161
 breathing mode 154, 163
 C_2H_2 molecule 164–166
 CH_4 molecule 152, 153, 168
 clusters of 3 hydrogen atoms at
 corners of equilateral triangle
 149, 152, 176
 CO molecule 162, 164, 165
 degeneracies 147
 degrees of freedom 150
 dimensionality 150
 eigenfunction 149
 equivalence transformation 154
 for linear molecules 161
 H_2O molecule 153–156, 177
 infrared active 149, 151, 153,
 157–160, 176
 irreducible representation 150
 linear molecules 161–166, 177
 mode mixing between modes with
 same symmetry 168
 molecular rotation 151
 molecular translation 150, 151
 NH_3 molecule 166–168, 176, 177
 normal mode amplitudes 148
 normal mode frequencies 148
 normal mode matrix 150
 orthogonality 151
 orthonormality 152
 phase related normal modes 168
 planar NH_3 molecule 176
 projection operators 152
 Raman active 149, 151, 153,
 159–161, 176
 secular equation 148
 selection rules 151, 158
 symmetric stretch mode 154
 symmetry 147–151, 163
 tetrahedron 152, 153
- O_2 molecule 163
 equivalence transformation 163
 molecular vibration 163
 one-electron Hamiltonian 183
 invariant under symmetry operations
 183
 order of a class 10
 definition 10
 order of a group 6, 28, 40
 example for $P(3)$ 40
 proof of theorem 40
 order of a subgroup 8, 9
 order of an element 6
 definition 6
 order of group 40
 orthogonality of basis functions 99,
 100
 partners 99, 100
 scalar product 100
 selection rules 100
 orthogonality theorem 19, *see* Won-
 derful Orthogonality Theorem
 orthonormality relation 28
 overtones 156, 157
 CH_4 molecule 156, 157
 direct product 156
 infrared active 156, 157
 irreducible representations 156, 157
 Raman active 156, 157
- $P(3)$ 13, 16, 37, 42, 443–448, 543
 $P(4)$ 13, 448–451, 544
 $P(5)$ 451, 452, 544
 $P(6)$ 451–453, 545
 $P(7)$ 451–453, 546
 period of an element 6, 7
 periodic boundary conditions 211
 permutation group of three objects
 37, 42
 permutation groups 3, 5, 13, 15, 16,
 431–454
 antisymmetric representation 433
 antisymmetric states 432
 basis functions 434, 437–440, 443
 classes 434–437
 classification of many electron states
 431
 commutation of permutation
 operations with Hamiltonian 432

- cycle structure 434, 435
 equivalent electron and hole configuration 450, 451, 453
 example 13
 five-electron states 434, 451–454
 four-electron states 434, 448–451
 group operations 432
 identity 432
 inverse 432
 irreducible representations 434, 436, 438, 439
 multiplication 432
 notation 432, 440
 number of elements 432
 orbital states 442
 $P(3)$ 13, 16
 $P(4)$ 13
 Pauli principle 432, 433, 440, 442, 443
 regular representation 439, 440
 six-electron states 454
 Slater determinant 433, 440
 symmetric representation 433
 symmetric states 432
 symmetry properties of tensors 431, 458–463
 three-electron states 434, 444, 445, 447, 448
 two-electron states 434, 440–443
 Perovskite structure 247–250
 acoustic 242, 245
 equivalence transformation 247
 infrared activity 250
 LA mode 245
 LO mode 245
 optical 245
 phonon modes 247–250
 TA mode 245
 TO mode 245
 phonon dispersion relations 242, 243
 branches 244, 245
 for germanium 243
 high symmetry points 243
 mode degeneracies 243
 optical modes 242
 phonon branches stick together 243
 phonon modes *see also* lattice modes, 241–277
 2D graphite at K point 258
 α -quartz 262, 268, 269
 diamond structure 250
 graphene 262
 NaCl structure 246, 247
 nonsymmorphic structure 268
 Perovskite structure 247–250, 256
 tellurium 262, 268
 π -bonding 113, 134–141
 angular momentum states 137–139
 bond direction 135
 characters 135
 directed valence bonds 135, 137–140
 equilateral triangle 137, 138
 equivalence transformation 137, 138
 irreducible representation 135, 140
 linear combination of atomic orbitals 135, 137
 p -states 135
 polarization 140
 transformation of vector 139
 piezoelectric third rank tensor under various symmetries 476
 plane wave basis functions for double group representations 361, 362
 $Pm3m$ (O_h^1) group #255 FCC 222
 $Pm3m$ (O_h^{11}) group 223
 Brillouin zone 223
 high symmetry axes and points 223
 point group 29, 48, 49
 $C_{\infty v}$ and $D_{\infty h}$ groups 53
 classification 48–53
 cubic groups 50, 52
 cyclic groups 50
 Hermann–Mauguin notation 48–50
 hexagonal group 49, 481–483
 horizontal planes 50
 icosahedral groups 49, 52, 483–485
 improper rotation 50
 inversion symmetry 50
 monoclinic group 49, 480
 orthorhombic group 49, 480
 proper rotation 50
 rhombohedral group 49, 481
 Schoenflies notation 48–50
 stereogram 50, 52
 tetragonal groups 49, 480, 482
 triclinic groups 49, 479
 vertical mirror planes 50

- point group character tables 29–55,
479–487
- projection operators 64–67, 72, 117,
152
- action on arbitrary function 64–67
- action on irreducible representation
66, 67
- definition 64
- diagonal elements 65
- matrix representation 65
- partners 64
- quantum mechanics 70–72
- commuting operations 70
- finding linear combination of wave
functions 72
- group of Schrödinger's equation 70
- higher to lower symmetry 72
- matrix representation 70
- Raman effect 159–161
- anti-Stokes component 159
- basis functions 161
- diagonal components 160, 161
- electron–photon interaction 160
- electron–photon scattering 160
- first-order process 159
- induced dipole moment 159
- intermediate state 160
- inversion symmetry 160
- matrix elements 159, 160
- off-diagonal components 160, 161
- polarizability tensor 159–161
- Raman Hamiltonian 159–161
- second rank symmetric tensor
159–161
- second-order process 159, 160
- selection rules 160, 161
- Stokes component 159
- transformation properties 160
- Rayleigh scattering 159
- rearrangement theorem 7, 8, 21, 37
- reciprocal space 210, 211, 503
- bands sticking together 507
- Brillouin zone 211
- lattice vector 210
- orthonormality relation 210
- primitive translation vector 210
- reciprocal lattice vectors 210
- reducible representation 17, 18, 33, 34
- regular octahedron 85
- regular representation 37–40, 439
- decomposition theorem 39
- definition 37
- dimensions 439, 440
- example from $P(3)$ 37, 40
- irreducible representations of 39
- multiplication of two elements 37
- order of regular representation 40,
439, 440
- Slater determinant 440
- representation of translation group
211–213
- Abelian groups 211, 212
- Bloch theorem 212
- commuting operators 211
- crystal symmetry 212
- number of group elements 212
- number of irreducible representations
211, 212
- periodic boundary condition 212
- phase factors 212
- representation theory 15, 19
- basic theorem 15
- representations 5, 15, 17, 28, 29
- arbitrariness 29
- by a matrix 5
- definition 5, 15
- dimensionality 28, 29
- faithful 15
- irreducible representation 17
- reducible representation 17
- unfaithful 15
- vector space 28
- restoring forces 147
- rhombohedral graphite 502
- rigid rotator 170–172
- Hamiltonian 170, 171
- linear HCl molecule 171, 172
- optical transitions 171, 172
- principal moments of inertia 171
- selection rules 171
- Wigner–Eckart theorem 171
- rotational energy levels 170, 172
- infrared spectra 171–173
- Raman spectra 171–173
- rigid rotator 170–172
- selection rules 172, 173

- typical energy range 170
- rotational spectra 170–173
 - circular polarization 173
 - polarization effect 171, 173
 - rotational–vibrational interaction 171, 173
- Wigner–Eckart theorem 172, 173
- Schoenflies symmetry notation 31, 44, 479
- Schur’s lemma 19, 21–25
- screw axis 186, 187, 197, 198
 - diamond screw 198
 - left-hand 186
 - n -fold 187, 198
 - notation 187
 - right-hand 186
 - unit cell translation 188
- second orthogonality theorem 36, 37, 43, 55
- secular equation for valence band
 - of group IV semiconductor 375–377, 399
- \mathbf{k} -dependent spin–orbit splitting 377
- selection rules 97, 98, 105–107, 109, 110, 147, 173
 - cubic symmetry 98, 106, 109
 - definition 97
 - direct product 105, 107, 108
 - electric dipole 98, 106–110
 - electromagnetic interaction 97, 106, 108
- group of Schrödinger’s equation 105, 106, 109
 - higher to lower symmetry 107, 108
 - infrared active 147, 173
 - linear diatomic molecule 173
 - momentum 106
 - odd parity 107
 - orthogonality 105
 - polarization effects 108, 109
 - Raman active 147, 173
 - rotational transitions 173
 - tetragonal symmetry 108
 - transformation properties of vector 106–109
- self-conjugate 9
- self-conjugate subgroup 10, 13
- definition 10
- left coset 10
- right coset 10
- setting up character tables 41–43
 - number of classes 41
 - number of irreducible representations 41
- SF_6 molecule 133, 134, 143
- SH_6 molecule 129, 143
- σ -bonding 113, 134–139
 - characters 135
 - directed valence bonds 135, 137–139
 - equilateral triangle 137, 138
 - equivalence transformation 137, 138
 - example 136–139
 - irreducible representation 135
 - linear combination of atomic orbitals 135–137
 - p -states 135
 - s -states 135
- silent modes 160
- simple cubic lattice 225
 - basis functions 224
 - character tables at high symmetry points 224, 225
 - compatibility relations 227
 - group of the wave vector at high symmetry points 223, 226, 227
- site symmetries 196
- six-electron states 454, 545
- Slater–Koster method 305, 306, 389–400
 - angular momentum matrices 391, 392
 - basis matrices 391, 392
 - Bloch functions 391
 - connection to $\mathbf{k} \cdot \mathbf{p}$ perturbation theory 396
 - contributions to Fourier expansion 395–397
 - coupled bands 391
 - $E_n(\mathbf{k})$ is periodic in k space 389
 - energy bands at high symmetry points 389
 - energy dispersion for FCC structure at high symmetry points 400
 - energy eigenvalues found at all \mathbf{k} values by diagonalizing the matrix Hamiltonian 397

- evaluating expansion parameters
 by parsising energies to
 experiments theory 397
 expansion parameters 390, 391, 395,
 397
 Fourier expansion for $E(k)$ bands
 390, 394–399
 germanium 389, 390, 399
 Hamiltonian 391
 interacting p -bands 394–398
 interpolation method 389, 390
 irreducible representations 395
 matrices spanning space 391–394
 neighbor distances 390, 394, 395
 nondegenerate bands 391
 overlap integrals 390
 partners of irreducible representations
 392, 394
 reciprocal lattice vectors 394
 scalar products of symmetrized
 Fourier functions and basis
 functions 394
 secular determinant 391, 400
 silicon 389, 399
 solutions of matrix Hamiltonian 397
 symmetrized basis matrices 391,
 395–400
 symmetrized Fourier functions
 394–398
 symmetry restricted number of
 independent expansion coefficients
 390
 Taylor's expansion at high symmetry
 points 400
 tight binding approximation 390
 Slater–Koster model 305, 306
 small representations 221
 group of the wave vector 221
 SnO_2 275, 276
 crystal structure 276
 lattice modes 276
 sp^2 planar carbon bonding 136–139
 space group 211, 214–216
 space group determination 206, 208
 carbon nanotubes 208
 graphite 208
 International Crystallography Tables
 206
 site symmetries 206
 Wyckoff positions 206, 208
 space group operations 183–186, 189,
 190, 208
 associative law 185
 commutation 185
 definitions 184, 185
 glide plane 183, 187, 189
 identity 185
 inverse 185
 inversion 185
 matrix representation 185, 187
 multiplication 184, 185
 notation 183–185, 187, 189
 point group operations 183, 184, 189
 rotations 184
 screw axes 183, 186, 189
 translations 183, 184
 space groups 29, 183, 184, 189, 190,
 195, 198, 205, 206
 Bravais lattice 190–198, 207
 crystal structure determination
 205–207
 definitions 189
 diamond structure 195, 207
 direct product group 190
 equivalence transformation 206
 factor group 190
 group of the wave vector 214–219
 irreducible representations 190
 line group 204
 nonsymmorphic 183, 189, 190, 198,
 207
 point group operations 183, 190,
 214, 215
 semi-direct product 189
 subgroups 189, 190
 symmorphic 183, 189, 190, 198, 207
 translations 214
 two-dimensional 198–203, 207, 211
 wave vector 215
 space groups in reciprocal space 209
 Bravais lattices 209
 dispersion relations 209
 group of the wave vector 209
 nonsymmorphic 209
 symmorphic 209
 spherical harmonics 82
 spin Hamiltonian 426, 427
 magnetic field effect 426

- spin-orbit interaction 81, 337–339, 348
 addition of angular momentum 338
 band degeneracies 340
 doubly degenerate 348
 Dresselhaus spin-orbit term 340
 expectation value of $\mathbf{L} \cdot \mathbf{S}$ 338
 germanium along high symmetry axes 339, 340
 good quantum numbers 338
 half-integral spin 337, 338
 Hamiltonian breaks into block diagonal form 348
 $|j, \ell, s, m_j\rangle$ representation 338
 Kramers degeneracy 340, 348
 lifting degeneracy 338
 linear k term in $E(k)$ 348
 magnitude 339
 notation 340
 relativistic corrections 348
 spin and orbital wave functions 339
 spin angular momentum and magnetic moment 337
 spin-orbit splitting in crystals 339, 340, 348
 time reversal symmetry 340, 348
 wave vector dependence 339, 340
 Zeeman splitting in an external magnetic field 338, 339
- star of a wave vector 214, 215, 217, 235
 2D space groups 215, 217, 235
 at $\mathbf{k} = 0$ 215, 217
 at general \mathbf{k} point 215
 at high symmetry points 217
 at zone boundary 217
 definition 215
 effect of translations 214
 reciprocal lattice vector 214
 symmetry elements 218
 structure of nanotube 205
 achiral 205
 armchair 205
 chiral 205
 line group symmetry 205
 zigzag 205
 subgroup 6–8, 10
 definition 6
 self-conjugate 10
 symmetry based energy band models 305, 306, 316
- $\mathbf{k} \cdot \mathbf{p}$ perturbation theory 305, 306
 Slater-Koster model 305, 306
- symmetry lowering 194
 point group symmetry lowering 194
 symmetry notation 44–48
 abbreviated notation 47
 compound rotation–inversion 45
 dihedral plane 45
 Hermann–Mauguin 44, 46, 47
 identity operation 44
 improper rotation 45, 48
 mirror planes 47, 48
 proper rotation 48
 reflection in a plane 45
 rotating about an axis 44, 47, 48
 Schoenflies notation 44, 46, 47
 semi-infinite groups 46
 symmetry groups 46
 symmetry properties of tensors 455–477
 antisymmetric second rank tensor 458
 complete isotropy 457
 effect of crystal symmetry 457, 460
 effect of permutations 460
 elastic constant tensor 457, 459, 467–477
 electrical conductivity tensor 455, 456
 fourth rank tensor 455
 full rotation group 457
 fully symmetric irreducible representation $L = 0$ 463
 independent coefficients for various tensors and symmetries 457, 460–466, 471–476
 irreducible representation 459
 momentum configuration 459
 nonlinear elastic modulus under permutation symmetry 476
 number of times the totally symmetric representation is contained in the direct product of coupling tensors 462
 p^2 configuration 458
 p^3 configuration 458
 Pauli allowed state 459
 permutation symmetry 455
 piezoelectric tensor 456, 459, 476

- polarizability tensor 455, 456, 459
 second rank tensor 455, 456
 strain tensor 457
 stress tensor 457
 symmetric third rank tensor 455, 456, 458
 tensor components equal to one another 457
 theory of independent components of tensors 462
 transformation properties of tensors under permutations 458, 459
 symmorphic space groups 189, 192–194, 196, 198–203
 Bravais lattice 192, 194
 equivalence transformation site symmetry 196
 International Crystallographic Tables 192

 table of direct products for double groups O and T_d 523
 table of group of the wave vector at various symmetry points 508
 space group #166 509
 space group #194 509
 space group #221 508
 space group #225 508
 space group #227 508
 space group #229 508
 tables for 3D space groups 499–520
 character tables 510–520
 tables of double groups 521–532
 notation 521
 references 521
 tables of permutation groups 543–547
 T_d symmetry 125, 152
 tellurium 262–268
 Brillouin zone 264
 character table 262
 crystal structure 263
 equivalence transformation zone
 center mode 264–266
 infrared activity 264, 265, 267
 lattice modes 262, 264–267
 nonsymmorphic 262
 normal modes 265–268, 274
 phonon dispersion relations 264
 polarization 264–268

 Raman activity 264–267
 screw axis 262, 264, 265
 space group 262
 z -direction 265
 tetrahedron 153
 three-dimensional graphite 274
 compare 2D and 3D graphite 274
 compatibility relations 274
 infrared activity 274
 normal modes 274
 number of lattice modes 274
 symmetry operations 274
 three-electron states 444–448
 allowed states 446
 antisymmetric irreducible representation Γ_1^a 445
 classes 444
 direct products 445, 446
 group $P(3)$ 446
 irreducible representations 444, 445
 orbital angular momentum states 445
 Pauli principle 445, 447, 448
 permutations of three-electrons 444
 spin states 445
 symmetric irreducible representation Γ_1^s 445
 time reversal operator 21, 403, 404
 action on momenta 403
 action on orbital angular momentum 404
 action on spin angular momentum 404
 action on velocities 403
 action on wave function 403
 antilinear operator 404
 commutation with Hamiltonian 404, 405
 complex conjugation of wave functions 404
 Pauli matrices 404, 405
 properties of time reversal operator 404–407
 spin-orbit interaction effects 404, 405
 $\hat{T}^2 = +$ or -1 405
 time evolution 403, 404
 time-reversed conjugate 403
 unitary operator 405

- time reversal symmetry 403–418, 422–425, 427–429, 446
 antiunitary operator 406
 bands sticking together 408, 413
 breaking time reversal symmetry 427
 complex conjugation 404, 405
 degeneracies 413
 effect of inversion symmetry 413
 effect of time reversal 406–413
 examples 414–416
 ferrites 429
 Frobenius–Schur test 414–416
 graphite space group #194 427
 Hamiltonian 429
 Herring’s rules 408–410, 412–415
 Kramers degeneracy 407, 412
 magnetic field effect 428
 magnetic groups 403, 407, 416–418, 422–425, 429
 notation 415, 416
 operators ($\mathbf{p}, \mathbf{L}, \sigma$) odd under time reversal symmetry 406
 operators ($H, \mathbf{r}, V(\mathbf{r})$) even under time reversal symmetry 406
 properties of time reversal operator 404–407
 Raman effect probe 429
 spin effects 403, 406, 411, 412, 425
 spin Hamiltonian 403, 427
 time evolution factor 404
 time reversal operator 403, 405
 zinc blende structure 429
- trace 12, 29
 invariance 12
- Translation Group 188, 211–213, 217
 Abelian group 211–213
 basis function 213, 217
 Bloch theorem 212, 213
 commuting operator 211
 cyclic subgroup 211
 direct product 188
 eigenfunction 212
 eigenvalue of translation 213
 factor group cosets 188
 invariant subgroup 188
 irreducible representation 211–213, 217
 notation 188
- periodic boundary condition 212
 phase factor 213
 quantum number 212
 space group 188
 three dimensions 212
 wave vector 213
- translation subgroup 188
 translational symmetry of line groups 204
 translations in molecular vibrations 151
 transparent host crystal 79
 transposition 16
 two-band model 311–316
 band edge wave function 312
 degenerate first order perturbation theory 311, 312
 dependence of density of states on energy 316
 dependence of effective mass on energy and wave vector 315, 316
 Kane two-band model 314
 Lax two-band model 314, 316
 momentum matrix elements 314
 nearly degenerate set (NDS) 311
 nonparabolic effects 313–316
 number of independent matrix elements 313
 secular equation 312, 313
 Taylor expansion for small κ 313, 315
- two-dimensional Bravais lattices 199, 200
- two-dimensional space groups 198–200, 236, 489–498
 2D oblique space groups 200
 allowed n -fold rotations 200
 centered 200
 contrast group #11 ($p4mm$) and group #99 ($P4mm$) 236
 glide planes 200
 group of the wave vector at high symmetry points in the 2D Brillouin zone 236
 hexagonal 199, 496–498
 International Crystallography Tables 199
 mirror planes 200
 nonsymmorphic 236

- notation 199, 200, 236
 oblique 199, 489, 490
 primitive 200
 rectangular 199, 490–493
 sixfold rotations 200
 space group numbers 199
 special points 200
 square 199, 494–496
 symbols for rotation 200
 symmorphic 199, 236
 two-electron states 440–443
 antisymmetric states 440, 441
 classes 441
 Γ_1^a representation 441
 Γ_{n-1} representation 441
 ground state 440, 441
 irreducible representations 441
 notation 440
 orbital state 441
 Slater determinant 440
 spin state 441
 symmetric state 440
 table of transformation properties 441
- unit cell 210
 unitarity of representation 19–22
 theorem 19, 20
- valley–orbit interaction 328, 331–336
 donor states for multivalley semiconductors 331, 332
 ENDOR studies of impurity levels 334, 335
 equivalence transformation for valley sites 332
 example of valley–orbit interactions 328
 experimental spectrum for valley–orbit splitting of phosphorous donors in silicon 334, 335
 importance of tetrahedral bonding for *s* state 331, 332
 linear combination of valley wave function transforming as irreducible representation of the crystal field 331–335
 lower symmetry group not a subgroup of higher symmetry group 328
- spatial dependence of wave functions 334, 335
 symmetry of effective mass Hamiltonian for impurity perturbation for one valley 328
 transformation of a vector for T_d group 333–335
 transition from $1s$ to transverse $2p$ levels 334, 335
 transitions between impurity levels showing valley–orbit splitting 334, 335
 vector space 28
 vibration potential function 147
 equilibrium coordinates 147
 vibrational–rotational interaction 173–175
 anharmonic term 174
 combination modes 174, 175
 experimental spectrum for HCl 175
 harmonic restoring force 174
 schematic spectrum for diatomic molecule such as HCl 176
 unperturbed energies 175
- wave vector symmetry 214
 group of the wave vector 214
 star of a wave vector 214
 Wigner–Eckart theorem 172
 angular momentum states 172
 electric dipole transitions 173
 infrared activity 173
 principal quantum numbers 172, 173
 Raman activity 173
 reduced matrix element 172, 173
 selection rules 173
 Wigner coefficient 172, 173
 wonderful orthogonality theorem 21, 25–28, 31, 55
 wonderful orthogonality theorem for character 31, 32, 34–37, 41
 Wyckoff positions 201, 206–208, 506
 site symmetry 201, 206
 special points 201
- zinc blende space group #216
 Hermann–Mauguin notation 502
 Schoenflies notation 502

Wyckoff positions 502
zinc blende structure 252, 502
LO–TO splitting 252, 253

phonon modes 252, 253
space group 252, 502
symmorphic group 252